VNIVERSITAT DE VALÈNCIA

PROGRAMA DE DOCTORAT EN BIOMEDICINA I BIOTECNOLOGIA

Life under the sun: microbial ecology and applications of the solar panel microbiota

MEMÒRIA PRESENTADA PER KRISTIE SYLVIA ARACELI TANNER, CANDIDATA AL GRAU DE DOCTORA PER LA UNIVERSITAT DE VALÈNCIA

CO-DIRECTORS: DR. MANUEL PORCAR MIRALLES, DR. JULI PERETÓ MAGRANER, DRA. CRISTINA VILANOVA SERRADOR

VALÈNCIA, OCTUBRE 2020

“What got you here won’t get you there”

Marshall Goldsmith

El Dr. MANUEL PORCAR MIRALLES, Investigador Indefinido Doctor de la Universitat de València (Instituto de Biología Integrativa de Sistemas I2SysBio, UV-CSIC), la Dra. CRISTINA VILANOVA SERRADOR, Directora Científica de Darwin Bioprospecting Excellence S.L., el Dr. JULI PERETÓ MAGRANER, Catedrático de la Universitat de València y miembro del Instituto de Biología Integrativa de Sistemas (I2SysBio, UV-CSIC) y la Dra. EMILIA MATALLANA REDONDO, catedrática de Bioquímica y Biología Molecular en la Universitat de València y miembro del Instituto de Biología Integrativa de Sistemas (I2SysBio, UV-CSIC):

AUTORIZAN la presentación de la memoria titulada "Life under the sun: microbial ecology and applications of the solar panel microbiota" y CERTIFICAN que los resultados que incluye fueron obtenidos bajo la codirección de los doctores MANUEL PORCAR MIRALLES, CRISTINA VILANOVA SERRADOR, y JULI PERETÓ MAGRANER en el Instituto de Biología Integrativa de Sistemas (I2SysBio, UV-CSIC) y en Darwin Bioprospecting Excellence S.L. por KRISTIE SYLVIA ARACELI TANNER.

Y para que conste, firman el siguiente certificado en Paterna a 28 de octubre de 2020.

PATERNA, 28/10/20
Lugar, Fecha

Dr. Manuel Porcar Miralles (Director)

PATERNA, 28/10/20
Lugar, Fecha

Dra. Cristina Vilanova Serrador (Directora)

PATERNA, 28/10/20
Lugar, Fecha

Dr. Juli Peretó Magraner (Director)

PATERNA, 28/10/20
Lugar, Fecha

Dra. Emilia Matallana Redondo (Tutora)

Acknowledgements

On this journey, I have been lucky enough to be surrounded by some incredible, talented, kind people, that have continuously supported me in both professional and personal aspects and without whom this thesis would not have been possible.

First of all, I would like to thank my directors. Manel, thank you for always bringing out the best in me and for inspiring me with your unlimited creativity. Juli, thank you for always giving me your valuable insight on all my work and for guiding me throughout these four years. And Cristina, there are so many things I would like to thank you for, but mostly I want to thank you for always being there for me as a mentor, as a coworker, and as a friend. You are an amazing woman and role model that any person would be lucky to have in their life.

I believe that a key aspect of scientific research is the human team behind it. That is why I would like to thank all my coworkers, both in the I^2SysBio and in DARWIN. In particular, I would like to thank Esther and Àngela from the I^2SysBio for being there from almost the beginning of this journey, and for all the fun times that we have had together. As for DARWIN, every day I am amazed at what an excellent team we have. In particular, I would like to give a special thanks to Javi, Adriel, Marta and Helena for their support in microbial taxonomy, bioinformatics and wetlab and, even more importantly, for always bringing out a smile in me. I would also like to give a special thanks to Patricia Martorell and the *C. elegans* team from ADM-Biopolis, to Maria Jesús Rodrigo and her team from the Instituto de Agroquímica y Tecnología de Alimentos (IATA, CSIC), and to the Khalil lab, led by Mo Khalil, in Boston. These collaborations have been so fruitful, and it has been a pleasure to work with all of you.

This thesis would not have been possible without the loving environment that has surrounded me. First, I would like to thank mum and dad, for always believing in me and encouraging me to continuously push my boundaries and go one step further. I am so lucky to have you as my parents, and I love you so much. I would also like to thank my 'other' family from Denia, Mikel, Lola and Aingeru, for always supporting me, and I would like to give a very special thanks to David, for always being there for me and for mum.

Friends are the family we choose, and there aren't enough words to thank all my friends that have accompanied me in this journey. Carmen, Paula and Lali, thank you for all the good times and all the laughs we have had, you are amazing. Karen, Erin and Natalie, my lifelong friends from the village, I know we will always be there for each other in the good times and in the bad, and I thank you for that.

I would like to give a very special thanks to Sarah and Mark. You welcomed me into your home without even knowing me and made me feel like family. Those three months in Boston will always have a special place in my heart, and the best part of it all was meeting you. I know that this is just the beginning of our friendship, and I am so looking forward to all the times to come.

Finally, I want to thank a very special person who has been there for me for almost 11 years and who I love more than anything in this world. Aitor, thank you for your patience and your kindness, for your love and your cuddles, for always making me happy. And, especially, thank you for not only being my partner in life, but also my best friend.

To everyone that I have mentioned here and many other people that are in my life, when we have each other, we have everything.

Contents

Introduction

1. The bioprospecting landscape

The diversity of prokaryotic microorganisms on Earth is a subject of controversy. While the use of scaling laws predict that the Earth is home to 1 trillion (10^{12}) microbial species (Locey & Lennon, 2016), a recent study based on publicly available sequencing data calculated a global prokaryotic OTU richness six orders of magnitude lower (Louca et al., 2019). Independently of the exact number, what is clear is that the prokaryotic world is vast and diverse, and a large fraction of it still remains to be explored. Microbial diversity is everything except random: microorganisms are the result of evolution and adaptation. This diversity provides us with an incredible arsenal of unique and useful tools that can be used in a wide range of industrial and pharmaceutical applications. The search of these biological tools is what we know as bioprospecting.

1.1 Bioprospecting opportunities for business

Taking into account that only a fraction of the global microbial diversity has been explored to date (Locey and Lennon, 2016), the number of – yet to be discovered – strains, genetic tools or metabolites with biotechnological or biomedical applications is overwhelming. This opens a great market opportunity for the biotechnology industry and, particularly, for microbiology-based commercial developments. Despite this great potential, the commercialization of products derived from bioprospecting is a long and costly endeavor that must comply with several checkpoints along the way (Figure 1).

Any bioprospecting project must begin with the collection of biological samples from a target environment. There are several critical aspects to take into account, for example selecting the environment accordingly to the purposes of the project to ensure an adequate pre-adaptation of the microorganisms, or ensuring sterility and optimal transportation conditions until the processing of the samples in the laboratory. But, more importantly, it is critical to be aware of the implications of the Nagoya protocol in the specific country where the samples are being collected. The next step is to apply advanced culturing techniques in order to isolate the largest possible fraction of culturable microorganisms that will then be subjected to high-throughput screening to detect biological activities of interest. Once the microorganisms of interest have been selected, it is important to assess the regulations and safety issues associated to the use of these particular strains, for example, for human consumption. Regarding this issue, the European Food Safety Authority (EFSA) publishes, every year, a list of biological agents that can be intentionally added to food or feed and that are considered to be safe (QPS or Qualified Presumption of Safety) (EFSA BIOHAZ Panel., 2020). Beyond Europe, a similar regulation is provided by the United States Food and Drug Administration (FDA), in which the term 'GRAS' is used to designate food additives (biological agents and other substances) that are Generally Recognized As Safe. For a microbial

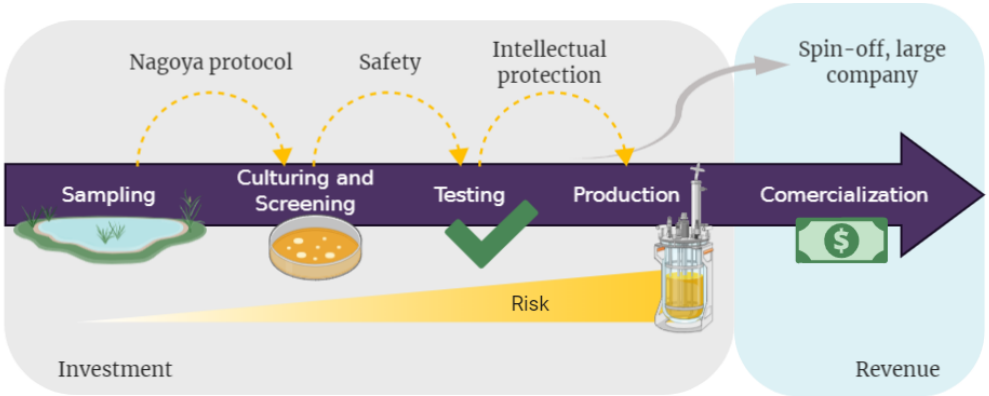

Figure 1. Bioprospecting process: from sampling to business.

strain to be considered QPS or GRAS it must display a certain genomic stability, be non-pathogenic, display no antimicrobial resistance, and not produce toxic substances (EFSA FEEDAP Panel et al., 2018).

The selected strains of interest may need to undergo a deep characterization to verify their biological activity *in vivo* using experimental models, from simple cell cultures and invertebrate models, to vertebrate models and clinical trials. Throughout this period, intellectual protection must be assessed and implemented for the applications of the promising strains, and the culturing of these strains must be scaled up, a step that is critical to obtain cost effectiveness when commercializing the final product. Furthermore, the translation to market requires the application of a specialized set of skills such as market trend analyses, business strategy, design, communication skills or financial expertise. For this reason, many bioprospecting projects often derive to an external company (i.e. large pharma companies) or to a spin-off company for this final phase. And, after a long investment with an increasing risk associated to each step, finally a revenue is obtained. Despite the complexity of bioprospecting projects, many companies have been successful in this endeavor (Table 1). For example, companies highly specialized in bioprospecting of innovative veterinary products (i.e. Aquilón Cyl, Spain) or bacteriocin-producing strains (i.e. BLIS Technologies, New Zealand), and also new start-up companies offering improved multi-omic analysis and culturing approaches (i.e. Darwin Bioprospecting Excellence S.L., Paterna, Spain) applied to any type of sample, are already part of the bioprospecting marketplace.

Table 1. Companies based on bioprospecting activities around the world.

Company	Founded	Country	Description
AB-BIOTICS	2004	Spain	Probiotics and functional ingredients for food and pharmaceutical industry
ADM-Biopolis	2003	Spain	Probiotics, novel ingredients and cell factories
Alimentary Health	1999	Ireland	Probiotic strains from human origin
Aquilón CyL	2012	Spain	Innovative veterinary products
ARTECHNO SA	1999	Belgium	Strains for food solutions, animal feed, and environmental applications
Barentzymes	2013	Norway	Enzyme-based solutions in industrial biotechnology
Bialactis	2012	Spain	Probiotics for human and animal consumption
BioCare Copenhagen	2012	Denmark	Microbial actives targeting GI disorders, metabolism, and immunity
BioGrowing	2006	China	High-quality probiotics production, research and development.
BIOHM Health	2016	USA	Novel probiotic products targeting microbiome's bacteria and fungi
Biosearch Life	2000	Spain	Probiotics for pharmaceutics, nutraceutics and functional food
BLIS Technologies	2000	New Zealand	Healthcare products based on bacteriocin-producing bacterial strains
Chr. Hansen	1874	Denmark	Cultures, enzymes, probiotics and natural colors for a range of applications
Danone Nutricia	1896	Netherlands	Nutritional solutions for infants, young children, pregnancy and the elderly
Darwin Bioprospecting Excellence S.L.	2016	Spain	Probiotics for agrifood, cosmetics and environmental applications
Deinove	2006	France	Use of *Deinococci* in production of biofuels and other compounds
EnzymatiX	2013	USA	Production of enzymes using fungi
FitBiomics	2015	USA	Probiotic bacteria for application in sports performance and recovery
Guardian Food	2010	USA	Probiotic for commercial livestock industry
ImmuneBiotech	2013	Sweden	Novel microbiome therapeutics based on probiotic lactic acid bacteria
JiangSu Wecare	2013	China	Novel probiotics and derivatives for human consumption and food starters
MetaboGen	2011	Sweden	Novel bacterial strains derived from the human gut microbiome
Microbion	2011	Italy	Innovative products in the field of agro-industrial microbiology
Noor Enzymes	2008	India	Enzymes targeted for industrial applications
Novozymes	2000	Denmark	Enzyme and microbial technologies
OptiBiotix	2012	United Kingdom	Microbial strains and compounds that modulate the human microbiome.
Organobalance	2001	Germany	Probiotics for human consumption
PharmaMar S.A.	1986	Spain	Antitumoral activities from marine microorganisms
Probi	1991	Sweden	Probiotic expertise from R&D to finished products
Probisearch	2011	Spain	New probiotics for human and veterinary applications
PROGE FARM	1992	Italy	Probiotic strains for gastrointestinal and gynecological applications
Pure Cultures	2013	USA	Custom fermentation company
Stratum Nutrition	1957	USA	Value-added ingredients for the supplement and pet food industries
Swissaustral Biotech	2009	USA	Development of highly stable extreme enzymes
SYNBIO Tech Inc.	2000	China	Probiotic manufacturer
THT	1991	Belgium	Lactic ferments used in healthcare and foodstuff
TwentyGreen	2015	Switzerland	New probiotic feed supplement for animal farming.
UBQ Madeira	2011	Portugal	Natural extracts from seaweeds
VF Bioscience	2011	France	Innovative functional ingredients and food supplements
Winclove	1991	Netherlands	Probiotic formulations

1.2 The bioprospecting process

The bioprospecting studies carried out in the present thesis have involved the first steps of the process described above: sampling, culturing and screening of microorganisms with potential applications in industry (Figure 1).

1.2.1 Sampling and regulations for the access to genetic resources

The Convention on Biological Diversity (CBD) was signed in 1992 with the goal of ensuring a sustainable use of biodiversity by supporting conservation of biodiversity sharing of benefits and knowledge/technology transfer through scientific cooperation. The Nagoya Protocol on Access and Benefit Sharing (ABS) came into force in October 2014, aiming to harmonize the implementation of the CBD by increasing legal certainty and transparency for the providers and users of genetic resources and associated traditional knowledge, while ensuring the correct allocation of benefits (monetary and non-monetary) that may derive from this use (Smith et al., 2017). Although the Nagoya Protocol arose from a global negotiation process, each country that ratifies it must implement its own regulations; in other words, it must decide whether or not it controls the access to the its resources. Country-specific information on access and benefit-sharing established by the Nagoya Protocol can be found on the ABS Clearing-House website (https://absch.cbd.int/). Currently (October 2020) a total of 127 countries have ratified the Nagoya Protocol.

Despite the good intentions of the Nagoya Protocol, there are several controversies dealing with its application to microbial diversity. Specifically, three of the central concepts of the Nagoya Protocol are hardly applicable to microorganisms (Overmann and Scholz, 2017):

- According to the Nagoya Protocol, biodiversity hotspots are mainly located in developing countries and can serve as providers of genetic resources that may derive in benefits for industrialized countries. Nevertheless, it is important to consider that the term "biodiversity hotspot" is based on the diversity of macroorganisms (i.e., plants or animals, among others) that are endemic and exclusive to a particular location, whereas - in general -microorganisms have not been proven to be endemic. In fact, high dispersal rates result in microorganisms being cosmopolitan, and high sequence identity has been detected in microbial strains isolated up to 18000 km apart (Griffin, 2007; Speth et al., 2012).
- The Nagoya Protocol creates economic incentive for the sustainable use of biodiversity by stressing that genetic resources have an inherent value. Nevertheless, as has been discussed previously, large investments are almost always required to fully develop and commercialize the products derived from these genetic resources, which can be at odds with the idea that the commercialization of these products is a straightforward process.
- Policies associated to the Nagoya Protocol tend to be very (almost patent-like) restrictive by covering all types of 'uses' of the resources, as they assume that commercialization can take place at any point of the bioprospecting process. The reality is that most access to genetic resources are without commercial purposes, and restrictive policies are in fact causing competitive disadvantages, as the cosmopolitan nature of microorganisms leads to the possibility of isolating the same microbial species in a different geographical location in which the policies are less restrictive or even inexistent.

Users of genetic resources must be aware of their responsibilities (ensure that the resources are acquired legally and that all benefits that may arise are shared fairly) and must comply with any regulations that are in place, which could be within Nagoya Protocol or, in countries where legislation is weak, it could be the CBD principles (Smith et al., 2017). When designing a bioprospecting project, the following aspects must be previously assessed to ensure correct practices: (1) are the resources going to be collected from a country in which the Nagoya Protocol is in place?; (2) what are the ABS regulations in that country?; (3) has Prior Informed Consent (PIC) and Mutually Agreed Terms (MAT) been acquired before accessing the resources?

In the frame of the present thesis, it is important to note two things:

(1) The Nagoya Protocol does not apply to research with exclusively taxonomic purposes, which includes: the application of principles and methods for the identification and classification of living beings, the study of their phylogenetic relationships, and the study of their evolutionary and ecological aspects by using morphological, physiological, genetic, behavioral, and environmental data.
(2) The requirements regarding access to Spanish genetic resources from wild taxa only apply to genetic resources accessed after 15th March 2017, date in which the Royal Decree 124/2017 came into force (published in the BOE on 14th March 2017 under reference number BOE-A-2017-2743). In other words, any microbial strain accessed prior to this date, and used by the same entity that isolated the strain, does not fall in the scope of this Royal Decree.

1.2.2 Culturing and screening

The development of innovative approaches for the mining of microbial communities has resulted in the discovery of new molecules and enzymes of outstanding interest. This is the case, for example, of *Entotheonella* sp., detected through single-cell genomics approaches and able to produce an unprecedented wide repertoire of bioactive compounds (Wilson et al., 2014), or the previously unculturable bacterium *Eleftheria terrae*, isolated from soil with an innovative culturing approach, and producer of the novel antibiotic teixobactin (Ling et al., 2015). These two cases exemplify the trade-off faced in all bioprospecting approaches: the use of culture-independent techniques (such as all the available –omic technologies), which allow a higher screening power although without physical isolation of the microbial strains; versus the use of culture-dependent approaches, limited by the fact that most of the existing microorganisms have not yet been cultured under laboratory conditions (Figure 2).

Metagenomics is the study of the metagenome, which is the collective genome of microorganisms from an environmental sample. This technology can lead to the detection of microbial taxa or functional genes of interest, for example, *Actinobacteria* and *Firmicutes* from mangroves and coastal microbial mats as sources for antimicrobial compounds, bacterial genes for cellulose and xylan hydrolysis from the hindgut microbiota of a wood-feeding termite, or cellulosic biomass-degrading genes and genomes from microbes adherent to plant fiber in cow rumen (Al-Amoudi et al., 2016; Warnecke et al., 2007; Hess et al., 2011). Other powerful –omic tools include metabolomics, metaproteomics and metatranscriptomics, aimed at studying metabolites, proteins and mRNA from any environmental sample, respectively. All these -omic tools, together, can provide an unprecedentedly complete characterization of the genes and gene expression patterns, microbial activities and complex metabolic pathways in a given environmental sample (Figure 2). Nevertheless, these tools have several limitations: (1) they often hide certain biological aspects, such as ecologically-relevant interactions among individual members of the community; (2) certain features are not correctly predicted due to the lack of complete reference genomic data in the databases (these are obtained through whole-genome sequencing of cultured isolates); and (3) the *in silico* predicted features must be tested experimentally (Vilanova & Porcar, 2016).

It is for these reasons that culture dependent and culture-independent techniques must complement each other in order to achieve an efficient bioprospecting process, which we could consider “next generation bioprospecting” (Figure 2). While culturing biotechnologically-relevant strains is essential for their later use in an industrial setting, culture-independent approaches can be used on not-yet culturable bacteria to perform physiological analysis that will improve the targeting of functional novelty (Overmann et al.,2017).

Isolating a microbial strain in laboratory conditions is not always straightforward task and, in fact, the cultivation of bacteria is biased toward a handful of phylogenetic groups. Currently, all cultivated species belong to 39 of the 112 currently recognized bacterial phyla (Parte 2018; https://gtdb.ecogenomic.org; both accessed May

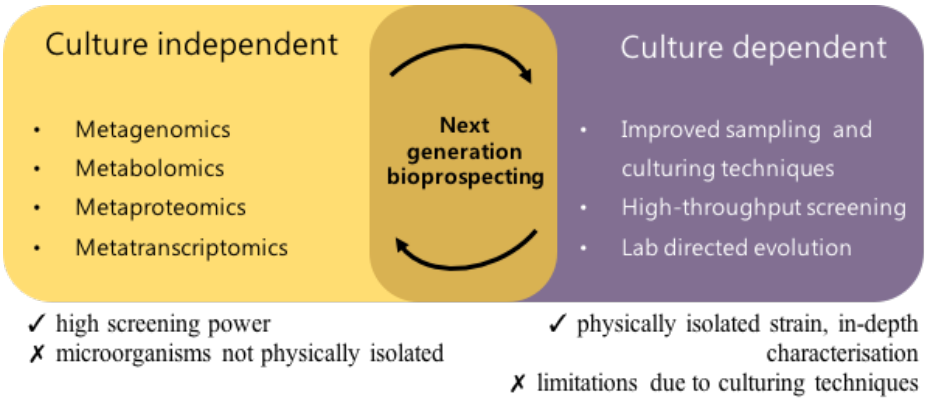

Figure 2. The bioprospecting trade-off: culture independent versus culture dependent approaches.

2020). This limited access to certain phyla is a consequence of the lack of appropriate laboratory incubation conditions, and results in unexplored taxa that are very likely to feature novel metabolic pathways with potential use in industry. Several cultivation concepts have been developed in the past years to overcome this limitation - to 'culture the unculturable' -, such as: low nutrient media, miniaturized cultivation platforms and disposable microfluidic cultivation devices for oligotrophic bacteria (Cho and Giovannoni 2004; Ingham et al., 2007; Grünberger et al., 2015); long incubation periods for slow-growing microorganisms (Puschen et al., 2017); size-selective filtration-based approaches to isolate ultramicrobacteria (smaller than 0.1 μm^3) (Geissinger et al., 2009); high-throughput culturing approaches – or culturomics – in which thousands of growth conditions are tested (Lagier et al., 2018); selective enrichment of biofilm-forming bacteria (Gich et al., 2012); dialysis units or agar beads to isolate strains that must be grown in coculture (Kealey et al., 2017; Lodhi et al., 2018); or *in situ* cultivation methods using diffusion chambers (Nichols et al., 2010; Bollmann et al., 2007).

Isolating microbial strains is only the first step and, for bioprospecting purposes, the screening method used is essential to select strains with biological activities of interest. Collections of microbial strains can be screened for biological activities of interest using *in vitro* and/or *in vivo* screening methods. Among the model organisms available for *in vivo* screening (i.e. *Danio rerio, Drosophila melanogaster, Mus musculus,* etc.), *Caenorhabditis elegans* provides many advantages, such as its small body size, completely sequenced genome (with more than 65 % of the genes associated with human disease), low cost, rapid development and aging, easy cultivation and genetic tractability (Park et al., 2017; Shen et al., 2018).

C. elegans has previously been used to study physiological processes, such as aging, lifespan, stress response, obesity or immunity (Park et al., 2017; Shen et al., 2018). In fact, a recent study has established a miniaturized assay protocol that allows for *in vivo* testing of natural products that can increase the survival of the nematode and suppress fat accumulation (Zwirchmayr et al., 2020). The conserved neurobiological system in this model organism has allowed it to be used as a model to identify molecular mechanisms that mediate drug-induced behavior (i.e. ethanol, nicotine, cocaine, etc.) and potential targets for medication development (Engleman et al., 2016). Furthermore, *C. elegans* has been used as a surrogate model to understand the conserved mechanisms in host-microbe interactions, due to morphological and functional similarities of *C. elegans* gut with the human gut (Kumar et al., 2019); to study genetics and developmental biology, including environmental epigenetics, environmental toxicology and genotoxin exposure (Weinhouse et al., 2018; Honnen 2017); and to perform biosafety assessments of nanoparticles (Wu et al., 2019).

1.3 Bioprospecting unusual environments

Many bioprospecting efforts have focused on well-known environments such as soil, a rich

source of antibiotic-producing microorganisms (Sherpa et al., 2015) and bacteria with insecticidal properties (Melo et al., 2014); or human gut, from which probiotic bacteria such as *Lactobacillus* spp. can be isolated (Halimi and Mirsalehian, 2016). Nevertheless, exotic and particular environments result in particular adaptations, and the understandable ease with which human or humanized environments can be sampled should not mask that most taxonomic and functional novelties lay somewhere else. Unusual environments remain poorly or unexplored to date although they are certainly valuable sources of novel products.

What is an unusual environment, or, more precisely, what is unusual enough? We consider an unusual environment as one that is both poorly explored, taxonomically distant from the human-associated microbiome and that is under extremophilic conditions. Interestingly, these three features tend to occur at the same time. It has to be stressed that some indoor or outdoor habitats (electrical appliances, sun-exposed surfaces, high-temperature saunas) fall into this category.

There are three reasons that make unusual environments especially interesting for bioprospecting studies. The first one is the large biodiversity they harbor, leading to a high probability of finding new taxa, as exemplified by the discovery of as many as 47 new phyla in aquifer sediments and groundwater in Colorado (Anantharaman et al., 2016). Second, these microorganisms are pre-adapted to stresses that often correlate with industrial needs. For example, sun-exposed environments tend to be very rich in pigmented bacteria, such as carotenoid-producing bacteria on solar panels or scytonemin-producing bacteria in microbial communities from the Atacama Desert, both of these pigment types with important applications in the food, cosmetic and pharmacological industries thanks to their antioxidant and UV-protection properties (Vítek et al., 2014; Rastogi et al., 2015; Tanner et al., 2019). Finally, a promising research field lies on developing new biofactories from the robust microorganisms able to resist a wide range of stresses (temperature, pH, salinity, etc.). Indeed, bacterial chassis based on *Deinococcus*, *Hymenobacter*, *Erythrobacter* and *Geobacillus* species – commonly present in extreme environments like desert soils (Rainey et al., 2005), Antarctic environments (Hirsch et al., 2004; Kojima et al., 2016), spacecraft surfaces (Stepanov et al., 2014), the troposphere (DeLeon-Rodriguez et al., 2013), solar salterns (Subhash et al., 2013) and mountain peaks (Marchant et al., 2002) – are already promising alternatives to classical *Escherichia coli* models for synthetic biology, although they still require further developments and standardization (Gerber et al., 2015; Hussein et al., 2015; Beal et al., 2020, Appendix D).

Biotechnologists are indebted to thermostable polymerases, such as the immensely popular Taq polymerase for polymerase chain reactions (PCRs), as well as Vent or Pfu DNA polymerases, all of them isolated from the extremophilic thermophiles *Thermus aquaticus*, *Thermococcus litoralis* or *Pyrococcus furiosus* respectively (Chien et al., 1976; Tindall and Kunkel, 1988; Lundberg et al., 1991; Kong et al., 1993). There are many other examples of valuable products obtained from unusual environments: from biofuel from hyperthermophilic archaea living in deep-sea hydrothermal vent chimneys (Nishimura and Sako, 2009), to latex-degrading bacteria from pine-tree forests (Vilanova et al., 2014) or cold-adapted plant growth promoting bacteria from extreme mountain environments (Pandey & Yarzábal, 2019).

During the last two decades, the discovery of novel microbial compounds has declined significantly, mainly as a consequence of the genetic and chemical redundancy detected in commonly analyzed environments (Zhang, 2005). Unusual and harsh environments hold great promise as unexploited, massively diverse targets for the discovery of biocompounds, microorganisms or consortia with potential commercial and/or industrial applications (Tanner et al., 2017, Appendix D; Molina-Menor et al., 2019, Appendix D).

2. Sun-exposed microbiota

The microbial communities associated to the first millimeters of many surfaces on Earth are subjected to a wide range of environmental stresses and, particularly, to a large amount of

radiation. Sunlight consists of visible, infrared and ultraviolet light, and the light that reaches the Earth's surface is composed of: around 55 % infrared, that contributes to heating our planet; 42-43 % visible, which is used, for example, for carbon fixation through photosynthesis; and 3-5 % ultraviolet light which, although required for synthesis of vitamin D in vertebrates, is also a well-known mutagenic agent that can cause DNA damage directly (i.e. by creating aberrant covalent bonds) or indirectly (i.e. by producing free radicals) (Bird and Hulstrom 1983; Markovitsi, 2016). These three components of sunlight are responsible for the three major selection pressures that sun-exposed organisms are subjected to: heating/desiccation, carbon assimilation opportunities, and DNA damage.

2.1 Stress-resistance mechanisms

Microorganisms living on sun-exposed surfaces display a wide range of mechanisms that enable them to resist these environmental stresses. Resistance to heat can be achieved, for example, through the accumulation of cytoplasmic solutes or through the formation of spores with low water content, high mineralization and saturation of DNA with small, acid-soluble proteins (SASP) (Pleitner et al., 2012; Setlow, 2006). Furthermore, biofilm formation confers resistance not only to extreme temperatures, but also to other environmental stresses, such as UV radiation, extreme pH values, high salinity, high pressure, and poor nutrient availability, among others (Yin et al., 2019). In extreme temperature conditions (both hot and cold), biofilms confer a so-called 'protective clothing', by resisting the external extreme temperatures and maintaining a stable interior that is suitable for microbial growth (Yin et al., 2019). Under oligotrophic conditions, biofilms can enhance microbial survival by preferentially distributing the limited nutrients (Yin et al., 2019). Other bacterial mechanisms to resist limited nutrient availability are spore formation, dormancy or extreme slow growth (Gray et al., 2019).

Regarding radiation resistance, UV radiation displays a reduced penetration into the biofilm matrix, which combined with the production of specialized compound such as mycosporine-like amino acids or pigments, can further protect microorganisms against this radiation (de Carvalho, 2017). On the other hand, a large fraction of prokaryotes accumulate polyhydroxyalkanoates (PHA) in the form of intracellular granules, which although involved in storing carbon and energy, can also enhance UV radiation resistance by scattering the radiation and by binding to DNA, providing a shield-like protection of their genomes (Slaninova et al., 2018). Other strategies to survive radiation-induced stress is the presence of efficient DNA repair mechanisms, oxidative stress defence, and spore formation (Nicholson et al., 2005; Lim et al., 2019).

Spore formation confers between 10 and 100-fold more resistance to UV radiation than the corresponding vegetative cells, and UV-resistance mechanisms in spores include, aside from efficient DNA repair mechanisms, the presence of SASP, and the accumulation of absorbing pigments (Nicholson et al., 2005). In fact, the role of pigments in UV protection, such as carotenoids, melanin, scytonemin, or prodigiosin, has been extensively studied (Ruan et al., 2004; Soule et al., 2009; Sandmann, 2015; Borić et al., 2011).

2.2 Sun-exposed microbiomes of human-made structures and the particular case of solar panel surfaces

The microbiome of sun exposed surfaces is not only shaped by the environmental conditions and selective pressures, but also by the substrate itself which, in some cases, can be very rich (i.e. the chemical composition and nutrient availability in biocrusts or the phyllosphere, among others). Nevertheless, human-made sun-exposed surfaces are inert, oligotrophic surfaces that can be used as a proxy to study surface microbiomes and the role of selective pressures in shaping these microbial communities.

A study of the microbiome composition of decayed historical church glass windows in a Mediterranean climate revealed the colonization of these surfaces by complex bacterial communities dominated by *Proteobacteria*, *Bacteroidetes*, *Firmicutes* and *Actinobacteria*, and a lower diversity of fungi, dominated by the

genera *Cladosporium* and *Phoma* (Piñar et al., 2013). In 2011, a study by Ragon et al. revealed that the microbial communities on sunlight-exposed concrete surfaces, characterized by *Actinobacteria, Alphaproteobacteria, Bacteroidetes, Acidobacteria* and *Deinococcales*, as well as green algae and ascomycete fungi, were very similar to the communities colonizing concrete surfaces from Chernobyl and exposed to different levels of radiation. These results suggest that biofilms growing on sun-exposed surfaces and that are naturally adapted to desiccation and ambient UV radiation, are pre-adapted to certain levels of ionizing radiation like those found in Chernobyl and are able to cope with increased mutation rates (Ragon et al., 2011). Finally, surface microbiomes of human-made structures can also be source of pigment producing microorganisms. In 2013, Kawasaki et al. isolated a eukaryotic microalga from the dry surface of heated asphalt in midsummer able to produce an astaxanthin-binding photooxidative stress-inducible aqueous carotenoprotein.

A particularly extreme case is the description of the microbiota that inhabits solar panel surfaces. Solar panel surfaces are smooth glass or glass-like surfaces with minimal water retention capacity and maximum sunlight exposure. These man-made structures can be found practically all over the world, and can be used as standard devices to study microbial communities and their colonization process in different geographical locations. Furthermore, solar panel surfaces are not only exposed to desiccation and high irradiation, but also to frequent temperature fluctuations, making them ideal sources of stress-resistant microorganisms.

According to a study by Dorado-Morales et al (2016), the microbial communities that live on solar panels surfaces are dominated by ascomycetes and a very diverse pool of bacteria, mainly *Novosphingobium, Sphingomonas, Rubellimicrobium, Hymenobacter, Segetibacter* or *Deinococcus*. The most frequent bacteria inhibiting solar panels are known to produce pigments, including carotenoids, but also sphingolipids, metabolites that play a role in both adhesion to the surface of the solar panels and in protection against oxidative stress (Moye et al., 2016). Both the functional and the taxonomic profiles of the solar panel microbial communities proved similar to other sunlight-exposed environments, such as polar microbial mats, the phylloplane, sun-oriented rocks as well as cold and hot desserts (Dorado-Morales et al., 2016). When analyzing specific *Deinococcus* sequences from the metagenomic data, low identity levels of solar panel pangenome with previously sequenced *Deinoccocus* species suggested the presence of previously undescribed species of this genus (Dorado-Morales et al., 2016). Furthermore, culturing of solar panel samples yielded a large number of colony-forming microorganisms, many of them displaying red, orange or pink pigmentation, and resistance to high salt concentrations (20-26 % w/v NaCl) and short exposures to UV light (Dorado-Morales et al., 2016). These results suggest that solar panel surfaces can be rich sources of novel microbial strains with biological activities of interest.

From a functional point of view, metagenomic data revealed similar functional profiles among different solar panels sampled in Valencia (Spain), whereas metaproteomic analysis revealed abundance of proteins involved in resistance to harsh conditions and biofilm formation, as well as differences between the protein composition in samples taken during the day and during the night, suggesting that microbial communities inhabiting these surfaces are biologically active and possess stress-response mechanisms (Dorado-Morales et al., 2016).

In a study in Sao Paulo, fungi were found to be a relevant component of SAB on photovoltaic panel surfaces after 6, 12 and 18 months of exposure, with melanized meristematic ascomycetes and pigmented bacterial species of the genera *Arthrobacter* and *Tetracococcus* being the major microorganisms (Shirakawa et al., 2015). Furthermore, significant reductions in solar panel efficiency were observed after 6, 12 and 18 months (7 % reduction after 6 and 12 months, and 11 % reduction after 18 months), and at 18 months the only detected taxa were meristematic *Dothydeomycetes*, *Ulothrix* and *Chlorella* (Shirakawa et al., 2015). Furthermore, four novel melanized fungal strains have been previously isolated from the microbial community inhabiting photocatalytic roof tiles (Ruibal et al., 2018).

The work performed in the present thesis aims to further explore the solar panel microbiota from both an ecological and an applied perspective. On one hand, the microbial communities inhabiting solar panels from different geographical locations have been analyzed in taxonomic and functional terms, and the colonization process of these surfaces has been studied in depth using a miniaturized solar farm. On the other hand, microbial strains have been isolated from this environment and further analyzed to determine biological activities of interest and to characterize and describe novel microbial species.

Objectives

This thesis aims at further characterizing the solar panel microbiota with a specific focus on two main aspects: microbial ecology of the communities inhabiting solar panel surfaces (Chapter I), and potential applications of these microbial communities (Chapter II).

The specific objectives of the present thesis are:

- Analyzing and comparing the functional and taxonomic diversity of microbial communities inhabiting solar panel surfaces located in distant geographical regions (Chapter I).
- Studying the microbial colonization process of solar panel surfaces and the effect of microbial growth on solar panel efficiency (Chapter I).
- Screening and characterizing microbial strains isolated from solar panel surfaces, with a special emphasis on stress-resistance and detection of antioxidant activities (Chapters I and II).
- Describing novel microbial species isolated from this sun-exposed environment (Chapter II).

Chapter I. Microbial ecology of solar panel surfaces

Publication I. **Tanner K**, Martí JM, Belliure J, Fernández-Méndez M, Molina-Menor E, Peretó J and Porcar M. (2018). Polar solar panels: Arctic and Antarctic microbiomes display similar taxonomic profiles. Environmental Microbiology Reports 10(1): 75-79.

Publication II. Porcar M, Louie KB, Kosina SM, Van Goethem MW, Bowen BP, **Tanner K** and Northen TR. (2018). Microbial Ecology on Solar Panels in Berkeley, CA, United States. Frontiers in Microbiology 9: 3043.

Publication III. **Tanner K**, Molina-Menor E, Latorre-Pérez A, Vidal-Verdú A, Vilanova C, Peretó J, Porcar M (2020). Extremophilic microbial communities on photovoltaic panel surfaces: a two-year study. Microbial Biotechnology

Original publication reprints can be found in Appendix A.

Supplementary figures can be found in Appendix B.

Publication I

Polar solar panels: Arctic and Antarctic microbiomes display similar taxonomic profiles

Kristie Tanner[1], Jose Manuel Martí[1], Josabel Belliure[2], Mar Fernéndez-Méndez[3], Esther Molina-Menor[1], Juli Peretó[1,4,5] and Manuel Porcar[1,5]

[1] Institute for Integrative Systems Biology (I2SysBio, University of Valencia-CSIC), Paterna, Valencia, Spain

[2] Ecology Section, Department of Life Sciences, University of Alcalá, Alcalá de Henares, Madrid, Spain

[3] Norwegian Polar Institute, Tromsø, Norway

[4] Department of Biochemistry and Molecular Biology, University of Valencia, Spain

[5] Darwin Bioprospecting Excellence SL, Paterna, Valencia, Spain

Abstract

Solar panels located on high (Arctic and Antarctic) latitudes combine the harshness of the climate with that of the solar exposure. We report here that these polar solar panels are inhabited by similar microbial communities in taxonomic terms, dominated by *Hymenobacter* spp., *Sphingomonas* spp. and *Ascomycota*. Our results suggest that solar panels, even on high latitudes, can shape a microbial ecosystem adapted to irradiation and desiccation.

Introduction

The microbial ecology of some artificial structures, including solar panels, has been poorly explored up to date (Shirakawa et al, 2015; Dorado-Morales et al, 2016). These reports suggest that photovoltaic surfaces display a diverse microbial community, highly tolerant to thermal fluctuations, ultraviolet (UV) irradiation and desiccation (Dorado-Morales et al, 2016). In this work, we aimed to study, through Next Generation Sequencing (NGS) and microbial culturing techniques, the microbiome of photovoltaic solar panels from two cold locations, lying close or inside the polar circles: Tromsø, Norway (698400 N 188560 E) and two Antarctic islands (62800S 58800W) (Figure I.1A).

Tromsø is the largest urban area in northern Norway. It is located on the coast, above the Arctic Circle, and experiences a subarctic climate. Average temperatures in winter range between 0.9 and -3.6 °C and in summer between 5.3 and 12.4 °C. The South Shetlands constitute a group of islands of the Maritime Antarctica. Monthly average temperature is between -3.1 and -10.9 °C from March to October, when the sea around the islands is closed by ice, and slightly warmer from November to February, with temperatures ranging between -1.7 and 0.5 °C.

Results and discussion

A total of 14 individual solar panels were sampled in January and May 2017 in Antarctica (9 panels, 3 from Deception Island and 6 from Livingston Island) and Tromsø (5 panels), respectively (Figure I.1A). Aliquots were spread on LB and R2A media and incubated at 4 °C for three weeks to select psychrotrophic and psychrophilic microorganisms (Figure I.1B). A collection of 44 isolates was characterized by genetic identification, growth ability and UV-light and desiccation resistance (Figure I.1C). A detailed explanation of all the experimental procedures used in this study can be found on the research group website that can be accessed using the following link: http://www.uv.es/synbio/solpan. The isolates from Antarctic panels able to grow at 4 °C were identified as either *Rhodotorula mucilaginosa* (pink pigmentation) or *Alcaligenes faecalis/Curtobacterium* sp. (yellow pigmentation). Samples from Tromsø yielded a larger diversity of microorganisms including

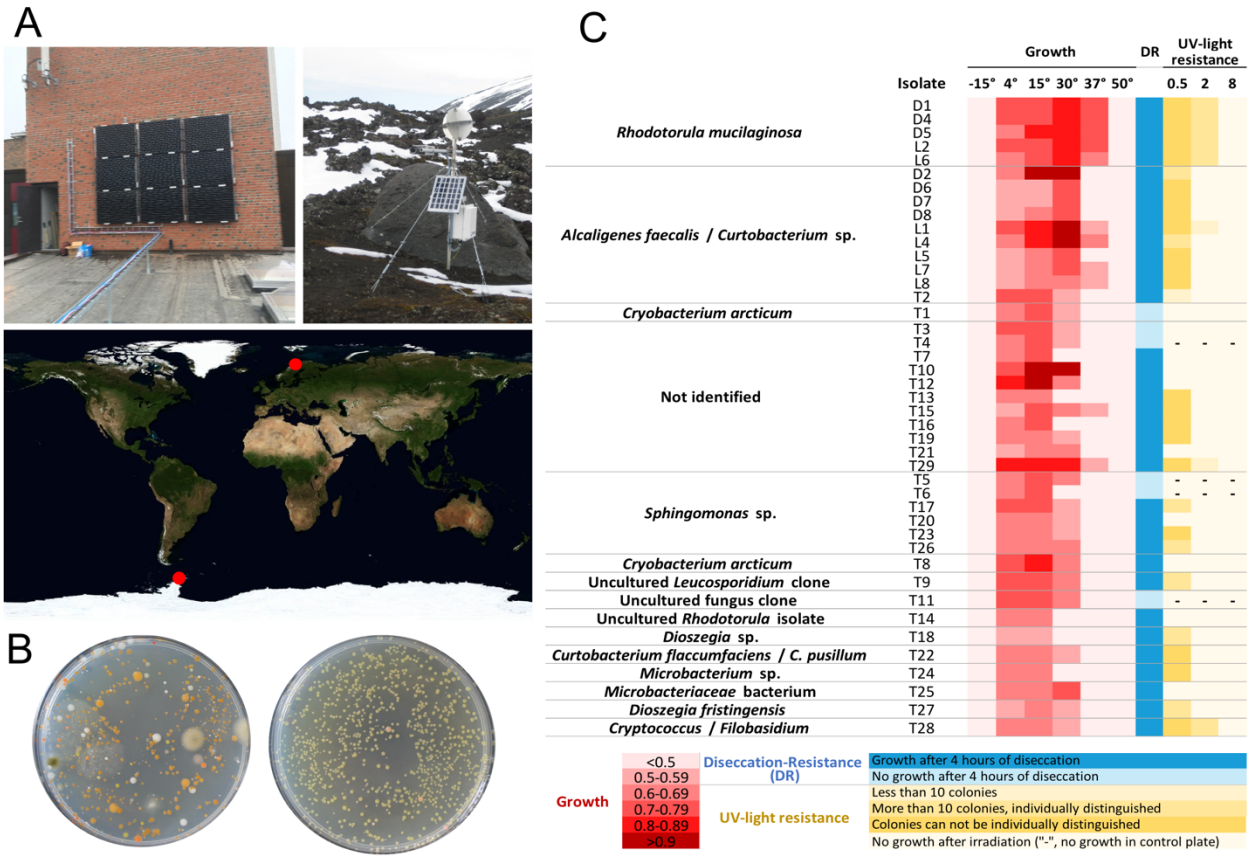

Figure I.1. (A) Solar panels sampled from Tromsø, Norway (top, left) and South Shetlands, Antarctica (top, right), indicated by red dots in the map below; (B) microbial colonies obtained culturing aliquots of surface biomass on R2A at 4 °C for 21 days (left, Tromsø; right, Antarctica); (C) heatmap displaying taxonomic identification, location ('D' Deception, Antarctica; 'L' Livingston, Antarctica; or 'T' Tromsø, Norway; followed by an identification number), growth (colony diameter in cm) at temperatures from 215 to 50 8C (data in red), resistance to desiccation (data in blue) and resistance to UV light (after 0.5, 2 and 8 min of irradiation; data in yellow) of the isolated colonies.

Cryobacterium arcticum, Sphingomonas sp., *Curtobacterium* sp., *Microbacterium* sp. and *Dioszegia fristingensis*, all of them able to grow at 15 °C. Interestingly, despite the low temperatures of their original habitats, 37 isolates were able to grow at 30 °C and 11 also grew at 37 °C. One of these was identified as *R. mucilaginosa*, a cold-adapted (with activity at up to 25 °C), carotenoid-producing, cosmopolitan, mesophilic yeast that has previously been isolated from a wide range of remote environments, including Antarctical ice cores or 11 000 m deep sea vents (Gadanho and Sampaio, 2005; Amato et al., 2009; Moline et al., 2012; Nunes et al., 2013; Connell et al., 2014; Yu et al., 2015). Regarding UV resistance, many of the isolates (a total of 30) were able to survive 30 s of irradiation with a monochromatic 254 nm light, whereas only seven isolates were able to survive two minutes of irradiation and none resisted eight minutes of irradiation. The most frequent isolate able to resist two minutes of UV irradiation was *R. mucilaginosa*, in which carotenoid accumulation may play an essential role in photoprotection against UV-light (Moline et al., 2010). Finally, desiccation-resistance assays revealed that 38 out of the 44 isolates were able to resist four hours of desiccation. *R. mucilaginosa* was present among these 38 isolates, an expected result when considering previous studies that describe this species as highly resistant to desiccation (Connell et al., 2008). The large heterogeneity in UV-resistance is in contrast with the high irradiance in the sampled site, suggesting that a tridimensional biofilm-like structure may play an important role, not only in survival under desiccation conditions, but also in UV-protection in the natural biocenosis (Gorbushina, 2007; Villa et al., 2015). Our results support the hypothesis of the existence of a specific solar panel microbial community adapted to the harsh conditions that characterize these artificial environments: UV-radiation and desiccation.

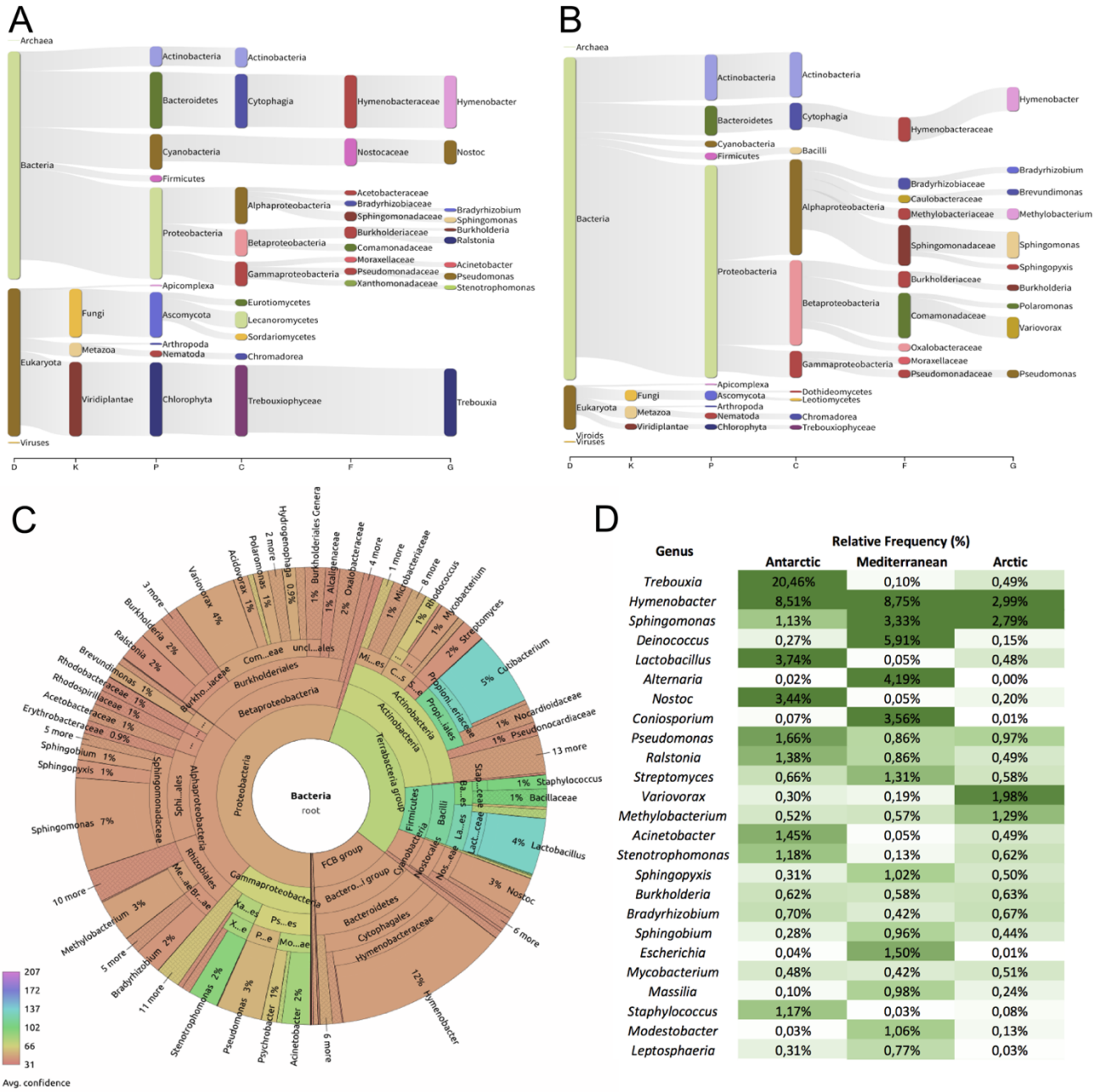

Figure I.2. Sankey diagram with the 10 most abundant taxa in different taxonomical levels (Domain D, Kingdom K, Phylum P, Class C, Family F, Genus G) in the solar panels of Livingston, Antarctica (A) and Tromsø, Norway (B); (C) Recentrifuge-Krona plot snapshot of the shared bacterial taxa at the genus level among all the polar panels (from Livingston and Tromsø), where the percentage shows the relative abundance at the genus level averaged for all the polar samples; (D) heatmap showing the 25 most abundant genera versus geographical location ordered by overall relative frequency; the average for all the solar panels sampled per location is given; the color scale is quasilogarithmic to improve visualization of taxa with similar order of magnitude among locations. Taxa under the clade *Streptophyta* have been removed throughout the figure to improve resolution at the microbial level.

The taxonomic profiles obtained through NGS of three panels from each location were analyzed (Breitwieser and Salzberg, 2016; Kim et al., 2016; Martí, 2017) and found to exhibit a rather low variation within locations, although both sites proved to differ in some taxa (Figure I.2A and I.2B). All the obtained Recentrifuge-Krona plots can be accessed on the research group's website through

the following link: http://www.uv.es/synbio/sol-pan. First, tree sequences were dominant in Tromsø and not in the Antarctica; similarly, sequences from Equisetum were found exclusively in the solar panels from Norway. This can be explained by the proximity and abundance of vegetation and the lack of it in Tromsø and Antarctica respectively, since Tromsø is in a forest area, whereas the South Shetlands are at least 800 km away from the nearest forest land (South America). Second, many more fungal sequences, including many yeasts, and, especially, the lichen-associated *Trebouxia* algae were more frequent in the Antarctica samples. Antarctica is not only characterized by its low temperatures but also by displaying very low values of environmental humidity, conditions which *Trebouxia* can easily overcome thanks to its cryo- and desiccation-resistant properties (Hájek et al., 2012; Carniel et al., 2016). Finally, other taxa that differed in frequency between the two locations were *Variovorax*, more frequent in Norway, and *Lactobacillus* and *Acinetobacter*, more frequent in the solar panels from Antarctica. Despite these differences, the global taxonomic profile of the two locations had relevant and abundant similarities (Figure I.2C and I.2D). Interestingly, many of the shared genera have also been found while reanalysing the sequences of the first NGS report of the solar panel microbiome (Dorado-Morales et al., 2016), carried out in a Mediterranean city (Figure I.2D). On the contrary, some other genera are more frequently found in Mediterranean solar panels than in the polar ones, such as *Alternaria*, *Coniosporium*, *Escherichia*, *Massilia* and *Modestobacter*.

Our results not only reveal the existence of a diverse community of microorganisms in solar panels from polar environments, which is in concordance with previous reports about the diversity of microbial life in polar regions, but it also highlights the importance of adaptation in extreme environments (Friedmann, 1982; 1993; Boetius et al., 2015). From the identification of a clear core of shared microbial taxa, it would be tempting to conclude that our results support the well-known microbial ecology mantra by Baas Becking 'everything is everywhere, but, the environment selects'. However, it has to be stressed that the location of the studied solar panels (either close or beyond the Antarctic and Arctic circles respectively) does not assure a common environment: both polar environments have different wind regimes and key differences in terms of climate or distance to other biomes (which is clearly reflected by the high frequency of tree sequences in the Tromsø samples, which were missing in Antarctica, for example). Yet, the striking co-presence of bacterial genera (Figure I.2D) such as *Sphingomonas*, *Pseudomonas*, *Ralstonia*, *Streptomyces*, *Methylobacterium* and, especially, *Hymenobacter* (the most abundant genus in solar panels from both poles as well as in those previously characterized in a Mediterranean city), indicates that solar panels are not mere stockers of wind-borne microorganisms. On the opposite, our results demonstrate that solar panels in extreme latitudes bear a similar, native microbiome, characterized by marker taxa shared with panels from other latitudes, fitting nicely with previous work performed on geothermal communities of Antarctica that aimed at assessing the role of aeolian transport and environmental selection in the establishment of microbial communities (Herbold et al., 2014). This fact suggests that the strong selection pressures – desiccation and irradiation, very likely – of the solar panels themselves – rather than their location – are what shape the microbiome developing on them.

Acknowledgements

Financial support from Spanish Government (grant Helios, reference: BIO2015–66960-C3-1-R co-financed by FEDER funds and Ministerio de Economía y Competitividad) is acknowledged. The data sets generated during and/or analysed during the current study are available from the corresponding author on reasonable request. The authors declare no conflict of interest.

References

Amato, P., Doyle, S., and Christner, B.C. (2009) Macromolecular synthesis by yeasts under frozen conditions. Environ Microbiol 11: 589–596.

Boetius, A., Anesio, A.M., Deming, J.W., Mikucki, J.A., and Rapp, J.Z. (2015) Microbial ecology of the cryosphere: sea ice and glacial habitats. Nat Rev Microbiol 13: 677–690.

Breitwieser, F.P., and Salzberg, S.L. (2016). Pavian: interactive analysis of metagenomics data for microbiomics and pathogen identification. bioRxiv: 084715.

Carniel, F.C., Gerdol, M., Montagner, A., Banchi, E., De Moro, G., Manfrin, C., et al. (2016) New features of desiccation tolerance in the lichen photobiont Trebouxia gelatinosa are revealed by a transcriptomic approach. Plant Mol Biol 91: 319–339.

Connell, L.B., Redman, R., Craig, S., Scorzetti, G., Iszard, M., and Rodriguez, R. (2008) Diversity of soil yeasts isolated from South Victoria Land, Antarctica. Microb Ecol 56: 448–459.

Connell, L.B., Rodriguez, R.R., Redman, R.S., and Dalluge, J.J. (2014). Cold-adapted yeasts in Antarctic Deserts. In Cold-Adapted Yeasts: Biodiversity, Adaptation Strategies and Biotechnological Significance. Buzzini, P., Margesin, R. (eds). Berlin Heidelberg: Springer-Verlag, pp. 75–98.

Dorado-Morales, P., Vilanova, C., Pereto, J., Codoñer, F.M., Ramón, D., and Porcar, M. (2016) A highly diverse, desert-like microbial biocenosis on solar panels in a Mediterranean city. Sci Rep 6: 29235.

Friedmann, E.I. (1982) Endolithic microorganisms in the Antarctic cold desert. Science 215: 1045–1053.

Friedmann, E.I. (1993). Antarctic Microbiology. 1st edn. California: Wiley-Liss.

Gadanho, M., and Sampaio, J.P. (2005) Occurrence and diversity of yeasts in the mid-atlantic ridge hydrothermal fields near the Azores Archipielago. Microb Ecol 50: 408–417.

Gorbushina, A.A. (2007) Life on the rocks. Environ Microbiol 9: 1613–1631.

Hájek, J., Váczi, P., Barták, M., and Jahnová, L. (2012) Interspecific differences in cryoresistance of lichen symbiotic algae of genus *Trebouxia* assessed by cell viability and chlorophyll fluorescence. Cryobiology 64: 215–222.

Herbold, C.W., Lee, C.K., McDonald, I.R., and Cary, S.C. (2014) Evidence of global-scale Aeolian dispersal and endemism in isolated geothermal microbial communities of Antarctica. Nat Commun 5: 3875.

Kim, D., Song, L., Breitwieser, F.P., and Salzberg, S.L. (2016) Centrifuge: rapid and sensitive classification of metagenomic sequences. Genome Res 26: 1721–1729.

Martí, J.M. (2017). Recentrifuge: robust comparative analy- sis and contamination removal for metagenomic data. bioRxiv DOI 10.1101/190934.

Moliné, M., Flores, M.R., Libkind, D., del Carmen Diéguez, M., Farías, M.E., and van Broock, M. (2010) Photoprotection by carotenoid pigments in the yeast *Rhodotorula mucilaginosa*: the role of torularhodin. Photochem Photobiol Sci 9: 1145–1151.

Moliné, M., Libkind, D., and van Broock, M. (2012) Production of torularhodin, torulene, and b-carotene by *Rhodotorula* yeasts. Methods Mol Biol 898: 275–283.

Nunes, J.M., Bizerra, F.C., Ferreira, R.C., and Colombo, A.L. (2013) Molecular identification, antifungal susceptibility profile, and biofilm formation of clinical and environ- mental *Rhodotorula* species isolates. Antimicrob Agents Chemother 57: 382–389.

Shirakawa, M.A., Zilles, R., Mocelin, A., Gaylarde, C.C., Gorbushina, A., Heidrich, G., et al. (2015) Microbial colonization affects the efficiency of photovoltaic panels in a tropical environment. J Environ Manage 157: 160–167.

Villa, F., Pitts, B., Lauchnor, E., Cappitelli, F., and Stewart, P.S. (2015) Development of a laboratory model of a phototroph-heterotroph mixed-species biofilm at the stone/air interface. Front Microbiol 6: 1251.

Yu, P., Wang, X.T., and Liu, J.W. (2015) Purification and characterization of a novel cold-adapted phytase from *Rhodotorula mucilaginosa* strain JMUY14 isolated from Antarctic. J Basic Microbiol 55: 1029–1039.

Publication II

Microbial Ecology on Solar Panels in Berkeley, CA, United States

Manuel Porcar[1,2,3], Katherine B. Louie[3], Suzanne M. Kosina[4], Marc W. Van Goethem[4], Benjamin P. Bowen[3,4], Kristie Tanner[2] and Trent R. Northen[3,4]

[1] Institute for Integrative Systems Biology (I2SysBio, University of Valencia-CSIC), Paterna, Valencia, Spain

[2] Darwin Bioprospecting Excellence S.L., Parc Científic de la Universitat de València, Paterna, Spain

[3] Joint Genome Institute, Lawrence Berkeley National Laboratory, Walnut Creek, CA, USA.

[4] Environmental Genomics and Systems Biology Division, Lawrence Berkeley National Laboratory, Berkeley, CA, USA.

Abstract

Solar panels can be found practically all over the world and represent a standard surface that can be colonized by microbial communities that are resistant to harsh environmental conditions, including high irradiation, temperature fluctuations and desiccation. These properties make them not only ideal sources of stress-resistant bacteria, but also standard devices to study the microbial communities and their colonization process from different areas of Earth. We report here a comprehensive description of the microbial communities associated with solar panels in Berkeley, CA, United States. Cultivable bacteria were isolated to characterize their adhesive capabilities, and UV- and desiccation-resistance properties. Furthermore, a parallel culture-independent metagenomic and metabolomic approach has allowed us to gain insight on the taxonomic and functional nature of these communities. Metagenomic analysis was performed using the Illumina HiSeq2500 sequencing platform, revealing that the bacterial population of the Berkeley solar panels is composed mainly of *Actinobacteria*, *Bacteroidetes* and *Proteobacteria*, as well as lower amounts of *Deinococcus-Thermus* and *Firmicutes*. Furthermore, a clear predominance of *Hymenobacter* sp. was also observed. A functional analysis revealed that pathways involved in the persistence of microbes on solar panels (i.e., stress response, capsule development, and metabolite repair) and genes assigned to carotenoid biosynthesis were common to all metagenomes. On the other hand, genes involved in photosynthetic pathways and general autotrophic subsystems were rare, suggesting that these pathways are not critical for persistence on solar panels. Metabolomics was performed using a liquid chromatography tandem mass spectrometry (LC-MS/MS) approach. When comparing the metabolome of the solar panels from Berkeley and from Valencia (Spain), a very similar composition in polar metabolites could be observed, although some metabolites appeared to be differentially represented (for example, trigonelline, pantolactone and 5-valerolactone were more abundant in the samples from Valencia than in the ones from Berkeley). Furthermore, triglyceride metabolites were highly abundant in all the solar panel samples, and both locations displayed similar profiles. The comparison of the taxonomic profile of the Californian solar panels with those previously described in Spain revealed striking similarities, highlighting the central role of both selective pressures and the ubiquity of microbial populations in the colonization and establishment of microbial communities.

Introduction

It has recently been calculated that there might be as many as one trillion different species on Earth, the vast majority of which are microorganisms (Locey and Lennon, 2016). Microorganisms are ubiquitous, and can even be found in extreme environments such as thermal springs (Kizilova et al., 2014), marine trenches (Felden et al., 2014) and man-made structures (Vilanova et al., 2015). Interestingly, solar panels have been reported to harbor a diverse microbial community, mainly composed of desiccation/irradiation-adapted

microorganisms, similar to those found in other highly irradiated environments, such as deserts, plant surfaces and polar microbial mats (Dorado-Morales et al., 2016; Tanner et al., 2018). The presence of biofilms on the surface of photovoltaic panels from Brazil has been shown to decrease the efficiency by 11% after 18 months (Shirakawa et al., 2015). Moreover, dust particle accumulation during drought seasons (a process known as "soiling") has been associated with a decrease in the yield of California photovoltaic panels, accounting for a loss of up to 0.1% of the power production per day (Mejia and Kleissl, 2013). Biofilm and dust accumulation on outdoor glass surfaces such as photovoltaic panels depend, among other factors, on the coating and angle (Mejia and Kleissl, 2013; Banerjee et al., 2015). Although the effect of biofilms on soiling in solar panels has not been quantified, it seems reasonable to hypothesize that biofilm growth might increase dust adhesion. Despite the economic benefits of understanding the association between the decreased yield of solar panels and the biofilms formed on them, little is known about how the latitude, climate, the physical characteristics of the panels affect the microbial communities in this still poorly characterized ecological niche.

Solar panels represent a particularly interesting environment due to their simple, yet standard structure and orientation (an equator-facing glass surface); their abundance worldwide; and the fact that these inert, non-porous bidimensional artificial surfaces are a proxy of sun-exposed natural environments such as rocks, the phyllosphere or the top layer of biological soil crusts. A previous study assessing the microbiome of solar panels from the North and South Poles revealed that despite the geographical distance between both environments, the composition of the solar panel microbiome is very similar (Tanner et al., 2018). Furthermore, solar panel surfaces can be used as sources for the isolation of interesting radiation- and desiccation-resistant bacteria. A study by Ragon et al. (2011) revealed that biofilms growing on sunlight-exposed surfaces are naturally resistant to Chernobyl ionizing-radiation levels which is due to their natural adaptation to periodical desiccation and UV-irradiation. Survival of ionizing radiation- and desiccation-resistant bacteria has been previously attributed to the ability of these microorganisms to protect their proteins from the oxidative damage generated during irradiation, leading to functioning repair systems that work more efficiently during recovery than those in bacteria that are sensitive to radiation (Fredrickson et al., 2008).

A previous description of the microbial community on solar panels from the Mediterranean city of Valencia, Spain revealed the presence of black fungi, some phototrophs and a surprising diversity of sun-adapted bacterial taxa, dominated by *Hymenobacter* spp., *Sphingomonas* spp., and *Deinococcus* spp. (Dorado-Morales et al., 2016). In order to shed light on the ecology of the solar panel microbiome and to further compare the microbial profiles on panels from distant geographical locations, we present here a comprehensive characterization of the microbial communities of solar panels in another coastal city distant from Valencia: Berkeley, CA, United States. Both cities share a Mediterranean climate, a relatively high humidity and a protracted dry summer season. They are also at similar altitudes and latitudes (Berkeley is less than two degrees south from Valencia: 37° 52′ and 39° 28′, respectively) and thus receive similar annual UV irradiation doses. In the present work, we have analyzed the functional and taxonomic diversity of the solar panels of the University of California in Berkeley through metagenomics; compared the microbial communities with those described on solar panels from Valencia (Dorado-Morales et al., 2016); identified several key compounds of its metabolome through mass spectrometry; and studied the adhesion, irradiation and desiccation resistance abilities of selected cultivable isolates in the laboratory.

Materials and Methods

Sampling

Sampling was carried out in August 2016 at the Lawrence Berkeley National Laboratory main campus (Berkeley, CA, United States). Three independent, adjacent photovoltaic solar panels of building 30 (installed and uncleaned for at least 18 months) were sampled by pouring sterile PBS on the surface and by strongly scraping the surface with autoclave-sterilized T-shaped rubber and

steel window cleaners (squeegees). Approximately 40 mL of soil panel dust slurry was collected from each solar panel using sterile pipettes, transferred into sterile polypropylene conical tubes and immediately transported to the laboratory for further processing. There, aliquots were taken for culturing and colonization experiments, and the remaining volume was split in two, centrifuged and the pellets stored at -80°C until required for metagenomic and metabolic analysis. The solar panels from Valencia (Spain) were sampled using the same procedure, obtaining a final volume of 5 mL that was sent on dry ice to the laboratory in Berkeley, CA, United States, for metabolomics analysis. The metagenomic sequences obtained in the previous report by Dorado-Morales et al. (2016) were used for the taxonomic comparison between the Spanish and Californian solar panels.

Culture Media and Conditions

A total of 300 µL aliquots of each sample were transferred into sterile 1.5 mL microcentrifuge tubes and let stand for 5 min at room temperature prior to spreading 50 µL of the supernatant on freshly prepared LB and R2A agar plates. A dual approach with nutrient-rich (LB) and nutrient-poor (R2A) media was used in order to allow microorganisms with different nutrient requirements to grow. All cultures were performed in duplicate and incubated at 4°C, room temperature (RT) (~22°C), 27 and 50°C for 22, 9, 5, and 3 days, respectively. Selected colonies corresponding to the most frequent phenotypes (i.e., light pink) on R2A were re-streaked on fresh R2A plates and pure cultures grown on solid medium were cryopreserved in 25% glycerol.

Pooled aliquots (10 µL) of the three samples were placed on microscope slides (VWR CAT No. 48393048, 22X40 mm) and dried at room temperature (RT) under sterile conditions. The slides were then washed with sterile water, dried again and subjected to 2 min of UV irradiation in the hood and at a distance of 46 cm from the UV light (Air Clean 600 PCR workstation equipped with a 254 nm short-wave UV light). The dried and irradiated microscope slides were kept in the hood at RT for 30 min and then transferred sample side down onto the surface of R2A agar plates, where they settled for 30 min before being removed. Plates were incubated at RT for 4 days. Surviving colonies, as well as the ten non-irradiated isolates selected among those growing in R2A plates were selected for further studies. Colonies were identified through amplification and sequencing of almost the full-length 16S rRNA gene (in exception of a small fragment of ~200 base pairs at the beginning of the V1 regions) through Sanger sequencing, followed by a taxonomic assignment using the NCBI Blast Tool. All but one of the sequences displayed 98–99% similarity with the closest match. The exception was an isolate belonging to the *Deinococcus* genus, which displayed 96% similarity with the closest match.

Colonization Experiments

A loopful of each selected isolate, grown for 1 week on R2A agar at room temperature, was suspended in liquid R2A and optical densities (600 nm) were adjusted to 0.1 absorbance units. A 10 µL droplet of each suspension was placed on a sterile glass slide and kept at RT for 1 h. Then, 10 µL of R2A were added to each droplet to prevent desiccation and the assay was continued for one more hour, after which droplets were removed by washing the slides three times with 1 mL of sterile water. The slides were allowed to completely dry in the hood for 1 h and were then either placed sample side down on the surface of R2A plates (glass colonization assay); subjected to UV irradiation (UV-resistance assay); or subjected to 72 h of further desiccation at RT (desiccation-resistance assay).

For the glass colonization assay, the slides were placed on solid R2A medium and incubated for 30 min at RT to allow for transfer of the bacteria to the solid medium. Then, the glass slides were removed and the plates were incubated at RT for 4 days. For the UV resistance assays, after washing and drying the slides (as described above), the 14 selected isolates were subjected to 2 min of irradiation with the UV lamp in the Air Clean 600 PCR workstation and at 15 cm distance from the lamp. UV-treated glass slides were placed on R2A agar plates and incubated as described above (30 min at room temperature) to allow the transfer of the bacteria. Finally, the desiccation-resistance assays were carried out with the 14 selected strains as described above (without UV irradiation) by air-drying washed droplets for 72 h inside the hood prior to transferring them to R2A plates, where they were incubated for 30 min at

room temperature to allow transfer of the bacteria.

DNA Isolation and Metagenomic Analysis

Metagenomic DNA was isolated from solar panels samples as previously described (Dorado-Morales et al., 2016). Briefly, pellets were thawed on ice, incubated with lysozyme in the PowerBead tubes solution without the beads (PowerSoil, MoBio) at 37°C for 10 min, and then transferred back to the PowerBead tubes containing the beads. The extraction was continued following the instructions of the manufacturer.

Metagenomic analysis and annotations were performed as follows. For the library construction, 10 ng of DNA was sheared to 300 bp using the Covaris LE220 (Covaris) and size selected using SPRI beads (Beckman Coulter). The fragments were treated with end-repair, A-tailing, and ligation of Illumina compatible adapters (IDT, Inc), and 5 cycles of PCR was used to enrich for the final library. The libraries were quantified and run on a Roche LightCycler 480 real-time PCR instrument, followed by preparation for sequencing on the Illumina HiSeq2500 sequencing platform using a TruSeq Rapid paired-end cluster kit, v.4. After sequencing, known Illumina adapters were removed and the reads were then processed using BBDuk filtering and trimming (where quality values were less than 12). Remaining reads were mapped to a masked version of human HG19 with BBMap, discarding all hits over 93% identity. Trimmed, screened, paired-end Illumina reads were assembled using megahit assembler using a range of Kmers (Li et al., 2015). The entire read set output from the previously described read pre-processing step were mapped to the final assembly and coverage information generated using BBMap. Annotation was performed using the DOE-JGI Metagenome Annotation Pipeline (MAP v.4) (Huntemann et al., 2016). Open reading frames (ORFs) were identified from each of the three assemblies using Prodigal v.2.6.3 software (Hyatt et al., 2010). Genes were subsequently annotated against the entire NCBI nr-database using DIAMOND (Buchfink et al., 2014).

Taxonomic information was obtained from the metagenomic data using the microbial classification engine “Centrifuge” (Kim et al., 2016), as well as the aforementioned NCBI non-redundant database. Taxonomic and functional affiliations were visualized in the MEGAN6 software environment (Huson et al., 2007). For comparison of solar panels from different locations, a radial tree representing phylogenetic distances between solar panels from Berkeley, CA, United States and Valencia, Spain was constructed using the JGI IMG/MER database tools, with a percent identity above 90%. Statistical analyses were performed both using STAMP (Parks et al., 2014) and in the R statistical environment.

Metabolite Extractions

Solar panel slurry pellets were collected by centrifugation of 5 mL (Valencia, Spain) or 10 mL (Berkeley, CA, United States) of solar panel dust slurry (2655 RCF for 5 min). Empty tubes were included as extraction controls to account for ions resulting from procedural methods.

For extraction of hydrophilic metabolites, the slurry pellets were extracted in methanol. Briefly, the pellets were resuspended in 2 mL of 100% methanol, vortexed for 10 s, sonicated for 20 min. in an ice bath, and then incubated at 4°C overnight. The following day, the methanol solutions were vortexed again and centrifuged at 6000 RCF for 3 min to pellet insoluble material. The supernatants were then dried under vacuum at room temperature for 6 h (Thermo SpeedVac Concentration and Trap) which each yielded ~10 µL of viscous yellow fluid. These were then resuspended in 150 µL of methanol with internal standards. The resuspensions were vortexed 10 s, sonicated 20 min in an ice bath and centrifuged at 6000 RCF for 3 min to pellet insoluble material; supernatants were filtered through a 0.22 µm microcentrifuge filtration devices (Pall, ODM02C34) and filtrates were transferred to glass vials for analysis. The internal standard mix used for the Valencia, Spain sample was a 2000-fold dilution of universally labeled 15N, 13C amino acid mix (Sigma, 767964). The internal standards used for the Berkeley, CA, United States samples included 1 µg/mL 2-amino-3-bromo-5-methylbenzoic acid (Sigma R435902), 5 µg/mL 3,6-dihydroxy-4-methylpyridazine (Sigma 668141), 5 µg/mL 13C-15N-L-phenylalanine (Sigma 608017), 10 µg/mL d4-lysine (Sigma 616192), 10 µg/mL d5-benzoic acid (Sigma 217158), and 2 µg/mL 9-anthracene carboxylic acid (Sigma A89405).

For triglycerides, chloroform extractions were performed on slurry pellets (collected as described

above) using a modified Bligh-Dyer approach (Bligh and Dyer, 1959). Briefly, 120 µL of water was added to each pellet, vortexed, then 450 µL of 2:1 MeOH:CH3Cl was added for a final ratio of 2:1:0.8 MeOH:CH3Cl:H2O followed by a brief vortex and incubation for 15 min in a sonicating water bath. An additional 150 µL CH3Cl and 150 µL H2O was added to create a final ratio of 1:1:0.9 MeOH:CH3Cl:H2O, then briefly vortexed and incubated for 10 min in a sonicating water bath. After centrifuging samples for 2 min at 2655 RCF, the lower lipid-enriched chloroform phase was transferred to a new tube. 300 µL of chloroform was then added to the remaining pellet (methanol-water layer), followed by repeat sonication and centrifugation, and the bottom chloroform phase was combined with the previously collected extract. Chloroform extracts of lipid were then dried in a SpeedVac (SPD111V, Thermo Scientific) and stored at -20°C. Prior to analysis, dried extracts were resuspended in 3:3:4 isopropanol:acetonitrile:methanol (IPA:ACN:MeOH), centrifuge-filtered through a 0.22 µm PVDF membrane (Millipore Ultrafree-MC) containing an internal standard mixture of 1 µg/mL 2-Amino-3-bromo-5-methylbenzoic acid (ABMBA) and 4 µM each of deuterated lipids including: 17:0-17:1-17:0 D5 triglyceride (Avanti 110544), 18:0-18:1 D5 phosphoglyceride (Avanti 110899), D9 oleic acid (Avanti 850809O), 1,3-16:1 D5 diglyceride (Avanti 110579), and dipalmitoyl glycerol trimethyl homoserine D9 (Avanti 857463). Filtrates were transferred to glass vials for analysis.

Liquid Chromatography Tandem Mass Spectrometry (LC-MS/MS) Based Metabolomics

Chromatographic separations were performed using an Agilent 1290 LC stack, with MS and MS/MS data collected using a Q Exactive hybrid Quadrupole-Orbitrap Mass Spectrometer equipped with a heated electrospray ionization (HESI-II) source probe (Thermo Scientific, San Jose, CA, United States). All chemicals and solvents were of LCMS or HPLC grade.

Polar metabolites were chromatographically separated using a 5 µm, 150 × 2.1 mm, 200Å ZIC-HILIC column containing sulfobetaine (zwitterionic) silica based stationary phase (Merck Millipore) under the following conditions: 0.45 mL/min. flow rate, 40°C column temperature, and a 2 µL injection volume. Mobile phases (A: 5 mM ammonium acetate in water, and B: 5 mM ammonium acetate, 95% v/v acetonitrile in water) were varied as follows: 1.5 min hold at 100% B, 13.5 min linear gradient to 65% B, 3 min linear gradient to 0% B, 5 min hold at 0% B, 2 min gradient to 100% B, and a 5 min reequilibration at 100% B.

Triglycerides were chromatographically separated using a 1.8 µm, 50 × 2.1 mm C18 column (Agilent ZORBAX Eclipse Plus C18, Rapid Resolution HD) under the following conditions: 0.4 mL/min flow rate, 55°C column temperature, and a 2 µL injection volume. Mobile phases (A: 40:60 water:acetonitrile with 5 mM ammonium acetate and 0.1% v/v formic acid, and B: 90:10 isopropanol:acetonitrile with 5 mM ammonium acetate and 0.1% v/v formic acid) were varied as follows: 1.5 min hold at 20% B, 2.5 min linear gradient to 55% B, 6 min linear gradient to 80% B, 2 min hold at 80% B, 1.5 min linear gradient to 100% B, 3.5 min hold at 100% B, 1.5 min linear gradient to 20% B and 1.5 min re-equilibration at 20% B.

For all chromatographies, eluted compounds were detected via ESI-MS/MS using the Q Exactive's data dependent MS2 Top2 function, where the two highest abundance precursor ions reaching at least 1e3 ions within the max ion transfer time (excluding ions with assigned charge ≥4) and not already fragmented in the previous 10 s are selected from a full MS pre-scan from m/z 70–1050 (HILIC) or 80–1200 (C18) at 70,000 resolution with an automatic gain control (AGC) target at 3e6 and 100 millisecond maximum ion transmission, followed by sequential MS/MS fragmentation of each of the two precursors with stepped normalized collision energies (stepped NCE) of 10, 20, and 30 (HILIC) or 10, 20, 40 (C18) at 17,000 resolution with an isolation window of 2 m/z and AGC target at 1e5 and 50 milliseconds; all spectra were stored in centroid data format. The source was set with the sheath gas flow at 55 (arbitrary units), aux gas flow at 20 (arbitrary units), sweep gas flow at 2 (arbitrary units), spray voltage at 3 |kV|, and capillary temperature at 400°C. Internal standards were used for quality control purposes.

Metabolomic Data Analysis

For HILIC data analysis, retention and fragmentation data were compared to a library of

pure reference standards analyzed under the same conditions. MS/MS fragmentation spectra, if collected for the compound of interest, were compared to internal and online spectral databases to confirm identification. A subset of the library was analyzed (as external standards) at the same time as the samples and used for generation of the theoretical retention times using linear regression (to account for retention shifts due to changes in tubing length, mobile phase batches and different lots of column from the manufacturer). Exact mass (+/- 25 ppm at peak apex) and retention time (+/- 0.5 min from theoretical) coupled with MS/MS fragmentation spectra were used to identify compounds with a python-based metabolite atlas analysis (Bowen and Northen, 2010; Yao et al., 2015). Python code is available at https://github.com/biorack/metatlas.

Exact mass and retention time coupled with MS/MS fragmentation spectra were used to identify lipids. Lipid class was determined based on characteristic fragment ions or neutral loss, and coupled with exact mass to determine specific lipid identity (number of carbons in fatty acid tails and degree of unsaturation). In positive ion mode, triglycerides ionized as a singly charged ammonium adduct with fatty acid tails detected in the MS/MS fragmentation spectra (McAnoy et al., 2005). Deuterated TG internal standard was used to verify fragmentation pattern and retention time range for the TG lipid class.

Availability of Data

Raw and processed data are available on the JGI Genome Portal: https://genome.jgi.doe.gov/portal/solcelcoanalysisunder proposal 503162 “solar cell community analysis.” Metabolomic results from solar panels in Berkeley and Valencia have been deposited under project ID 1196772. The metagenomics from the three Berkeley, CA, United States solar panel communities are available under project IDs: 1123560, 1123562, and 1123564.

Results

Cultivable Isolates and Colonization Experiments

Solar panels proved very rich in cultivable bacteria on LB and, particularly, R2A media (Figure II.1). A large diversity of colony phenotypes was observed at temperatures from 4°C to 27°C, with very few cultivable isolates growing at higher temperatures (50°C). Many of the isolates displayed yellow, orange or pink colors, particularly on R2A. In fact, R2A plates incubated at temperatures from 4°C to 27°C displayed numerous pink-pigmented colonies.

Due to the diverse microbial growth observed on the R2A plates, this media was selected for all the further studies and isolates were re-streaked exclusively from R2A plates. Specifically, seven isolates from the R2A plates grown at RT (SPB1-SPB7) were randomly selected along with three pink-pigmented isolates from the R2A plates grown at 4°C (SPB8-SPB10). Additionally, four isolates previously selected from the solar panels samples by UV irradiating for 5 min (as described in Materials and Methods) were selected as well (data not shown) (SPB11-SPB14). In total, 14 isolates were identified by 16S rRNA gene sequencing as follows: *Arthrobacter* (SPB1), *Hymenobacter* (SPB2), *Hymenobacter* (SPB3), *Rhodococcus* (uranium-contaminated site) (SPB4), *Methylobacterium* (SPB5), *Deinococcus* (SPB6), *Arthrobacter agilis* (SPB7), *Hymenobacter* (SPB8), *Hymenobacter* (SPB9), *Hymenobacter perfusus-uranium* (SPB10), *Hymenobacter perfusus-uranium* (SPB11), *Curtobacterium* (SPB12), *Curtobacterium* (SPB13), and *Arthrobacter agilis* (SPB14).

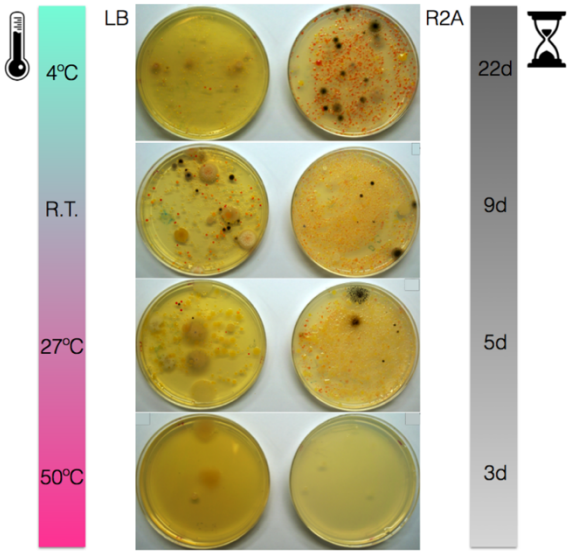

Figure II.1. Solar panel samples grown on LB and R2A media and incubated at 4°C, room temperature (22°C), 27 and 50°C for 22, 9, 5, and 3 days, respectively.

The 14 isolates were then screened for their glass-colonization abilities. After 2 days of incubation, strains SPB1, SPB5, and SPB6 exhibited very faint but visible colonies. After 4 days, all but one strain were able to grow, indicating some adhesion ability to the glass surfaces (Figure II.2A). The strains with the highest glass colonization ability, as deduced by a fully compact growth on the slide were SPB1, SPB5, and SPB6, and to a lesser extent, SPB11 and SPB3 (Figure II.2A). When subjected to 2 min of UV irradiation, only one strain (SPB1), exhibited high resistance as deduced by numerous colonies (>10) growing after transfer to R2A solid medium (Figure II.2, left). Three other isolates resulted ≤ three colonies each (SPB6, SPB11 and SPB12) and the rest of isolates did not yield viable cells after irradiation (Figure II.2B).

As it was the case with UV radiation, 72 h desiccation tests yielded a decrease in viability of most of the strains. Only strain SPB5 exhibited vigorous growth, concentered around the spot on which the suspension was placed; followed by SPB1, with hundreds of surviving colonies. The remaining isolates exhibited very low (<20 colonies for SPB7, 12, 13, 14) to no survival to desiccation (Figure II.2C).

Metagenomic Analysis

Between 590 and 775 Mb were sequenced for each sample and assembled into around 710.000 and 1 million scaffolds. Approximately one million ORFs were predicted for each metagenome: 99.11% of the ORFs corresponded to protein-coding genes, and the remaining 0.89% to RNA genes. Taxonomic analysis (Figure II.3) revealed that the sequences corresponded mainly to bacteria, although there was also a substantial proportion of Eukaryota, in which predominant sequences corresponded to fungi and, more specifically, to *Ascomycota* (~31.9% of annotated contigs across the three metagenomes). In the case of bacteria, the predominant phyla were *Actinobacteria* (15.6%), *Bacteroidetes* (22.6%), and *Proteobacteria* (14.8%), and to a lesser extent, *Deinococcus* (6.3%) *Cyanobacteria* and *Firmicutes*. Furthermore, there was a clear predominance of *Hymenobacter* spp. amongst the microbial community of the Berkeley solar panels (19.7%), with other constituents including *Deinococcus* spp. (6.3%), *Modestobacter marinus* (1.25%), *Kineococcus radiotolerans* (3.13%), *Friedmanniella sagamiharensis* (4.98%) and *Alternaria alternata* (2.19%), among others. The results of our metagenomic sequencing clearly support our culture-based approach, as all our cultured isolates are represented in our assembled metagenomes.

When comparing the taxonomic information of the solar panels from Berkeley with the data obtained from solar panels in Valencia (Dorado-Morales et al., 2016), the taxonomic profiles

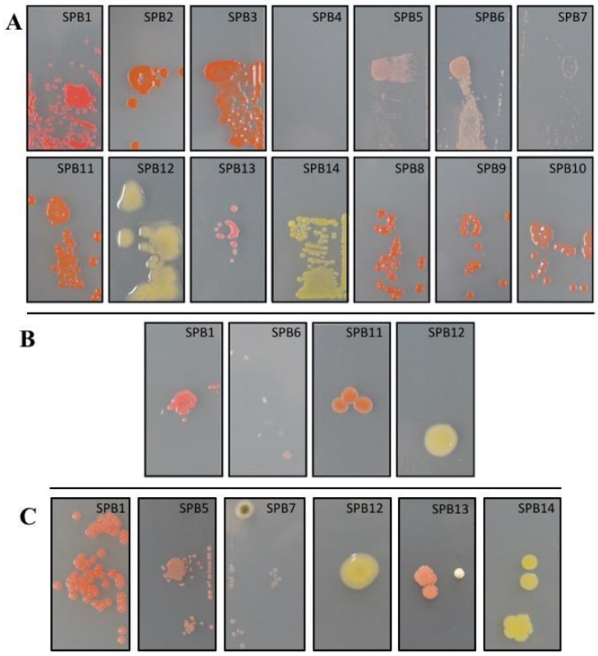

Figure II.2. (A) Glass-adhesion test performed as described in M&M. From left to right, top: isolates SPB1, SPB2, SPB3, SPB4, SPB5, SPB6, SPB7; bottom: SPB11, SPB12, SPB13, SPB14, SPB8, SPB9, and SPB10. (B) UV-resistance test performed on glass-adhering cells as described in M&M. From left to right isolates SPB1, SPB6, SPB11, and SPB12. The three later correspond to the growth of only 1-3 UV-resistant colonies each. (C) Desiccation-resistance test performed on glass-adhering cells as described in M&M. From left to right isolates SPB1, SPB5, SPB7, SPB12, SPB13, and SPB14. Isolates correspond to: SPB1, *Arthrobacter*; SPB2, *Hymenobacter*; SPB3, *Hymenobacter*; SPB4, *Rhodococcus* (uranium-contaminated site); SPB5, *Methylobacterium*; SPB6, *Deinococcus*; SPB7, *Arthrobacter agilis*; SPB8, *Hymenobacter*; SPB9, *Hymenobacter*; SPB10, H*ymenobacter perfusus-uranium*; SPB11, *Hymenobacter perfusus-uranium*; SPB12, *Curtobacterium*; SPB13, *Curtobacterium*; and SPB14, *Arthrobacter agilis*. The images are representative of the microscope slides (size 22X40 mm).

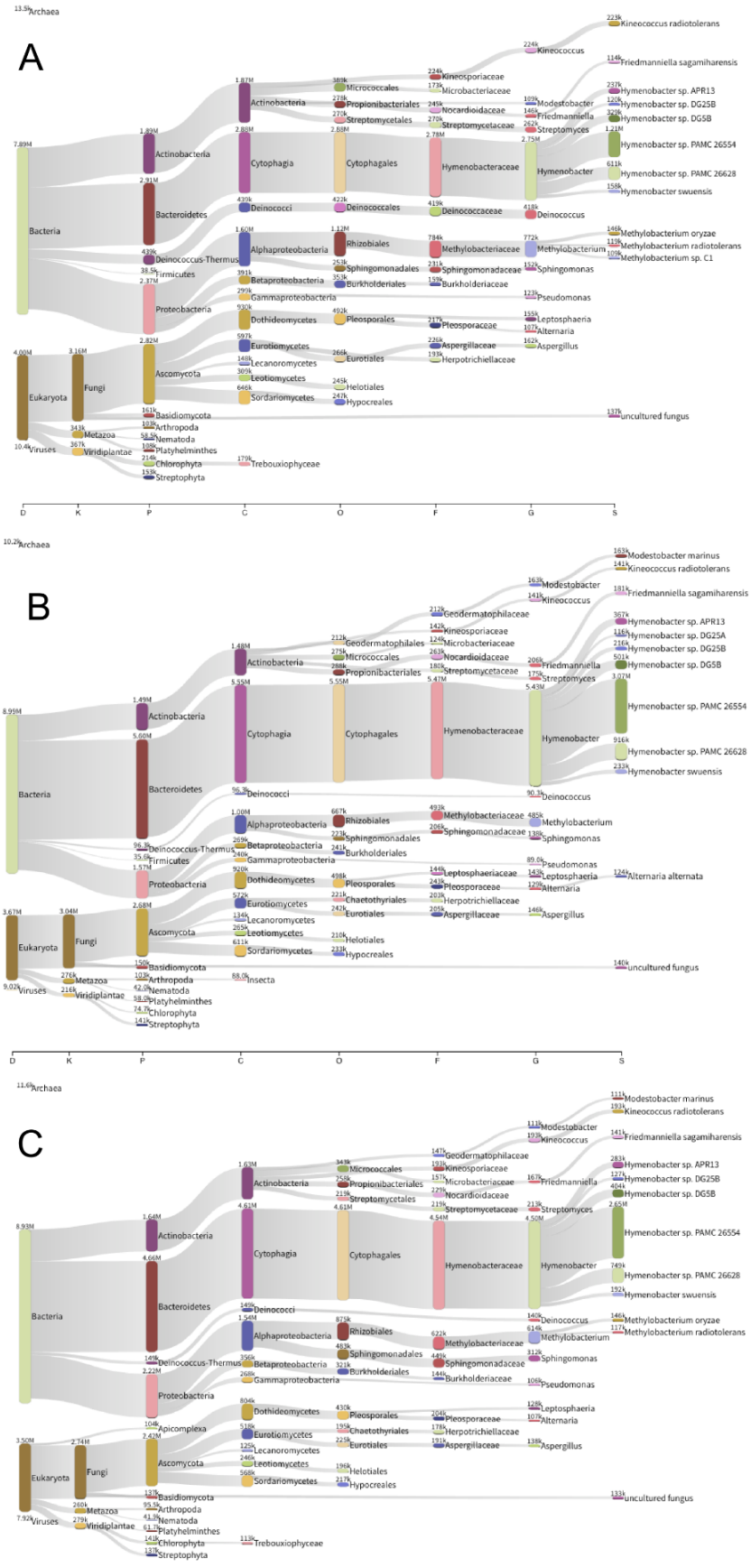

Figure II.3. Taxonomic composition of three solar panel microbial communities from Berkeley, CA, United States. The thickness of the lines is representative of the relative abundance of the taxa. (A) Left solar panel. (B) Center solar panel. (C) Right solar panel.

proved very similar both in community composition and taxon abundance (Figure II.4). Specifically, the most abundant taxa in all five samples were *Actinobacteria, Bacteroidetes* (mainly *Cytophagales*), *Cyanobacteria, Deinococcus* (mainly *Deinococcales*), *Firmicutes, Proteobacteria* and *Ascomycota*; and the subdivisions of these taxa were very similar in the solar panels from both locations (Figure II.4). Despite these general similarities, we found a number of significant differences between localities at various taxonomic levels. Specifically, members of the *Ascomycota* and *Bacteroidetes* were significantly enriched in the Berkeley samples compared to the Valencia communities (Welch's two-sided t-test, $P < 0.05$). By contrast, *Alphaproteobacteria* were significantly more common in the Valencia metagenomes than the Berkeley counterparts ($P < 0.05$), as were *Sphingomonas* spp. ($P < 0.05$) (Figure II.5A). Statistical analyses indicate that these communities differ significantly in their composition according to sampling location (Valencia vs. California; PERMANOVA, $P < 0.001$).

Consistent with the observed taxonomic variations between the solar panel communities, we found marked differences in the functional attributes of the solar panel communities. Firstly, comparisons of our genes against the SEED subsystems database (Figure II.5B) showed that pathways involved in the persistence of microbes on solar panels, such as stress response (3.1% of annotated open reading frames), capsule development (2.8%) and metabolite repair (2.1%), were common to all metagenomes. We also found evidence of genes for carotenoid biosynthesis and, by contrast, genes assigned to photosynthetic pathways were rare (0.07%) as were those assigned to general autotrophic subsystems (0.02%) suggesting that these pathways are not critical for persistence on solar panels.

Notwithstanding these dominant processes, we found significant over-representation of catalases, cAMP- binding proteins and 3-oxoacyl-[acyl-carrier protein] reductases in the Berkeley metagenomes compared to the Valencia samples (Welch's two-sided t-test, $P < 0.05$). The opposite trend was observed for DNA-dependent RNA polymerases and TonB-dependent receptors ($P < 0.05$), which were more abundant in the metagenomes from Valencia. Cumulatively, the differences in gene content between the

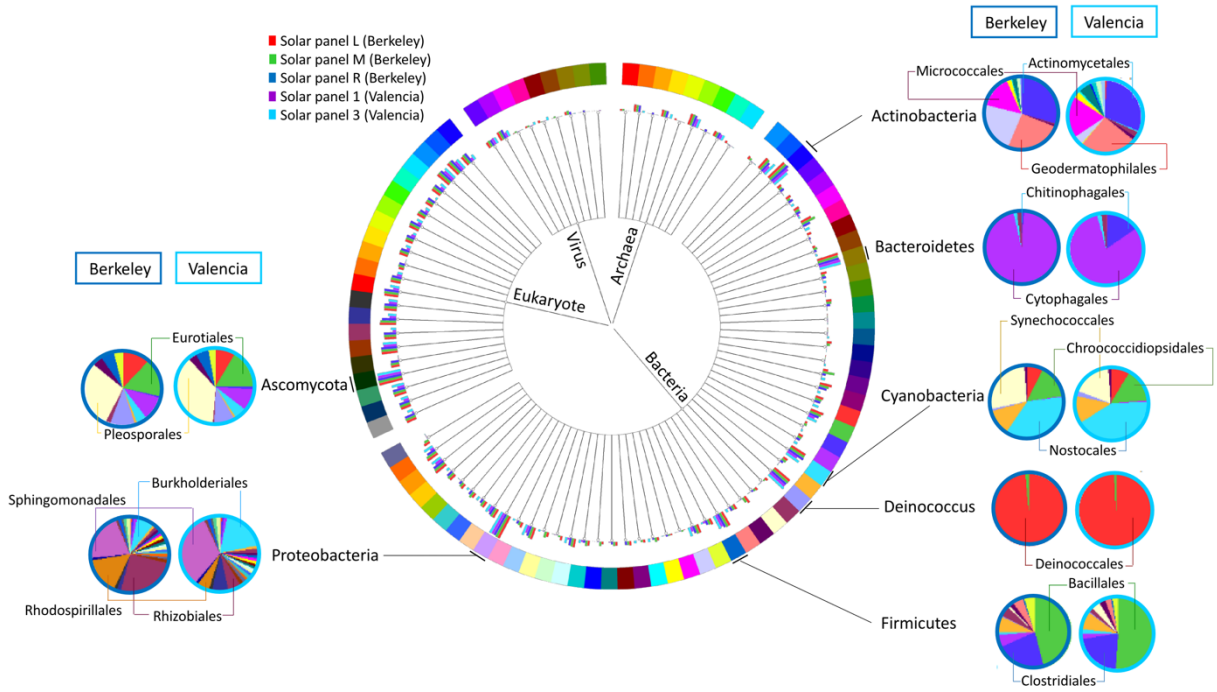

Figure II.4. Comparison of the taxonomic profiles of solar panels from Berkeley, CA, United States (red, green, and dark blue bars – three replicates) and Valencia, Spain (purple and light blue bars – two replicates). Most abundant taxa are indicated, and subdivisions of those taxa in one replicate from each location are represented (Berkeley and Valencia replicates in the dark and light blue circles, respectively).

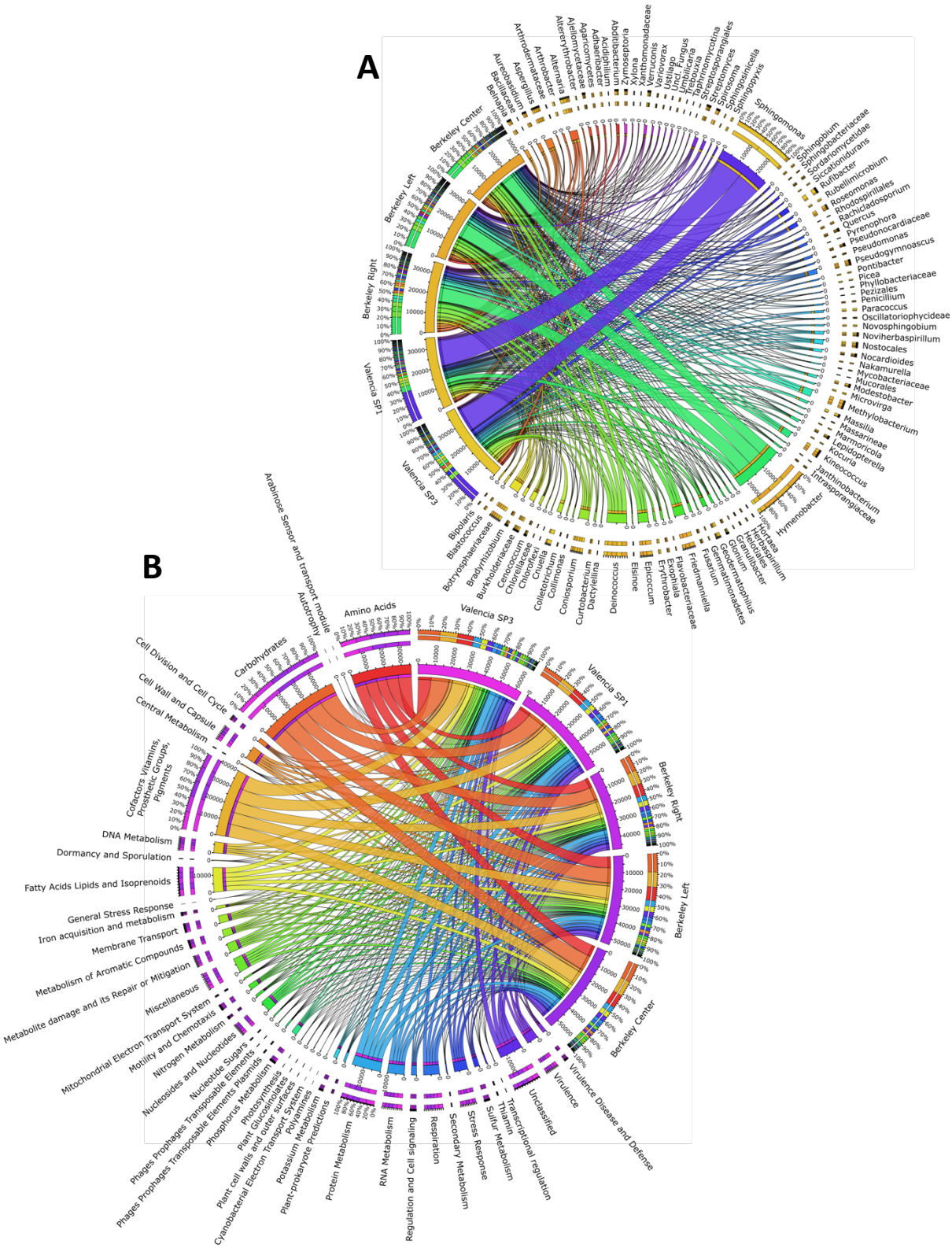

Figure II.5. Circos graph connecting (A) microbial taxa at the genus level and (B) SEED functional subsystems to the different metagenomes analyzed in this work (three solar panels from Berkeley, CA, United States, and two solar panels from Valencia, Spain).

communities were sufficient to explain >70% of the variation between the metagenomes collected from Valencia and Berkeley (PCA, First principal component = 70.7%; PERMANOVA, $P < 0.05$).

A more targeted analysis of the functional components of these metagenomes revealed diverse mechanisms for dealing with the extreme climatic conditions imposed by living on solar

panels. We found numerous genes encoding heat shock chaperone proteins (e.g., dnaK, dnaJ, grpE; combined genes across Berkeley metagenomes, n = 187) which belonged to a range of taxa, but were primarily affiliated with *Deinococcus* spp. and *Sphingomonas* spp. Mechanisms of combatting oxidative stress were equally abundant in both locations and included a variety of superoxide dismutases (n = 50), most of which belonged to *Kineococcus radiotolerans* and *Deinococcus* spp., as well as a group of peroxidases and peroxide stress regulators, which were assigned exclusively to members of the *Methylobacteria*. Perhaps the most ubiquitous stress responses were those involved in DNA damage repair which provided between 459 and 519 genes per metagenome. DNA mismatch repair genes mutL and mutS were very common features within the metagenomes and could be assigned to a diverse set of dominant bacterial groups including *Hymenobacter* spp. and *Sphingomonas* spp., among others.

Finally, our functional data strongly corroborate our metabolomics results (described in the section below). Pathways for allantoin utilization were common to all metagenomes and include allantoinase and allantoicase, two hydrolase families involved in the biogenesis and degradation of ureides. As observed in the metabolomics data, we found more genes involved in allantoin metabolism in the Berkeley samples than in the Valencian samples. For example, allantoate amidohydrolase and allantoin racemase were present exclusively in the Berkeley metagenomes. These processes appear to be carried out by both dominant (i.e., *Deinococcus* spp.) and rare (i.e., *Thermobispora bispora*) community members, indicating a widespread gene catalog for key processes that permit colonization in an extreme environment.

Metabolomic Results

Most of the detected polar metabolites were present in both locations, although a few were detected primarily in a single location (Figure II.6A). In both locations, common primary metabolites such as amino acids, nucleobases and sugars were detected. Interestingly, both locations contained nicotine, which may be linked to outdoor smoking. A number of aliphatic dicarboxylic acids of variable chain lengths (maleic acid, azelaic acid, suberic acid, pimelic acid) were present in both. Compatible solutes, such as ectoine, sugar alcohols, di- and tri-saccharides, were detected in both, which may play a role in protection against desiccation, heat and/or UV stress. A few compounds, sphinganine, sphingomyelin, an unidentified hexose and UDP-acetylhexosamine were detected only in the Berkeley samples while trigonelline, pantolactone, 5-valerolactone, and threonic acid and 4-guanidinobutyric acid had higher relative abundance in the Valencian sample. Triglyceride (TG) metabolites were highly abundant in both locations, and the most abundant triglycerides were similar between both locations (Figure II.6B). The metagenomic and metabolomic data are publicly available in the JGI database under accession number ID: 503162, and can be accessed with the following URL: https://genome.jgi.doe.gov/portal/solcelcoanalysis/solcelcoanalysis.info.html.

Discussion

Samples isolated from solar panels in Berkeley, CA, United States proved very rich in culturable bacteria despite the harsh environmental conditions they are subjected to, a result that is consistent with the previous work done on solar panels from Valencia, Spain and polar regions (Dorado-Morales et al., 2016; Tanner et al., 2018). Interestingly, the vast majority of the culturable microorganisms were not thermotolerant, but mesophilic or even psychrotolerant. This has important implications for the ecology of an environment that is prone to have thermal stress and daily peaks of extreme heat, particularly in summer (Dorado-Morales et al., 2016), when sampling was performed. Taking into account that peaks of heat on the panels tend to correlate with drought, our results suggest that microbial growth may be concentrated during the night, when water availability is higher and temperatures much cooler, even in Mediterranean climates. The average low temperature in Berkeley in August is just 12.4°C (Western Regional Climate Center, accessed May 5th 2017). This preference for mild growth temperatures was also observed in the isolates from Spain (Dorado-Morales et al., 2016). Taken together, both reports strongly suggest a thermoresistant -but not thermophilic- solar panel-adapted community.

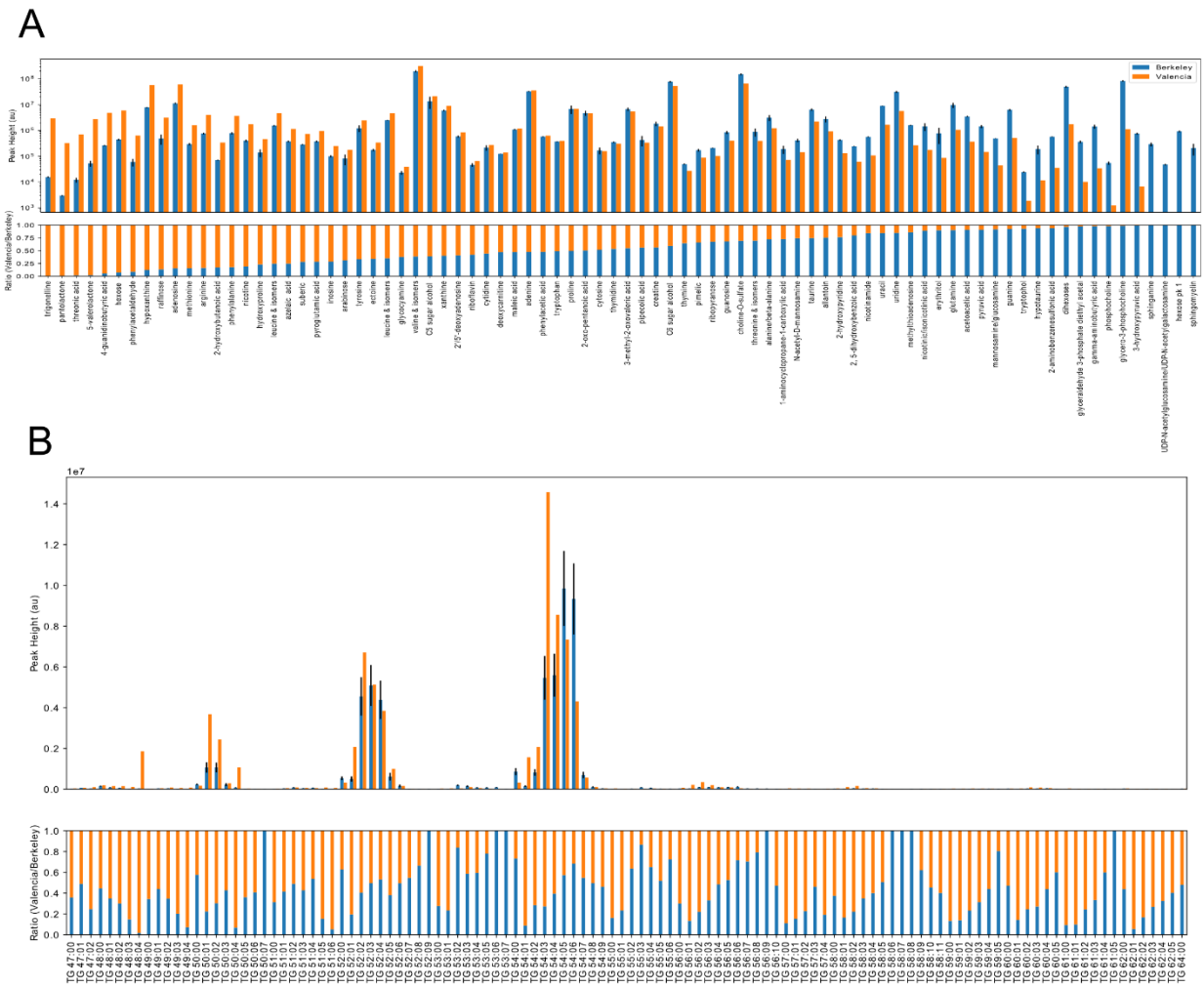

Figure II.6. Metabolomics analyses of the Californian and Valencian solar panel samples. Ion abundance results for polar metabolites (A) and triacylglycerol lipids (B). Absolute ion abundances (upper panels, log scale) and relative ion abundances (lower panels, scaled to 1) corresponding to the identified metabolites are indicated in orange (Valencia, Spain) and blue (Berkeley, CA, United States). Without quantification, ion abundances cannot be used to compare between metabolites due to differences in ionization efficiencies. Here, ion abundances of identified metabolites may be used to compare relative abundances between Berkeley and Valencia. Polar metabolites (A) are ranked by relative abundance and triacylglycerol lipids are sorted by chain length followed by degree of unsaturation.

Growth on both LB and R2A media yielded a large proportion of pigmented colonies. Interestingly, the highest number of pigmented colonies was observed when the samples were grown on R2A medium at 4°C, which could be explained by the increased accumulation of carotenoids at low temperatures as a cryoprotection strategy through the modulation of membrane fluidity (Jagannadham et al., 2000; Dieser et al., 2010). Furthermore, growth of *Hymenobacter* on R2A medium and at temperatures between 4 and 25°C is consistent with previous reports (Srinivasan et al., 2015; Lee et al., 2016) and suggests the preference of this bacterium for low nutrient culture media. The well-known role of carotenoids as UV sunscreens and the abundance of pigmented strains in panels strongly suggests their involvement in radiation protection during the day.

Besides heat-, radiation- and drought-resistance, microorganisms living on a smooth, flat surface fully exposed to the harsh climate must firmly attach to the substrate. Such attachment can involve binding to dust and other inorganic particles, but at least in the first stages of

colonization, strong adhesion to the glass surface is likely to be a major selective force. In order to characterize the glass-adhesion abilities as well as the resistance to UV light and desiccation of glass-bound cells, we developed an ad hoc test for some of the culturable strains from the solar panels. As expected, almost all of the isolated strains tested positive for adhesion to glass, with the exception of *Rhodococcus*, which is surprising taking into account that this genus typically produces extracellular polysaccharides that have a role in adhesion to surfaces (Urai et al., 2007). On the other hand, UV-radiation experiments resulted in the selection of only four UV-resistance isolates under our conditions (*Arthrobacter* spp., *Deinococcus* spp., *Hymenobacter* spp., and *Curtobacterium* spp.), whose extreme radiation-resistance properties have previously been reported (Jacobs and Sundin, 2001; Mongodin et al., 2006; Chung et al., 2010; Gerber et al., 2015). The lack of a higher number of UV-resistant isolates from a highly irradiated source environment is intriguing, and it could be explained by the effect of dust or sub-aerial biofilms shadowing on bacteria, thus mediating survival of low-resistant organisms (Osman et al., 2008). Desiccation experiments on glass revealed *Arthrobacter* and *Methylobacterium* as the most resistant isolates, consistent with previous reports concerning the desiccation-resistance properties of these two genera (Makhalanyane et al., 2013; SantaCruz-Calvo et al., 2013).

These results suggest that sun-exposed surfaces such as solar panels can be rich reservoirs of biotechnologically interesting bacteria thanks to their adhesion, radiation-resistance and desiccation-resistant properties, as well as to the production of sunscreens and/or antioxidant compounds such as carotenoids. This potential could of course increase when considering the non-culturable fraction of the sampled microbiomes. In order to further characterize the solar panels from California, a culture-independent approach combining metagenomic sequencing and metabolomics was set in place.

High-throughput sequencing of the solar panel samples revealed that these structures are composed of a rather diverse microbial population. In concordance with the culture-based characterization described above, the microbiome was dominated by *Hymenobacter* spp. and, to a lesser extent, by well-known radiation-resistant organisms, such as: *Modestobacter marinus*, an *Actinobacterium* that grows on calcareous stone surfaces (Normand et al., 2012); *Kineococcus radiotolerans*, previously isolated from radioactive areas (Phillips et al., 2002); or *Alternaria alternata*, a plant pathogenic fungus also found to grow inside the Chernobyl reactor (Mironenko et al., 2000).

Regarding the metabolomics analysis, although most of the detected polar compounds are common intracellular metabolites, a few were differentially expressed between the two locations. For example, trigonelline, a thermally labile secondary metabolite that is present in leguminous and, to a lesser extent, non-leguminous plants (Ashihara and Watanabe, 2014), as well as mammal urine, have been shown to inhibit attachment of bacteria to surfaces (Daglia et al., 2002). There have been previous reports on the ability of rhizosphere microorganisms to perform trigonelline catabolism (Boivin et al., 1991; Goldmann et al., 1991), but there are no reports (to the best of our knowledge) of microorganisms able to produce trigonelline. Pantolactone, 5-valerolactone, threonic acid and 4-guanidinobutyric acid were >10-fold more abundant in the Valencia sample. Threonic acid is a product of ascorbic acid metabolism (vitamin C), a well-known antioxidant compound; the degradation of ascorbic acid has been described in a variety of bacteria, including Lactobacillus spp., a genus detected in the Valencian sample (Englard and Seifter, 1986; Montaño et al., 2013). On the other hand, 5-valerolactone in an intermediate in the metabolism of cyclopentanone, a pathway that has been previously described in *Pseudomonas* spp. (Griffin and Trudgill, 1972) and *Comamonas* spp. (Iwaki et al., 2002). Interestingly, dye-sensitized solar cells have been previously fabricated with 4-guanidinobutyric acid as co-adsorbent, leading to an approximately 50 mV increase in open-circuit voltage in comparison to cells without GBA cografting (Zhang et al., 2005). This molecule could also be present due to conversion from L-arginine by means of the L-arginine oxidase, an enzyme that has been previously described in *Pseudomonas* spp. (Matsui et al., 2016) and cyanobacteria (Schriek et al., 2007). Compounds including sphingomyelin,

sphinganine, N-acetylhexosamine and were only detected in the Berkeley, CA, United States samples. Sphingomyelin is the most frequently occurring mammalian sphingolipid, although it has previously been described in *B. thetaiotaomicron* (Olsen and Jantzen, 2001). Interestingly, sphinganine has proven to inhibit bacterial adherence and to negatively affect biofilm formation in Staphylococcus aureus, Streptococcus mitis and *Streptococcus mutans* (Bibel et al., 1992; Cukkemane et al., 2015). N-acetylglucosamine, is an important component of the bacterial and fungal cell walls, and along with insect chitin may play a signaling role across multiple kingdoms (Konopka, 2012).

There were also a few metabolites detected from both Valencia and Berkeley that were of special interest given the environmental conditions on the solar panels. Interestingly, a number of medium chain length dicarboxylic acids were detected in samples from both Berkeley and Valencia. Only a single transporter was found in the metagenome for a short chain dicarboxylic acid. Azelaic acid, a bactericidal agent produced in fungi, plants and animals, can also be utilized as a sole carbon source by *Burkholderia* spp. (Estrada-de los Santos et al., 2001), a genus identified in both Berkeley and Valencia samples. The presence of compatible solutes in both locations is not surprising given the exposure to high heat and UV irradiation. Ectoine and 5-hydroxyectoine are produced by bacteria for protection against osmotic stress and more recently have been demonstrated to protect mammalian DNA from UV damage (Czech et al., 2018); however, only a single gene, assigned to *Bradyrhizobium*, was found in the Valencia, Spain metagenome for production of 5-hydroxyectoine from ectoine. Polyols, many of which were present in both Berkeley and Valencia samples, accumulate in yeasts in response to osmotic stress (Tekolo et al., 2010). Thus it was not surprising that numerous genes involved in polyol and trehalose biosynthesis, utilization and degradation were detected across a diverse set of bacteria. Pipecolic acid, a precursor to secondary metabolites, is produced in both bacteria and fungi (He, 2006). Allantoin is utilized by some bacteria as a secondary source of nitrogen under nutrient-limiting conditions (Ma et al., 2016). Tryptophol may act as a signaling molecule and precursor to secondary metabolites in fungi and yeasts (Palmieri and Petrini, 2018).

Triglyceride metabolites were detected in both locations, and this is not surprising, given that cells enduring an environmental stress such as desiccation (as found on a solar panel) often shift metabolic energy to a more quiescent state and toward carbon storage, e.g., TG accumulation and fatty acid storage in TGs (Rittershaus et al., 2013). The most abundant triglycerides were similar among both locations, and this may be attributed to the strikingly similar taxonomic profiles of the solar panels between Spain and California (Figure II.4), since lipid composition is characteristic of species and often similar between species from the same taxa (Sohlenkamp and Geiger, 2016).

As recently described for solar panels in the North and South Poles (Tanner et al., 2018), there is also a striking similarity between the taxonomic and functional profiles from solar panels from two same-latitude locations: Berkeley, CA, United States and in the distant Mediterranean city of Valencia, Spain (Figure II.4). This is certainly related to the common environmental conditions, including the climate and the selective pressures associated to a fully sun-exposed habitat on a glass surface: thermal fluctuations and heat peaks, high irradiation and circadian cycles of wetting and desiccation. These common stressors, which also include limited C and N availability, have created communities that are strikingly similar in terms of their functional capacity (Figure II.5B), even though we observed nuanced differences for some essential processes. This indicates a high degree of functional redundancy, whereby the variety of stress response adaptations occur in multiple individual microbial groups within each community. Although common selective pressures are expected to yield adaptive convergence, as observed in our results, rather than a taxonomic similarity, the comparison between the Valencian and Berkeley solar panels strongly suggests that, besides the climate, there must be similar inocula involved in the colonization process (Figure II.5A). As previously reported elsewhere, the wind is a major source of air-borne bacteria (Hervàs et al., 2009; Barberán et al., 2015; Meola et al., 2015), which, along with birds, insects and other animals, might be the main source of inocula for the solar panel microbiome to develop. Our results are in

concordance with a world-wide distribution of bacterial diversity, which is shaped in situ, by the specific pressure of living on a solar panel.

Author Contributions

MP and TN designed the project. MP, KL, and SK performed the experiments. MP, BB, KL, SK, MG, and KT analyzed the data. MP, KL, SK, BB, KT, MG, and TN wrote and revised the manuscript. TN and MP provided the funding.

Funding

Financial support from the Spanish Government (Grant Helios, Reference: BIO2015-66960-C3-1-R co-financed by FEDER funds and Ministerio de Ciencia, Innovación y Universidades) is acknowledged. Work performed at Lawrence Berkeley National Laboratory under the Office of Science Early Career Program (awarded to TN) and at the U.S. Department of Energy Joint Genome Institute, a Department of Energy Office of Science User Facility, and with use of resources at the National Energy Research Scientific Computing Center, a Department of Energy Office of Science User Facility, is supported by the U.S. Department of Energy, Office of Science, Office of Biological and Environmental Research under contract number DE-AC02-05CH11231.

Conflict of Interest Statement

The authors declare that the research was conducted in the absence of any commercial or financial relationships that could be construed as a potential conflict of interest.

Acknowledgments

We are very grateful to Thomas Price, Jeffery Knight, and Jesse Knight for their kind assistance in sampling the solar panels. We also thank Jose Manuel Martí Martínez for his help with the metagenomics analysis.

References

Ashihara, H., and Watanabe, S. (2014). Accumulation and function of trigonelline in non-leguminous plants. Nat. Prod. Commun. 9, 795–798.

Banerjee, S., Dionysiou, D. D., and Pillai, S. C. (2015). Self-cleaning applications of TiO2 by photo-induced hydrophilicity and photocatalysis. Appl. Catal. B. 176, 396–428. doi: 10.1016/j.apcatb.2015.03.058

Barberán, A., Ladau, J., Leff, J. W., Pollard, K. S., Meninger, H. L., Dunn, R. R., et al. (2015). Continental-scale distributions of dust-associated bacteria and fungi. Proc. Natl. Acad. Sci. U.S.A. 112, 5756–5761. doi: 10.1073/pnas.1420815112

Bibel, D. J., Aly, R., and Shinefield, H. R. (1992). Inhibition of microbial adherence by sphinganine. Can. J. Microbiol. 38, 983–985. doi: 10.1139/m92-158

Bligh, E. G., and Dyer, W. J. (1959). A rapid method of total lipid extraction and purification. Can J. Biochem. Physiol. 37, 911–917. doi: 10.1139/o59-099

Boivin, C., Barran, L. R., Malpica, C. A., and Rosenberg, C. (1991). Genetic analysis of a region of the Rhizobium meliloti pSym plasmid specifying catabolism oftrigonelline, a secondary metabolite present in legumes. J. Bacteriol. 173, 2808–2817. doi: 10.1128/jb.173.9.2809-2817.1991

Bowen, B. P., and Northen, T. R. (2010). Dealing with the unknown: metabolomics and metabolite atlases. J. Am. Soc. Mass Spectrom. 21, 1471–1476. doi: 10.1016/j.jasms.2010.04.003

Buchfink, B., Xie, C., and Huson, D. H. (2014). Fast and sensitive protein alignment using DIAMOND. Nat. Methods 12, 59–60. doi: 10.1038/nmeth.3176

Chung, A. P., Lopes, A., Nobre, M. F., and Morais, P. V. (2010). Hymenobacter perfusus sp. nov., Hymenobacter flocculans sp. nov. and Hymenobacter metalli sp. nov. three new species isolated from a uranium mine waste water treatment system. Syst. Appl. Microbiol. 33, 436–443. doi: 10.1016/j.syapm.2010.09.002

Cukkemane, N., Bikker, F. J., Nazmi, K., Brand, H. S., Sotres, J., Lindh, L., et al. (2015). Anti-adherence and bactericidal activity of sphingolipids against Streptococcus mutans. Eur. J. Oral Sci. 123, 221–227. doi: 10.1111/eos.12200

Czech, L., Hermann, L., Stöveken, N., Richter, A. A., Höppner, A., Smits, S. H. J., et al. (2018). Role of the extremolytes ectoine and hydroxyectoine as stress protectants and nutrients: genetics, phylogenomics, biochemistry, and structural analysis. Genes 9, 1–58. doi: 10.3390/genes9040177

Daglia, M., Tarsi, R., Papetti, A., Grisoli, P., Dacarro, C., Pruzzo, C., et al. (2002). Antiadhesive effect of green and roasted coffee on Streptococcus mutans' adhesive properties on saliva-coated hydroxyapatite beads. J. Agric. Food Chem. 50, 1225–1229. doi: 10.1021/jf010958t

Dieser, M., Greenwood, M., and Foreman, C. M. (2010). Carotenoid pigmentation in antarctic heterotrophic bacteria as a strategy to withstand environmental

stresses. Arct. Antarct. Alp. Res. 42, 396–405. doi: 10.1657/1938-4246-42.4.396

Dorado-Morales, P., Vilanova, C., Peretó, J., Codoñer, F. M., Ramón, D., and Porcar, M. (2016). A highly diverse, desert-like microbial biocenosis on solar panels in a Mediterranean city. Sci. Rep. 6:29235. doi: 10.1038/srep29235

Englard, S., and Seifter, S. (1986). The biochemical functions of ascorbic acid. Ann. Rev. Nutr. 6, 365–406. doi: 10.1146/annurev.nu.06.070186.002053

Estrada-de los Santos, P., Bustillos-Cristales, R., and Caballero-Mellado, J. (2001). Burkholderia, a genus rich in plant-associated nitrogen fixers with wide environmental and geographic distribution. Appl. Environ. Microbiol. 67, 2790–2798. doi: 10.1128/AEM.67.6.2790-2798.2001

Felden, J., Ruff, S. E., Ertefai, T., Inagaki, F., Hinrichs, K. U., and Wenzhöfer, F. (2014). Anaerobic methanotrophic community of a 5346-m-deep vesicomyid clam colony in the Japan Trench. Geobiology 12, 183–199. doi: 10.1111/gbi.12078

Fredrickson, J. K., Li, S. M., Gaidamakova, E. K., Matrosova, V. Y., Zhai, M., Sulloway, H. M., et al. (2008). Protein oxidation: key to bacterial desiccation resistance? SME J. 2, 393–403. doi: 10.1038/ismej.2007.116

Gerber, E., Bernard, R., Castang, S., Chabot, N., Coze, F., Dreux-Zigha, A., et al. (2015). Deinococcus as new chassis for industrial biotechnology: biology, physiology and tools. J. Appl. Microbiol. 119, 1–10. doi: 10.1111/jam.12808

Goldmann, A., Boivin, C., Fleury, V., Message, B., Lecoeur, L., Maille, M., et al. (1991). Betaine use by rhizosphere bacteria: genes essential for trigonelline, stachydrine, and carnitine catabolism in Rhizobium meliloti are located on pSym in the symbiotic region. Mol. Plant Microbe Interact. 4, 571–578. doi: 10.1094/MPMI-4-571

Griffin, M., and Trudgill, P. W. (1972). The metabolism of cyclopentanol by Pseudomonas sp. N.C.I.B. 9872. Biochem. J. 129, 595–603.

He, M. (2006). Pipecolic acid in microbes: biosynthetic routes and enzymes. J. Ind. Microbiol. Biotechnol. 33, 401–407. doi: 10.1007/s10295-006-0078-3

Hervàs, A., Camarero, L., Reche, I., and Casamayor, E. O. (2009). Viability and potential for immigration of airborne bacteria from Africa that reach high mountain lakes in Europe. Environ. Microbiol. 11, 1612–1623. doi: 10.1111/j.1462-2920.2009.01926.x

Huntemann, M., Ivanova, N. N., Mavromatis, K., Tripp, H. J., Paez-Espino, D., Tennessen, K., et al. (2016). The standard operating procedure of the DOE-JGI metagenome annotation pipeline (MAP v.4). Stand. Genomic Sci. 11:17. doi: 10.1186/s40793-016-0138-x

Huson, D. H., Auch, A. F., and Schuster, S. C. (2007). Megan analysis of metagenomic data. Genome Res. 17, 377–386. doi: 10.1101/gr.5969107

Hyatt, D., Chen, G. L., Locascio, P. F., Land, M. L., Larimer, F. W., and Hauser, L. J. (2010). Prodigal: prokaryotic gene recognition and translation initiation site identification. BMC Bioinformatics 11:119. doi: 10.1186/1471-2105-11-119

Iwaki, H., Hasegawa, Y., Wang, S., Kayser, M. M., and Lau, P. C. (2002). Cloning and characterization of a gene cluster involved in cyclopentanol metabolism in Comamonas sp. Strain NCIMB 9872 and biotransformations effected by Escherichia coli-expressed cyclopentanone 1,2-monooxygenase. Appl. Environ. Microbiol. 68, 5671–5684. doi: 10.1128/AEM.68.11.5671-5684.2002

Jacobs, J. L., and Sundin, G. W. (2001). Effect of solar UV-B radiation on a phyllosphere bacterial community. Appl. Environ. Microbiol. 67, 5488–5496. doi: 10.1128/AEM.67.12.5488-5496.2001

Jagannadham, M. V., Chattopadhyay, M. K., Subbalakshmi, C., Vairamani, M., Narayanan, K., Rao, C. M., et al. (2000). Carotenoids of an antarctic psychrotolerant bacterium, Sphingomonas antarticus, and a mesophilic bacterium, Sphingobacterium multivorum. Arch. Microbiol. 173, 418–424. doi: 10.1007/s002030000163

Kim, D., Song, L., Breitwieser, F. P., and Salzberg, S. L. (2016). Centrifuge: a rapid and sensitive classification of metagenomic sequences. Genome Res. 26, 1721–1729. doi: 10.1101/gr.210641.116

Kizilova, A. K., Sukhacheva, M. V., Pimenov, N. V., Yurkov, A. M., and Kravchenko, I. K. (2014). Methane oxidation activity and diversity of aerobic methanotrophs in pH-neutral and semi-neutral thermal springs of the Kunashir Island Russian Far East. Extremophiles 18, 207–218. doi: 10.1007/s00792-013-0603-z

Konopka, J. B. (2012). N-acetylglucosamine (GlcNAc) functions in cell signaling. Scientifica 2012, 631–632. doi: 10.6064/2012/489208

Lee, J., Kang, M., Joo, E. S., Jung, H., and Kim, M. K. (2016). Hymenobacter sedentarius sp. nov., isolated from a soil. J. Microbiol. 54, 283–289. doi: 10.1007/s12275-016-5386-3

Li, D., Liu, C. M., Luo, R., Sadakane, K., and Lam, T. W. (2015). MEGAHIT: an ultra-fast single-node solution for large and complex metagenomics assembly via succinct

de Bruijn graph. Bioinformatics 31, 1674–1676. doi: 10.1093/bioinformatics/btv033

Locey, K. J., and Lennon, J. T. (2016). Scaling laws predict global microbial diversity. Proc. Natl. Acad. Sci. U.S.A. 113, 5970–5975. doi: 10.1073/pnas.1521291113

Ma, P., Patching, S. G., Ivanova, E., Baldwin, J. M., Sharples, D., Baldwin, S. A., et al. (2016). Allantoin transport protein, Pucl, from Bacillus subtillis: evolutionary relationships, amplified expression, activity and specificity. Microbiology 162, 823–836. doi: 10.1099/mic.0.000266

Makhalanyane, T. P., Valverde, A., Birkeland, N., Cary, S. C., Tuffin, M., and Cowan, D. A. (2013). Evidence for successional development in Antarctic hypolithic bacterial communities. ISME J. 7, 2080–2090. doi: 10.1038/ismej.2013.94

Matsui, D., Terai, A., and Asano, Y. (2016). L-Arginine oxidase from Pseudomonas sp. TPU 7192: characterization, gene cloning, heterologous expression, and application to L-arginine determination. Enzyme Microb. Technol. 82, 151–157. doi: 10.1016/j.enzmictec.2015.10.002

McAnoy, A. M., Wu, C. C., and Murphy, R. C. (2005). Direct qualitative analysis of triacylglycerols by electrospray mass spectrometry using a linear ion trap. J. Am. Soc. Mass Spectrom. 16, 1498–1509. doi: 10.1016/j.jasms.2005.04.017

Mejia, F. A., and Kleissl, J. (2013). Soiling losses for solar photovoltaic systems in California. Sol. Energy 95, 357–363. doi: 10.1016/j.solener.2013.06.028

Meola, M., Lazzaro, A., and Zeyer, J. (2015). Bacterial composition and survival on Sahara dust particles transported to the European Alps. Front. Microbiol. 6:1454. doi: 10.3389/fmicb.2015.01454

Mironenko, N. V., Alekhina, I. A., Zhdanova, N. N., and Bulat, S. A. (2000). Intraspecific variation in gamma-radiation resistance and genomic structure in the filamentous fungus Alternaria alternata: a case study of strains inhabiting Chernobyl reactor no. 4. Ecotoxicol. Environ. Saf. 45, 177–187. doi: 10.1006/eesa.1999.1848

Mongodin, E. F., Shapir, N., Daugherty, S. C., DeBoy, R. T., Emerson, J. B., Shvartzbeyn, A., et al. (2006). Secrets of soil survival revealed by the genome sequence of Arthrobacter aurescens TC1. PLoS Genet. 2:e214. doi: 10.1371/journal.pgen.0020214

Montaño, A., Sánchez, A. H., Casado, F. J., Beato, V. M., and de Castro, A. (2013). Degradation of ascorbic acid and potassium sorbate different Lactobacillus species isolated from packed Green olives. Food Microbiol. 34, 7–11. doi: 10.1016/j.fm.2012.11.006

Normand, P., Gury, J., Pujic, P., Chouaia, B., Crotti, E., Brusetti, L., et al. (2012). Genome sequence of radiation-resistant Modestobacter marinus strain BC501, a representative actinobacterium that thrives on calcareous stone surfaces. J. Bacteriol. 194, 4773–4774. doi: 10.1128/JB.01029-12

Olsen, I., and Jantzen, E. (2001). Sphingolipids in bacteria and fungi. Anaerobe 7, 103–112. doi: 10.1006/anae.2001.0376

Osman, S., Peeters, Z., La Duc, M. T., Mancinelli, R., Ehrenfreund, P., and Venkateswaran, K. (2008). Effect of shadowing on survival of bacteria under conditions simulating the Martian atmosphere and UV radiation. Appl. Environ. Microbiol. 74, 959–970. doi: 10.1128/AEM.01973-07

Palmieri, A., and Petrini, M. (2018). Tryptophol and derivatives: natural occurrence and applications to the synthesis of bioactive compounds. Nat. Prod. Rep. doi: 10.1039/c8np00032h [Epub ahead of print].

Parks, D. H., Tyson, G. W., Hugenholtz, P., and Beiko, R. G. (2014). STAMP: statistical analysis of taxonomic and functional profiles. Bioinformatics 30, 3123–3124. doi: 10.1093/bioinformatics/btu494

Phillips, R. W., Wiegel, J., Berry, C. J., Fliermans, C., Peacock, A. D., White, D. C., et al. (2002). Kineococcus radiotolerans sp. nov., a radiation-resistant, gram-positive bacterium. Int. J. Syst. Evol. Microbiol. 52, 933–938.

Ragon, M., Restoux, G., Moreira, D., Møller, A. P., and López-García, P. (2011). Sunlight-exposed biofilm microbial communities are naturally resistant to chernobyl ionizing-radiation levels. PLoS One 6:e21764. doi: 10.1371/journal.pone.0021764

Rittershaus, E. S., Baek, S. H., and Sassetti, C. M. (2013). The normalcy of dormancy: common themes in microbial quiescence. Cell Host Microbe 13, 643–651. doi: 10.1016/j.chom.2013.05.012

SantaCruz-Calvo, L., González-López, J., and Manzanera, M. (2013). Arthrobacter siccitolerans sp. nov., a highly desiccation-tolerant, xeroprotectant-producing strain isolated from dry soil. Int. J. Syst. Evol. Micorbiol. 63, 4174–4180. doi: 10.1099/ijs.0.052902-0

Schriek, S., Rückert, C., Staiger, D., Pistorius, E. K., and Michel, K. P. (2007). Bioinformatic evaluation of L-arginine catabolic pathways in 24 cyanobacteria and transcriptional analysis of genes encoding enzymes of L-arginine catabolism in the cyanobacterium Synechocystis sp. PCC 6803. BMC Genomics 8:437. doi: 10.1186/1471-2164-8-437

Shirakawa, M. A., Zilles, R., Mocelin, A., Gaylarde, C. C., Gorbushina, A., Heidrich, G., et al. (2015). Microbial colonization affects the efficiency of photovoltaic

panels in a tropical environment. J. Environ. Manage. 157, 160–167. doi: 10.1016/j.jenvman.2015.03.050

Sohlenkamp, C., and Geiger, O. (2016). Bacterial membrane lipids: diversity in structures and pathways. FEMS Microbiol. Rev. 40, 133–159. doi: 10.1093/femsre/fuv008

Srinivasan, S., Joo, E. S., Lee, J., and Kim, M. K. (2015). Hymenobacter humi sp. nov., a bacterium isolated from soil. Antonie van Leeuwenhoek 107, 1411–1419. doi: 10.1007/s10482-015-0436-0

Tanner, K., Martí, J. M., Belliure, J., Fernandez-Mendez, M., Molina-Menor, E., Peretó, J., et al. (2018). Polar solar panels: Arctic and Antarctic microbiomes display similar taxonomic profiles. Environ. Microbiol. Rep. 10, 75–79. doi: 10.1111/1758-2229.12608

Tekolo, O. M., Mckenzie, J., Botha, A., and Prior, B. A. (2010). The osmotic stress tolerance of basidiomycetous yeasts. FEMS Yeast Res. 10, 482–491. doi: 10.1111/j.1567-1364.2010.00612.x

Urai, M., Yoshizaki, H., Anzai, H., Ogihara, J., Iwabuchi, N., Harayama, S., et al. (2007). Structural analysis of mucoidan, an acidic extracellular polysaccharide produced by a pristane-assimilating marine bacterium, Rhodococcus erythropolis PR4. Carbohydr. Res. 342, 927–932. doi: 10.1016/j.carres.2007.02.002

Vilanova, C., Iglesias, A., and Porcar, M. (2015). The coffee-machine bacteriome: biodiversity and colonization of the wasted coffee tray leach. Sci. Rep. 5:17163. doi: 10.1038/srep17163

Yao, Y., Sun, T., Wang, T., Ruebel, O., Northen, T., and Bowen, B. P. (2015). Analysis of metabolomics datasets with high-performance computing and metabolite atlases. Metabolites 5, 431–442. doi: 10.3390/metabo5030431

Zhang, Z., Zakeeruddin, S. M., O'Regan, B. C., Humphry-Baker, R., and Grätzel, M. (2005). Influence of 4-Guanidinobutyric acid as coadsorbent in reducing recombination in dye-sensitized solar cells. J. Phys. Chem. B. 109, 21818–21824. doi: 10.1021/jp054305h

Publication III

Extremophilic microbial communities on photovoltaic panel surfaces: a two-year study

Kristie Tanner[1,2 †], Esther Molina-Menor[2 †], Adriel Latorre-Pérez[1], Àngela Vidal-Verdú[2], Cristina Vilanova[1], Juli Peretó[1,2,3], and Manuel Porcar[1,2*]

[1] Darwin Bioprospecting Excellence S.L., Parc Científic de la Universitat de València, Paterna, Spain

[2] Institute for Integrative Systems Biology (I2SysBio, University of Valencia-CSIC), Paterna, Spain

[3] Department of Biochemistry and Molecular Biology, University of Valencia, Dr. Moliner 50, 46100 Burjassot, Spain

[†] These authors contributed equally to this work

Abstract

Solar panel surfaces can be colonized by microorganisms adapted to desiccation, temperature fluctuations and solar radiation. Although the taxonomic and functional composition of these communities has been studied, the microbial colonization process remains unclear. In the present work, we have monitored this microbial colonization process during 24 months by performing weekly measurements of the photovoltaic efficiency, carrying out 16S rRNA gene high-throughput sequencing, and studying the effect of antimicrobial compounds on the composition of the microbial biocenosis. This is the first time a long-term study of the colonization process of solar panels has been performed, and our results reveal that species richness and biodiversity exhibit seasonal fluctuations and that there is a trend towards an increase or decrease of specialist (solar panel-adapted) and generalist taxa, respectively. On the former, extremophilic bacterial genera *Deinococcus*, *Hymenobacter* and *Roseomonas* and fungal *Neocatenulostroma, Symmetrospora* and *Sporobolomyces* tended to dominate the biocenosis; whereas *Lactobacillus* sp or *Stemphyllium* exhibited a decreasing trend. This profile was deeply altered by washing the panels with chemical agents (Virkon), but this did not lead to an increase of the solar panels efficiency. Our results show that solar panels are extreme environments that force the selection of a particular microbial community.

Introduction

Extreme environments are characterized by their strong selective pressures, which can include physical (i.e., temperature or radiation), geochemical (i.e., desiccation or salinity) and/or biological stresses (i.e., limited nutrient availability) (Lynn and Rocco, 2001). The microorganisms that inhabit these environments, known as extremophiles or extremotolerants, are selected due a variety of mechanisms, such as biofilm formation (Flemming et al., 2016; Blanco et al., 2019); the production of extremolytes and extremozymes (Gabani and Singh, 2013); or highly efficient DNA repair systems (Singh and Gabani, 2011). Microorganisms inhabiting extreme environments evolve faster than those inhabiting 'benign' environments, mainly due to the high mutation rates associated to stressful environmental conditions (Li et al., 2014), and this could lead to these microorganisms being rich sources of new specialized metabolites (Sayed et al., 2019).

A diversity of physical, geochemical and biological extremes (solar radiation, temperature fluctuations, desiccation and limited nutrient availability) concur on solar panel surfaces. A study performed on subaerial solar panel biofilms in São Paulo revealed that dust, pollen and other debris covering the solar panel surfaces accumulated in time and included abundant fungi and pigmented bacterial genera, and this was associated with a decrease in the photovoltaic power efficiency, especially after 12 and 18 months (loss of 7% and 11% power respectively) (Shirakawa et al., 2015). This process – the accumulation of dust particles and microorganisms on a surface – is known as soiling, and it affects photovoltaic efficiency especially

under dry and arid conditions, such as those in the Atacama Desert, resulting in an annual energy loss of up 39% in regions with infrequent rainfalls (Cordero et al., 2018).

Microbial colonization of solar panel surfaces is of great interest not only from an energetic point of view, but also from an ecological perspective. The widespread distribution around the world of these artificial devices, as well as their relatively standard design, has enabled them to be used as ubiquitous sampling devices for microbial ecologists in the recent years. A previous study of solar panels located in Valencia (Spain) revealed that these surfaces are inhabited by diverse, desert-like microbial communities that show different day/night proteomic profiles and are adapted to high temperatures, desiccation and solar radiation (Dorado-Morales et al., 2016). The microbial communities present on the solar panels from Valencia proved rather similar, in taxonomic terms, to those on solar panels located in Arctic and Antarctic regions, with the most abundant genera being *Hymenobacter, Sphingomonas* and *Deinococcus* in all cases (Tanner et al., 2018). Furthermore, the microbiome of solar panel surfaces from Berkeley (California, USA) also displayed similar profiles, both in taxonomic and functional terms, to those observed on the Spanish solar panels, highlighting the role of selective pressures in the establishment of these microbial communities (Porcar et al., 2018). Nevertheless, and despite the previous taxonomic and functional characterization of the solar panel microbiome, little is known about the colonization process of these surfaces.

In the present study, we have weekly monitored the photovoltaic efficiency of 54 small-sized solar panels, and we have analysed the microbiome composition – including fungi and bacteria – every seven weeks, throughout a period of two years, with the aim of studying in detail the microbial colonization process and its effect on photovoltaic efficiency. Furthermore, we have assessed the effect on the solar panel microbiome of periodically treating the solar panel surfaces with a disinfectant.

Results

Solar panel efficiency, originally of roughly 20 Volts (V), displayed significant fluctuations in time and decreased during the first months of the experiment, but then recovered, and exhibited a very similar pattern during the next year (Figure III.1A). The efficiency was lower in the spring/summer months (between April and September), and this pattern was detected in both annuities, coinciding with the temperature

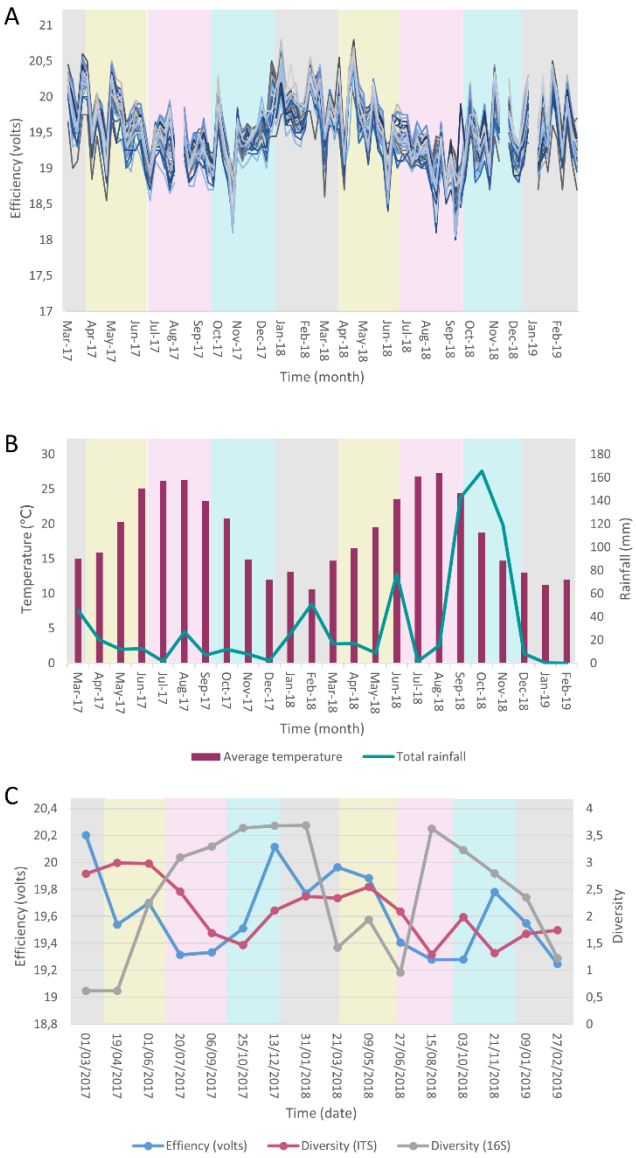

Figure III.1. (A) Variations in solar panel voltage throughout time (measures of the 54 panels were taken every week for a total of 106 weeks). (B) Climate graph of Valencia city, displaying the mean annual temperatures and rainfall values (data source: AVAMET MX). (C) Solar panel voltage is shown and compared to Shannon diversity values at genus level of the detected 16S (grey line) and ITS (pink line) sequences. Seasons in which each sampling was performed are indicated in grey (winter), green (spring), pink (summer) and blue (autumn).

increase and rainfall decrease recorded in Valencia, Spain (Figure III.1B). Bacterial diversity (Figure III.1C) and richness (Supplementary Figure III.1A) increased during these spring/summer months and decreased during the autumn/winter period. In the case of fungi, the opposite pattern was observed: both the diversity (Figure III.1D) and the richness (Supplementary Figure III.1B) decreased during the spring/summer months and increased during the autumn/winter period. Furthermore, seasonal decreases in bacterial richness and diversity (Supplementary Figure III.2A) coincided with an increase in chloroplast sequences (Supplementary Figure III.2B).

The mean relative abundance for each genus in time was calculated and the 15 most abundant bacteria and fungi were selected for further analysis (Table III.1). The most abundant bacterial genera were *Modestobacter* (2.72%), *Deinococcus* (2.52%), *Sphingomonas* (2.44%), *Hymenobacter* (2.38%) and *Rubellimicrobium* (2.29%). On the other hand, the most abundant fungal genus was, by far, *Alternaria*, with 55.4% of mean relative abundance, followed by an unidentified fungi (5.6%) and an unidentified *Pleosporales* (5.4%) and by 13 other taxa that displayed between 0.5 and 2.5% of mean relative abundance.

Table III.1. Fifteen bacterial and fungal genera with the highest mean relative abundance (MRA) throughout time obtained through 16S rRNA and ITS gene sequencing, respectively.

Bacteria		Fungi	
Genus	**MRA (%)**	**Genus**	**MRA (%)**
Modestobacter	2,72	*Alternaria*	55,45
Deinococcus	2,52	*unidentified*	13,41
Sphingomonas	2,44	*Stemphylium*	2,56
Hymenobacter	2,38	*Cladosporium*	1,96
Rubellimicrobium	2,29	*Neocatenulostroma*	1,60
Methylobacterium	2,15	*Aureobasidium*	1,56
Lactobacillus	1,62	*Filobasidium*	1,49
Skermanella	1,41	*Coniosporium*	1,44
Roseomonas	1,29	*Nigrospora*	1,29
Geodermatophilus	1,15	*Knufia*	1,26
Arthrobacter	1,14	*Phaeosphaeria*	0,75
Blastococcus	1,09	*Sporobolomyces*	0,58
Bacillus	1,39	*Vishniacozyma*	0,55
Microbispora	1,12	*Symmetrospora*	0,54
Paracoccus	0,95	*Trebouxia*	0,51

Fluctuations throughout time were observed for the 15 most abundant bacterial and fungal taxa (Supplementary Figure III.3). A close-up look at the most abundant taxa during the first 21 weeks (Supplementary Figure III.4), revealed that *Lactobacillus*, *Bacillus*, *Sphingomonas* and *Hymenobacter* are among the first to arrive, and that the abundance of *Sphingomonas* increases during the first 14 weeks, remaining more or less stable after that. On the other hand, on weeks 14 and 21, there is a general increase in abundance of the most abundant taxa, although this increase is especially pronounced for *Rubellimicrobium*, *Modestobacter*, *Skermanella* and *Microbispora*, whereas other taxa, such as *Sphingomonas*, *Hymenobacter* or *Deinococcus* remain constant. Interestingly, several of the most abundant bacteria displayed similar temporal profiles: *Sphingomonas* and *Deinococcus* (Figure III.2A), *Arthrobacter* and *Blastococcus* (Figure III.2B), *Cellulomonas* and *Rubellimicrobium* (Figure III.2C), and *Skermanella* and *Microbispora* (Figure III.2D).

Despite the fluctuations observed, only several bacterial and fungal taxa displayed statistically significant increases or decreases throughout time (Figures III.3 and III.4). Specifically, *Deinococcus*, *Hymenobacter* and *Roseomonas* increased with time, whereas *Lactobacillus* decreased (Prais-Winsten, P-value < 0.05) (Figure III.3). Regarding fungi, *Neocatenulostroma*, *Symmetrospora*, *Sporobolomyces* and *Comoclathris* increased throughout time, whereas *Stemphylium* decreased (Figure III.4) (Prais–Winsten, P-value < 0.05).

The effect of using a disinfectant on the microbial composition was studied using Rely + On Virkon (DuPont, Michigan, USA), a disinfectant that is routinely used to disinfect hard surfaces. This choice of disinfectant was based on the fact that Virkon does not generate fumes or strong odours, it is compatible with most hard non-porous surfaces, it cleans and disinfects in one step, it has a long shelf life (2 years for the tablet format) and it is effective as determined by European EN standards (bactericidal, fungicidal and virucidal efficacy). Furthermore, in a 1% solution it is non-irritating to eyes and skin. Solar panels that were cleaned with Virkon displayed very different bacterial profiles (Figure III.5A) when compared with the two types of controls (either dipped in

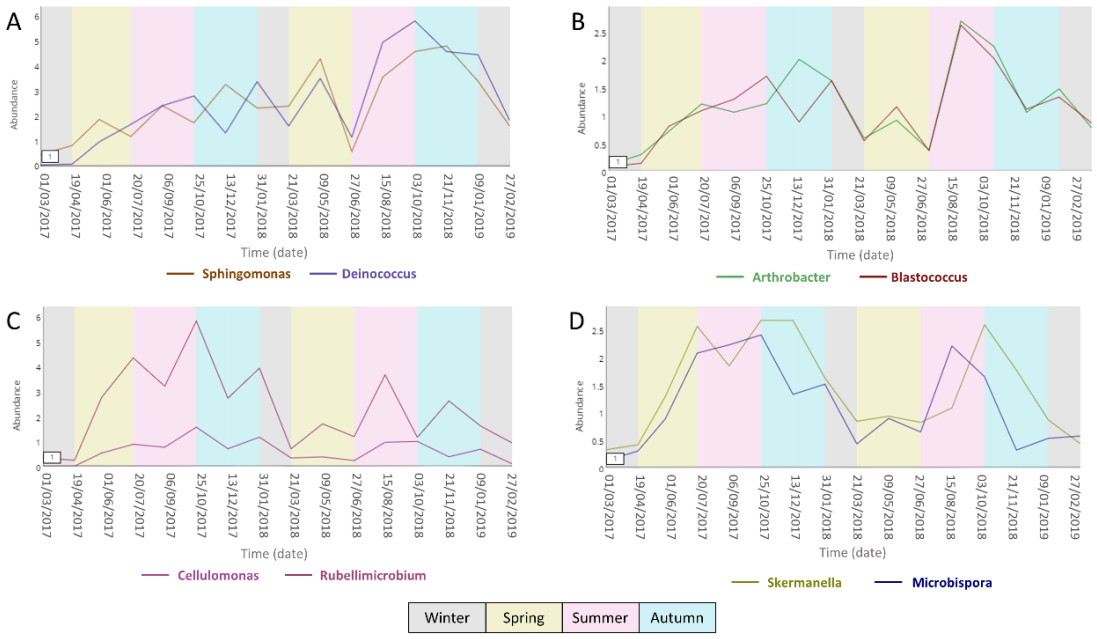

Figure III.2. Trend plots of taxa that display a similar behavior over time: (A) *Sphingomonas* and *Deinococcus*, (B) *Arthrobacter* and *Blastococcus*, (C) *Cellulomonas* and *Rubellimicrobium*, and (D) *Skermanella* and *Microbispora*. These taxa were identified with TIME using a Dynamic Time Warping (DTW) algorithm (Baksi et al., 2018). Seasons in which each sampling was performed are indicated in grey (winter), green (spring), pink (summer) and blue (autumn).

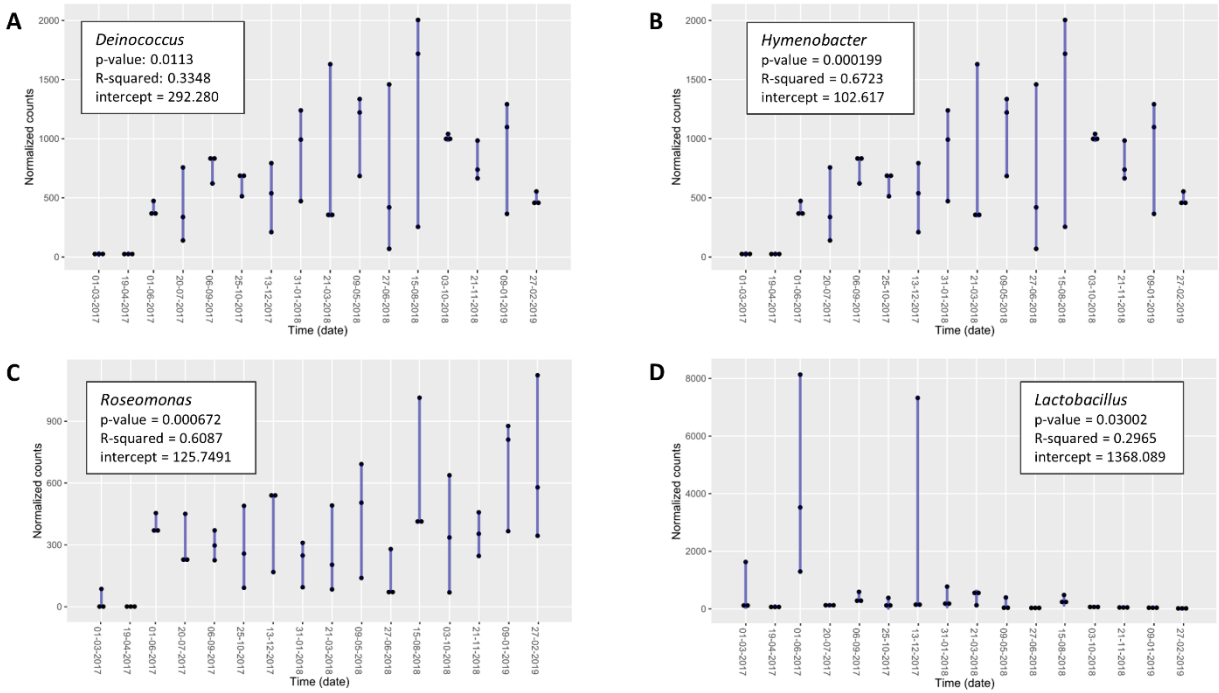

Figure III.3. Statistically significant positive (A,B,C) and negative (D) trends observed in bacterial genera throughout time and calculated using Prais-Winsten estimation (p-value < 0.05) Reported P-values were calculated by applying the normalization of EdgeR package. R-squared and intercept values are also indicated. The black dots indicate the normalized abundance for each of the three replicates.

sterile water or untreated, both of which displayed a more distant profile in comparison with the Virkon-treated solar panels). Specifically, the panels treated with Virkon were characterized by the almost complete disappearance of *Deinococcus*, and by the increase of 'other' taxa,

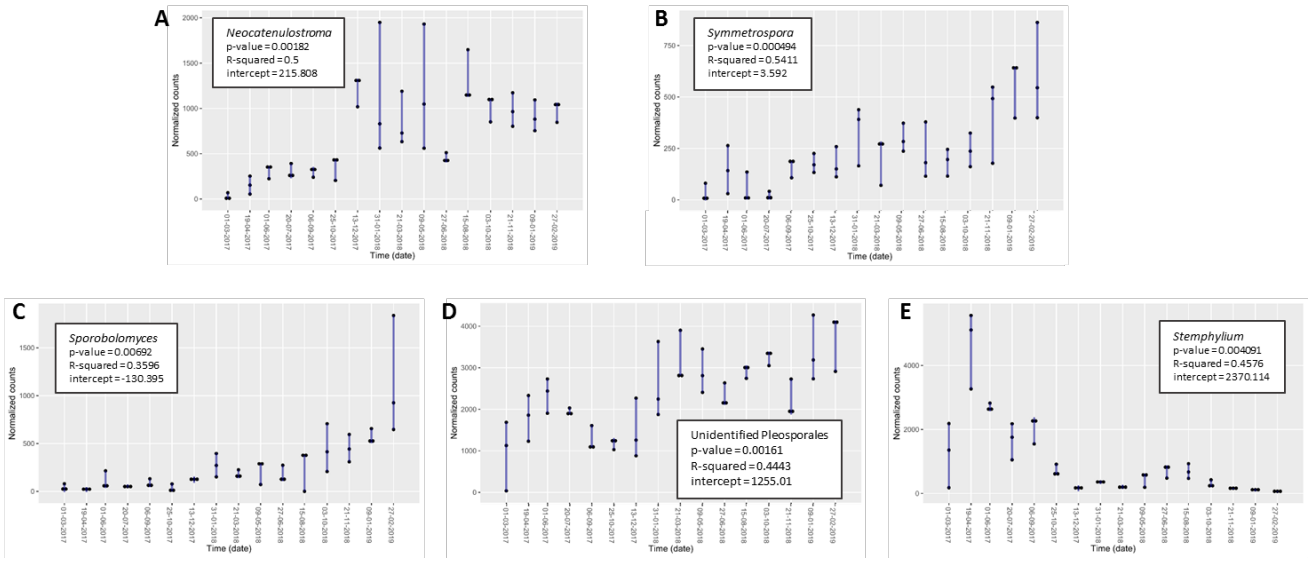

Figure III.4. Statistically significant positive (A,B,C,D) and negative (E) trends observed in fungal genera throughout time and calculated using Prais-Winsten estimation (p-value < 0.05). Reported P-values were calculated by applying the normalization of EdgeR package. R-squared and intercept values are also indicated. The black dots indicate the normalized abundance for each of the three replicates.

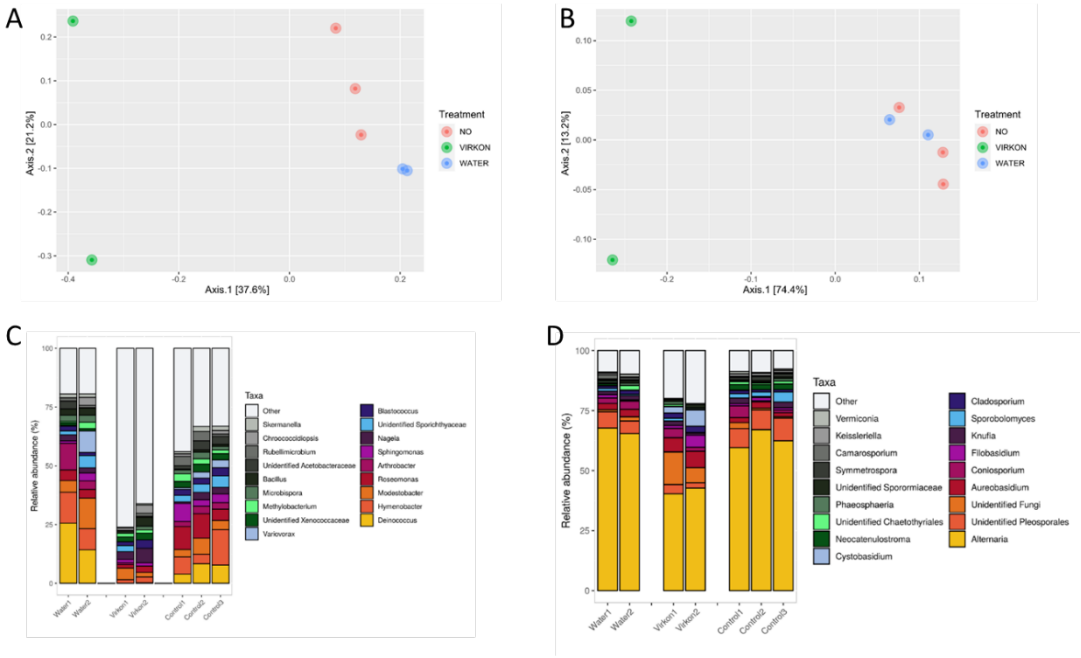

Figure III.5. PCoA (using Bray-Curtis dissimilarities and full data) showing the variations in bacterial (A) and fungal (B) communities on solar panel surfaces as a result of not washing the surfaces in a period of 24 months, or washing them with water/Virkon every seven weeks. Taxonomic analysis of the bacterial (C) and fungal (D) communities in the three different conditions (surfaces unwashed for two years or washed with Virkon/water).

which corresponded mainly to the phyla *Proteobacteria, Bacteroidetes, Firmicutes* and *Actinobacteria* (Figure III.5C). On the other hand, differences were also observed in the fungal communities of the Virkon-treated panels in comparison with the control treatments (Figure III.5B). Specifically, Virkon-treated surfaces displayed a decrease in general diversity, an increase in the relative abundance of *Cystobasidium* and *Filobasidium*, as well as a slight increase in the abundance of taxa assigned to 'other', which corresponded mainly to the phyla *Pleosporales, Dothideales, Capnodiales* and *Tremellales* (Figure III.5D). It is important to note

that the PCoA plots did not change substantially when only the most abundant 15 genera were used (data not shown). Regarding the effect on efficiency of cleaning the solar panels with water or Virkon, in general the produced voltage increased after cleaning, independently of the method used (Supplementary Figure III.5).

Discussion

Our results reveal that the microbial communities inhabiting solar panel surfaces change in time and experience seasonal variations. The microbial composition is characterized by a set of highly resistant bacterial genera (*Deinococcus, Hymenobacter, Roseomonas*) and fungi (*Alternaria*, among others), which are marginally present on the panels at the beginning of the experiment, but increase in frequency and become dominant by the end of the experiment. Some of the most abundant bacterial genera, such as *Hymenobacter, Modestobacter* and *Deinococcus*, have in fact previously been isolated from warm, irradiated environments, such as arid soil crusts or hyper-arid desert soils (Reddy and Garcia-Pichel, 2013; Busarakam et al., 2016; Gundlapally and Garcia-Pichel, 2017), and they have also been reported as frequent taxa inhabiting solar panel surfaces (Dorado-Morales et al., 2016; Tanner et al., 2018; Porcar et al., 2018). In fact, the microbial communities inhabiting solar panel surfaces around the world are similar in both functional and phylogenetic terms (Tanner et al., 2018; Porcar et al., 2018), suggesting the presence of not only common strong selective pressures (leading to functional similarity), but also of common structuring principles (leading to phylogenetic conservation) that include, among others, assembly history (the timing and order in which species arrive) and priority effects (the imprint of arrival order on community structure) (Carlström et al., 2019). Interestingly, *Deinococcus* and *Hymenobacter* have been proposed as biomarkers for desert airborne bacteria (Meola et al., 2015), indicating that a possible source of the solar panel microbiome could be the airborne transport of dust particles from deserts.

The most abundant bacterial taxa detected in this work (mean value throughout time) are consistent with those previously described to inhabit solar panel surfaces (Dorado-Morales et al., 2016; Tanner et al., 2018; Porcar et al., 2018) and other radiation-exposed environments, suggesting that the strong selection pressure imposed by solar radiation and other factors, such as desiccation, temperature or limited nutrient availability, is what shapes the microbial communities in these environments. For example, a previous study reported that concrete walls exposed to sunlight and ionizing radiation in Chernobyl proved to harbor similar communities to those present in a sun-exposed environment from a control area (without ionizing radiation), and these were dominated by *Actinobacteria*, *Deinococcales* and pigmented ascomycete fungi (Ragon et al., 2011). Similar communities, dominated by Acti*nobacteria, Cyanobacteria, Proteobacteria* and *Deinococcus-Thermus*, have also been detected on other stone surfaces around the world, including Roman stone ruins in North Africa (Louati et al., 2019) and historic Scottish monuments (Suihko et al., 2007).

During the first weeks of colonization, members of the genus *Sphingomonas* were among the first taxa whose abundance increased on solar panel surfaces, suggesting a crucial role of this taxa in the establishment of the subaerial biofilm. This is not the first time that *Sphingomonas* spp. has been described to initiate biofilm formation (Bereschenko et al., 2010), and its contribution to biofilm formation is largely associated to its ability to secrete exopolysaccharides (EPS) (Venugopalan et al., 2005). At a larger time-scale (24-months), the most abundant taxa detected on solar panel surfaces were *Modestobacter*, *Deinococcus*, *Sphingomonas*, *Hymenobacter*, *Rubellimicrobium* and *Methylobacterium*, several of which (*Deinococcus*, *Hymenobacter* and *Roseomonas*) displayed an increase in abundance throughout time. These genera are known to contain radiation-resistant (Su et al., 2014; Lee et al., 2017; Kim et al., 2018; Lim et al., 2019) and biofilm-forming (Kolari et al., 2002; Saarimaa et al., 2006; Simões et al., 2010) species, traits that could contribute to their success in this environment. In the case of *Methylobacterium* species, these have shown the ability to form biofilms, adhere to polystyrene surfaces and tolerate desiccation and low nutrient conditions (Kolari et al., 2002; Simões et al., 2010; Yano et al., 2013). On the other hand, *Deinococcus* has been found to adhere to paper

surfaces in industrial environments, acting as an intermediate for the adhesion of other bacteria (Kolari et al., 2002; Saarimaa et al., 2006). Thus, *Deinococcus* may play a role in both establishing and intermediating in the biofilm formation on solar panels. Furthermore, previous glass-adhesion experiments with strains isolated from solar panel surfaces revealed that species belonging to the genus *Arthrobacter*, *Methylobacterium*, *Deinococcus* and *Hymenobacter* displayed a high ability to colonize glass surfaces (Dorado-Morales et al., 2016).

The increase in abundance of several marker taxa is linked to the hypothesis that, after inoculation on the surface (i.e., via wind carrying desert soil, as suggested by the presence of *Deinococcus* and *Hymenobacter*), some of these taxa, namely those able to resist the extreme conditions inherent to solar panel surfaces, begin to form biofilm structures. In fact, high temperatures and poor nutrient conditions, as the ones that characterize solar panel surfaces, have been described to enhance biofilm formation (Yin et al., 2019), and these biofilms could in turn protect the microbial community from other environmental stressors. For example, in *Deinococcus geothermalis*, biofilm formation has been linked to an increased desiccation resistance, although it has also been linked to a decrease in UV resistance due to the photodissociation of water molecules retained in the EPS matrix, leading to increased ROS concentrations (Frösler et al., 2017). On the other hand, biofilm structures have also been described to protect against UV-radiation due to physical shading (Yin et al., 2019). Interestingly, several bacterial taxa displayed very similar profiles throughout time, suggesting an interdependence between these genera. Whether this dependence is nutritional (i.e., auxotrophic complementation), physical (protection through biofilm formation) or due to another cause remains unknown. A recent study by Carlström et al. (2019) on the assembly rules of phyllosphere microbiota revealed that, once established, an initial microbial community is relatively robust and difficult to perturb through the introduction of new species. Nevertheless, in this previous study, single-strain drop out experiments revealed the importance of key taxa in shaping community structures, mainly by affecting (either positively or negatively) strains with low abundance. In this sense, the initial weeks of colonization of solar panel surfaces are critical for the establishment of the final community, and the perturbation of certain strains due to seasonal/environmental variations could lead to the similar profiles observed for several bacterial taxa throughout time. In fact, Carlström et al. (2019) described predominantly (around 75%) inhibitory interactions among strains, although one of the two strains displaying positive interactions was found to be *Arthrobacter*, which we also detected in our experimental conditions, displaying a similar behaviour to *Blastococcus* (possibly due to a positive interaction).

In general, bacteria dominated the surface of the panels during the spring/summer period, whereas fungi were more abundant in autumn and winter, very likely linked to the moisture levels during the typically rainy autumn period and the relatively cool Mediterranean winter. Soiling has been reported to increase during low rainfall periods which, as well as affecting the performance of photovoltaic systems (Kimber et al., 2006), could also act as a nutrient source, leading to a larger accumulation of bacteria on the surfaces. On the other hand, fungi displayed an increase in richness and diversity in the autumn/winter period, which is consistent with several previous studies. For example, members of the genera *Alternaria*, *Cladosporium* and *Stemphylium*, among others, display increased ambient concentrations during high relative humidity periods (Llorente et al., 2012; Priyamvada et al., 2017). Furthermore, it has been shown that filamentous fungi can form biofilms when they grow on surfaces (Harding et al., 2009). Indeed, fungi are great candidates to live on surfaces as they secrete extracellular enzymes, they have an absorptive nutrition mode and they can easily invade surfaces due to the apical hyphal growth (Wessels, 1993). The most abundant taxa belonged to the genus *Alternaria*, consistent with the observation by Shirakawa et al. (2015), in which melanized *Ascomycetes* dominated the subaerial biofilms located on solar panel surfaces. The abundance of *Alternaria* on solar panel surfaces and other subaerial biofilms could be explained by the abundance within the species belonging to this genus of pathways for melanin biosynthesis, a pigment that confers protection against UV radiation and other environmental stressors (Kawamura et al., 1999;

Tseng et al., 2011). Interestingly, some bacterial colonizers displayed significant tendencies to decrease throughout time. For example, the genus *Lactobacillus*, not known to be radiation resistant, generally associated to the human microbiota and characterized by including facultative anaerobic or microaerophilic bacteria, tended to decrease during the 2-year experiment.

In our experimental conditions, seasonal fluctuations of solar panel efficiency (open circuit voltage) were observed, which we hypothesize are associated mainly to climatic conditions (specifically, reduced efficiency due to high temperatures, as previously reported) (Skoplaki and Palyvos, 2009; Omubo-Pepple et al., 2009) and, to a lesser extent, to soiling and/or biofilm formation (a slight increase in efficiency was observed after rinsing the solar panels periodically with either water or Virkon). Nevertheless, although the use of water or Virkon yielded a similar increase in efficiency, the microbial community after each of those treatment was different. Specifically, the surfaces treated with water displayed a similar microbial composition than the untreated plates, whereas the ones treated with Virkon suffered from changes such as a clear decrease of the genus *Deinococcus*, which was not detected after cleaning the surfaces with water. On the other hand, the fact that the water-treated surfaces were similar, in taxonomic terms, to the untreated surfaces could provide an explanation regarding the stability throughout time of the solar panel microbiome: although rainfall (cleaning with water being a proxy of this) reduces soiling, is not enough to disrupt the microbial community inhabiting solar panel surfaces. Our results thus indicate that chemical agents can strongly modify the microbial composition of the panels, but do not seem to have an important effect on electric production, which is largely dependent on non-biological factors such as dust accumulation and temperature fluctuations.

Taking into account these results, we hypothesize that solar panel surfaces are colonized by microorganisms that arrive through the deposition of soil and dust particles transported via wind. Then, in a very short time period, the microorganisms able to resist radiation and desiccation are selected by the environment and form robust biofilm structures. These biofilms then support the accumulation of other, lesser-abundant organisms, leading to a stable community that is not altered by rainfall and, therefore, is robust throughout time.

This is the first work specifically designed to study, at a large scale and throughout a 2-year time period, the colonization process of solar panel surfaces, focusing on both the fungal and bacterial communities. The most abundant bacterial genera detected (*Modestobacter, Deinococcus, Sphingomonas, Hymenobacter* and *Rubellimicrobium*) and the most abundant fungal genera (*Alternaria*, among others) are consistent with previous studies on solar panel microbiomes. Our results allow us to conclude that the presence of such taxa on solar panels is not the result of their mere accumulation from the surrounding environment, but corresponds to the final step of an ecological succession, in the frame of which extremophilic taxa adapted to the harsh conditions of solar panels are selected. Indeed, a significant increase of solar panel-adapted genera such as *Deinococcus, Hymenobacter, Roseomonas* and *Neocatenulostroma*) as well as the decrease of non-resistant, ubiquitous taxa (*Lactobacillus* or *Stemphyllium*) was recorded throughout the experiment. Nevertheless, this accumulation of microorganisms is not linked to a significant reduction in photovoltaic efficiency, which exhibits a seasonal variation and that is not improved by antiseptic compounds. It can be concluded that the microbial community is clearly modified by such compounds but that this fact is not linked to a clear benefit in terms of enhanced electric efficiency, at least under the Mediterranean conditions of our study.

Experimental procedures

Small-scale solar farm construction

For this work, a small-scale solar farm was built using 54 small-sized solar panels (SOLARPOWER 5W-12V, Xunzel Soluciones S.L., Mendaro-Guipuzcoa, Spain) mounted on an aluminium frame designed *ad hoc* by the ICMUV Institute (Valencia, Spain; Figure III.6A). The surfaces of the panels were sterilized on-site by cleaning them with 70% ethanol. Then, they were placed in the metallic structure (Figure III.6B), which had previously been placed on the roof of one of the

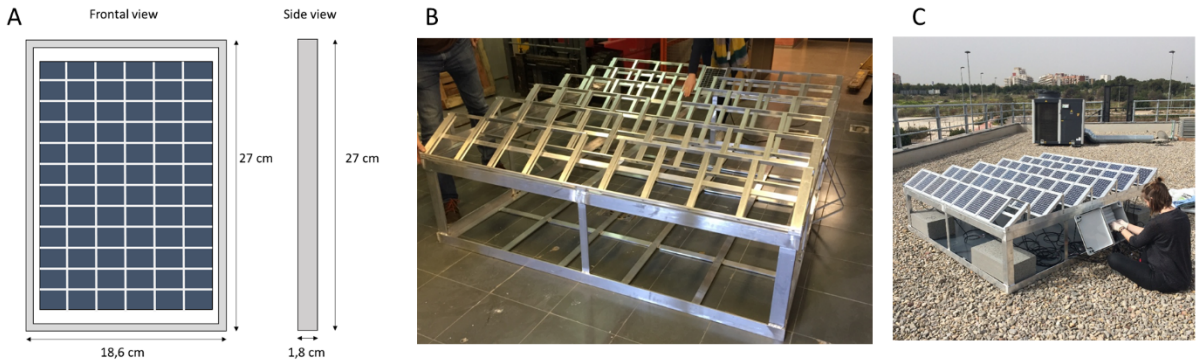

Figure III.6. Experimental set-up: 54 small-sized solar panels (A) were set up on an aluminum chassis (B) and placed on the rooftop of a building in the Scientific Park of the University of Valencia in Paterna, Spain (C).

buildings belonging to the Scientific Park of the University of Valencia (39°30'56.0"N 0°25'28.4"W) in an equator-facing position (Figure III.6C). Furthermore, all the solar panels were electrically connected to two connection boxes placed at either side of the structure and that were sealed in order to avoid the entrance of water or environmental particles. Once a week (except on cloudy days), and for a period of two years, the efficiency of each solar panel was measured twice and both values were recorded.

Solar panel sampling

Throughout the two-year time period, the surfaces of four of the solar panels were subjected to a treatment with either a disinfectant or water, with the goal of comparing, at the end of the experiment, the microbial taxonomy of both groups. Every seven weeks, two solar panel surfaces were soaked in sterile distilled water for 10 min, and another two were soaked in a solution of Rely + On Virkon disinfectant at 10 g l−1, the working concentration recommended by the manufacturers (DuPont, Michigan, USA) for 10 min, followed by a rinse with sterile distilled water. After cleaning, these solar panels were left to dry in the sun for 10 min and then placed again in the metal structure. At the end of the 2-year period, these four solar panels were sampled together with the final three (uncleaned during 2 years).

Additionally, every seven weeks, three solar panels were randomly selected and sampled. The selected solar panels were removed from the metallic frame, placed in sterile bags and transported to the laboratory. Then, the panels were placed in a laminar flow hood and the surfaces were washed with sterile phosphate-buffered saline (PBS) using a sterile window cleaner. The resulting liquid was concentrated into a pellet by centrifugation, and all pellets were frozen at −20°C until required.

DNA extraction, sequencing and bioinformatic analysis

All DNA extractions were performed using the Power Soil DNA isolation kit (MO BIO Laboratories, Carlsbad, CA, USA), and the resulting DNA was quantified using the QUBIT dsDNA HS-high sensitivity kit (Invitrogen, CA, USA). NextSeq Illumina libraries were constructed, targeting the hypervariable V3 and V4 regions of the 16S gene (Forward = 5' TCGTCGGCAGCGTCAGATGTGTATAAGAGACAGCC TACGGGNGGCWGCAG; Reverse = 5' GTCTCGTGGGCTCGGAGATGTGTATAAGAGACAGG ACTACHVGGGTATCTAATCC) and targeting the ITS region (Forward = 5'CTTGGTCATTTAGAGGAAGTAA3'; Reverse = 5'GCTGCGTTCTTCATCGATGC3'). Then, Illumina sequencing adaptors and dual-index barcodes (Nextera XT index kit v2, FC-131-2001) were added, and libraries were normalized and pooled. The pools were loaded onto the MiSeq reagent cartridge v3 (MS-102-3003), spiked with 10% PhiX control and sequencing was conducted using paired-ends on an Illumina MiSeq sequencing system. Rarefaction curves were saturated for all samples, indicating that sequencing was deep enough to assess all microbial diversity (Supplementary Figure III.6). Mean values of 36 533 and 52 192 sequences were obtained for the 16S gene and the ITS region, respectively, with a

minimum of 9669 and a maximum of 61 764 sequences for the 16S gene, and a minimum of 25 640 and a maximum of 68 942 sequences for the ITS region.

Raw Illumina sequences were analysed using Qiime2 (Boylen et al., 2019). Briefly, the quality of the reads was assessed with the Demux plugin, and the sequences subsequently corrected and trimmed via Dada2. The taxonomy of each sequence variant was assigned employing the classify-Sklearn module from the feature-classifier plugin. GreenGenes (v. 13.8.99) and uniite (v. 7_99_01.12.2017) were used as reference databases for 16S rRNA and ITS taxonomic assignment respectively. For the time-series analysis, taxonomy was collapsed into the genus level. For each sampling time and genus, an average of the three replicates sequence count was calculated. The web application TIME (Temporal Insights into Microbial Ecology) was used to analyse and represent the temporal distributions of the taxonomic profiles (Baksi et al., 2018), dividing the time period in four seasons: spring (21 March to 20 June), summer (21 June to 20 September), autumn (21 September to 20 December) and winter (21 December to 20 March).

The 15 most abundant genera were selected in order to study their temporary trends. Average sequence counts were calculated for each sampling time, and Prais–Winsten estimation was carried out for each genus using the 'Prais' R package. This linear model was applied for its ability to handle autocorrelation, which is usually found in time-series data. Regressions were calculated using three approaches: with the raw abundance data, normalizing the data through rarefaction with respect to the sample with the lowest sequencing depth and applying the normalization of EdgeR package. All three approaches yielded the same result, and the P-values indicated in Figures III.3 and III.4 were calculated with the edgeR approach. In all the statistically significant tendencies observed for bacteria and fungi, independently of the approach used, the P-value was below 0.05.

Acknowledgements

Financial support from the Spanish Government (grant Helios. reference: BIO2015-66960-C3-1-R co-financed by FEDER funds and Ministerio de Economía y Competitividad) and from the European CSA on biological standardization BIOROBOOST (EU grant number 820699) are acknowledged. KT is a recipient of a Doctorado Industrial fellowship from the Ministerio de Ciencia, Innovación y Universidades (Spain), with reference DI-16-08976. AL is a recipient of a Doctorado Industrial fellowship from the Ministerio de Ciencia, Innovación y Universidades (Spain), with reference DI-17-09613. EMM is funded with a Formación de Profesorado Universitario (FPU) grant from the Spanish Government (Ministerio de Ciencia, Innovación y Universidades), with reference FPU17/04184. AVV is funded with a Formación de Profesorado Universitario (FPU) grant from the Spanish Government (Ministerio de Ciencia, Innovación y Universidades), with reference FPU18/02578. CV is a recipient of a Torres Quevedo fellowship from the Ministerio de Ciencia, Innovación y Universidades (Spain), with reference PTQ-16-08227. MP is indebted to Wim Mertens for life-long musical support. We would like to thank Julian Heredero and Joaquin Baixeras for their help in setting up the solar farm.

Conflict of interest

The authors declare no conflict of interest.

References

Baksi, K.D., Kuntal, B.K., and Mande, S.S. (2018) 'TIME': A Web Application for Obtaining Insights into Microbial Ecology Using Longitudinal Microbiome Data. Front Microbiol 9: 36.

Bereschenko, L.A., Stams, A.J.M., Euverink, G.J.W., and van Loosdrecht, M.C.M. (2010) Biofilm formation on reverse osmosis membranes is initiated and dominated by Sphingomonas spp. Appl Environ Microbiol 76(8): 2623-2632.

Blanco, Y., Rivas, L.A., González-Toril, E., Ruiz-Bermejo, M., Moreno-Paz, M., Parro, V., et al. (2019) Environmental parameters, and not phylogeny, determine the composition of extracellular substances in microbial mats from extreme environments. Sci Total Environ 650(1): 384-393.

Boylen, E., Rideout, J., Dillon, M., Bokulich, N., Abnet, C., Al-Ghalith, G., et al. (2019). Reproducible, interactive, scalable and extensible microbiome data science using QIIME 2. Nat Biotechnol 37(8): doi: 10.1038/s41587-019-0209-9.

Busarakam, K., Bull, A.T., Trujillo, M.E., Riesco, R., Sangal, V., van Wezel, G.P., and Goodfellow, M. (2016) *Modestobacter caceresii* sp. nov., novel actinobacteria with an insight into their adaptive mechanisms for survival in extreme hyper-arid Atacama Desert soils. Syst Appl Microbiol 39(4): 243-251.

Carlström, C.I., Field, C.M., Bortfeld-Miller, M., Müller, B., Sunagawa, S., and Vorhold, J.A. (2019) Synthetic microbiota reveal priority effects and keystone strains in the *Arabidopsis* phyllosphere. Nat Ecol Evol 3: 1445-1454.

Cordero, R.R., Damiani, A., Laroze, D., MacDonell, S., Jorquera, J., Sepúlveda, E., et al. (2018) Effects of soiling on photovoltaic (PV) modules in the Atacama Desert. Sci Rep 8: 13943.

Dorado-Morales, P., Vilanova, C., Peretó, J., Codoñer, F.M., Ramón, D., and Porcar, M. (2016) A highly diverse, desert-like microbial biocenosis on solar panels in a Mediterranean city. Sci Rep 6: 29235.

Flemming, H., Wingender, J., Szewzyk, U., Steinberg, P., Rice, S.A., and Kjelleberg, S. (2016) Biofilms: an emergent form of bacterial life. Nat Rev Microbiol 14: 563-575.

Frösler, J., Panitz, C., Wingender, J., Flemming, H., and Rettberg, P. (2017) Survival of *Deinococcus geothermalis* in biofilms under desiccation and simulated space and Martial conditions. Astrobiology 17(5): 431-447.

Gabani, P. and Singh, O.V. (2013) Radiation-resistant extremophiles and their potential in biotechnology and therapeutics. Appl Microbiol Biotechnol 97(3): 993-1004.

Gundlapally, S.R. and Garcia-Pichel, F. (2017) Description of *Deinococcus oregonensis* sp. nov., from biological soil crusts in the Southwestern arid lands of the United States of America. Arch Microbiol 199(1): 69-76.

Harding, M.W., Marques, L.L.R., Howard, R.J., and Olson, M.E. (2009) Can filamentous fungi form biofilms? Trends Microbiol 17(11): 475-480.

Kawamura, C., Tsujimoto, T., and Tsuge, T. (1999) Targeted disruption of a melanin biosynthesis gene affects conidial development and UV tolerance in the Japanese pear pathotype of *Alternaria alternata*. Mol Plant Microbe Interac 12(1): 59-63.

Kim, J.Y., Kim, D.U., Kang, M.S., Jang, J.H., Kim, S.J., Kim, M.J., et al. (2018) *Roseomonas radiodurans* sp. nov., a gamma-radiation-resistant bacterium isolated from gamma ray-irradiated soil. Int J Syst Evol Microbiol 68(8): 2443-2447.

Kimber, A., Mitchell, L., Nogradi, S., and Wenger, H. (2006) The effect of soiling on large grid-connected photovoltaic systems in California and the southwest region of the United States. IEEE 4th World Conference on Photovoltaic Energy Conversion, Waikoloa.

Kolari, M., Schmidt, U., Kuismanen, E., and Salkinoja-Salonen, M.S. (2002) Firm but slippery attachment of *Deinococcus geothermalis*. J Bacteriol 184(9): 2473-2480.

Lee, J.J., Park, S.J., Lee, Y.H., Lee, S.Y., Ten, L.N., and Jung, H.Y. (2017) *Hymenobacter aquaticus* sp. nov., a radiation-resistant bacterium isolated from a river. Int J Syst Evol Microbiol 67: 1206-1211.

Li, S., Hua, Z., Huang, L., Li, J., Shi, S., Chen, L., et al. (2014) Microbial communities evolve faster in extreme environments. Sci Rep 4: 6205.

Lim, S., Jung, J.H., Blanchard, L., and de Groot, A. (2019) Conservation and diversity of radiation and oxidative stress resistance mechanisms in *Deinococcus* species. FEMS Microbiol Rev 43(1): 19-52.

Llorente, I., Moragrega, C., Ruz, L., and Montesinos, E. (2012) An update on control of brown spot of pear. Trees (Berl West) 26(1): 239-245.

Louati, M., Ennis, N.J., Ghodhbane-Gtari, F., Hezbri, K., Sevigny, J.L., Fahnestock, M.F., et al. (2019) Elucidating the ecological networks in stone-dwelling microbiomes. Environ Microbiol: doi: 10.1111/1462-2920.14700

Lynn, J.R. and Rocco, L.M. (2001) Life in extreme environments. Nature 409: 1092-1101.

Omubo-Pepple, V.B., Israel-Cookey, C., and Alaminokuma, G.I. (2009) Effects of temperature, solar flux and relative humidity on the efficient conversión of solar energy to electricity. Eur J Sci Res 35(2): 173-180.

Porcar, M., Louie, K.B., Kosina, S.M., Van Goethem, M.W., Bowen, B.P., Tanner, K., and Northen, T.R. (2018) Microbial ecology on solar panels in Berkeley, CA, United States. Front Microbiol 9: 3043.

Priyamvada, H., Singh, R.K., Akila, M., Ravikrishna, R., Verma, R.S., and Gunthe, S.S. (2017) Seasonal variation of the dominant allergenic fungal aerosols – One year study from southern Indian region. Sci Rep 7: 11171.

Meola, M., Lazzaro, A., and Zeyer, J. (2015) Bacterial composition and survival on Sahara dust particles transported to the European Alps. Front Microbiol 6: 1454.

Ragon, M., Restoux, G., Moreira, D., Moller, A.P., and López-García, P. (2011) Sunlight-exposed biofilm microbial communities are natural resistant to Chernobyl ionizing-radiation levels. PLoS One 6(7): e21764.

Reddy, G.S.N. and Garcia-Pichel, F. (2013) Description of *Hymenobacter arizonensis* sp. nov. from the southwestern arid lands of the United States of America. Antonie van Leeuwenhoek 103(2): 321-330.

Saarimaa, C., Perolta, M., Raulio, M., Neu, T.R., Salkinoja-Salonen, M.S., and Neubauer, P. (2006) Characterization of adhesión threads of *Deinococcus geothermalis* as Type IV pili. J Bacteriol 188(19): 7016-7021.

Sayed, A.M., Hassan, M.H.A., Alhadrami, H.A., Hassan, H.M., Goodfellow, M., and Rateb, M.E. (2019) Extreme environments: microbiology leading to specialized metabolites. J Appl Microbiol: doi: 10.1111/jam.14386.

Shirakawa, M.A., Zilles, R., Mocelin, A., Gaylarde, C.C., Gorbushina, A., Heidrich, G., et al. (2015) Microbial colonization affects the efficiency of photovoltaic panels in a tropical environment. J Environ Manage 157: 160-167.

Simões, L.C., Simões, M., and Vieira, M.J. (2010) Adhesion and biofilm formation on polystyrene by drinking water-isolated bacteria. Antonie van Leeuwenhoek 98: 317

Singh, O.V. and Gabani, P. (2011) Extremophiles: radiation resistance microbial reserves and therapeutic implications. J Appl Microbiol. 110: 851-861.

Skoplaki, E. and Palyvos, J.A. (2009) On the temperature dependence of photovoltaic module electrical performance: A review of efficiency/power correlations. Solar Energy 83: 614-624.

Su, S., Chen, M., Teng, C., Jiang, S., Zhang, C., Lin, M., and Zhang, W. (2014) *Hymenobacter kanuolensis* sp. nov., a novel radiation-resistant bacterium. Int J Syst Evol Microbiol 64: 2108-2112.

Suihko, M., Alakomi, H., Gorbushina, A., Fortune, I., Marquardt, J., and Saarela, M. (2007) Characterization of aerobic bacterial and fungal microbiota on surfaces of historic Scottish monuments. Syst Appl Microbiol 30(6): 494-508.

Tanner, K., Martí, J.M., Belliure, J., Fernández-Méndez, M., Molina-Menor, E., Peretó, J., and Porcar, M. (2018) Polar solar panels: Arctic and Antarctic microbiomes display similar taxonomic profiles. Environ Microbiol Rep. 10(1): 75-59.

Tseng, M.N., Chung, P.C. and Tzean, S.S. (2011) Enhancing the stress tolerance and virulence of an entomopathogen by metabolic engineering of dihydroxynaphthalene melanin biosynthesis genes. Appl Environ Microbiol 77(13): 4508-4519.

Venugopalan, V.P., Kuehn, M., Hausner, M., Springael, D., Wilderer, P.A., and Wuertz, S. (2005) Architecture of a nascent *Sphingomonas* sp. Biofilm under varied hydrodynamic conditions. Appl Environ Microbiol 71(5): 2677-2686.

Wessels, J.G.H. (1993) Tansley review no. 45 – wall growth, protein excretion and morphogenesis in fungi. New Phytol 123(3): 397–413.

Yano, T., Kuboota, H., Hanai, J., Hitomi, J., and Tokuda, H. (2013) Stress tolerance of *Methylobacterium* biofilms in bathrooms. Microbes Environ 28(1): 87-95.

Yin, W., Wang, Y., Liu, L., and He, J. (2019) Biofilms: The microbial "protective clothing" in extreme environments. Int J Mol Sci 20(14): 3423.

Chapter II. Bioprospecting the solar panel microbiome: a source of antioxidant bacteria and new bacterial species

Publication IV. **Tanner K**, Martorell P, Genovés S, Ramón D, Zacarías L, Rodrigo MJ, Peretó J and Porcar M (2019). Bioprospecting the solar panel microbiome: high-throughput screening for antioxidant bacteria in a *Caenorhabditis elegans* model. Frontiers in Microbiology 10: 986.

Publication V. **Tanner K**, Mancuso CP, Peretó J, Khalil AS, Vilanova C and Pascual J (2020). *Sphingomonas solaris* sp. nov., isolated from a solar panel in Boston, Massachusetts. International Journal of Systematic and Evolutionary Microbiology. doi: 10.1099/ijsem.0.003977

Original publication reprints can be found in Appendix A.

Supplementary figures can be found in Appendix B.

Publication IV

Bioprospecting the solar panel microbiome: high-throughput screening for antioxidant bacteria in a *Caenorhabditis elegans* model

Kristie Tanner[1], Patricia Martorell[2], Salvador Genovés[2], Daniel Ramón[2], Lorenzo Zacarías[3], María Jesús Rodrigo[3], Juli Peretó[1,4,5], and Manuel Porcar[1,4]

[1] Darwin Bioprospecting Excellence S.L., Parc Científic de la Universitat de València, Paterna, Spain

[2] ADM Biopolis S.L., Paterna, Spain

[3] Instituto de Agroquímica y Tecnología de Alimentos (IATA-CSIC), Paterna, Spain

[4] Institute for Integrative Systems Biology (I2SysBio, University of Valencia-CSIC), Paterna, Spain

[5] Department of Biochemistry and Molecular Biology, University of Valencia, Burjassot, Spain

Abstract

Microbial communities that are exposed to sunlight typically share a series of adaptations to deal with the radiation they are exposed to, including efficient DNA repair systems, pigment production and protection against oxidative stress, which makes these environments good candidates for the search of novel antioxidant microorganisms. In this research project, we isolated potential antioxidant pigmented bacteria from a dry and highly-irradiated extreme environment: solar panels. High-throughput in vivo assays using *Caenorhabditis elegans* as an experimental model demonstrated the high antioxidant and ultraviolet-protection properties of these bacterial isolates that proved to be rich in carotenoids. Our results suggest that solar panels harbor a microbial community that includes strains with potential applications as antioxidants.

Introduction

Antioxidants are molecules that can protect cells against oxidative stress. For example, they can play a protective role against the biological damage derived from an excessive cellular production of reactive oxygen species (ROS). ROS are unstable metabolites of molecular oxygen (i.e., superoxide radical, hydroxyl radical, or hydrogen peroxide) that are constantly generated in the cells as by-products of normal aerobic metabolism, but whose levels can increase under certain stress situations (for example, alcohol consumption, smoking, or exposure to environmental pollutants) and become harmful for the cell (Al-Gubory, 2014; Rahal et al., 2014; Zorov et al., 2014; Chen et al., 2015). In humans, chronic oxidative stress has been associated on many occasions with the initiation and progression of a variety of diseases, including Alzheimer's and cardiovascular diseases (such as hypertension and atherosclerosis) or cancer (Chen and Zhong, 2014; Milkovic et al., 2014; Dandekar et al., 2015; Siti et al., 2015).

The discovery of new antioxidants from natural sources (i.e., plants or microorganisms) is of high interest for the pharmacological and food industries (Finley et al., 2011; Lin et al., 2014). The search for novel natural molecules with biotechnological applications is known as bioprospecting and, in the past, microorganisms have proved to be rich sources of natural products that have been used for the fabrication of commercial products (antibiotics, probiotics, sustainable agriculture, fermentation processes, etc.) with a wide range of applications (Mahajan and Balachandran, 2012; Kanchiswamy et al., 2015; Katz and Baltz, 2016; Choudhary et al., 2017; Gupta and Bajaj, 2017). Microorganisms living in harsh environments typically exhibit strategies to cope with the environmental stresses

they are exposed to. In the case of microbial communities exposed to sunlight (i.e., to radiation and desiccation), these adaptations include efficient DNA repair systems, pigment production and protection from oxidative stress (Lebre et al., 2017), suggesting that highly-irradiated environments may be good sources of novel antioxidant-producing microorganisms. In fact, tolerances to desiccation and radiation are mechanistically correlated (Mattimore and Battista, 1996; Ragon et al., 2011; Slade and Radman, 2011), particularly through protection strategies against protein oxidation (Fredrickson et al., 2008; Fagliarone et al., 2017). For these reasons, in the present research we selected a highly-irradiated environment as a potential source of antioxidant-producing microorganisms: solar panels. Solar panels are man-made structures that are exposed to desiccation and high amounts of solar radiation. These harsh conditions shape the surface-inhabiting microbiome toward a highly diverse microbial community with many drought-, heat-, and radiation-resistant bacteria (Dorado-Morales et al., 2016; Porcar et al., 2018; Tanner et al., 2018a). The cultivable microorganisms isolated from solar panels typically display red, orange, or yellow pigmentation, which is assumed to be linked to the production of carotenoids (CRTs), natural pigments that may play a role in the protection of these microorganisms against harmful ionizing radiation and oxidative stress (Britton, 1995; Sandmann, 2015; Dorado-Morales et al., 2016).

Taking into account the need of screening a large number of pigment-producing bacteria isolated from the solar panels, *Caenorhabditis elegans* was chosen as an experimental organism, as it is suitable for these high-throughput screenings. *C. elegans* is a nematode which has previously been used for testing potential antioxidant compounds such as selenite (Li et al., 2014), cocoa products (Martorell et al., 2013), tyrosol (Cañuelo et al., 2012), or CRTs such as astaxanthin (Yazaki et al., 2011) or β-carotene (Lashmanova et al., 2015). The use of *C. elegans* as an experimental model has many advantages, such as the low cost, simplicity, and quickness of the methods. Nevertheless, there is one more advantage that is of particular interest in this study: the fact that this nematode is naturally a bacteria eater, worms can directly be fed with selected bacterial strains. Laboratory *C. elegans* have a basal diet of *Escherichia coli*, but it is possible to supplement the growth medium with many ingredients of interest, including other bacteria, in order to analyze their biological activity. This functional screening method has previously been used in order to identify new antioxidant probiotic strains, such as *Lactobacillus rhamnosus* CNCM I-3690 strain (Grompone et al., 2012) or *Bifidobacterium animalis* subsp. *lactis* CECT 8145 strain (Martorell et al., 2016).

The research we present here aimed at establishing a collection of pigmented bacteria isolated from solar panels in order to select those with promising biological activities as antioxidants. For this, bacterial isolates with no record of opportunistic infections were subjected to a high-throughput antioxidant screening in *C. elegans* using the tracking device WMicrotracker-One™ (PhylumTech, Santa Fé, Argentina), which uses photo-beam interruptions to assess movement of nematodes in multi-well plates. Specifically, the WMicrotracker-One™ (WT) device was used to quantify the survival of the worms after the addition of hydrogen peroxide to the medium. Isolates with the highest antioxidant activity were then selected for further characterization through oxidative stress and UV-protection assays. Finally, a preliminary identification of the CRTs from the selected isolates was performed. This is the first study focused on bioprospecting the solar panel microbiome aiming at obtaining microorganisms with high potential as antioxidants.

Materials and Methods

Sampling

Samples were collected from six solar panels located on the rooftop of the Faculty of Economics of the University of Valencia on the 30th November 2015. Sampling was performed by washing the solar panels with sterile Phosphate-Buffered Saline (PBS) and by scraping the surface with sterile glass wipers as previously described (Dorado-Morales et al., 2016). The resulting liquid was collected using sterile pipettes and stored in 50 mL Falcon tubes, which were then transported

to the laboratory on ice, where cultivation, isolation, and identification of the strains was performed.

Cultivation and Isolation of Pigmented Bacterial Strains

Solar panel samples were cultivated on Luria-Bertani medium (LB), Reasoner's 2A (R2A) agar (Reasoner and Geldereich, 1985), and Marine Agar (MA) medium, by spreading 50 µL of the collected liquid to each plate. Then, samples were left to settle for 30 min, allowing the larger sized particles – including many fungi – to sediment, and 50 µL of the supernatant were plated on LB, R2A agar, and MA. By allowing the samples to settle, fungal growth was reduced when cultivating the samples on the different culture media. Plates were incubated at room temperature for 1 week and, after incubation, individual colonies were selected and isolated in pure culture by re-streaking on fresh medium. Morphological characteristics of the colonies (color, texture, and size) were taken into account in order to isolate as many different microorganisms as possible. The pure isolates were conserved at -80°C in 20% glycerol for future use.

16S rDNA Sequencing

For 16S rDNA sequencing, a 500-bp fragment of the hypervariable region V1-V3 of the isolates was amplified by colony PCR, using universal primers 28F (5'-GAG TTT GAT CNT GGC TCA G-3') and 519R (5'-GTN TTA CNG CGG CKG CTG-3'). Isolates whose 16S rDNA failed to amplify from colony templates were amplified again with the same PCR program plus an initial step of incubation for 10 min at 100°C. Amplicons were checked in 1.4% agarose gel and then precipitated overnight in isopropanol 1:1 (vol:vol) and potassium acetate 3 M pH 5 1:10 (vol:vol). Precipitated DNA was washed with 70% ethanol, resuspended in Milli-Q water (Merck Millipore Ltd, Tullagreen, Cork, Ireland) and quantified with a Nanodrop-1000 Spectrophotometer (Thermo Fisher Scientific, Wilmington, DE, United States). Amplicons were tagged using BigDye®Terminator v3.1 Cycle Sequencing Kit (Applied Biosystems, Carlsbad, CA, United States) and sequenced with the Sanger method by the Sequencing Service (SCSIE) of the University of Valencia (Spain). The resulting sequences were manually edited using Pregap4 (Staden Package, 2002) to eliminate low-quality base calls. The EzBioCloud online tool (Yoon et al., 2017) was used to determine the closest neighbor with valid name for each isolate. The partial 16S rDNA sequence of the isolates was deposited in the GenBank/EMBL/DDBJ databases, under accession numbers MK621939-MK622006.

Oxidative Stress Assays With Worm Tracker

Experiments were carried out with the wild-type *C. elegans* strain N2 (Bristol), which was routinely propagated at 20°C on Nematode Growth Medium (NGM) plates supplemented with *E. coli* strain OP50 as the regular food source. Worms were synchronized by isolating eggs from gravid adults at 20°C. Synchronization was performed on NGM plates with *E. coli* OP50 as a negative control, *E. coli* OP50 plus vitamin C (vitC) at 20 µg/mL as a positive control (Supplementary Figure IV.2A), or *E. coli* OP50 plus the pigmented isolates in order to test antioxidant properties of the bacteria. The isolates were grown overnight in liquid LB medium at 28°C and 180 rpm, optical density at 600 nm (OD_{600}) was adjusted to 30 and to 60, and 50 µL of the bacterial suspension was added to the plates. The synchronized worms were incubated for a total of 3 days on the previously described plates, until reaching young adult stage.

Young adult worms were collected and washed three times with M9 buffer, and finally resuspended in 100–200 µL of the buffer. Worms were then transferred by pipetting to 96-well plates (10–30 worms per well) containing M9 buffer. After transferring all the worms, hydrogen peroxide was added to the wells, reaching a final concentration of 1.2 mM of hydrogen peroxide (Supplementary Figure IV.2B). Mobility of the worms was measured with the WT device during 60 min (four measurements of 15 min). This device detects the movement of organisms through the interference they cause in an array of microbeams of infrared light (patented technology, #US12515723, EP208640881). In this experiment, data was collected in the form of "worm activity" (or relative locomotive activity), and was normalized by the number of worms in each well. All assays were performed with two biological replicates.

Manual Oxidative Stress Assays

Manual assays were also carried out with the wild-type *C. elegans* strain N2 (Bristol), routinely propagated and synchronized as previously described (on NGM with *E. coli* OP50 as a negative control, and supplemented with pigmented isolates at an OD_{600} of 30 for biological assays), except for the positive control, which in this case was vitC at 10 µg/mL. Young adult worms were transferred to fresh plates once every 2 days, until reaching 5-day adult stage. Then, these worms were transferred to plates containing basal medium supplemented with 2 mM hydrogen peroxide and incubated for 5 h at 20°C. After incubation, the survival rate of the worms for each condition (negative control, positive control and fed with pigmented bacteria) was calculated by manually assessing survival of the worms. Two biological replicates were performed for every condition.

UV-Protection Assays

Wild-type *C. elegans* strain N2 (Bristol) worms were synchronized on NGM plates with *E. coli* OP50 as a negative control, *E. coli* OP50 plus vitC (0.1 µg/mL) or plus chlorogenic acid (CGA) (0.1 µg/mL) as positive controls, or *E. coli* OP50 plus the pigmented isolates (50 µL of an over-night culture adjusted to OD 30) in order to test the UV light protection properties of the bacteria.

Synchronized worms were propagated for 15 days on the different types of medium, irradiated daily for 45 s in the laminar flow hood with UV light and transferred to new medium every 2 days, as previously described (Iriondo-DeHond et al., 2016). Survival rate of the worms was manually recorded every day and the assay was performed with biological duplicates.

Pigment Extraction

Carotenoid extraction was performed with two types of bacterial cultures: grown on solid (S) and in liquid (L) medium for 1 week and 12 h (overnight), respectively. For CRTs extraction from isolates grown on solid medium, bacterial cells were collected from solid LB medium after 1 week of incubation at room temperature. Cells were resuspended in PBS and concentrated through centrifugation at 13000 rpm for 3 min. The supernatant was discarded and pellets were dried completely with a vacuum-connected centrifuge (DNA Speed Vac, DNA120, Savant). Then, dry weight was determined. For the exponential phase samples, overnight cultures of selected isolates were collected and the wet weight was determined for each sample.

Bacterial pellets were resuspended and washed in Tris-Buffered Saline (TBS) solution, and centrifuged. Pelleted cells were frozen in liquid nitrogen (N_2) three times, followed by addition of methanol (Sharlau, HPLC grade) (ten times the volume of the pellet) and sonication in a XUBA3 ultrasonic water bath (35 W; Grant Instruments, Cambridge, United Kingdom) for 5 min, in order to break the bacterial cells. Samples were vigorously shaken and centrifuged, and then the upper layer of colored methanol was transferred to a clean tube. This step was performed several times until a non-colored pellet was obtained.

Dicloromethane (HPLC grade) and water (Milli Q grade) (both at ten times the volume of the original pellet) were added to the methanol extract in order to separate organic and aqueous phases. Samples were vigorously shaken, centrifuged, and the aqueous phase was discarded. This step was performed twice, finally yielding CRT extracts in dicloromethane. Samples were then dried under N_2 and kept at -20°C until analysis by HPLC-PDA. All steps were performed under dim light to avoid CRTs modifications such as photodegradation, isomerizations or structural changes.

HPLC-PDA Analysis

Carotenoid composition of each sample was analyzed by using an HPLC with a Waters liquid chromatography system (Waters, Barcelona, Spain) equipped with a 600E pump and a 2998 photodiode array detector (PDA). Empower software (Waters, Barcelona, Spain) was used for HPLC program set up and chromatogram analysis. A C_{30} CRT column (250 mm × 4.6 mm, 5 µm) coupled to a C_{30} guard column (20 mm × 4.0 mm, 5 µm) (YMC GmbH, Germany) was used. Samples were prepared for HPLC analysis by dissolving the CRT extracts in $CHCl_3$:MeOH:acetone (3:2:1, v:v:v), followed by centrifugation for 2 min at 13000 rpm in order to discard any solid residues. CRT separation was performed with a ternary gradient elution, with an initial solvent composition of 90% methanol (MeOH), 5% water and 5% methyl tert-butyl ether (MTBE). Solvent composition changed during the analysis as described by Carmona et al.

(2012) and Alquezar et al. (2008). After each analysis, the initial conditions were re-established and equilibrated before the next injection. The flow rate was 1 mL min^{-1} and column temperature was 25°C. A volume of 20 µL of each sample was injected and the PDA was set to scan from 250 to 540 nm. A Maxplot chromatogram was obtained for each sample that plots each CRT peak at its corresponding maximum absorbance wavelength.

Carotenoids were identified by comparison of the absorption spectra and retention times with the available standards or with data obtained in similar experimental conditions and described in the literature (Britton et al., 1998). For quantification, the chromatographic peaks of each CRT were integrated in their maximum wavelength and the resulting area of the peak was interpolated in different calibration curves that were already set up in the laboratory. The available calibration curves were: canthaxanthin (Sigma), lutein (Sigma), β-carotene (Sigma), β-cryptoxanthin (Extrasynthese). Standards of phytoene and phytofluene were obtained from peel extracts of orange fruits (Rodrigo et al., 2003) and HPLC purified. Quantification of adonirubin, astaxanthin, and echineone was performed using the calibration curve of β-carotene, with values expressed as equivalents of β-carotene. As for the non-identified CRTs, they were quantified using either the β-carotene or the lutein calibration curves depending on their retention times and spectra.

This article had been previously published as a preprint (Tanner et al., 2018b).

Results

Isolation of Pigmented Bacteria

Culturing of the solar panel samples yielded a high amount of colony-forming pigmented microorganisms on all three media (LB, R2A, and MA) as previously described (Dorado-Morales et al., 2016), although the isolates growing on LB media displayed more intense pigmentation. On the other hand, fungal growth was much lower on LB medium than on R2A or MA, facilitating the isolation of pure bacterial cultures from samples grown on LB medium rather than from the other two media. A total of 87 isolates were selected, obtained in pure culture, cryo-preserved in 20% glycerol and subjected to taxonomic identification through 16S rDNA sequencing, with 68 isolates being successfully identified and comprising a wide range of species belonging to the following genera: *Agrococcus*, *Arthrobacter*, *Bacillus*, *Cellulosimicrobium*, *Curtobacterium*, *Frigoribacterium*, *Glutamicibacter*, *Kocuria*, *Leucobacter*, *Microbacterium*, *Pantoea*, *Paracoccus*, *Pedobacter*, *Planomicrobium*, *Plantibacter*, *Pontibacter*, *Pseudoclavibacter*, *Rhodobacter*, *Sanguibacter*, and *Sphingomonas* (Supplementary Table IV.1).

Oxidative Stress Assays

After identification, 14 isolates with no record of opportunistic infections were selected for biological activity assays in *C. elegans*. For example, *Erwinia persicina* was not selected for these assays due to its capacity of infecting plants, causing chlorosis and necrosis in leaves (González et al., 2007). Isolates from the *Kocuria* genus were not selected due to increasing incidence of different types of *Kocuria* infection, mostly in immunocompromised hosts or hosts with severe underlying diseases, causing infections such as peritonitis, bacteremia or endocarditis (Purty et al., 2013). Finally, isolation from clinical specimens of bacteria from the genera *Microbacterium*, *Cellulosimicrobium*, and *Curtobacterium* have been reported, therefore isolates from these species were not selected for biological activity assays (Gneiding et al., 2008; Francis et al., 2011; Zamora and Camps, 2018).

The selected isolates for high-throughput biological assays were the following (Table IV.1): PS1 (*Planomicrobium* sp.), PS83 (*Bacillus* sp.), PS75 (*Bacillus* sp.), PS21 (*Rhodobacter* sp.), PS20 (*Curtobacterium* sp.), PS13 (*Sanguibacter* sp.), PS19 (*Sanguibacter* sp.), PS30 (*Arthrobacter* sp.), PS17 (*Arthrobacter* sp.), PS47 (*Arthrobacter* sp.), PS63 (*Arthrobacter* sp.), PS10 (*Glutamicibacter* sp.), PS66 (*Agrococcus* sp.) and PS57 (*Sphingomonas* sp.). All these isolates were individually tested with an oxidative stress assay using the WT device, which is able to automatically assess survival of the worms through the detection of omega bends and reversals in the

Table IV.1 Selected isolates for high-throughput biological assays in *C. elegans*.

Phylum	Isolate number	Closest neighbor (accession number)	% similarity
Actinobacteria	PS66	*Agrococcus citreus* IAM 15145 (AB279547)	99.70
	PS30	*Arthrobacter agilis* DSM 20550 (X80748)	99.26
	PS63	*Arthrobacter agilis* DSM 20550 (X80748)	98.87
	PS17	*Arthrobacter pityocampae* Tp2 (EU855749)	97.77
	PS47	*Arthrobacter subterraneus* CH7 (DQ097525)	97.95
	PS10	*Glutamicibacter arilaitensis* Re117 (FQ311875)	100
	PS20	*Curtobacterium herbarum* P 420/07 (AJ310413)	98.37
	PS13	*Sanguibacter inulinus* ST50 (X79451)	100
	PS19	*Sanguibacter inulinus* ST50 (X79451)	100
Firmicutes	PS75	*Bacillus megaterium* NBRC 15308 (JJMH01000057)	100
	PS83	*Bacillus aryabhattai* B8W22 (EF114313)	99.77
	PS1	*Planomicrobium glaciei* 423 (EU036220)	97.38
Proteobacteria	PS21	*Rhodobacter maris* JA276 (AM745438)	98.89
Bacteroidetes	PS57	*Sphingomonas aerolata* NW12 (AJ429240)	99.76

Percentage of similarity with the closest neighbor (species, strain, and accession number) is indicated.

worm's locomotion (Huang et al., 2006). Survival under oxidative stress conditions was measured after incubation of the worms for 3 days on NGM supplemented with each bacterial isolate at OD_{600} of 30 or of 60. Isolate PS57 did not grow well in liquid culture and was therefore discarded from the assay. After 3 days of incubation with the selected pigmented isolates, some worms had not reached young adult phase and were de-synchronized. Specifically, this was the case of worms incubated with PS66, PS47, PS19, and PS20. The most extreme case was PS66, so this one was not measured in the WT device. Nevertheless, PS47, PS19, and PS20 displayed only slight differences in growth and were therefore tested. Worm activity after oxidative stress was best measured at 30 min after addition of hydrogen peroxide to the medium, as it is at this point when larger differences could be observed between the positive and negative controls (Figure IV.1).

In general, there was no significant differences in antioxidant activity between the worms incubated with the isolates at an OD of 30 or of 60 (Figure IV.1A), although a lower OD was beneficial for worm movement and, therefore, was the OD of choice for further experiments. After 30 min of incubation, PS30 did not display significant differences in activity per worm in comparison to the negative control, and PS10 displayed lower mobility than the negative control, indicating more worm mortality. On the other hand, incubation of the worms with PS1, PS13, PS21, PS75, PS17, PS47, PS19, PS20, PS63, and PS83 resulted in a higher protection of these worms against oxidative stress, with significant differences with respect to the negative control, and in some cases, with significantly higher protection in comparison to the positive control (Figure IV.1A). In order to compare all experiments, an antioxidant index (AI) was calculated for each isolate by dividing the average activity per worm at 30 min when incubated with the isolate at OD 30 or 60 (the highest activity was used) by the average activity per worm of the positive control (Figure IV.1B). Nine out of the ten tested isolates displayed higher antioxidant activity than the positive control (AI > 1), although three of these (PS47, PS19, and PS20) could not be compared to the rest due to the worms being smaller and, in some cases, not correctly synchronized.

The WT is a device that measures survival of the worms through their mobility, although this is not the most precise way to measure survival due to the fact that worms tend to have reduced mobility in liquid culture in comparison to solid medium. Therefore, the device may detect false negative results. For this reason, the best isolates according to results with the WT were selected for further, in depth characterization with the manual oxidative stress assay in order to confirm the results. Specifically, PS1, PS75, and PS21 were selected. For the manual assays, oxidative stress is applied to 5-day old adult worms instead of young adult worms, in accordance with the protocol described by Martorell et al. (2013).

Incubation with hydrogen peroxide resulted in a survival of approximately 37% of the worms grown on NGM with *E. coli*, whereas the survival of worms grown on NGM with *E. coli* supplemented with vitamin C (vitC) was higher, with approximately 51% survival (Figure IV.1C), confirming the antioxidant effect of the positive control (vitC). Furthermore, the selected isolates also displayed a high antioxidant effect: incubation with PS75 resulted in around 57%

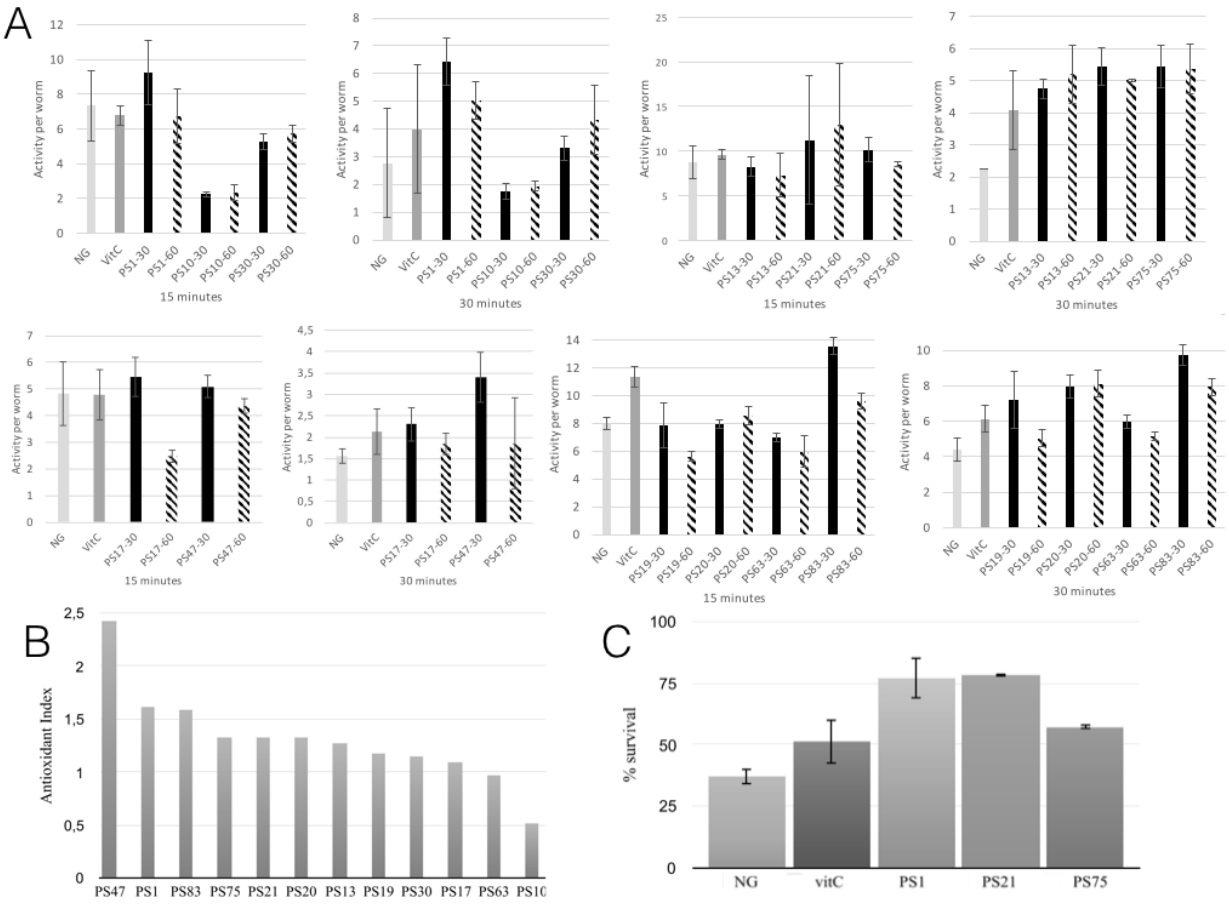

Figure IV.1. (A) Oxidative stress assays of the selected isolates using the WT device. Worms were fed with the selected isolates at either an OD600 of 30 or 60. Survival rate is represented in the Y-axis in the form of activity per worm, and results are shown after 15 and 30 minutes of incubation with hydrogen peroxide. Error bars indicate standard deviation. (B) Antioxidant index (AI) of the pigmented bacterial isolates from solar panels. AI was calculated by dividing the highest activity average (at an OD600 of 30 or 60) of each isolate by the average activity of the positive control (vitC) after 30 minutes of incubation with hydrogen peroxide. (C) Manual oxidative stress assay results. Y-axis indicates percentage of survival of the worms after 5 hours of incubation in nematode growth medium supplemented with 20 mM hydrogen peroxide. NG (Nematode growth), negative control. VitC (vitamin C), positive control. Error bars indicate standard deviation.

survival, whereas incubation with PS1 and PS21 resulted in a survival rate of as much as 78%. These results confirm that isolates PS1, PS21, and PS75 confer a very high protection against oxidative stress in *C. elegans* and, therefore, validate the WT protocol that was designed for this project.

UV-Protection Assays

The photo-protective effects of the isolated pigmented bacteria were tested *in vivo* in *C. elegans* using a UV-protection assay (Figure IV.2).

There was a natural decrease in survival rate over time in the non-irradiated control (NG-C), with a survival rate at day 14 of 54% (Figure IV.2A). Despite a general decrease of survival rate over the first 9 days (Figure IV.2A), day 11 showed the largest decrease of the negative control survival rate (worms grown on NGM with *E. coli* and subjected to irradiation) in comparison to the survival rate of the positive controls and of the worms fed with the selected isolates (Figure IV.2B). Worms fed with PS1 and PS21 displayed a survival rate of around 55% at day 11, suggesting that these isolates are able to confer resistance against UV irradiation. On the other hand, although PS75 is also able to confer protection to UV-light, the survival rates are lower than the ones obtained with PS1 and PS21 (Figure IV.2A). These results correlate with the previous ones regarding effectiveness of the strains in protecting *C. elegans* against oxidative stress: PS1 and PS21 are

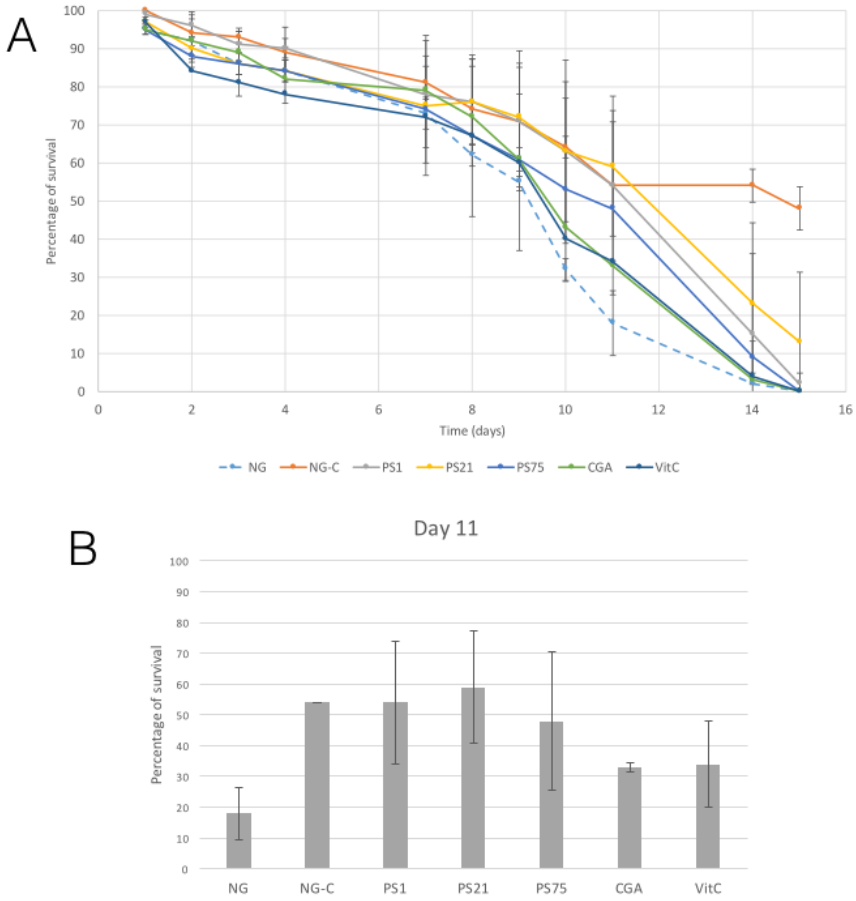

Figure IV.2. UV-light protection assay. Error bars indicate standard deviation. **(A)** Y-axis indicates percentage of survival of *C. elegans* irradiated with UV-light for 45 seconds every day over a period of 15 days (X-axis). NG-C indicates the non-irradiated controls: the basal survival rate of the worms over the 15-day period. NG refers to the negative control: worms incubated in NGM with no supplements and irradiated during the 15 days. CGA and VitC are two positive controls: worms incubated with antioxidant compounds (chlorogenic acid and vitamin C) and irradiated during 15 days. Finally, PS1, PS21 and PS75 (*Planomicrobium* sp., *Rhodobacter* sp. and *Bacillus* sp., respectively) indicate worms incubated with pigmented solar panel isolates and irradiated over the 15-day period in order to test the protective effect of these isolates against UV-light. **(B)** Results at day 11, in which the largest differences between the negative control and the worms fed with the pigmented isolates were observed.

the isolates which confer the highest resistance, followed by PS75.

Preliminary Characterization of the Carotenoid Content of Selected Isolates

The three selected isolates (PS1, PS21, and PS75) were further studied in two different types of bacterial culture: liquid culture and solid culture. For this, pigments were extracted and analyzed by HPLC-PDA. The resulting chromatogram of each sample, together with examples of characteristic absorption spectra for CRTs peaks can be seen in Supplementary Figure IV.1. For each sample, the peaks with a characteristic CRT spectrum were integrated at their maximum wavelength and, if possible, their probable identities were assigned according to the absorbance spectrum and retention time compared to commercial standards or reported in similar chromatographic conditions. Peaks with a characteristic CRT spectrum but without assigned identity were reported as "not identified" (NI) in the profile description. Peaks were quantified by interpolating the area of the peaks into calibration curves, as explained in Materials and Methods. The relative abundance of each carotenoid can be seen in Figure IV.3, and all details (identification, peaks, maximum wavelengths, numeric indication of the spectral shape, and quantification) of the CRTs tentatively

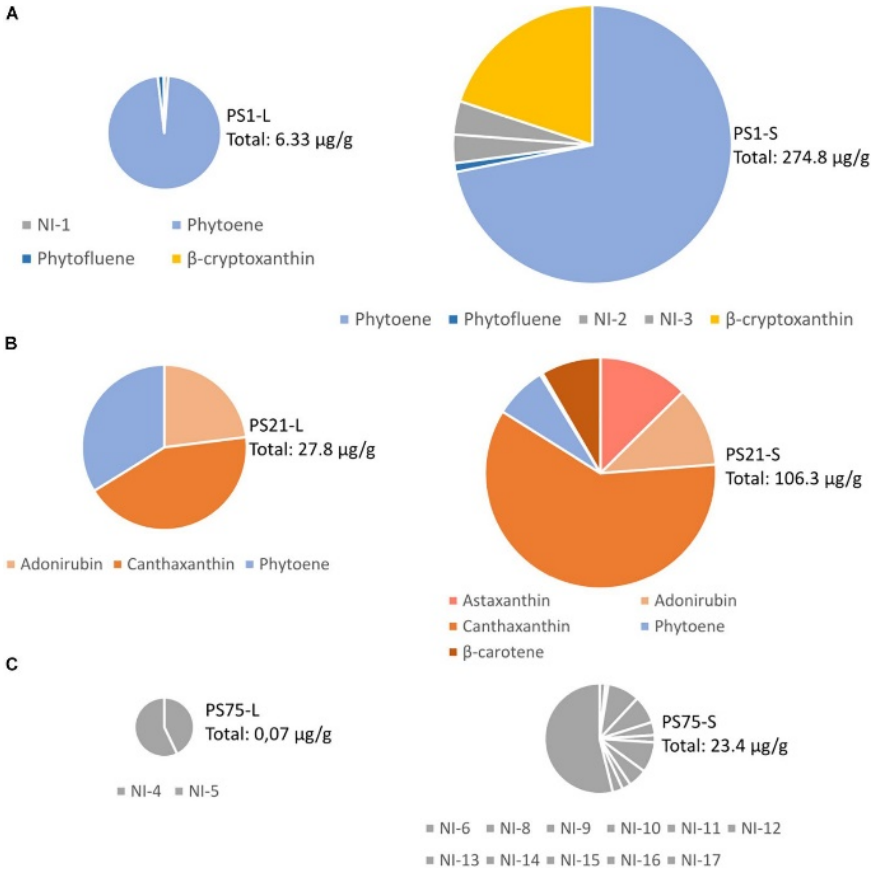

Figure IV.3. Tentative identification and quantification of the carotenoid content from the three selected isolates (A - PS1, B - PS21, C- PS75) after harvesting from liquid (L) or solid (S) culture. The total amount of CRTs is indicated next to each chart in µg per gram of cellular pellet (dry pellet in the samples harvested from solid culture, and wet pellet in the samples harvested from liquid culture). Further details on the concentration of each carotenoid can be found in Supplementary Table IV.2

identified (TI) of each sample can be found in Supplementary Table IV.2.

Discussion

Despite the harsh conditions, solar panels harbor a wide range of pigmented bacteria that are also shared by other harsh environments. *Microbacterium radiodurans* is a UV radiation-tolerant bacterium that was isolated for the first time from the upper sand layers of the Gobi desert in China (Zhang et al., 2010). Other isolates are characteristic of polar environments, such as *Planomicrobium glaciei*, a psychrotolerant bacterium that was first isolated from a glacier in China (Zhang et al., 2009), *Arthrobacter agilis* (Brambilla et al., 2001) or *Sphingomonas aerolata* (Busse et al., 2003); and others are characteristic of soil environments, such as *P. agri* (Roh et al., 2008) or many species of the *Frigoribacterium* (Kämpfer et al., 2000; Dastager et al., 2008), *Arthrobacter* (Park et al., 2014; Siddiqi et al., 2014) and *Curtobacterium* genera (Kim et al., 2008). Pigmentation of the bacterial isolates may play a protective role in their survival in environments with extreme temperature fluctuations and subjected to large amounts of irradiation. An intensification in the pigmentation was observed after the plates were incubated in the refrigerator for several days. In fact, previous studies suggest that pigments such as CRTs not only play an important role in radiation protection but also in cryoprotection (Dieser et al., 2010) due to their ability to modulate membrane fluidity in bacteria when grown under low temperature conditions (Jagannadham et al., 2000).

The diversity of genera found on the solar panel surfaces is consistent with other studies focusing on naturally irradiated environments. For example, several members of the *Bacillus*, *Micrococcus*,

and *Pseudomonas* genera that proved to be resistant to UV-B irradiation have previously been isolated from high-altitude Andean wetlands, an environment that is characterized to have high UV radiation (Dib et al., 2008). On the other hand, UV-C resistant microorganisms including *Arthrobacter* sp. and *Curtobacterium* sp. have been isolated from sun-exposed rock varnish from the hot desert of the Whipple Mountains (Kuhlman et al., 2005). Furthermore, it is important to stress that 48 of the 68 isolates identified in the present study were Actinobacteria, a class that has been previously associated to UV-exposed environments including soil and high-altitude freshwater lakes (Warnecke et al., 2005; Rasuk et al., 2017; Bull et al., 2018).

Oxidative-stress assays with *C. elegans* revealed the antioxidant properties of these isolates, making them of great interest for the pharmacological and food industries: extracts of these isolates or even the bacteria themselves could be used as promising treatments for conditions in which oxidative stress plays an important role. On the other hand, the UV-protection assays suggest that the pigmented bacteria isolated from solar panels could also play a protecting role in this type of stress, which is of high interest for the cosmetic industry, specifically in the fabrication of products that protect against sunlight-induced skin damage. The three isolates selected for UV-light protection assays due to the promising results obtained in the oxidative-stress tests (*Planomicrobium* sp. or PS1, *Rhodobacter* sp. or PS21 and *Bacillus* sp. or PS75) were further tested through HPLC-PDA analysis to shed light on their CRTs composition.

PS1 was found to be 97,38% similar to *Planomicrobium glaciei*, a species that was first described by Zhang et al. (2009), who indicated that it displayed yellow-to-orange pigmentation. Our results suggest that the main CRTs present in PS1 may be phytoene and β-cryptoxanthin, and previous studies have demonstrated the antioxidant and free radical scavenging properties of β-cryptoxanthin, phytoene and phytofluene (Martínez et al., 2014; Ni et al., 2014). It would be interesting to consider whether the high antioxidant capacity of this isolate could be related to the presence of phytoene together with the colored CRT, β-cryptoxanthin.

PS21 was found to be 98.89% similar to *Rhodobacter maris*, a bacterium previously isolated from a marine habitat and described to produce CRTs (Ramana et al., 2008). Interestingly, although *Rhodobacter* PS21 harvested from liquid culture was seen to be rich in pigments probably corresponding to adonirubin (TI), canthaxanthin, and phytoene, when harvested from solid medium CRT composition included also astaxanthin (T) and β-carotene. The CRTs present in PS1 and PS21 could be commercially valuable as they have many applications (Sandmann, 2015): β-carotene and canthaxanthin are used as food colorants and feed additives, especially in aquaculture, whereas astaxanthin and phytoene are widely used in the cosmetic industry.

Finally, the closest neighbor of PS75 was identified as *B. megaterium* (100% similarity), a spore-forming species (Mitchell et al., 1986). Although no identity was assigned to CRT peaks in PS75 extracts, the absorbance spectrum and retention time in the used chromatographic conditions of NI-17 and other minor peaks (NI-14 to -16) in solid culture, and NI-4 and 5 in liquid culture, are compatible with methyl esters of glycosyl-apo-8'-lycopene, orange colored derivatives of a C30 apo-8'-carotenoid pathway that occurs in certain *Bacillus* species (Pérez-Fons et al., 2011). Moreover, the NI-6 to NI-13 compounds and phytoene-like may also correspond to glycosyl-3-4-dehydro-8'-apolycopene esters and apo-8-phytoene which have been identified in vegetative cells and spores of *Bacillus* sp. species (Pérez-Fons et al., 2011). In relation to the oxidative stress and UV-resistant assays, this isolate had less antioxidant activity in comparison to PS1 and PS21.

Conclusion

In conclusion, after selecting a number of pigmented isolates from solar panels according to their low biological risk and testing them *in vivo* in order to elucidate their biological activity, nine out of the ten selected isolates displayed a higher antioxidant activity than the positive control. The isolates with highest antioxidant activity, PS1 (*Planomicrobium* sp.), PS21 (*Rhodobacter* sp.), and PS75 (*Bacillus* sp.) were validated with a manual oxidative stress assay, confirming the

previous results and validating the protocol designed and used for oxidative stress assay in the WT device. Furthermore, the three selected strains also displayed UV-protection properties, with values once again higher than the positive control in the case of PS1 and PS21. The high antioxidant properties of these isolates are promising from a pharmacological point of view. Specifically, extracts of these bacteria or artificial combinations of their active compounds, could be useful for the design of new treatments against diseases in which oxidative stress plays a crucial role.

Taken together, our results provide new data on the biological activity of bacterial strains from solar panels with very high antioxidant and UV-protection properties. This is the first report describing the biotechnological potential of pigmented bacterial strains from solar panels using a *C. elegans*-based model.

Author Contributions

The project was designed by MP, JP, and DR. Sampling and isolation/identification of the strains was performed by MP, JP, and KT. Experiments involving *C. elegans* were performed by SG, PM, DR, and KT. Characterization of the pigment content was performed by MR, LZ, and KT. Manuscript has been written and revised by all the authors.

Funding

Financial support from the Spanish Government (grant Helios, reference: BIO2015-66960-C3-1-R co-financed by FEDER funds and Ministerio de Ciencia, Innovación y Universidades) and from the Regional Government of Valencia (grant MICROBIOSOL, reference: IFIDUA/2015/10 financed by IVACE) are acknowledged. Furthermore, KT is a recipient of a Doctorado Industrial fellowship from the Ministerio de Ciencia, Innovación y Universidades (Spain), with reference DI-16-08976. MR and LZ are members of the CaRed Excellence Network (BIO2017-90877-REDT) and EUROCAROTEN European COST Action (CA15113).

Conflict of Interest Statement

KT was employed at the time of research by the company Darwin Bioprospecting Excellence S.L., whereas JP and MP are co-founders of the company Darwin Bioprospecting Excellence S.L. PM, SG, and DR were employed by the company ADM Biopolis S.L.

The remaining authors declare that the research was conducted in the absence of any commercial or financial relationships that could be construed as a potential conflict of interest.

Acknowledgments

We are very grateful to Cristina Vilanova for her kind assistance in the taxonomic identification of the isolates.

References

Al-Gubory, K.H. (2014). Environmental pollutants and lifestyle factors induce oxidative stress and poor prenatal development. Reprod. Biomed. Online 29(1), 17-31.

Alquezar, B., Rodrigo, M. J., and Zacarías, L. (2008). Regulation of carotenoid biosynthesis during fruit maturation in the red-fleshed orange mutant *Cara cara*. Phytochemistry, 69(10), 1997–2007.

Brambilla, E., Hippe, H., Hagelstein, A., Tindal, B.J. and Stackerbrandt, E. (2001). 16S rRNA diversity of cultured and uncultured prokaryotes of a mat sample from Lake Fryxell, McMurdo Dry Valleys, Antarctica. Extremophiles 5(1), 23-33.

Britton, G. (1995). Structure and properties of carotenoids in relation to function. FASEB J 9(15), 1551-1558.

Britton, G., Liaaen-Jensen, S., and Pfander, H. (1998). Carotenoids: biosynthesis and metabolism, vol. 3. Basel, Switzerland: Birkhäuser.

Bull, A.T., Idris, H., Sanderson, R., Asenjo, J., Andrews, B., and Goodfellow, M. (2018). High altitude, hyper-arid soils of the Central-Andes harbor mega-diverse communities of Actinobacteria. Extremophiles 22(1): 47-57.

Busse, H.J., Denner, E.B.M., Buczolits, S., Salkinoja-Salonen, M., Bennasar, A, et al. (2003*). Sphingomonas aurantiaca* sp. nov., *Sphingomonas aerolata* sp. nov. and *Sphingomonas faeni* sp. nov., air- and dustborne and Antarctic, orange-pigmented, psychrotolerant

bacteria, and emended description of the genus *Sphingomonas*. Int. J. Syst. Evol. Microbiol. 53, 1253-1260.

Cañuelo, A., Gilbert-López, B., Pacheco-Liñán, P., Martínez-Lara, E., Siles, E., et al. (2012). Tyrosol, a main phenol present in extra virgin olive oil, increases lifespan and stress resistance in *Caenorhabditis elegans.* Mech. Ageing. Dev. 133, 563-574.

Carmona, L., Zacarías, L. and Rodrigo, M.J. (2012). Stimulation of coloration and carotenoid biosynthesis during postharvest storage of 'Navelina' orange fruit at 12ºC. Postharvest Biol. Technol. 74, 108-117.

Chen, Z., Wang, D., Liu, X., Pei, W., Li, J., et al. (2015). Oxidative DNA damage is involved in cigarette smoke-induced lung injury in rats. Environ. Health. Prev. Med. 20(5), 318-324.

Chen, Z. and Zhong, C. (2014). Oxidative stress in Alzheimer's disease. Neurosci. Bull. 30(2), 271-281.

Choudhary, J., Singh, S., and Nain, L. (2017). Bioprospecting thermotolerant ethanologenic yeasts for simultaneous saccharification and fermentation from diverse environments. J. Biosci. Bioeng. 123(3), 342-346.

Dandekar A., Mendez R., and Zhang K. (2015). "Cross Talk Between ER Stress, Oxidative Stress, and Inflammation in Health and Disease", in Stress Responses. Methods in Molecular Biology, ed. C. Oslowski (New York, NY: Humana Press), 205-214.

Dastager, S.G., Lee, J.C., Ju, Y.J., Park, D.J. and Kim, C.J. (2008). *Frigoribacterium mesophilum* sp. nov., a mesophilic actinobacterium isolated from Bigeum Island, Korea. Int. J. Syst. Evol. Microbiol. 58, 1869-1872.

Dib, J., Motok, J., Zenoff, V.F., Ordoñez, O., Farías, M.E. (2008). Occurrence of resistance to antibiotics, UV-B, and arsenic in bacteria isolated from extreme environments in high-altitude (above 4400 m) Andean wetlands. Curr. Microbiol. 56(5): 510-7.

Dieser, M., Greenwood, M. and Foreman, C.M. (2010). Carotenoid pigmentation in Antarctic heterotrophic bacteria as a strategy to withstand environmental stresses. Arct. Antarct. Alp. Res. 42(4), 396-405.

Dorado-Morales, P., Vilanova, C., Peretó, J., Codoñer, F.M., Ramón, D., et al. (2016). A highly diverse, desert-like microbial biocenosis on solar panels in a Mediterranean city. Sci. Rep. 6, 29235. doi: 10.1038/srep29235.

Fagliarone, C., Mosca, C., Ubaldi, I., Verseux, C., Baqué, M., Wilmotte, A. and Billi, D. (2017). Avoidance of protein oxidation correlates with the desiccation and radiation resistance of hot and cold desert strains of the cyanobacterium *Chroococcidiopsis*. Extremophiles 21(6): 981-991.

Finley, J.W., Kong, A., Hintze, K.J., Jeffery, E.H., Ji, L.L., et al. (2011). Antioxidants in foods: state of the science important to the food industry. J. Agric. Food Chem. 59(13), 6837-6846.

Francis, M.J., Doherty, R.R., Patel, M., Hamblin, J.F., Ojaimi, S and Korman, T.M. (2011). *Curtobacterium flaccumfaciens* septic arthritis following puncture with a Coxspur Hawthorn thorn. J. Clin. Microbiol. 49(7): 2759-2760.

Fredrickson, J. K., Shu-mei, W. L., Gaidamakova, E. K., Matrosova, V. Y., Zhai, M., Sulloway, H. M., et al. (2008). Protein oxidation: key to bacterial desiccation resistance? ISME J. 2(4): 393-403.

González, A.J., Tello, J.C. and Rodicio, M.R. (2007). *Erwinia persicina* causing chlorosis and necrotic spots in leaves and tendrils of Pisum sativum in southeastern Spain. Plant Dis. 91(4), 460.

Gneiding, K., Frodl, R., and Funke, G. (2008) Identities of Microbacterium spp. encountered in human clinical specimens. J. Clin. Microbiol. 46(11): 3646-3652.

Grompone, G., Martorell, P., Llopis, S., González, N., Genovés, S., Mulet, A. P. et al. (2012). Anti-inflammatory *Lactobacillus rhamnosus* CNCM I-3690 strains protects against oxidative stress and increases lifespan in *Caenorhabditis elegans*. PLoS ONE 7(12): e52493.

Gupta, M., and Bajaj, B.K. (2017). Functional characterization of potential probiotic lactic acid bacteria isolated from Kalarei and development of probiotic fermented oat flour. Probiotics Antimicrob. Proteins. doi: 10.1007/s12602-017-9306-6

Huang, K., Cosman, P. and Schafer, W.R. (2006). Machine vision based detection of omega bends and reversals in *C. elegans*. J. Neurosci. Methods 158(2): 323-336.

Iriondo-DeHond, A., Martorell, P., Genovés, S., Ramón, D., Stamatakis, K., Fresno, M., et al. (2016). Coffee silverskin extract protects against accelerated aging caused by oxidative agents. Molecules 21(6): 721. doi: 10.3390/molecules21060721

Jagannadham, M.V., Chattopadhyay, M.K., Subbalakshmi, C., Vairamani, M., Narayanan, K., Rao, C.M. and Shivaji, S. (2000). Carotenoids of an Antarctic psychrotolerant bacterium, *Sphingomonas antarticus*, and a mesophilic bacterium, *Sphingobacterium multivorum.* Arch. Microbiol. 173(5-6): 418-424.

Kämpfer, P., Rainey, F.A., Andersson, M.A., Nurmiaho, L.E.L., Ulrych, U., Busse, H.J. et al. (2000). *Frigoribacterium faeni* gen. nov., sp. nov., a

novel psychrophilic genus of the family *Microbacteriaceae*. Int. J. Syst. Evol. Microbiol. 50: 355-363.

Kanchiswamy, C.N., Malnoy, M., and Maffei, M.E. (2015). Bioprospecting bacterial and fungal volatiles for sustainable agriculture. Trends Plant Sci. 20(4): 206-211.

Katz, L. and Baltz, R.H. (2016). Natural product discovery: past, present and future. J Ind Microbiol Biotechnol 43: 155-176.

Kim, M.K., Kim, Y.J., Kim, H.B., Kim, S.Y., Yi, T.H., and Yang, D.C. (2008). *Curtobacterium ginsengisoli* sp. nov., isolated from soil of a ginseng field. Int. J. Syst. Evol. Microbiol. 58: 2393-2397.

Kuhlman, K.R., Allenbach, L.B., Ball, C.L., Fusco, W.G., La Duc, M.T., Kuhlman, G.M., et al. (2005). Enumeration, isolation, and characterization of ultraviolet (UV-C) resistant bacteria from rock varnish in the Whipple Mountains, California. Icarus 174(2): 585-595.

Lashmanova, E., Proshkina, E., Zhikrivetskaya, S., Shevchenko, O., Marusich, E., Leonov, S., et al. (2015). Fucoxanthin increases lifespan of *Drosophila melanogaster* and *Caenorhabditis elegans*. Pharmacol. Res. 100: 228-241.

Lebre, P. H., De Maayer, P. and Cowan, D. A. (2017). Xerotolerant bacteria: surviving through a dry spell. Nature. Rev. Microbiol. 15(5): 285-296.

Li, W.H., Shi, Y.C., Chang, C.H., Huang, C.W., and Hsiu-Chuan Liao, V. (2014). Selenite protects Caenorhabditis elegans from oxidative stress via DAF-16 and TRXR-1. Mol. Nutr. Food Res. 58: 863-874.

Lin, Y., Jain, R., and Yan, Y. (2014). Microbial production of antioxidant food ingredients via metabolic engineering. Curr. Opin. Biotechnol. 26: 71-78.

Mahajan, G.B. and Balachandran, L. (2012). Antibacterial agents from actinomycetes – a review. Front. Biosci. 4: 240-253.

Martínez, A., Stinco, C.M. and Meléndez-Martínez, A.J. (2014). Free radical scavenging properties of phytofluene and phytoene isomers as compared to lycopene: a combined experimental and theoretical study. J. Phys. Chem. 118(33): 9819-9825.

Martorell, P., Bataller, E., Llopis, S., Gonzalez, N., Álvarez, B., Montón, F. et al. (2013). A cocoa peptide protects *Caenorhabditis elegans* from oxidative stress and β-amyloid peptide toxicity. PLoS ONE 8(5): e63283. doi:10.1371/journal.pone.0063283

Martorell, P., Llopis, S., González, N., Chenoll, E., López-Carreras, N., Aleixandre, A. et al. (2016). Probiotic strain *Bifidobacterium animalis* subsp. lactis CECT 8145 reduces fat content and modulates lipid metabolism and antioxidant response in *Caenorhabditis elegans*. J. Agric. Food Chem. 64: 3462-3472.

Mattimore, V. and Battista, J. R. (1996). Radioresistance of *Deinococcus radiodurans*: functions necessary to survive ionizing radiation are also necessary to survive prolonged desiccation. J. Bacteriol. 178(3): 633-637.

Milkovic, L., Siems, W., Siems, R., and Zarkovic, N. (2014). Oxidative stress and antioxidants in carcinogenesis and integrative therapy of cancer. Curr. Pharm. Des. 20(42): 6529-6542.

Mitchell, C., Lyer, S., Skomurski, J. F. and Vary, J. C. (1986). Red pigment in *Bacillus megaterium* spores. Appl. Environ. Microbiol. 52(1): 64-67.

Ni, Y., Nagashimada, M., Zhan, L., Nagata, N., Kobori, M., Sugiura, M. et al. (2014). Prevention and reversal of lipotoxicity-induced hepatic insulin resistance and steatohepatitis in mice by an antioxidant carotenoid, β-cryptoxanthin. Endocrinology 156(3): 987-999.

Park, Y., Kook, M., Ngo, H.T., Kim, K.Y., Park, S.Y., Mavlonov, G.T., and Yi, T.H. (2014). *Arthrobacter bambusae* sp. nov., isolated from soil of a bamboo grove. Int. J. Syst. Evol. Microbiol. 64: 3069-3074.

Pérez-Fons, L., Steiger, S., Khaneja, R., Bramley, P. M., Cutting, S. M., Sandmann, G. and Fraser, P. D. (2011). Identification and the developmental formation of carotenoid pigments in the yellow/orange *Bacillus* spore-formers. Biochem. Biophys. Acta 1811(3): 177-185.

Porcar, M., Louie, K.B., Kosina, S.M., Van Goethem, M.W., Bowen, B.P., Tanner, K., and Northen, T.R. (2018). Microbial Ecology on Solar Panels in Berkeley, CA, United States. Front. Microbiol. https://doi.org/10.3389/fmicb.2018.03043

Purty, S., Saranathan, R., Prashanth, K., Narayanan, K., Asir, J., Devi, C.S. and Amarnath, S.K. (2013). The expanding spectrum of human infections caused by *Kocuria* species: a case report and literature review. Emerg. Microbes Infect. 2(10): e71.

Ragon, M., Restoux, G., Moreira, D., Møller, A.P., and López-García, P. (2011). Sunlight-exposed biofilm microbial communities are naturally resistant to chernobyl ionizing-radiation levels. PLoS One 6(7):e21764.

Rahal, A., Kumar, A., Singh, V., Yadav, B., Tiwari, R., Charkraborty, S. and Dhama, K. (2014). Oxidative stress, prooxidants and antioxidants: the interplay. BioMed Res. Int. 2014: 761264.

Ramana, V.V., Sasikala, C., and Ramana, C.V. (2008). *Rhodobacter maris* sp. nov., a phototrophic

alphaproteobacterium isolated from a marine habitat of India. Int. J. Syst. Evol. Microbiol. 58: 1719-1722.

Rasuk, M.C., Ferrer, G.M., Kurth, D., Portero, L.R., Farías, M.E., Albarracín, V.H. (2017). UV-resistant Actinobacteria from high-altitude Andean lakes: isolation, characterization and antagonistic activities. Photochem. Photobiol. 93(3): 865-880.

Reasoner, D.J. and Geldereich, E.E. (1985). A new medium for the enumeration and subculture of bacteria from potable water. Appl. Environ. Microbiol. 49(1): 1-7.

Rodrigo, M., Marcos, J., Alferez, F., Mallent, M. D., and Zacarias, L. (2003). Characterization of Pinalate, a novel *Citrus sinensis* mutant with a fruit-specific alteration that results in yellow pigmentation and decreased ABA content. J. Exp. Bot. 54(383): 727–738. http://doi.org/10.1093/jxb/erg083

Roh, S.W., Quan, Z.X., Nam, Y.D., Chang, H.W., Kim, K.H., Kim, M.K., et al. (2008). *Pedobacter agri* sp. nov., from soil. Int. J. Syst. Evol. Microbiol. 58: 1640-1643.

Sandmann, G. (2015). Carotenoids of biotechnological importance. Adv. Biochem. Eng. Biotechnol. 148: 449-467.

Siddiqi, M.Z., Kim, Y.J., Hoang, V.A., Siddiqi, M.H., Huq, M.A., and Yang, D.C. (2014). *Arthrobacter ginsengisoli* sp. nov., isolated from soil of a ginseng field. Arch. Microbiol. 496(12): 863-870.

Siti, H.N., Kamisah, Y., and Kamsiah, J. (2015). The role of oxidative stress, antioxidants and vascular inflammation in cardiovascular disease (a review). Vascul. Pharmacol. 71: 40-56.

Slade, D. and Radman, M. (2011). Oxidative stress resistance in *Deinococcus radiodurans*. Microbiol. Mol. Biol. Rev. 75(1): 133-191.

Tanner, K., Martí, J.M., Belliure, J., Fernández-Méndez, M., Molina-Menor, E., Peretó, J., and Porcar, M. (2018). Polar solar panels: Arctic and Antarctic microbiomes display similar taxonomic profiles. Environ. Microbiol. Rep. 10(1): 75-79.

Tanner, K., Martorell, P., Genovés, S., Ramón, D., Zacarías, L., Rodrigo, M.J., Peretó, J., and Porcar, M. Bioprospecting the solar panel microbiome: high-throughput screening for antioxidant bacteria in a *Caenorhabditis elegans* model. bioRxiv. doi: https://doi.org/10.1101/423731

Warnecke, F., Sommaruga, R., Sekar, R., Hofer, J.S., and Pernthaler, J. (2005). Abundances, identity, and growth state of Actinobacteria in mountain lakes of different UV transparency. Applied and Environmental Microbiology 71(9): 5551-5559.

Yazaki, K., Yoshikoshi, C., Oshiro, S. and Yanase, S. (2011). Supplemental cellular protection by a carotenoid extends lifespan via Ins/IGF-1 signaling in Caenorhabditis *elegans*. Oxid. Med. Cell. Longev. 2011: 596240.

Yoon, S.H., Ha, S.M., Kwon, S., Lim, J., Kim, Y., Seo, H., Chun, J. (2017). Introducing EzBioCloud: A taxonomically united database of 16S rRNA and whole genome assemblies. Int. J. Syst. Evol. Microbiol. 67: 1613-1617.

Zamora, J.A.G., and Camps, N. (2018). Bacteremia caused by cellulosimicrobium in a bone marrow transplant patient: A case report and literature review. IDCases 11: 64-66.

Zhang, D.C., Liu, H.C., Xin, Y.H., Yu, Y., Zhou, P.J. and Zhou, Y.G. (2009). Planomicrobium glaciei sp. nov., a psychrotolerant bacterium isolated from a glacier. Int. J. Syst. Evol. Microbiol. 59: 1387-1390.

Zhang, W., Zhu, H.H., Yuan, M., Yao, Q., Tang, R., Lin, M., Yang, S.Z., Li, Z.K., and Chen, M. (2010) *Microbacterium radiodurans* sp. nov., a UV radiation-resistant bacterium isolated from soil. Int. J. Syst. Evol. Microbiol. 60(Pt 11):2665-2670.

Zorov, D.B., Juhaszova, M. and Sollott, S.J. (2014). Mitochondrial reactive oxygen species (ROS) and ROS-induced ROS release. Physiol. Rev. 94(3): 909-950.

Publication V

Sphingomonas solaris sp. nov., isolated from a solar panel in Boston, Massachusetts

Kristie Tanner[1,2,3,4], Christopher P. Mancuso[5,6], Juli Peretó[1,4,7], Ahmad S. Khalil[3,5,6], Cristina Vilanova[1], and Javier Pascual[1]

[1] Darwin Bioprospecting Excellence S.L., Parc Científic de la Universitat de València, Paterna, Spain

[2] Real Colegio Complutense at Harvard University, Cambridge, MA, USA

[3] Wyss Institute for Biologically Inspired Engineering, Harvard University, Boston, MA, USA

[4] Institute for Integrative Systems Biology (I2SysBio, University of Valencia-CSIC), Paterna, Spain

[5] Biological Design Center, Boston University, Boston, MA, USA

[6] Department of Biomedical Engineering, Boston University, Boston, MA, USA

[7] Department of Biochemistry and Molecular Biology, University of Valencia, Burjassot, Spain

Abstract

Solar panel surfaces, although subjected to a range of extreme environmental conditions, are inhabited by a diverse microbial community adapted to solar radiation, desiccation and temperature fluctuations. This is the first time a new bacterial species has been isolated from this environment. Strain R4DWN^T belongs to the genus *Sphingomonas* and was isolated from a solar panel surface in Boston, MA, USA. Strain R4DWN^T is a Gram-negative, non-motile and rod-shaped bacteria that tested positive for oxidase and catalase and forms round-shaped, shiny and orange-coloured colonies. It is mesophilic, neutrophilic and non-halophilic, and presents a more stenotrophic metabolism than its closest neighbours. The major fatty acids in this strain are $C_{18:1}\omega7c/C_{18:1}\omega6c$, $C_{16:1}\omega7c/C_{16:1}\omega6c$, $C_{14:0}$ 2OH and $C_{16:0}$. Comparison of 16S rRNA gene sequences revealed that the closest type strains to R4DWN^T are *Sphingomonas fennica* , *Sphingomonas formosensis* , *Sphingomonas prati* , *Sphingomonas montana* and *Sphingomonas oleivorans* with 96.3, 96.1, 96.0, 95.9 and 95.7 % pairwise similarity, respectively. The genomic G+C content of R4DWN^T is 67.9 mol%. Based on these characteristics, strain R4DWN^T represents a novel species of the genus *Sphingomonas* for which the name *Sphingomonas solaris* sp. nov. is proposed with the type strain R4DWN^T (=CECT 9811^T=LMG 31344^T).

In 1990, Yabuuchi *et al.* [1] described for the first time the genus *Sphingomonas*, with the type species being *Sphingomonas paucimobilis*. This genus is classified in the class *Alphaproteobacteria* [2] and is characterized by having ubiquinone Q-10 as the major respiratory quinone and by having an outer membrane that contains glycosphingolipids but lacks lipopolysaccharides [1, 3]. A total of 122 different *Sphingomonas* species have been described up to date (Source: EzBioCloud [4]). They are gram negative, rod shaped, non-sporulating, strictly aerobic, and display pigmented colonies that range from light yellow/whitish, to intense yellow and orange. Several members of the genus *Sphingomonas* have been shown to hold promise in bioremediation applications, including degradation of polycyclic aromatic hydrocarbons (PAH's), bisphenol A and heavy metal pollutants [5, 6, 7].

In this study we have characterized a new isolate belonging to the genus *Sphingomonas* from the surface of a solar panel. Solar panels from the Hunnewell Building at The Arnold Arboretum of Harvard University, Boston, MA, USA (42° 18' 28.3" N, 71° 07' 14.5" W), were sampled by cleaning the surfaces with sterile Phosphate-Buffered Saline (PBS) and using a sterile window cleaner. The resulting liquid was collected in sterile tubes and transported to the laboratory on ice. The samples were then left to settle for 5 minutes in order to allow fungi to sediment, and

serial dilutions were performed and plated on LB agar and R2A agar. After incubation at room temperature for 6 days, individual colonies were selected and re-streaked in fresh medium in order to obtain pure cultures. Strain R4DWN^T was among the isolates selected the from R2A agar plates.

The complete sequence of the 16S rRNA gene of the isolate was extracted from the draft genome and, according to the EZBioCloud online tool [4], the closest type strains to R4DWN^T are *Sphingomonas fennica* (96.3 %)*, Sphingomonas formosensis* (96.1 %)*, Sphingomonas prati* (96.0 %), *Sphingomonas montana* (95.9 %)*,* and *Sphingomonas oleivorans* (95.7 %). With the aim of establishing the accurate taxonomic position of R4DWN^T, this isolate was characterized using a polyphasic approach. For this, the reference strains of the two closest species, *Sphingomonas fennica* and *Sphingomonas formosensis*, were acquired from the DSMZ Collection (Leibniz Institute DSMZ, Germany) with reference numbers DSM 13665^T and DSM 24164^T, respectively. All three strains were grown on R2A medium at 25 °C for all studies (unless specified otherwise).

For temperature growth tests, all three strains were grown on R2A medium and incubated at 4, 15, 25, 30 and 37 °C. Salt tolerance was determined by cultivating the three strains on R2A medium supplemented with NaCl 0, 1, 2 and 3 % (w/v), and pH tolerance (between 4.0 and 11.0) was determined by cultivating the strains in liquid R2A media buffered with MES (pH 4-6), HEPES (pH 7-8) or CHES (pH 9-11). Catalase activity was determined by detecting bubble production when colonies were mixed with 30 % (v/v) hydrogen peroxide. Oxidase activity was determined using Oxidase Sticks for microbiology (PanReac AppliChem, Barcelona, Spain), and Gram type was determined by assessing cell lysis in KOH 3 % (w/v). All three strains were characterized using API 20NE and API ZYM strips (bioMérieux, Marcy-l'Étoile, France), as well as BIOLOG GENIII MicroPlates (BIOLOG Inc., Hayward, CA, USA). The differential phenotypic characteristics between strain R4DWN^T and the closest species are shown in Table V.1, and the detailed results obtained from the API galleries and BIOLOG GEN III utilization tests are detailed in the protologue of the new species and in Supplementary Table V.1.

Strain R4DWN^T cells were observed to be gram-negative, non-motile and rod-shaped (1.2-4.5 µm length x 1.2 µm wide). In old cultures, some cells grew in the form of a long rod shape of approximately 30 µm. Colonies were found to be round-shaped, shiny, orange-coloured, convex, and 1 mm in diameter after 7 days of incubation at 25 °C. Strain R4DWN^T displayed several characteristics that allows it to be differentiated from other closely related species of the genus (Table V.1), including growth at a smaller range of temperatures (growing only up to 25 °C as opposed to the 30 or 37 °C of other species), assimilation of potassium gluconate and malic acid, and valine arylamidase and β-glucosidase activities. Furthermore, BIOLOG assays revealed that strain R4DWN^T is only able to assimilate 7 out of the 71 tested carbon sources, mainly organic acids and simple sugars (glucuronamide, acetoacetic acid, D-fructose-6-PO4, L-malic acid, L-galactonic acid lactone, β-hydroxy-D,L-butyric acid and D-glucose-6-PO4), whereas *S. fennica* DSM 13665^T and *S. formosensis* DSM 24164^T are able to assimilate 19 and 39 out of the 71 tested carbon sources, respectively. This suggests that the strain R4DWN^T displays a more stenotrophic metabolism than the closest neighbours.

For fatty acid analysis, the three strains were grown on R2A plates at 25 °C for 5 days. Then, the cells were harvested and fatty acid profiles were obtained using the standard MIDI Microbial Identification System protocol [8]. Fatty acids were analysed on an Agilent 6850 gas chromatography system and using the MIDI method TSBA6 [9]. The major fatty acids in strain R4DWN^T were $C_{18:1}$ *ω7c*/$C_{18:1}$ *ω6c* (48.9 %), $C_{16:1}$ *ω7c*/$C_{16:1}$ *ω6c* (21.2%), $C_{14:0}$ 2OH (12.0 %) and $C_{16:0}$ (10.3 %) (Table V.2), a profile that is consistent with other members of the genus *Sphingomonas* [10, 11]. Nevertheless, the lack of $C_{17:1}$ *ω6c* differentiates R4DWN^T from the type species *S. fennica* DSM 13665^T, whereas the large amount of $C_{16:1}$ *ω7c*/$C_{16:1}$ *ω6c* differentiates R4DWN^T from the type species *S. formosensis* DSM 24164^T, which displayed only low amounts of these fatty acids.

The total DNA of the strain R4DWN^T was extracted using the protocol described by Latorre *et al.* [12], quantified using the QUBIT dsDNA HS-high sensitivity kit (Invitrogen), and the 16S rRNA gene was amplified by PCR reaction using the following

Table V.1. Phenotypic comparisons of strain R4DWN^T and the type strains of closely related *Sphingomonas* species. Strains: 1, R4DWN^T; 2, *S. fennica* DSM 24164^T; 3, *S. formosensis* DSM 24164^T; 4, *S. prati* DSM 103336^T; 5, *S. montana* DSM 103337^T; 6, *S. oleivorans* HAMBI 3659^T. Analysis of strains 1, 2 and 3 was conducted under the same conditions in this study, whereas data from strains 4, 5 and 6 was taken from the original species description papers [27, 28, 29]. All strains were positive for the following characteristics: alkaline phosphatase, esterase (C4), esterase lipase (C8), leucine arylamidase, acid phosphatase and naphtol-AS-BI-phosphohydrolase. All strains are negative for the following characteristics: Gram reaction, nitrate reduction, glucose fermentation, activity of arginine dihydrolase, urease, gelatin hydrolysis, assimilation of adipic acid, trisodium citrate and phenylacetic acid, lipase (C14), N-acetyl-β-glycosaminidase, α-mannosidase, and α-fucosidase. +, Positive; –, negative; W, weakly positive.

Characteristic	**1**	**2**	**3**	**4**	**5**	**6**
Isolation source	Solar panel surface	Groundwater *	Soil†	Soil	Soil	Soil
Motility	No	No	No	No	Yes	No
Cell size	1.2-4.5 µm length, 1.2 µm wide	0.9–1.5 µm length, 0.5–0.9 µm wide*	1.4 µm length, 0.4 µm wide†	1.1 µm length, 0.7 µm wide	1.2 µm length, 0.9 µm wide	1.6-2.4 µm length, 0.4-0.85 µm wide
Colour	Orange	Light yellow	Yellow	Orange	Orange	Light yellow
Catalase	+	+	+	W	+	-
Oxidase	+	+	-	W	+	-
Growth temperature (°C)	4-25	4-30	4-37	4-30	4-30	4-37
pH range	6-9	6-7	5-11	5-10	5-9	5-9
NaCl (%, w/V)	0-1	0	0-3	0-1	0-1	0-2
Enzymatic Activity (API 20NE)						
Indole production	-	-	-	W	-	-
Aesculin hydrolisis	W	-	+	+	+	-
β-galactosidase	+	-	-	W	+	-
Enzymatic Activity (API ZYM)						
Valine arylamidase	W	-	-	W	W	+
Cystein arylamidase	-	-	-	-	-	+
Trypsin	-	W	+	+	-	+
α-chymotrypsin	-	-	-	W	-	-
α-galactosidase	-	-	-	W	W	-
β-galactosidase	+	-	-	-	+	+
β-glucuronidase	-	-	+	-	-	-
α-glucosidase	-	-	W	-	-	+
β-glucosidase	+	-	+	+	+	-
Carbon source utilization (API 20NE)						
Glucose	+	-	+	-	-	-
Arabinose	+	-	+	-	+	-
Mannose	-	-	-	-	-	+
Manitol	+	-	-	-	-	+
N-acetyl-glucosamine	+	-	+	-	-	+
Maltose	+	-	-	-	-	+
Potassium gluconate	W	-	-	-	-	-
Capric acid	-	-	-	-	-	+
Malic acid	W	-	-	-	-	-

Table V.2. Cellular fatty acid composition (%) of strain R4DWN^T and related type strains. Strains: 1, R4DWN^T; 2, *S. fennica* DSM 13665^T; 3, *S. formosensis* DSM 24164^T; 4, *S. prati* DSM 103336^T; 5, *S. montana* DSM 103337^T; 6, *S. oleivorans* HAMBI 3659^T. Data from strains 1, 2 and 3 are from this study, whereas data from 4, 5 and 6 are from the original species description papers [27, 28, 29]. tr, <1.0 %; "-" indicates not detected.

Fatty acid	1	2	3	4	5	6
Saturated						
$C_{14:0}$	1.6	1.1	5.3	tr	tr	tr
$C_{16:0}$	10.3	15.6	12.6	4.5	7.0	14.6
$C_{17:00}$	-	-	-	-	-	1.1
$C_{18:0}$	-	-	1.1	-	tr	tr
Unsaturated						
$C_{16:1}$ *ω5c*	1.2	1.1	4.7	1.9	1.3	tr
$C_{17:1}$ *ω6c*	-	2.8	-	-	tr	14.0
$C_{18:1}$ *ω7c* 11-methyl	3.5	1.5	10.3	1.5	3.1	4.0
$C_{18:1}$ *ω5c*	-	tr	tr	-	1.3	1.0
$C_{18:1}$ *ω6c*	-	-	-	-	-	43.1
$C_{19:0}$ cyclo *ω8c*	-	6.9	tr	-	tr	tr
Hydroxy						
$C_{14:0}$ 2OH	12.0	12.5	8.2	14.9	4.5	11.1
$C_{16:0}$ iso 3OH	1.3	1.0	-	-	-	
$C_{15:0}$ 2OH	-	tr	-	-	-	3.2
$C_{16:0}$ 2OH	-	-	-	1.5	-	1.3
$C_{16:1}$ 2OH				-	1.0	-
$C_{18:0}$ 2OH	-	-	-	1.1	-	-
$C_{18:1}$ 2OH				-	1.3	tr
iso-16:0 3-OH	-	-	-	2.3	1.4	-
Summed features*						
3	21.2	14.7	1.3	48.1	36.7	TR
8	48.9	41.3	54.0	21.9	39.2	-

primers [13]: 8f (5´-AGAGTTTGATCCTGGCTCAG-3´), 1492r (5´-GGTTACCTTGTTACGACTT-3´), 1055f (5´-ATGGCTGTCGTCAGCT-3´), and 341r (5´-CTGCTGCCTCCCGTAGG-3´). The almost complete sequence of the 16S rDNA gene of the isolate was obtained through Sanger Sequencing. The sequence length was of 1,470 base pairs, and it can be accessed in the GenBank/EMBL/DDBJ databases under accession number MK569518. The online SINA (SILVA) tool [14] was used to perform a multiple alignment of the sequences, and the maximum-likelihood (ML) (Figure V.1) and neighbour-joining (NJ) (Supplementary Figure V.1) trees were constructed using RaxML [15] and MEGA6 [16], respectively. The GTR algorithm was used for the ML tree, whereas Kimura 2-parameter model was used for the NJ tree. Reliability of the branch patterns was assessed using bootstrap analyses based on 1000 resamplings. Based on the 16S rRNA sequence analysis, R4DWN^T does not have a clear phylogenetic position within the genus *Sphingomonas*. The closest neighbour is *S. formosensis* in both the ML (Figure V.1) and NJ (Supplementary Figure V.1) trees, whereas *S. fennica* (the closest neighbour according to the 16S rRNA sequencing) appears grouped with *S. oleivorans* forming an external group. Nevertheless, these branches are not supported by high bootstrap values.

The draft genome of strain R4DWN^T was sequenced using MiSeq sequencer (Illumina), and the Nextera XT Prep Kit protocol was used for library preparation. FastQC was utilized to assess the quality of the sequence reads. Genome assembly of 284,541 paired reads was performed using SPAdes 3.12.0 [17]. The draft genome of R4DWN^T consists of 229 contigs yielding a total length of 4,444,219 bp, with a G+C content of 67.9 % and an N50 value of 38,937 bp. This genomic G+C content is in agreement with the closest neighbours and confirms the adscription of R4DWN^T to the genus *Sphingomonas* [10, 11]. The maximum contig length was 136,617 bp, and all the contigs were annotated using the RAST tool kit (RASTtk) integrated in PATRIC v.3.5.41 (https://www.patricbrc.org). A total of 4,455 coding sequences (CDS) were predicted, of which 2,602 were proteins with functional assignments. A total of 45 tRNA and 3 rRNA genes (one single ribosomal operon) were identified. This Whole Genome Shotgun project has been deposited at GenBank/EMBL/DDBJ under the accession VNIM00000000. The version described in this paper is version VNIM01000000. The completeness and levels of contamination of the genome were analyzed with the bioinformatic tool

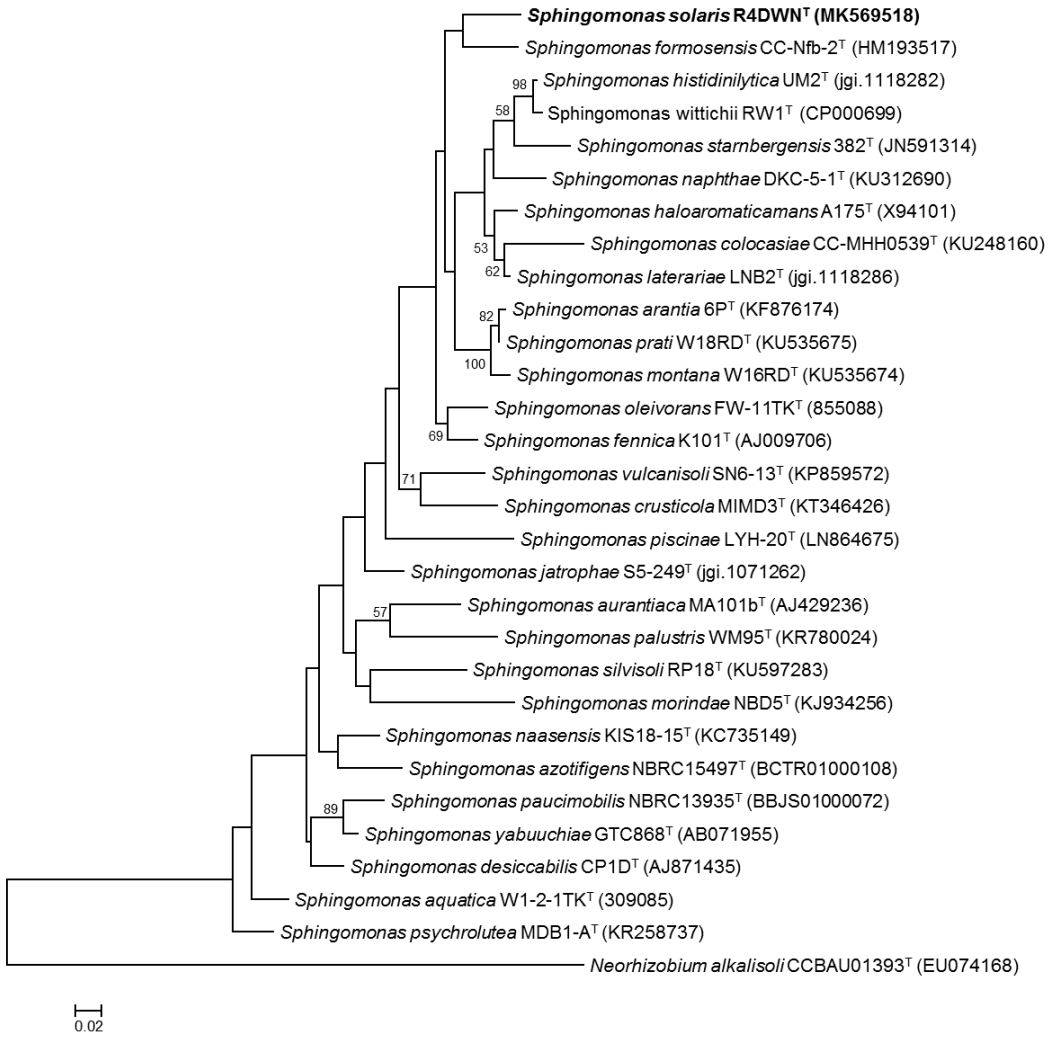

Figure V.1. Maximum-likelihood tree illustrating the phylogenetic position of strain R4DWN^T and related members of the genus *Sphingomonas* based on almost-complete 16S rRNA gene sequences. The optimal evolutionary model of nucleotide substitution applied is GTR. Bar, 0.02 expected nucleotide substitutions per site. *Neorhizobium alkalisoli* was used as outgroup. Only bootstrap values above 50 % are indicated (1000 resamplings) at branchings.

CheckM v1.0.6 [18], revealing values of 99.095 % and 0.603, respectively. Therefore, the draft genome showed enough quality for further analyses [19]. The complete 16S rRNA gene was extracted from this draft genome and, according to the EZBioCloud online tool [4], the closest type strains of R4DWN^T are *Sphingomonas fennica* K101^T*, Sphingomonas formosensis* CC-Nfb-2^T*, , Sphingomonas prati* W18RD^T, *Sphingomonas montana* W16RD^T*,* and *Sphingomonas oleivorans* FW-11^T with 96.3, 96.1, 96.0, 95.9 and 95.7 % of pairwise similarity, respectively. Taking into account that the similarity between R4DWN^T and the closest type strain (*S. fennica*) is lower than 98.7 %, this isolate can be considered a new species [19, 20].

With the purposes of obtaining a more accurate phylogenetic inference of the strain R4DWN^T, a phylogenomic tree based on nucleotidic sequences was generated. The UBCG v. 3.0 pipeline (up-to-date bacterial core gene set) [21] was used to construct a maximum likelihood tree based on a multiple alignment of a set of 92 universal and single copy gene sequences with the tool FastTree v2,10,1 (Figure V.2). According to the phylogenomic tree, the closest neighbor to R4DWN^T is *Sphingomonas montana*, and this is supported by high bootstrap values. *S. fennica* and *S. olveirans,* two of the closest neighbors according to the 16S rRNA sequence, have an external position with regards to the clade formed

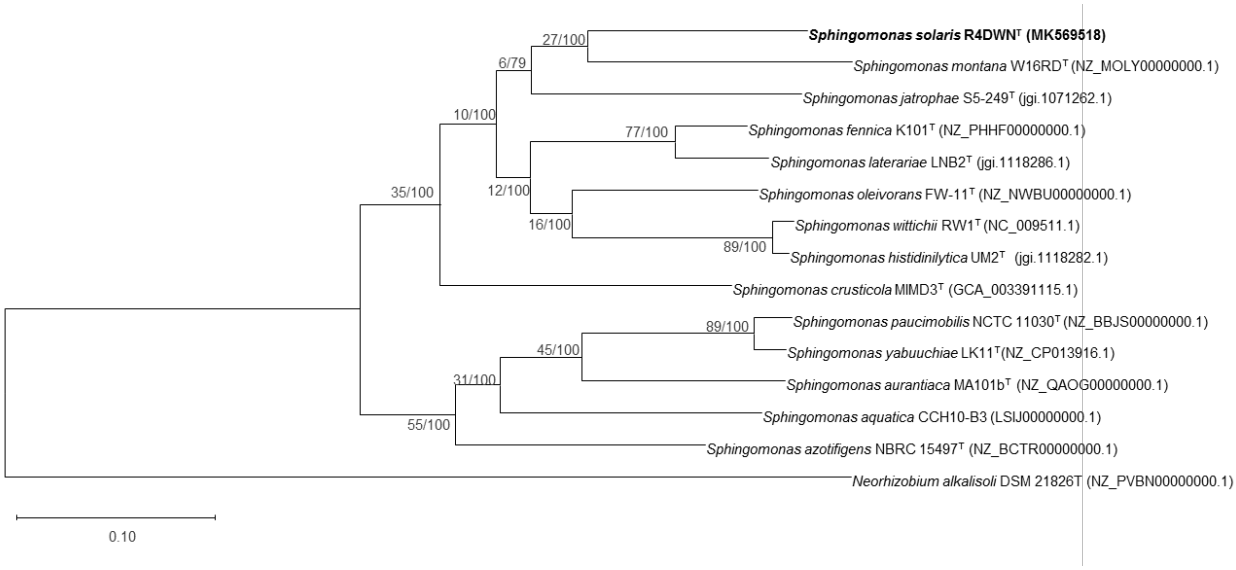

Figure V.2. Phylogenomic tree of strain R4DWN^T. Unrooted maximum-likelihood phylogenetic tree based on a multiple alignment of a set of 92 gene sequences (concatenation of 85 764 nucleotides) from using the ubcg version 3.0 pipeline [21]. Bootstrap analysis was carried out using 100 replications. Gene support indices (max. value 92 genes) and percentage bootstrap values (max. value 100%) are given at branching points. Bar, 0.10 substitutions per position.

by *S. montana* and R4DWN^T, along with other species.

In order to investigate if our isolate belongs to a known species, pairwise average nucleotide identity values (ANIb) [22] were calculated between strain R4DWN^T and its closest type strains, by using the JSpeciesWS online tool [23]. Additionally, digital DNA-DNA hybridization (dDDH) pairwise values were also obtained using the Genome-to-Genome Distance Calculator 2.1 (GGDC) tool [24]. As recommended for incompletely sequenced genomes, formula 2 was used for calculating the digital DDH values [24]. The ANI and digital DDH values between strain R4DWN^T and the type strains of phylogenetically close species were higher than the threshold established to circumscribe prokaryotic species (Supplementary Table V.2), namely 95% for ANI values [25] and 70% for dDDH [24]. Therefore, both genome-related indexes [26] confirmed the adscription of strain R4DWN^T to a hitherto unknown species.

Analysis of the draft genome of strain R4DWN^T allowed to predict its ability to synthesise phosphatidylethanolamine, diphosphatidilglycerol, phosphatidylglycerol, phosphatidylglycerolphosphate and a sphingolipid, due to the presence of genes coding for phosphatidylserine decarboxylase [EC 4.1.1.65], cardiolipin synthase A/B [EC:2.7.8.-], ribosomal-protein-serine acetyltransferase [EC 2.3.1.-], CDP-diacylglycerol-glycerol-3-phosphate 3-phosphatidyltransferase [EC 2.7.8.5], and serine palmitoyl transferase [EC 2.3.1.50]. This polar lipids profile is in agreement with the polar lipid analyses available for other species of the genus *Sphingomonas* with validly published names [10, 11]. As described previously in *Sphingomonas fennica* [10], strain R4DWN^T is not able to synthesize phosphatidylcholine due to the absence of phosphatidylcholine synthase [EC 2.7.8.24], a unique feature of these closely related strains. Furthermore, spermidine synthase [EC 2.5.1.16] was detected in the draft genome of strain R4DWN^T, suggesting that this strain could produce spermidine as the major polyamine. On the other hand, no genes related to homospermidine synthesis were detected. The strain R4DWN^T has all the enzymatic repertory, including the enzymes 2-methoxy-6-polyprenyl-1,4-benzoquinol methylase [EC 2.1.1.201], ubiquinone biosynthesis monooxygenase Coq6 [EC 1.14.13.-] and 3-demethylubiquinol 3-O-methyltransferase [EC 2.1.1.64], to synthetize ubiquinones as the main isoprenoid quinone.

The comparison of the phenotypic, genomic and phylogenetic characteristics of the strain R4DWN^T with those of its closes phylogenetic neighbours revealed that this strain represents a new species

belonging to the genus *Sphingomonas* for which the name of *Sphingomonas solaris* sp. nov. is proposed.

Description of *Sphingomonas solaris* sp. nov.

Sphingomonas solaris [so.la.ris. N.L. fem. adj. *solaris*, pertaining to the sun, referring to the origin of the type strain, isolated from the surface of solar panels].

Cells are gram-negative, non-motile and rod-shaped (1.2-4.5 µm length x 1.2 µm wide). In old cultures, some cells grow in the form of a long rod shape of approximately 30 µm. After 7 days of incubation at 25 °C, colonies are round-shaped, shiny, orange-coloured, convex, and 1 mm in diameter. This species is able to grow between 4 and 25 °C (optimum at 15-25 °C), and tolerates up to 1 % NaCl (w/v), with optimum at 0 % NaCl (w/v). The pH for optimum growth ranges between 6 and 9, and oxidase and catalase tests were positive. Alkaline phosphatase, esterase (C4), esterase lipase (C8), leucine arylamidase, valine arylamidase, acid phosphatase, naphthol-AS-BI-phosphohydrolase, β-galactosidase and β-glucosidase activities are detected, whereas lipase (C14), cystine arylamidase, trypsin, α-chymotrypsin, α-galactosidase, β-glucuronidase, α-glucosidase, N-acetyl-beta-glucosaminidase, α-mannosidase and α-fucosidase activities are not detected. Using API 20NE, this species is positive for the assimilation of glucose, arabinose, mannitol, N-acetyl-glucosamine, maltose; weak for the assimilation of potassium gluconate and malic acid, and negative for the assimilation of mannose, capric acid, adipic acid, trisodium citrate and phenylacetic acid. Using BIOLOG GENIII MicroPlates, this species is positive for the utilization of glucuronamide, acetoacetic acid, D-fructose-6-PO4 and L-malic acid; weakly positive for the utilization of L-galactonic acid lactone, β-hydroxy-D,L-butyric acid and D-glucose-6-PO4; and negative for the utilization of D-raffinose, α-D-glucose, D-sorbitol, gelatin, pectin, p-hydroxy-phenylacetic acid, tween 40, dextrin, α-D-lactose, D-mannose, D-mannitol, glycyl-L-proline, D-galacturonic acid, methyl pyruvate, ɣ-amino-butyric acid, D-maltose, D-melibiose, D-fructose, D-arabitol, L-alanine, D-lactic acid methyl ester, α-hydroxy-butyric acid, D-trehalose, β-methyl-D-glucoside, D-galactose, myo-inositol, L-arginine, D-gluconic acid, L-lactic acid, D-cellobiose, D-salicin, 3-methyl glucose, glycerol, L-aspartic acid, D-glucuronic acid, citric acid, α-keto-butyric acid, gentiobiose, N-acetyl-D-glucosamine, D-fucose, L-glutamic acid, α-keto-glutaric acid, sucrose, N-acetyl-β-D-mannosamine, L-fucose, L-histidine, mucic acid, D-malic acid, propionic acid, D-turanose, N-acetyl-D-galactosamine, L-rhamnose, D-aspartic acid, L-pyroglutamic acid, quinic acid, acetic acid, stachyose, N-acetyl neuraminic acid, inosine, D-serine, L-serine, D-saccharic acid, bromo-succinic acid and formic acid. The major fatty acids are $C_{18:1}$ *ω7c*/$C_{18:1}$ *ω6c*, $C_{16:1}$ *ω7c*/$C_{16:1}$ *ω6c*, $C_{14:0}$ 2OH and $C_{16:0}$. The type strain is R4DWN^T (= CECT 9811^T = LMG 31344^T), isolated from the surface of a solar panel in Boston, MA, USA. The GenBank/EMBL/DDBJ accession number for the 16S rRNA gene sequence of strain R4DWN^T is MK569518, and the genome accession number is VNIM00000000. The genomic G+C content of the type strain is 67.9 %.

Funding

Financial support from the Real Colegio Complutense at Harvard University (Visiting Research Fellowship) is acknowledged. Kristie Tanner is a recipient of a Doctorado Industrial fellowship from the Ministerio de Ciencia, Innovación y Universidades (Spain), with reference DI-16-08976. Financial support from Spanish Government (grant Helios. reference: BIO2015-66960-C3-1-R co-financed by FEDER funds and Ministerio de Economía y Competitividad) is acknowledged. This work was supported by DARPA BRICS grants HR0011-15-C-0091 and HR0011-18-2-0014 (to A.S.K.) and IARPA FELIX grant N66001-18-C-4503 (to A.S.K.). A.S.K. also acknowledges funding from the NIH Director's New Innovator Award (1DP2AI131083-01) and an NSF CAREER Award (MCB-1350949).

Acknowledgements

We acknowledge the Arnold Arboretum of Harvard University for providing access to the solar panels sampled in this project. We thank Manuel Porcar for his help in writing this manuscript and his continuous support throughout this project.

Conflict of interest statement: The authors declare that there are no conflicts of interest.

Ethical statement: This research did not contain any studies with humans or animals performed by any of the authors.

References

[1] Yabuuchi E, Yano I, Oyaizu H, Hashimoto Y, Ezaki T, *et al*. Proposals of *Sphingomonas paucimobilis* gen. nov. and comb. nov., *Sphingomonas parapaucimobilis* sp. nov., *Sphingomonas yanoikuyae* sp. nov., *Sphingomonas adhaesiva* sp. nov., *Sphingomonas capsulata* comb. nov., and two genospecies of the genus *Sphingomonas*. *Microbiol Immunol* 1990;34:99-119.

[2] Takeuchi M, Sawada H, Oyaizu H, Yokota A. Phylogenetic evidence for Sphingomonas and Rhizomonas as nonphotosynthetic members of the alpha-4 subclass of the Proteobacteria. *Int J Syst Evol Microbiol* 1994;44:308-314.

[3] White DC, Sutton SD, Ringelberg DB. The genus *Sphingomonas*: physiology and ecology. *Curr Opin Biotechnol* 1996;7:301-306.

[4] Yoon SH, Ha SM, Kwon S, Lim J, Kim Y, *et al*. Introducing EzBioCloud: A taxonomically united database of 16S rRNA and whole genome assemblies. *Int J Syst Evol Microbiol* 2017;67:1613-1617.

[5] Zhao Q, Yue S, Bilal M, Hu H, Wang W, *et al*. Comparative genomic analysis of 26 *Sphingomonas* and *Sphingobium* strains: Dissemination of bioremediation capabilities, biodegradation potential and horizontal gene transfer. *Sci Total Environ* 2017;609:1238-1247.

[6] Fujiwara H, Soda S, Fujita M, Ike M. Kinetics of bisphenol A degradation by *Sphingomonas paucimobilis* FJ-4. *J Biosci Bioeng* 2016;122:341-344.

[7] Waigi MG, Sun K, Gao Y. Sphingomonads in microbe-assisted phytoremediation: tackling soil pollution. *Trends Biotechnol* 2017;35:883-899.

[8] Sasser M (1990). Identification of bacteria by gas chromatography of cellular fatty acids, MIDI Technical Note 101. Newark: DE: MIDI Inc

[9] MIDI (2008). Sherlock Microbial Identification System Operating Manual, version 6.1. Newark, DE: MIDI Inc.

[10] Wittich R, Busse H, Kämpfer P, Macedo A, Tiirola M, *et al*. *Sphingomonas fennica* sp. nov. and *Sphingomonas haloaromaticans* sp. nov., outliers of the genus *Sphingomonas. Int J Syst Evol Microbiol* 2007;57:1740-1746.

[11] Lin S, Shen F, Lai W, Zhu Z, Chen W, *et al. Sphingomonas formosensis* sp. nov., a polycyclic aromatic hydrocarbon-degrading bacterium isolated from agricultural soil. *In J Syst Evol Microbiol* 2012;62:1581-1586.

[12] Latorre A, Moya A, Ayala F. Evolution of mitochondrial DNA in *Drosophila subobscura*. *P Natl Acad Sci* 1986;83:8649–53.

[13] Pascual J, Wüst PK, Geppert A, Foesel BU, Huber KJ, *et al*. Novel isolates double the number of chemotrophic species and allow the first description of higher taxa in Acidobacteria subdivision 4. *Syst Appl Microbiol* 2015;38:531-544.

[14] Pruesse E, Peplies J, Glöckner FO. SINA: Accurate high-throughput multiple sequence alignment of ribosomal RNA genes. *Bioinformatics* 2012;28:18123-1829.

[15] Kozlov AM, Darriba D, Flouri T, Morel B, Stamatakis A. RAxML-NG: A fast, scalable, and user-friendly tool for maximum likelihood phylogenetic inference. bioRxiv 2018; doi:10.1101/447110

[16] Tamura K, Stecher G, Peterson D, Filipski A, Kumar S. MEGA6: Molecular Evolutionary Genetics Analysis version 6.0. *Mol Biol Evol* 2013;12:2725-2729.

[17] Nurk S, Bankevich A, Antipov D, Gurevich A, Korobeynikov A *et al*. Assembling genomes and mini-metagenomes from highly chimeric reads. In Annual International Conference on Research in Computational Molecular Biology 2013; pp. 158-170. Springer, Berlin, Heidelberg.

[18] Parks DH, Imelfort M, Skennerton CT, Hugenholtz P, Tyson GW. Assessing the quality of microbial genomes recovered from isolates, single cells, and metagenomes. *Genome Res* 2014; 25:1043–1055

[19] Chun J, Oren A, Ventosa A, Christensen H, Arahal DR *et al*. Proposed minimal standards for the use of genome data for the taxonomy of prokaryotes. *Int J Syst Evol Microbiol* 2018;68:461–466.

[20] Kim M, Oh HS, Park SC, Chun J. Towards a taxonomic coherence between average nucleotide identity and 16S rRNA gene sequence similarity for species demarcation of prokaryotes. *Int J Syst Evol Microbiol* 2014;64:346–351.

[21] Na SI, Kim YO, Yoon SH, Ha SM, Baek I, *et al*. UBCG: Up-to-date bacterial core gene set and pipeline for phylogenomic tree reconstruction. *J Microbiol.* 2018;56:280 –285.

[22] Goris J, Konstantinidis KT, Klappenbach JA, Coenye T, Vandamme P, *et al*. DNA–DNA hybridization values and their relationship to whole-genome sequence similarities. *Int J Syst Evol Microbiol* 2007;57:81–91.

[23] Richter M, Rosselló-Mora R, Glöckner FO, Peplies J. JSpeciesWS: a web server for prokaryotic species

circumscription based on pairwise genome comparison. *Bioinformatics* 2015; pii: btv681.

[24] Meier-Kolthoff JP, Auch AF, Klenk HP, Göker M. Genome sequence-based species delimitation with confidence intervals and improved distance functions. *BMC Bioinformatics* 2013;14:60.

[25] Richter M, Rosselló-Mora R. Shifting the genomic gold standard for the prokaryotic species definition. *Proc Natl Acad Sci U S A* 2009;106:19126–19131.

[26] Chun J, Rainey FA. Integrating genomics into the taxonomy and systematics of the Bacteria and Archaea. *Int J Syst Evol Microbiol* 2014;64:316–324.

[27] Manandhar P, Zhang G, Hu Y, Lama A, Gao F, *et al*. *Sphingomonas prati* sp. nov., isolated from alpine meadow soil. *Int J Syst Evol Microbiol* 2016;66:4269-4275.

[28] Manandhar P, Zhang G, Lama A, Liu F, Hu Y. *Sphingomoans montana* sp. nov., isolated from a soil sample from the Tanggula Mountain in the Qinghai Tibetan Plateau. *Antonie van Leeuwenhoek* 2017;110:1659-1668.

[29] Chen L, Chen WF, Xu ZL, Li W, Zhang XY, et al. *Sphingomonas oleivorans* sp. nov., isolated from oil-contaminated soil. *Int J Syst Evol Microbiol* 2018;68:3720-3725.

General Results and Discussion

1. The taxonomic core of the solar panel microbiota

Solar panel surfaces are extreme environments (exposed to UV-radiation, desiccation, temperature fluctuations, and nutrient limitation) that are inhabited by a suprising diversity of stress-adapted microorganisms. The standard structure and orientation (equator-facing) of solar panels all over the world, and their inert bidimentional surfaces, make them a proxy of the harshest natural sun-exposed environments. The use of artificial devices for the study of surface-inhabiting microbial communities has previously been described, for example, in artificial phyllosphere (plant surface) studies (Doan and Leveau, 2015). These artificial phyllospheres include from more complex microstructured surfaces, to more simple surfaces such as nutrient agar, inert surfaces (i.e. stainless steel), or even plastic plants (Ottesen et al., 2016; Soffe et al., 2019). In the latter case, the study revealed that there was a high level of shared taxonomy between the live tomato plants and the adjacent inanimate controls, suggesting that environmental forces play an important role in the introduction of microbes on plant surfaces (Ottesen et al., 2016).

A similar conclusion has been drawn in the present study when analyzing the communities inhabiting solar panel surfaces from distant geographical locations, namely, Berkeley (California, USA), Valencia (Spain), Tromsø (Norway) and the Antarctic islands Deception and Livingston. Despite the physical distance between these solar panels, microbial communities inhabiting their surfaces proved to be very similar in both taxonomic and, especially, functional terms (Figure I.2; Figure II.4; Figure II.5), with the most abundant phyla being *Actinobacteria, Bacteroidetes, Deinococcus, Cyanobacteria, Firmicutes, Proteobacteria* and *Ascomycota* (Figure I.2; Figure II.3, Figure II.4, Figure III.1).

Interestingly, the comparison of the most abundant genera from each study has revealed that several taxa are shared among all the geographical locations (Figure 3). Furthermore, this analysis includes the microbial communities

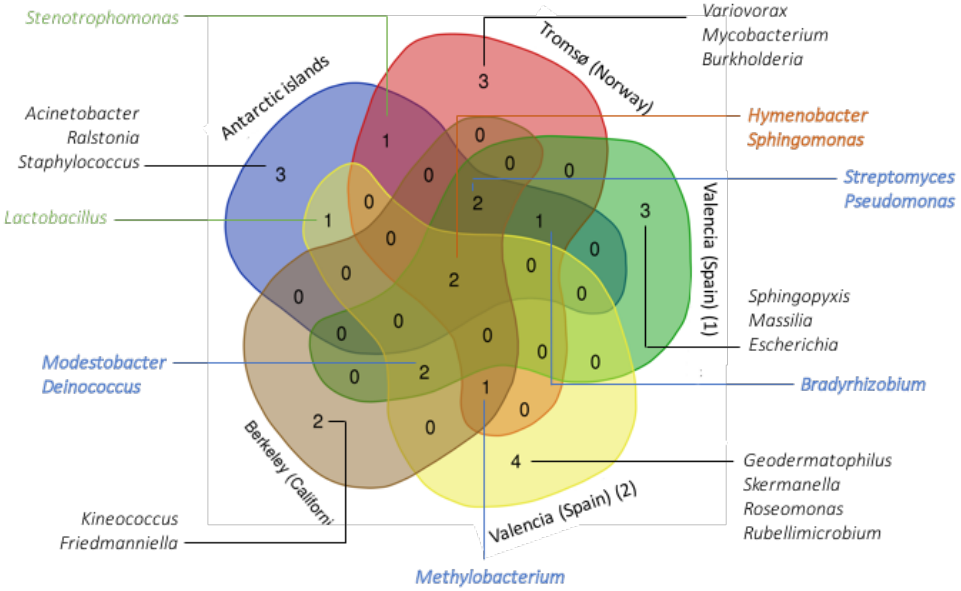

Figure 3. Venn diagram representing the 9-10 most abundant genera inhabiting solar panel surfaces in: Tromsø (Norway) and the Antarctic islands Deception and Livingston (Publication I); Berkeley, California, USA (Publication II); and in Valencia, Spain, with data from Dorado-Morales et al, 2016 reprsented in Valencia (Spain) (1), and data from Publication III represented in Valencia (Spain) (2). Genera in orange are present in all locations, genera in blue are present in 4/5 samples, genera in green are present in 2 samples, and genera in black are exclusive to one location.

previously described by Dorado-Morales et al. (2016), in which the surfaces of solar panels from Valencia were analysed for the first time, represented in Figure 3 as 'Valencia (Spain) (1)'. The genera *Hymenobacter* and *Sphingomonas* are present among the most abundant taxa in all locations, whereas the genera *Streptomyces, Pseudomonas, Bradyrhizobium, Methylobacterium, Modestobacter* and *Deinococcus* are among the most abundant taxa present in 4 out of the 5 locations sampled (Figure 3), suggesting that there is a microbial core on solar panel surfaces composed by these 8 genera.

2. Stress resistance properties on sun-exposed surfaces

The most abundant genera on solar panel surfaces are characterized for their stress resistant properties. Members of the genera *Deinococcus* and *Hymenobacter* show high levels of resistance to both gamma and UV radiation (Rainey et al., 2005; Batista 1997; Maeng et al., 2020). In fact, environmental exposure appears to facilitate adaptation. In the study by Rainey et al. (2005), microorganisms isolated from desert soil survived doses of up to 30 kGy of radiation, while no isolates were recovered from nonarid forest soil after doses larger than 13 kGy. *Sphingomonas* (a biofilm-forming, xenobiotic-degrader and EPS-producing genus) and *Methylobacterium* produce carotenoids, are very resistant to desiccation and UV light, and can thrive at a wide range of temperatures (Lee et al., 2014; Grube et al., 2009; Csotonyi et al., 2010). Members of the genera *Pseudomonas* and *Modestobacter* thrive on UV-exposed surfaces (Franklin et al., 2005; Alonso-Sáez et al., 2006; Santos et al., 2012; Normand et al., 2012), whereas members of the genus *Streptomyces* and *Bradyrhizobium*, found predominantly in soil and the rhizosphere, respectively, have been described to tolerate dehydration (Orellana *et al.,* 2018; Sugawara et al., 2010; Jeon et al., 2015).

In the present work, representatives of several microbial genera (many of them, pigmented) have been isolated from solar panel surfaces, and their stress-resistant properties have been assessed. Members of the genera *Rhodotorula, Deinococcus, Hymenobacter, Arthrobacter* and *Cryptococcus* and, to a lesser extent, *Alcaligenes, Sphingomonas, Dioszegia, Curtobacterium* and *Microbacterium*, displayed UV-resistance (Figure I.1.C; Figure II.2B). On the other hand, almost all of the strains isolated from the polar solar panels were able to resist desiccation (Figure I.1.C), whereas only *Methylobacterium* and *Arthrobacter* isolated from Berkeley (California, USA) were able to survive desiccation under our experimental conditions (Figure II.2C).

Multi-omic analysis (metagenomics and metabolomics) in the present study revealed some of the stress-resistance mechanisms present in these microbial communities. Specifically, pathways involved in the persistence of microbes on solar panels surfaces (i.e. stress response, capsule development, metabolite repair heat shock chaperone proteins) were detected, as well as genes for carotenoid biosynthesis and other mechanisms to combat oxidative stress (i.e. superoxide dismutases and peroxidases) (Figure II.5). Furthermore, metabolomics analysis revealed the presence of compatible solutes (i.e. ectoine, sugar alcohols, di- and tri-saccharides), that may play a role in protection against desiccation, heat and/or UV-stress (II.6). In the work by Dorado-Morales et al. (2016), additional stress-resistance mechanisms were detected through metagenomic and metaproteomic analysis, including membrane-bound proton-translocating pyrophosphatase (mPP), heat- and cold-shock proteins, S-layer proteins, lipoproteins and biofilm formation. Together, these studies have allowed to gain insight on the stress-resistance profiles of these microbial communities (Figure 4).

Other sun-exposed environments share similarities with solar panel surfaces in terms of dominant environmental stresses and most abundant microbial taxa. For example, a recent study described that *Hymenobacter*, *Sphingomonas* and *Rhizobiales* are among the core phyllosphere microbiome across distant populations of the tea tree *Leptospermum scoparium*, indigenous to New Zealand (Noble et al., 2020). Furthermore, in the study by Ottesen et al. (2016), the three most abundant taxa in the phyllosphere of both the live plants and their inanimate controls were *Pseudomonas, Erwinia* and *Sphingomonas.* It is important to stress that, in fact, plant leaves are biological 'solar panels' that share some of the ecological conditions of

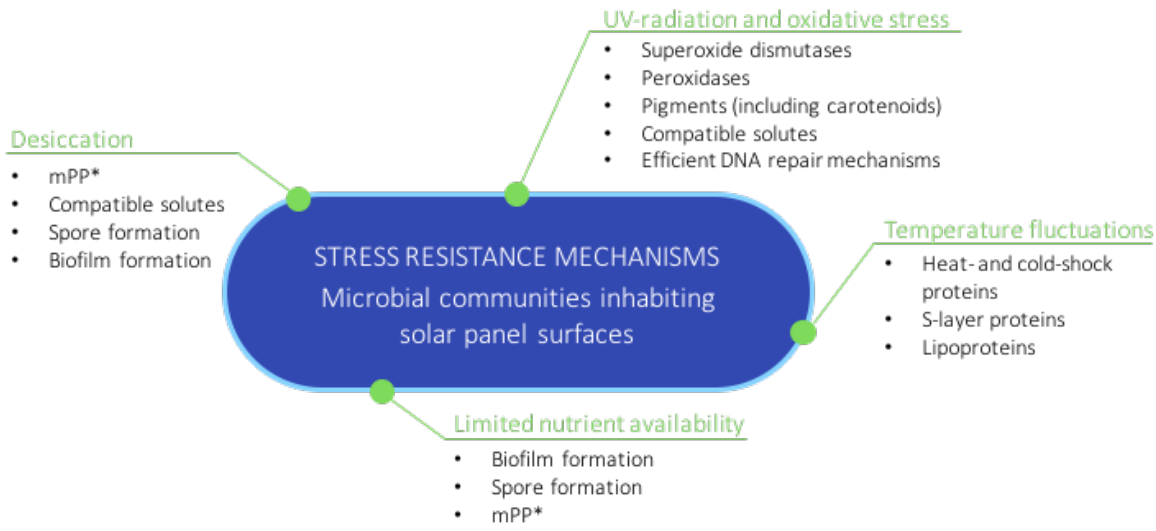

Figure 4. Stress resistance mechanisms in the microbial communities inhabiting solar panel surfaces as described in Publication II and in the publication by Dorado-Morales et al. (2016). *Membrane-bound proton-translocating pyrophosphatase

artificial, photovoltaic devices. On the other hand, surface microlayers are inhabited by bacterioneuston and located at the air-water interface, where availability of organic matter, UV radiation and wind speed have been suggested to influence the community composition (Zäncker et al., 2018; Santos et al., 2012; Santos et al., 2014). Previous studies have revealed a high similarity between bacterioneuston and airborne bacteria, supporting the hypothesis that airborne inputs can be an important source of bacteria for surface environments (Hervas and Casamayor, 2009), and *Pseudomonas* has been described to be among the most abundant genera in freshwater bacterioneuston (Azevedo et al., 2012). Regarding desertic regions, the radiation- and desiccation-tolerant genera *Deinococcus* and *Rubrobacter* have been found to dominate the soil biota of McKelvey Valley, one of the coldest hyperarid deserts on Earth located in Artarctic (Pointing et al., 2009). Furthermore, taking into account the whole microbial community analysed through high-throughput sequencing (not only the most abundant taxa) and including higher taxonomic levels (i.e. phylum), the previous study by Dorado-Morales et al. (2016) reported that surface environments, including solar panels, deserts, polar microbial mats and phyllobiomes, show low phyllogenomic distance and are clearly divergent from non-surface-associated environments such as human, marine sediments or rainforest soil.

A report by Gibbons (2017) stressed on the importance of the functional, rather than taxonomic, component in the establishment of microbiomes. Nevertheless, the results obtained in the present work show that there are not only common adaptations, but also taxonomic similarities among the microbial communities inhabiting solar panels from distant geographical regions (Publication I and II). The strong selective pressure under which surface microbial communities have to survive and the ease of spread of airborne bacterial communities (Griffin, 2007; Speth et al., 2012) make it tempting to hypothesize that a "taxonomic and functional surface biome" partially conserved among all superficial locations exists. In this sense, the Earth surface and, more specifically, the sun-adapted upper part of the biosphere, could be considered as a world-wide biome by its own, the so-called *Hymenosphere* (Porcar et al., manuscript in preparation).

3. Colonizing solar panel surfaces

Despite the fact that the microbial communities inhabiting solar panel surfaces are largely conserved, these communities do display seasonal variations. In particular, bacteria and fungi display a higher relative abundance during the spring/summer and the autumn/winter periods, respectively (Publication III). This is likely linked to higher levels of *soiling* in the low rainfall periods (spring/summer), and higher moisture levels

during the typically rainy Mediterranean autumn/winter period. Even with these seasonal variations, a clear transition has been observed in the present work from a more generalistic community at the beginning of the colonization experiment, to a more specialized community composed of highly resistant bacterial and fungal genera. This supports the hypothesis that the strong selection pressures that characterize these surfaces are what shape the microbial community. According to our results, members of the *Sphingomonas* genus (one of the core taxa of this microbial community, as previously described) are the first to arrive on solar panel surfaces. This taxon may play a crucial role in establishing the subaerial biofilm due to its ability to secrete EPS and to resist UV radiation and desiccation (Bereschenko et al., 2010; Venugopalan et al., 2005). After 24 months, the most abundant taxa detected on these surfaces were *Modestobacter*, *Deinococcus*, *Sphingomonas*, *Hymenobacter*, *Rubellimicrobium* and *Methylobacterium*, with *Deinococcus, Hymenobacter* and *Roseomonas* displaying a significative increase in abundance throughout time (Table III.1; Figure III.3), coinciding with the most abundant taxa observed on the solar panels analysed in the present work (Publications I and II). In fact, *Deinococcus* and *Hymenobacter* have been proposed as biomarkers for desert airborne bacteria (Meola et al., 2015), suggesting that airborne transport of dust particles from deserts could be a possible source of the microorganisms that inhabit solar panel surfaces.

Regarding fungal colonization of the solar panel surfaces in Valencia (Spain), several genera (*Neocatenulostroma*, *Symmetrospora*, *Sporobolomyces* and *Comoclathris*) displayed a significant increase throughout time, although the most abundant genus by far was *Alternaria.* This could be explained by the abundance of species within the *Alternaria* genus that are able to produce melanin, a pigment that confers protection against UV-radiation and other environmental stressors (Kawamura et al., 1999; Tseng et al., 2011). This result is consistent with the observation by Shirakawa et al. (2015), in which melanized *Ascomycetes* dominated the subaerial biofilms located on solar panel surfaces. In fact, *Ascomycetes* were also among the most abundant fungi on the solar panel surfaces in Tromsø, Antarctica and Berkeley, California. Indeed, fungi are great candidates to live on surfaces as they have an absorptive nutrition mode and they can form biofilms when they grow on surfaces (Harding et al., 2009).

According to our results, the establishment of a solar panel surface microbiota does not affect solar panel efficiency (measured as open circuit voltage), as this parameter did not tend to decrease throughout the 24-month period we analyzed (Figure III.1). Nevertheless, seasonal fluctuations in efficiency were observed, with a reduced efficiency in the summer periods. We hypothesize that this is due to a combination of high temperatures (previously reported to reduce solar panel efficiency) and soiling (Omubo-Pepple et al., 2009; Skoplaki and Palyvos, 2009). In fact, cleaning the solar panels with water or Virkon led to a slight increase in efficiency. Interestingly, although cleaning with Virkon resulted in an alteration of the microbial community composition (i.e. a decrease in the abundance of *Deinococcus*), cleaning with water did not (Figure III.5). This could provide an explanation regarding the stability observed in the composition of the microbial communities inhabiting solar panel surfaces (Publications I and II): although rainfall (cleaning with water being a proxy of this) reduces soiling, it may not be enough to disrupt the microbial community inhabiting solar panel surfaces.

4. Bioprospecting the solar panel microbiota

Extreme and unusual environments, such as solar panel surfaces, can act as sources of industrially-relevant microorganisms that are pre-adapted to harsh microbial conditions. In fact, several of the genera isolated in pure culture in the present study display potential applications in industry, including production of enzymes, production of antioxidant pigments (including carotenoids), bioremediation, plant growth promotion, or as biocontrol agents (Table 2, Publication IV). Nevertheless, it must be noted that despite the high temperatures reached on solar panel surfaces (temperatures of up to 50 °C have been recorded), most of the isolated microorganisms grew well between 4 and 30 °C, only a fraction of them grew well at 37 °C, and no growth was

Table 2. Potential applications of some of the microbial genera isolated in the present work.

Genus	Potential applications	Referencias
Alcaligenes	Biocontrol of plant and fish pathogens, enzyme production (i.e. nitrilase, amidase, laccase, chitinase), biorremediation (n-octane, toluene, xylene, mineral oils and crude oil, ammonium-rich wastewater, polychlorinated biphenyl congeners), plant growth promotion	Yokoyama et al., 2013; Liu et al., 2014; Mishra et al., 2016; Mehandia et al., 2019; Toledo & Calvo et al., 2008; Zhao et al., 2017; Annamalai et al., 2011; Salimizadeh et al., 2018; Mastan et al., 2020; Annamali et al., 2011
Arthrobacter	Biorremediation (i.e. degradatino of atrazine, nicotine, acrylamide, terbuthylazine, bisphenols), enzyme production (i.e. urease, chndroitin AC exolyase, hyaluronate lyase, α-Amylase), plant growth promotion, pigment production	Zhao et al., 2018; Rajendran et al., 2019; Ruan et al., 2018; Xu et al., 2018; Afra et al., 2017; Chen et al., 2019; Bedade & Singhal, 2017; Zhu et al., 2017; Viegas et al., 2019; Kim et al., 2017; Ren et al., 2016
Bacillus	Biopesticides, enzyme production (i.e. proteases, phytases), probiotics, fermented food production, cellular factories, plant growth promotion, inhibition of fungal and bacterial growth, biosurfactant production	Melo et al., 2014; Contesini et al., 2018; Jeżewska-Frąckowiak et al., 2018; Kimura & Yokoyama, 2019; Gu et al., 2018; Lopes et al., 2018; Ye et al., 2018; Fu et al., 2008; Jemil et al., 2016
Curtobacterium	Plant growth promotion, olefin synthesis	Irizarry & White, 2017; Surget et al., 2020; Bulgari et al., 2014
Deinococcus	Resistant chassis cells for industrial biotechnology, stress resistant enzyme production (i.e. UV-resistant manganese superoxide dismutase for skin care applications or thermostable lipases)	Jin et al., 2019; Gerber et al., 2015; Palmieri et al., 2019; Shao & Yan, 2014
Glutamicibacter	Enzyme production (i.e. carboxymethyl cellulase for lignocellulosic waste biomass saccharification), exopolysaccharide production, plant growth promotion, biorremediation (i.e. phenol biodegradation), olefin biosynthesis	Aarti et al., 2018; Xiong et al., 2020; Duraisamy et al., 2020; Surger et al., 2020
Hymenobacter	Source of novel photolyases, biorremediatino (i.e. degradation of imidacloprid)	Marizcurrena et al., 2017; Guo et al., 2014
Methylobacterium	Use of methanol to generate added-value products, biorremediation (i.e. degradation of formaldehyde), plant growth promotion	Ochsner et al., 2015; Shao et al., 2019; Kwak et al., 2014
Microbacterium	Enzyme production (i.e. mannanase, enolase, metalloprotease, polysaccaride bioflocculants, manganese oxides), antifungal activity, in situ biorremediation (i.e. sulfamethoxazole and other sulfonamides, hexavalent chromium, benzo(a)pyrene, iprodione), antioxidant pigment production	Purohit & Yadav, 2020; Logeshwaran et al., 2020; Saggu et al., 2019; Savi et al., 2019; Fenu et al., 2015; Liu et al., 2017; Sarkar et al., 2016; Jayaraman et al., 2020; Qin et al., 2017; Liang et al., 2017; Cao et al., 2018
Planomicrobium	Biorremediation (i.e. degradation of high melting explosive, diesel oil), plant growth promotion, production of alginate lyase	Nagar et al., 2018; Sahid et al., 2018; Das & Tiwary et al., 2013; Wang et al., 2017
Rhodobacter	Lycogen production (an anti-oxidant and anti-inflammatory compound), biorremediation (i.e. removal of cadmium and zinc from contaminated soils), exopolysaccharide production	Wang et al., 2018; Peng et al., 2018; Govarthanan et al., 2019
Rhodococcus	Biorremediation, (i.e. degradation of hydrocarbons, plasticizer compounds. Aflatoxin B1, zearalenone, arsenite, diesel oil, steroids), biocatalytic production of high-value chemicals from low-value materials, enzyme production (i.e. DyP type peroxidase), biosynthesis activities (i.e. production of biosurfactants, bioflocculants, carotenoids, triacyglycerols, siderophores, antimicrobials, among others)	Kim et al., 2018; Sahinkaya et al., 2019; Busch et al., 2019; Kuyukina et al., 2015; Zampolli et al., 2019; Risa et al., 2018; Retamal-Morales et al., 2018; Cappelletti et al., 2020; Kumari et al., 2019; Kis et al., 2017; Ye et al., 2019
Sanguibacter	Cold-active chitinase production	Tao et al., 2006; Han et al., 2011
Sphingomonas	Enzyme production (i.e. β-xylosidase, dehydrogenase, alginate lyase, chitinase, chitosanase), exopolysaccharide production (i.e. sphingans), biorremediation (i.e. degradation of fungicides, acetochlor, fenvalerate, pentachlorophenol, phenanthrene), plant growth promotion, antioxidant pigment production	Li et al., 2018; Beer et al., 2018; Fialho et al., 2008; He et al., 2018; Perruchon et al., 2016; Luo et al., 2019; Wang et al., 2018; Jayaraman et al., 2020; Yu et al., 2013; Yang et al., 2006; Zhao et al., 2008; Zhu et al., 2007

observed when the isolates were incubated at 50 °C, suggesting that these isolates are thermotolerant but not thermophilic (Figure I.1C).

In particular, the antioxidant properties of solar panel isolates were assessed in the present work using an *in vivo* model base on *C. elegans.* As previously mentioned, the use of high-throughput screening strategies is key for en efficient bioprospecting process, as it allows to assess the biological activity of a large number of isolates at a time. For this reason, a high-throughput oxidative stress assay was performed using the WMicrotracker-One™ device (PhylumTech, Santa Fe, Argentina). This device allows the automatic detection of survival in *C. elegans* worms, a step that is usually performed manually in oxidative stress assays and that requires a substantial investment of time. This assay revealed that *Arthrobacter* sp. (PS47), *Planomicrobium* sp. (PS1), *Bacillus aryabhattai* (PS83), *Bacillus megaterium* (PS75), *Rhodobacter maris* (PS21) and *Curtobacterium* sp. (PS20) were the isolates with the highest antioxidant activity among the 14 tested isolates (Table IV.1; Figure IV.1A and B). The antioxidant activity of PS1, PS21 and PS75 was confirmed with a manual oxidative stress assay, in which *C. elegans* was incubated with hydrogen peroxide and survival was determined manually (Figure IV.1C). Furthermore, these three isolates also displayed UV-protection properties, as determined through analyzing the survival of *C. elegans* when fed with these microbial strains and irradiated with UV light (Figure IV.2).

When isolating cultivable microorganisms from the solar panels sampled in this work, a large fraction of them displayed an orange/yellow/red pigmentation (Publications I, II and IV). Although there are several pigments that display reddish-yellow pigmentation (i.e. the red pigment prodigiosin or the yellow-green scytonemin), these colours are often due to carotenoid production. In the present work, the abundance of microbial isolates displaying this type of pigmentation, the identification and quantification through HPLC of the carotenoids produced by several microbial strains, and the detection of carotenoid biosynthesis genes through metagenomics analysis (Publication II) suggests that carotenoids are widespread among these microbial communities and may play an essential role in UV-protection on solar panel surfaces.

In particular, we hypothesize that the carotenoid content of the antioxidant isolates studied in Publication IV (phytoene, β-cryptoxathin and phytofluene in PS1; canthaxanthin, astaxanthin, β-carotene, adonirubin and phytoene in PS21; and unidentified carotenoids in PS75) could partially explain the antioxidant and UV-protecting effects observed in *C. elegans* (Figure IV.3). The antioxidant and free radical scavenging properties of coloured carotenoids has been extensively studied in the past (Ni et al.,2014; Sandmann et al., 2015), whereas colourless carotenoids have lacked attention and are of special interest due to their abundance in these microbial strains (i.e. phytoene and phytofluene). It has been demonstrated that phytoene and phytofluene posses free radical scavenging properties, although these are lower than those of coloured carotenoids (Martínez et al., 2014). It would be very interesting to consider whether the high antioxidant capacity of PS1 could be related to the presence of phytoene together with the coloured carotenoid, β-cryptoxanthin.

5. Unexplored environments as a source of novel microbial species

Solar panel surfaces harbor bacteria that haven't been studied up to date and that can, in fact, be identified as new microbial species. This is the case, for example, of the orange-coloured *Sphingomonas solaris* R4DWN sp. nov. described in the present work and isolated from a solar panel surface in Boston (Massachusetts, USA). Interestingly, the *Sphingomonas* genus is not only a member of the core taxa inhabiting solar panels, but is also one of the first to arrive during the colonization of these surfaces (Publications I, II and III). Carbon-assimilation assays revealed that this strain is only able to assimilate 7 out of the 71 tested carbon sources, far less than the closest type species *S. fennica* DSM 13665^T and *S. formosensis* DSM 24164^T, able to assimilate 19 and 39 out of the 71 tested sources (Table V.1). *S. fennica* DSM 13665^T was originally isolated from a Dutch drinking water well (Wittich et al., 2007),

whereas *S. formosensis* DSM 24164^T was isolated from agricultural soil and displayed polycyclic aromatic hydrocarbon-degrading properties (Lin et al., 2012). It is possible the the larger availability of nutrients in these environments in comparison to solar panel surfaces shaped these strains to be able to assimilate a larger variety of carbon sources.

Sphingomonas solaris R4DWN is only one of the many potential new species isolated from solar panel surfaces during the present work. According to a publication by Kim et al. (2014), a 16S rRNA gene sequence similarity lower than 98.65 % can be considered the threshold for differentiating two species. With this threshold in mind, 12 out of the 68 strains isolated in Publication IV are potential new species (Supplementary Table IV.1), whereas 5 out of the 40 strains isolated from solar panel surfaces in Boston (Publication V), are also potential new species (Supplementary Table V.3). It must be noted that this % of similarity must be confirmed through sequencing of the full 16S rRNA gene, as these isolates have been initially identified through partial sequencing of this gene. Whether the abundance of potential new species is related to a higher mutation rate associated to UV-irradiation, or to the fact that solar panels are unusual environments that have been hardly explored up to date, remains yet to be determined. In line with this, a thorough compilation of new microbial species described in recent years and their isolation sources should be carried out to further analyse the potential of extreme and unusual environments as sources of novel microbial species.

6. Ongoing/future work

Although the work in the present thesis has allowed to gain insight into the microbial ecology and potential applications of the microbial communities inhabiting solar panel surfaces, further work must be done in order to fully understand and exploit these microbial communities. On one hand, a comparative functional and taxonomic analysis of the microbial communities colonizing solar panels and other sun-exposed surfaces in different geographical locations would be of great interest to further pursue the idea of a surface-adapted microbiome. On the other hand, biotechnological potential of the microbial strains isolated from this environment can be further improved, for example, to increase their carotenoid production. Up to date, the chemical synthesis of a number of carotenoids has not yet been achieve, and these can only be produced via natural sources (i.e. plants, algae, fungi, and bacteria), which to date are less cost-efficient and provide a lower yield than using chemical synthesis (Sandmann, 2015). The need to search for more efficient carotenoid-producing microbial strains, the increase in consumer demand for naturally produced carotenoids, and the projected growth of the global carotenoids market (from USD 1.5 billion in 2019 to USD 2.0 billion by 2026) has led to a special interest in searching for novel natural sources of carotenoids (Source: Carotenoids Market by Type, Application, Source, Formulation, and Region - Global Forecast to 2026).

Nevertheless, the natural production of carotenoids in bacteria is frequently several hundred-fold lower than in other organisms, such as plants or algae (Lee and Schmidt-Dannert, 2002). This limitation can be overcome through the use of genetic engineering approaches aiming to improve natural carotenoid production or even clone entire carotenoid-biosynthesis pathways in non-carotenogenic microorganisms (Ruther et al., 1997; Henke et al., 2016). Although effective, genetic engineering of microorganisms can still lead to a reduced carotenoid production yield, and the genetically engineered microorganisms (GEMs) are subjected to a number of regulations that could limit their use. For example, the regulatory frameworks in the USA and the EU consider many foods produced with GEMs as novel foods, and therefore they must undergo the novel food evaluation process, that includes assessment of the entire manufacturing process, including the production organism, fermentation media, equipment, filters, and formulation ingredients, among others (Hanlon and Sewalt, 2020).

An alternative to genetic engineering is to use adaptive evolution strategies in order to ‘naturally’ evolve microbial strains towards an enhanced production of a carotenoids. Previous studies have revealed that exposure to certain environmental stresses, such as hydrogen

peroxide or UV-radiation, lead to an increase in carotenoid production (Jeong et al., 1999; Ligusa et al., 2005; Sankari et al., 2017). Therefore, the use of an increasing selective pressures (such as increasing hydrogen peroxide or UV-radiation levels), coupled to a continuous culture assay could be effective in the selection of stress-adapted bacteria and, in particular, in the increase of carotenoid production (Mozzetti et al., 2010). Although long term evolution experiments using continuous culture can be carried out manually, these can be tedious and require a large amount of time and effort. As a result of this, the use of automation in this field is gaining popularity, and an example is the development of the eVOLVER platform: a scalable DIY framework that can be configured to carry out high-throughput growth experiments with a precise and automated control of the growth conditions (Wong et al., 2018; Heins et al., 2019). In the framework of the present thesis, the eVOLVER platform has been used to evolve microbial strains isolated from solar panel surfaces in Boston with the aim of increasing carotenoid production (work in progress, unpublished and preliminary data in Appendix C). In this work, adaptive evolution has been performed by applying saline stress as a selective pressure. Saline stress has been seen to increase carotenogenesis in algae and fungi (Mao et al., 2020; Li et al., 2019) and, according to our results, it could also be used to increase carotenoid production in bacteria (Appendix C).

Another research line that would be worth pursuing is to further characterize the biological activity of carotenoids *in vivo,* in order to fully comprehend the mechanisms with which these strains can confer protection against oxidative stress and UV-radiation. For example, the effect of combinations of carotenoids versus the application of individual carotenoids could be further explored in a *C. elegans* model in order to detect possible synergistic effects of combining certain carotenoids. Previous studies have demonstrated the synergistic effects (increased antioxidant activity) of combining different carotenoids (Stahl et al., 1998), and of combining carotenoids with other substances, such as phenolic compounds or with vitamin E derivatives (Kogure 2019; Milde et al., 2007). Furthermore, it has been proposed that the potent antioxidant properties of fruit and vegetables are a result of the additive and synergistic effects caused by the complex mixture of phytochemicals they display (Liu RH, 2013).

Despite the benefits of using *C. elegans* as a model organism (i.e. the low cost, simplicity and quickness of the methods), other model organisms are becoming increasingly popular in the recent years. A particular case is *G. mellonella*, that displays several advantages over the use of other model organisms such as *Drosophila melanogaster, Danio rerio* or *C. elegans:* it is able to grow at 37 °C (similar to the physiological temperature of the human body), it allows the inoculation of an exact quantity of microorganisms or compounds through injections or force-feeding, it can be easily dissected to separate specific tissues and organs, and it displays both humoral and cell-mediated immunity (Junqueira et al., 2012; Mikulak et al., 2018; Trevijano-Contador and Zaragoza, 2018; Jorjão et al., 2018). Despite these advantages, the use of *G. mellonella* as a model organism is still under development and requires an important effort to standardize the procedures associated to its use (i.e. feed, dosage, or mortality/morbility record) (Champion et al., 2018). Up to date, this organism has mainly been used as a model to study virulence factors in pathogen-induced diseases and to study the efficacy of antimicrobial compounds in infection scenarios (Junqueira et al., 2012; Mesa-Arango et al., 2013; Pereira et al., 2015). The existence of a measurable oxidative stress response in this organism would be of great use to further characterize the antioxidant effects and associated molecular mechanisms of the carotenoid-producing microorganisms isolated in the present work. In fact, this model is being developed and coordinated by this researcher at Darwin Bioprospecting Excellence S.L. (work in progress, data not shown).

The final goal in any company-driven bioprospecting project is usually commercialization. In this context, the carotenoid-producing isolates characterized in the present study could be commercially valuable in several market sectors. On one hand, the pigmented microbial strains and/or their extracts could be used as antioxidants in the pharmacological industry (for example the β-carotene-producing PS1 strain, Publication IV) to treat conditions in

which oxidative stress plays an important role. Carotenoids have a protective effect against certain ROS-mediated disorders, and have been seen to reduce the risk of several chronic diseases, several types of cancer, cardiovascular and photosensitive disorders, and eye related diseases (Fiedor and Burda, 2014). On the other hand, carotenoids are valuable pigments in the feed and food industry, as they are used as food colorants and feed additives, especially in aquaculture (Sandmann, 2015). In particular, the carotenoids β-carotene, canthaxanthin and astaxanthin, produced by isolates PS1 and PS21 (Publication IV), are widely used in this sector.

These carotenoid-producing strains and/or their extracts could also be used in the cosmetic industry, for example, for protection against sunlight-induced skin damage. Both the topical application of phytochemicals to the skin and the supplementation of phytochemicals through the diet have previously been studied and have revealed promising results (Stahl and Sies, 2012; Afaq et al., 2002). In fact, the Norwegian company Promar AS has patented the manufacture and use in sunscreens of a carotenoid-producing *Micrococcus luteus* extract (patent US8834855B2). Finally, a previous study even described the possibility of using carotenoids produced by UV-resistant bacteria, specifically *Hymenobacter* sp. (red pigment) and *Chryseobacterium* sp. (yellow pigment), as photosensitizers in green solar cells, as these pigments displayed a high photostability and generated an open circuit voltage of 435.0 mV and 548.8 mV for the red and yellow pigments, respectively (Órdenes-Aenishanslins et al., 2016).

Indeed, unusual environments hold great promise as unexploited, diverse targets for the discovery of novel compounds, microorganisms or consortia with potential commercial and/or industrial applications, and new microbial species. In this context, we envisage xenomicrobial bioprospecting (the bioprospecting of foreign/unusual environments) as revolutionary field for both microbial ecologists and entrepreneurs of tomorrow's bioeconomy (Tanner et al., 2017; Appendix D).

Conclusions

In this thesis, the ecological aspects and the biotechnological potential of microbial communities inhabiting solar panel surfaces have been assessed. The general conclusions emerging from our work are listed below:

- Despite the physical distance, solar panel surfaces from around the world display microbiomes with taxonomic and functional similarities. The most abundant phyla include *Actinobacteria, Bacteroidetes, Deinococcus, Cyanobacteria, Firmicutes, Proteobacteria* and *Ascomycota*, and common functional traits include mainly stress-defense pathways involved in the persistence of microbes on solar panels surfaces.
- The genera *Hymenobacter, Sphingomonas, Streptomyces, Pseudomonas, Bradyrhizobium, Methylobacterium, Modestobacter* and *Deinococcus* constitute the core of the solar panel microbiota.
- The microbial communities inhabiting solar panel surfaces display several stress-resistance mechanisms as revealed through multi-omic (metagenomics and metabolomics) analyses. These mechanisms include stress response, capsule development, metabolite repair heat shock chaperone proteins, genes for carotenoid biosynthesis, superoxide dismutases, peroxidases and compatible solutes.
- The composition of the solar panel microbiota is not the result of a mere accumulation of taxa from the surrounding environment, but corresponds to the equilibrium point in an ecological succession, in the frame of which extremophilic taxa adapted to the harsh conditions of solar panels (UV-radiation, desiccation and temperature fluctuations) are selected.
- The microbial communities inhabiting solar panel surfaces display seasonal variations: bacteria dominate solar panel surfaces during the spring/summer period, whereas fungi are more abundant in the autumn/winter period.
- In the colonization process of solar panel surfaces, there is a transition from an initial generalistic community, to a final specialized community composed of highly resistant bacterial and fungal genera.
- The presence of microbial communities on solar panel surfaces is not linked to a significant reduction in photovoltaic efficiency.
- A large fraction of the microorganisms inhabiting solar panel surfaces are able to produce pigments, among which we highlight the production of commercially valuable carotenoids including β-carotene, canthaxanthin and astaxanthin, among others.
- Several of the microbial strains isolated from solar panel surfaces displayed antioxidant and UV-protection properties validated in an *C. elegans* model. In particular, worms fed with isolates PS1 (97.38 % similar to *Planomicrobium glaciei*) and PS21 (98.89 % similar to *Rhodobacter maris*) displayed a higher resistance to oxidative stress and UV-radiation than the worms fed with *E. coli* (basal diet) or with *E. coli* supplemented with antioxidants.
- Solar panel surfaces can be a source of new microbial taxa, as is the case of *Sphingomonas solaris* R4DWN, isolated from a solar panel surface in Boston (Massachusetts, USA).

Resumen en Castellano

Introducción

1. El panorama de la bioprospección

La diversidad de microorganismos procariotas en la Tierra es objeto de controversia. Si bien el uso de leyes de escalado predice que la Tierra alberga 1 billón (10^{12}) de especies microbianas (Locey y Lennon, 2016), un estudio reciente basado en datos de secuenciación disponibles públicamente calculó una riqueza de OTUs procariotas global seis órdenes de magnitud menor (Louca et al., 2019). Independientemente del número exacto, lo que está claro es que el mundo procariota es amplio y diverso, y aún queda por explorar una gran fracción del mismo. La diversidad microbiana existente es el resultado de la evolución y la adaptación. Esta diversidad nos proporciona un increíble arsenal de herramientas únicas y útiles que se pueden utilizar en una amplia gama de aplicaciones, tanto industriales como farmacéuticas. La búsqueda de estas herramientas biológicas es lo que conocemos como bioprospección.

1.1. La bioprospección como negocio

Teniendo en cuenta que hasta la fecha solo se ha explorado una fracción de la diversidad microbiana mundial (Locey y Lennon, 2016), la cantidad de cepas microbianas, herramientas genéticas o metabolitos con aplicaciones biotecnológicas o biomédicas, que quedan aún por descubrir, es abrumadora. Esto abre una gran oportunidad de mercado para las industrias biotecnológicas y, en particular, para los desarrollos comerciales basados en la microbiología aplicada. A pesar de este gran potencial, la comercialización de productos derivados de la bioprospección es un esfuerzo largo y costoso que debe cumplir, a lo largo de su camino, con varios controles.

Cualquier proyecto de bioprospección debe comenzar con la recolección de muestras biológicas. Hay varios aspectos críticos a tener en cuenta, por ejemplo, seleccionar el ambiente acorde a los propósitos del proyecto para asegurar una adecuada pre adaptación de los microorganismos, o asegurar la esterilidad y las condiciones óptimas de transporte hasta el procesamiento de las muestras en el laboratorio. Además, es fundamental estar al tanto de las implicaciones del protocolo de Nagoya en el país específico donde se recolectan las muestras. El siguiente paso es aplicar técnicas de cultivo avanzadas para aislar la mayor fracción posible de microorganismos cultivables, que luego se someterán a cribados masivos para detectar actividades biológicas de interés. Una vez seleccionados los microorganismos de interés, es importante evaluar las normativas y los problemas de seguridad asociados al uso de estas cepas, por ejemplo, para el consumo humano. Respecto a este tema, la Autoridad Europea de Seguridad Alimentaria (EFSA) publica, cada año, una lista de agentes biológicos que pueden añadirse intencionalmente a alimentos o piensos y que se consideran seguros (QPS o Presunción Cualificada de Seguridad) (EFSA BIOHAZ Panel, 2020). Más allá de Europa, la Administración de Drogas y Alimentos de los Estados Unidos (FDA) proporciona una regulación similar, en la que el término "GRAS" se utiliza para designar los aditivos alimentarios (agentes biológicos y otras sustancias) que generalmente se reconocen como seguros. Para que una cepa microbiana se considere QPS o GRAS debe mostrar una cierta estabilidad genómica, no ser patógena, no presentar resistencia a antibióticos, y no producir sustancias tóxicas (EFSA FEEDAP Panel et al., 2018).

Las cepas de interés seleccionadas se deben someter a una caracterización profunda para verificar su actividad biológica *in vivo* utilizando modelos experimentales, desde cultivos celulares simples y modelos invertebrados, hasta modelos vertebrados y ensayos clínicos. A lo largo de este período, se debe evaluar e implementar la protección intelectual para las aplicaciones de las cepas seleccionadas. Además, el cultivo de estas cepas debe escalarse, un paso que es fundamental

para obtener rentabilidad a la hora de comercializar el producto final. Finalmente, el lanzamiento del producto al mercado requiere la aplicación de un conjunto especializado de habilidades como análisis de tendencias de mercado, estrategia comercial, diseño, habilidades de comunicación o experiencia financiera. Por esta razón, muchos proyectos de bioprospección a menudo derivan de una empresa externa (por ejemplo, grandes empresas farmacéuticas) para esta fase final. Y, tras una larga inversión con un riesgo creciente asociado a cada paso, finalmente se obtiene un ingreso. A pesar de la complejidad de los proyectos de bioprospección, muchas empresas han tenido éxito en este esfuerzo. Por ejemplo, existen empresas altamente especializadas en bioprospección de productos veterinarios innovadores (por ejemplo, Aquilón Cyl, España) o cepas productoras de bacteriocinas (por ejemplo, BLIS Technologies, Nueva Zelanda), así como empresas de nueva creación que ofrecen estrategias innovadoras en bioprospección microbiana aplicada a cualquier tipo de muestra (por ejemplo, la empresa Darwin Bioprospecting Excellence SL, Paterna, España).

1.2. El proceso de bioprospección

Los estudios de bioprospección realizados en la presente tesis han cubierto los primeros pasos del proceso descrito anteriormente: muestreo, cultivo y cribado de microorganismos con potenciales aplicaciones en la industria.

1.2.1 Muestreo y regulaciones para el acceso a los recursos genéticos

El Convenio sobre la Diversidad Biológica (CDB) se firmó en 1992 con el objetivo de garantizar un uso sostenible de la diversidad biológica mediante el apoyo a la conservación de la diversidad biológica, el intercambio de beneficios y la transferencia de conocimientos/tecnología a través de la cooperación científica. El Protocolo de Nagoya sobre Acceso y Distribución de Beneficios (ABS) entró en vigor en octubre de 2014, con el objetivo de armonizar la implementación del CDB aumentando la seguridad jurídica y la transparencia para los proveedores y usuarios de los recursos genéticos y de los conocimientos tradicionales asociados, así como para garantizar la asignación correcta de los beneficios (monetarios y no monetarios) que puedan derivarse de este uso (Smith et al., 2017). Si bien el Protocolo de Nagoya surgió de un proceso de negociación global, cada país que lo ratifica debe implementar sus propias regulaciones; en otras palabras, debe decidir si controla o no el acceso a sus recursos (https://absch.cbd.int/). Actualmente (octubre de 2020) un total de 127 países han ratificado el Protocolo de Nagoya.

A pesar de las buenas intenciones del Protocolo de Nagoya, existen varias controversias relacionadas con su aplicación a la diversidad microbiana. En concreto, tres de los conceptos centrales del Protocolo de Nagoya apenas son aplicables a los microorganismos (Overmann y Scholz, 2017):

- Según el Protocolo de Nagoya, los puntos calientes de biodiversidad se encuentran principalmente en países en desarrollo y pueden servir como proveedores de recursos genéticos que pueden derivar en beneficios para los países industrializados. Sin embargo, es importante considerar que el término “punto caliente de biodiversidad” se basa en la diversidad de macroorganismos (plantas, animales, etc.) que son endémicos y exclusivos de un lugar en particular, mientras que, en general, no se ha demostrado que los microorganismos sean endémicos. De hecho, las altas tasas de dispersión dan como resultado que los microorganismos sean cosmopolitas, y se ha detectado una alta identidad de secuencia en cepas microbianas aisladas a una distancia de hasta 18000 km (Griffin, 2007; Speth et al., 2012).

- El Protocolo de Nagoya crea un incentivo económico para el uso sostenible de la biodiversidad al enfatizar que los recursos genéticos tienen un valor inherente. No obstante, como se ha comentado anteriormente, casi siempre se requieren grandes inversiones para desarrollar y comercializar plenamente los productos derivados de estos recursos genéticos, lo que puede contradecir la idea de que la comercialización de estos productos es un proceso sencillo.

- Las políticas asociadas al Protocolo de Nagoya tienden a ser muy restrictivas al cubrir todos los tipos de "usos" de los recursos, ya que asumen que la comercialización puede tener lugar en cualquier punto del proceso de bioprospección. La realidad es que la mayoría de los accesos a los recursos genéticos no tienen fines comerciales, y las políticas restrictivas están provocando desventajas competitivas, ya que la naturaleza cosmopolita de los microorganismos conduce a la posibilidad de aislar las mismas especies microbianas en una ubicación geográfica donde las políticas asociadas sean menos restrictivas o, incluso, inexistentes.

Los usuarios de los recursos genéticos deben ser conscientes de sus responsabilidades (por ejemplo, asegurarse de que los recursos se adquieran legalmente y de que todos los beneficios que puedan surgir se compartan de manera justa) y deben cumplir con todas las regulaciones vigentes, que podrían estar dentro del Protocolo de Nagoya o, en los países donde la legislación es débil, podrían ser los principios del CDB (Smith et al., 2017).

1.2.2 Cultivo y cribado

El desarrollo nuevas estrategias innovadoras para la minería de comunidades microbianas ha resultado en el descubrimiento de nuevas moléculas y enzimas de gran interés. Este es el caso, por ejemplo, de *Entotheonella* sp., detectada mediante enfoques de genómica unicelular y capaz de producir un amplio repertorio de compuestos bioactivos (Wilson et al., 2014), o la bacteria *Eleftheria terrae*, que no se había podido cultivar en condiciones de laboratorio y se aisló de suelo con un enfoque de cultivo innovador y describió su capacidad de producir un nuevo antibiótico, la teixobactina (Ling et al., 2015). Estos dos casos ejemplifican el compromiso al cual tienen que enfrentarse todos los proyectos de bioprospección: el uso de técnicas independientes del cultivo, que permiten un mayor poder de detección, aunque sin aislamiento físico de las cepas microbianas; versus el uso de enfoques dependientes del cultivo, limitado por el hecho de que la mayoría de los microorganismos existentes aún no se han cultivado en condiciones de laboratorio.

La metagenómica es el estudio del metagenoma, que es el genoma colectivo de microorganismos de una muestra ambiental. Esta tecnología puede conducir a la detección de taxones microbianos o genes funcionales de interés. Algunos ejemplos son la detección de *Actinobacteria* y *Firmicutes* de manglares y zonas costeras como fuentes de compuestos antimicrobianos, la identificación de genes bacterianos para la hidrólisis de celulosa y xilano de la microbiota intestinal de una termita que se alimenta de madera, o el descubrimiento de genes para la degradación de la biomasa celulósica de microbios adheridos a la fibra vegetal en el rumen de la vaca (Al-Amoudi et al., 2016; Warnecke et al., 2007; Hess et al., 2011). Otras herramientas económicas poderosas incluyen la metabolómica, la metaproteómica y la metatranscriptómica, dirigidas al estudio de metabolitos, proteínas y ARNm de cualquier muestra ambiental, respectivamente. Todas estas herramientas -ómicas, juntas, pueden proporcionar una caracterización completa sin precedentes de los genes y los patrones de expresión génica, las actividades microbianas y las vías metabólicas complejas en una muestra ambiental determinada. Sin embargo, estas herramientas tienen varias limitaciones: (1) a menudo ocultan ciertos aspectos biológicos, como interacciones ecológicamente relevantes entre miembros individuales de la comunidad; (2) ciertas características no se predicen correctamente debido a la falta de datos genómicos de referencia en las bases de datos (estos se obtienen mediante la secuenciación del genoma completo de cultivos aislados); y (3) las características predichas *in silico* deben probarse experimentalmente (Vilanova & Porcar, 2016).

Es por estas razones que las técnicas dependientes e independientes de cultivo deben complementarse entre sí para lograr un proceso de bioprospección eficiente, que podríamos considerar como “bioprospección de segunda generación” o “next generation bioprospecting”. Si bien el cultivo de cepas biotecnológicamente relevantes es esencial para su uso posterior en un entorno industrial, se pueden utilizar enfoques

independientes de cultivo en bacterias aún no cultivadas para realizar análisis fisiológicos que mejorarán la orientación de la novedad funcional (Overmann et al., 2017).

El aislamiento de una cepa microbiana en condiciones de laboratorio no siempre es una tarea sencilla y, de hecho, el cultivo de bacterias está sesgado hacia un número relativamente bajo de grupos filogenéticos. Hasta la fecha, todas las especies cultivadas pertenecen a 39 de los 112 filos bacterianos actualmente reconocidos (Parte 2018; https://gtdb.ecogenomic.org; datos consultados en mayo 2020). Este acceso limitado a ciertos phyla es una consecuencia de la falta de condiciones de incubación adecuadas, y resulta en un gran número de taxones inexplorados que probablemente posean nuevas vías metabólicas con uso potencial en la industria. Se han desarrollado varios conceptos de cultivo en los últimos años para superar esta limitación - 'cultivar lo incultivable' -, tales como: medios con bajo contenido de nutrientes, plataformas de cultivo miniaturizadas y dispositivos de cultivo desechables basados en microfluídica para bacterias oligotróficas (Cho y Giovannoni 2004; Ingham et al. ., 2007; Grünberger et al., 2015); largos períodos de incubación para poder aislar microorganismos de crecimiento lento (Puschen et al., 2017); enfoques basados en filtración selectiva por tamaño para aislar ultramicrobacterias (menores de 0,1 µm3) (Geissinger et al., 2009); estrategias de cultivo de alto rendimiento, o culturomics, en los que se prueban miles de condiciones de crecimiento (Lagier et al., 2018); enriquecimiento selectivo de bacterias formadoras de biofilms (Gich et al., 2012); unidades de diálisis o perlas de agar para aislar cepas que deben cultivarse en cocultivo (Kealey et al., 2017; Lodhi et al., 2018); o métodos de cultivo *in situ* que utilizan cámaras de difusión (Nichols et al., 2010; Bollmann et al., 2007).

El aislamiento de las cepas microbianas es solo el primer paso y, a efectos de la bioprospección, el método de cribado utilizado es fundamental para seleccionar cepas con actividades biológicas de interés. Las colecciones de cepas microbianas se pueden cribar para actividades biológicas de interés usando métodos de cribado *in vitro* y/o *in vivo*. Entre los organismos modelo disponibles para el cribado *in vivo* (es decir, *Danio rerio*, *Drosophila melanogaster, Mus musculus*, etc.), *Caenorhabditis elegans* ofrece muchas ventajas, como su pequeño tamaño corporal y su genoma completamente secuenciado (con más del 65% de los genes asociados con enfermedades humanas), así como su bajo coste o su rápido desarrollo y envejecimiento (Park et al., 2017; Shen et al., 2018).

C. elegans se ha utilizado hasta la fecha para estudiar procesos fisiológicos, como el envejecimiento, la esperanza de vida, la respuesta al estrés, la obesidad o la inmunidad (Park et al., 2017; Shen et al., 2018). De hecho, un estudio reciente ha establecido un protocolo de ensayo miniaturizado que permite realizar pruebas *in vivo* de productos naturales que pueden aumentar la supervivencia del nematodo y suprimir la acumulación de grasa (Zwirchmayr et al., 2020). El sistema neurobiológico conservado en este organismo modelo ha permitido su utilización como modelo para identificar los mecanismos moleculares que median el comportamiento inducido por drogas (como etanol, nicotina, cocaína, etc.) y para identificar posibles dianas para el desarrollo de medicamentos (Engleman et al., 2016). Además, *C. elegans* se ha utilizado como modelo para: comprender los mecanismos conservados en las interacciones huésped-microorganismo, debido a las similitudes morfológicas y funcionales del intestino de *C. elegans* con el intestino humano (Kumar et al., 2019); estudiar la genética y la biología del desarrollo, incluida la epigenética ambiental, la toxicología ambiental y la exposición a genotoxinas (Weinhouse et al., 2018; Honnen 2017); y realizar evaluaciones de bioseguridad de nanopartículas (Wu et al., 2019).

1.3. Bioprospección de ambientes inusuales

Muchos esfuerzos de bioprospección se han centrado en entornos bien conocidos como el suelo, una fuente muy rica de microorganismos productores de antibióticos (Sherpa et al., 2015) y bacterias con propiedades insecticidas (Melo et al., 2014); o como el intestino humano, del cual se han aislado bacterias probióticas como *Lactobacillus* spp. (Halimi y Mirsalehian, 2016). No obstante, los entornos exóticos y particulares dan

lugar a adaptaciones particulares, y la facilidad con la que se pueden muestrear los entornos humanos o humanizados no debe ocultar que la mayoría de las novedades taxonómicas y funcionales se encuentran en otro lugar. Los entornos inusuales siguen estando muy inexplorados hasta la fecha, a pesar de ser fuentes valiosas de productos novedosos.

¿Qué es un entorno inusual o, más precisamente, qué es lo suficientemente inusual? Consideramos un entorno inusual como uno que está escasamente explorado, taxonómicamente distante del microbioma asociado con los humanos y que se encuentra en condiciones extremófilas. Curiosamente, las tres características tienden a ocurrir al mismo tiempo. Cabe destacar que algunos hábitats interiores o exteriores (aparatos eléctricos, superficies expuestas al sol, saunas de alta temperatura) entran en esta categoría.

Hay tres razones que hacen que los entornos inusuales sean especialmente interesantes para los estudios de bioprospección. El primero es la gran biodiversidad que albergan, lo que conduce a una alta probabilidad de encontrar nuevos taxones, como lo demuestra el descubrimiento de hasta 47 nuevos phyla en sedimentos de acuíferos y aguas subterráneas en Colorado (Anantharaman et al., 2016). En segundo lugar, estos microorganismos están preadaptados a diferentes condiciones de estrés que, a menudo, se correlaciona con las necesidades industriales. Finalmente, un campo de investigación prometedor radica en el desarrollo de nuevas biofactorías a partir de microorganismos robustos capaces de resistir una amplia gama de tensiones (temperatura, pH, salinidad, etc.).

Los biotecnólogos están en deuda con las polimerasas termoestables, como la inmensamente popular *Taq* polimerasa para las reacciones en cadena de la polimerasa (PCR), así como las polimerasas *Vent* o *Pfu*, todas ellas aisladas a partir de los microorganismos extremófilos *Thermus aquaticus, Thermococcus litoralis* y *Pyrococcus furiosus,* respectivamente (Chien et al., 1976; Tindall y Kunkel, 1988; Lundberg et al., 1991; Kong et al., 1993). Hay muchos otros ejemplos de productos valiosos obtenidos de entornos inusuales: desde el biocombustible de arqueas hipertermófilas que viven en chimeneas hidrotermales de aguas profundas (Nishimura y Sako, 2009), hasta bacterias promotoras del crecimiento vegetal adaptadas al frío y aisladas a partir de entornos montañosos extremos (Pandey & Yarzábal, 2019). No obstante, durante las últimas dos décadas, el descubrimiento de nuevos compuestos microbianos ha disminuido significativamente, principalmente como consecuencia de la redundancia genética y química detectada en entornos comúnmente analizados (Zhang, 2005). Los entornos inusuales son muy prometedores como dianas con una alta diversidad microbiana sin explotar para el descubrimiento de biocompuestos, microorganismos o consorcios con posibles aplicaciones comerciales y/o industriales (Tanner et al., 2017, Apéndice D; Molina-Menor et al., 2019, Apéndice D).

2. Microbiomas expuestos al sol

Los microbiomas asociados a los primeros milímetros de muchas superficies de la Tierra están sometidos a una amplia gama de estreses ambientales y, en particular, a una gran cantidad de radiación. La luz solar está formada por luz visible, infrarroja y ultravioleta, y la luz que llega a la superficie de la Tierra está compuesta por: aproximadamente un 55% de luz infrarroja, que contribuye a calentar nuestro planeta; un 42-43% de luz visible, que se utiliza, por ejemplo, para la fijación de carbono mediante fotosíntesis; y un 3-5% de luz ultravioleta que, aunque es necesaria para la síntesis de vitamina D en vertebrados, también es un agente mutagénico bien conocido (Bird y Hulstrom 1983; Markovitsi, 2016). Estos tres componentes de la luz solar son responsables de las tres principales presiones de selección a las que están sujetos los organismos expuestos al sol: calentamiento/desecación, baja cantidad de nutrientes y daño del ADN.

2.1. Mecanismos de resistencia al estrés

Los microorganismos que viven en superficies expuestas al sol muestran una amplia gama de mecanismos que les permiten resistir estos estreses ambientales. La resistencia al calor se puede lograr, por ejemplo, mediante la

acumulación de solutos citoplasmáticos o mediante la formación de esporas con bajo contenido de agua, alta mineralización y saturación del ADN con proteínas pequeñas solubles en ácido (SASP) (Pleitner et al., 2012; Setlow, 2006). Además, la formación de biofilms confiere resistencia no solo a temperaturas extremas, sino también a otros estreses ambientales, como radiación UV, valores extremos de pH, alta salinidad, alta presión y escasa disponibilidad de nutrientes, entre otros (Yin et al., 2019). En condiciones de temperaturas extremas (tanto calientes como frías), los biofilms confieren una denominada "ropa protectora", al resistir las temperaturas extremas externas y mantener un interior estable que es adecuado para el crecimiento microbiano (Yin et al., 2019). En condiciones oligotróficas, los biofilms pueden mejorar la supervivencia microbiana al distribuir de forma eficiente los nutrientes limitados (Yin et al., 2019). Otros mecanismos bacterianos para resistir la disponibilidad limitada de nutrientes son la formación de esporas, la latencia o el crecimiento extremadamente lento (Gray et al., 2019).

En cuanto a la resistencia a la radiación, la radiación UV muestra una penetración reducida en la matriz del biofilm, lo que combinado con la producción de compuestos especializados como aminoácidos o pigmentos similares a las micosporinas, puede proteger aún más a los microorganismos contra esta radiación (de Carvalho, 2017). Por otro lado, una gran fracción de procariotas acumula polihidroxialcanoatos (PHA) en forma de gránulos intracelulares, que aunque participan en el almacenamiento de carbono y energía, también pueden mejorar la resistencia a la radiación UV dispersando la radiación y uniéndose al ADN, proporcionando una protección similar a un escudo de sus genomas (Slaninova et al., 2018). Otras estrategias para sobrevivir al estrés inducido por la radiación es la presencia de mecanismos eficientes de reparación del ADN, mecanismos de defensa contra el estrés oxidativo y la formación de esporas (Nicholson et al., 2005; Lim et al., 2019).

La formación de esporas confiere entre 10 y 100 veces más resistencia a la radiación UV que las células vegetativas correspondientes, y los mecanismos de resistencia a los rayos UV en las esporas incluyen, además de los mecanismos eficientes de reparación del ADN, la presencia de SASP y la acumulación de pigmentos absorbentes (Nicholson et al., 2005). De hecho, el papel de los pigmentos en la protección UV, como los carotenoides, la melanina, la escitonemina o la prodigiosina, se ha estudiado ampliamente (Ruan et al., 2004; Soule et al., 2009; Sandmann, 2015; Borić et al., 2011).

2.2. Microbiomas expuestos al sol de estructuras artificiales y el caso particular de las superficies de los paneles solares

El establecimiento de la microbiota en superficies expuestas al sol no solo está determinado por las condiciones ambientales y las presiones selectivas, sino también por el propio sustrato que. Sin embargo, las superficies artificiales expuestas al sol son superficies oligotróficas inertes que se pueden utilizar como sustituto para estudiar los microbiomas superficiales y el papel de las presiones selectivas en la configuración de estas comunidades microbianas.

Un estudio de la composición del microbioma de las vidrieras de iglesias históricas en descomposición en un clima mediterráneo reveló la colonización de estas superficies por comunidades bacterianas complejas dominadas por *Proteobacteria*, *Bacteroidetes*, *Firmicutes* y *Actinobacteria*, y una menor diversidad de hongos, dominada por los géneros *Cladosporium* y *Phoma*. (Piñar et al., 2013). En 2011, un estudio de Ragon et al. reveló que las comunidades microbianas en superficies de hormigón expuestas a la luz solar, caracterizadas por *Actinobacteria, Alphaproteobacteria, Bacteroidetes, Acidobacteria* y *Deinococcales*, así como algas verdes y hongos ascomicetos, eran muy similares a las comunidades que colonizan superficies de hormigón en Chernobyl y que están expuestas a diferentes niveles de radiación. Estos resultados sugieren que los biofilms que crecen en superficies expuestas al sol y que se adaptan a la desecación y a la radiación ultravioleta ambiental, están preadaptados a ciertos niveles de radiación ionizante como las que se encuentran en Chernobyl y son capaces de hacer frente al

aumento de las tasas de mutación (Ragon et al. al., 2011).

Un caso particularmente extremo es la descripción de la microbiota que habita las superficies de las placas solares. Las superficies de las placas solares son superficies lisas de vidrio o similares al vidrio con una capacidad mínima de retención de agua y una exposición máxima a la luz solar. Estas estructuras artificiales se pueden encontrar prácticamente en todo el mundo y se pueden utilizar como dispositivos estándar para estudiar las comunidades microbianas y su proceso de colonización en diferentes ubicaciones geográficas. Además, las superficies de las placas solares no solo están expuestas a la desecación y la alta irradiación, sino también a las frecuentes fluctuaciones de temperatura, lo que las convierte en fuentes ideales de microorganismos resistentes al estrés.

Según un estudio de Dorado-Morales et al (2016), las comunidades microbianas que viven en las superficies de las placas solares están dominadas por ascomicetos y una variedad de bacterias, principalmente *Novosphingobium, Sphingomonas, Rubellimicrobium, Hymenobacter, Segetibacter* o *Deinococcus*. Este estudio también reveló que bacterias que habitan en las placas solares producen pigmentos, por ejemplo carotenoides, y esfingolípidos, metabolitos que juegan un papel tanto en la adhesión a la superficie de los paneles solares como en la protección contra el estrés oxidativo (Moye et al., 2016). Tanto los perfiles funcionales como los taxonómicos de las comunidades microbianas de las placas solares son similares a otros entornos expuestos a la luz solar, como las esteras microbianas polares, el filoplano, las rocas orientadas al sol, los desiertos calientes y fríos (Dorado-Morales et al., 2016). Además, el cultivo de muestras de placas solares dio lugar a una gran cantidad de microorganismos formadores de colonias, muchos de ellos con pigmentación roja, naranja o rosa, y con resistencia a altas concentraciones de sal y exposiciones breves a la luz ultravioleta. (Dorado-Morales et al., 2016). Estos resultados sugieren que las superficies de los paneles solares pueden ser fuentes ricas en nuevas cepas microbianas con actividades biológicas de interés.

Desde un punto de vista funcional, los datos metagenómicos revelaron perfiles funcionales similares entre las diferentes placas solares muestreadas en Valencia (España), mientras que el análisis metaproteómico reveló abundantes proteínas involucradas en la resistencia a condiciones adversas y en la formación de biofilms, así como diferencias entre la composición proteica en muestras tomadas durante el día y durante la noche, lo que sugiere que las comunidades microbianas que habitan estas superficies son biológicamente activas y poseen mecanismos de respuesta al estrés (Dorado-Morales et al., 2016).

En un estudio en Sao Paulo, se encontró que los hongos son un componente relevante de SAB en superficies de placas fotovoltaicos después de 6, 12 y 18 meses de exposición, siendo los ascomicetos meristemáticos melanizados y las especies bacterianas pigmentadas de los géneros *Arthrobacter* y *Tetracococcus* los principales microorganismos (Shirakawa et al., 2015). Además, se observaron reducciones significativas en la eficiencia de las placas solares después de 6, 12 y 18 meses (reducción del 7% después de 6 y 12 meses, y reducción del 11% después de 18 meses), y a los 18 meses los únicos taxones detectados fueron *Dothydeomycetes meristemáticos, Ulothrix* y *Chlorella* (Shirakawa et al., 2015). Además, se han aislado previamente cuatro nuevas cepas de hongos melanizados de la comunidad microbiana que habita las tejas fotocatalíticas (Ruibal et al., 2018).

El trabajo realizado en la presente tesis tiene como objetivo profundizar en la exploración de la microbiota de los paneles solares desde una perspectiva tanto ecológica como aplicada. Por un lado, se han analizado en términos taxonómicos y funcionales las comunidades microbianas que habitan paneles solares de diferentes ubicaciones geográficas, y se ha estudiado en profundidad el proceso de colonización de estas superficies mediante una granja solar miniaturizada. Por otro lado, se han aislado cepas microbianas de este entorno y se han analizado más a fondo para determinar las actividades biológicas de interés y para caracterizar y describir nuevas especies microbianas.

Resultados y discusión

1. El núcleo taxonómico de la microbiota de los paneles solares

Las superficies de los paneles solares son ambientes extremos (expuestos a radiación ultravioleta, desecación, fluctuaciones de temperatura y limitación de nutrientes) que están habitados por una sorprendente diversidad de microorganismos adaptados al estrés. La estructura y orientación estándar (frente al ecuador) de los paneles solares en todo el mundo, y sus superficies bidimensionales inertes, los convierten en un sustituto de los entornos naturales expuestos al sol. El uso de dispositivos artificiales para el estudio de comunidades microbianas que habitan en la superficie se ha descrito previamente, por ejemplo, en estudios de filosfera artificial (superficie de la planta) (Doan y Leveau, 2015). Estas filosferas artificiales incluyen desde superficies microestructuradas más complejas, hasta superficies más simples como agar nutritivo, superficies inertes (es decir, acero inoxidable) o incluso plantas de plástico (Ottesen et al., 2016; Soffe et al., 2019). En el último caso, el estudio reveló que había un alto nivel de taxonomía compartida entre las plantas de tomate vivas y los controles inanimados adyacentes, lo que sugiere que las fuerzas ambientales juegan un papel importante en la introducción de microorganismos en la superficie de las plantas (Ottesen et al., 2016).

Se ha llegado a una conclusión similar en el presente estudio al analizar las comunidades que habitan en superficies de paneles solares de ubicaciones geográficas distantes, a saber, Berkeley (California, EE. UU.), Valencia (España), Tromsø (Noruega) y las islas antárticas Decepción y Livingston. A pesar de la distancia física entre estos paneles solares, las comunidades microbianas que habitan en sus superficies resultaron ser muy similares tanto en términos taxonómicos como funcionales, con los filos más abundantes siendo *Actinobacteria*, *Bacteroidetes, Deinococcus, Cyanobacteria, Firmicutes, Proteobacteria* y *Ascomycota*.

Curiosamente, la comparación de los géneros más abundantes de cada estudio ha revelado que varios taxones se comparten entre todas las ubicaciones geográficas. Los géneros *Hymenobacter* y *Sphingomonas* se encuentran entre los taxones más abundantes en todos los lugares, mientras que los géneros *Streptomyces, Pseudomonas, Bradyrhizobium, Methylobacterium, Modestobacter* y *Deinococcus* se encuentran entre los taxones más abundantes presentes en 4 de los 5 lugares muestreados, lo que sugiere que hay un núcleo microbiano en las superficies de los paneles solares compuestos por estos 8 géneros.

2. Propiedades de resistencia al estrés en superficies expuestas al sol

Los géneros más abundantes en las superficies de los paneles solares se caracterizan por sus propiedades de resistencia al estrés. Los miembros de los géneros *Deinococcus* e *Hymenobacter* muestran altos niveles de resistencia tanto a la radiación gamma como a la UV (Rainey et al., 2005; Batista 1997; Maeng et al., 2020). De hecho, la exposición ambiental parece facilitar la adaptación. En el estudio de Rainey et al. (2005), los microorganismos aislados de suelos desérticos sobrevivieron a dosis de hasta 30 kGy de radiación, mientras que no se recuperaron aislados de suelos de bosques no áridos después de dosis superiores a 13 kGy. Miembros de los géneros *Sphingomonas* (un género que forma biofilms, degrada xenobióticos y produce EPS) y *Methylobacterium* producen carotenoides, son muy resistentes a la desecación y a la luz ultravioleta, y pueden prosperar en un amplio rango de temperaturas (Lee et al., 2014; Grube et al., 2009; Csotonyi et al., 2010). Los miembros de los géneros *Pseudomonas* y *Modestobacter* prosperan en superficies expuestas a los rayos UV (Franklin et al., 2005; Alonso-Sáez et al., 2006; Santos et al., 2012; Normand et al., 2012), mientras que los miembros de los géneros *Streptomyces* y *Bradyrhizobium*, abundantes en el suelo y la rizosfera, respectivamente, toleran la deshidratación (Orellana et al., 2018; Sugawara et al., 2010; Jeon et al., 2015).

En el presente trabajo, representantes de varios géneros microbianos (muchos de ellos

pigmentados) se han aislado de las superficies de los paneles solares y se han evaluado sus propiedades de resistencia al estrés. Miembros de los géneros *Rhodotorula, Deinococcus, Hymenobacter, Arthrobacter* y *Cryptococcus* y, en menor medida, *Alcaligenes, Sphingomonas, Dioszegia, Curtobacterium* y *Microbacteria*, mostraron resistencia a los rayos UV. Por otro lado, casi todas las cepas aisladas de los paneles solares polares fueron capaces de resistir la desecación, mientras que solo *Methylobacterium* y *Arthrobacter* aisladas de Berkeley (California, EE. UU.) pudieron sobrevivir a la desecación bajo nuestras condiciones experimentales.

El análisis multiómico (metagenómica y metabolómica) en el presente estudio reveló algunos de los mecanismos de resistencia al estrés presentes en estas comunidades microbianas. Específicamente, se detectaron vías involucradas en la persistencia de los microorganismos en las superficies de los paneles solares, así como genes para la biosíntesis de carotenoides y otros mecanismos para combatir el estrés oxidativo. Además, el análisis metabolómico reveló la presencia de solutos, que pueden desempeñar un papel en la protección contra la desecación, el calor y/o el estrés por radiación UV. En el trabajo de Dorado-Morales et al. (2016), se detectaron mecanismos adicionales de resistencia al estrés mediante análisis metagenómico y metaproteómico, por ejemplo la producción de pirofosfatasa translocadora de protones unida a la membrana (mPP), proteínas de choque térmico y frío, proteínas de la capa S, lipoproteínas y formación de biofilms. Juntos, estos estudios han permitido conocer mejor los perfiles de resistencia al estrés de estas comunidades microbianas.

Otros ambientes expuestos al sol comparten similitudes con las superficies de los paneles solares en términos de estrés ambiental dominante y taxones microbianos más abundantes. Por ejemplo, un estudio reciente describió que *Hymenobacter*, *Sphingomonas* y *Rhizobiales* se encuentran entre el microbioma de la filosfera central en poblaciones distantes del árbol del té *Leptospermum scoparium*, autóctono de Nueva Zelanda (Noble et al., 2020). Además, en el estudio de Ottesen et al. (2016), los tres taxones más abundantes en la filosfera tanto de las plantas vivas como de sus controles inanimados fueron *Pseudomonas, Erwinia* y *Sphingomonas*. Es importante destacar que, de hecho, las hojas de las plantas son "paneles solares" biológicos que comparten algunas de las condiciones de estrés observadas en los dispositivos fotovoltaicos artificiales. Por otro lado, las microcapas superficiales están habitadas por bacterioneuston y ubicadas en la interfaz aire-agua, donde se ha sugerido que la disponibilidad de materia orgánica, la radiación UV y la velocidad del viento influyen en la composición de la comunidad (Zäncker et al., 2018; Santos et al., 2012; Santos et al., 2014). Estudios previos han revelado una gran similitud entre las bacterias que forman el bacterioneuston y las que son transportadas por el aire, apoyando la hipótesis de que el aire puede ser una fuente importante de bacterias para los ambientes superficiales (Hervas y Casamayor, 2009), y se ha descrito que *Pseudomonas* se encuentra entre los géneros más abundantes en bacterioneuston de agua dulce (Azevedo et al., 2012). En cuanto a las regiones desérticas, se ha descubierto que los géneros *Deinococcus* y *Rubrobacter*, tolerantes a la radiación y la desecación, dominan la biota del suelo del valle de McKelvey, uno de los desiertos hiperáridos más fríos de la Tierra ubicado en el Artártico (Pointing et al., 2009). Además, teniendo en cuenta toda la comunidad microbiana analizada mediante secuenciación de alto rendimiento (no solo los taxones más abundantes) e incluyendo niveles taxonómicos más altos (por ejemplo, a nivel de phylum), el estudio anterior de Dorado-Morales et al. (2016) reveló que los entornos superficiales, incluyendo los paneles solares, los desiertos, las esteras microbianas polares y la filosfera, muestran una distancia filogenómica baja y son claramente divergentes de los entornos no superficiales, como los ambientes asociados al cuerpo humano, los sedimentos marinos o el suelo de la selva tropical.

Un informe de Gibbons (2017) destacó la importancia del componente funcional, más que el taxonómico, en el establecimiento de microbiomas. Sin embargo, los resultados obtenidos en el presente trabajo muestran que no solo existen adaptaciones comunes, sino también similitudes taxonómicas entre las comunidades microbianas que habitan paneles solares de

regiones geográficas distantes. La fuerte presión selectiva bajo la cual las comunidades microbianas de la superficie tienen que sobrevivir y la facilidad de propagación de las comunidades bacterianas transportadas por el aire (Griffin, 2007; Speth et al., 2012) hacen que sea tentador plantear la hipótesis de que existe un "bioma de superficie taxonómico y funcional" parcialmente conservado entre todas las localizaciones superficiales. En este sentido, la superficie de la Tierra y, más específicamente, la parte superior de la biosfera adaptada al sol, podría considerarse como un bioma mundial por sí mismo, la denominada *Himenosfera* (Porcar et al., manuscrito en preparación).

3. Colonización de las superficies de paneles solares

A pesar de que las comunidades microbianas que habitan las superficies de los paneles solares se conservan en gran medida, estas comunidades muestran variaciones estacionales. En particular, las bacterias y los hongos muestran una mayor abundancia relativa durante los períodos de primavera/verano y otoño/invierno, respectivamente. Esto probablemente esté relacionado con niveles más altos de suciedad en los períodos de poca lluvia (primavera/verano) y niveles más altos de humedad durante el otoño/invierno típicamente lluvioso característico del mediterráneo. Incluso con estas variaciones estacionales, en el presente trabajo se ha observado una clara transición de una comunidad más generalista al comienzo del experimento de colonización, a una comunidad más especializada compuesta por géneros bacterianos y fúngicos altamente resistentes. Esto apoya la hipótesis de que las fuertes presiones de selección que caracterizan estas superficies son las que dan forma a la comunidad microbiana. Según nuestros resultados, los miembros del género *Sphingomonas* (uno de los taxones centrales de esta comunidad microbiana, como se describió anteriormente) son los primeros en llegar a las superficies de los paneles solares. Este taxón puede desempeñar un papel crucial en el establecimiento de un biofilm debido a su capacidad para secretar EPS y para resistir la radiación UV y la desecación (Bereschenko et al., 2010; Venugopalan et al., 2005). Después de 24 meses, los taxones más abundantes detectados en estas superficies fueron *Modestobacter*, *Deinococcus*, *Sphingomonas, Hymenobacter, Rubellimicrobium* y *Methylobacterium*, mostrando *Deinococcus, Hymenobacter* y *Roseomonas* un aumento significativo en abundancia a lo largo del tiempo, coincidiendo con los taxones más abundantes observados en los paneles solares analizados en el presente trabajo. De hecho, *Deinococcus* e *Hymenobacter* se han propuesto como biomarcadores para las bacterias transportadas por el aire del desierto (Meola et al., 2015), lo que sugiere que el transporte de partículas de polvo desde los desiertos por el aire podría ser una posible fuente de microorganismos para las comunidades microbianas que habitan en las superficies de los paneles solares.

En cuanto a la colonización fúngica de las superficies de los paneles solares en Valencia (España), varios géneros (*Neocatenulostroma, Symmetrospora, Sporobolomyces* y *Comoclathris*) mostraron un aumento significativo a lo largo del tiempo, aunque el género más abundante con diferencia fue *Alternaria*. Esto podría deberse a la abundancia de especies dentro del género *Alternaria* que son capaces de producir melanina, un pigmento que confiere protección contra la radiación UV y otros estresores ambientales (Kawamura et al., 1999; Tseng et al., 2011). Este resultado es consistente con la observación de Shirakawa et al. (2015), en el que los *Ascomycetes* melanizados dominaron los biofilms subaéreos ubicados en las superficies de los paneles solares. De hecho, los ascomicetos también se encontraban entre los hongos más abundantes en las superficies de los paneles solares en Tromsø, las islas antárticas y Berkeley, California. De hecho, los hongos son excelentes candidatos para vivir en superficies, ya que tienen un modo de nutrición absorbente y pueden formar biofilms cuando crecen en superficies (Harding et al., 2009).

Según nuestros resultados, el establecimiento de una microbiota en la superficie de un panel solar no afecta la eficiencia del panel solar (medida como voltaje de circuito abierto), ya que este parámetro no tendió a disminuir durante el período de 24 meses que analizamos. No obstante, se observaron fluctuaciones estacionales en la eficiencia, con una eficiencia

reducida en los períodos estivales. Presumimos que esto se debe a una combinación de altas temperaturas y suciedad (Omubo-Pepple et al., 2009; Skoplaki y Palyvos, 2009). Curiosamente, aunque la limpieza con Virkon resultó en una alteración de la composición de la comunidad microbiana (es decir, una disminución en la abundancia de *Deinococcus*), la limpieza con agua no lo hizo. Esto podría proporcionar una explicación con respecto a la estabilidad observada en la composición de las comunidades microbianas que habitan las superficies de los paneles solares: aunque la lluvia (la limpieza con agua siendo un proxy de esto) reduce la suciedad, no es capaz de alterar la comunidad microbiana que habita las superficies de los paneles solares.

4. Bioprospección de la microbiota de paneles solares

Los entornos extremos e inusuales, como las superficies de los paneles solares, pueden actuar como fuentes de microorganismos de importancia industrial que están preadaptados a las duras condiciones ambientales. De hecho, varios de los géneros aislados en cultivo puro en el presente estudio presentan aplicaciones potenciales en la industria, como la producción de enzimas, la producción de pigmentos antioxidantes (incluidos los carotenoides), la biorremediación, la promoción del crecimiento de las plantas o como agentes de control biológico.

En particular, las propiedades antioxidantes de los aislados de paneles solares se evaluaron en el presente trabajo utilizando un modelo *in vivo* basado en *C. elegans*. Como se mencionó anteriormente, el uso de estrategias de cribado de alto rendimiento es clave para un proceso de bioprospección eficiente, ya que permite evaluar la actividad biológica de una gran cantidad de aislamientos a la vez. Por esta razón, se realizó un ensayo de estrés oxidativo de alto rendimiento utilizando el dispositivo WMicrotracker-OneTM (PhylumTech, Santa Fe, Argentina), que permite la detección automática de supervivencia en *C. elegans*. Este ensayo reveló que *Arthrobacter* sp. (PS47), *Planomicrobium* sp. (PS1), *Bacillus aryabhattai* (PS83), *Bacillus megaterium* (PS75), *Rhodobacter maris* (PS21) y *Curtobacterium* sp. (PS20) fueron los aislados con mayor actividad antioxidante entre las 14 cepas tesatdas. La actividad antioxidante de PS1, PS21 y PS75 se confirmó con un ensayo de estrés oxidativo manual, en el que *C. elegans* se incubó con peróxido de hidrógeno y la supervivencia se determinó manualmente. Además, estos tres aislados también mostraron propiedades de protección contra los rayos ultravioleta.

Al aislar microorganismos cultivables de los paneles solares muestreados en este trabajo, una gran fracción de ellos mostró una pigmentación naranja/amarilla/roja. Aunque hay varios pigmentos que muestran una pigmentación amarillo-rojiza (es decir, el pigmento rojo prodigiosina o la escitonemina amarillo-verde), estos colores a menudo se deben a la producción de carotenoides. En el presente trabajo, la abundancia de aislados microbianos que presentan este tipo de pigmentación, la identificación y cuantificación mediante HPLC de los carotenoides producidos por varias cepas microbianas, y la detección de genes de biosíntesis de carotenoides mediante análisis metagenómico sugiere que los carotenoides están muy extendidos entre estas comunidades microbianas y pueden desempeñar un papel esencial en la protección UV en las superficies de los paneles solares.

En particular, planteamos la hipótesis de que el contenido de carotenoides de los aislados de antioxidantes estudiados en la Publicación IV (fitoeno, β-criptoxatina y fitoflueno en PS1; cantaxantina, astaxantina, β-caroteno, adonirrubina y fitoeno en PS21; y carotenoides no identificados en PS75) podría ser parcialmente explicar los efectos antioxidantes y protectores de los rayos UV observados en *C. elegans*. Las propiedades antioxidantes y de captación de radicales libres de los carotenoides de color se han estudiado ampliamente en el pasado (Ni et al., 2014; Sandmann et al., 2015), mientras que los carotenoides incoloros (por ejemplo, fitoeno y fitoflueno) han carecido de atención y son de especial interés debido a su abundancia en las cepas microbianas estudiadas. Se ha demostrado que el fitoeno y el fitoflueno poseen propiedades captadoras de radicales libres, aunque estas son menores que las de los carotenoides coloreados (Martínez et al., 2014). Sería muy interesante

considerar si la alta capacidad antioxidante de PS1 podría estar relacionada con la presencia de fitoeno junto con el carotenoide coloreado, β-criptoxantina.

5. Ambientes inexplorados como fuente de nuevas especies microbianas

Las superficies de los paneles solares albergan bacterias que no se han estudiado hasta la fecha y que, de hecho, pueden identificarse como nuevas especies microbianas. Este es el caso, por ejemplo, de *Sphingomonas solaris* R4DWN sp. nov., una bacteria de color naranja descrita en el presente trabajo y aislado de la superficie de un panel solar en Boston (Massachusetts, EE.UU.). Curiosamente, el género *Sphingomonas* no solo es un miembro de los taxones centrales que habitan los paneles solares, sino que también es uno de los primeros en llegar durante la colonización de estas superficies. Los ensayos de asimilación de carbono revelaron que esta cepa solo es capaz de asimilar 7 de las 71 fuentes de carbono analizadas, mucho menos que la especie tipo más cercana *S. fennica* DSM 13665T y S*. formosensis* DSM 24164T, capaz de asimilar 19 y 39 de las 71 fuentes probadas (Cuadro V.1). *S. fennica* DSM 13665T se aisló originalmente de un pozo de agua potable holandés (Wittich et al., 2007), mientras que *S. formosensis* DSM 24164T se aisló de suelo agrícola y mostró propiedades de degradación de hidrocarburos aromáticos policíclicos (Lin et al., 2012). Es posible que la mayor disponibilidad de nutrientes en estos entornos en comparación con las superficies de los paneles solares haya dado forma a estas cepas para poder asimilar una mayor variedad de fuentes de carbono.

Sphingomonas solaris R4DWN es solo una de las muchas potenciales especies nuevas aisladas de las superficies de los paneles solares durante el presente trabajo. Según una publicación de Kim et al. (2014), una similitud de la secuencia del gen del ARNr 16S inferior al 98,65% puede considerarse el umbral para diferenciar dos especies. Con este umbral en mente, 12 de las 68 cepas aisladas en la Publicación IV son posibles nuevas especies, mientras que 5 de las 40 cepas aisladas de las superficies de paneles solares en Boston (Publicación V), también podrían ser nuevas especies. Cabe señalar que este % de similitud debe confirmarse mediante la secuenciación del gen completo del ARNr 16S, ya que estos aislados se han identificado inicialmente mediante la secuenciación parcial de este gen. Aún no se ha determinado si la abundancia de nuevas especies potenciales está relacionada con una mayor tasa de mutación asociada a la irradiación UV, o con el hecho de que los paneles solares son entornos inusuales que apenas se han explorado hasta la fecha. En consonancia con esto, debería llevarse a cabo una recopilación exhaustiva de las nuevas especies microbianas descritas en los últimos años y sus fuentes de aislamiento para analizar más a fondo el potencial de los entornos extremos e inusuales como fuentes de nuevas especies microbianas.

Los entornos inusuales son fuentes prometedoras de nuevos compuestos, microorganismos o consorcios microbianos con posibles aplicaciones comerciales y/o industriales, y nuevas especies microbianas. En este contexto, visualizamos la bioprospección xenomicrobiana (la bioprospección de entornos extraños/inusuales) como un campo revolucionario tanto para los ecólogos microbianos como para los emprendedores de la bioeconomía del futuro (Tanner et al., 2017, Apéndice D).

Conclusiones

En esta tesis se han evaluado los aspectos ecológicos y el potencial biotecnológico de las comunidades microbianas que habitan las superficies de los paneles solares. Las conclusiones generales que surgen de nuestro trabajo se enumeran a continuación:

• A pesar de la distancia física, las superficies de los paneles solares de todo el mundo muestran microbiomas con similitudes taxonómicas y funcionales. Los phyla más abundantes incluyen *Actinobacteria, Bacteroidetes, Deinococcus, Cyanobacteria, Firmicutes*, *Proteobacteria* y *Ascomycota*, y las características funcionales comunes incluyen principalmente vías de defensa contra el estrés involucradas en la persistencia de microbios en las superficies de los paneles solares.

• Los géneros *Hymenobacter, Sphingomonas, Streptomyces, Pseudomonas, Bradyrhizobium,*

Methylobacterium, Modestobacter y *Deinococcus* constituyen el núcleo de la microbiota de las placas solares.

• Las comunidades microbianas que habitan en las superficies de los paneles solares muestran varios mecanismos de resistencia al estrés, tal y como revelan los análisis multiómicos realizados (metagenómica y metabolómica). Estos mecanismos incluyen el desarrollo de cápsulas, así como la producción de chaperonas de choque térmico, de solutos compatibles, de carotenoides, de superóxido dismutasas y peroxidasas.

• La composición de la microbiota de los paneles solares no es el resultado de una mera acumulación de taxones microbianos del entorno circundante, sino que corresponde al punto de equilibrio en una sucesión ecológica, en el marco del cual se seleccionan los taxones extremófilos adaptados a las duras condiciones de los paneles solares (radiación UV, desecación y fluctuaciones de temperatura).

• Las comunidades microbianas que habitan las superficies de los paneles solares muestran variaciones estacionales: las bacterias dominan las superficies de los paneles solares durante el período de primavera/verano, mientras que los hongos son más abundantes en el período de otoño/invierno.
• En el proceso de colonización de superficies de paneles solares, hay una transición de una comunidad generalista inicial a una comunidad especializada final compuesta por géneros bacterianos y fúngicos altamente resistentes.

• La presencia de comunidades microbianas en las superficies de los paneles solares no está vinculada a una reducción significativa de la eficiencia fotovoltaica.

• Una gran fracción de los microorganismos que habitan las superficies de los paneles solares son capaces de producir pigmentos, entre los que destacamos la producción de carotenoides comercialmente valiosos como β-caroteno, cantaxantina y astaxantina, entre otros.

• Varias de las cepas microbianas aisladas de las superficies de los paneles solares mostraron propiedades antioxidantes y de protección UV validadas en un modelo de *C. elegans*. En particular, los gusanos alimentados con las cepas PS1 (97,38% similar a *Planomicrobium glaciei*) y PS21 (98,89% similar a *Rhodobacter maris*) mostraron una mayor resistencia al estrés oxidativo y a la radiación UV que los gusanos alimentados con *E. coli* (dieta basal) o con *E. coli* complementado con antioxidantes.

• Las superficies de los paneles solares pueden ser una fuente de nuevos taxones microbianos, como es el caso de *Sphingomonas solaris* R4DWN, aislado de la superficie de un panel solar en Boston (Massachusetts, EE. UU.).

References

Aarti C, Khusro A, Agastian P (2018). Carboxymethyl cellulase production optimization from *Glutamicibacter arilaitensis* strain ALA4 and its application in lignocellulosic waste biomass saccharification. Prep Biochem Biotechnol 48(9): 853-866.

Afaq F, Adhami VM, Ahmad N, and Mukhtar H (2002). Botanical antioxidants for chemoprevention of photocarcinogenesis. Frontiers in Bioscience 7: 789-792.

Afra S, Makhdoumi A, Matin MM, Feizy J (2017). A novel red pigment from marine *Arthrobacter* sp. G20 with specific anticancer activity. J Appl Microbiol 123(5): 1228-1236.

Al-Amoudi S, Razali R, Essack M, Amini MS, Bougoffa S, Archer JAC, et al. (2016). Metagenomics as a preliminary screen for antimicrobial bioprospecting. Gene 594(2): 248-258.

Annamalai N, Kumar A, Saravanakumar A, Vijaylakshmi S, Balasubramanian T (2011). Characterization of protease from *Alcaligens faecalis* and its antibacterial activity on fish pathogens. J Environ Biol. 32(6):781-6.

Annamalai N, Veeramuthu Rajeswari M, Vijayalakshmi S, Balasubramanian T (2011). Purification and characterization of chitinase from *Alcaligenes faecalis* AU02 by utilizing marine wastes and its antioxidant activity. Ann Microbiol 61(4):801-807.

Anantharaman K, Brown CT, Hug LA, Sharon I, Castelle CJ, Probst AJ, et al (2016). Thousands of microbial genomes shed light on interconnected biogeochemical processes in an aquifer system. Nature Communications 7: 13219.

Azevedo JS, Ramos I, Araújo S, Oliveria CS, Correia A, and Henriques IS (2012). Spatial and temporal analysis of estuarine bacterioneuston and bacterioplankton using culture-dependent and culture-independent methodologies. Antonie van Leeuwenhoek 101: 819-835.

Batista JR (1994). AGAINST ALL ODDS: the survival strategies of *Deinococcus radiodurans.* Annual Review of Microbiology 51: 203-224.

Bedade DK, Singhal RS (2017). Isolation and Characterization of Acrylamidase from *Arthrobacter* sp. DBV1 and Its Ability to Biodegrade Acrylamide. Appl Biochem Biotechnol 182(2): 570-585.

Beer B, Pick A, Döring M, Lommes P, Sieber V (2018). Substrate scope of a dehydrogenase from *Sphingomonas species* A1 and its potential application in the synthesis of rare sugars and sugar derivatives. Microb Biotechnol. 11(4): 747-758.

Belnap J, Büdel B, and Lange OL (2002). Biological soil crusts: characteristics and distribution. *In* Biological soil crusts: structure, function, and management. Belnap J and Lange OL (eds). Berlin-Heidelberg: Springer, pp. 3-30.

Bereschenko LA, Stams AJM, Euverink GJW, and van Loosdrecht MCM (2010) Biofilm formation on reverse osmosis membranes is initiated and dominated by Sphingomonas spp. Applield and Environmental Microbiology 76(8): 2623-2632.

Bird RE and Hulstrom LR (1983). Terrestrial Solar Spectral Data Sets. Solar Energy 30: 563.

Bollmann A, Lewis K, and Epstein SS (2007). Incubation of environmental samples in a diffusion chamber increases the diversity of recovered isolates. Applied and Environmental Microbiology 73(20): 6386-6390.

Borić M, Danevčič T, and Stopar D (2011). Prodigiosin from *Vibrio* sp. DSM 14379; a new UV-protective pigment. Microbial Ecology 62(3): 528-36.

Bulgari D, Minio A, Casati P, Quaglino F, Delledonne M, Bianco PA (2014). *Curtobacterium* sp. Genome Sequencing Underlines Plant Growth Promotion-Related Traits. Genome Announcements 2(4): e00592-14.

Busch H, Hagedoorn PL, Hanefeld U (2019). *Rhodococcus* as A Versatile Biocatalyst in Organic Synthesis. Int J Mol Sci 20(19): 4787.

Cao L, Shi W, Shu R, Pang J, Liu Y, Zhang X, Lei Y (2018). Isolation and characterization of a bacterium able to degrade high concentrations of iprodione. Can J Microbiol 64(1):49-56.

Cappelletti M, Presentato A, Piacenza E, Firrincieli A, Turner RJ, Zannoni D (2020). Biotechnology of *Rhodococcus* for the production of valuable compounds. Appl Microbiol Biotechnol 104(20): 8567-8594.

Carlström CI, Field CM, Bortfeld-Miller M, Müller B, Sunagawa S, and Vorhold JA (2019) Synthetic microbiota reveal priority effects and keystone strains in the *Arabidopsis* phyllosphere. Nature Ecology and Evolution 3: 1445-1454.

Champion OL, Titball RW, and Bates S (2018). Standardization of *G. mellonella* larvae to provide reliable and reproducible results in the study of fungal pathogens. Journal of Fungi 4(3): 108.

Chaud LC, Lario LD, Bonugli-Santos RC, Sette LD, Pessoa Junior A, Felipe MD (2016). Improvement in extracellular protease production by the marine antarctic yeast *Rhodotorula mucilaginosa* L7. N Biotechnol 33(6): 807-814.

Chen LZ, Shi CQ, Yin FX, Wang FS, Sheng JZ (2019). Cloning and Characterization of a Chondroitin AC Exolyase from *Arthrobacter* sp. SD-04. Mol Biotechnol 61(10): 791-800.

Chien A, Edgar DB and Trela JM (1976). Deoxyribonucleic acid polymerase from the extreme thermophile *Thermus aquaticus*. Journal of Bacteriology 127: 1550–1557.

Cho JC and Giovannoni SJ (2004). Cultivation and growth characteristics of a diverse group of oligrotrophic marine Gemmaproteobacteria. Applied and Environmental Microbiology 70: 432-440.

Contesini FJ, Melo RR, Sato HH (2017). An overview of *Bacillus* proteases: from production to application. Crit Rev Biotechnol 38(3): 321-334.

Csotonyi JT, Swiderski J, Stackebrandt E, and Yurkov V (2010). A new environment for aerobic anoxygenic phototrophic bacteria: biological soil crusts. Environmental Microbiology Reports 2(5): 651-656.

Das R, Tiwary BN (2013). Isolation of a novel strain of *Planomicrobium* chinense from diesel contaminated soil of tropical environment. J Basic Microbiol 53(9): 723-32.

De Carvalho CCCR (2017). iofilms: Microbial Strategies for Surviving UV Exposure. Advances in Experimental Medicina and Biology 996: 233-239.

DeLeon-Rodriguez N, Lathem TL, Rodriguez-R LM, Barazesh JM, Anderson BE, Beyersdorf AJ, et al (2013). Microbiome of the upper troposphere: species composition and prevalence, effects of tropical storms, and atmospheric implications. Proceedings of the National Academy of Sciences of the United States of America 110: 2575–2580.

Doan HK and Leveau JH (2015). Artificial surfaces in phyllosphere microbiology. Phytopathology 105(8): 1036-1042.

Dorado-Morales P, Vilanova C, Peretó J, Codoñer FM, Ramón D and Porcar M (2016). A highly diverse, desert-like microbial biocenosis on solar panels in a Mediterranean city. Scientific Reports 6: 29235.

Duraisamy P, Sekar J, Arunkumar AD, Ramalingam PV (2020). Kinetics of Phenol Biodegradation by Heavy Metal Tolerant Rhizobacteria *Glutamicibacter nicotianae* MSSRFPD35 From Distillery Effluent Contaminated Soils. Frontiers in Microbiology 11: 1573.

EFSA BIOHAZ Panel (EFSA Panel on Biological Hazards), Koutsoumanis K, Allende A, Alvarez-Ordóñez A, Bolton D, Bover-Cid S, et al. (2020). Statement on the update of the list of QPS-recommended biological agents intentionally added to food or feed as notified to EFSA 11: suitability of taxonomic units notified to EFSA until September2019. EFSA Journal 18(2): 5965.

EFSA FEEDAP Panel (EFSA Panel on Additives and Products or Substances usedin Animal Feed), Rychen G, Aquilina G, Azimonti G, Bampidis V, Bastos ML, et al. (2018). Guidance on the characterisation of microorganismsused as feed additives or as production organisms. EFSA Journal 16(3): 5206.

Engleman EA, Katner SN, and Neal-Beliveau BSN (2016). *Caenorhabditis elegans* as a model to study the molecular and genetic mechanisms of drug addiction. Progress in Molecular Biology and Translational Science 137: 229-252.

Fenu A, Donckels BM, Beffa T, Bemfohr C, Weemaes M (2015). Evaluating the application of *Microbacterium* sp. strain BR1 for the removal of sulfamethoxazole in full-scale membrane bioreactors. Water Sci Technol 72(10): 1754-61.

Fialho AM, Moreira LM, Granja AT, Popescu AO, Hoffmann K, Sá-Correia I (2008). Occurrence, production, and applications of gellan: current state and perspectives. Appl Microbiol Biotechnol79(6): 889-900.

Fiedor J and Burda K (2014). Potential role of carotenoids as antioxidants in human health and disease. Nutrients 6: 466-488.

Franklin MP, McDonald IR, Bourne DG, Owens NJP, Upstill-Goddard RC, and Murrell JC (2005). Bacterial diversity in the bacterioneuston (sea surface microlayer): the bacterioneuston through the looking glass. Environmental Microbiology 7(5): 723-36.

Fu S, Sun J, Qian L, Li Z (2008). *Bacillus* phytases: present scenario and future perspectives. Appl Biochem Biotechnol 151(1):1-8.

Garza-Gonzalez MT, Barboza Perez D, Vazquez Rodriguez A, Garcia-Gutierrez DI, Zarate X, Cantú Cardenas ME, et al. (2016). Metal-Induced Production of a Novel Bioadsorbent Exopolysaccharide in a Native *Rhodotorula mucilaginosa* from the Mexican Northeastern Region. PLoS One 11(2): e0148430.

Geissinger O, Herlemann DPR, Mörschel E, Maier UG, and Brune A (2009). The ultramicrobacterium "*Elusimicrobium minitum*" gen. nov., sp. Nov., the first cultivated representative of the termite group 1 phylum. Applied and Environmental Microbiology 75: 2831-2840.

Gerber E, Bernard R, Castang S, Chabot N, Coze F, Dreux-Zigha A, et al (2015). *Deinococcus* as new chassis for industrial biotechnology: biology, physiology and tools. Journal of Applied Microbiology 119: 1–10.

Gibbons SM (2017). Microbial community ecology: function over phylogeny. Nature Ecology and Evolution 1: 0032.

Gich F, Janys MA, König M, and Overmann J (2012). Enrichment of previously uncultured bacteria from natural complex communities by adhesion to solid surfaces. Environmental Microbiology 14: 2984-2997.

Govarthanan M, Kamala-Kannan S, Selvankumar T, Mythili R, Srinivasan P, Kim H (2019). Effect of blue light on growth and exopolysaccharides production in phototrophic *Rhodobacter* sp. BT18 isolated from brackish water. Int J Biol Macromol 131: 74-80.

Gray DA, Dugar G, Gamba P, Strahl H, Jonker MJ, and Hamoen LW (2019). Extreme slow growth as alternative strategy to survive deep starvation in bacteria. Nature Communications 10(1): 890.

Griffin DW (2007). Atmospheric movement of microorganisms in clouds of desert dust and implications for human health. Clinical Microbiology Reviews 30: 459–477.

Grube M, Cardinale M, de Castro JV Jr, Müller H, and Berg G (2009). Species-specific structural and functional diversity of bacterial communities in lichen symbioses. ISME Journal 3(9): 1105-15.

Grünberger A, Probst C, Helfrich S, Nanda A, Stute B, et al. (2015). Spatiotemporal microbial single-cell analysis using a high-throughput microfluidics cultivation platform. Cytometry A87: 1101-1115.

Gu Y, Xu X, Wu Y, Niu T, Liu Y, Li J, Du G, Liu L (2018). Advances and prospects of *Bacillus subtilis* cellular factories: From rational design to industrial applications. Metab Eng 50: 109-121.

Guo L, Dai Z, Guo J, Yang W, Ge F, Dai Y (2020). Oligotrophic bacterium *Hymenobacter latericoloratus* CGMCC 16346 degrades the neonicotinoid imidacloprid in surface water. AMB Express 10(1): 7.

Halimi S and Mirsalehian A (2016). Assessment and comparison of probiotic potential of four *Lactobacillus* species isolated from feces samples of Iranian infants. Microbiology and Immunology 60: 73–81.

Han SJ, Park H, Lee SG, Lee HK, Yim JH (2011). Optimization of cold-active chitinase production from the Antarctic bacterium, *Sanguibacter antarcticus* KOPRI 21702. Appl Microbiol Biotechnol 89(3): 613-21.

Hanlon P and Sewalt V. GEMs: genetically engineered microorganisms and the regulatory oversight of their uses in modern food production. Critical Reviews in Food Science and Nutrition, online ahead of print, 1-12.

Harding MW, Marques LLR, Howard RJ, and Olson ME (2009). Can filamentous fungi form biofilms? Trends in Microbiology 17(11): 475-480.

He M, Guo M, Zhang X, Chen K, Yan J, Irbis C (2018). Purification and characterization of alginate lyase from *Sphingomonas* sp. ZH0. J Biosci Bioeng 126(3): 310-316.

Heins ZJ, Mancuso CP, Kiriakov S, Wong BG, Bashor CJ, and Khalil AS (2019). Designing automated, high-throughput, continuous cell growth experiments using eVOLVER. Journal of Visualized Experiments 147: 10.3791/59652.

Henke NA, Heider SAE, Peters-Wendisch P, and Wendisch VF (2016). Production of the marine carotenoid astaxanthin by metabolically engineered *Corynebacterium glutamicum*. Marine Drugs 14(7): 124.

Hervas A and Casamayor EO (2009). High similarity between bacterioneuston and airborne bacterial community compositions in a high mountain lake area. FEMS Microbiology Ecology 67(2): 219-228.

Hess M, Sczyrba A, Egan R, Kim T, Chokhawala H, Schroth G, et al. (2011). Metagenomic discovery of biomass-degrading genes and genomes from cow rumen. Science 331 (6016), 463-467.

Hirsch P, Gallikowski CA, Siebert J, Peissl K, Kroppenstedt R, Schumann P, et al (2004). *Deinococcus frigens* sp. nov., *Deinococcus saxicola* sp. nov., and *Deinococcus marmoris* sp. nov., Low Temperature and Draught-tolerating, UV-resistant Bacteria from Continental Antarctica. Systematic and Applied Microbiology 27: 636–645.

Honnen S (2017). *Caenorhabditis elegans* as a powerful alternative model organism to promote research in genetic toxicology and biomedicine. Arch Toxicol 91(5): 2029-2044.

Hu K, Zhu XL, Mu H, Ma Y, Ullah N, Tao YS (2016) A novel extracellular glycosidase activity from *Rhodotorula mucilaginosa*: its application potential in wine aroma enhancement. Lett Appl Microbiol 62(2): 169-76.

Hussein AH, Lisowska BK, and Leak DJ (2015). The genus *Geobacillus* and their biotechnological potential. Advances in Applied Microbiology 92: 1–48.

Ingham CJ, Sprenkels A, Bomer J, Molenaar D, van der Berg A, et al. (2007). The micro-Petri dish, a million-well growth chip for the culture and high-throughput screening of microorganisms. PNAS 104: 18217-18222.

Irizarry I, White JF (2017). Application of bacteria from non-cultivated plants to promote growth, alter root architecture and alleviate salt stress of cotton. Journal of Applied Microbiology 122(4): 1110-1120.

Jarboui R, Baati H, Fetoui F, Gargouri A, Gharsallah N, Ammar E (2012). Yeast performance in wastewater treatment: case study of *Rhodotorula mucilaginosa*. Environ Technol 33(7-9): 951-60.

Jayaraman JD, Sigamani S, Arul D, Nedunchelizan K, Pachiappan P, Ramamurthy D (2020). Molecular characterization and antioxidant assay of pigment producing bacteria, *Sphingomonas paucimobilis* and *Microbacterium arborescens* isolated from fresh water sediments. Nat Prod Res 34(8):1192-1196.

Jemil N, Ben Ayed H, Hmidet N, Nasri M (2016). Characterization and properties of biosurfactants produced by a newly isolated strain *Bacillus methylotrophicus* DCS1 and their applications in enhancing solubility of hydrocarbon. World J Microbiol Biotechnol 32(11):175.

Jeon J, Lee H, Sadowsky MJ, Sugawara M, and Chang W (2015). Characterization of a functional role of the *Bradyrhizobium japonicum* isocitrate lyase in desiccation tolerance. International Journal of Molecular Sciences 16(7): 16695-16709.

Jeong J, Lee I, Kim S, and Park Y (1999). Stimulation of β-carotene synthesis by hydrogen peroxide in *Blakesle trispora*. Biotechnology Letters 21(8): 683-686.

Jeżewska-Frąckowiak J, Seroczyńska K, Banaszczyk J, Jedrzejczak G, Żylicz-Stachula A, Skowron PM (2018). The promises and risks of probiotic *Bacillus* species. Acta Biochim Pol 65(4): 509-519.

Jin M, Xiao A, Zhu L, Zhang Z, Huang H, Jiang L (2019). The diversity and commonalities of the radiation-resistance mechanisms of *Deinococcus* and its up-to-date applications. AMB Express 9(1): 138.

Jorjão AL, Oliveira LD, Scorzoni L, Figueiredo-Godoi L, Prata CA, Jorge MA and Junqueira JC (2018). From moths to caterpillars: ideal conditions for *Galleria mellonella* rearing for in vivo microbiological studies. Virulence 9(1): 383–389.

Junqueira JC (2012). *Galleria mellonella* as a model host for human pathogens: recent studies and new perspectives. Virulence 3(6): 474-476.

Kawahara H, Hirai A, Minabe T, Obata H (2013). Stabilization of astaxanthin by a novel biosurfactant produced by *Rhodotorula mucilaginosa* KUGPP-1. Biocontrol Sci 18(1): 21-8.

Kawamura C, Tsujimoto T, and Tsuge T (1999) Targeted disruption of a melanin biosynthesis gene affects conidial development and UV tolerance in the Japanese pear pathotype of *Alternaria alternata*. Molecular Plant-Microbe Interactions 12(1): 59-63.

Kawasaki S, Mizuguchi K, Sato M, Kono T, and Shimizu H (2013). A novel astaxanthin-binding photooxidative stress-inducible aqueous carotenoprotein from a eukaryotic microalga isolated from asphalt in midsummer. Plant and Cell Physiology 54(7): 1027-40.

Kealey C, Creaven CA, Murphy CD, and Brady CB (2017). New approaches to antibiotic discovery. Biotechnology Letters 39: 805-817.

Khot M, Ghosh D (2017). Lipids of *Rhodotorula mucilaginosa* IIPL32 with biodiesel potential: Oil yield, fatty acid profile, fuel properties. J Basic Microbiol 57(4):345-352.

Kiehl JT and Trenberth KE (1997). Earth's Annual Global Mean Energy Budget. Bulletin of the American Meteorological Society 78: 197–208.

Kim D, Choi KY, Yoo M, Zylstra GJ, Kim E (2018). Biotechnological Potential of *Rhodococcus* Biodegradative Pathways. J Microbiol Biotechnol 28(7): 1037-1051.

Kim M, Oh HS, Park SC, Chun J (2014). Towards a taxonomic coherence between average nucleotide identity and 16S rRNA gene sequence similarity for species demarcation of prokaryotes. Int J Syst Evol Microbiol 64: 346–351.

Kim SM, Park H, Choi JI (2017). Cloning and Characterization of Cold-Adapted α-Amylase from Antarctic Arthrobacter agilis. Appl Biochem Biotechnol. 181(3):1048-1059.

Kimura K, Yokoyama S (2019). Trends in the application of *Bacillus* in fermented foods. Curr Opin Biotechnol 56: 36-42.

Kis ÁE, Laczi K, Zsíros S, Kós P, Tengölics R, Bounedjoum N, Kovács T, Rákhely G, Perei K (2017). Characterization of the *Rhodococcus* sp. MK1 strain and its pilot application for bioremediation of diesel oil-contaminated soil. Acta Microbiol Immunol Hung 64(4): 463-482.

Kogure K (2019). Novel Antioxidative Activity of Astaxanthin and Its Synergistic Effect with Vitamin E. Journal of Nutritional Science and Vitaminology 65: S109-S112.

Kojima H, Watanabe M, Tokizawa R, Shinohara A, and Fukui M (2016). *Hymenobacter nivis* sp. nov., isolated from red snow in Antarctica. International Journal of Systematic and Evolutionary Microbiology 66, 4821–4825.

Kong H, Kucera RB and Jack WE (1993). Characterization of a DNA polymerase from the hyperthermophile Archaea *Thermococcus litoralis*. The Journal of Biological Chemistry 268: 1965–1975.

Kumar A, Baruah A, Tomioka M, Iino Y, Kalita MC, and Khan M (2019). *Caenorhabditis elegans*: a model to understand host-microbe interactions. Cell Mol Life Sci 77(7): 1229-1249.

Kumari N, Rana A, Jagadevan S (2019). Arsenite biotransformation by *Rhodococcus* sp.: Characterization, optimization using response surface methodology and mechanistic studies. Science of the Total Environment 687: 577-589.

Kuyukina MS, Ivshina IB, Baeva TA, Kochina OA, Gein SV, Chereshnev VA (2015). Trehalolipid biosurfactants from nonpathogenic *Rhodococcus* actinobacteria with diverse immunomodulatory activities. N Biotechnol 32(6): 559-68.

Kwak MJ, Jeong H, Madhaiyan M, Lee Y, Sa TM, Oh TK, Kim JF (2014). Genome information of *Methylobacterium oryzae*, a plant-probiotic methylotroph in the phyllosphere. PLoS One 9(9): e106704.

Lagier JC, Duborg G, Million M, Cadoret F, Bilen M, Fenollar F, et al. (2018). Culturing the human microbiota and culturomics. Nature Reviews in Microbiology 16: 540-550.

Lee KC, Archer SDJ, Boyle RH, Lecap-Bugler DC, Belnap J, and Pointing SB (2016). Niche filtering of bacteria in soil and rock habitats of the Colorado Plateau Desert, Utah, USA. Frontiers in Microbiology 7: 1489.

Lee PC, and Schmidt-Dannert C (2002). Metabolic engineering towards biotechnological production of carotenoids in microorganisms. Applied Microbiology and Biotechnology 60: 1-11.

Lee YM, Kim EH, Lee HK, and Hong SG (2014). Biodiversity and physiological characteristics of Antarctic and Arctic lichens-associated bacteria. World Journal of Microbiology and Biotechnology 30(10): 2711-21.

Li N, Han X, Xu S, Li C, Wei X, Liu Y, Zhang R, Tang X, Zhou J, Huang Z (2018). Glycoside Hydrolase Family 39 β-Xylosidase of *Sphingomonas* Showing Salt/Ethanol/Trypsin Tolerance, Low-pH/Low-Temperature Activity, and Transxylosylation Activity. J Agric Food Chem 66(36): 9465-9472.

Ligusa H, Yoshida Y, and Hasunuma K (2005). Oxygen and hydrogen peroxide enhance light-induced carotenoid synthesis in *Neurospora crassa*. FEBS Letters 579(18): 4012-4016.

Lim S, Jung J, Blanchard L, and de Groot A. Conservation and diversity of radiation and oxidative stress resistance mechanisms in Deinococcus species. FEMS Microbiology Reviews 43(1): 19-52.

Liu W, Liu C, Sun D (2017). Complete Genome Sequence of a Novel Bioflocculant-Producing Strain, *Microbacterium paludicola* CC3. Genome Announc 5(38): e01008-17.

Lodhi AF, Zhang Y, Adil M, and Deng Y (2018). Antibiotic discovery: combining isolation chip (iChip) technology and co-culture technique. Applied Microbiology and Biotechnology 102(17): 7333-7341.

Li C, Li B, Zhang N, Wei N, Wang Q, Wang W, Xie Y, and Zou H (2019). Salt stress increases carotenoid production of Sporidiobolus pararoseus NGR via torulene biosynthetic pathway. The Journal of General and Applied Microbiology 65(3): 111-120.

Liang G, Yang Y, Wu S, Jiang Y, Xu Y (2017). The generation of biogenic manganese oxides and its application in the removal of As(III) in groundwater. Environ Sci Pollut Res Int 24(21): 17935-17944.

Lin S, Shen F, Lai W, Zhu Z, Chen W, *et al.* (2012). *Sphingomonas formosensis* sp. nov., a polycyclic aromatic hydrocarbon-degrading bacterium isolated from agricultural soil. International Journal of Systematic and Evolutionary Microbiology 62: 1581-1586.

Ling LL, Schneider T, Peoples AJ, Spoering AL, Engels I, Conlon BP, et al (2015). A new antibiotic kills pathogens without detectable resistance. Nature 517, 455–459.

Liu RH (2013). Health-promoting components of fruits and vegetables in the diet. Advances in Nutrition 4(3): 384S-392S.

Liu Z, Zhang X, Xue Y, Xu M, and Zheng Y (2014). Improvement of *Alcaligenes faecalis* nitrilase by gene site saturation mutagenesis and its application in stereospecific biosynthesis of (R)-(-)-mandelic acid. Journal of Agricultural and Food Chemistry 62(20): 4685-4694.

Locey KJ and Lennon JT (2016). Scaling laws predict global microbial diversity. PNAS 113(21): 5970-5975.

Lopes R, Tsui S, Gonçalves PJRO, de Queiroz MV (2018). A look into a multifunctional toolbox: endophytic *Bacillus* species provide broad and underexploited benefits for plants. World J Microbiol Biotechnol 34(7):94.

Louca S, Mazel F, Doebeli M, and Parfrey LW (2019). A census-based estimate of Earth's bacterial and archaeal diversity. PLOS Biology 17(2): e3000106.

Lundberg KS, Shoemaker DD, Adams MW, Short JM, Sorge JA, and Mathur EJ (1991). High-fidelity amplification using a thermostable DNA polymerase isolated from *Pyrococcus furiosus*. Gene 108: 1–6.

Luo Y, Wang F, Huang Y, Zhou M, Gao J, Yan T, Sheng H, An L (2019). *Sphingomonas* sp. Cra20 Increases Plant Growth Rate and Alters Rhizosphere Microbial Community Structure of *Arabidopsis thaliana* Under Drought Stress. Frontiers in Microbiology 10: 1221.

Maeng S, Kim MK, Subramani G (2020). *Hymenobacter jejuensis* sp. Nov., a UV radiation-tolerant bacterium isolated from Jeju island. Antonie Van Leeuwenhoek 113(4): 553-561.

Makhalanyane TP, Valverde A, Gunnigle E, Frossard A, Ramond JB, and Cowan DA (2015). Microbial ecology of hot desert edaphic systems. FEMS Microbiology Reviews 39: 203–221.

Mao X, Zhang Y, Wang X and Liu J (2020). Novel insights into salinity-induced lipogenesis and carotenogenesis in the oleaginous astaxanthin-producing alga Chromochloris zofingiensis: a multi-omics study. Biotechnology for Biofuels 13: 73.

Marchant R, Banat IM, Rahman TJ and Berzano M (2002). The frequency and characteristics of highly thermophilic bacteria in cool soil environments. Environmental Microbiology 4: 595–602.

Marizcurrena JJ, Morel MA, Braña V, Morales D, Martinez-López W, Castro-Sowinski S (2017). Searching for novel photolyases in UVC-resistant Antarctic bacteria. Extremophiles 21(2): 409-418.

Markovitsi D (2016). UV-induced DNA Damage: The Role of Electronic Excited States. Photochemistry and Photobiology 92(1): 45-51.

Martínez A, Stinco CM, and Meléndez-Martínez AJ (2014). Free radical scavenging properties of phytofluene and phytoene isomers as compared to lycopene: a combined experimental and theoretical study. The Journal of Physical Chemistry 118(33): 9819-9825.

Mastan A, Rane D, Dastager SG, Vivek Babu CS (2020). Plant Probiotic Bacterial Endophyte, Alcaligenes faecalis, Modulates Plant Growth and Forskolin Biosynthesis in Coleus forskohlii. Probiotics Antimicrob Proteins 12(2):481-493.

Mehandia S, Sharma SC, and Arya SK (2019). Isolation and characterization of an alkali and thermostable laccase from a novel *Alcaligenes faecalis* and its application in decolorization of synthetic dyes. Biotechnology Reports (Amsterdam) 25: e00413.

Melo ALD, Soccol VT, and Soccol CR (2014). *Bacillus thuringiensis*: mechanism of action, resistance and new applications: a review. Critical Reviews in Biotechnology 36: 317–326.

Mesa-Arango AC, Forastiero A, Bernal-Martínez L, Cuenca-Estrella M, Mellado E, Zaragoza O (2013). The non-mammalian host *Galleria mellonella* can be used to study the virulence of the fungal pathogen *Candida tropicalis* and the efficacy of antifungal drugs during infection by this pathogenic yeast. Medical Mycology 51(5): 461-472.

Mikulak E, Gliniewicz A, Przygodzka M, Solecka J (2018). *Galleria mellonella* as model organism used in biomedical and other studies. Przegląd epidemiologiczny 72(1): 57-73.

Milde J, Estner EF, and Grassmann J (2007). Synergistic effects of phenolics and carotenoids on human low-density lipoprotein oxidation. Molecular Nutrition & Food Research 51(8): 956-961.

Mishra P, Kaur S, Sharma AN, and Jolly RS (2016). Characterization of an indole-3-acetamide hydrolase from *Alcaligenes faecalis* subsp. *parafaecalis* and its application in efficient preparation of both enantiomers of chiral building block 2,3-dihydro-1,4-benzodioxin-2-carboxylic acid. PLoS One 11(7): e0159009.

Moliné M, Libkind D, van Broock M (2012). Production of torularhodin, torulene, and β-carotene by *Rhodotorula* yeasts. Methods Mol Biol 898: 275-83.

Moye ZD, Valiuskyte K, Dewhirst FE, Nichols FC, and Davey ME (2016). Synthesis of sphingolipids impacts survival of *Porphyromonas gingivalis* and the presentation of surface polysaccharides. Frontiers in Microbiology 7: 1919.

Mozzetti V, Grattepanche F, Moine D, Bernard B, Rezzonico E, Meile L, et al. (2010). New method for selection of hydrogen peroxide adapted bifidobacteria cells using continuous culture and immobilized cell technology. Microbial Cell Factories 9: 60.

Nagar S, Shaw AK, Anand S, Celin SM, Rai PK (2018). Aerobic biodegradation of HMX by *Planomicrobium flavidum*. 3 Biotech 8(11): 455.

Ni Y, Nagashimada M, Zhaz L, Nagata N, Kobori M, Sugiura M, et al. (2014). Prevention and reversal of lipotoxicity-induced hepatic insulin resistance and steatohepatitis in mice by an antioxidant carotenoid, β-cryptoxanthin. Endocrinology 156(3): 987-999.

Nicholson WL, Schuerger AC, and Setlow P. (2005). The solar UV environment and bacterial spore UV resistance: considerations for Earth-to-Mars transport by natural processes and human spaceflight. Mutation Research 571: 249-264.

Nichols D, Cahoon N, Trakhtenberg EM, Pham L, Mehta A, Belanger A, et al. (2010). Use of Ichip for high-throughput *in* situ cultivation of "uncultivable" microbial species. Applied and Environmental Microbiology 76 (8): 2445-2450.

Nishimura H and Sako Y (2009). Purification and characterization of the oxygen-thermostable hydrogenase from the aerobic hyperthermophilic archaeon *Aeropyrum*

camini. Journal of Bioscience and Bioengineering 108, 299–303.

Noble AS, Noe S, Clearwater MJ, and Lee CK (2020). A core phyllosphere microbiome exists across distant populations of a tree species indigenous to New Zealand. PLoS ONE 15(8): e0237079.

Normand P, Gury J, Pujic P, Chouaia B, Crotti E, Brusetti L, et al. (2012). Genome sequence of radiation-resistant *Modestobacter marinus* strain BC501, a representative *Actinobacterium* that thrives on calcareous stone surfaces. Journal of Bacteriology 194(17): 4773-4774.

Omubo-Pepple, V.B., Israel-Cookey, C., and Alaminokuma, G.I. (2009) Effects of temperature, solar flux and relative humidity on the efficient conversión of solar energy to electricity. Eur J Sci Res 35(2): 173-180.

Orellana R, Macaya C, Bravo G, Dorochesi F, Cumsille A, Valencia R, Rojas C, and Seeger M (2018). Living at the frontiers of life: extremophiles in chile and their potential for bioremediation. Frontiers in Microbiology 9: 2309.

Órdenes-Aenishanslins N, Anziani-Ostuni G, Vargas-Reyes M, Alarcón J, Tello A, and Pérez-Donoso JM (2016). Pigments from UV-resistant Antarctic bacteria as photosensitizers in Dye Sensitized Solar Cells. Journal of Photochemistry and Photobiology B 162: 707-14.

Ochsner AM, Sonntag F, Buchhaupt M, Schrader J, Vorholt JA (2015). *Methylobacterium extorquens*: methylotrophy and biotechnological applications. Appl Microbiol Biotechnol 99(2): 517-34.

Ottesen AR, Gorham S, Reed E, Newell MJ, Ramachandran P, Canida T, Allard M, Evans P, Brown E, and White JR (2016). Using a control to better understand phyllosphere microbiota. PLoS ONE 11(9): e0163482.

Overmann J, Abt B, and Sikorski J (2017). Present and future of culturing bacteria. Annual Review of Microbiology 71: 11-30.

Overmann J and Scholz AH (2017). Microbiological research under the Nagoya Protocol: facts and fiction. Trends in Microbiology 25(2): 85-88.

Pacia MZ, Pukalski J, Turnau K, Baranska M, Kaczor A (2016). Lipids, hemoproteins and carotenoids in alive *Rhodotorula mucilaginosa* cells under pesticide decomposition - Raman imaging study. Chemosphere. 164:1-6.

Palmieri G, Arciello S, Bimonte M, Carola A, Tito A, Gogliettino M, et al. (2019). The extraordinary resistance to UV radiations of a manganese superoxide dismutase of *Deinococcus radiodurans* offers promising potentialities in skin care applications. J Biotechnol. 302: 101-111.

Pandey A and Yarzábal LA (2019). Bioprospecting cold-adapted plant growth promoting microorganisms from mountain environments. Applied Microbiology and Biotechnology 103: 643–657.

Park HH, Jung Y and Lee SV (2017). Survival assays using *Caenorhabditis elegans*. Mol Cells 40(2): 90-99.

Parte AC (2018). LPSN — List of Prokaryotic names with Standing in Nomenclature (bacterio.net), 20 years on. International Journal of Systematic and Evolutionary Microbiology, 68, 1825-1829.

Peng W, Li X, Song J, Jiang W, Liu Y, Fan W (2018). Bioremediation of cadmium- and zinc-contaminated soil using *Rhodobacter sphaeroides*. Chemosphere 197: 33-41.

Pereira MF, Rossi CC, de Queiroz MV, Martins GF, Isaac C, Bosse JT, et al. (2015). *Galleria mellonella* is an effective model to study *Actinobacillus pleuropneumoniae* infection. Microbiology 161(Pt 2): 387–400.

Perruchon C, Patsioura V, Vasileiadis S, Karpouzas DG (2016). Isolation and characterisation of a *Sphingomonas* strain able to degrade the fungicide ortho-phenylphenol. Pest Manag Sci 72(1): 113-24.

Piñar G, Garcia-Valles M, Gimeno-Torrente D, Fernandez-Turiel JL, Ettenauer J, and Sterflinger K (2013). Microscopic, chemical, and molecular-biological investigation of the decayed medieval stained window glasses of two Catalonian churches. International Biodeterioration & Biodegradation 84(100): 388-400.

Pleitner A, Zhai Y, Winter R, Ruan L, McMullen LM, and Gänzle MG (2012). Compatible solutes contribute to heat resistance and ribosome stability in *Escherichia coli* AW1.7. Biochimica et Biophysica Acta 1824(12): 1351-1357.

Pointing SB, Chan Y, Lacap DC, Lau MCY, Jurgens JA, and Farrell RL (2009). Highly specialized microbial diversity in hyper-arid polar desert. Proceedings of the National Academy of Sciences of the United States of America 106(47): 19964-19969.

Porcar M, Tanner K, and Northen T. The Hymenosphere: the microbial skin of the Earth. *Manuscript in preparation*.

Purohit A, Yadav SK (2020). Characterization of a thermotolerant and acidophilic mannanase producing *Microbacterium* sp. CIAB417 for mannooligosachharide production from agro-residues and dye decolorization. Int J Biol Macromol 163: 1154-1161.

Qin W, Fan F, Zhu Y, Wang Y, Liu X, Ding A, Dou J (2017). Comparative proteomic analysis and characterization of benzo(a)pyrene removal by *Microbacterium* sp. strain M.CSW3 under denitrifying conditions. Bioprocess Biosyst Eng 40(12): 1825-1838.

Rainey FA, Ray K, Ferreira M, Gatz BZ, Nobre MF, Bagaley D, et al (2005). Extensive diversity of ionizing-radiation-resistant bacteria recovered from Sonoran desert soil and description of nine new species of the genus *Deinococcus* obtained from a single soil sample. Applied and Environmental Microbiology 71: 5225–5235.

Rajendran R, Pandi A, Ramchary A, Thiagarajan H, Panneerselvam J, Niraikulam A, et al. (2019). Extracellular urease from *Arthrobacter creatinolyticus* MTCC 5604: scale up, purification and its cytotoxic effect thereof. Mol Biol Rep 46(1):133-141.

Rastogi RP, Sonani RR, and Madamwar D (2015). Cyanobacterial sunscreen scytonemin: role in photoprotection and biomedical research. Applied Biochemistry and Biotechnology 176: 1551–1563.

Ren L, Jia Y, Ruth N, Shi Y, Wang J, Qiao C, Yan Y (2016). Biotransformations of bisphenols mediated by a novel *Arthrobacter* sp. strain YC-RL1. Appl Microbiol Biotechnol. 100(4):1967-1976.

Retamal-Morales G, Heine T, Tischler JS, Erler B, Gröning JAD, Kaschabek SR, Schlömann M, Levicán G, Tischler D (2018). Draft genome sequence of *Rhodococcus erythropolis* B7g, a biosurfactant producing actinobacterium. J Biotechnol 280: 38-41.

Risa A, Krifaton C, Kukolya J, Kriszt B, Cserháti M, Táncsics A (2018). Aflatoxin B1 and Zearalenone-Detoxifying Profile of *Rhodococcus* Type Strains. Curr Microbiol 75(7): 907-917.

Ruan A, Gao Y, Fang C, Xu Y (2018). Isolation and characterization of a novel nicotinophilic bacterium, *Arthrobacter* sp. aRF-1 and its metabolic pathway. Biotechnol Appl Biochem 65(6):848-856.

Ruan L, Yu Z, Fang B, He W, Wang Y, and Shen P (2004). Melanin pigment formation and increased UV resistance in *Bacillus thuringiensis* following high temperature induction. Systematic and Applied Microbiology 27(3): 286-289.

Ruibal C, Selbmann L, Avci S, Martin-Sanchez PM, and Gorbushina AA (2018). Roof-inhabiting cousins of rock-inhabiting fungi: novel melanized microcolonial fungal species from photocatalytically reactive subaerial surfaces. Life 8(3): 30.

Ruther A, Misawa N, Boger P, and Sandmann G (1997). Production of zeaxanthin in *Escherichia coli* transformed with different carotenogenic plasmids. Applied Microbiology and Biotechnology 48: 162-167.

Sahinkaya M, Colak DN, Ozer A, Canakci S, Deniz I, Belduz AO (2019). Cloning, characterization and paper pulp applications of a newly isolated DyP type peroxidase from *Rhodococcus* sp. T1. Mol Biol Rep 46(1): 569-580.

Salimizadeh M, Shirvani M, Shariatmadari H, Nikaeen M, Leili Mohebi Nozar S (2018). Coupling of bioaugmentation and phytoremediation to improve PCBs removal from a transformer oil-contaminated soil. Int J Phytoremediation 20(7):658-665.

Sandmann, G. (2015). Carotenoids of biotechnological importance. Advances in Biochemical Engineering and Biotechnology 148: 449-467.

Sankari M, Hridya H, Sneha P, George PDC, and Siva R. (2017) Effect of UV radiation and its implications on carotenoid pathway in *Bixa orellana* L. Journal of Photochemistry and Photobiology B: Biology

Santos AL, Baptista I, Lopes S, Henriques I, Gomes NCM, Almeida A, et al. (2012). The UV responses of bacterioneuston and bacterioplankton isolates depend on the physiological condition and involve a metabolic shift. FEMS Microbiology Ecology 80(3): 646-58.

Santos AL, Baptista I, Newton CMG, Henriques I, Almeida A, Correia A, and Cunha A (2014). Contribution of chemical water properties to the differential responses of bacterioneuston and bacterioplankton to ultraviolet-B radiation. FEMS Microbiology Ecology 87(2): 517-35.

Sarkar A, Sar P, Islam E (2016). Hexavalent Chromium Reduction by *Microbacterium oleivorans* A1: A Possible Mechanism of Chromate -Detoxification and -Bioremediation. Recent Pat Biotechnol 9(2): 116-29.

Savi DC, Shaaban KA, Gos FMW, Thorson JS, Glienke C, Rohr J (2018). Secondary metabolites produced by *Microbacterium* sp. LGMB471 with antifungal activity against the phytopathogen *Phyllosticta citricarpa*. Folia Microbiol (Praha) 64(3): 453-460.

Setlow P (2006). Spores of *Bacillus subtilis*: their resistance to and killing by radiation, heat and chemicals. Journal of Applied Microbiology 101(3): 514-525.

Shahid M, Akram MS, Khan MA, Zubair M, Shah SM, Ismail M, et al. (2018). A phytobeneficial strain *Planomicrobium* sp. MSSA-10 triggered oxidative stress responsive mechanisms and regulated the growth of pea plants under induced saline environment. J Appl Microbiol 124(6): 1566-1579.

Shao Y, Wang Y, Yi F, Zhang Y, Liu W, Yang C, Meng H, Cui P, Zhong W (2019). Gaseous Formaldehyde Degrading by *Methylobacterium* sp. XJLW. Appl Biochem Biotechnol 189(1): 262-272.

Shao H, Xu L, Yan Y (2014). Thermostable lipases from extremely radioresistant bacterium *Deinococcus radiodurans*: cloning, expression, and biochemical characterization. J Basic Microbiol. 54(9): 984-95.

Shen P, Yue Y, and Park Y. (2018). A living model for obesity and aging research: *Caenorhabditis elegans.* Critical Reviews in Food Science and Nutrition 58(5): 741-754.

Sherpa RT, Reese CJ, and Montazaeri AH (2015). Application of iChip to grow "uncultivable" microorganisms and its impact on antibiotic discovery. Journal of Pharmacy & Pharmaceutical Sciences 18: 303–315.

Shirakawa MA, Zilles R, Mocelin A, Gaylarge CC, Gorbushina A, Heidrich G, Giudice MC, Del Negro GMB, and John VM (2015). Journal of Environmental Mannagement 157: 160-167.

Skoplaki, E. and Palyvos, J.A. (2009) On the temperature dependence of photovoltaic module electrical performance: A review of efficiency/power correlations. Solar Energy 83: 614-624.

Slaninova E, Sedlacek P, Mravec F, Mullerova L, Samek O, Koller M, et al. (2018). Light scattering on PHA granules protects bacterial cells against the harmful effects of UV radiation. Applied Microbiology and Biotechnology 102(4): 1923-1931.

Smith D, da Silva M, Jackson J, and Lyal C. (2017). Explanation of the Nagoya Protocol on Access and Benefit Sharing and its implication for microbiology. Microbiology 163: 289-296.

Soffe R, Bernach M, Remus-Emsermann MNP, and Nock V (2019). Replicating Arabidopsis model leaf surfaces for phyllosphere microbiology. Scientific Reports 9: 14420.

Soule T, Garcia-Pichel F, and Stout V (2009). Melanin pigment formation and increased UV resistance in Bacillus thuringiensis following high temperature induction. Journal of Bacteriology 191(14): 4639-4646.

Speth DE, Hu B, Bosch N, Keltjens JT, Stunnenberg HG, and Jetten MSM (2012). Comparative genomics of two independently enriched "Candidatus Kuenenia Stuttgartiensis" anammox bacteria. Frontiers in Microbiology 3: 307.

Stahl W, and Helmut S (2012). β-Carotene and other carotenoids in protection from sunlight. The Americal Journal of Clinical Nutrition 96(5): 1179S-1184S.

Stahl W, Junghans A, de Boer B, Driomina ES, Briviba K, and Sies H (1998). Carotenoid mixtures protect multilamellar liposomes against oxidative damage: synergistic effects of lycopene and lutein. FEBS Letters 427: 305-308.

Stepanov VG, Vaishampayan P, Venkateswaran K, and Fox GE (2014). Draft genome sequence of *Deinococcus phoenicis*, a novel strain isolated during the Phoenix Lander spacecraft assembly. Genome Announcements 2, e00301-14.

Subhash Y, Tushar L, Sasikala C, and Ramana CV (2013). *Erythrobacter odishensis* sp. nov. and *Pontibacter odishensis* sp. nov. isolated from dry soil of a solar saltern. International Journal of Systematic and Evolutionary Microbiology 63: 4524–4532.

Sugawara M, Cytryn EJ, and Sadowsky MJ (2010). Functional role of *Bradyrhizobium japonicum* trehalose biosynthesis and metabolism genes during physiological stress and nodulation. Applied and Environmental Microbiology 76(4): 1071-1081.

Surger M, Angelov A, Liebl W (2020). Distribution and diversity of olefins and olefin-biosynthesis genes in Gram-positive bacteria. Biotechnol for Biofuels 13: 70.

Tanner K, Vilanova C, and Porcar M (2017). Bioprospecting challenges in unusual environments. Microbial Biotechnology 10(4): 671-673.

Tao Y, Jin H, Long ZF, Zhang L, Ding XQ, Tao K, Liu SG (2006). Cloning and expression of a chitinase gene from *Sanguibacter* sp. C4. Yi Chuan Xue Bao 33(11):1037-46.

Tindall KR and Kunkel TA (1988). Fidelity of DNA synthesis by the *Thermus aquaticus* DNA polymerase. Biochemistry 27: 6008–6013.

Toledo FL, Gonzalez-Lopez J, Calvo C (2008). Production of bioemulsifier by *Bacillus subtilis, Alcaligenes faecalis* and *Enterobacter* species in liquid culture. Bioresour Technol 99(17):8470-5.

Trevijano-Contador N and Zaragoza O (2018). Immune response of *Galleria mellonella* against human fungal pathogens. Journal of fungi (Basel, Switzerland) 5(1): 3.

Tseng MN, Chung PC and Tzean SS (2011). Enhancing the stress tolerance and virulence of an entomopathogen by metabolic engineering of dihydroxynaphthalene melanin biosynthesis genes. Applied and Environmental Microbiology 77(13): 4508-4519.

Venugopalan VP, Kuehn M, Hausner M, Springael D, Wilderer PA, and Wuertz S (2005) Architecture of a nascent *Sphingomonas* sp. Biofilm under varied hydrodynamic conditions. Applied and Environmental Microbiology 71(5): 2677-2686.

Viegas CA, Silva VP, Varela VM, Correia V, Ribeiro R, Moreira-Santos M (2019). Evaluating formulation and storage of *Arthrobacter aurescens* strain TC1 as a bioremediation tool for terbuthylazine contaminated soils: Efficacy on abatement of aquatic ecotoxicity. Sci Total Environ. 668:714-722.

Vilanova C, Marín M, Baixeras J, Latorre A, and Porcar M (2014). Selecting microbial strains from pine tree resin: biotechnological applications from a terpene world. PLoS ONE 9: e100740.

Vilanova C and Porcar M (2016). Are multi-omics enough? Nature Microbiology 1(8):16101.

Vítek P, Jehlička J, Ascaso C, Mašek V, Gómez-Silva B, Olivares H, and Wierzchos J (2014). Distribution of scytonemin in endolithic microbial communities from halite crusts in the hyperarid zone of the Atacama Desert, Chile. FEMS Microbiology Ecology 90: 351–366.

Wang M, Chen L, Zhang Z, Wang X, Qin S, Yan P (2017). Screening of alginate lyase-excreting microorganisms from the surface of brown algae. AMB Express 7(1): 74.

Wang H, Jiang K, Zhu Z, Jiang W, Yang Z, Zhu S, et al. (2018). Optimization of fed-batch fermentation and direct spray drying in the preparation of microbial inoculant of acetochlor-degrading strain *Sphingomonas* sp. DC-6. 3 Biotech 8(7): 294.

Wang CT, Wang YY, Liu WS, Cheng CM, Chiu KH, Liu LL, et al. (2018). *Rhodobacter sphaeroides* Extract Lycogen™ Attenuates Testosterone-Induced Benign Prostate Hyperplasia in Rats. Int J Mol Sci 19(4): 1137.

Weinhouse C, Truong L, Meyer JN, and Allard P. *Caenorhabditis elegans* as an emerging model system in environmental epigenetics. Environ Mol Mutagen 59(7): 560-575.

Wilson MC, Mori T, Rückert C, Uria AR, Helf MJ, Takada K, et al (2014). An environmental bacterial taxon with a large and distinct metabolic repertoire. Nature 506: 58–62.

Wittich R, Busse H, Kämpfer P, Macedo A, Tiirola M, *et al*. (2007). *Sphingomonas fennica* sp. nov. and *Sphingomonas haloaromaticans* sp. nov., outliers of the genus *Sphingomonas.* International Journal of Systematic and Evolutionary Microbiology 57: 1740-1746.

Wong BG, Mancuso CP, Kiriakov S, Bashor CJ, and Khalil A (2018). Precise, automated control of conditions for high-throughput growth of yeast and bacteria with eVOLVER. Nature Biotechnology 36: 614-623.

Wu T, Xu H, Liang X, and Tang M (2019). *Caenorhabditis elegans* as a complete model organism for biosafety assessments of nanoparticles. Chemosphere 221: 708-726.

Wu Q, Zhao Y, Wang D, Xu Y (2013). Immobilized *Rhodotorula mucilaginosa*: a novel urethanase-producing strain for degrading ethyl carbamate. Appl Biochem Biotechnol 171(8): 2220-32.

Xiong YW, Ju XY, Li XW, Gong Y, Xu MJ, Zhang CM, Yuan B, Lv ZP, Qin S (2019). Fermentation conditions optimization, purification, and antioxidant activity of exopolysaccharides obtained from the plant growth-promoting endophytic actinobacterium *Glutamicibacter halophytocola* KLBMP 5180. Int J Biol Macromol 153: 1176-1185.

Xu X, Xu M, Zhao Q, Xia Y, Chen C, Shen Z (2018). Complete Genome Sequence of Cd(II)-Resistant *Arthrobacter* sp. PGP41, a Plant Growth-Promoting Bacterium with Potential in Microbe-Assisted Phytoremediation. Curr Microbiol 75(9): 1231-1239.

Yang CF, Lee CM, Wang CC (2006). Isolation and physiological characterization of the pentachlorophenol degrading bacterium *Sphingomonas chlorophenolica*. Chemosphere 62(5): 709-14.

Ye X, Peng T, Feng J, Yang Q, Pratush A, Xiong G, Huang T, Hu Z (2019). A novel dehydrogenase 17β-HSDx from *Rhodococcus* sp. P14 with potential application in bioremediation of steroids contaminated environment. J Hazard Mater 362: 170-177.

Ye M, Tang X, Yang R, Zhang H, Li F, Tao F, Li F, Wang Z (2018). Characteristics and Application of a Novel Species of *Bacillus: Bacillus velezensis*. ACS Chem Biol 13(3): 500-505.

Yin W, Wang Y, Liu L, and He J (2019). Biofilms: The Microbial "Protective Clothing" in Extreme Environments. Internatinoal Journal of Molecular Sciences 20(14): 3423.

Yokoyama S, Adachi Y, Asakura S, and Kohyama E (2013). Characterization of *Alcaligenes faecalis* strain AD15 indicating biocontrol activity against plant pathogens. The Journal of General and Applied Microbiology 59(2): 89-95.

Yu FB, Shan SD, Luo LP, Guan LB, Qin H (2013). Isolation and characterization of a *Sphingomonas* sp. strain F-7 degrading fenvalerate and its use in bioremediation of contaminated soil. J Environ Sci Health B 48(3): 198-207.

Zampolli J, Zeaiter Z, Di Canito A, Di Gennaro P (2019). Genome analysis and -omics approaches provide new insights into the biodegradation potential of *Rhodococcus*. Appl Microbiol Biotechnol 103(3): 1069-1080.

Zäncker B, Cunliffe M, and Engel A (2018). Bacterial community composition in the sea surface microlayer off the Peruvian coast. Frontiers in Microbiology 9: 2699.

Zhang L (2005). Integrated approaches for discovering novel drugs from microbial natural products. *In* Natural Projects. Zhang L and Demain AL (eds). New Jersey: Humana Press, pp. 33-35.

Zhang XN, Ran QQ, Zhang X (2015). Screening and identification of a cutinase-producing *Rhodotorula mucilaginosa* and properties of the cutinase. Appl Biochem Biotechnol 175(2): 1221-33.

Zhao B, Tian M, An Q, Ye J, Guo JS (2017). Characteristics of a heterotrophic nitrogen removal bacterium and its potential application on treatment of ammonium-rich wastewater. Bioresour Technol 226:46-54.

Zhao X, Wang L, Ma F, Yang J (2018). Characterisation of an efficient atrazine-degrading bacterium, *Arthrobacter* sp. ZXY-2: an attempt to lay the foundation for potential bioaugmentation applications. Biotechnoly for Biofuels 11: 113.

Zhao HP, Wang L, Ren JR, Li Z, Li M, Gao HW (2008). Isolation and characterization of phenanthrene-degrading strains *Sphingomonas* sp. ZP1 and *Tistrella* sp. ZP5. J Hazard Mater 152(3): 1293-300.

Zhu C, Zhang J, Li L, Zhang J, Jiang Y, Shen Z, Guan H, Jiang X (2017). Purification and Characterization of Hyaluronate Lyase from *Arthrobacter globiformis* A152. Appl Biochem Biotechnol 182(1): 216-228.

Zhu XF, Zhou Y, Feng JL (2007). Analysis of both chitinase and chitosanase produced by *Sphingomonas* sp. CJ-5. J Zhejiang Univ Sci B. 8(11): 831-8.

Zwirchmayr J, Kirchweger B, Lehner T, Tahir A, Pretsch D, and Rollinger JM (2020). A robust and miniaturized screening platform to study natural products affecting metabolism and survival in *Caenorhabditis elegans*. Scientific Reports 10(1): 12323.

Appendix A

Original publication reprints

environmental microbiology reports

Environmental Microbiology Reports (2018) **10**(1), 75–79 doi:10.1111/1758-2229.12608

Polar solar panels: Arctic and Antarctic microbiomes display similar taxonomic profiles

Kristie Tanner,[1] Jose Manuel Martí,[1] Josabel Belliure,[2] Mar Fernández-Méndez,[3] Esther Molina-Menor,[1] Juli Peretó[1,4,5] and Manuel Porcar[1,5]*

[1]*Institute for Integrative Systems Biology (I2SysBio, University of Valencia-CSIC), Paterna, Valencia, Spain.*
[2]*Ecology Section, Department of Life Sciences, University of Alcalá, Alcalá de Henares, Madrid, Spain.*
[3]*Norwegian Polar Institute, Tromsø, Norway.*
[4]*Department of Biochemistry and Molecular Biology, University of Valencia, Spain.*
[5]*Darwin Bioprospecting Excellence SL, Paterna, Valencia, Spain.*

Summary

Solar panels located on high (Arctic and Antarctic) latitudes combine the harshness of the climate with that of the solar exposure. We report here that these polar solar panels are inhabited by similar microbial communities in taxonomic terms, dominated by *Hymenobacter* spp., *Sphingomonas* spp. and Ascomycota. Our results suggest that solar panels, even on high latitudes, can shape a microbial ecosystem adapted to irradiation and desiccation.

Introduction

The microbial ecology of some artificial structures, including solar panels, has been poorly explored up to date (Shirakawa *et al*, 2015; Dorado-Morales *et al*, 2016). These reports suggest that photovoltaic surfaces display a diverse microbial community, highly tolerant to thermal fluctuations, ultraviolet (UV) irradiation and desiccation (Dorado-Morales *et al*, 2016). In this work, we aimed to study, through Next Generation Sequencing (NGS) and microbial culturing techniques, the microbiome of photovoltaic solar panels from two cold locations, lying close or inside the polar circles: Tromsø, Norway (69°40′N 18°56′E) and two Antarctic islands (62°0′S 58°0′W) (Fig. 1A).

Received 5 October, 2017; accepted 23 November, 2017. *For correspondence E-mail: manuel.porcar@uv.es; Tel. +34 963544473.

© 2017 Society for Applied Microbiology and John Wiley & Sons Ltd

Tromsø is the largest urban area in northern Norway. It is located on the coast, above the Arctic Circle, and experiences a subarctic climate. Average temperatures in winter range between 0.9 and −3.6 °C and in summer between 5.3 and 12.4 °C. The South Shetlands constitute a group of islands of the Maritime Antarctica. Monthly average temperature is between −3.1 and −10.9 °C from March to October, when the sea around the islands is closed by ice, and slightly warmer from November to February, with temperatures ranging between −1.7 and 0.5 °C.

Results and discussion

A total of 14 individual solar panels were sampled in January and May 2017 in Antarctica (9 panels, 3 from Deception Island and 6 from Livingston Island) and Tromsø (5 panels), respectively (Fig. 1A). Aliquots were spread on LB and R2A media and incubated at 4 °C for three weeks to select psychrotrophic and psychrophilic microorganisms (Fig. 1B). A collection of 44 isolates was characterized by genetic identification, growth ability and UV-light and desiccation resistance (Fig. 1C). A detailed explanation of all the experimental procedures used in this study can be found on the research group website that can be accessed using the following link: http://www.uv.es/synbio/solpan. The isolates from Antarctic panels able to grow at 4 °C were identified as either *Rhodotorula mucilaginosa* (pink pigmentation) or *Alcaligenes faecalis*/*Curtobacterium* sp. (yellow pigmentation). Samples from Tromsø yielded a larger diversity of microorganisms including *Cryobacterium arcticum*, *Sphingomonas* sp., *Curtobacterium* sp., *Microbacterium* sp. and *Dioszegia fristingensis*, all of them able to grow at 15 °C. Interestingly, despite the low temperatures of their original habitats, 37 isolates were able to grow at 30 °C and 11 also grew at 37 °C. One of these was identified as *R. mucilaginosa*, a cold-adapted (with activity at up to −5 °C), carotenoid-producing, cosmopolitan, mesophilic yeast that has previously been isolated from a wide range of remote environments, including Antarctical ice cores or 11 000 m deep sea vents (Gadanho and Sampaio, 2005; Amato *et al*., 2009; Moliné *et al*., 2012; Nunes *et al*., 2013; Connell *et al*., 2014; Yu *et al*., 2015).

Regarding UV resistance, many of the isolates (a total of 30) were able to survive 30 s of irradiation with

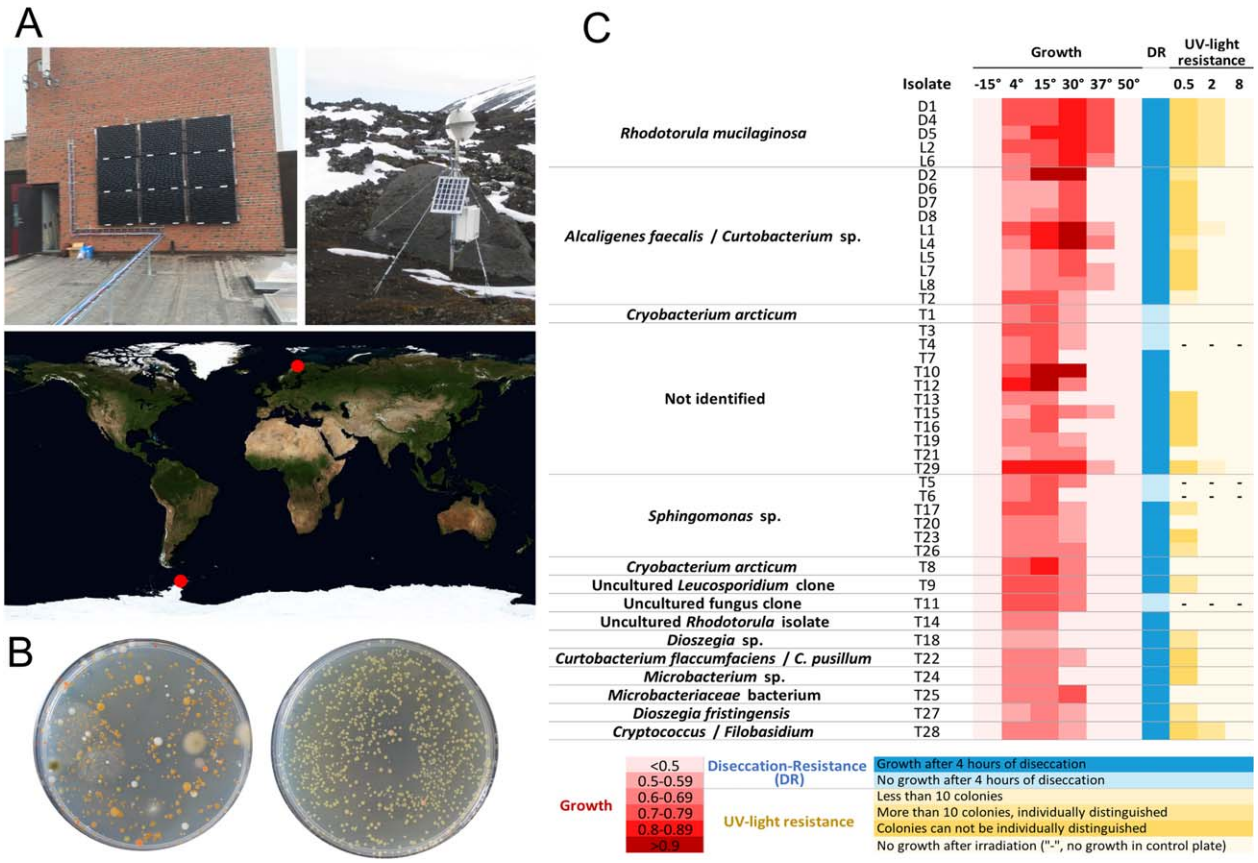

Fig. 1. (A) Solar panels sampled from Tromsø, Norway (top, left) and South Shetlands, Antarctica (top, right), indicated by red dots in the map below; (B) microbial colonies obtained culturing aliquots of surface biomass on R2A at 4 °C for 21 days (left, Tromsø; right, Antarctica); (C) heatmap displaying taxonomic identification, location ('D' Deception, Antarctica; 'L' Livingston, Antarctica; or 'T' Tromsø, Norway; followed by an identification number), growth (colony diameter in cm) at temperatures from −15 to 50 °C (data in red), resistance to desiccation (data in blue) and resistance to UV light (after 0.5, 2 and 8 min of irradiation; data in yellow) of the isolated colonies.

a monochromatic 254 nm light, whereas only seven isolates were able to survive two minutes of irradiation and none resisted eight minutes of irradiation. The most frequent isolate able to resist two minutes of UV irradiation was *R. mucilaginosa*, in which carotenoid accumulation may play an essential role in photoprotection against UV-light (Moliné *et al.*, 2010). Finally, desiccation-resistance assays revealed that 38 out of the 44 isolates were able to resist four hours of desiccation. *R. mucilaginosa* was present among these 38 isolates, an expected result when considering previous studies that describe this species as highly resistant to desiccation (Connell *et al.*, 2008). The large heterogeneity in UV-resistance is in contrast with the high irradiance in the sampled site, suggesting that a tridimensional biofilm-like structure may play an important role, not only in survival under desiccation conditions, but also in UV-protection in the natural biocenosis (Gorbushina, 2007; Villa *et al.*, 2015). Our results support the hypothesis of the existence of a specific solar panel microbial community adapted to the harsh conditions that characterize these artificial environments: UV-radiation and desiccation.

The taxonomic profiles obtained through NGS of three panels from each location were analysed (Breitwieser and Salzberg, 2016; Kim *et al.*, 2016; Martí, 2017) and found to exhibit a rather low variation within locations, although both sites proved to differ in some taxa (Fig. 2A and B). All the obtained Recentrifuge-Krona plots can be accessed on the research group's website through the following link: http://www.uv.es/synbio/solpan. First, tree sequences were dominant in Tromsø and not in the Antarctica; similarly, sequences from *Equisetum* were found exclusively in the solar panels from Norway. This can be explained by the proximity and abundance of vegetation and the lack of it in Tromsø and Antarctica respectively, since Tromsø is in a forest area, whereas the South Shetlands are at least 800 km away from the nearest forest land (South America). Second, many more fungal sequences, including many yeasts, and, especially, the lichen-associated *Trebouxia* algae were more frequent in the Antarctica

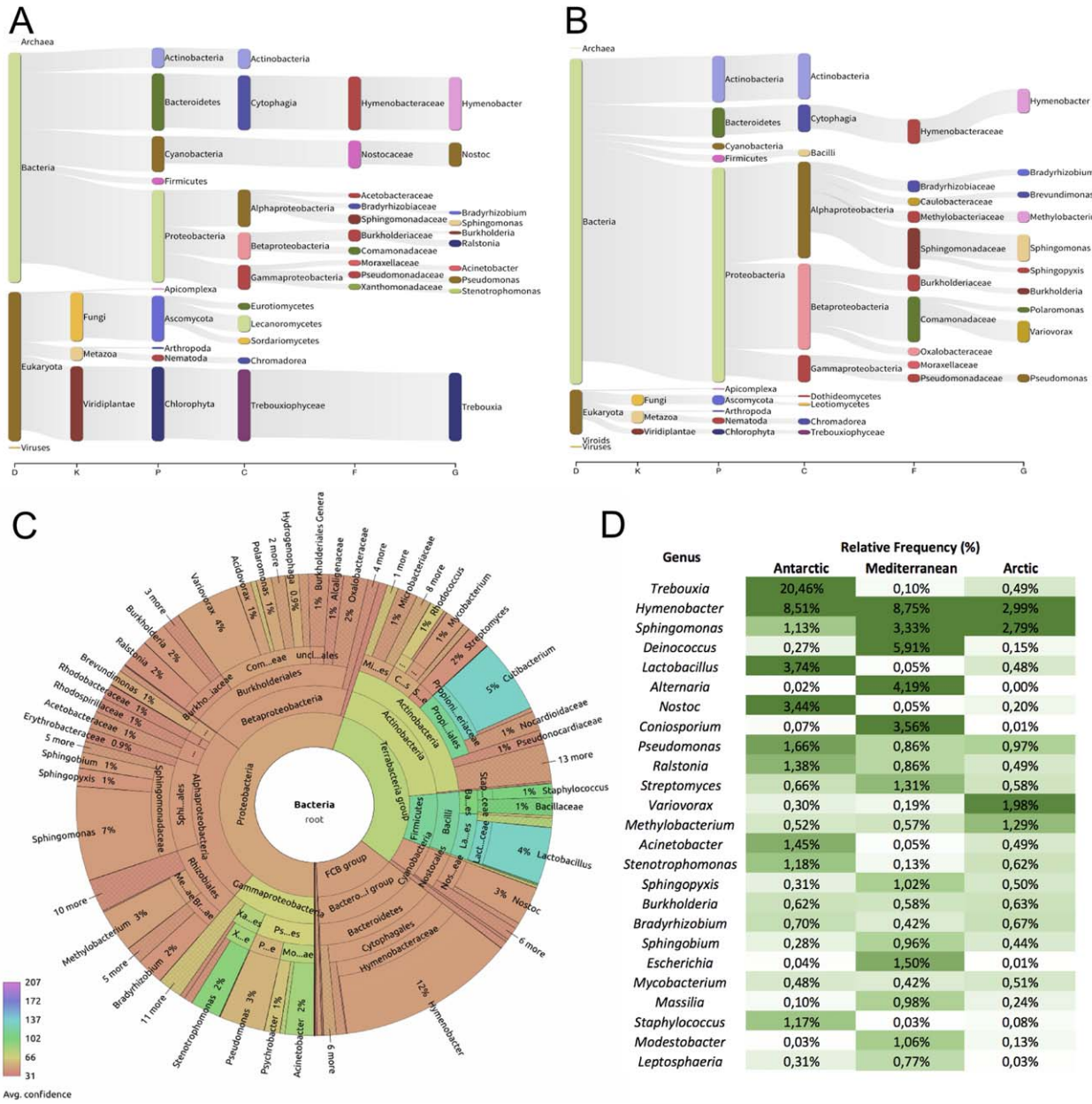

Genus	Relative Frequency (%)		
	Antarctic	Mediterranean	Arctic
Trebouxia	20,46%	0,10%	0,49%
Hymenobacter	8,51%	8,75%	2,99%
Sphingomonas	1,13%	3,33%	2,79%
Deinococcus	0,27%	5,91%	0,15%
Lactobacillus	3,74%	0,05%	0,48%
Alternaria	0,02%	4,19%	0,00%
Nostoc	3,44%	0,05%	0,20%
Coniosporium	0,07%	3,56%	0,01%
Pseudomonas	1,66%	0,86%	0,97%
Ralstonia	1,38%	0,86%	0,49%
Streptomyces	0,66%	1,31%	0,58%
Variovorax	0,30%	0,19%	1,98%
Methylobacterium	0,52%	0,57%	1,29%
Acinetobacter	1,45%	0,05%	0,49%
Stenotrophomonas	1,18%	0,13%	0,62%
Sphingopyxis	0,31%	1,02%	0,50%
Burkholderia	0,62%	0,58%	0,63%
Bradyrhizobium	0,70%	0,42%	0,67%
Sphingobium	0,28%	0,96%	0,44%
Escherichia	0,04%	1,50%	0,01%
Mycobacterium	0,48%	0,42%	0,51%
Massilia	0,10%	0,98%	0,24%
Staphylococcus	1,17%	0,03%	0,08%
Modestobacter	0,03%	1,06%	0,13%
Leptosphaeria	0,31%	0,77%	0,03%

Fig. 2. Sankey diagram with the 10 most abundant taxa in different taxonomical levels (Domain D, Kingdom K, Phylum P, Class C, Family F, Genus G) in the solar panels of Livingston, Antarctica (A) and Tromsø, Norway (B); (C) Recentrifuge-Krona plot snapshot of the shared bacterial taxa at the genus level among all the polar panels (from Livingston and Tromsø), where the percentage shows the relative abundance at the genus level averaged for all the polar samples; (D) heatmap showing the 25 most abundant genera versus geographical location ordered by overall relative frequency; the average for all the solar panels sampled per location is given; the colour scale is quasilogarithmic to improve visualization of taxa with similar order of magnitude among locations. Taxa under the clade Streptophyta have been removed throughout the figure to improve resolution at the microbial level.

samples. Antarctica is not only characterized by its low temperatures but also by displaying very low values of environmental humidity, conditions which *Trebouxia* can easily overcome thanks to its cryo- and desiccation-resistant properties (Hájek *et al.*, 2012; Carniel *et al.*, 2016). Finally, other taxa that differed in frequency between the two locations were *Variovorax*, more frequent in Norway, and *Lactobacillus* and *Acinetobacter*, more frequent in the solar panels from Antarctica.

Despite these differences, the global taxonomic profile of the two locations had relevant and abundant similarities (Fig. 2C and D). Interestingly, many of the shared genera have also been found while reanalysing the sequences of the first NGS report of the solar panel

microbiome (Dorado-Morales *et al*., 2016), carried out in a Mediterranean city (Fig. 2D). On the contrary, some other genera are more frequently found in Mediterranean solar panels than in the polar ones, such as *Alternaria*, *Coniosporium*, *Escherichia*, *Massilia* and *Modestobacter*.

Our results not only reveal the existence of a diverse community of microorganisms in solar panels from polar environments, which is in concordance with previous reports about the diversity of microbial life in polar regions, but it also highlights the importance of adaptation in extreme environments (Friedmann, 1982; 1993; Boetius *et al*., 2015). From the identification of a clear core of shared microbial taxa, it would be tempting to conclude that our results support the well-known microbial ecology *mantra* by Baas Becking '*everything is everywhere, but, the environment selects'*. However, it has to be stressed that the location of the studied solar panels (either close or beyond the Antarctic and Arctic circles respectively) does not assure a common environment: both polar environments have different wind regimes and key differences in terms of climate or distance to other biomes (which is clearly reflected by the high frequency of tree sequences in the Tromsø samples, which were missing in Antarctica, for example). Yet, the striking co-presence of bacterial genera (Fig. 2D) such as *Sphingomonas*, *Pseudomonas*, *Ralstonia*, *Streptomyces*, *Methylobacterium* and, especially, *Hymenobacter* (the most abundant genus in solar panels from both poles as well as in those previously characterized in a Mediterranean city), indicates that solar panels are not mere stockers of wind-borne microorganisms. On the opposite, our results demonstrate that solar panels in extreme latitudes bear a similar, native microbiome, characterized by marker taxa shared with panels from other latitudes, fitting nicely with previous work performed on geothermal communities of Antarctica that aimed at assessing the role of aeolian transport and environmental selection in the establishment of microbial communities (Herbold *et al*., 2014). This fact suggests that the strong selection pressures – desiccation and irradiation, very likely – of the solar panels themselves – rather than their location – are what shape the microbiome developing on them.

Acknowledgements

Financial support from Spanish Government (grant Helios, reference: BIO2015–66960-C3-1-R co-financed by FEDER funds and Ministerio de Economía y Competitividad) is acknowledged. The data sets generated during and/or analysed during the current study are available from the corresponding author on reasonable request. The authors declare no conflict of interest.

References

Amato, P., Doyle, S., and Christner, B.C. (2009) Macromolecular synthesis by yeasts under frozen conditions. *Environ Microbiol* **11**: 589–596.

Boetius, A., Anesio, A.M., Deming, J.W., Mikucki, J.A., and Rapp, J.Z. (2015) Microbial ecology of the cryosphere: sea ice and glacial habitats. *Nat Rev Microbiol* **13**: 677–690.

Breitwieser, F.P., and Salzberg, S.L. (2016). Pavian: interactive analysis of metagenomics data for microbiomics and pathogen identification. bioRxiv: 084715.

Carniel, F.C., Gerdol, M., Montagner, A., Banchi, E., De Moro, G., Manfrin, C., *et al*. (2016) New features of desiccation tolerance in the lichen photobiont *Trebouxia gelatinosa* are revealed by a transcriptomic approach. *Plant Mol Biol* **91**: 319–339.

Connell, L.B., Redman, R., Craig, S., Scorzetti, G., Iszard, M., and Rodriguez, R. (2008) Diversity of soil yeasts isolated from South Victoria Land, Antarctica. *Microb Ecol* **56**: 448–459.

Connell, L.B., Rodriguez, R.R., Redman, R.S., and Dalluge, J.J. (2014). Cold-adapted yeasts in Antarctic Deserts. In *Cold-Adapted Yeasts: Biodiversity, Adaptation Strategies and Biotechnological Significance*. Buzzini, P., Margesin, R. (eds). Berlin Heidelberg: Springer-Verlag, pp. 75–98.

Dorado-Morales, P., Vilanova, C., Peretó, J., Codoñer, F.M., Ramón, D., and Porcar, M. (2016) A highly diverse, desert-like microbial biocenosis on solar panels in a Mediterranean city. *Sci Rep* **6**: 29235.

Friedmann, E.I. (1982) Endolithic microorganisms in the Antarctic cold desert. *Science* **215**: 1045–1053.

Friedmann, E.I. (1993). *Antarctic Microbiology*. 1st edn. California: Wiley-Liss.

Gadanho, M., and Sampaio, J.P. (2005) Occurrence and diversity of yeasts in the mid-atlantic ridge hydrothermal fields near the Azores Archipielago. *Microb Ecol* **50**: 408–417.

Gorbushina, A.A. (2007) Life on the rocks. *Environ Microbiol* **9**: 1613–1631.

Hájek, J., Váczi, P., Barták, M., and Jahnová, L. (2012) Interspecific differences in cryoresistance of lichen symbiotic algae of genus *Trebouxia* assessed by cell viability and chlorophyll fluorescence. *Cryobiology* **64**: 215–222.

Herbold, C.W., Lee, C.K., McDonald, I.R., and Cary, S.C. (2014) Evidence of global-scale Aeolian dispersal and endemism in isolated geothermal microbial communities of Antarctica. *Nat Commun* **5**: 3875.

Kim, D., Song, L., Breitwieser, F.P., and Salzberg, S.L. (2016) Centrifuge: rapid and sensitive classification of metagenomic sequences. *Genome Res* **26**: 1721–1729.

Martí, J.M. (2017). Recentrifuge: robust comparative analysis and contamination removal for metagenomic data. bioRxiv DOI 10.1101/190934.

Moliné, M., Flores, M.R., Libkind, D., del Carmen Diéguez, M., Farías, M.E., and van Broock, M. (2010) Photoprotection by carotenoid pigments in the yeast *Rhodotorula mucilaginosa*: the role of torularhodin. *Photochem Photobiol Sci* **9**: 1145–1151.

Moliné, M., Libkind, D., and van Broock, M. (2012) Production of torularhodin, torulene, and β-carotene by *Rhodotorula* yeasts. *Methods Mol Biol* **898**: 275–283.

Nunes, J.M., Bizerra, F.C., Ferreira, R.C., and Colombo, A.L. (2013) Molecular identification, antifungal susceptibility profile, and biofilm formation of clinical and environmental *Rhodotorula* species isolates. *Antimicrob Agents Chemother* **57**: 382–389.

Shirakawa, M.A., Zilles, R., Mocelin, A., Gaylarde, C.C., Gorbushina, A., Heidrich, G., *et al*. (2015) Microbial colonization affects the efficiency of photovoltaic panels in a tropical environment. *J Environ Manage* **157**: 160–167.

Villa, F., Pitts, B., Lauchnor, E., Cappitelli, F., and Stewart, P.S. (2015) Development of a laboratory model of a phototroph-heterotroph mixed-species biofilm at the stone/air interface. *Front Microbiol* **6**: 1251.

Yu, P., Wang, X.T., and Liu, J.W. (2015) Purification and characterization of a novel cold-adapted phytase from *Rhodotorula mucilaginosa* strain JMUY14 isolated from Antarctic. *J Basic Microbiol* **55**: 1029–1039.

frontiers in Microbiology

ORIGINAL RESEARCH
published: 11 December 2018
doi: 10.3389/fmicb.2018.03043

Microbial Ecology on Solar Panels in Berkeley, CA, United States

Manuel Porcar[1,2,3], Katherine B. Louie[3], Suzanne M. Kosina[4], Marc W. Van Goethem[4], Benjamin P. Bowen[3,4], Kristie Tanner[2] and Trent R. Northen[3,4]**

[1] Institute for Integrative Systems Biology (I2SysBio), University of Valencia-CSIC, Paterna, Spain, [2] Darwin Bioprospecting Excellence S.L., Parc Científic de la Universitat de València, Paterna, Spain, [3] Lawrence Berkeley National Laboratory, Joint Genome Institute, Walnut Creek, CA, United States, [4] Environmental Genomics and Systems Biology Division, Lawrence Berkeley National Laboratory, Berkeley, CA, United States

Solar panels can be found practically all over the world and represent a standard surface that can be colonized by microbial communities that are resistant to harsh environmental conditions, including high irradiation, temperature fluctuations and desiccation. These properties make them not only ideal sources of stress-resistant bacteria, but also standard devices to study the microbial communities and their colonization process from different areas of Earth. We report here a comprehensive description of the microbial communities associated with solar panels in Berkeley, CA, United States. Cultivable bacteria were isolated to characterize their adhesive capabilities, and UV- and desiccation-resistance properties. Furthermore, a parallel culture-independent metagenomic and metabolomic approach has allowed us to gain insight on the taxonomic and functional nature of these communities. Metagenomic analysis was performed using the Illumina HiSeq2500 sequencing platform, revealing that the bacterial population of the Berkeley solar panels is composed mainly of Actinobacteria, Bacteroidetes and Proteobacteria, as well as lower amounts of Deinococcus-Thermus and Firmicutes. Furthermore, a clear predominance of *Hymenobacter* sp. was also observed. A functional analysis revealed that pathways involved in the persistence of microbes on solar panels (i.e., stress response, capsule development, and metabolite repair) and genes assigned to carotenoid biosynthesis were common to all metagenomes. On the other hand, genes involved in photosynthetic pathways and general autotrophic subsystems were rare, suggesting that these pathways are not critical for persistence on solar panels. Metabolomics was performed using a liquid chromatography tandem mass spectrometry (LC-MS/MS) approach. When comparing the metabolome of the solar panels from Berkeley and from Valencia (Spain), a very similar composition in polar metabolites could be observed, although some metabolites appeared to be differentially represented (for example, trigonelline, pantolactone and 5-valerolactone were more abundant in the samples from Valencia than in the ones from Berkeley). Furthermore, triglyceride metabolites were highly abundant in all the solar panel samples, and both locations displayed similar profiles. The comparison of the taxonomic profile of the Californian solar panels with those previously described in Spain revealed striking similarities, highlighting the central role of both selective pressures and the ubiquity of microbial populations in the colonization and establishment of microbial communities.

Keywords: solar panels, microbiome, metabolomics, metagenomics, stress-resistant bacteria

OPEN ACCESS

Edited by:
Claudio Christian Vásquez, Universidad de Santiago de Chile, Chile

Reviewed by:
Charles K. Lee, University of Waikato, New Zealand
Robert Heyer, Otto-von-Guericke-Universität Magdeburg, Germany

****Correspondence:***
Manuel Porcar
manuel.porcar@uv.es
Trent R. Northen
TRNorthen@lbl.gov

Specialty section:
This article was submitted to Extreme Microbiology, a section of the journal Frontiers in Microbiology

Received: *12 July 2018*
Accepted: *26 November 2018*
Published: *11 December 2018*

Citation:
Porcar M, Louie KB, Kosina SM, Van Goethem MW, Bowen BP, Tanner K and Northen TR (2018) Microbial Ecology on Solar Panels in Berkeley, CA, United States. Front. Microbiol. 9:3043. doi: 10.3389/fmicb.2018.03043

INTRODUCTION

It has recently been calculated that there might be as many as one trillion different species on Earth, the vast majority of which are microorganisms (Locey and Lennon, 2016). Microorganisms are ubiquitous, and can even be found in extreme environments such as thermal springs (Kizilova et al., 2014), marine trenches (Felden et al., 2014) and man-made structures (Vilanova et al., 2015). Interestingly, solar panels have been reported to harbor a diverse microbial community, mainly composed of desiccation/irradiation-adapted microorganisms, similar to those found in other highly irradiated environments, such as deserts, plant surfaces and polar microbial mats (Dorado-Morales et al., 2016; Tanner et al., 2018). The presence of biofilms on the surface of photovoltaic panels from Brazil has been shown to decrease the efficiency by 11% after 18 months (Shirakawa et al., 2015). Moreover, dust particle accumulation during drought seasons (a process known as "soiling") has been associated with a decrease in the yield of California photovoltaic panels, accounting for a loss of up to 0.1% of the power production per day (Mejia and Kleissl, 2013). Biofilm and dust accumulation on outdoor glass surfaces such as photovoltaic panels depend, among other factors, on the coating and angle (Mejia and Kleissl, 2013; Banerjee et al., 2015). Although the effect of biofilms on soiling in solar panels has not been quantified, it seems reasonable to hypothesize that biofilm growth might increase dust adhesion. Despite the economic benefits of understanding the association between the decreased yield of solar panels and the biofilms formed on them, little is known about how the latitude, climate, the physical characteristics of the panels affect the microbial communities in this still poorly characterized ecological niche.

Solar panels represent a particularly interesting environment due to their simple, yet standard structure and orientation (an equator-facing glass surface); their abundance worldwide; and the fact that these inert, non-porous bidimensional artificial surfaces are a proxy of sun-exposed natural environments such as rocks, the phyllosphere or the top layer of biological soil crusts. A previous study assessing the microbiome of solar panels from the North and South Poles revealed that despite the geographical distance between both environments, the composition of the solar panel microbiome is very similar (Tanner et al., 2018). Furthermore, solar panel surfaces can be used as sources for the isolation of interesting radiation- and desiccation-resistant bacteria. A study by Ragon et al. (2011) revealed that biofilms growing on sunlight-exposed surfaces are naturally resistant to Chernobyl ionizing-radiation levels which is due to their natural adaptation to periodical desiccation and UV-irradiation. Survival of ionizing radiation- and desiccation-resistant bacteria has been previously attributed to the ability of these microorganisms to protect their proteins from the oxidative damage generated during irradiation, leading to functioning repair systems that work more efficiently during recovery than those in bacteria that are sensitive to radiation (Fredrickson et al., 2008).

A previous description of the microbial community on solar panels from the Mediterranean city of Valencia, Spain revealed the presence of black fungi, some phototrophs and a surprising diversity of sun-adapted bacterial taxa, dominated by *Hymenobacter* spp., *Sphingomonas* spp., and *Deinococcus* spp. (Dorado-Morales et al., 2016). In order to shed light on the ecology of the solar panel microbiome and to further compare the microbial profiles on panels from distant geographical locations, we present here a comprehensive characterization of the microbial communities of solar panels in another coastal city distant from Valencia: Berkeley, CA, United States. Both cities share a Mediterranean climate, a relatively high humidity and a protracted dry summer season. They are also at similar altitudes and latitudes (Berkeley is less than two degrees south from Valencia: 37° 52′ and 39° 28′, respectively) and thus receive similar annual UV irradiation doses. In the present work, we have analyzed the functional and taxonomic diversity of the solar panels of the University of California in Berkeley through metagenomics; compared the microbial communities with those described on solar panels from Valencia (Dorado-Morales et al., 2016); identified several key compounds of its metabolome through mass spectrometry; and studied the adhesion, irradiation and desiccation resistance abilities of selected cultivable isolates in the laboratory.

MATERIALS AND METHODS

Sampling

Sampling was carried out in August 2016 on the Lawrence Berkeley National Laboratory main campus (Berkeley, CA, United States). Three independent, adjacent photovoltaic solar panels of building 30 (installed and uncleaned for at least 18 months) were sampled by pouring sterile PBS on the surface and by strongly scraping the surface with autoclave-sterilized T-shaped rubber and steel window cleaners (squeegees). Approximately 40 mL of soil panel dust slurry was collected from each solar panel using sterile pipettes, transferred into sterile polypropylene conical tubes and immediately transported to the laboratory for further processing. There, aliquots were taken for culturing and colonization experiments, and the remaining volume was split in two, centrifuged and the pellets stored at −80°C until required for metagenomic and metabolic analysis. The solar panels from Valencia (Spain) were sampled using the same procedure, obtaining a final volume of 5 mL that was sent on dry ice to the laboratory in Berkeley, CA, United States, for metabolomics analysis. The metagenomic sequences obtained in the previous report by Dorado-Morales et al. (2016) were used for the taxonomic comparison between the Spanish and Californian solar panels.

Culture Media and Conditions

A total of 300 μL aliquots of each sample were transferred into sterile 1.5 mL microcentrifuge tubes and let stand for 5 min at room temperature prior to spreading 50 μL of the supernatant on freshly prepared LB and R2A agar plates. A dual approach with nutrient-rich (LB) and nutrient-poor (R2A) media was used in order to allow microorganisms with different nutrient requirements to grow. All cultures were performed in duplicate and incubated at 4°C, room temperature (RT) (∼22°C), 27 and 50°C for 22, 9, 5, and 3 days, respectively. Selected

colonies corresponding to the most frequent phenotypes (i.e., light pink) on R2A were re-streaked on fresh R2A plates and pure cultures grown on solid medium were cryopreserved in 25% glycerol.

Pooled aliquots (10 μL) of the three samples were placed on microscope slides (VWR CAT No. 48393048, 22X40 mm) and dried at room temperature (RT) under sterile conditions. The slides were then washed with sterile water, dried again and subjected to 2 min of UV irradiation in the hood and at a distance of 46 cm from the UV light (Air Clean 600 PCR workstation equipped with a 254 nm short-wave UV light). The dried and irradiated microscope slides were kept in the hood at RT for 30 min and then transferred sample side down onto the surface of R2A agar plates, where they settled for 30 min before being removed. Plates were incubated at RT for 4 days. Surviving colonies, as well as the ten non-irradiated isolates selected among those growing in R2A plates were selected for further studies. Colonies were identified through amplification and sequencing of almost the full-length 16S rRNA gene (in exception of a small fragment of ∼200 base pairs at the beginning of the V1 regions) through Sanger sequencing, followed by a taxonomic assignment using the NCBI Blast Tool. All but one of the sequences displayed 98–99% similarity with the closest match. The exception was an isolate belonging to the *Deinococcus* genus, which displayed 96% similarity with the closest match.

Colonization Experiments

A loopful of each selected isolate, grown for 1 week on R2A agar at room temperature, was suspended in liquid R2A and optical densities (600 nm) were adjusted to 0.1 absorbance units. A 10 μL droplet of each suspension was placed on a sterile glass slide and kept at RT for 1 h. Then, 10 μL of R2A were added to each droplet to prevent desiccation and the assay was continued for one more hour, after which droplets were removed by washing the slides three times with 1 mL of sterile water. The slides were allowed to completely dry in the hood for 1 h and were then either placed sample side down on the surface of R2A plates (glass colonization assay); subjected to UV irradiation (UV-resistance assay); or subjected to 72 h of further desiccation at RT (desiccation-resistance assay).

For the glass colonization assay, the slides were placed on solid R2A medium and incubated for 30 min at RT to allow for transfer of the bacteria to the solid medium. Then, the glass slides were removed and the plates were incubated at RT for 4 days. For the UV resistance assays, after washing and drying the slides (as described above), the 14 selected isolates were subjected to 2 min of irradiation with the UV lamp in the Air Clean 600 PCR workstation and at 15 cm distance from the lamp. UV-treated glass slides were placed on R2A agar plates and incubated as described above (30 min at room temperature) to allow the transfer of the bacteria. Finally, the desiccation-resistance assays were carried out with the 14 selected strains as described above (without UV irradiation) by air-drying washed droplets for 72 h inside the hood prior to transferring them to R2A plates, where they were incubated for 30 min at room temperature to allow transfer of the bacteria.

DNA Isolation and Metagenomic Analysis

Metagenomic DNA was isolated from solar panels samples as previously described (Dorado-Morales et al., 2016). Briefly, pellets were thawed on ice, incubated with lysozyme in the PowerBead tubes solution without the beads (PowerSoil, MoBio) at 37°C for 10 min, and then transferred back to the PowerBead tubes containing the beads. The extraction was continued following the instructions of the manufacturer.

Metagenomic analysis and annotations were performed as follows. For the library construction, 10 ng of DNA was sheared to 300 bp using the Covaris LE220 (Covaris) and size selected using SPRI beads (Beckman Coulter). The fragments were treated with end-repair, A-tailing, and ligation of Illumina compatible adapters (IDT, Inc), and 5 cycles of PCR was used to enrich for the final library. The libraries were quantified and run on a Roche LightCycler 480 real-time PCR instrument, followed by preparation for sequencing on the Illumina HiSeq2500 sequencing platform using a TruSeq Rapid paired-end cluster kit, v.4. After sequencing, known Illumina adapters were removed and the reads were then processed using BBDuk filtering and trimming (where quality values were less than 12). Remaining reads were mapped to a masked version of human HG19 with BBMap, discarding all hits over 93% identity. Trimmed, screened, paired-end Illumina reads were assembled using megahit assembler using a range of Kmers (Li et al., 2015). The entire read set output from the previously described read pre-processing step were mapped to the final assembly and coverage information generated using BBMap. Annotation was performed using the DOE-JGI Metagenome Annotation Pipeline (MAP v.4) (Huntemann et al., 2016). Open reading frames (ORFs) were identified from each of the three assemblies using Prodigal v.2.6.3 software (Hyatt et al., 2010). Genes were subsequently annotated against the entire NCBI nr-database using DIAMOND (Buchfink et al., 2014).

Taxonomic information was obtained from the metagenomic data using the microbial classification engine "Centrifuge" (Kim et al., 2016), as well as the aforementioned NCBI non-redundant database. Taxonomic and functional affiliations were visualized in the MEGAN6 software environment (Huson et al., 2007). For comparison of solar panels from different locations, a radial tree representing phylogenetic distances between solar panels from Berkeley, CA, United States and Valencia, Spain was constructed using the JGI IMG/MER database tools, with a percent identity above 90%. Statistical analyses were performed both using STAMP (Parks et al., 2014) and in the R statistical environment.

Metabolite Extractions

Solar panel slurry pellets were collected by centrifugation of 5 mL (Valencia, Spain) or 10 mL (Berkeley, CA, United States) of solar panel dust slurry (2655 RCF for 5 min). Empty tubes were included as extraction controls to account for ions resulting from procedural methods.

For extraction of hydrophilic metabolites, the slurry pellets were extracted in methanol. Briefly, the pellets were resuspended in 2 mL of 100% methanol, vortexed for 10 s, sonicated for

20 min. in an ice bath, and then incubated at 4°C overnight. The following day, the methanol solutions were vortexed again and centrifuged at 6000 RCF for 3 min to pellet insoluble material. The supernatants were then dried under vacuum at room temperature for 6 h (Thermo SpeedVac Concentration and Trap) which each yielded ∼10 μL of viscous yellow fluid. These were then resuspended in 150 μL of methanol with internal standards. The resuspensions were vortexed 10 s, sonicated 20 min in an ice bath and centrifuged at 6000 RCF for 3 min to pellet insoluble material; supernatants were filtered through a 0.22 μm microcentrifuge filtration devices (Pall, ODM02C34) and filtrates were transferred to glass vials for analysis. The internal standard mix used for the Valencia, Spain sample was a 2000-fold dilution of universally labeled 15N, 13C amino acid mix (Sigma, 767964). The internal standards used for the Berkeley, CA, United States samples included 1 μg/mL 2-amino-3-bromo-5-methylbenzoic acid (Sigma R435902), 5 μg/mL 3,6-dihydroxy-4-methylpyridazine (Sigma 668141), 5 μg/mL 13C-15N-L-phenylalanine (Sigma 608017), 10 μg/mL d4-lysine (Sigma 616192), 10 μg/mL d5-benzoic acid (Sigma 217158), and 2 μg/mL 9-anthracene carboxylic acid (Sigma A89405).

For triglycerides, chloroform extractions were performed on slurry pellets (collected as described above) using a modified Bligh-Dyer approach (Bligh and Dyer, 1959). Briefly, 120 μL of water was added to each pellet, vortexed, then 450 μL of 2:1 MeOH:CH_3Cl was added for a final ratio of 2:1:0.8 MeOH:CH_3Cl:H_2O followed by a brief vortex and incubation for 15 min in a sonicating water bath. An additional 150 μL CH_3Cl and 150 μL H_2O was added to create a final ratio of 1:1:0.9 MeOH:CH_3Cl:H_2O, then briefly vortexed and incubated for 10 min in a sonicating water bath. After centrifuging samples for 2 min at 2655 RCF, the lower lipid-enriched chloroform phase was transferred to a new tube. 300 μL of chloroform was then added to the remaining pellet (methanol-water layer), followed by repeat sonication and centrifugation, and the bottom chloroform phase was combined with the previously collected extract. Chloroform extracts of lipid were then dried in a SpeedVac (SPD111V, Thermo Scientific) and stored at −20°C. Prior to analysis, dried extracts were resuspended in 3:3:4 isopropanol:acetonitrile:methanol (IPA:ACN:MeOH), centrifuge-filtered through a 0.22 μm PVDF membrane (Millipore Ultrafree-MC) containing an internal standard mixture of 1 μg/mL 2-Amino-3-bromo-5-methylbenzoic acid (ABMBA) and 4 μM each of deuterated lipids including: 17:0-17:1-17:0 D5 triglyceride (Avanti 110544), 18:0-18:1 D5 phosphoglyceride (Avanti 110899), D9 oleic acid (Avanti 850809O), 1,3-16:1 D5 diglyceride (Avanti 110579), and dipalmitoyl glycerol trimethyl homoserine D9 (Avanti 857463). Filtrates were transferred to glass vials for analysis.

Liquid Chromatography Tandem Mass Spectrometry (LC-MS/MS) Based Metabolomics

Chromatographic separations were performed using an Agilent 1290 LC stack, with MS and MS/MS data collected using a Q Exactive hybrid Quadrupole-Orbitrap Mass Spectrometer equipped with a heated electrospray ionization (HESI-II) source probe (Thermo Scientific, San Jose, CA, United States). All chemicals and solvents were of LCMS or HPLC grade.

Polar metabolites were chromatographically separated using a 5 μm, 150 × 2.1 mm, 200Å ZIC-HILIC column containing sulfobetaine (zwitterionic) silica based stationary phase (Merck Millipore) under the following conditions: 0.45 mL/min. flow rate, 40°C column temperature, and a 2 μL injection volume. Mobile phases (A: 5 mM ammonium acetate in water, and B: 5 mM ammonium acetate, 95% v/v acetonitrile in water) were varied as follows: 1.5 min hold at 100% B, 13.5 min linear gradient to 65% B, 3 min linear gradient to 0% B, 5 min hold at 0% B, 2 min gradient to 100% B, and a 5 min reequilibration at 100% B.

Triglycerides were chromatographically separated using a 1.8 μm, 50 × 2.1 mm C18 column (Agilent ZORBAX Eclipse Plus C18, Rapid Resolution HD) under the following conditions: 0.4 mL/min flow rate, 55°C column temperature, and a 2 μL injection volume. Mobile phases (A: 40:60 water:acetonitrile with 5 mM ammonium acetate and 0.1% v/v formic acid, and B: 90:10 isopropanol:acetonitrile with 5 mM ammonium acetate and 0.1% v/v formic acid) were varied as follows: 1.5 min hold at 20% B, 2.5 min linear gradient to 55% B, 6 min linear gradient to 80% B, 2 min hold at 80% B, 1.5 min linear gradient to 100% B, 3.5 min hold at 100% B, 1.5 min linear gradient to 20% B and 1.5 min re-equilibration at 20% B.

For all chromatographies, eluted compounds were detected via ESI-MS/MS using the Q Exactive's data dependent MS2 Top2 function, where the two highest abundance precursor ions reaching at least 1e3 ions within the max ion transfer time (excluding ions with assigned charge ≥4) and not already fragmented in the previous 10 s are selected from a full MS pre-scan from m/z 70–1050 (HILIC) or 80–1200 (C18) at 70,000 resolution with an automatic gain control (AGC) target at 3e6 and 100 millisecond maximum ion transmission, followed by sequential MS/MS fragmentation of each of the two precursors with stepped normalized collision energies (stepped NCE) of 10, 20, and 30 (HILIC) or 10, 20, 40 (C18) at 17,000 resolution with an isolation window of 2 m/z and AGC target at 1e5 and 50 milliseconds; all spectra were stored in centroid data format. The source was set with the sheath gas flow at 55 (arbitrary units), aux gas flow at 20 (arbitrary units), sweep gas flow at 2 (arbitrary units), spray voltage at 3 |kV|, and capillary temperature at 400°C. Internal standards were used for quality control purposes.

Metabolomics Data Analysis

For HILIC data analysis, retention and fragmentation data were compared to a library of pure reference standards analyzed under the same conditions. MS/MS fragmentation spectra, if collected for the compound of interest, were compared to internal and online spectral databases to confirm identification. A subset of the library was analyzed (as external standards) at the same time as the samples and used for generation of the theoretical retention times using linear regression (to account for retention shifts due to changes in tubing length, mobile phase batches and different lots of column from the manufacturer). Exact mass (+/− 25 ppm at peak apex) and retention time (+/− 0.5 min from theoretical) coupled with MS/MS fragmentation spectra

were used to identify compounds with a python-based metabolite atlas analysis (Bowen and Northen, 2010; Yao et al., 2015). Python code is available at https://github.com/biorack/metatlas.

Exact mass and retention time coupled with MS/MS fragmentation spectra were used to identify lipids. Lipid class was determined based on characteristic fragment ions or neutral loss, and coupled with exact mass to determine specific lipid identity (number of carbons in fatty acid tails and degree of unsaturation). In positive ion mode, triglycerides ionized as a singly charged ammonium adduct with fatty acid tails detected in the MS/MS fragmentation spectra (McAnoy et al., 2005). Deuterated TG internal standard was used to verify fragmentation pattern and retention time range for the TG lipid class.

Availability of Data

Raw and processed data are available on the JGI Genome Portal: https://genome.jgi.doe.gov/portal/solcelcoanalysisunder proposal 503162 "solar cell community analysis." Metabolomic results from solar panels in Berkeley and Valencia have been deposited under project ID 1196772. The metagenomics from the three Berkeley, CA, United States solar panel communities are available under project IDs: 1123560, 1123562, and 1123564.

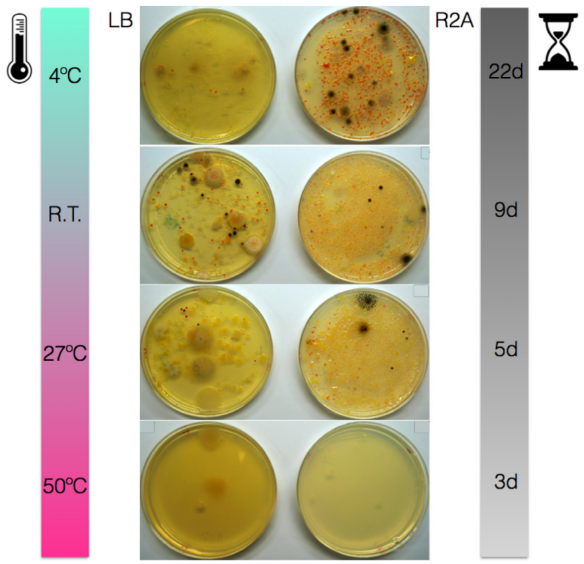

FIGURE 1 | Solar panel samples grown on LB and R2A media and incubated at 4°C, room temperature (22°C), 27 and 50°C for 22, 9, 5, and 3 days, respectively.

RESULTS

Cultivable Isolates and Colonization Experiments

Solar panels proved very rich in cultivable bacteria on LB and, particularly, R2A media (**Figure 1**). A large diversity of colony phenotypes was observed at temperatures from 4°C to 27°C, with very few cultivable isolates growing at higher temperatures (50°C). Many of the isolates displayed yellow, orange or pink colors, particularly on R2A. In fact, R2A plates incubated at temperatures from 4°C to 27°C displayed numerous pink-pigmented colonies.

Due to the diverse microbial growth observed on the R2A plates, this media was selected for all the further studies and isolates were re-streaked exclusively from R2A plates. Specifically, seven isolates from the R2A plates grown at RT (SPB1-SPB7) were randomly selected along with three pink-pigmented isolates from the R2A plates grown at 4°C (SPB8-SPB10). Additionally, four isolates previously selected from the solar panels samples by UV irradiating for 5 min (as described in Materials and Methods) were selected as well (data not shown) (SPB11-SPB14). In total, 14 isolates were identified by 16S rRNA gene sequencing as follows: *Arthrobacter* (SPB1), *Hymenobacter* (SPB2), *Hymenobacter* (SPB3), *Rhodococcus* (uranium-contaminated site) (SPB4), *Methylobacterium* (SPB5), *Deinococcus* (SPB6), *Arthrobacter agilis* (SPB7), *Hymenobacter* (SPB8), *Hymenobacter* (SPB9), *Hymenobacter perfusus*-uranium (SPB10), *Hymenobacter perfusus*-uranium (SPB11), *Curtobacterium* (SPB12), *Curtobacterium* (SPB13), and *Arthrobacter agilis* (SPB14).

The 14 isolates were then screened for their glass-colonization abilities. After 2 days of incubation, strains SPB1, SPB5, and SPB6 exhibited very faint but visible colonies. After 4 days, all but one strain were able to grow, indicating some adhesion ability to the glass surfaces (**Figure 2A**). The strains with the highest glass colonization ability, as deduced by a fully compact growth on the slide were SPB1, SPB5, and SPB6, and to a lesser extent, SPB11 and SPB3 (**Figure 2A**). When subjected to 2 min of UV irradiation, only one strain (SPB1), exhibited high resistance as deduced by numerous colonies (>10) growing after transfer to R2A solid medium (**Figure 2**, left). Three other isolates resulted $\leq$ three colonies each (SPB6, SPB11 and SPB12) and the rest of isolates did not yield viable cells after irradiation (**Figure 2B**).

As it was the case with UV radiation, 72 h desiccation tests yielded a decrease in viability of most of the strains. Only strain SPB5 exhibited vigorous growth, concentered around the spot on which the suspension was placed; followed by SPB1, with hundreds of surviving colonies. The remaining isolates exhibited very low (<20 colonies for SPB7, 12, 13, 14) to no survival to desiccation (**Figure 2C**).

Metagenomic Analysis

Between 590 and 775 Mb were sequenced for each sample and assembled into around 710.000 and 1 million scaffolds. Approximately one million ORFs were predicted for each metagenome: 99.11% of the ORFs corresponded to protein-coding genes, and the remaining 0.89% to RNA genes. Taxonomic analysis (**Figure 3**) revealed that the sequences corresponded mainly to bacteria, although there was also a substantial proportion of eukaryota, in which predominant sequences corresponded to fungi and, more specifically, to Ascomycota (~31.9% of annotated contigs across the three metagenomes). In the case of bacteria, the predominant phyla were Actinobacteria (15.6%), Bacteroidetes (22.6%), and Proteobacteria (14.8%), and to a lesser extent, Deinococcus (6.3%) Cyanobacteria

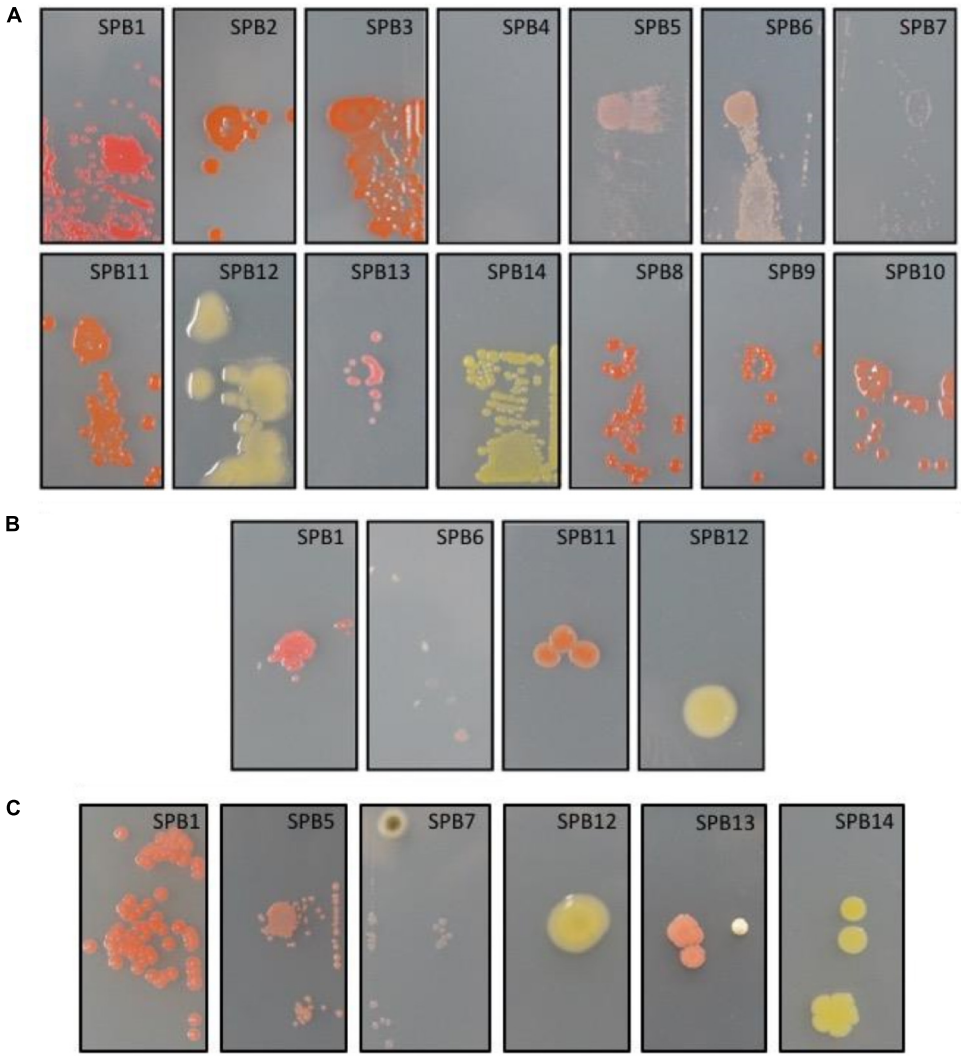

FIGURE 2 | (A) Glass-adhesion test performed as described in M&M. From left to right, top: isolates SPB1, SPB2, SPB3, SPB4, SPB5, SPB6, SPB7; bottom: SPB11, SPB12, SPB13, SPB14, SPB8, SPB9, and SPB10. **(B)** UV-resistance test performed on glass-adhering cells as described in M&M. From left to right isolates SPB1, SPB6, SPB11, and SPB12. The three later correspond to the growth of only 1-3 UV-resistant colonies each. **(C)** Desiccation-resistance test performed on glass-adhering cells as described in M&M. From left to right isolates SPB1, SPB5, SPB7, SPB12, SPB13, and SPB14. Isolates correspond to: SPB1, *Arthrobacter*; SPB2, *Hymenobacter*; SPB3, *Hymenobacter*; SPB4, *Rhodococcus* (uranium-contaminated site); SPB5, *Methylobacterium*; SPB6, *Deinococcus*; SPB7, *Arthrobacter agilis*; SPB8, *Hymenobacter*; SPB9, *Hymenobacter*; SPB10, *Hymenobacter perfusus-uranium*; SPB11, *Hymenobacter perfusus-uranium*; SPB12, *Curtobacterium*; SPB13, *Curtobacterium*; and SPB14, *Arthrobacter agilis*. The images are representative of the microscope slides (size 22X40 mm).

and Firmicutes. Furthermore, there was a clear predominance of *Hymenobacter* spp. amongst the microbial community of the Berkeley solar panels (19.7%), with other constituents including *Deinococcus* spp. (6.3%), *Modestobacter marinus* (1.25%), *Kineococcus radiotolerans* (3.13%), *Friedmanniella sagamiharensis* (4.98%) and *Alternaria alternata* (2.19%), among others. The results of our metagenomic sequencing clearly support our culture-based approach, as all our cultured isolates are represented in our assembled metagenomes.

When comparing the taxonomic information of the solar panels from Berkeley with the data obtained from solar panels in Valencia (Dorado-Morales et al., 2016), the taxonomic profiles proved very similar both in community composition and taxon abundance (**Figure 4**). Specifically the most abundant taxa in all five samples were Actinobacteria, Bacteroidetes (mainly Cytophagales), Cyanobacteria, Deinococcus (mainly Deinococcales), Firmicutes, Proteobacteria and Ascomycota; and the subdivisions of these taxa were very similar in the solar panels from both locations (**Figure 4**). Despite these general similarities, we found a number of significant differences between localities at various taxonomic levels. Specifically, members of the Ascomycota and Bacteroidetes were significantly enriched in the Berkeley samples compared to the Valencia communities (Welch's two-sided t-test, $P < 0.05$). By contrast, Alphaproteobacteria were significantly more common in the Valencia metagenomes than the Berkeley counterparts ($P < 0.05$),

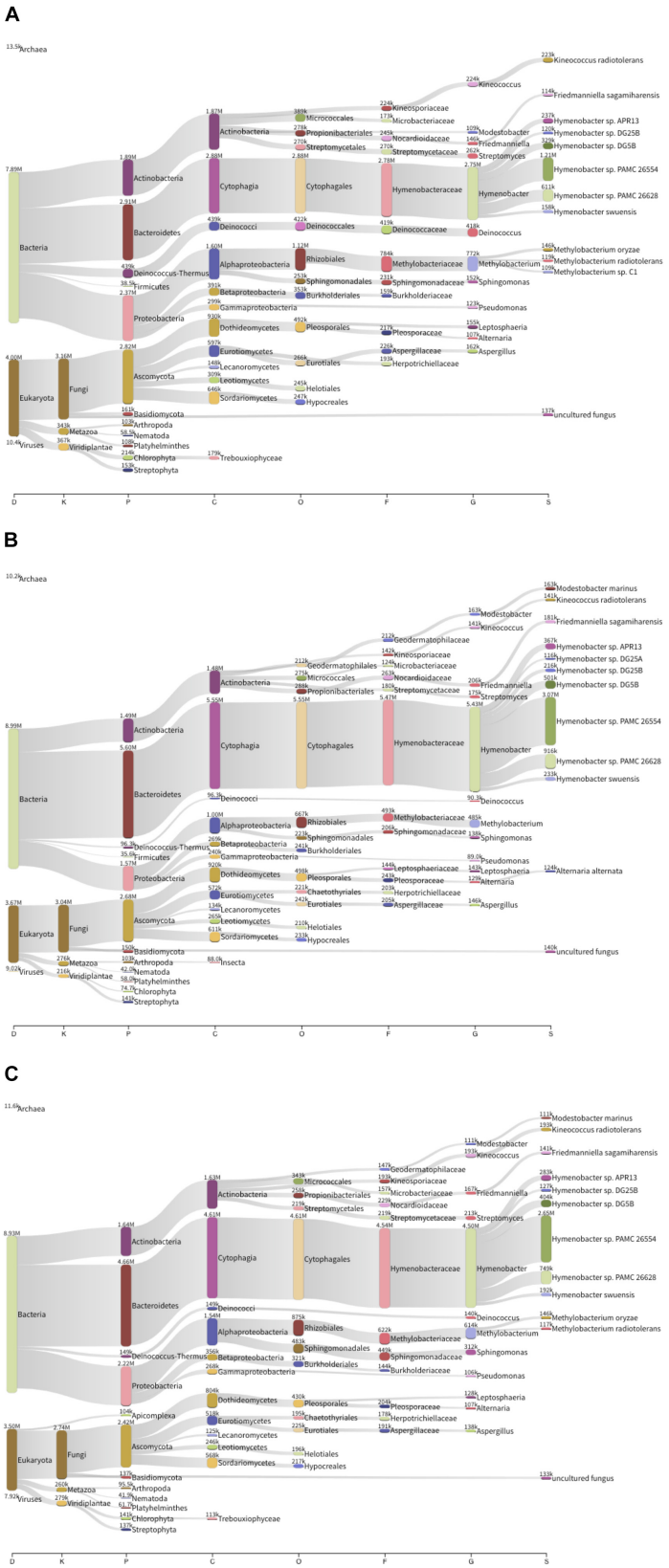

FIGURE 3 | Taxonomic composition of three solar panel microbial communities from Berkeley, CA, United States. The thickness of the lines is representative of the relative abundance of the taxa. **(A)** Left solar panel. **(B)** Center solar panel. **(C)** Right solar panel.

as were *Sphingomonas* spp. ($P < 0.05$) (**Figure 5A**). Statistical analyses indicate that these communities differ significantly in their composition according to sampling location (Valencia vs. California; PERMANOVA, $P < 0.001$).

Consistent with the observed taxonomic variations between the solar panel communities, we found marked differences in the functional attributes of the solar panel communities. Firstly, comparisons of our genes against the SEED subsystems database (**Figure 5B**) showed that pathways involved in the persistence of microbes on solar panels, such as stress response (3.1% of annotated open reading frames), capsule development (2.8%) and metabolite repair (2.1%), were common to all metagenomes. We also found evidence of genes for carotenoid biosynthesis and, by contrast, genes assigned to photosynthetic pathways were rare (0.07%) as were those assigned to general autotrophic subsystems (0.02%) suggesting that these pathways are not critical for persistence on solar panels.

Notwithstanding these dominant processes, we found significant over-representation of catalases, cAMP-binding proteins and 3-oxoacyl-[acyl-carrier protein] reductases in the Berkeley metagenomes compared to the Valencia samples (Welch's two-sided *t*-test, $P < 0.05$). The opposite trend was observed for DNA-dependent RNA polymerases and TonB-dependent receptors ($P < 0.05$), which were more abundant in the metagenomes from Valencia. Cumulatively, the differences in gene content between the communities were sufficient to explain >70% of the variation between the metagenomes collected from Valencia and Berkeley (PCA, First principal component = 70.7%; PERMANOVA, $P < 0.05$).

A more targeted analysis of the functional components of these metagenomes revealed diverse mechanisms for dealing with the extreme climatic conditions imposed by living on solar panels. We found numerous genes encoding heat shock chaperone proteins (e.g., *dnaK, dnaJ, grpE*; combined genes across Berkeley metagenomes, $n = 187$) which belonged to a range of taxa, but were primarily affiliated with *Deinococcus* spp. and *Sphingomonas* spp. Mechanisms of combatting oxidative stress were equally abundant in both locations and included a variety of superoxide dismutases ($n = 50$), most of which belonged to *Kineococcus radiotolerans* and *Deinococcus* spp., as well as a group of peroxidases and peroxide stress regulators, which were assigned exclusively to members of the *Methylobacteria*. Perhaps the most ubiquitous stress responses were those involved in DNA damage repair which provided between 459 and 519 genes per metagenome. DNA mismatch repair genes *mutL* and *mutS* were very common features within the metagenomes and could be assigned to a diverse set of dominant bacterial groups including *Hymenobacter* spp. and *Sphingomonas* spp., among others.

Finally, our functional data strongly corroborate our metabolomics results (described in the section below). Pathways for allantoin utilization were common to all metagenomes and include allantoinase and allantoicase, two hydrolase families involved in the biogenesis and degradation of ureides. As observed in the metabolomics data, we found more genes involved in allantoin metabolism in the Berkeley samples than in the Valencian samples. For example, allantoate amidohydrolase and allantoin racemase were present exclusively in the Berkeley metagenomes. These processes appear to be carried out by both dominant (i.e., *Deinococcus* spp.) and rare (i.e., *Thermobispora bispora*) community members, indicating a widespread gene catalog for key processes that permit colonization in an extreme environment.

Metabolomics Results

Most of the detected polar metabolites were present in both locations, although a few were detected primarily in a single location (**Figure 6A**). In both locations, common primary metabolites such as amino acids, nucleobases and sugars were detected. Interestingly, both locations contained nicotine, which may be linked to outdoor smoking. A number of aliphatic dicarboxylic acids of variable chain lengths (maleic acid, azelaic acid, suberic acid, pimelic acid) were present in both. Compatible solutes, such as ectoine, sugar alcohols, di- and tri-saccharides, were detected in both, which may play a role in protection against desiccation, heat and/or UV stress. A few compounds, sphinganine, sphingomyelin, an unidentified hexose and UDP-acetylhexosamine were detected only in the Berkeley samples while trigonelline, pantolactone, 5-valerolactone, and threonic acid and 4-guanidinobutyric acid had higher relative abundance in the Valencian sample. Triglyceride (TG) metabolites were highly abundant in both locations, and the most abundant triglycerides were similar between both locations (**Figure 6B**). The metagenomic and metabolomic data are publicly available in the JGI database under accession number ID: 503162, and can be accessed with the following URL: https://genome.jgi.doe.gov/portal/solcelcoanalysis/solcelcoanalysis.info.html.

DISCUSSION

Samples isolated from solar panels in Berkeley, CA, United States proved very rich in culturable bacteria despite the harsh environmental conditions they are subjected to, a result that is consistent with the previous work done on solar panels from Valencia, Spain and polar regions (Dorado-Morales et al., 2016; Tanner et al., 2018). Interestingly, the vast majority of the culturable microorganisms were not thermotolerant, but mesophilic or even psychrotolerant. This has important implications for the ecology of an environment that is prone to have thermal stress and daily peaks of extreme heat, particularly in summer (Dorado-Morales et al., 2016), when sampling was performed. Taking into account that peaks of heat on the panels tend to correlate with drought, our results suggest that microbial growth may be concentrated during the night, when water availability is higher and temperatures much cooler, even in Mediterranean climates. The average low temperature in Berkeley in August is just 12.4°C (Western Regional Climate Center, accessed May 5th 2017). This preference for mild growth temperatures was also observed in the isolates from Spain (Dorado-Morales et al., 2016). Taken together, both reports strongly suggest a thermoresistant -but not thermophilic- solar panel-adapted community.

Growth on both LB and R2A media yielded a large proportion of pigmented colonies. Interestingly, the highest number of

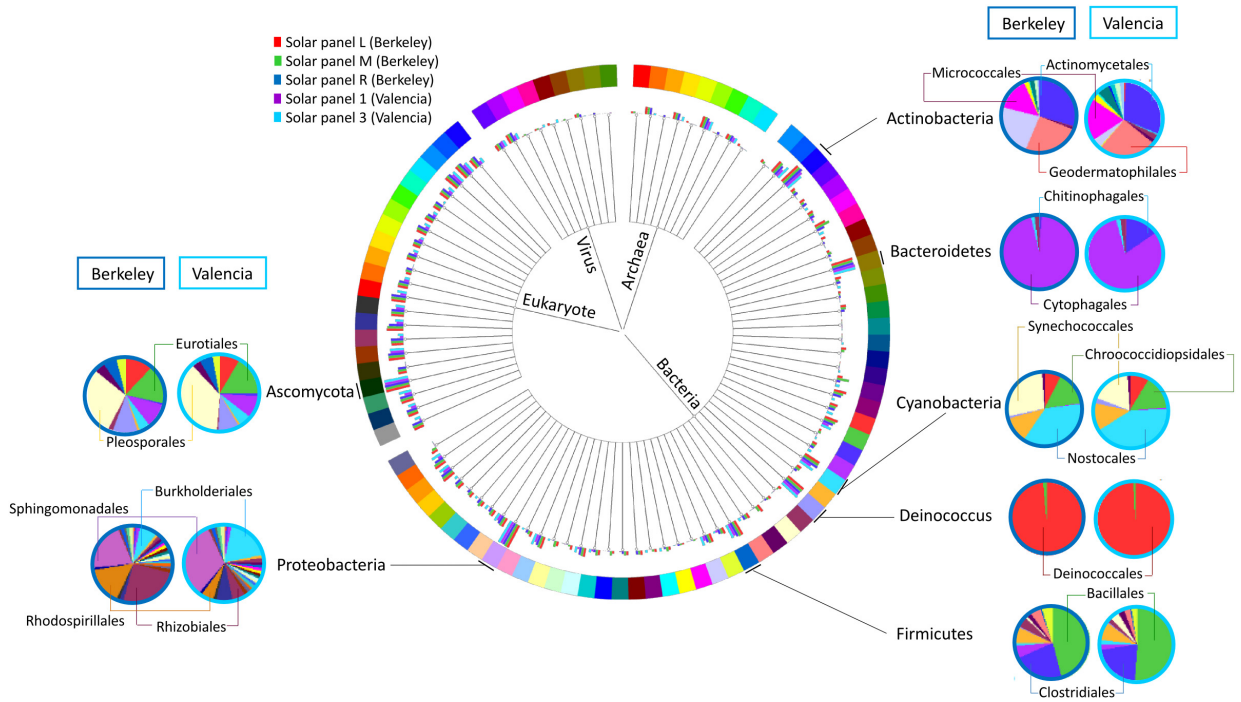

FIGURE 4 | Comparison of the taxonomic profiles of solar panels from Berkeley, CA, United States (red, green, and dark blue bars – three replicates) and Valencia, Spain (purple and light blue bars – two replicates). Most abundant taxa are indicated, and subdivisions of those taxa in one replicate from each location are represented (Berkeley and Valencia replicates in the dark and light blue circles, respectively).

pigmented colonies was observed when the samples were grown on R2A medium at 4°C, which could be explained by the increased accumulation of carotenoids at low temperatures as a cryoprotection strategy through the modulation of membrane fluidity (Jagannadham et al., 2000; Dieser et al., 2010). Furthermore, growth of *Hymenobacter* on R2A medium and at temperatures between 4 and 25°C is consistent with previous reports (Srinivasan et al., 2015; Lee et al., 2016) and suggests the preference of this bacterium for low nutrient culture media. The well-known role of carotenoids as UV sunscreens and the abundance of pigmented strains in panels strongly suggests their involvement in radiation protection during the day.

Besides heat-, radiation- and drought-resistance, microorganisms living on a smooth, flat surface fully exposed to the harsh climate must firmly attach to the substrate. Such attachment can involve binding to dust and other inorganic particles, but at least in the first stages of colonization, strong adhesion to the glass surface is likely to be a major selective force. In order to characterize the glass-adhesion abilities as well as the resistance to UV light and desiccation of glass-bound cells, we developed an *ad hoc* test for some of the culturable strains from the solar panels. As expected, almost all of the isolated strains tested positive for adhesion to glass, with the exception of *Rhodococcus*, which is surprising taking into account that this genus typically produces extracellular polysaccharides that have a role in adhesion to surfaces (Urai et al., 2007). On the other hand, UV-radiation experiments resulted in the selection of only four UV-resistance isolates under our conditions (*Arthrobacter* spp., *Deinococcus* spp., *Hymenobacter* spp., and *Curtobacterium* spp.), whose extreme radiation-resistance properties have previously been reported (Jacobs and Sundin, 2001; Mongodin et al., 2006; Chung et al., 2010; Gerber et al., 2015). The lack of a higher number of UV-resistant isolates from a highly irradiated source environment is intriguing, and it could be explained by the effect of dust or sub-aerial biofilms shadowing on bacteria, thus mediating survival of low-resistant organisms (Osman et al., 2008). Desiccation experiments on glass revealed *Arthrobacter* and *Methylobacterium* as the most resistant isolates, consistent with previous reports concerning the desiccation-resistance properties of these two genera (Makhalanyane et al., 2013; SantaCruz-Calvo et al., 2013).

These results suggest that sun-exposed surfaces such as solar panels can be rich reservoirs of biotechnologically interesting bacteria thanks to their adhesion, radiation-resistance and desiccation-resistant properties, as well as to the production of sunscreens and/or antioxidant compounds such as carotenoids. This potential could of course increase when considering the non-culturable fraction of the sampled microbiomes. In order to further characterize the solar panels from California, a culture-independent approach combining metagenomic sequencing and metabolomics was set in place.

High-throughput sequencing of the solar panel samples revealed that these structures are composed of a rather diverse microbial population. In concordance with the culture-based characterization described above, the microbiome was dominated by *Hymenobacter* spp. and, to a lesser extent, by well-known

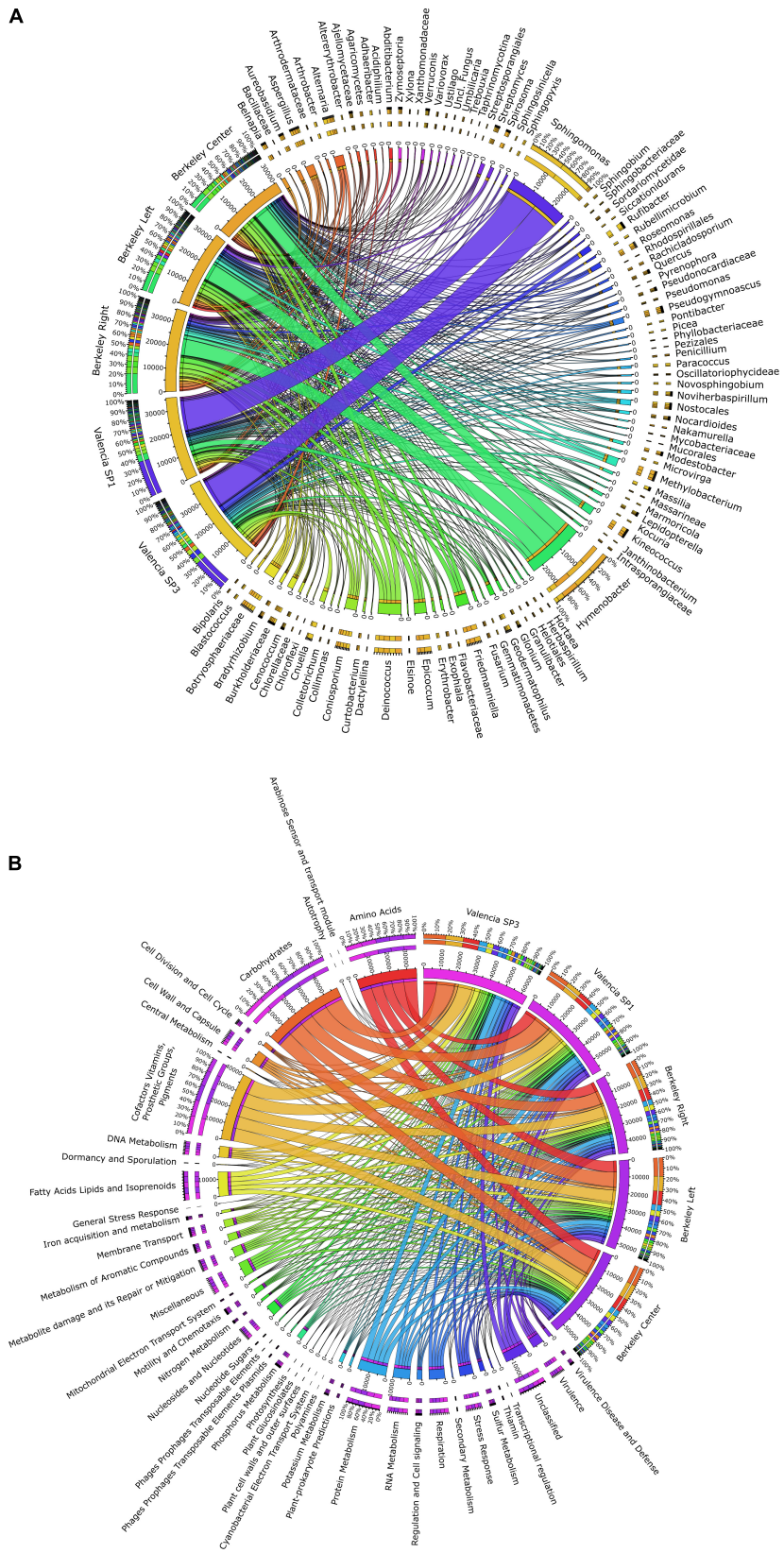

FIGURE 5 | Circos graph connecting **(A)** microbial taxa at the genus level and **(B)** SEED functional subsystems to the different metagenomes analyzed in this work (three solar panels from Berkeley, CA, United States, and two solar panels from Valencia, Spain).

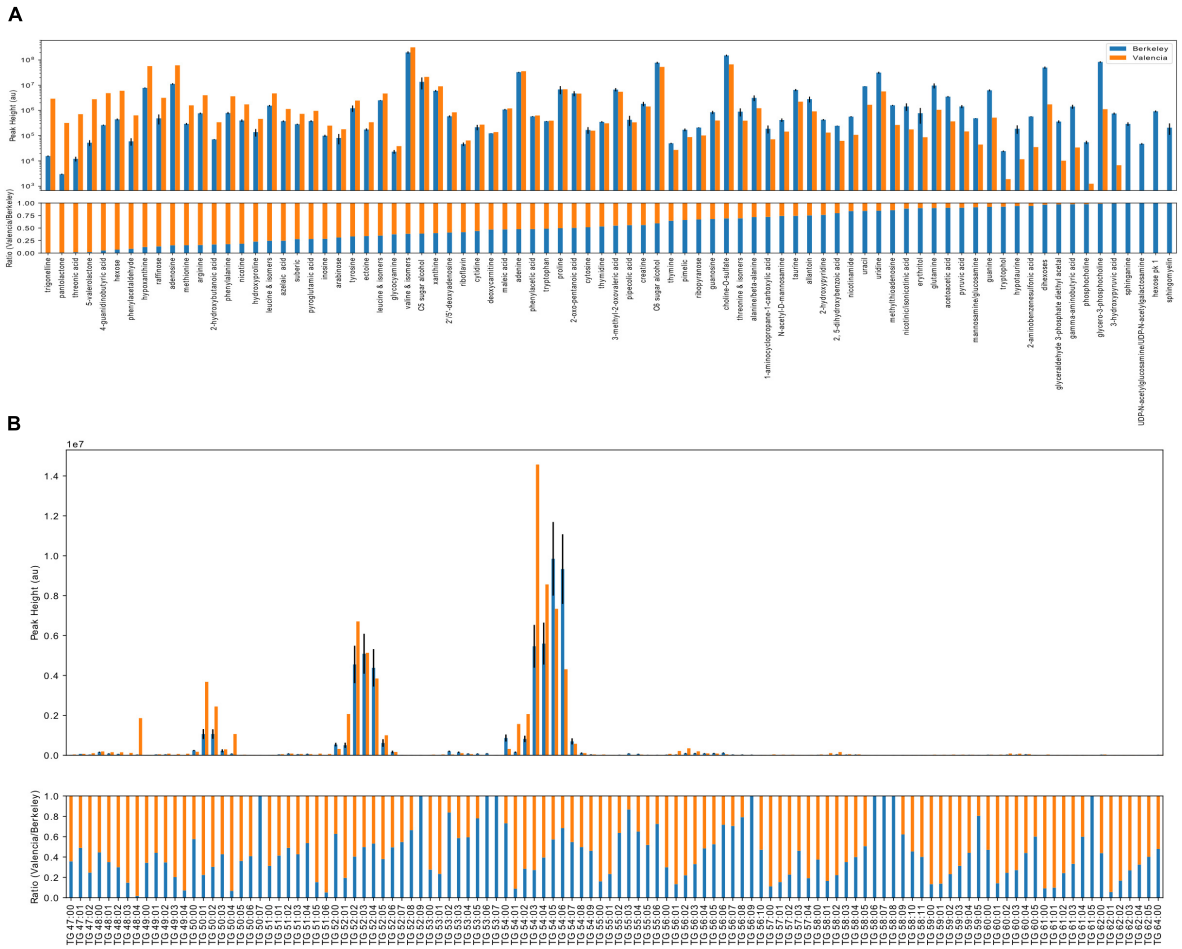

FIGURE 6 | Metabolomics analyses of the Californian and Valencian solar panel samples. Ion abundance results for polar metabolites **(A)** and triacylglycerol lipids **(B)**. Absolute ion abundances (upper panels, log scale) and relative ion abundances (lower panels, scaled to 1) corresponding to the identified metabolites are indicated in orange (Valencia, Spain) and blue (Berkeley, CA, United States). Without quantification, ion abundances cannot be used to compare between metabolites due to differences in ionization efficiencies. Here, ion abundances of identified metabolites may be used to compare relative abundances between Berkeley and Valencia. Polar metabolites **(A)** are ranked by relative abundance and triacylglycerol lipids are sorted by chain length followed by degree of unsaturation.

radiation-resistant organisms, such as: *Modestobacter marinus*, an *Actinobacterium* that grows on calcareous stone surfaces (Normand et al., 2012); *Kineococcus radiotolerans*, previously isolated from radioactive areas (Phillips et al., 2002); or *Alternaria alternata*, a plant pathogenic fungus also found to grow inside the Chernobyl reactor (Mironenko et al., 2000).

Regarding the metabolomics analysis, although most of the detected polar compounds are common intracellular metabolites, a few were differentially expressed between the two locations. For example, trigonelline, a thermally labile secondary metabolite that is present in leguminous and, to a lesser extent, non-leguminous plants (Ashihara and Watanabe, 2014), as well as mammal urine, have been shown to inhibit attachment of bacteria to surfaces (Daglia et al., 2002). There have been previous reports on the ability of rhizosphere microorganisms to perform trigonelline catabolism (Boivin et al., 1991; Goldmann et al., 1991), but there are no reports (to the best of our knowledge) of microorganisms able to produce trigonelline. Pantolactone, 5-valerolactone, threonic acid and 4-guanidinobutyric acid were >10-fold more abundant in the Valencia sample. Threonic acid is a product of ascorbic acid metabolism (vitamin C), a well-known antioxidant compound; the degradation of ascorbic acid has been described in a variety of bacteria, including *Lactobacillus* spp., a genus detected in the Valencian sample (Englard and Seifter, 1986; Montaño et al., 2013). On the other hand, 5-valerolactone in an intermediate in the metabolism of cyclopentanone, a pathway that has been previously described in *Pseudomonas* spp. (Griffin and Trudgill, 1972) and *Comamonas* spp. (Iwaki et al., 2002). Interestingly, dye-sensitized solar cells have been previously fabricated with 4-guanidinobutyric acid as co-adsorbent, leading to an approximately 50 mV increase in open-circuit voltage in comparison to cells without GBA cografting (Zhang et al., 2005). This molecule could also be present due to conversion from L-arginine by means of the L-arginine oxidase, an enzyme that has been previously described in *Pseudomonas* spp. (Matsui et al., 2016) and cyanobacteria

(Schriek et al., 2007). Compounds including sphingomyelin, sphinganine, N-acetylhexosamine and were only detected in the Berkeley, CA, United States samples. Sphingomyelin is the most frequently occurring mammalian sphingolipid, although it has previously been described in *B. thetaiotaomicron* (Olsen and Jantzen, 2001). Interestingly, sphinganine has proven to inhibit bacterial adherence and to negatively affect biofilm formation in *Staphylococcus aureus, Streptococcus mitis* and *Streptococcus mutans* (Bibel et al., 1992; Cukkemane et al., 2015). N-acetylglucosamine, is an important component of the bacterial and fungal cell walls, and along with insect chitin may play a signaling role across multiple kingdoms (Konopka, 2012).

There were also a few metabolites detected from both Valencia and Berkeley that were of special interest given the environmental conditions on the solar panels. Interestingly, a number of medium chain length dicarboxylic acids were detected in samples from both Berkeley and Valencia. Only a single transporter was found in the metagenome for a short chain dicarboxylic acid. Azelaic acid, a bactericidal agent produced in fungi, plants and animals, can also be utilized as a sole carbon source by Burkholderia spp. (Estrada-de los Santos et al., 2001), a genus identified in both Berkeley and Valencia samples. The presence of compatible solutes in both locations is not surprising given the exposure to high heat and UV irradiation. Ectoine and 5-hydroxyectoine are produced by bacteria for protection against osmotic stress and more recently have been demonstrated to protect mammalian DNA from UV damage (Czech et al., 2018); however, only a single gene, assigned to Bradyrhizobium, was found in the Valencia, Spain metagenome for production of 5-hydroxyectoine from ectoine. Polyols, many of which were present in both Berkeley and Valencia samples, accumulate in yeasts in response to osmotic stress (Tekolo et al., 2010). Thus it was not surprising that numerous genes involved in polyol and trehalose biosynthesis, utilization and degradation were detected across a diverse set of bacteria. Pipecolic acid, a precursor to secondary metabolites, is produced in both bacteria and fungi (He, 2006). Allantoin is utilized by some bacteria as a secondary source of nitrogen under nutrient-limiting conditions (Ma et al., 2016). Tryptophol may act as a signaling molecule and precursor to secondary metabolites in fungi and yeasts (Palmieri and Petrini, 2018).

Triglyceride metabolites were detected in both locations, and this is not surprising, given that cells enduring an environmental stress such as desiccation (as found on a solar panel) often shift metabolic energy to a more quiescent state and toward carbon storage, e.g., TG accumulation and fatty acid storage in TGs (Rittershaus et al., 2013). The most abundant triglycerides were similar among both locations, and this may be attributed to the strikingly similar taxonomic profiles of the solar panels between Spain and California (**Figure 4**), since lipid composition is characteristic of species and often similar between species from the same taxa (Sohlenkamp and Geiger, 2016).

As recently described for solar panels in the North and South Poles (Tanner et al., 2018), there is also a striking similarity between the taxonomic and functional profiles from solar panels from two same-latitude locations: Berkeley, CA, United States and in the distant Mediterranean city of Valencia, Spain (**Figure 4**). This is certainly related to the common environmental conditions, including the climate and the selective pressures associated to a fully sun-exposed habitat on a glass surface: thermal fluctuations and heat peaks, high irradiation and circadian cycles of wetting and desiccation. These common stressors, which also include limited C and N availability, have created communities that are strikingly similar in terms of their functional capacity (**Figure 5B**), even though we observed nuanced differences for some essential processes. This indicates a high degree of functional redundancy, whereby the variety of stress response adaptations occur in multiple individual microbial groups within each community. Although common selective pressures are expected to yield adaptive convergence, as observed in our results, rather than a taxonomic similarity, the comparison between the Valencian and Berkeley solar panels strongly suggests that, besides the climate, there must be similar inocula involved in the colonization process (**Figure 5A**). As previously reported elsewhere, the wind is a major source of air-borne bacteria (Hervàs et al., 2009; Barberán et al., 2015; Meola et al., 2015), which, along with birds, insects and other animals, might be the main source of inocula for the solar panel microbiome to develop. Our results are in concordance with a world-wide distribution of bacterial diversity, which is shaped *in situ*, by the specific pressure of living on a solar panel.

AUTHOR CONTRIBUTIONS

MP and TN designed the project. MP, KL, and SK performed the experiments. MP, BB, KL, SK, MG, and KT analyzed the data. MP, KL, SK, BB, KT, MG, and TN wrote and revised the manuscript. TN and MP provided the funding.

FUNDING

Financial support from the Spanish Government (Grant Helios, Reference: BIO2015-66960-C3-1-R co-financed by FEDER funds and Ministerio de Ciencia, Innovación y Universidades) is acknowledged. Work performed at Lawrence Berkeley National Laboratory under the Office of Science Early Career Program (awarded to TN) and at the U.S. Department of Energy Joint Genome Institute, a Department of Energy Office of Science User Facility, and with use of resources at the National Energy Research Scientific Computing Center, a Department of Energy Office of Science User Facility, is supported by the U.S. Department of Energy, Office of Science, Office of Biological and Environmental Research under contract number DE-AC02-05CH11231.

ACKNOWLEDGMENTS

We are very grateful to Thomas Price, Jeffery Knight, and Jesse Knight for their kind assistance in sampling the solar panels. We also thank Jose Manuel Martí Martínez for his help with the metagenomics analysis.

REFERENCES

Ashihara, H., and Watanabe, S. (2014). Accumulation and function of trigonelline in non-leguminous plants. *Nat. Prod. Commun.* 9, 795–798.

Banerjee, S., Dionysiou, D. D., and Pillai, S. C. (2015). Self-cleaning applications of TiO2 by photo-induced hydrophilicity and photocatalysis. *Appl. Catal. B.* 176, 396–428. doi: 10.1016/j.apcatb.2015.03.058

Barberán, A., Ladau, J., Leff, J. W., Pollard, K. S., Meninger, H. L., Dunn, R. R., et al. (2015). Continental-scale distributions of dust-associated bacteria and fungi. *Proc. Natl. Acad. Sci. U.S.A.* 112, 5756–5761. doi: 10.1073/pnas.1420815112

Bibel, D. J., Aly, R., and Shinefield, H. R. (1992). Inhibition of microbial adherence by sphinganine. *Can. J. Microbiol.* 38, 983–985. doi: 10.1139/m92-158

Bligh, E. G., and Dyer, W. J. (1959). A rapid method of total lipid extraction and purification. *Can J. Biochem. Physiol.* 37, 911–917. doi: 10.1139/o59-099

Boivin, C., Barran, L. R., Malpica, C. A., and Rosenberg, C. (1991). Genetic analysis of a region of the *Rhizobium meliloti* pSym plasmid specifying catabolism oftrigonelline, a secondary metabolite present in legumes. *J. Bacteriol.* 173, 2808–2817. doi: 10.1128/jb.173.9.2809-2817.1991

Bowen, B. P., and Northen, T. R. (2010). Dealing with the unknown: metabolomics and metabolite atlases. *J. Am. Soc. Mass Spectrom.* 21, 1471–1476. doi: 10.1016/j.jasms.2010.04.003

Buchfink, B., Xie, C., and Huson, D. H. (2014). Fast and sensitive protein alignment using DIAMOND. *Nat. Methods* 12, 59–60. doi: 10.1038/nmeth.3176

Chung, A. P., Lopes, A., Nobre, M. F., and Morais, P. V. (2010). *Hymenobacter perfusus* sp. nov., *Hymenobacter flocculans* sp. nov. and *Hymenobacter metalli* sp. nov. three new species isolated from a uranium mine waste water treatment system. *Syst. Appl. Microbiol.* 33, 436–443. doi: 10.1016/j.syapm.2010.09.002

Cukkemane, N., Bikker, F. J., Nazmi, K., Brand, H. S., Sotres, J., Lindh, L., et al. (2015). Anti-adherence and bactericidal activity of sphingolipids against *Streptococcus mutans*. *Eur. J. Oral Sci.* 123, 221–227. doi: 10.1111/eos.12200

Czech, L., Hermann, L., Stöveken, N., Richter, A. A., Höppner, A., Smits, S. H. J., et al. (2018). Role of the extremolytes ectoine and hydroxyectoine as stress protectants and nutrients: genetics, phylogenomics, biochemistry, and structural analysis. *Genes* 9, 1–58. doi: 10.3390/genes9040177

Daglia, M., Tarsi, R., Papetti, A., Grisoli, P., Dacarro, C., Pruzzo, C., et al. (2002). Antiadhesive effect of green and roasted coffee on Streptococcus mutans' adhesive properties on saliva-coated hydroxyapatite beads. *J. Agric. Food Chem.* 50, 1225–1229. doi: 10.1021/jf010958t

Dieser, M., Greenwood, M., and Foreman, C. M. (2010). Carotenoid pigmentation in antarctic heterotrophic bacteria as a strategy to withstand environmental stresses. *Arct. Antarct. Alp. Res.* 42, 396–405. doi: 10.1657/1938-4246-42.4.396

Dorado-Morales, P., Vilanova, C., Peretó, J., Codoñer, F. M., Ramón, D., and Porcar, M. (2016). A highly diverse, desert-like microbial biocenosis on solar panels in a Mediterranean city. *Sci. Rep.* 6:29235. doi: 10.1038/srep29235

Englard, S., and Seifter, S. (1986). The biochemical functions of ascorbic acid. *Ann. Rev. Nutr.* 6, 365–406. doi: 10.1146/annurev.nu.06.070186.002053

Estrada-de los Santos, P., Bustillos-Cristales, R., and Caballero-Mellado, J. (2001). Burkholderia, a genus rich in plant-associated nitrogen fixers with wide environmental and geographic distribution. *Appl. Environ. Microbiol.* 67, 2790–2798. doi: 10.1128/AEM.67.6.2790-2798.2001

Felden, J., Ruff, S. E., Ertefai, T., Inagaki, F., Hinrichs, K. U., and Wenzhöfer, F. (2014). Anaerobic methanotrophic community of a 5346-m-deep vesicomyid clam colony in the Japan Trench. *Geobiology* 12, 183–199. doi: 10.1111/gbi.12078

Fredrickson, J. K., Li, S. M., Gaidamakova, E. K., Matrosova, V. Y., Zhai, M., Sulloway, H. M., et al. (2008). Protein oxidation: key to bacterial desiccation resistance? *SME J.* 2, 393–403. doi: 10.1038/ismej.2007.116

Gerber, E., Bernard, R., Castang, S., Chabot, N., Coze, F., Dreux-Zigha, A., et al. (2015). Deinococcus as new chassis for industrial biotechnology: biology, physiology and tools. *J. Appl. Microbiol.* 119, 1–10. doi: 10.1111/jam.12808

Goldmann, A., Boivin, C., Fleury, V., Message, B., Lecoeur, L., Maille, M., et al. (1991). Betaine use by rhizosphere bacteria: genes essential for trigonelline, stachydrine, and carnitine catabolism in *Rhizobium meliloti* are located on pSym in the symbiotic region. *Mol. Plant Microbe Interact.* 4, 571–578. doi: 10.1094/MPMI-4-571

Griffin, M., and Trudgill, P. W. (1972). The metabolism of cyclopentanol by Pseudomonas sp. N.C.I.B. 9872. *Biochem. J.* 129, 595–603.

He, M. (2006). Pipecolic acid in microbes: biosynthetic routes and enzymes. *J. Ind. Microbiol. Biotechnol.* 33, 401–407. doi: 10.1007/s10295-006-0078-3

Hervàs, A., Camarero, L., Reche, I., and Casamayor, E. O. (2009). Viability and potential for immigration of airborne bacteria from Africa that reach high mountain lakes in Europe. *Environ. Microbiol.* 11, 1612–1623. doi: 10.1111/j.1462-2920.2009.01926.x

Huntemann, M., Ivanova, N. N., Mavromatis, K., Tripp, H. J., Paez-Espino, D., Tennessen, K., et al. (2016). The standard operating procedure of the DOE-JGI metagenome annotation pipeline (MAP v.4). *Stand. Genomic Sci.* 11:17. doi: 10.1186/s40793-016-0138-x

Huson, D. H., Auch, A. F., and Schuster, S. C. (2007). Megan analysis of metagenomic data. *Genome Res.* 17, 377–386. doi: 10.1101/gr.5969107

Hyatt, D., Chen, G. L., Locascio, P. F., Land, M. L., Larimer, F. W., and Hauser, L. J. (2010). Prodigal: prokaryotic gene recognition and translation initiation site identification. *BMC Bioinformatics* 11:119. doi: 10.1186/1471-2105-11-119

Iwaki, H., Hasegawa, Y., Wang, S., Kayser, M. M., and Lau, P. C. (2002). Cloning and characterization of a gene cluster involved in cyclopentanol metabolism in Comamonas sp. Strain NCIMB 9872 and biotransformations effected by *Escherichia coli*-expressed cyclopentanone 1,2-monooxygenase. *Appl. Environ. Microbiol.* 68, 5671–5684. doi: 10.1128/AEM.68.11.5671-5684.2002

Jacobs, J. L., and Sundin, G. W. (2001). Effect of solar UV-B radiation on a phyllosphere bacterial community. *Appl. Environ. Microbiol.* 67, 5488–5496. doi: 10.1128/AEM.67.12.5488-5496.2001

Jagannadham, M. V., Chattopadhyay, M. K., Subbalakshmi, C., Vairamani, M., Narayanan, K., Rao, C. M., et al. (2000). Carotenoids of an antarctic psychrotolerant bacterium, *Sphingomonas antarticus*, and a mesophilic bacterium, *Sphingobacterium multivorum*. *Arch. Microbiol.* 173, 418–424. doi: 10.1007/s002030000163

Kim, D., Song, L., Breitwieser, F. P., and Salzberg, S. L. (2016). Centrifuge: a rapid and sensitive classification of metagenomic sequences. *Genome Res.* 26, 1721–1729. doi: 10.1101/gr.210641.116

Kizilova, A. K., Sukhacheva, M. V., Pimenov, N. V., Yurkov, A. M., and Kravchenko, I. K. (2014). Methane oxidation activity and diversity of aerobic methanotrophs in pH-neutral and semi-neutral thermal springs of the Kunashir Island Russian Far East. *Extremophiles* 18, 207–218. doi: 10.1007/s00792-013-0603-z

Konopka, J. B. (2012). N-acetylglucosamine (GlcNAc) functions in cell signaling. *Scientifica* 2012, 631–632. doi: 10.6064/2012/489208

Lee, J., Kang, M., Joo, E. S., Jung, H., and Kim, M. K. (2016). Hymenobacter sedentarius sp. nov., isolated from a soil. *J. Microbiol.* 54, 283–289. doi: 10.1007/s12275-016-5386-3

Li, D., Liu, C. M., Luo, R., Sadakane, K., and Lam, T. W. (2015). MEGAHIT: an ultra-fast single-node solution for large and complex metagenomics assembly via succinct de Bruijn graph. *Bioinformatics* 31, 1674–1676. doi: 10.1093/bioinformatics/btv033

Locey, K. J., and Lennon, J. T. (2016). Scaling laws predict global microbial diversity. *Proc. Natl. Acad. Sci. U.S.A.* 113, 5970–5975. doi: 10.1073/pnas.1521291113

Ma, P., Patching, S. G., Ivanova, E., Baldwin, J. M., Sharples, D., Baldwin, S. A., et al. (2016). Allantoin transport protein, Pucl, from *Bacillus subtillis*: evolutionary relationships, amplified expression, activity and specificity. *Microbiology* 162, 823–836. doi: 10.1099/mic.0.000266

Makhalanyane, T. P., Valverde, A., Birkeland, N., Cary, S. C., Tuffin, M., and Cowan, D. A. (2013). Evidence for successional development in Antarctic hypolithic bacterial communities. *ISME J.* 7, 2080–2090. doi: 10.1038/ismej.2013.94

Matsui, D., Terai, A., and Asano, Y. (2016). L-Arginine oxidase from Pseudomonas sp. TPU 7192: characterization, gene cloning, heterologous expression, and application to L-arginine determination. *Enzyme Microb. Technol.* 82, 151–157. doi: 10.1016/j.enzmictec.2015.10.002

McAnoy, A. M., Wu, C. C., and Murphy, R. C. (2005). Direct qualitative analysis of triacylglycerols by electrospray mass spectrometry using a linear ion trap. *J. Am. Soc. Mass Spectrom.* 16, 1498–1509. doi: 10.1016/j.jasms.2005.04.017

Mejia, F. A., and Kleissl, J. (2013). Soiling losses for solar photovoltaic systems in California. *Sol. Energy* 95, 357–363. doi: 10.1016/j.solener.2013.06.028

Meola, M., Lazzaro, A., and Zeyer, J. (2015). Bacterial composition and survival on Sahara dust particles transported to the European Alps. *Front. Microbiol.* 6:1454. doi: 10.3389/fmicb.2015.01454

Mironenko, N. V., Alekhina, I. A., Zhdanova, N. N., and Bulat, S. A. (2000). Intraspecific variation in gamma-radiation resistance and genomic structure in the filamentous fungus Alternaria alternata: a case study of strains inhabiting Chernobyl reactor no. 4. *Ecotoxicol. Environ. Saf.* 45, 177–187. doi: 10.1006/eesa.1999.1848

Mongodin, E. F., Shapir, N., Daugherty, S. C., DeBoy, R. T., Emerson, J. B., Shvartzbeyn, A., et al. (2006). Secrets of soil survival revealed by the genome sequence of *Arthrobacter aurescens* TC1. *PLoS Genet.* 2:e214. doi: 10.1371/journal.pgen.0020214

Montaño, A., Sánchez, A. H., Casado, F. J., Beato, V. M., and de Castro, A. (2013). Degradation of ascorbic acid and potassium sorbate different Lactobacillus species isolated from packed Green olives. *Food Microbiol.* 34, 7–11. doi: 10.1016/j.fm.2012.11.006

Normand, P., Gury, J., Pujic, P., Chouaia, B., Crotti, E., Brusetti, L., et al. (2012). Genome sequence of radiation-resistant Modestobacter marinus strain BC501, a representative actinobacterium that thrives on calcareous stone surfaces. *J. Bacteriol.* 194, 4773–4774. doi: 10.1128/JB.01029-12

Olsen, I., and Jantzen, E. (2001). Sphingolipids in bacteria and fungi. *Anaerobe* 7, 103–112. doi: 10.1006/anae.2001.0376

Osman, S., Peeters, Z., La Duc, M. T., Mancinelli, R., Ehrenfreund, P., and Venkateswaran, K. (2008). Effect of shadowing on survival of bacteria under conditions simulating the Martian atmosphere and UV radiation. *Appl. Environ. Microbiol.* 74, 959–970. doi: 10.1128/AEM.01973-07

Palmieri, A., and Petrini, M. (2018). Tryptophol and derivatives: natural occurrence and applications to the synthesis of bioactive compounds. *Nat. Prod. Rep.* doi: 10.1039/c8np00032h [Epub ahead of print].

Parks, D. H., Tyson, G. W., Hugenholtz, P., and Beiko, R. G. (2014). STAMP: statistical analysis of taxonomic and functional profiles. *Bioinformatics* 30, 3123–3124. doi: 10.1093/bioinformatics/btu494

Phillips, R. W., Wiegel, J., Berry, C. J., Fliermans, C., Peacock, A. D., White, D. C., et al. (2002). Kineococcus radiotolerans sp. nov., a radiation-resistant, gram-positive bacterium. *Int. J. Syst. Evol. Microbiol.* 52, 933–938.

Ragon, M., Restoux, G., Moreira, D., Møller, A. P., and López-García, P. (2011). Sunlight-exposed biofilm microbial communities are naturally resistant to chernobyl ionizing-radiation levels. *PLoS One* 6:e21764. doi: 10.1371/journal.pone.0021764

Rittershaus, E. S., Baek, S. H., and Sassetti, C. M. (2013). The normalcy of dormancy: common themes in microbial quiescence. *Cell Host Microbe* 13, 643–651. doi: 10.1016/j.chom.2013.05.012

SantaCruz-Calvo, L., González-López, J., and Manzanera, M. (2013). Arthrobacter siccitolerans sp. nov., a highly desiccation-tolerant, xeroprotectant-producing strain isolated from dry soil. *Int. J. Syst. Evol. Micorbiol.* 63, 4174–4180. doi: 10.1099/ijs.0.052902-0

Schriek, S., Rückert, C., Staiger, D., Pistorius, E. K., and Michel, K. P. (2007). Bioinformatic evaluation of L-arginine catabolic pathways in 24 cyanobacteria and transcriptional analysis of genes encoding enzymes of L-arginine catabolism in the cyanobacterium Synechocystis sp. PCC 6803. *BMC Genomics* 8:437. doi: 10.1186/1471-2164-8-437

Shirakawa, M. A., Zilles, R., Mocelin, A., Gaylarde, C. C., Gorbushina, A., Heidrich, G., et al. (2015). Microbial colonization affects the efficiency of photovoltaic panels in a tropical environment. *J. Environ. Manage.* 157, 160–167. doi: 10.1016/j.jenvman.2015.03.050

Sohlenkamp, C., and Geiger, O. (2016). Bacterial membrane lipids: diversity in structures and pathways. *FEMS Microbiol. Rev.* 40, 133–159. doi: 10.1093/femsre/fuv008

Srinivasan, S., Joo, E. S., Lee, J., and Kim, M. K. (2015). Hymenobacter humi sp. nov., a bacterium isolated from soil. *Antonie van Leeuwenhoek* 107, 1411–1419. doi: 10.1007/s10482-015-0436-0

Tanner, K., Martí, J. M., Belliure, J., Fernandez-Mendez, M., Molina-Menor, E., Peretó, J., et al. (2018). Polar solar panels: Arctic and Antarctic microbiomes display similar taxonomic profiles. *Environ. Microbiol. Rep.* 10, 75–79. doi: 10.1111/1758-2229.12608

Tekolo, O. M., Mckenzie, J., Botha, A., and Prior, B. A. (2010). The osmotic stress tolerance of basidiomycetous yeasts. *FEMS Yeast Res.* 10, 482–491. doi: 10.1111/j.1567-1364.2010.00612.x

Urai, M., Yoshizaki, H., Anzai, H., Ogihara, J., Iwabuchi, N., Harayama, S., et al. (2007). Structural analysis of mucoidan, an acidic extracellular polysaccharide produced by a pristane-assimilating marine bacterium, *Rhodococcus erythropolis* PR4. *Carbohydr. Res.* 342, 927–932. doi: 10.1016/j.carres.2007.02.002

Vilanova, C., Iglesias, A., and Porcar, M. (2015). The coffee-machine bacteriome: biodiversity and colonization of the wasted coffee tray leach. *Sci. Rep.* 5:17163. doi: 10.1038/srep17163

Yao, Y., Sun, T., Wang, T., Ruebel, O., Northen, T., and Bowen, B. P. (2015). Analysis of metabolomics datasets with high-performance computing and metabolite atlases. *Metabolites* 5, 431–442. doi: 10.3390/metabo5030431

Zhang, Z., Zakeeruddin, S. M., O'Regan, B. C., Humphry-Baker, R., and Grätzel, M. (2005). Influence of 4-Guanidinobutyric acid as coadsorbent in reducing recombination in dye-sensitized solar cells. *J. Phys. Chem. B.* 109, 21818–21824. doi: 10.1021/jp054305h

Conflict of Interest Statement: The authors declare that the research was conducted in the absence of any commercial or financial relationships that could be construed as a potential conflict of interest.

Copyright © 2018 Porcar, Louie, Kosina, Van Goethem, Bowen, Tanner and Northen. This is an open-access article distributed under the terms of the Creative Commons Attribution License (CC BY). The use, distribution or reproduction in other forums is permitted, provided the original author(s) and the copyright owner(s) are credited and that the original publication in this journal is cited, in accordance with accepted academic practice. No use, distribution or reproduction is permitted which does not comply with these terms.

microbial biotechnology

Open Access

Extremophilic microbial communities on photovoltaic panel surfaces: a two-year study

Kristie Tanner,[1,2,†] Esther Molina-Menor,[2,†] Adriel Latorre-Pérez,[1] Àngela Vidal-Verdú,[2] Cristina Vilanova,[1] Juli Peretó[1,2,3] and Manuel Porcar[1,2*]

[1]*Darwin Bioprospecting Excellence S.L., Calle Catedrático Agustín Escardino 9, Paterna, 46980, Spain.*
[2]*Institute for Integrative Systems Biology I2SysBio, University of Valencia – CSIC, Catedrático José Beltrán 2, Paterna, 46980, Spain.*
[3]*Department of Biochemistry and Molecular Biology, University of Valencia, Dr. Moliner 50, Burjassot, 46100, Spain.*

Summary

Solar panel surfaces can be colonized by microorganisms adapted to desiccation, temperature fluctuations and solar radiation. Although the taxonomic and functional composition of these communities has been studied, the microbial colonization process remains unclear. In the present work, we have monitored this microbial colonization process during 24 months by performing weekly measurements of the photovoltaic efficiency, carrying out 16S rRNA gene high-throughput sequencing, and studying the effect of antimicrobial compounds on the composition of the microbial biocenosis. This is the first time a long-term study of the colonization process of solar panels has been performed, and our results reveal that species richness and biodiversity exhibit seasonal fluctuations and that there is a trend towards an increase or decrease of specialist (solar panel-adapted) and generalist taxa, respectively. On the former, extremophilic bacterial genera *Deinococcus*, *Hymenobacter* and *Roseomonas* and fungal *Neocatenulostroma*, *Symmetrospora* and *Sporobolomyces* tended to dominate the biocenosis; whereas *Lactobacillus* sp or *Stemphyllium* exhibited a decreasing trend. This profile was deeply altered by washing the panels with chemical agents (Virkon), but this did not lead to an increase of the solar panels efficiency. Our results show that solar panels are extreme environments that force the selection of a particular microbial community.

Received 20 March, 2020; revised 2 June, 2020; accepted 9 June, 2020.
*For correspondence. E-mail manuel.porcar@uv.es; Tel. +34 628821813.
†These authors contributed equally to this work.
Microbial Biotechnology (2020) **13**(6), 1819–1830
doi:10.1111/1751-7915.13620
Funding information
Financial support from the Spanish Government (grant Helios. reference: BIO2015-66960-C3-1-R co-financed by FEDER funds and Ministerio de Economía y Competitividad) and from the European CSA on biological standardization BIOROBOOST (EU grant number 820699) are acknowledged. KT is a recipient of a Doctorado Industrial fellowship from the Ministerio de Ciencia, Innovación y Universidades (Spain), with reference DI-16-08976. AL is a recipient of a Doctorado Industrial fellowship from the Ministerio de Ciencia, Innovación y Universidades (Spain), with reference DI-17-09613. EMM is funded with a Formación de Profesorado Universitario (FPU) grant from the Spanish Government (Ministerio de Ciencia, Innovación y Universidades), with reference FPU17/04184. AVV is funded with a Formación de Profesorado Universitario (FPU) grant from the Spanish Government (Ministerio de Ciencia, Innovación y Universidades), with reference FPU18/02578. CV is a recipient of a Torres Quevedo fellowship from the Ministerio de Ciencia, Innovación y Universidades (Spain), with reference PTQ-16-08227.

Introduction

Extreme environments are characterized by their strong selective pressures, which can include physical (i.e., temperature or radiation), geochemical (i.e., desiccation or salinity) and/or biological stresses (i.e., limited nutrient availability) (Lynn and Rocco, 2001). The microorganisms that inhabit these environments, known as extremophiles or extremotolerants, are selected due a variety of mechanisms, such as biofilm formation (Flemming *et al.*, 2016; Blanco *et al.*, 2019); the production of extremolytes and extremozymes (Gabani and Singh, 2013); or highly efficient DNA repair systems (Singh and Gabani, 2011). Microorganisms inhabiting extreme environments evolve faster than those inhabiting 'benign' environments, mainly due to the high mutation rates associated to stressful environmental conditions (Li *et al.*, 2014), and this could lead to these microorganisms being rich sources of new specialized metabolites (Sayed *et al.*, 2019).

A diversity of physical, geochemical and biological extremes (solar radiation, temperature fluctuations, desiccation and limited nutrient availability) concur on solar panel surfaces. A study performed on subaerial solar panel biofilms in São Paulo revealed that dust, pollen and other debris covering the solar panel surfaces accumulated in time and included abundant fungi and pigmented bacterial genera, and this was associated with a

© 2020 The Authors. *Microbial Biotechnology* published by Society for Applied Microbiology and John Wiley & Sons Ltd
This is an open access article under the terms of the Creative Commons Attribution License, which permits use, distribution and reproduction in any medium, provided the original work is properly cited.

decrease in the photovoltaic power efficiency, especially after 12 and 18 months (loss of 7% and 11% power respectively) (Shirakawa *et al*., 2015). This process – the accumulation of dust particles and microorganisms on a surface – is known as soiling, and it affects photovoltaic efficiency especially under dry and arid conditions, such as those in the Atacama Desert, resulting in an annual energy loss of up 39% in regions with infrequent rainfalls (Cordero *et al*., 2018).

Microbial colonization of solar panel surfaces is of great interest not only from an energetic point of view, but also from an ecological perspective. The widespread distribution around the world of these artificial devices, as well as their relatively standard design, has enabled them to be used as ubiquitous sampling devices for microbial ecologists in the recent years. A previous study of solar panels located in Valencia (Spain) revealed that these surfaces are inhabited by diverse, desert-like microbial communities that show different day/night proteomic profiles and are adapted to high temperatures, desiccation and solar radiation (Dorado-Morales *et al*., 2016). The microbial communities present on the solar panels from Valencia proved rather similar, in taxonomic terms, to those on solar panels located in Arctic and Antarctic regions, with the most abundant genera being *Hymenobacter*, *Sphingomonas* and *Deinococcus* in all cases (Tanner *et al*., 2018). Furthermore, the microbiome of solar panel surfaces from Berkeley (California, USA) also displayed similar profiles, both in taxonomic and functional terms, to those observed on the Spanish solar panels, highlighting the role of selective pressures in the establishment of these microbial communities (Porcar *et al*., 2018). Nevertheless, and despite the previous taxonomic and functional characterization of the solar panel microbiome, little is known about the colonization process of these surfaces.

In the present study, we have weekly monitored the photovoltaic efficiency of 54 small-sized solar panels, and we have analysed the microbiome composition – including fungi and bacteria – every seven weeks, throughout a period of two years, with the aim of studying in detail the microbial colonization process and its effect on photovoltaic efficiency. Furthermore, we have assessed the effect on the solar panel microbiome of periodically treating the solar panel surfaces with a disinfectant.

Results

Solar panel efficiency, originally of roughly 20 Volts (V), displayed significant fluctuations in time and decreased during the first months of the experiment, but then recovered, and exhibited a very similar pattern during the next year (Fig. 1A). The efficiency was lower in the spring/summer months (between April and September), and this pattern was detected in both annuities, coinciding with the temperature increase and rainfall decrease recorded in Valencia, Spain (Fig. 1B). Bacterial diversity (Fig. 1C) and richness (Fig. S1A) increased during these spring/summer months and decreased during the autumn/winter period. In the case of fungi, the opposite pattern was observed: both the diversity (Fig. 1D) and the richness (Fig. S1B) decreased during the spring/summer months and increased during the autumn/winter period. Furthermore, seasonal decreases in bacterial richness and diversity (Fig. S2A) coincided with an increase in chloroplast sequences (Fig. S2B).

The mean relative abundance for each genus in time was calculated and the 15 most abundant bacteria and fungi were selected for further analysis (Table 1). The most abundant bacterial genera were *Modestobacter* (2.72%), *Deinococcus* (2.52%), *Sphingomonas* (2.44%), *Hymenobacter* (2.38%) and *Rubellimicrobium* (2.29%). On the other hand, the most abundant fungal genus was, by far, *Alternaria*, with 55.4% of mean relative abundance, followed by an unidentified fungi (5.6%) and an unidentified *Pleosporales* (5.4%) and by 13 other taxa that displayed between 0.5 and 2.5% of mean relative abundance.

Fluctuations throughout time were observed for the 15 most abundant bacterial and fungal taxa (Fig. S3). A close-up look at the most abundant taxa during the first 21 weeks (Fig. S4), revealed that *Lactobacillus*, *Bacillus, Sphingomonas* and *Hymenobacter* are among the first to arrive, and that the abundance of *Sphingomonas* increases during the first 14 weeks, remaining more or less stable after that. On the other hand, on weeks 14 and 21, there is a general increase in abundance of the most abundant taxa, although this increase is especially pronounced for *Rubellimicrobium, Modestobacter, Skermanella* and *Microbispora*, whereas other taxa, such as *Sphingomonas*, *Hymenobacter* or *Deinococcus* remain constant. Interestingly, several of the most abundant bacteria displayed similar temporal profiles: *Sphingomonas* and *Deinococcus* (Fig. 2A), *Arthrobacter* and *Blastococcus* (Fig. 2B), *Cellulomonas* and *Rubellimicrobium* (Fig. 2C), and *Skermanella* and *Microbispora* (Fig. 2D).

Despite the fluctuations observed, only several bacterial and fungal taxa displayed statistically significant increases or decreases throughout time (Figs 3 and 4). Specifically, *Deinococcus, Hymenobacter* and *Roseomonas* increased with time, whereas *Lactobacillus* decreased (Prais-Winsten, P-value < 0.05) (Fig. 3). Regarding fungi, *Neocatenulostroma, Symmetrospora, Sporobolomyces* and *Comoclathris* increased throughout time, whereas *Stemphylium* decreased (Fig. 4) (Prais–Winsten, P-value < 0.05).

© 2020 The Authors. *Microbial Biotechnology* published by Society for Applied Microbiology and John Wiley & Sons Ltd,

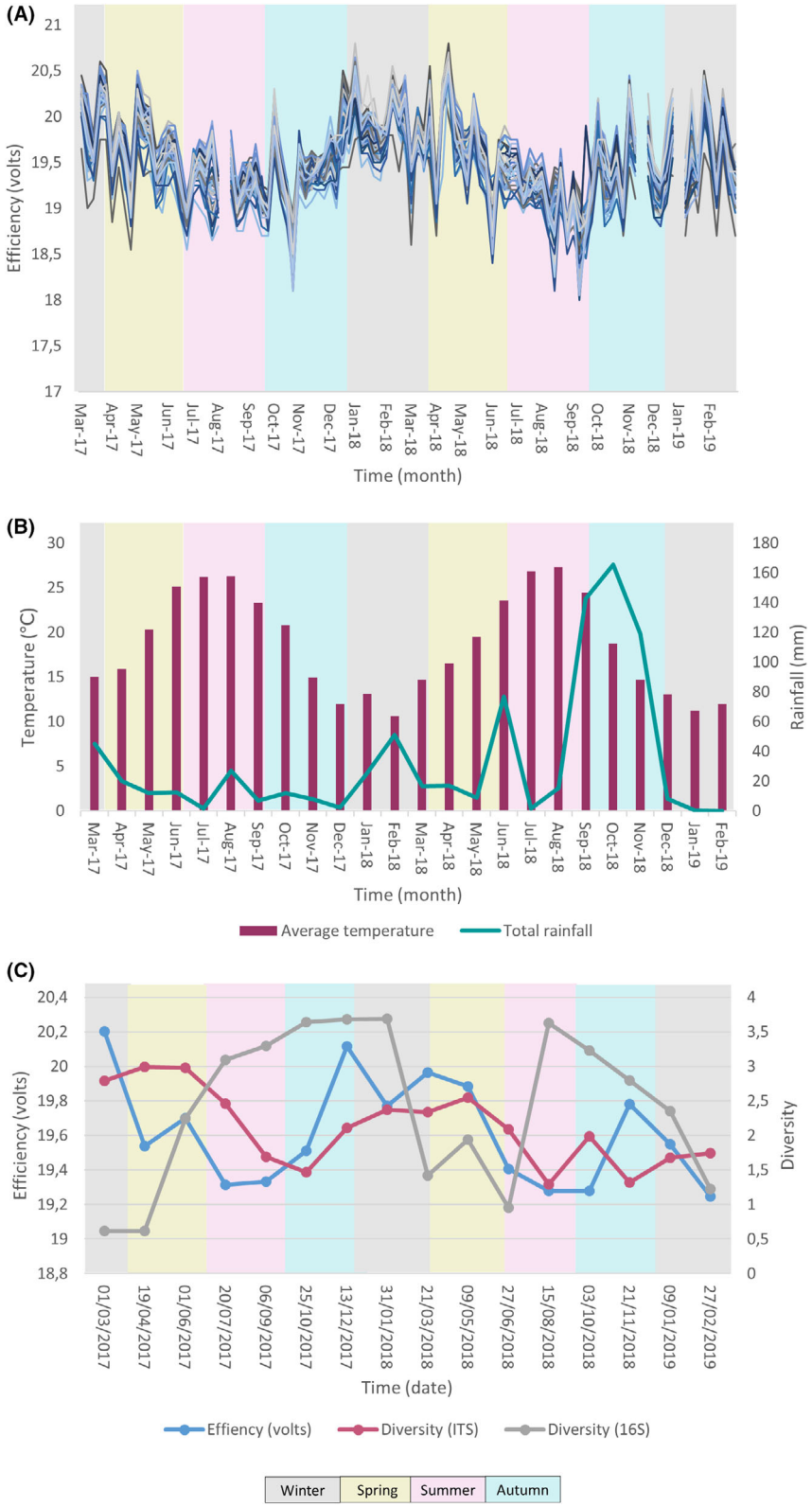

Fig. 1. (A) Variations in solar panel voltage throughout time (measures of the 54 panels were taken every week for a total of 106 weeks). (B) Climate graph of Valencia city, displaying the mean annual temperatures and rainfall values (data source: AVAMET MX). (C) Solar panel voltage is shown and compared to Shannon diversity values at genus level of the detected 16S (grey line) and ITS (pink line) sequences. Seasons in which each sampling was performed are indicated in grey (winter), green (spring), pink (summer) and blue (autumn).

© 2020 The Authors. *Microbial Biotechnology* published by Society for Applied Microbiology and John Wiley & Sons Ltd,

Table 1. Fifteen bacterial and fungal genera with the highest mean relative abundance (MRA) throughout time obtained through 16S rRNA and ITS gene sequencing respectively.

Bacteria		Fungi	
Genus	MRA (%)	Genus	MRA (%)
Modestobacter	2.72	*Alternaria*	55.45
Deinococcus	2.52	*unidentified*	13.41
Sphingomonas	2.44	*Stemphylium*	2.56
Hymenobacter	2.38	*Cladosporium*	1.96
Rubellimicrobium	2.29	*Neocatenulostroma*	1.60
Methylobacterium	2.15	*Aureobasidium*	1.56
Lactobacillus	1.62	*Filobasidium*	1.49
Skermanella	1.41	*Coniosporium*	1.44
Roseomonas	1.29	*Nigrospora*	1.29
Geodermatophilus	1.15	*Knufia*	1.26
Arthrobacter	1.14	*Phaeosphaeria*	0.75
Blastococcus	1.09	*Sporobolomyces*	0.58
Bacillus	1.39	*Vishniacozyma*	0.55
Microbispora	1.12	*Symmetrospora*	0.54
Paracoccus	0.95	*Trebouxia*	0.51

The effect of using a disinfectant on the microbial composition was studied using Rely + On Virkon (DuPont, Michigan, USA), a disinfectant that is routinely used to disinfect hard surfaces. This choice of disinfectant was based on the fact that Virkon does not generate fumes or strong odours, it is compatible with most hard non-porous surfaces, it cleans and disinfects in one step, it has a long shelf life (2 years for the tablet format) and it is effective as determined by European EN standards (bactericidal, fungicidal and virucidal efficacy). Furthermore, in a 1% solution it is non-irritating to eyes and skin. Solar panels that were cleaned with Virkon displayed very different bacterial profiles (Fig. 5A) when compared with the two types of controls (either dipped in sterile water or untreated, both of which displayed a more distant profile in comparison with the Virkon-treated solar panels). Specifically, the panels treated with Virkon were characterized by the almost complete disappearance of *Deinococcus*, and by the increase of 'other' taxa, which corresponded mainly to the phyla *Proteobacteria, Bacteroidetes, Firmicutes* and *Actinobacteria* (Fig. 5C). On the other hand, differences were also observed in the fungal communities of the Virkon-treated panels in comparison with the control treatments (Fig. 5B). Specifically, Virkon-treated surfaces displayed a decrease in general diversity, an increase in the relative abundance

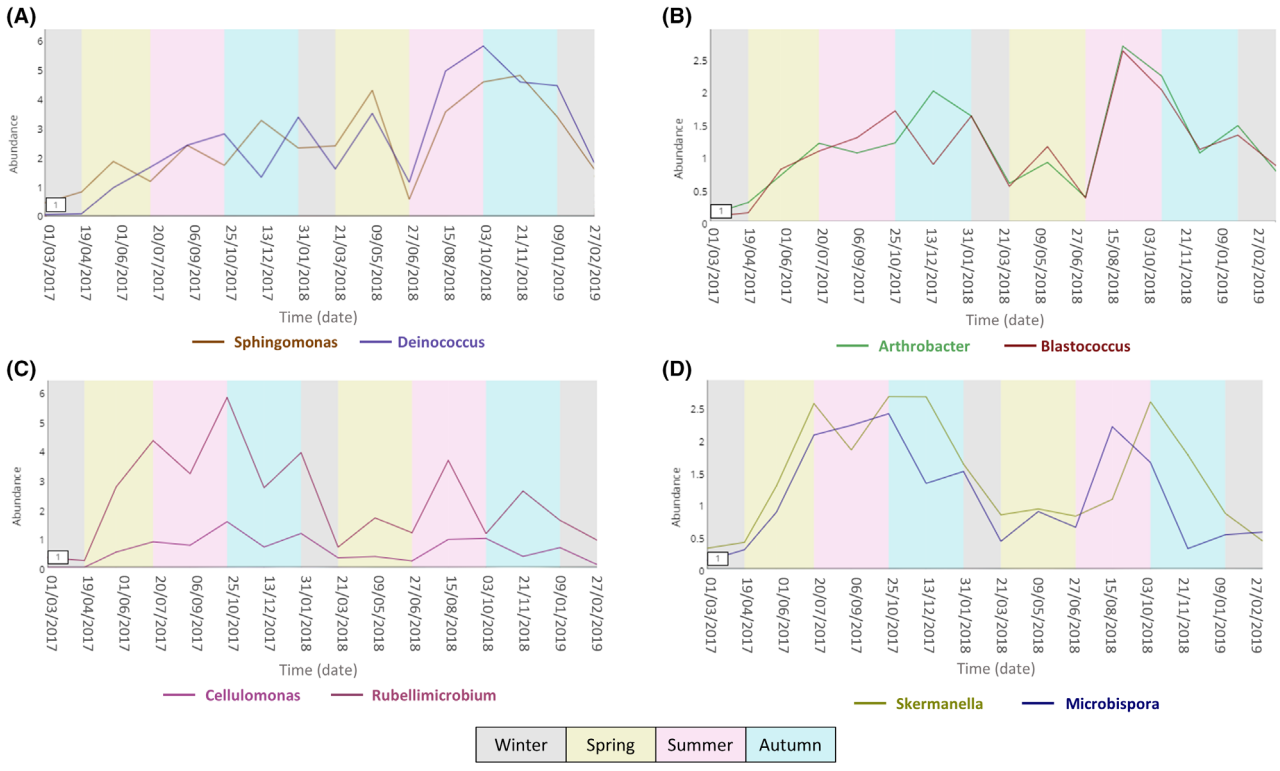

Fig. 2. Trend plots of taxa that display a similar behaviour over time.
A. *Sphingomonas* and *Deinococcus*.
B. *Arthrobacter* and *Blastococcus*.
C. *Cellulomonas* and *Rubellimicrobium*.
D. *Skermanella* and *Microbispora*. These taxa were identified with TIME using a dynamic time warping (DTW) algorithm (Baksi *et al.*, 2018). Seasons in which each sampling was performed are indicated in grey (winter), green (spring), pink (summer) and blue (autumn).

© 2020 The Authors. *Microbial Biotechnology* published by Society for Applied Microbiology and John Wiley & Sons Ltd,

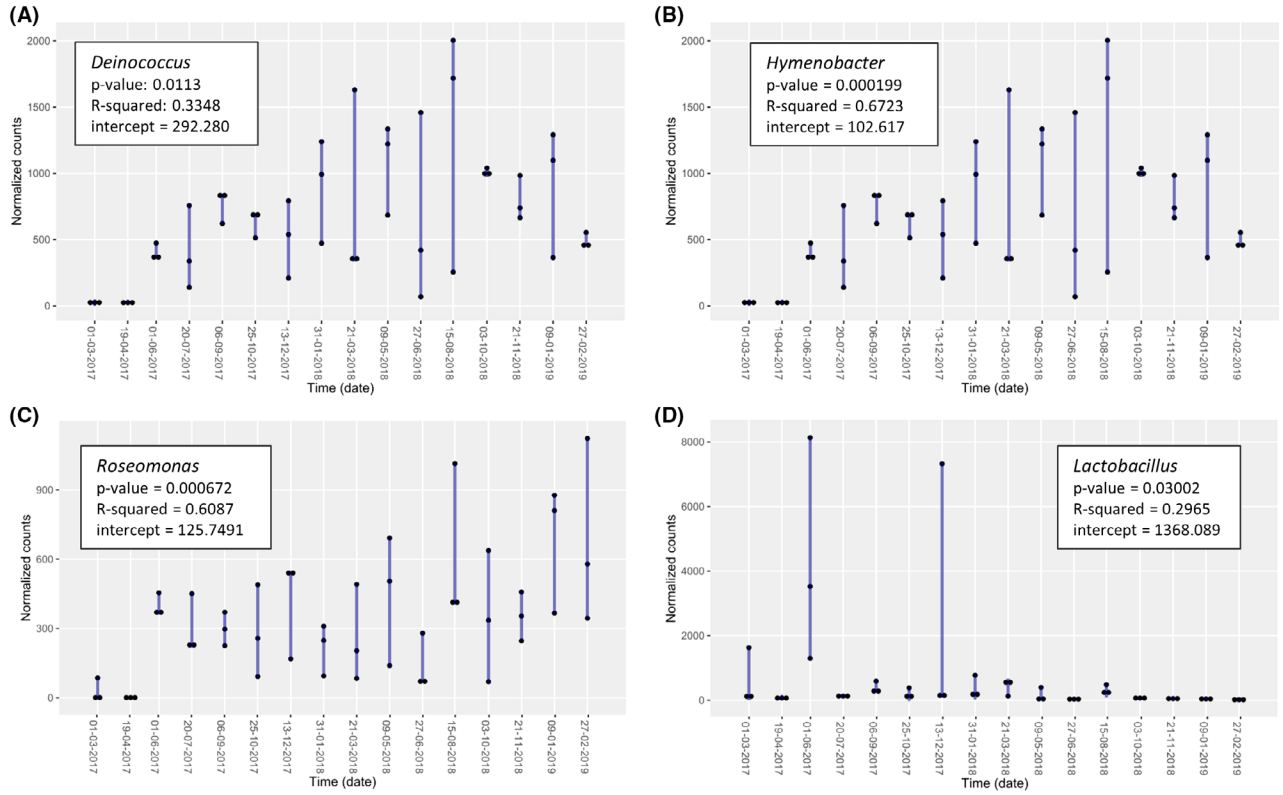

Fig. 3. Statistically significant positive (A,B,C) and negative (D) trends observed in bacterial genera throughout time and calculated using Prais–Winsten estimation (P-value < 0.05) Reported P-values were calculated by applying the normalization of EdgeR package. R-squared and intercept values are also indicated. The black dots indicate the normalized abundance for each of the three replicates.

of *Cystobasidium* and *Filobasidium,* as well as a slight increase in the abundance of taxa assigned to 'other', which corresponded mainly to the phyla *Pleosporales, Dothideales, Capnodiales and Tremellales* (Fig. 5D). It is important to note that the PCoA plots did not change substantially when only the most abundant 15 genera were used (data not shown). Regarding the effect on efficiency of cleaning the solar panels with water or Virkon, in general the produced voltage increased after cleaning, independently of the method used (Fig. S5).

Discussion

Our results reveal that the microbial communities inhabiting solar panel surfaces change in time and experience seasonal variations. The microbial composition is characterized by a set of highly resistant bacterial genera (*Deinococcus, Hymenobacter, Roseomonas*) and fungi (*Alternaria*, among others), which are marginally present on the panels at the beginning of the experiment, but increase in frequency and become dominant by the end of the experiment. Some of the most abundant bacterial genera, such as *Hymenobacter, Modestobacter* and *Deinococcus*, have in fact previously been isolated from warm, irradiated environments, such as arid soil crusts or hyper-arid desert soils (Reddy and Garcia-Pichel, 2013; Busarakam *et al*., 2016; Gundlapally and Garcia-Pichel, 2017), and they have also been reported as frequent taxa inhabiting solar panel surfaces (Dorado-Morales *et al*., 2016; Tanner *et al*., 2018; Porcar *et al*., 2018). In fact, the microbial communities inhabiting solar panel surfaces around the world are similar in both functional and phylogenetic terms (Tanner *et al*., 2018; Porcar *et al*., 2018), suggesting the presence of not only common strong selective pressures (leading to functional similarity), but also of common structuring principles (leading to phylogenetic conservation) that include, among others, assembly history (the timing and order in which species arrive) and priority effects (the imprint of arrival order on community structure) (Carlström *et al*., 2019). Interestingly, *Deinococcus* and *Hymenobacter* have been proposed as biomarkers for desert airborne bacteria (Meola *et al*., 2015), indicating that a possible source of the solar panel microbiome could be the airborne transport of dust particles from deserts.

The most abundant bacterial taxa detected in this work (mean value throughout time) are consistent with those previously described to inhabit solar panel

© 2020 The Authors. *Microbial Biotechnology* published by Society for Applied Microbiology and John Wiley & Sons Ltd,

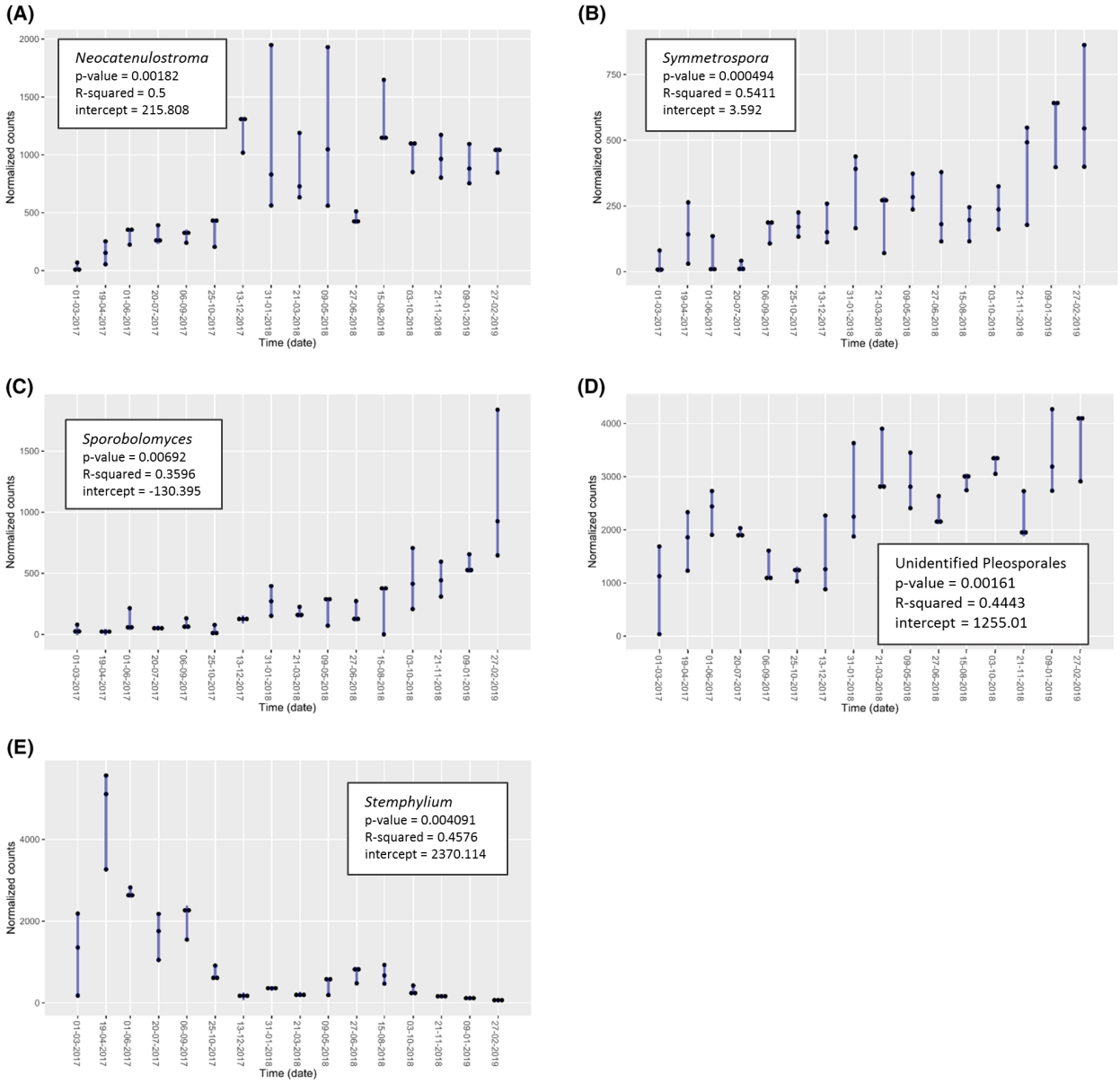

Fig. 4. Statistically significant positive (A,B,C,D) and negative (E) trends observed in fungal genera throughout time and calculated using Prais–Winsten estimation (P-value < 0.05). Reported P-values were calculated by applying the normalization of EdgeR package. R-squared and intercept values are also indicated. The black dots indicate the normalized abundance for each of the three replicates.

surfaces (Dorado-Morales *et al.*, 2016; Tanner *et al.*, 2018; Porcar *et al.*, 2018) and other radiation-exposed environments, suggesting that the strong selection pressure imposed by solar radiation and other factors, such as desiccation, temperature or limited nutrient availability, is what shapes the microbial communities in these environments. For example, a previous study reported that concrete walls exposed to sunlight and ionizing radiation in Chernobyl proved to harbour similar communities to those present in a sun-exposed environment from a control area (without ionizing radiation), and these were dominated by *Actinobacteria*, *Deinococcales* and pigmented ascomycete fungi (Ragon *et al.*, 2011). Similar communities, dominated by *Actinobacteria, Cyanobacteria, Proteobacteria* and *Deinococcus-Thermus*, have also been detected on other stone surfaces around the world, including Roman stone ruins in North Africa (Louati *et al.*, 2019) and historic Scottish monuments (Suihko *et al.*, 2007).

During the first weeks of colonization, members of the genus *Sphingomonas* were among the first taxa whose abundance increased on solar panel surfaces,

© 2020 The Authors. *Microbial Biotechnology* published by Society for Applied Microbiology and John Wiley & Sons Ltd,

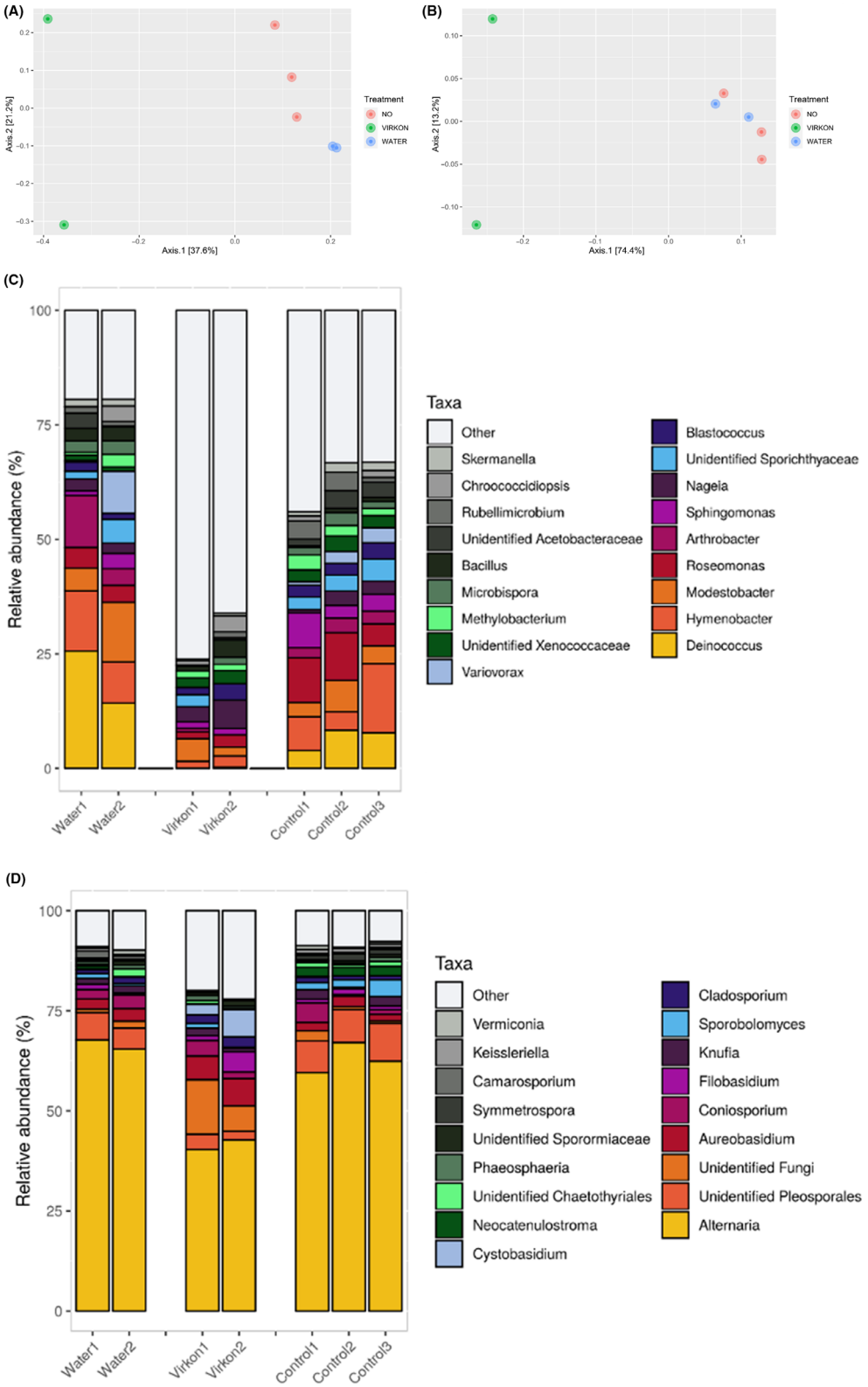

Fig. 5. PCoA (using Bray–Curtis dissimilarities and full data) showing the variations in bacterial (A) and fungal (B) communities on solar panel surfaces as a result of not washing the surfaces in a period of 24 months, or washing them with water/Virkon every seven weeks. Taxonomic analysis of the bacterial (C) and fungal (D) communities in the three different conditions (surfaces unwashed for 2 years or washed with Virkon/water).

© 2020 The Authors. *Microbial Biotechnology* published by Society for Applied Microbiology and John Wiley & Sons Ltd,

suggesting a crucial role of this taxa in the establishment of the subaerial biofilm. This is not the first time that *Sphingomonas* spp. has been described to initiate biofilm formation (Bereschenko *et al*., 2010), and its contribution to biofilm formation is largely associated to its ability to secrete exopolysaccharides (EPS) (Venugopalan *et al*., 2005). At a larger time-scale (24-months), the most abundant taxa detected on solar panel surfaces were *Modestobacter, Deinococcus, Sphingomonas, Hymenobacter, Rubellimicrobium* and *Methylobacterium,* several of which (*Deinococcus*, *Hymenobacter* and *Roseomonas*) displayed an increase in abundance throughout time. These genera are known to contain radiation-resistant (Su *et al*., 2014; Lee *et al*., 2017; Kim *et al*., 2018; Lim *et al*., 2019) and biofilm-forming (Kolari *et al*., 2002; Saarimaa *et al*., 2006; Simões *et al*., 2010) species, traits that could contribute to their success in this environment. In the case of *Methylobacterium* species, these have shown the ability to form biofilms, adhere to polystyrene surfaces and tolerate desiccation and low nutrient conditions (Kolari *et al*., 2002; Simões *et al*., 2010; Yano *et al*., 2013). On the other hand, *Deinococcus* has been found to adhere to paper surfaces in industrial environments, acting as an intermediate for the adhesion of other bacteria (Kolari *et al*., 2002; Saarimaa *et al*., 2006). Thus, *Deinococcus* may play a role in both establishing and intermediating in the biofilm formation on solar panels. Furthermore, previous glass-adhesion experiments with strains isolated from solar panel surfaces revealed that species belonging to the genus *Arthrobacter*, *Methylobacterium*, *Deinococcus* and *Hymenobacter* displayed a high ability to colonize glass surfaces (Dorado-Morales *et al*., 2016).

The increase in abundance of several marker taxa is linked to the hypothesis that, after inoculation on the surface (i.e., via wind carrying desert soil, as suggested by the presence of *Deinococcus* and *Hymenobacter*), some of these taxa, namely those able to resist the extreme conditions inherent to solar panel surfaces, begin to form biofilm structures. In fact, high temperatures and poor nutrient conditions, as the ones that characterize solar panel surfaces, have been described to enhance biofilm formation (Yin *et al*., 2019), and these biofilms could in turn protect the microbial community from other environmental stressors. For example, in *Deinococcus geothermalis,* biofilm formation has been linked to an increased desiccation resistance, although it has also been linked to a decrease in UV resistance due to the photodissociation of water molecules retained in the EPS matrix, leading to increased ROS concentrations (Frösler *et al*., 2017). On the other hand, biofilm structures have also been described to protect against UV-radiation due to physical shading (Yin *et al*., 2019). Interestingly, several bacterial taxa displayed very similar profiles throughout time, suggesting an interdependence between these genera. Whether this dependence is nutritional (i.e., auxotrophic complementation), physical (protection through biofilm formation) or due to another cause remains unknown. A recent study by Carlström *et al*. (2019) on the assembly rules of phyllosphere microbiota revealed that, once established, an initial microbial community is relatively robust and difficult to perturb through the introduction of new species. Nevertheless, in this previous study, single-strain drop out experiments revealed the importance of key taxa in shaping community structures, mainly by affecting (either positively or negatively) strains with low abundance. In this sense, the initial weeks of colonization of solar panel surfaces are critical for the establishment of the final community, and the perturbation of certain strains due to seasonal/environmental variations could lead to the similar profiles observed for several bacterial taxa throughout time. In fact, Carlström *et al*. (2019) described predominantly (around 75%) inhibitory interactions among strains, although one of the two strains displaying positive interactions was found to be *Arthrobacter,* which we also detected in our experimental conditions, displaying a similar behaviour to *Blastococcus* (possibly due to a positive interaction).

In general, bacteria dominated the surface of the panels during the spring/summer period, whereas fungi were more abundant in autumn and winter, very likely linked to the moisture levels during the typically rainy autumn period and the relatively cool Mediterranean winter. Soiling has been reported to increase during low rainfall periods which, as well as affecting the performance of photovoltaic systems (Kimber *et al*., 2006), could also act as a nutrient source, leading to a larger accumulation of bacteria on the surfaces. On the other hand, fungi displayed an increase in richness and diversity in the autumn/winter period, which is consistent with several previous studies. For example, members of the genera *Alternaria, Cladosporium* and *Stemphylium,* among others, display increased ambient concentrations during high relative humidity periods (Llorente *et al*., 2012; Priyamvada *et al*., 2017). Furthermore, it has been shown that filamentous fungi can form biofilms when they grow on surfaces (Harding *et al*., 2009). Indeed, fungi are great candidates to live on surfaces as they secrete extracellular enzymes, they have an absorptive nutrition mode and they can easily invade surfaces due to the apical hyphal growth (Wessels, 1993). The most abundant taxa belonged to the genus *Alternaria*, consistent with the observation by Shirakawa *et al*. (2015), in which melanized *Ascomycetes* dominated the subaerial biofilms located on solar panel surfaces. The abundance of *Alternaria* on solar panel surfaces and other subaerial biofilms could be explained by the abundance within the species belonging to this genus of pathways for melanin biosynthesis, a pigment that

© 2020 The Authors. *Microbial Biotechnology* published by Society for Applied Microbiology and John Wiley & Sons Ltd,

confers protection against UV radiation and other environmental stressors (Kawamura *et al*., 1999; Tseng *et al*., 2011). Interestingly, some bacterial colonizers displayed significant tendencies to decrease throughout time. For example, the genus *Lactobacillus*, not known to be radiation resistant, generally associated to the human microbiota and characterized by including facultative anaerobic or microaerophilic bacteria, tended to decrease during the 2-year experiment.

In our experimental conditions, seasonal fluctuations of solar panel efficiency (open circuit voltage) were observed, which we hypothesize are associated mainly to climatic conditions (specifically, reduced efficiency due to high temperatures, as previously reported) (Skoplaki and Palyvos, 2009; Omubo-Pepple *et al*., 2009) and, to a lesser extent, to soiling and/or biofilm formation (a slight increase in efficiency was observed after rinsing the solar panels periodically with either water or Virkon). Nevertheless, although the use of water or Virkon yielded a similar increase in efficiency, the microbial community after each of those treatment was different. Specifically, the surfaces treated with water displayed a similar microbial composition than the untreated plates, whereas the ones treated with Virkon suffered from changes such as a clear decrease of the genus *Deinococcus,* which was not detected after cleaning the surfaces with Virkon. On the other hand, the fact that the water-treated surfaces were similar, in taxonomic terms, to the untreated surfaces could provide an explanation regarding the stability throughout time of the solar panel microbiome: although rainfall (cleaning with water being a proxy of this) reduces soiling, is not enough to disrupt the microbial community inhabiting solar panel surfaces. Our results thus indicate that chemical agents can strongly modify the microbial composition of the panels, but do not seem to have an important effect on electric production, which is largely dependent on non-biological factors such as dust accumulation and temperature fluctuations.

Taking into account these results, we hypothesize that solar panel surfaces are colonized by microorganisms that arrive through the deposition of soil and dust particles transported via wind. Then, in a very short time period, the microorganisms able to resist radiation and desiccation are selected by the environment and form robust biofilm structures. These biofilms then support the accumulation of other, lesser-abundant organisms, leading to a stable community that is not altered by rainfall and, therefore, is robust throughout time.

This is the first work specifically designed to study, at a large scale and throughout a 2-year time period, the colonization process of solar panel surfaces, focusing on both the fungal and bacterial communities. The most abundant bacterial genera detected (*Modestobacter, Deinococcus, Sphingomonas, Hymenobacter* and *Rubellimicrobium*) and the most abundant fungal genera (*Alternaria,* among others) are consistent with previous studies on solar panel microbiomes. Our results allow us to conclude that the presence of such taxa on solar panels is not the result of their mere accumulation from the surrounding environment, but corresponds to the final step of an ecological succession, in the frame of which extremophilic taxa adapted to the harsh conditions of solar panels are selected. Indeed, a significant increase of solar panel-adapted genera such as *Deinococcus*, *Hymenobacter*, *Roseomonas* and *Neocatenulostroma)* as well as the decrease of non-resistant, ubiquitous taxa (*Lactobacillus* or *Stemphyllium*) was recorded throughout the experiment. Nevertheless, this accumulation of microorganisms is not linked to a significant reduction in photovoltaic efficiency, which exhibits a seasonal variation and that is not improved by antiseptic compounds. It can be concluded that the microbial community is clearly modified by such compounds but that this fact is not linked to a clear benefit in terms of enhanced electric efficiency, at least under the Mediterranean conditions of our study.

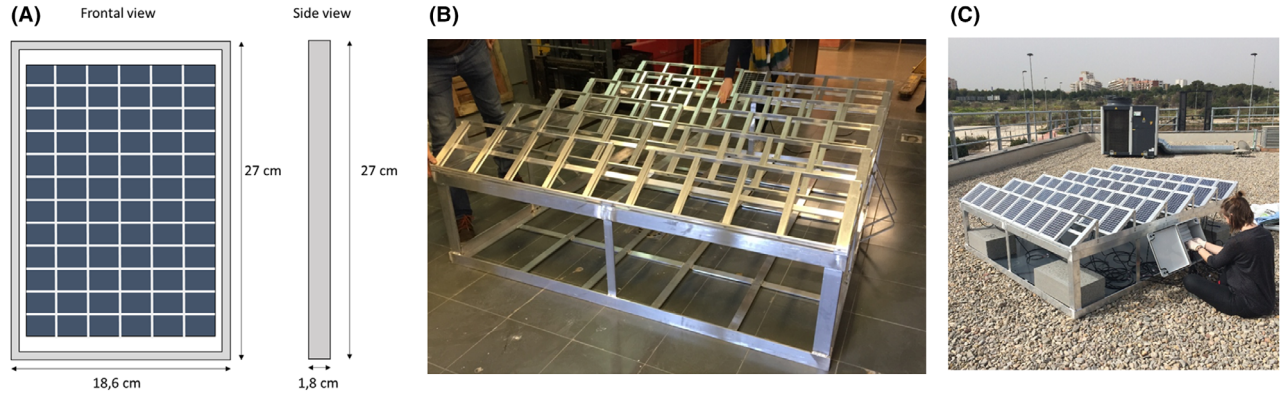

Fig. 6. Experimental set-up: 54 small-sized solar panels (A) were set up on an aluminum chassis (B) and placed on the rooftop of a building in the Scientific Park of the University of Valencia in Paterna, Spain (C).

© 2020 The Authors. *Microbial Biotechnology* published by Society for Applied Microbiology and John Wiley & Sons Ltd,

Experimental procedures

Small-scale solar farm construction

For this work, a small-scale solar farm was built using 54 small-sized solar panels (SOLARPOWER 5W-12V, Xunzel Soluciones S.L., Mendaro-Guipuzcoa, Spain) mounted on a aluminium frame designed *ad hoc* by the ICMUV Institute (Valencia, Spain; Fig. 6A). The surfaces of the panels were sterilized on-site by cleaning them with 70% ethanol. Then, they were placed in the metallic structure (Fig. 6B), which had previously been placed on the roof of one of the buildings belonging to the Scientific Park of the University of Valencia (39°30′56.0″N 0°25′28.4″W) in an equator-facing position (Fig. 6C). Furthermore, all the solar panels were electrically connected to two connection boxes placed at either side of the structure and that were sealed in order to avoid the entrance of water or environmental particles. Once a week (except on cloudy days), and for a period of two years, the efficiency of each solar panel was measured twice and both values were recorded.

Solar panel sampling

Throughout the two-year time period, the surfaces of four of the solar panels were subjected to a treatment with either a disinfectant or water, with the goal of comparing, at the end of the experiment, the microbial taxonomy of both groups. Every seven weeks, two solar panel surfaces were soaked in sterile distilled water for 10 min, and another two were soaked in a solution of Rely + On Virkon disinfectant at 10 g l^{-1}, the working concentration recommended by the manufacturers (DuPont, Michigan, USA) for 10 min, followed by a rinse with sterile distilled water. After cleaning, these solar panels were left to dry in the sun for 10 min and then placed again in the metal structure. At the end of the 2-year period, these four solar panels were sampled together with the final three (uncleaned during 2 years).

Additionally, every seven weeks, three solar panels were randomly selected and sampled. The selected solar panels were removed from the metallic frame, placed in sterile bags and transported to the laboratory. Then, the panels were placed in a laminar flow hood and the surfaces were washed with sterile phosphate-buffered saline (PBS) using a sterile window cleaner. The resulting liquid was concentrated into a pellet by centrifugation, and all pellets were frozen at −20°C until required.

DNA extraction, sequencing and bioinformatic analysis

All DNA extractions were performed using the Power Soil DNA isolation kit (MO BIO Laboratories, Carlsbad, CA, USA), and the resulting DNA was quantified using the QUBIT dsDNA HS-high sensitivity kit (Invitrogen, CA, USA). NextSeq Illumina libraries were constructed, targeting the hypervariable V3 and V4 regions of the 16S gene (Forward = 5′ TCGTCGGCAGCGTCAGATGTGTATAAGAGACAGCCTACGGGNGGCWGCAG; Reverse = 5′ GTCTCGTGGGCTCGGAGATGTGTATAAGAGACAGGACTACHVGGGTATCTAATCC) and targeting the ITS region (Forward = 5′CTTGGTCATTTAGAGGAAGTAA3′; Reverse = 5′GCTGCGTTCTTCATCGATGC3′). Then, Illumina sequencing adaptors and dual-index barcodes (Nextera XT index kit v2, FC-131-2001) were added, and libraries were normalized and pooled. The pools were loaded onto the MiSeq reagent cartridge v3 (MS-102-3003), spiked with 10% PhiX control and sequencing was conducted using paired-ends on an Illumina MiSeq sequencing system. Rarefaction curves were saturated for all samples, indicating that sequencing was deep enough to assess all microbial diversity (Fig. S6). Mean values of 36 533 and 52 192 sequences were obtained for the 16S gene and the ITS region, respectively, with a minimum of 9669 and a maximum of 61 764 sequences for the 16S gene, and a minimum of 25 640 and a maximum of 68 942 sequences for the ITS region.

Raw Illumina sequences were analysed using Qiime2 (Boylen *et al*., 2019). Briefly, the quality of the reads was assessed with the Demux plugin, and the sequences subsequently corrected and trimmed via DADA2. The taxonomy of each sequence variant was assigned employing the classify-Sklearn module from the feature-classifier plugin. GREENGENES (v. 13.8.99) and UNIITE (v. 7_99_01.12.2017) were used as reference databases for 16S rRNA and ITS taxonomic assignment respectively. For the time-series analysis, taxonomy was collapsed into the genus level. For each sampling time and genus, an average of the three replicates sequence count was calculated. The web application TIME (Temporal Insights into Microbial Ecology) was used to analyse and represent the temporal distributions of the taxonomic profiles (Baksi *et al*., 2018), dividing the time period in four seasons: spring (21 March to 20 June), summer (21 June to 20 September), autumn (21 September to 20 December) and winter (21 December to 20 March).

The 15 most abundant genera were selected in order to study their temporary trends. Average sequence counts were calculated for each sampling time, and Prais–Winsten estimation was carried out for each genus using the 'Prais' R package. This linear model was applied for its ability to handle autocorrelation, which is usually found in time-series data. Regressions were calculated using three approaches: with the raw abundance data, normalizing the data through rarefaction with respect to the sample with the lowest sequencing depth and applying the normalization of EdgeR package. All

© 2020 The Authors. *Microbial Biotechnology* published by Society for Applied Microbiology and John Wiley & Sons Ltd,

three approaches yielded the same result, and the *P*-values indicated in Figures 3 and 4 were calculated with the edgeR approach. In all the statistically significant tendencies observed for bacteria and fungi, independently of the approach used, the *P*-value was below 0.05.

Acknowledgements

Financial support from the Spanish Government (grant Helios. reference: BIO2015-66960-C3-1-R co-financed by FEDER funds and Ministerio de Economía y Competitividad) and from the European CSA on biological standardization BIOROBOOST (EU grant number 820699) are acknowledged. KT is a recipient of a Doctorado Industrial fellowship from the Ministerio de Ciencia, Innovación y Universidades (Spain), with reference DI-16-08976. AL is a recipient of a Doctorado Industrial fellowship from the Ministerio de Ciencia, Innovación y Universidades (Spain), with reference DI-17-09613. EMM is funded with a Formación de Profesorado Universitario (FPU) grant from the Spanish Government (Ministerio de Ciencia, Innovación y Universidades), with reference FPU17/04184. AVV is funded with a Formación de Profesorado Universitario (FPU) grant from the Spanish Government (Ministerio de Ciencia, Innovación y Universidades), with reference FPU18/02578. CV is a recipient of a Torres Quevedo fellowship from the Ministerio de Ciencia, Innovación y Universidades (Spain), with reference PTQ-16-08227. MP is indebted to Wim Mertens for life-long musical support. We would like to thank Julian Heredero and Joaquin Baixeras for their help in setting up the solar farm.

Conflict of interest

The authors declare no conflict of interest.

References

Baksi, K.D., Kuntal, B.K., and Mande, S.S. (2018) 'TIME': A web application for obtaining insights into microbial ecology using longitudinal microbiome data. *Front Microbiol* **9:** 36.

Bereschenko, L.A., Stams, A.J.M., Euverink, G.J.W., and van Loosdrecht, M.C.M. (2010) Biofilm formation on reverse osmosis membranes is initiated and dominated by *Sphingomonas* spp. *Appl Environ Microbiol* **76:** 2623–2632.

Blanco, Y., Rivas, L.A., González-Toril, E., Ruiz-Bermejo, M., Moreno-Paz, M., Parro, V., *et al*. (2019) Environmental parameters, and not phylogeny, determine the composition of extracellular substances in microbial mats from extreme environments. *Sci Total Environ* **650:** 384–393.

Boylen, E., Rideout, J., Dillon, M., Bokulich, N., Abnet, C., Al-Ghalith, G., *et al*. (2019) Reproducible, interactive, scalable and extensible microbiome data science using QIIME 2. *Nat Biotechnol* **37:** 852–857.

Busarakam, K., Bull, A.T., Trujillo, M.E., Riesco, R., Sangal, V., van Wezel, G.P., and Goodfellow, M. (2016) *Modestobacter caceresii* sp. nov., novel actinobacteria with an insight into their adaptive mechanisms for survival in extreme hyper-arid Atacama Desert soils. *Syst Appl Microbiol* **39:** 243–251.

Carlström, C.I., Field, C.M., Bortfeld-Miller, M., Müller, B., Sunagawa, S., and Vorhold, J.A. (2019) Synthetic microbiota reveal priority effects and keystone strains in the *Arabidopsis* phyllosphere. *Nat Ecol Evol* **3:** 1445–1454.

Cordero, R.R., Damiani, A., Laroze, D., MacDonell, S., Jorquera, J., Sepúlveda, E., *et al*. (2018) Effects of soiling on photovoltaic (PV) modules in the Atacama Desert. *Sci Rep* **8:** 13943.

Dorado-Morales, P., Vilanova, C., Peretó, J., Codoñer, F.M., Ramón, D., and Porcar, M. (2016) A highly diverse, desert-like microbial biocenosis on solar panels in a Mediterranean city. *Sci Rep* **6:** 29235.

Flemming, H., Wingender, J., Szewzyk, U., Steinberg, P., Rice, S.A., and Kjelleberg, S. (2016) Biofilms: an emergent form of bacterial life. *Nat Rev Microbiol* **14:** 563–575.

Frösler, J., Panitz, C., Wingender, J., Flemming, H., and Rettberg, P. (2017) Survival of *Deinococcus geothermalis* in biofilms under desiccation and simulated space and Martial conditions. *Astrobiology* **17:** 431–447.

Gabani, P., and Singh, O.V. (2013) Radiation-resistant extremophiles and their potential in biotechnology and therapeutics. *Appl Microbiol Biotechnol* **97:** 993–1004.

Gundlapally, S.R., and Garcia-Pichel, F. (2017) Description of *Deinococcus oregonensis* sp. nov., from biological soil crusts in the Southwestern arid lands of the United States of America. *Arch Microbiol* **199:** 69–76.

Harding, M.W., Marques, L.L.R., Howard, R.J., and Olson, M.E. (2009) Can filamentous fungi form biofilms? *Trends Microbiol* **17:** 475–480.

Kawamura, C., Tsujimoto, T., and Tsuge, T. (1999) Targeted disruption of a melanin biosynthesis gene affects conidial development and UV tolerance in the Japanese pear pathotype of *Alternaria alternata*. *Mol Plant Microbe Interac* **12:** 59–63.

Kim, J.Y., Kim, D.U., Kang, M.S., Jang, J.H., Kim, S.J., Kim, M.J., *et al*. (2018) *Roseomonas radiodurans* sp. nov., a gamma-radiation-resistant bacterium isolated from gamma ray-irradiated soil. *Int J Syst Evol Microbiol* **68:** 2443–2447.

Kimber, A., Mitchell, L., Nogradi, S., and Wenger, H. (2006) The effect of soiling on large grid-connected photovoltaic systems in California and the southwest region of the United States. IEEE 4th World Conference on Photovoltaic Energy Conversion, Waikoloa.

Kolari, M., Schmidt, U., Kuismanen, E., and Salkinoja-Salonen, M.S. (2002) Firm but slippery attachment of *Deinococcus geothermalis*. *J Bacteriol* **184:** 2473–2480.

Lee, J.J., Park, S.J., Lee, Y.H., Lee, S.Y., Ten, L.N., and Jung, H.Y. (2017) *Hymenobacter aquaticus* sp. nov., a radiation-resistant bacterium isolated from a river. *Int J Syst Evol Microbiol* **67:** 1206–1211.

Li, S., Hua, Z., Huang, L., Li, J., Shi, S., Chen, L., *et al*. (2014) Microbial communities evolve faster in extreme environments. *Sci Rep* **4:** 6205.

Lim, S., Jung, J.H., Blanchard, L., and de Groot, A. (2019) Conservation and diversity of radiation and oxidative stress resistance mechanisms in *Deinococcus* species. *FEMS Microbiol Rev* **43:** 19–52.

© 2020 The Authors. *Microbial Biotechnology* published by Society for Applied Microbiology and John Wiley & Sons Ltd,

Llorente, I., Moragrega, C., Ruz, L., and Montesinos, E. (2012) An update on control of brown spot of pear. *Trees* **26:** 239–245.

Louati, M., Ennis, N.J., Ghodhbane-Gtari, F., Hezbri, K., Sevigny, J.L., Fahnestock, M.F., *et al*. (2019) Elucidating the ecological networks in stone-dwelling microbiomes. *Environ Microbiol* **22:** 1467–1480.

Lynn, J.R., and Rocco, L.M. (2001) Life in extreme environments. *Nature* **409:** 1092–1101.

Meola, M., Lazzaro, A., and Zeyer, J. (2015) Bacterial composition and survival on Sahara dust particles transported to the European Alps. *Front Microbiol* **6:** 1454.

Omubo-Pepple, V.B., Israel-Cookey, C., and Alaminokuma, G.I. (2009) Effects of temperature, solar flux and relative humidity on the efficient conversión of solar energy to electricity. *Eur J Sci Res* **35:** 173–180.

Porcar, M., Louie, K.B., Kosina, S.M., Van Goethem, M.W., Bowen, B.P., Tanner, K., and Northen, T.R. (2018) Microbial ecology on solar panels in Berkeley, CA, United States. *Front Microbiol* **9:** 3043.

Priyamvada, H., Singh, R.K., Akila, M., Ravikrishna, R., Verma, R.S., and Gunthe, S.S. (2017) Seasonal variation of the dominant allergenic fungal aerosols – One year study from southern Indian region. *Sci Rep* **7:** 11171.

Ragon, M., Restoux, G., Moreira, D., Moller, A.P., and López-García, P. (2011) Sunlight-exposed biofilm microbial communities are natural resistant to Chernobyl ionizing-radiation levels. *PLoS One* **6:** e21764.

Reddy, G.S.N., and Garcia-Pichel, F. (2013) Description of *Hymenobacter arizonensis* sp. nov. from the southwestern arid lands of the United States of America. *Antonie Van Leeuwenhoek* **103:** 321–330.

Saarimaa, C., Perolta, M., Raulio, M., Neu, T.R., Salkinoja-Salonen, M.S., and Neubauer, P. (2006) Characterization of adhesión threads of *Deinococcus geothermalis* as Type IV pili. *J Bacteriol* **188:** 7016–7021.

Sayed, A.M., Hassan, M.H.A., Alhadrami, H.A., Hassan, H.M., Goodfellow, M., and Rateb, M.E. (2019) Extreme environments: microbiology leading to specialized metabolites. *J Appl Microbiol* **128:** 630–657.

Shirakawa, M.A., Zilles, R., Mocelin, A., Gaylarde, C.C., Gorbushina, A., Heidrich, G., *et al*. (2015) Microbial colonization affects the efficiency of photovoltaic panels in a tropical environment. *J Environ Manage* **157:** 160–167.

Simões, L.C., Simões, M., and Vieira, M.J. (2010) Adhesion and biofilm formation on polystyrene by drinking water-isolated bacteria. *Antonie Van Leeuwenhoek* **98:** 317.

Singh, O.V., and Gabani, P. (2011) Extremophiles: radiation resistance microbial reserves and therapeutic implications. *J Appl Microbiol* **110:** 851–861.

Skoplaki, E., and Palyvos, J.A. (2009) On the temperature dependence of photovoltaic module electrical performance: A review of efficiency/power correlations. *Sol Energy* **83:** 614–624.

Su, S., Chen, M., Teng, C., Jiang, S., Zhang, C., Lin, M., and Zhang, W. (2014) *Hymenobacter kanuolensis* sp. nov., a novel radiation-resistant bacterium. *Int J Syst Evol Microbiol* **64:** 2108–2112.

Suihko, M., Alakomi, H., Gorbushina, A., Fortune, I., Marquardt, J., and Saarela, M. (2007) Characterization of aerobic bacterial and fungal microbiota on surfaces of historic Scottish monuments. *Syst Appl Microbiol* **30:** 494–508.

Tanner, K., Martí, J.M., Belliure, J., Fernández-Méndez, M., Molina-Menor, E., Peretó, J., and Porcar, M. (2018) Polar solar panels: Arctic and Antarctic microbiomes display similar taxonomic profiles. *Environ Microbiol Rep* **10:** 75–59.

Tseng, M.N., Chung, P.C., and Tzean, S.S. (2011) Enhancing the stress tolerance and virulence of an entomopathogen by metabolic engineering of dihydroxynaphthalene melanin biosynthesis genes. *Appl Environ Microbiol* **77:** 4508–4519.

Venugopalan, V.P., Kuehn, M., Hausner, M., Springael, D., Wilderer, P.A., and Wuertz, S. (2005) Architecture of a nascent *Sphingomonas* sp. Biofilm under varied hydrodynamic conditions. *Appl Environ Microbiol* **71:** 2677–2686.

Wessels, J.G.H. (1993) Tansley review no. 45 – wall growth, protein excretion and morphogenesis in fungi. *New Phytol* **123:** 397–413.

Yano, T., Kuboota, H., Hanai, J., Hitomi, J., and Tokuda, H. (2013) Stress tolerance of *Methylobacterium* biofilms in bathrooms. *Microbes Environ* **28:** 87–95.

Yin, W., Wang, Y., Liu, L., and He, J. (2019) Biofilms: The microbial "protective clothing" in extreme environments. *Int J Mol Sci* **20:** 3423.

Supporting information

Additional supporting information may be found online in the Supporting Information section at the end of the article.

Fig. S1. Solar panel efficiency measurements (blue dots) are shown and compared to the Richness at genus level of the detected 16S (grey dots) and ITS (pink dots) sequences (these measurements correspond to days in which samples were taken from the surface for genomic analysis). Seasons in which each sampling was performed are indicated in grey (winter), green (spring), pink (summer) and blue (autumn).

Fig. S2. (A) *Y*-axes indicates bacterial Richness (green) and Shannon diversity index (purple) at genus level throughout time. (B) Taxonomic distribution of bacteria in time at class level. Seasons in which each sampling was performed are indicated in grey (winter), green (spring), pink (summer) and blue (autumn).

Fig. S3. Variation in % of abundance throughout time of the 15 bacterial (A) and fungal (B) genera with highest mean abundance. Graphs are separated for 5 genera at a time to facilitate visualization of the data and are ordered from more abundant (top) to less abundant (bottom). Seasons in which each sampling was performed are indicated in grey (winter), green (spring), pink (summer) and blue (autumn).

Fig. S4. Close up of the most abundant genera in the first 21 weeks of sampling.

Fig. S5. Change in open voltage (% of increase or decrease) after cleaning with Virkon or water. Values are shown for the two replicates of each condition (blue dots for plates treated with Virkon and orange dots for plates treated with water).

Fig. S6. Rarefaction curves for sequences corresponding to the 16S gene (A) and ITS region (B).

© 2020 The Authors. *Microbial Biotechnology* published by Society for Applied Microbiology and John Wiley & Sons Ltd,

frontiers in Microbiology

ORIGINAL RESEARCH
published: 07 May 2019
doi: 10.3389/fmicb.2019.00986

Bioprospecting the Solar Panel Microbiome: High-Throughput Screening for Antioxidant Bacteria in a *Caenorhabditis elegans* Model

*Kristie Tanner[1], Patricia Martorell[2], Salvador Genovés[2], Daniel Ramón[2], Lorenzo Zacarías[3], María Jesús Rodrigo[3], Juli Peretó[1,4,5] and Manuel Porcar[1,4]**

[1] Darwin Bioprospecting Excellence S.L., Paterna, Spain, [2] ADM Biopolis S.L., Paterna, Spain, [3] Instituto de Agroquímica y Tecnología de Alimentos (IATA-CSIC), Paterna, Spain, [4] Institute for Integrative Systems Biology (I2SysBio), University of Valencia-CSIC, Paterna, Spain, [5] Department of Biochemistry and Molecular Biology, University of Valencia, Burjassot, Spain

Microbial communities that are exposed to sunlight typically share a series of adaptations to deal with the radiation they are exposed to, including efficient DNA repair systems, pigment production and protection against oxidative stress, which makes these environments good candidates for the search of novel antioxidant microorganisms. In this research project, we isolated potential antioxidant pigmented bacteria from a dry and highly-irradiated extreme environment: solar panels. High-throughput *in vivo* assays using *Caenorhabditis elegans* as an experimental model demonstrated the high antioxidant and ultraviolet-protection properties of these bacterial isolates that proved to be rich in carotenoids. Our results suggest that solar panels harbor a microbial community that includes strains with potential applications as antioxidants.

Keywords: microbiome, sun-exposed environment, bioprospecting, antioxidant, *Caenorhabditis elegans*

OPEN ACCESS

Edited by:
Davide Zannoni,
University of Bologna, Italy

Reviewed by:
Virginia Helena Albarracín,
Center for Electron Microscopy (CIME), Argentina
Birinchi Kumar Sarma,
Banaras Hindu University, India

***Correspondence:**
Manuel Porcar
manuel.porcar@uv.es

Specialty section:
This article was submitted to Extreme Microbiology, a section of the journal Frontiers in Microbiology

Received: *20 December 2018*
Accepted: *18 April 2019*
Published: *07 May 2019*

Citation:
Tanner K, Martorell P, Genovés S, Ramón D, Zacarías L, Rodrigo MJ, Peretó J and Porcar M (2019) Bioprospecting the Solar Panel Microbiome: High-Throughput Screening for Antioxidant Bacteria in a Caenorhabditis elegans Model. Front. Microbiol. 10:986. doi: 10.3389/fmicb.2019.00986

INTRODUCTION

Antioxidants are molecules that can protect cells against oxidative stress. For example, they can play a protective role against the biological damage derived from an excessive cellular production of reactive oxygen species (ROS). ROS are unstable metabolites of molecular oxygen (i.e., superoxide radical, hydroxyl radical, or hydrogen peroxide) that are constantly generated in the cells as by-products of normal aerobic metabolism, but whose levels can increase under certain stress situations (for example, alcohol consumption, smoking, or exposure to environmental pollutants) and become harmful for the cell (Al-Gubory, 2014; Rahal et al., 2014; Zorov et al., 2014; Chen et al., 2015). In humans, chronic oxidative stress has been associated on many occasions with the initiation and progression of a variety of diseases, including Alzheimer's and cardiovascular diseases (such as hypertension and atherosclerosis) or cancer (Chen and Zhong, 2014; Milkovic et al., 2014; Dandekar et al., 2015; Siti et al., 2015).

The discovery of new antioxidants from natural sources (i.e., plants or microorganisms) is of high interest for the pharmacological and food industries (Finley et al., 2011; Lin et al., 2014). The search for novel natural molecules with biotechnological applications is known as bioprospecting and, in the past, microorganisms have proved to be rich sources of natural products that have been

used for the fabrication of commercial products (antibiotics, probiotics, sustainable agriculture, fermentation processes, etc.) with a wide range of applications (Mahajan and Balachandran, 2012; Kanchiswamy et al., 2015; Katz and Baltz, 2016; Choudhary et al., 2017; Gupta and Bajaj, 2017). Microorganisms living in harsh environments typically exhibit strategies to cope with the environmental stresses they are exposed to. In the case of microbial communities exposed to sunlight (i.e., to radiation and desiccation), these adaptations include efficient DNA repair systems, pigment production and protection from oxidative stress (Lebre et al., 2017), suggesting that highly-irradiated environments may be good sources of novel antioxidant-producing microorganisms. In fact, tolerances to desiccation and radiation are mechanistically correlated (Mattimore and Battista, 1996; Ragon et al., 2011; Slade and Radman, 2011), particularly through protection strategies against protein oxidation (Fredrickson et al., 2008; Fagliarone et al., 2017). For these reasons, in the present research we selected a highly-irradiated environment as a potential source of antioxidant-producing microorganisms: solar panels. Solar panels are man-made structures that are exposed to desiccation and high amounts of solar radiation. These harsh conditions shape the surface-inhabiting microbiome toward a highly diverse microbial community with many drought-, heat-, and radiation-resistant bacteria (Dorado-Morales et al., 2016; Porcar et al., 2018; Tanner et al., 2018a). The cultivable microorganisms isolated from solar panels typically display red, orange, or yellow pigmentation, which is assumed to be linked to the production of carotenoids (CRTs), natural pigments that may play a role in the protection of these microorganisms against harmful ionizing radiation and oxidative stress (Britton, 1995; Sandmann, 2015; Dorado-Morales et al., 2016).

Taking into account the need of screening a large number of pigment-producing bacteria isolated from the solar panels, *Caenorhabditis elegans* was chosen as an experimental organism, as it is suitable for these high-throughput screenings. *C. elegans* is a nematode which has previously been used for testing potential antioxidant compounds such as selenite (Li et al., 2014), cocoa products (Martorell et al., 2013), tyrosol (Cañuelo et al., 2012), or CRTs such as astaxanthin (Yazaki et al., 2011) or β-carotene (Lashmanova et al., 2015). The use of *C. elegans* as an experimental model has many advantages, such as the low cost, simplicity, and quickness of the methods. Nevertheless, there is one more advantage that is of particular interest in this study: the fact that this nematode is naturally a bacteria eater, worms can directly be fed with selected bacterial strains. Laboratory *C. elegans* have a basal diet of *Escherichia coli*, but it is possible to supplement the growth medium with many ingredients of interest, including other bacteria, in order to analyze their biological activity. This functional screening method has previously been used in order to identify new antioxidant probiotic strains, such as *Lactobacillus rhamnosus* CNCM I-3690 strain (Grompone et al., 2012) or *Bifidobacterium animalis* subsp. *lactis* CECT 8145 strain (Martorell et al., 2016).

The research we present here aimed at establishing a collection of pigmented bacteria isolated from solar panels in order to select those with promising biological activities as antioxidants. For this, bacterial isolates with no record of opportunistic infections were subjected to a high-throughput antioxidant screening in *C. elegans* using the tracking device WMicrotracker-One^{TM} (PhylumTech, Santa Fé, Argentina), which uses photo-beam interruptions to assess movement of nematodes in multi-well plates. Specifically, the WMicrotracker-One^{TM} (WT) device was used to quantify the survival of the worms after the addition of hydrogen peroxide to the medium. Isolates with the highest antioxidant activity were then selected for further characterization through oxidative stress and UV-protection assays. Finally, a preliminary identification of the CRTs from the selected isolates was performed. This is the first study focused on bioprospecting the solar panel microbiome aiming at obtaining microorganisms with high potential as antioxidants.

MATERIALS AND METHODS

Sampling

Samples were collected from six solar panels located on the rooftop of the Faculty of Economics of the University of Valencia on the 30th November 2015. Sampling was performed by washing the solar panels with sterile Phosphate-Buffered Saline (PBS) and by scraping the surface with sterile glass wipers as previously described (Dorado-Morales et al., 2016). The resulting liquid was collected using sterile pipettes and stored in 50 mL Falcon tubes, which were then transported to the laboratory on ice, where cultivation, isolation, and identification of the strains was performed.

Cultivation and Isolation of Pigmented Bacterial Strains

Solar panel samples were cultivated on Luria-Bertani medium (LB), Reasoner's 2A (R2A) agar (Reasoner and Geldereich, 1985), and Marine Agar (MA) medium, by spreading 50 μL of the collected liquid to each plate. Then, samples were left to settle for 30 min, allowing the larger sized particles – including many fungi – to sediment, and 50 μL of the supernatant were plated on LB, R2A agar, and MA. By allowing the samples to settle, fungal growth was reduced when cultivating the samples on the different culture media. Plates were incubated at room temperature for 1 week and, after incubation, individual colonies were selected and isolated in pure culture by re-streaking on fresh medium. Morphological characteristics of the colonies (color, texture, and size) were taken into account in order to isolate as many different microorganisms as possible. The pure isolates were conserved at −80°C in 20% glycerol for future use.

16S rDNA Sequencing

For 16S rDNA sequencing, a 500-bp fragment of the hypervariable region V1-V3 of the isolates was amplified by colony PCR, using universal primers 28F (5′-GAG TTT GAT CNT GGC TCA G-3′) and 519R (5′-GTN TTA CNG CGG CKG CTG-3′). Isolates whose 16S rDNA failed to amplify from colony templates were amplified again with the same PCR program plus an initial step of incubation for 10 min

at 100°C. Amplicons were checked in 1.4% agarose gel and then precipitated overnight in isopropanol 1:1 (vol:vol) and potassium acetate 3 M pH 5 1:10 (vol:vol). Precipitated DNA was washed with 70% ethanol, resuspended in Milli-Q water (Merck Millipore Ltd, Tullagreen, Cork, Ireland) and quantified with a Nanodrop-1000 Spectrophotometer (Thermo Fisher Scientific, Wilmington, DE, United States). Amplicons were tagged using BigDye®Terminator v3.1 Cycle Sequencing Kit (Applied Biosystems, Carlsbad, CA, United States) and sequenced with the Sanger method by the Sequencing Service (SCSIE) of the University of Valencia (Spain). The resulting sequences were manually edited using Pregap4 (Staden Package, 2002) to eliminate low-quality base calls. The EzBioCloud online tool (Yoon et al., 2017) was used to determine the closest neighbor with valid name for each isolate. The partial 16S rDNA sequence of the isolates was deposited in the GenBank/EMBL/DDBJ databases, under accession numbers MK621939-MK622006.

Oxidative Stress Assays With Worm Tracker

Experiments were carried out with the wild-type *C. elegans* strain N2 (Bristol), which was routinely propagated at 20°C on Nematode Growth Medium (NGM) plates supplemented with *E. coli* strain OP50 as the regular food source. Worms were synchronized by isolating eggs from gravid adults at 20°C. Synchronization was performed on NGM plates with *E. coli* OP50 as a negative control, *E. coli* OP50 plus vitamin C (vitC) at 20 μg/mL as a positive control (**Supplementary Figure 2A**), or *E. coli* OP50 plus the pigmented isolates in order to test antioxidant properties of the bacteria. The isolates were grown overnight in liquid LB medium at 28°C and 180 rpm, optical density at 600 nm (OD_{600}) was adjusted to 30 and to 60, and 50 μL of the bacterial suspension was added to the plates. The synchronized worms were incubated for a total of 3 days on the previously described plates, until reaching young adult stage.

Young adult worms were collected and washed three times with M9 buffer, and finally resuspended in 100–200 μL of the buffer. Worms were then transferred by pipetting to 96-well plates (10–30 worms per well) containing M9 buffer. After transferring all the worms, hydrogen peroxide was added to the wells, reaching a final concentration of 1.2 mM of hydrogen peroxide (**Supplementary Figure 2B**). Mobility of the worms was measured with the WT device during 60 min (four measurements of 15 min). This device detects the movement of organisms through the interference they cause in an array of microbeams of infrared light (patented technology, #US12515723, EP208640881). In this experiment, data was collected in the form of "worm activity" (or relative locomotive activity), and was normalized by the number of worms in each well. All assays were performed with two biological replicates.

Manual Oxidative Stress Assays

Manual assays were also carried out with the wild-type *C. elegans* strain N2 (Bristol), routinely propagated and synchronized as previously described (on NGM with *E. coli* OP50 as a negative control, and supplemented with pigmented isolates at an OD_{600} of 30 for biological assays), except for the positive control, which in this case was vitC at 10 μg/mL. Young adult worms were transferred to fresh plates once every 2 days, until reaching 5-day adult stage. Then, these worms were transferred to plates containing basal medium supplemented with 2 mM hydrogen peroxide and incubated for 5 h at 20°C. After incubation, the survival rate of the worms for each condition (negative control, positive control and fed with pigmented bacteria) was calculated by manually assessing survival of the worms. Two biological replicates were performed for every condition.

UV-Protection Assays

Wild-type *C. elegans* strain N2 (Bristol) worms were synchronized on NGM plates with *E. coli* OP50 as a negative control, *E. coli* OP50 plus vitC (0.1 μg/mL) or plus chlorogenic acid (CGA) (0.1 μg/mL) as positive controls, or *E. coli* OP50 plus the pigmented isolates (50 μL of an over-night culture adjusted to OD 30) in order to test the UV light protection properties of the bacteria.

Synchronized worms were propagated for 15 days on the different types of medium, irradiated daily for 45 s in the laminar flow hood with UV light and transferred to new medium every 2 days, as previously described (Iriondo-DeHond et al., 2016). Survival rate of the worms was manually recorded every day and the assay was performed with biological duplicates.

Pigment Extraction

Carotenoid extraction was performed with two types of bacterial cultures: grown on solid (S) and in liquid (L) medium for 1 week and 12 h (overnight), respectively. For CRTs extraction from isolates grown on solid medium, bacterial cells were collected from solid LB medium after 1 week of incubation at room temperature. Cells were resuspended in PBS and concentrated through centrifugation at 13000 rpm for 3 min. The supernatant was discarded and pellets were dried completely with a vacuum-connected centrifuge (DNA Speed Vac, DNA120, Savant). Then, dry weight was determined. For the exponential phase samples, overnight cultures of selected isolates were collected and the wet weight was determined for each sample.

Bacterial pellets were resuspended and washed in Tris-Buffered Saline (TBS) solution, and centrifuged. Pelleted cells were frozen in liquid nitrogen (N_2) three times, followed by addition of methanol (Sharlau, HPLC grade) (ten times the volume of the pellet) and sonication in a XUBA3 ultrasonic water bath (35 W; Grant Instruments, Cambridge, United Kingdom) for 5 min, in order to break the bacterial cells. Samples were vigorously shaken and centrifuged, and then the upper layer of colored methanol was transferred to a clean tube. This step was performed several times until a non-colored pellet was obtained.

Dicloromethane (HPLC grade) and water (Milli Q grade) (both at ten times the volume of the original pellet) were added to the methanol extract in order to separate organic and aqueous phases. Samples were vigorously shaken, centrifuged, and the aqueous phase was discarded. This step was performed twice, finally yielding CRT extracts in dicloromethane. Samples were then dried under N_2 and kept at −20°C until analysis by HPLC-PDA. All steps were performed under dim light to avoid

CRTs modifications such as photodegradation, isomerizations or structural changes.

HPLC-PDA Analysis

Carotenoid composition of each sample was analyzed by using an HPLC with a Waters liquid chromatography system (Waters, Barcelona, Spain) equipped with a 600E pump and a 2998 photodiode array detector (PDA). Empower software (Waters, Barcelona, Spain) was used for HPLC program set up and chromatogram analysis. A C_{30} CRT column (250 mm × 4.6 mm, 5 μm) coupled to a C_{30} guard column (20 mm × 4.0 mm, 5 μm) (YMC GmbH, Germany) was used. Samples were prepared for HPLC analysis by dissolving the CRT extracts in $CHCl_3$:MeOH:acetone (3:2:1, v:v:v), followed by centrifugation for 2 min at 13000 rpm in order to discard any solid residues. CRT separation was performed with a ternary gradient elution, with an initial solvent composition of 90% methanol (MeOH), 5% water and 5% methyl tert-butyl ether (MTBE). Solvent composition changed during the analysis as described by Carmona et al. (2012) and Alquezar et al. (2008). After each analysis, the initial conditions were re-established and equilibrated before the next injection. The flow rate was 1 mL min^{-1} and column temperature was 25°C. A volume of 20 μL of each sample was injected and the PDA was set to scan from 250 to 540 nm. A Maxplot chromatogram was obtained for each sample that plots each CRT peak at its corresponding maximum absorbance wavelength.

Carotenoids were identified by comparison of the absorption spectra and retention times with the available standards or with data obtained in similar experimental conditions and described in the literature (Britton et al., 1998). For quantification, the chromatographic peaks of each CRT were integrated in their maximum wavelength and the resulting area of the peak was interpolated in different calibration curves that were already set up in the laboratory. The available calibration curves were: canthaxanthin (Sigma), lutein (Sigma), β-carotene (Sigma), β-cryptoxanthin (Extrasynthese). Standards of phytoene and phytofluene were obtained from peel extracts of orange fruits (Rodrigo et al., 2003) and HPLC purified. Quantification of adonirubin, astaxanthin, and echineone was performed using the calibration curve of β-carotene, with values expressed as equivalents of β-carotene. As for the non-identified CRTs, they were quantified using either the β-carotene or the lutein calibration curves depending on their retention times and spectra.

This article had been previously published as a preprint (Tanner et al., 2018b).

RESULTS

Isolation of Pigmented Bacteria

Culturing of the solar panel samples yielded a high amount of colony-forming pigmented microorganisms on all three media (LB, R2A, and MA) as previously described (Dorado-Morales et al., 2016), although the isolates growing on LB media displayed more intense pigmentation. On the other hand, fungal growth was much lower on LB medium than on R2A or MA, facilitating the isolation of pure bacterial cultures from samples grown on LB medium rather than from the other two media. A total of 87 isolates were selected, obtained in pure culture, cryo-preserved in 20% glycerol and subjected to taxonomic identification through 16S rDNA sequencing, with 68 isolates being successfully identified and comprising a wide range of species belonging to the following genera: *Agrococcus*, *Arthrobacter*, *Bacillus*, *Cellulosimicrobium*, *Curtobacterium*, *Frigoribacterium*, *Glutamicibacter*, *Kocuria*, *Leucobacter*, *Microbacterium*, *Pantoea*, *Paracoccus*, *Pedobacter*, *Planomicrobium*, *Plantibacter*, *Pontibacter*, *Pseudoclavibacter*, *Rhodobacter*, *Sanguibacter*, and *Sphingomonas* (**Supplementary Table 1**).

Oxidative Stress Assays

After identification, 14 isolates with no record of opportunistic infections were selected for biological activity assays in *C. elegans*. For example, *Erwinia persicina* was not selected for these assays due to its capacity of infecting plants, causing chlorosis and necrosis in leaves (González et al., 2007). Isolates from the *Kocuria* genus were not selected due to increasing incidence of different types of *Kocuria* infection, mostly in immunocompromised hosts or hosts with severe underlying diseases, causing infections such as peritonitis, bacteremia or endocarditis (Purty et al., 2013). Finally, isolation from clinical specimens of bacteria from the genera *Microbacterium*, *Cellulosimicrobium*, and *Curtobacterium* have been reported, therefore isolates from these species were not selected for biological activity assays (Gneiding et al., 2008; Francis et al., 2011; Zamora and Camps, 2018).

The selected isolates for high-throughput biological assays were the following (**Table 1**): PS1 (*Planomicrobium* sp.), PS83 (*Bacillus* sp.), PS75 (*Bacillus* sp.), PS21 (*Rhodobacter* sp.), PS20 (*Curtobacterium* sp.), PS13 (*Sanguibacter* sp.), PS19 (*Sanguibacter* sp.), PS30 (*Arthrobacter* sp.), PS17 (*Arthrobacter* sp.), PS47 (*Arthrobacter* sp.), PS63 (*Arthrobacter* sp.), PS10 (*Glutamicibacter* sp.), PS66 (*Agrococcus* sp.) and PS57 (*Sphingomonas* sp.). All these isolates were individually tested with an oxidative stress assay using the WT device, which is able to automatically assess survival of the worms through the detection of omega bends and reversals in the worm's locomotion (Huang et al., 2006). Survival under oxidative stress conditions was measured after incubation of the worms for 3 days on NGM supplemented with each bacterial isolate at OD_{600} of 30 or of 60. Isolate PS57 did not grow well in liquid culture and was therefore discarded from the assay. After 3 days of incubation with the selected pigmented isolates, some worms had not reached young adult phase and were de-synchronized. Specifically, this was the case of worms incubated with PS66, PS47, PS19, and PS20. The most extreme case was PS66, so this one was not measured in the WT device. Nevertheless, PS47, PS19, and PS20 displayed only slight differences in growth and were therefore tested. Worm activity after oxidative stress was best measured at 30 min after addition of hydrogen peroxide to the medium, as it is at this point when larger differences could be observed between the positive and negative controls (**Figure 1**).

In general, there was no significant differences in antioxidant activity between the worms incubated with the isolates at an OD

of 30 or of 60 (**Figure 1A**), although a lower OD was beneficial for worm movement and, therefore, was the OD of choice for further experiments. After 30 min of incubation, PS30 did not display significant differences in activity per worm in comparison to the negative control, and PS10 displayed lower mobility than the negative control, indicating more worm mortality. On the other hand, incubation of the worms with PS1, PS13, PS21, PS75, PS17, PS47, PS19, PS20, PS63, and PS83 resulted in a higher protection of these worms against oxidative stress, with significant differences with respect to the negative control, and in some cases, with significantly higher protection in comparison to the positive control (**Figure 1A**). In order to compare all experiments, an antioxidant index (AI) was calculated for each isolate by dividing the average activity per worm at 30 min when incubated with the isolate at OD 30 or 60 (the highest activity was used) by the average activity per worm of the positive control (**Figure 1B**). Nine out of the ten tested isolates displayed higher antioxidant activity than the positive control (AI $>$ 1), although three of these (PS47, PS19, and PS20) could not be compared to the rest due to the worms being smaller and, in some cases, not correctly synchronized.

The WT is a device that measures survival of the worms through their mobility, although this is not the most precise way to measure survival due to the fact that worms tend to have reduced mobility in liquid culture in comparison to solid medium. Therefore, the device may detect false negative results. For this reason, the best isolates according to results with the WT were selected for further, in depth characterization with the manual oxidative stress assay in order to confirm the results. Specifically, PS1, PS75, and PS21 were selected. For the manual assays, oxidative stress is applied to 5-day old adult worms instead of young adult worms, in accordance with the protocol described by Martorell et al. (2013).

Incubation with hydrogen peroxide resulted in a survival of approximately 37% of the worms grown on NGM with *E. coli*, whereas the survival of worms grown on NGM with *E. coli* supplemented with vitamin C (vitC) was higher, with approximately 51% survival (**Figure 1C**), confirming the antioxidant effect of the positive control (vitC). Furthermore, the selected isolates also displayed a high antioxidant effect: incubation with PS75 resulted in around 57% survival, whereas incubation with PS1 and PS21 resulted in a survival rate of as much as 78%. These results confirm that isolates PS1, PS21, and PS75 confer a very high protection against oxidative stress in *C. elegans* and, therefore, validate the WT protocol that was designed for this project.

TABLE 1 | Selected isolates for high-throughput biological assays in *C. elegans*.

Phylum	Isolate number	Closest neighbor (accession number)	% similarity
Actinobacteria	PS66	*Agrococcus citreus* IAM 15145 (AB279547)	99.70
	PS30	*Arthrobacter agilis* DSM 20550 (X80748)	99.26
	PS63	*Arthrobacter agilis* DSM 20550 (X80748)	98.87
	PS17	*Arthrobacter pityocampae* Tp2 (EU855749)	97.77
	PS47	*Arthrobacter subterraneus* CH7 (DQ097525)	97.95
	PS10	*Glutamicibacter arilaitensis* Re117 (FQ311875)	100
	PS20	*Curtobacterium herbarum* P 420/07 (AJ310413)	98.37
	PS13	*Sanguibacter inulinus* ST50 (X79451)	100
	PS19	*Sanguibacter inulinus* ST50 (X79451)	100
Firmicutes	PS75	*Bacillus megaterium* NBRC 15308 (JJMH01000057)	100
	PS83	*Bacillus aryabhattai* B8W22 (EF114313)	99.77
	PS1	*Planomicrobium glaciei* 423 (EU036220)	97.38
Proteobacteria	PS21	*Rhodobacter maris* JA276 (AM745438)	98.89
Bacteroidetes	PS57	*Sphingomonas aerolata* NW12 (AJ429240)	99.76

Percentage of similarity with the closest neighbor (species, strain, and accession number) is indicated.

UV-Protection Assays

The photo-protective effects of the isolated pigmented bacteria were tested *in vivo* in *C. elegans* using a UV-protection assay (**Figure 2**).

There was a natural decrease in survival rate over time in the non-irradiated control (NG-C), with a survival rate at day 14 of 54% (**Figure 2A**). Despite a general decrease of survival rate over the first 9 days (**Figure 2A**), day 11 showed the largest decrease of the negative control survival rate (worms grown on NGM with *E. coli* and subjected to irradiation) in comparison to the survival rate of the positive controls and of the worms fed with the selected isolates (**Figure 2B**). Worms fed with PS1 and PS21 displayed a survival rate of around 55% at day 11, suggesting that these isolates are able to confer resistance against UV irradiation. On the other hand, although PS75 is also able to confer protection to UV-light, the survival rates are lower than the ones obtained with PS1 and PS21 (**Figure 2A**). These results correlate with the previous ones regarding effectiveness of the strains in protecting *C. elegans* against oxidative stress: PS1 and PS21 are the isolates which confer the highest resistance, followed by PS75.

Preliminary Characterization of the Carotenoid Content of Selected Isolates

The three selected isolates (PS1, PS21, and PS75) were further studied in two different types of bacterial culture: liquid culture and solid culture. For this, pigments were extracted and analyzed by HPLC-PDA. The resulting chromatogram of each sample, together with examples of characteristic absorption spectra for CRTs peaks can be seen in **Supplementary Figure 1**. For each sample, the peaks with a characteristic CRT spectrum were integrated at their maximum wavelength and, if possible, their

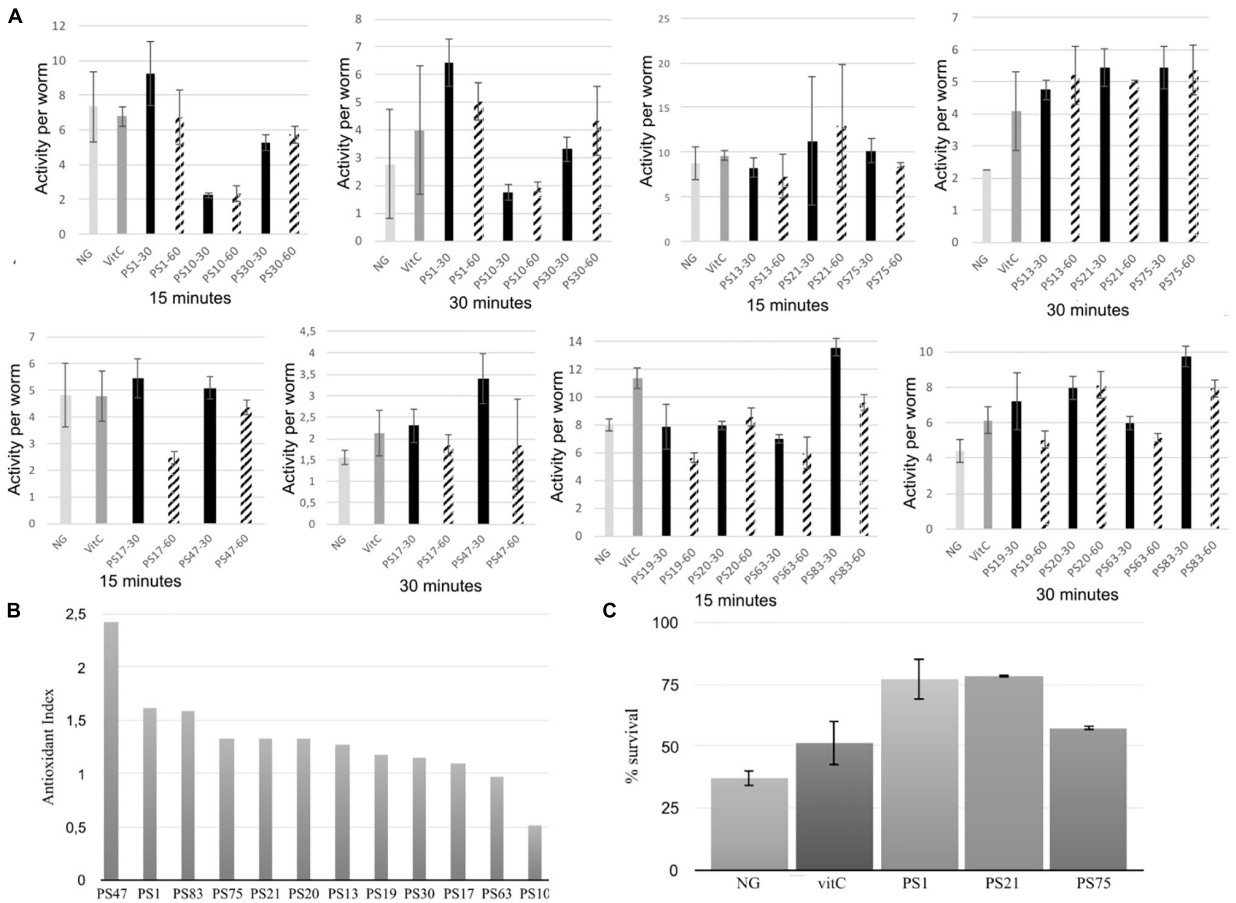

FIGURE 1 | (A) Oxidative stress assays of the selected isolates using the WT device. Worms were fed with the selected isolates at either an OD_{600} of 30 or 60. Survival rate is represented in the Y-axis in the form of activity per worm, and results are shown after 15 and 30 min of incubation with hydrogen peroxide. Error bars indicate standard deviation. **(B)** Antioxidant index (AI) of the pigmented bacterial isolates from solar panels. AI was calculated by dividing the highest activity average (at an OD_{600} of 30 or 60) of each isolate by the average activity of the positive control (vitC) after 30 min of incubation with hydrogen peroxide. **(C)** Manual oxidative stress assay results. Y-axis indicates percentage of survival of the worms after 5 h of incubation in nematode growth medium supplemented with 20 mM hydrogen peroxide. NG (Nematode growth), negative control. VitC (vitamin C), positive control. Error bars indicate standard deviation.

probable identities were assigned according to the absorbance spectrum and retention time compared to commercial standards or reported in similar chromatographic conditions. Peaks with a characteristic CRT spectrum but without assigned identity were reported as "not identified" (NI) in the profile description. Peaks were quantified by interpolating the area of the peaks into calibration curves, as explained in Materials and Methods. The relative abundance of each carotenoid can be seen in **Figure 3**, and all details (identification, peaks, maximum wavelengths, numeric indication of the spectral shape, and quantification) of the CRTs tentatively identified (TI) of each sample can be found in **Supplementary Table 2**.

DISCUSSION

Despite the harsh conditions, solar panels harbor a wide range of pigmented bacteria that are also shared by other harsh environments. *Microbacterium radiodurans* is a UV radiation-tolerant bacterium that was isolated for the first time from the upper sand layers of the Gobi desert in China (Zhang et al., 2010). Other isolates are characteristic of polar environments, such as *Planomicrobium glaciei*, a psychrotolerant bacterium that was first isolated from a glacier in China (Zhang et al., 2009), *Arthrobacter agilis* (Brambilla et al., 2001) or *Sphingomonas aerolata* (Busse et al., 2003); and others are characteristic of soil environments, such as *P. agri* (Roh et al., 2008) or many species of the *Frigoribacterium* (Kämpfer et al., 2000; Dastager et al., 2008), *Arthrobacter* (Park et al., 2014; Siddiqi et al., 2014) and *Curtobacterium* genera (Kim et al., 2008). Pigmentation of the bacterial isolates may play a protective role in their survival in environments with extreme temperature fluctuations and subjected to large amounts of irradiation. An intensification in the pigmentation was observed after the plates were incubated in the refrigerator for several days. In fact, previous studies suggest that pigments such as CRTs not only play an important role in radiation protection but also in cryoprotection

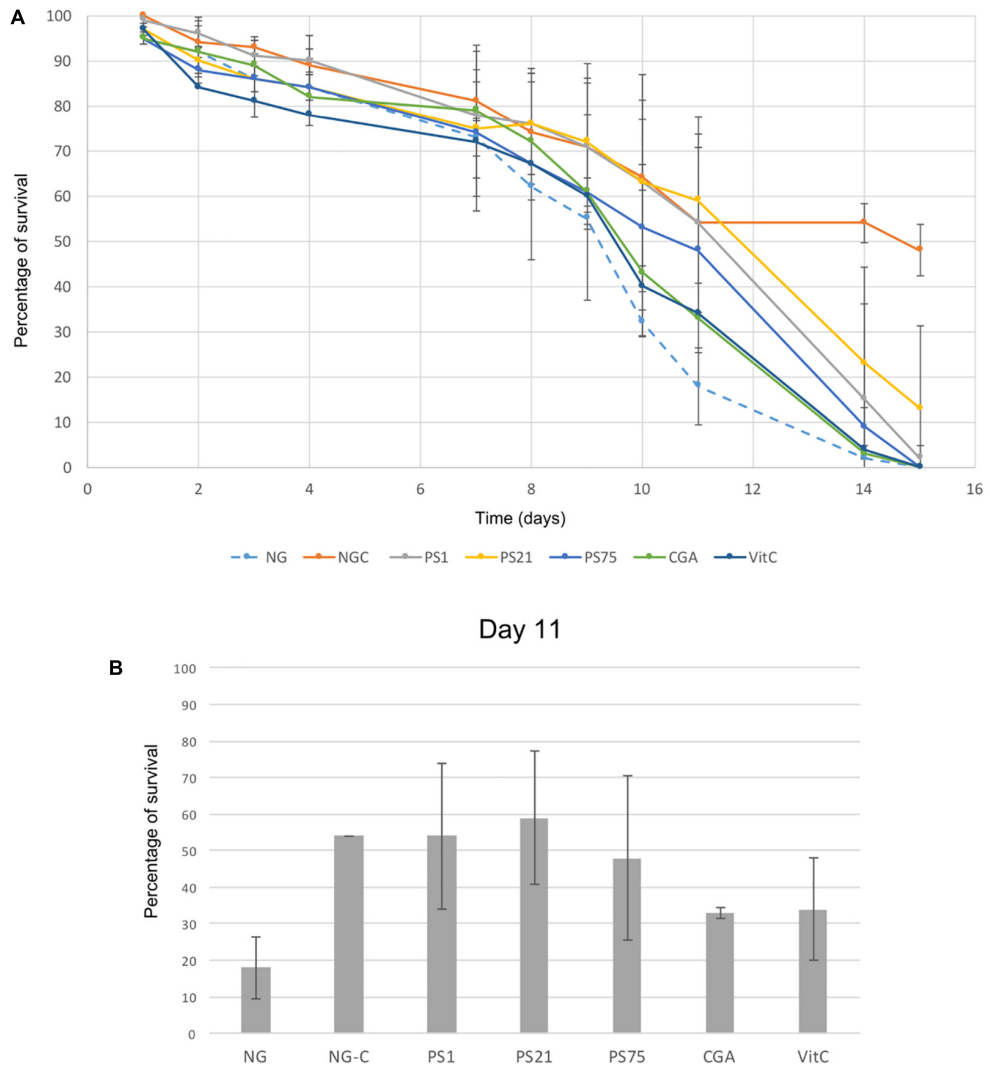

FIGURE 2 | UV-light protection assay. Error bars indicate standard deviation. **(A)** Y-axis indicates percentage of survival of *C. elegans* irradiated with UV-light for 45 s every day over a period of 15 days (X-axis). NG-C indicates the non-irradiated controls: the basal survival rate of the worms over the 15-day period. NG refers to the negative control: worms incubated in NGM with no supplements and irradiated during the 15 days. CGA and VitC are two positive controls: worms incubated with antioxidant compounds (chlorogenic acid and vitamin C) and irradiated during 15 days. Finally, PS1, PS21, and PS75 (*Planomicrobium* sp., *Rhodobacter* sp., and *Bacillus* sp., respectively) indicate worms incubated with pigmented solar panel isolates and irradiated over the 15-day period in order to test the protective effect of these isolates against UV-light. **(B)** Results at day 11, in which the largest differences between the negative control and the worms fed with the pigmented isolates were observed.

(Dieser et al., 2010) due to their ability to modulate membrane fluidity in bacteria when grown under low temperature conditions (Jagannadham et al., 2000).

The diversity of genera found on the solar panel surfaces is consistent with other studies focusing on naturally irradiated environments. For example, several members of the *Bacillus*, *Micrococcus*, and *Pseudomonas* genera that proved to be resistant to UV-B irradiation have previously been isolated from high-altitude Andean wetlands, an environment that is characterized to have high UV radiation (Dib et al., 2008). On the other hand, UV-C resistant microorganisms including *Arthrobacter* sp. and *Curtobacterium* sp. have been isolated from sun-exposed rock varnish from the hot desert of the Whipple Mountains (Kuhlman et al., 2005). Furthermore, it is important to stress that 48 of the 68 isolates identified in the present study were Actinobacteria, a class that has been previously associated to UV-exposed environments including soil and high-altitude freshwater lakes (Warnecke et al., 2005; Rasuk et al., 2017; Bull et al., 2018).

Oxidative-stress assays with *C. elegans* revealed the antioxidant properties of these isolates, making them of great interest for the pharmacological and food industries: extracts of these isolates or even the bacteria themselves could be used as promising treatments for conditions in which oxidative stress plays an important role. On the other hand, the UV-protection assays suggest that the pigmented bacteria isolated from solar panels could also play a protecting role in this type of stress,

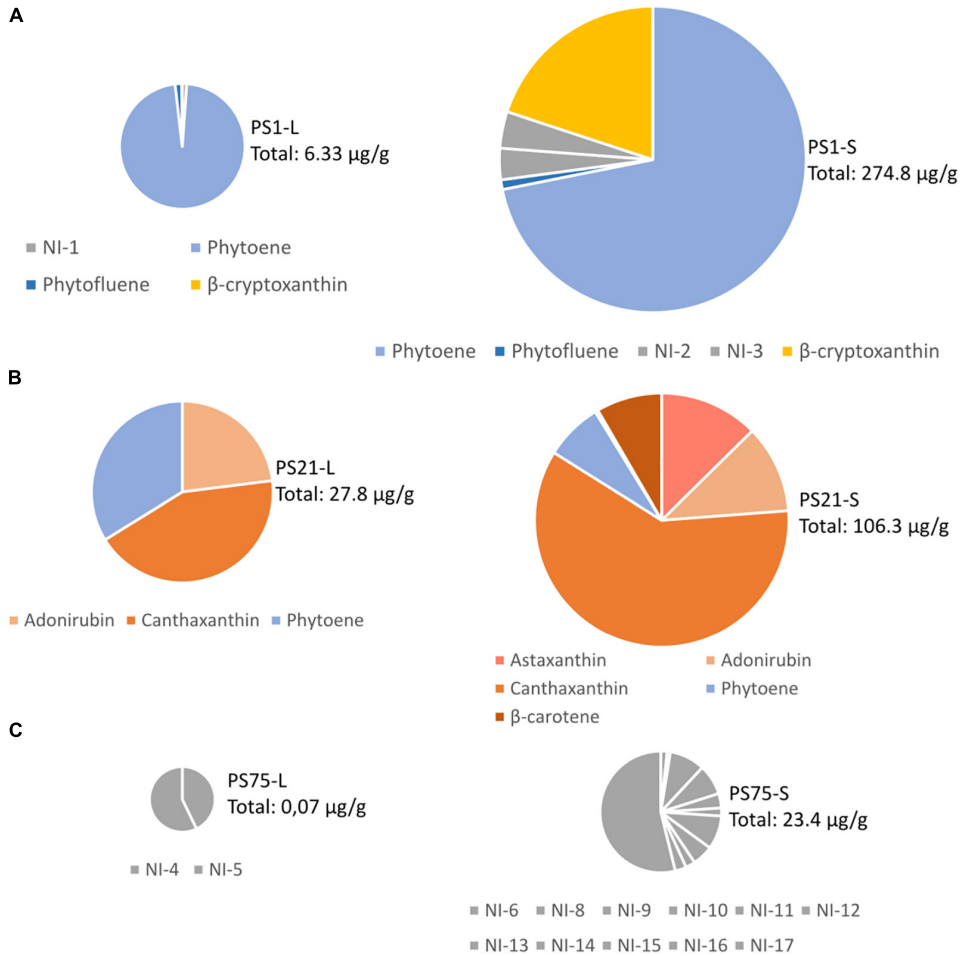

FIGURE 3 | Tentative identification and quantification of the carotenoid content from the three selected isolates **(A)** PS1, **(B)** PS21, **(C)** PS75) after harvesting from liquid (L) or solid (S) culture. The total amount of CRTs is indicated next to each chart in µg per gram of cellular pellet (dry pellet in the samples harvested from solid culture, and wet pellet in the samples harvested from liquid culture). Further details on the concentration of each carotenoid can be found in **Supplementary Table 2**.

which is of high interest for the cosmetic industry, specifically in the fabrication of products that protect against sunlight-induced skin damage. The three isolates selected for UV-light protection assays due to the promising results obtained in the oxidative-stress tests (*Planomicrobium* sp. or PS1, *Rhodobacter* sp. or PS21 and *Bacillus* sp. or PS75) were further tested through HPLC-PDA analysis to shed light on their CRTs composition.

PS1 was found to be 97,38% similar to *Planomicrobium glaciei*, a species that was first described by Zhang et al. (2009), who indicated that it displayed yellow-to-orange pigmentation. Our results suggest that the main CRTs present in PS1 may be phytoene and β-cryptoxanthin, and previous studies have demonstrated the antioxidant and free radical scavenging properties of β-cryptoxanthin, phytoene and phytofluene (Martínez et al., 2014; Ni et al., 2014). It would be interesting to consider whether the high antioxidant capacity of this isolate could be related to the presence of phytoene together with the colored CRT, β-cryptoxanthin.

PS21 was found to be 98.89% similar to *Rhodobacter maris*, a bacteria previously isolated from a marine habitat and described to produce CRTs (Ramana et al., 2008). Interestingly, although Paracoccus PS21 harvested from liquid culture was seen to be rich in pigments probably corresponding to adonirubin (TI), canthaxanthin, and phytoene, when harvested from solid medium CRT composition included also astaxanthin (T) and β-carotene. The CRTs present in PS1 and PS21 could be commercially valuable as they have many applications (Sandmann, 2015): β-carotene and canthaxanthin are used as food colorants and feed additives, especially in aquaculture, whereas astaxanthin and phytoene are widely used in the cosmetic industry.

Finally, the closest neighbor of PS75 was identified as *B. megaterium* (100% similarity), a spore-forming species (Mitchell et al., 1986). Although no identity was assigned to CRT peaks in PS75 extracts, the absorbance spectrum and retention time in the used chromatographic conditions of NI-17 and other minor peaks (NI-14 to -16) in solid culture,

and NI-4 and 5 in liquid culture, are compatible with methyl esters of glycosyl-apo-8′-lycopene, orange colored derivatives of a C30 apo-8′-carotenoid pathway that occurs in certain *Bacillus* species (Pérez-Fons et al., 2011). Moreover, the NI-6 to NI-13 compounds and phytoene-like may also correspond to glycosyl-3-4-dehydro-8′-apolycopene esters and apo-8-phytoene which have been identified in vegetative cells and spores of *Bacillus* sp. species (Pérez-Fons et al., 2011). In relation to the oxidative stress and UV-resistant assays, this isolate had less antioxidant activity in comparison to PS1 and PS21.

CONCLUSION

In conclusion, after selecting a number of pigmented isolates from solar panels according to their low biological risk and testing them *in vivo* in order to elucidate their biological activity, nine out of the ten selected isolates displayed a higher antioxidant activity than the positive control. The isolates with highest antioxidant activity, PS1 (*Planomicrobium* sp.), PS21 (*Rhodobacter* sp.), and PS75 (*Bacillus* sp.) were validated with a manual oxidative stress assay, confirming the previous results and validating the protocol designed and used for oxidative stress assay in the WT device. Furthermore, the three selected strains also displayed UV-protection properties, with values once again higher than the positive control in the case of PS1 and PS21. The high antioxidant properties of these isolates are promising from a pharmacological point of view. Specifically, extracts of these bacteria or artificial combinations of their active compounds, could be useful for the design of new treatments against diseases in which oxidative stress plays a crucial role.

Taken together, our results provide new data on the biological activity of bacterial strains from solar panels with very high antioxidant and UV-protection properties. This is the first report describing the biotechnological potential of pigmented bacterial strains from solar panels using a *C. elegans*-based model.

AUTHOR CONTRIBUTIONS

The project was designed by MP, JP, and DR. Sampling and isolation/identification of the strains was performed by MP, JP, and KT. Experiments involving *C. elegans* were performed by SG, PM, DR, and KT. Characterization of the pigment content was performed by MR, LZ, and KT. Manuscript has been written and revised by all the authors.

FUNDING

Financial support from the Spanish Government (grant Helios, reference: BIO2015-66960-C3-1-R co-financed by FEDER funds and Ministerio de Ciencia, Innovación y Universidades) and from the Regional Government of Valencia (grant MICROBIOSOL, reference: IFIDUA/2015/10 financed by IVACE) are acknowledged. Furthermore, KT is a recipient of a Doctorado Industrial fellowship from the Ministerio de Ciencia, Innovación y Universidades (Spain), with reference DI-16-08976. MR and LZ are members of the CaRed Excellence Network (BIO2017-90877-REDT) and EUROCAROTEN European COST Action (CA15113).

ACKNOWLEDGMENTS

We are very grateful to Cristina Vilanova for her kind assistance in the taxonomic identification of the isolates.

SUPPLEMENTARY MATERIAL

The Supplementary Material for this article can be found online at: https://www.frontiersin.org/articles/10.3389/fmicb.2019.00986/full#supplementary-material

REFERENCES

Al-Gubory, K. H. (2014). Environmental pollutants and lifestyle factors induce oxidative stress and poor prenatal development. *Reprod. Biomed.* 29, 17–31. doi: 10.1016/j.rbmo.2014.03.002

Alquezar, B., Rodrigo, M. J., and Zacarías, L. (2008). Regulation of carotenoid biosynthesis during fruit maturation in the red-fleshed orange mutant *Cara cara*. *Phytochemistry* 69, 1997–2007. doi: 10.1016/j.phytochem.2008.04.020

Brambilla, E., Hippe, H., Hagelstein, A., Tindal, B. J., and Stackerbrandt, E. (2001). 16S rRNA diversity of cultured and uncultured prokaryotes of a mat sample from Lake Fryxell, McMurdo Dry Valleys, Antarctica. *Extremophiles* 5, 23–33. doi: 10.1007/s007920000169

Britton, G. (1995). Structure and properties of carotenoids in relation to function. *FASEB J.* 9, 1551–1558. doi: 10.1096/fasebj.9.15.8529834

Britton, G., Liaaen-Jensen, S., and Pfander, H. (1998). *Carotenoids: Biosynthesis and Metabolism*, Vol. 3. Basel: Birkhäuser.

Bull, A. T., Idris, H., Sanderson, R., Asenjo, J., Andrews, B., and Goodfellow, M. (2018). High altitude, hyper-arid soils of the Central-Andes harbor mega-diverse communities of Actinobacteria. *Extremophiles* 22, 47–57. doi: 10.1007/s00792-017-0976-5

Busse, H. J., Denner, E. B., Buczolits, S., Salkinoja-Salonen, M., Bennasar, A., and Kämpfer, P. (2003). *Sphingomonas aurantiaca* sp. nov., *Sphingomonas aerolata* sp. nov. and *Sphingomonas faeni* sp. nov., air- and dustborne and Antarctic, orange-pigmented, psychrotolerant bacteria, and emended description of the genus Sphingomonas. *Int. J. Syst. Evol. Microbiol.* 53, 1253–1260. doi: 10.1099/ijs.0.02461-0

Cañuelo, A., Gilbert-López, B., Pacheco-Liñán, P., Martínez-Lara, E., Siles, E., and Miranda-Vizuete, A. (2012). Tyrosol, a main phenol present in extra virgin olive oil, increases lifespan and stress resistance in *Caenorhabditis elegans*. *Mech. Ageing Dev.* 133, 563–574. doi: 10.1016/j.mad.2012.07.004

Carmona, L., Zacarías, L., and Rodrigo, M. J. (2012). Stimulation of coloration and carotenoid biosynthesis during postharvest storage of 'Navelina' orange fruit at 12°C. *Postharvest Biol. Technol.* 74, 108–117. doi: 10.1016/j.postharvbio.2012.06.021

Chen, Z., Wang, D., Liu, X., Pei, W., Li, J., Cao, Y., et al. (2015). Oxidative DNA damage is involved in cigarette smoke-induced lung injury in rats. *Environ. Health. Prev. Med.* 20, 318–324. doi: 10.1007/s12199-015-0469-z

Chen, Z., and Zhong, C. (2014). Oxidative stress in Alzheimer's disease. *Neurosci. Bull.* 30, 271–281.

Choudhary, J., Singh, S., and Nain, L. (2017). Bioprospecting thermotolerant ethanologenic yeasts for simultaneous saccharification and fermentation from diverse environments. *J. Biosci. Bioeng.* 123, 342–346. doi: 10.1016/j.jbiosc.2016.10.007

Dandekar, A., Mendez, R., and Zhang, K. (2015). "Cross talk between ER stress, oxidative stress, and inflammation in health and disease," in *Stress Responses.*

Methods in Molecular Biology, ed. C. Oslowski (New York, NY: Humana Press), 205–214. doi: 10.1007/978-1-4939-2522-3_15

Dastager, S. G., Lee, J. C., Ju, Y. J., Park, D. J., and Kim, C. J. (2008). Frigoribacterium mesophilum sp. nov., a mesophilic actinobacterium isolated from Bigeum Island, Korea. *Int. J. Syst. Evol. Microbiol.* 58, 1869–1872. doi: 10.1099/ijs.0.65637-0

Dib, J., Motok, J., Zenoff, V. F., Ordoñez, O., and Farías, M. E. (2008). Occurrence of resistance to antibiotics, UV-B, and arsenic in bacteria isolated from extreme environments in high-altitude (above 4400 m) Andean wetlands. *Curr. Microbiol.* 56, 510–517. doi: 10.1007/s00284-008-9103-2

Dieser, M., Greenwood, M., and Foreman, C. M. (2010). Carotenoid pigmentation in Antarctic heterotrophic bacteria as a strategy to withstand environmental stresses. *Arct. Antarct. Alp. Res.* 42, 396–405. doi: 10.1657/1938-4246-42.4.396

Dorado-Morales, P., Vilanova, C., Peretó, J., Codoñer, F. M., Ramón, D., and Porcar, M. (2016). A highly diverse, desert-like microbial biocenosis on solar panels in a Mediterranean city. *Sci. Rep.* 6, 29235. doi: 10.1038/srep29235

Fagliarone, C., Mosca, C., Ubaldi, I., Verseux, C., Baqué, M., Wilmotte, A., et al. (2017). Avoidance of protein oxidation correlates with the desiccation and radiation resistance of hot and cold desert strains of the cyanobacterium *Chroococcidiopsis*. *Extremophiles* 21, 981–991. doi: 10.1007/s00792-017-0957-8

Finley, J. W., Kong, A. N., Hintze, K. J., Jeffery, E. H., Ji, L. L., and Lei, X. G. (2011). Antioxidants in foods: state of the science important to the food industry. *J. Agric. Food Chem.* 59, 6837–6846. doi: 10.1021/jf2013875

Francis, M. J., Doherty, R. R., Patel, M., Hamblin, J. F., Ojaimi, S., and Korman, T. M. (2011). *Curtobacterium flaccumfaciens* septic arthritis following puncture with a Coxspur Hawthorn thorn. *J. Clin. Microbiol.* 49, 2759–2760. doi: 10.1128/JCM.00340-11

Fredrickson, J. K., Shu-mei, W. L., Gaidamakova, E. K., Matrosova, V. Y., Zhai, M., Sulloway, H. M., et al. (2008). Protein oxidation: key to bacterial desiccation resistance? *ISME J.* 2, 393–403. doi: 10.1038/ismej.2007.116

Gneiding, K., Frodl, R., and Funke, G. (2008). Identities of Microbacterium spp. encountered in human clinical specimens. *J. Clin. Microbiol.* 46, 3646–3652. doi: 10.1128/JCM.01202-08

González, A. J., Tello, J. C., and Rodicio, M. R. (2007). *Erwinia persicina* causing chlorosis and necrotic spots in leaves and tendrils of Pisum sativum in southeastern Spain. *Plant Dis.* 91:460. doi: 10.1094/PDIS-91-4-0460A

Grompone, G., Martorell, P., Llopis, S., González, N., Genovés, S., Mulet, A. P., et al. (2012). Anti-inflammatory *Lactobacillus rhamnosus* CNCM I-3690 strains protects against oxidative stress and increases lifespan in *Caenorhabditis elegans*. *PLoS One* 7:e52493. doi: 10.1371/journal.pone.0052493

Gupta, M., and Bajaj, B. K. (2017). Functional characterization of potential probiotic lactic acid bacteria isolated from Kalarei and development of probiotic fermented oat flour. *Probiotics Antimicrob. Proteins* 10, 654–661. doi: 10.1007/s12602-017-9306-6

Huang, K., Cosman, P., and Schafer, W. R. (2006). Machine vision based detection of omega bends and reversals in *C. elegans*. *J. Neurosci. Methods* 158, 323–336. doi: 10.1016/j.jneumeth.2006.06.007

Iriondo-DeHond, A., Martorell, P., Genovés, S., Ramón, D., Stamatakis, K., Fresno, M., et al. (2016). Coffee silverskin extract protects against accelerated aging caused by oxidative agents. *Molecules* 21:721. doi: 10.3390/molecules21060721

Jagannadham, M. V., Chattopadhyay, M. K., Subbalakshmi, C., Vairamani, M., Narayanan, K., Rao, C. M., et al. (2000). Carotenoids of an Antarctic psychrotolerant bacterium, *Sphingomonas antarticus*, and a mesophilic bacterium, *Sphingobacterium multivorum*. *Arch. Microbiol.* 173, 418–424. doi: 10.1007/s002030000163

Kämpfer, P., Rainey, F. A., Andersson, M. A., Nurmiaho, L. E. L., Ulrych, U., Busse, H. J., et al. (2000). *Frigoribacterium faeni* gen. nov., sp. nov., a novel psychrophilic genus of the family Microbacteriaceae. *Int. J. Syst. Evol. Microbiol.* 50, 355–363. doi: 10.1099/00207713-50-1-355

Kanchiswamy, C. N., Malnoy, M., and Maffei, M. E. (2015). Bioprospecting bacterial and fungal volatiles for sustainable agriculture. *Trends Plant Sci.* 20, 206–211. doi: 10.1016/j.tplants.2015.01.004

Katz, L., and Baltz, R. H. (2016). Natural product discovery: past, present and future. *J. Ind. Microbiol. Biotechnol.* 43, 155–176. doi: 10.1007/s10295-015-1723-5

Kim, M. K., Kim, Y. J., Kim, H. B., Kim, S. Y., Yi, T. H., and Yang, D. C. (2008). *Curtobacterium ginsengisoli* sp. nov., isolated from soil of a ginseng field. *Int. J. Syst. Evol. Microbiol.* 58, 2393–2397. doi: 10.1099/ijs.0.65591-0

Kuhlman, K. R., Allenbach, L. B., Ball, C. L., Fusco, W. G., La Duc, M. T., Kuhlman, G. M., et al. (2005). Enumeration, isolation, and characterization of ultraviolet (UV-C) resistant bacteria from rock varnish in the Whipple Mountains, California. *Icarus* 174, 585–595. doi: 10.1016/j.icarus.2004.11.022

Lashmanova, E., Proshkina, E., Zhikrivetskaya, S., Shevchenko, O., Marusich, E., Leonov, S., et al. (2015). Fucoxanthin increases lifespan of *Drosophila melanogaster* and *Caenorhabditis elegans*. *Pharmacol. Res.* 100, 228–241. doi: 10.1016/j.phrs.2015.08.009

Lebre, P. H., De Maayer, P., and Cowan, D. A. (2017). Xerotolerant bacteria: surviving through a dry spell. *Nat. Rev. Microbiol.* 15, 285–296. doi: 10.1038/nrmicro.2017.16

Li, W. H., Shi, Y. C., Chang, C. H., Huang, C. W., and Hsiu-Chuan Liao, V. (2014). Selenite protects Caenorhabditis elegans from oxidative stress via DAF-16 and TRXR-1. *Mol. Nutr. Food Res.* 58, 863–874. doi: 10.1002/mnfr.201300404

Lin, Y., Jain, R., and Yan, Y. (2014). Microbial production of antioxidant food ingredients via metabolic engineering. *Curr. Opin. Biotechnol.* 26, 71–78. doi: 10.1016/j.copbio.2013.10.004

Mahajan, G. B., and Balachandran, L. (2012). Antibacterial agents from actinomycetes – a review. *Front. Biosci.* 4:240–253. doi: 10.2741/e373

Martínez, A., Stinco, C. M., and Meléndez-Martínez, A. J. (2014). Free radical scavenging properties of phytofluene and phytoene isomers as compared to lycopene: a combined experimental and theoretical study. *J. Phys. Chem.* 118, 9819–9825. doi: 10.1021/jp503227j

Martorell, P., Bataller, E., Llopis, S., Gonzalez, N., Álvarez, B., Montón, F., et al. (2013). A cocoa peptide protects *Caenorhabditis elegans* from oxidative stress and β-amyloid peptide toxicity. *PLoS One* 8:e63283. doi: 10.1371/journal.pone.0063283

Martorell, P., Llopis, S., González, N., Chenoll, E., López-Carreras, N., Aleixandre, A., et al. (2016). Probiotic strain *Bifidobacterium animalis* subsp. *lactis CECT* 8145 reduces fat content and modulates lipid metabolism and antioxidant response in *Caenorhabditis elegans*. *J. Agric. Food Chem.* 64, 3462–3472. doi: 10.1021/acs.jafc.5b05934

Mattimore, V., and Battista, J. R. (1996). Radioresistance of *Deinococcus radiodurans*: functions necessary to survive ionizing radiation are also necessary to survive prolonged desiccation. *J. Bacteriol.* 178, 633–637. doi: 10.1128/jb.178.3.633-637.1996

Milkovic, L., Siems, W., Siems, R., and Zarkovic, N. (2014). Oxidative stress and antioxidants in carcinogenesis and integrative therapy of cancer. *Curr. Pharm. Des.* 20, 6529–6542. doi: 10.2174/13816128206614082615 2822

Mitchell, C., Lyer, S., Skomurski, J. F., and Vary, J. C. (1986). Red pigment in *Bacillus megaterium* spores. *Appl. Environ. Microbiol.* 52, 64–67.

Ni, Y., Nagashimada, M., Zhan, L., Nagata, N., Kobori, M., Sugiura, M., et al. (2014). Prevention and reversal of lipotoxicity-induced hepatic insulin resistance and steatohepatitis in mice by an antioxidant carotenoid, β-cryptoxanthin. *Endocrinology* 156, 987–999. doi: 10.1210/en.2014-1776

Park, Y., Kook, M., Ngo, H. T., Kim, K. Y., Park, S. Y., Mavlonov, G. T., et al. (2014). *Arthrobacter bambusae* sp. nov., isolated from soil of a bamboo grove. *Int. J. Syst. Evol. Microbiol.* 64, 3069–3074. doi: 10.1099/ijs.0.064550-0

Pérez-Fons, L., Steiger, S., Khaneja, R., Bramley, P. M., Cutting, S. M., Sandmann, G., et al. (2011). Identification and the developmental formation of carotenoid pigments in the yellow/orange *Bacillus* spore-formers. *Biochem. Biophys. Acta* 1811, 177–185. doi: 10.1016/j.bbalip.2010.12.009

Porcar, M., Louie, K. B., Kosina, S. M., Van Goethem, M. W., Bowen, B. P., Tanner, K., et al. (2018). Microbial ecology on solar panels in Berkeley, CA, United States. *Front. Microbiol.* 9:3043. doi: 10.3389/fmicb.2018.03043

Purty, S., Saranathan, R., Prashanth, K., Narayanan, K., Asir, J., Devi, C. S., et al. (2013). The expanding spectrum of human infections caused by *Kocuria* species: a case report and literature review. *Emerg. Microbes Infect.* 2:e71.

Ragon, M., Restoux, G., Moreira, D., Møller, A. P., and López-García, P. (2011). Sunlight-exposed biofilm microbial communities are naturally resistant to chernobyl ionizing-radiation levels. *PLoS One* 6:e21764. doi: 10.1371/journal.pone.0021764

Rahal, A., Kumar, A., Singh, V., Yadav, B., Tiwari, R., Charkraborty, S., et al. (2014). Oxidative stress, prooxidants and antioxidants: the interplay. *Biomed. Res. Int.* 2014:761264. doi: 10.1155/2014/761264

Ramana, V. V., Sasikala, C., and Ramana, C. V. (2008). *Rhodobacter maris* sp. nov., a phototrophic alphaproteobacterium isolated from a marine habitat of India. *Int. J. Syst. Evol. Microbiol.* 58, 1719–1722. doi: 10.1099/ijs.0.65638-0

Rasuk, M. C., Ferrer, G. M., Kurth, D., Portero, L. R., Farías, M. E., and Albarracín, V. H. (2017). UV-resistant Actinobacteria from high-altitude Andean lakes: isolation, characterization and antagonistic activities. *Photochem. Photobiol.* 93, 865–880. doi: 10.1111/php.12759

Reasoner, D. J., and Geldereich, E. E. (1985). A new medium for the enumeration and subculture of bacteria from potable water. *Appl. Environ. Microbiol.* 49, 1–7.

Rodrigo, M., Marcos, J., Alferez, F., Mallent, M. D., and Zacarias, L. (2003). Characterization of Pinalate, a novel *Citrus sinensis* mutant with a fruit-specific alteration that results in yellow pigmentation and decreased ABA content. *J. Exp. Bot.* 54, 727–738. doi: 10.1093/jxb/erg083

Roh, S. W., Quan, Z. X., Nam, Y. D., Chang, H. W., Kim, K. H., Kim, M. K., et al. (2008). *Pedobacter agri* sp. nov., from soil. *Int. J. Syst. Evol. Microbiol.* 58, 1640–1643. doi: 10.1099/ijs.0.65783-0

Sandmann, G. (2015). Carotenoids of biotechnological importance. *Adv. Biochem. Eng. Biotechnol.* 148, 449–467. doi: 10.1007/10_2014_277

Siddiqi, M. Z., Kim, Y. J., Hoang, V. A., Siddiqi, M. H., Huq, M. A., and Yang, D. C. (2014). *Arthrobacter ginsengisoli* sp. nov., isolated from soil of a ginseng field. *Arch. Microbiol.* 496, 863–870. doi: 10.1007/s00203-014-1025-8

Siti, H. N., Kamisah, Y., and Kamsiah, J. (2015). The role of oxidative stress, antioxidants and vascular inflammation in cardiovascular disease (a review). *Vascul. Pharmacol.* 71, 40–56. doi: 10.1016/j.vph.2015.03.005

Slade, D., and Radman, M. (2011). Oxidative stress resistance in *Deinococcus radiodurans*. *Microbiol. Mol. Biol. Rev.* 75, 133–191. doi: 10.1128/MMBR.00015-10

Tanner, K., Martí, J. M., Belliure, J., Fernández-Méndez, M., Molina-Menor, E., Peretó, J., et al. (2018a). Polar solar panels: arctic and Antarctic microbiomes display similar taxonomic profiles. *Environ. Microbiol. Rep.* 10, 75–79. doi: 10.1111/1758-2229.12608

Tanner, K., Martorell, P., Genovés, S., Ramón, D., Zacarías, L., Rodrigo, M. J., et al. (2018b). Bioprospecting the solar panel microbiome: high-throughput screening for antioxidant bacteria in a *Caenorhabditis elegans* model. *bioRxiv* [Preprint]. doi: 10.1101/423731

Warnecke, F., Sommaruga, R., Sekar, R., Hofer, J. S., and Pernthaler, J. (2005). Abundances, identity, and growth state of Actinobacteria in mountain lakes of different UV transparency. *Appl. Environ. Microbiol.* 71, 5551–5559. doi: 10.1128/aem.71.9.5551-5559.2005

Yazaki, K., Yoshikoshi, C., Oshiro, S., and Yanase, S. (2011). Supplemental cellular protection by a carotenoid extends lifespan via Ins/IGF-1 signaling in *Caenorhabditis elegans*. *Oxid. Med. Cell. Longev.* 2011:596240. doi: 10.1155/2011/596240

Yoon, S. H., Ha, S. M., Kwon, S., Lim, J., Kim, Y., Seo, H., et al. (2017). Introducing EzBioCloud: a taxonomically united database of 16S rRNA and whole genome assemblies. *Int. J. Syst. Evol. Microbiol.* 67, 1613–1617. doi: 10.1099/ijsem.0.001755

Zamora, J. A. G., and Camps, N. (2018). Bacteremia caused by cellulosimicrobium in a bone marrow transplant patient: a case report and literature review. *IDCases* 11, 64–66. doi: 10.1016/j.idcr.2018.01.007

Zhang, D. C., Liu, H. C., Xin, Y. H., Yu, Y., Zhou, P. J., and Zhou, Y. G. (2009). *Planomicrobium glaciei* sp. nov., a *Psychrotolerant bacterium* isolated from a glacier. *Int. J. Syst. Evol. Microbiol.* 59, 1387–1390. doi: 10.1099/ijs.0.002592-0

Zhang, W., Zhu, H. H., Yuan, M., Yao, Q., Tang, R., Lin, M., et al. (2010). *Microbacterium radiodurans* sp. nov., a UV radiation-resistant bacterium isolated from soil. *Int. J. Syst. Evol. Microbiol.* 60(Pt 11), 2665–2670. doi: 10.1099/ijs.0.017400-0

Zorov, D. B., Juhaszova, M., and Sollott, S. J. (2014). Mitochondrial reactive oxygen species (ROS) and ROS-induced ROS release. *Physiol. Rev.* 94, 909–950. doi: 10.1152/physrev.00026.2013

Conflict of Interest Statement: KT was employed at the time of research by the company Darwin Bioprospecting Excellence S.L., whereas JP and MP are co-founders of the company Darwin Bioprospecting Excellence S.L. PM, SG, and DR were employed by the company ADM Biopolis S.L.

The remaining authors declare that the research was conducted in the absence of any commercial or financial relationships that could be construed as a potential conflict of interest.

Copyright © 2019 Tanner, Martorell, Genovés, Ramón, Zacarías, Rodrigo, Peretó and Porcar. This is an open-access article distributed under the terms of the Creative Commons Attribution License (CC BY). The use, distribution or reproduction in other forums is permitted, provided the original author(s) and the copyright owner(s) are credited and that the original publication in this journal is cited, in accordance with accepted academic practice. No use, distribution or reproduction is permitted which does not comply with these terms.

INTERNATIONAL JOURNAL OF SYSTEMATIC AND EVOLUTIONARY MICROBIOLOGY

TAXONOMIC DESCRIPTION

Tanner *et al.*, *Int. J. Syst. Evol. Microbiol.* 2020;70:1814–1821

DOI 10.1099/ijsem.0.003977

MICROBIOLOGY SOCIETY

Sphingomonas solaris sp. nov., isolated from a solar panel in Boston, Massachusetts

Kristie Tanner[1,2,3,4], Christopher P. Mancuso[5,6], Juli Peretó[1,4,7], Ahmad S. Khalil[3,5,6], Cristina Vilanova[1] and Javier Pascual[1,*]

Abstract

Solar panel surfaces, although subjected to a range of extreme environmental conditions, are inhabited by a diverse microbial community adapted to solar radiation, desiccation and temperature fluctuations. This is the first time a new bacterial species has been isolated from this environment. Strain R4DWN^T belongs to the genus *Sphingomonas* and was isolated from a solar panel surface in Boston, MA, USA. Strain R4DWN^T is a Gram-negative, non-motile and rod-shaped bacteria that tested positive for oxidase and catalase and forms round-shaped, shiny and orange-coloured colonies. It is mesophilic, neutrophilic and non-halophilic, and presents a more stenotrophic metabolism than its closest neighbours. The major fatty acids in this strain are $C_{18:1}\omega7c/C_{18:1}\omega6c$, $C_{16:1}\omega7c/C_{16:1}\omega6c$, $C_{14:0}$ 2OH and $C_{16:0}$. Comparison of 16S rRNA gene sequences revealed that the closest type strains to R4DWN^T are *Sphingomonas fennica*, *Sphingomonas formosensis*, *Sphingomonas prati*, *Sphingomonas montana* and *Sphingomonas oleivorans* with 96.3, 96.1, 96.0, 95.9 and 95.7 % pairwise similarity, respectively. The genomic G+C content of R4DWN^T is 67.9 mol%. Based on these characteristics, strain R4DWN^T represents a novel species of the genus *Sphingomonas* for which the name *Sphingomonas solaris* sp. nov. is proposed with the type strain R4DWN^T (=CECT 9811^T=LMG 31344^T).

In 1990, Yabuuchi *et al.* [1] described the genus *Sphingomonas* for the first time, with the type species being *Sphingomonas paucimobilis*. This genus is classified in the class *Alphaproteobacteria* [2] and is characterized by having ubiquinone Q-10 as the major respiratory quinone and by having an outer membrane that contains glycosphingolipids but lacks lipopolysaccharides [1, 3]. A total of 122 different *Sphingomonas* species have been described up to date (EzBioCloud [4]). They are Gram-negative, rod shaped, non-sporulating, strictly aerobic and display pigmented colonies that range from light yellow/whitish, to intense yellow and orange. Several members of the genus *Sphingomonas* have been shown to hold promise in bioremediation applications, including degradation of polycyclic aromatic hydrocarbon, bisphenol A and heavy metal pollutants [5–7].

In this study we have characterized a new isolate belonging to the genus *Sphingomonas* from the surface of a solar panel. Solar panels from the Hunnewell Building at The Arnold Arboretum of Harvard University, Boston, MA, USA (42° 18′ 28.3″ N, 71° 07′ 14.5″ W), were sampled by cleaning the surfaces with sterile PBS and using a sterile window cleaner. The resulting liquid was collected in sterile tubes and transported to the laboratory on ice. The samples were then left to settle for 5 min in order to allow fungi to sediment, and serial dilutions were performed and plated on Luria–Bertani agar and Reasoner's 2A (R2A) agar. After incubation at room temperature for 6 days, individual colonies were selected and restreaked on fresh medium in order to obtain pure cultures. Strain R4DWN^T was among the isolates selected from the R2A agar plates.

The complete sequence of the 16S rRNA gene of the isolate was extracted from the draft genome and, according to the EZBioCloud online tool [4], the closest type strains to R4DWN^T are *Sphingomonas fennica* (96.3 %), *Sphingomonas*

Author affiliations: [1]Darwin Bioprospecting Excellence S.L., Calle Catedrático Agustín Escardino, 9, 46980 Paterna, Spain; [2]Real Colegio Complutense at Harvard University, 26 Trowbridge St, Cambridge, MA 02138, USA; [3]Wyss Institute for Biologically Inspired Engineering, Harvard University, Harvard University, 3 Blackfan Cir, Boston, MA 02115, USA; [4]Institute for Integrative Systems Biology (I2SysBio, University of Valencia-CSIC), Calle del Catedratico Agustín Escardino Benlloch 9, 46980 Paterna, Spain; [5]Biological Design Center, Boston University, 610 Commonwealth Avenue, Boston, MA 02215, USA; [6]Department of Biomedical Engineering, Boston University, 44 Cummington Mall, Boston, MA 02215, USA; [7]Department of Biochemistry and Molecular Biology, University of Valencia, Calle del Dr. Moliner 50, 46100 Burjassot, Spain.
***Correspondence:** Javier Pascual, jpascual@darwinbioprospecting.com
Keywords: *Sphingomonas solaris*; solar panel.
Abbreviations: ANIb, average nucleotide identity; CDS, coding sequences; dDDH, digital DNA–DNA hybridization; GGDC, Genome-to-Genome Distance Calculator; ML, maximum-likelihood; NJ, neighbour-joining; R2A, Reasoner's 2A; UBCG, up-to-date bacterial core gene set.
Colección Española de Cultivos Tipo (CECT), Belgian Co-ordinated Collections of Micro-organisms (BCCM/LMG). The GenBank/EMBL/DDBJ accession number for the 16S rRNA gene sequence of strain R4DWN^T is MK569518, and the genome accession number is VNIM00000000.
Two supplementary tables and one supplementary figure are available with the online version of this article.

003977 © 2020 The Authors

formosensis (96.1 %), *Sphingomonas prati* (96.0 %), *Sphingomonas montana* (95.9 %) and *Sphingomonas oleivorans* (95.7 %). With the aim of establishing the accurate taxonomic position of R4DWN^T, this isolate was characterized using a polyphasic approach. For this, the reference strains of the two closest species, *S. fennica* and *S. formosensis*, were acquired from the DSMZ Collection (Leibniz Institute DSMZ, Germany) with reference numbers DSM 13665^T and DSM 24164^T, respectively. All three strains were grown on R2A medium at 25 °C for all studies (unless specified otherwise).

For temperature growth tests, all three strains were grown on R2A medium and incubated at 4, 15, 25, 30 and 37 °C. Salt tolerance was determined by cultivating the three strains on R2A medium supplemented with NaCl 0, 1, 2 and 3% (w/v). pH tolerance (between pH 4.0 and 11.0) was determined by cultivating the strains in liquid R2A media buffered with MES (pH 4–6), HEPES (pH 7–8) or CHES (pH 9–11). Catalase activity was determined by detecting bubble production when colonies were mixed with 30% (v/v) hydrogen peroxide. Oxidase activity was determined using Oxidase Sticks for microbiology (PanReac AppliChem), and Gram type was determined by assessing cell lysis in KOH 3% (w/v). All three strains were characterized using API 20NE and API ZYM strips (bioMérieux), as well as Biolog GENIII MicroPlates. The differential phenotypic characteristics between strain R4DWN^T and its closest species are shown in Table 1, and the detailed results obtained from the API galleries and Biolog GEN III utilization tests are detailed in the species description and in Table S1 (available in the online version of this article).

Strain R4DWN^T cells were observed to be Gram-negative, non-motile and rod-shaped (1.2–4.5 µm length x 1.2 µm wide). In old cultures, some cells grew in the form of a long rod shape of approximately 30 µm. Colonies were found to be round-shaped, shiny, orange-coloured, convex and 1 mm in diameter after 7 days of incubation at 25 °C. Strain R4DWN^T displayed several characteristics that allows it to be differentiated from other closely related species of the genus (Table 1), including growth at a smaller range of temperatures (growing only up to 25 °C as opposed to the 30 or 37 °C of other species), assimilation of potassium gluconate and malic acid, and valine arylamidase and β-glucosidase activities. Furthermore, Biolog assays revealed that strain R4DWN^T is only able to assimilate seven out of the 71 tested carbon sources, mainly organic acids and simple sugars (glucuronamide, acetoacetic acid, D-fructose-6-PO4, L-malic acid, L-galactonic acid lactone, β-hydroxy-D,L-butyric acid and D-glucose-6-PO4), whereas *S. fennica* DSM 13665^T and *S. formosensis* DSM 24164^T are able to assimilate 19 and 39 out of the 71 tested carbon sources, respectively. This suggests that strain R4DWN^T displays a more stenotrophic metabolism than its closest neighbours.

For fatty acid analysis, the three strains were grown on R2A plates at 25 °C for 5 days. Then, the cells were harvested and fatty acid profiles were obtained using the standard MIDI Microbial Identification System protocol [8]. Fatty acids were analysed on an Agilent 6850 gas chromatography system and using the MIDI method (TSBA6) [9]. The major fatty acids in strain R4DWN^T were $C_{18:1}\omega7c/C_{18:1}\omega6c$ (48.9 %), $C_{16:1}\omega7c/C_{16:1}\omega6c$ (21.2 %), $C_{14:0}$ 2OH (12.0 %) and $C_{16:0}$ (10.3 %) (Table 2), a profile that is consistent with other members of the genus *Sphingomonas* [10, 11]. Nevertheless, the lack of $C_{17:1}\omega6c$ differentiates R4DWN^T from the type species *S. fennica* DSM 13665^T, whereas the large amount of $C_{16:1}\omega7c/C_{16:1}\omega6c$ differentiates R4DWN^T from the type species *S. formosensis* DSM 24164^T, which displayed only low amounts of these fatty acids.

The total DNA of strain R4DWN^T was extracted using the protocol described by Latorre *et al.* [12], quantified using the QUBIT dsDNA HS-high sensitivity kit (Invitrogen), and the 16S rRNA gene was amplified by PCR reaction using the following primers [13]: 8F (5′-AGAGTTTGATCCTGGCTCAG-3′), 1492R (5′-GGTTACCTTGTTACGACTT-3′), 1055F (5′-ATGGCTGTCGTCAGCT-3′) and 341R (5′-CTGCTGCCTCCCGTAGG-3′). The almost-complete sequence of the 16S rRNA gene of the isolate was obtained through Sanger sequencing. The sequence length was 1470 base pairs, and it can be accessed in the GenBank/EMBL/DDBJ databases under accession number MK569518. The online SINA (SILVA) tool [14] was used to perform a multiple alignment of the sequences, and the maximum-likelihood (ML) (Fig. 1) and neighbour-joining (NJ) (Fig. S1) trees were reconstructed using RaxML [15] and MEGA6 [16], respectively. The GTR algorithm was used for the ML tree, whereas Kimura's two-parameter model was used for the NJ tree. Reliability of the branch patterns was assessed using bootstrap analyses based on 1000 resamplings. Based on the 16S rRNA sequence analysis, R4DWN^T does not have a clear phylogenetic position within the genus *Sphingomonas*. The closest neighbour is *S. formosensis* in both the ML (Fig. 1) and NJ (Fig. S1) trees, whereas *S. fennica* (the closest neighbour according to the 16S rRNA sequencing) appears grouped with *S. oleivorans* forming an external group. Nevertheless, these branches are not supported by high bootstrap values.

The draft genome of strain R4DWN^T was sequenced using the MiSeq sequencer (Illumina), and the Nextera XT Prep Kit protocol was used for library preparation. FastQC was utilized to assess the quality of the sequence reads. Genome assembly of 284 541 paired reads was performed using SPAdes 3.12.0 [17]. The draft genome of R4DWN^T consists of 229 contigs yielding a total length of 4 444 219 bp, with a G+C content of 67.9mol% and an N50 value of 38 937 bp. This genomic G+C content is in agreement with the closest neighbours and confirms the adscription of R4DWN^T to the genus *Sphingomonas* [10, 11]. The maximum contig length was 136 617 bp, and all the contigs were annotated using the RAST tool kit (RASTtk) integrated in PATRIC version 3.5.41 (www.patricbrc.org). A total of 4455 coding sequences (CDS) were predicted, of which 2602 were proteins with functional assignments. A total of 45 tRNA and three rRNA genes (one single ribosomal operon) were identified. This Whole Genome Shotgun project has been deposited at GenBank/EMBL/DDBJ under the accession VNIM00000000. The version described in this paper is version VNIM01000000. The completeness and levels of contamination of the genome were analysed

Table 1. Phenotypic comparisons of strain R4DWN^T and the type strains of closely related *Sphingomonas* species

Strains: 1, R4DWN^T; 2, *Sphingomonas fennica* DSM 24164^T; 3, *Sphingomonas formosensis* DSM 24164^T; 4, *Sphingomonas prati* DSM 103336^T; 5, *Sphingomonas montana* DSM 103337^T; 6, *Sphingomonas oleivorans* HAMBI 3659^T. Analysis of strains 1, 2 and 3 was conducted under the same conditions in this study, whereas data from strains 4, 5 and 6 was taken from the original species description papers [27–29]. All strains were positive for the following characteristics: alkaline phosphatase, esterase (C4), esterase lipase (C8), leucine arylamidase, acid phosphatase and naphtol-AS-BI-phosphohydrolase. All strains were negative for the following characteristics: Gram reaction, nitrate reduction, glucose fermentation, activity of arginine dihydrolase, urease, gelatin hydrolysis, assimilation of adipic acid, trisodium citrate and phenylacetic acid, lipase (C14), *N*-acetyl-*β*-glycosaminidase, α-mannosidase, and α-fucosidase. +, Positive; –, negative; w, weakly positive.

Characteristic	1	2	3	4	5	6
Isolation source	Solar panel surface	Groundwater*	Soil†	Soil	Soil	Soil
Motility	No	No	No	No	Yes	No
Cell size (μm)	1.2–4.5×1.2	0.9–1.5×0.5–0.9*	1.4×0.4†	1.1×0.7	1.2×0.9	1.6–2.4×0.4–0.85
Colour	Orange	Light yellow	Yellow	Orange	Orange	Light yellow
Catalase	+	+	+	w	+	–
Oxidase	+	+	–	w	+	–
Growth temperature (°C)	4–25	4–30	4–37	4–30	4–30	4–37
pH range for growth	6–9	6–7	5–11	5–10	5–9	5–9
NaCl tolerance (%, w/V)	0–1	0	0–3	0–1	0–1	0–2
Enzymatic activity (API 20NE):						
Indole production	–	–	–	w	–	–
Aesculin hydrolysis	w	–	+	+	+	–
β-Galactosidase	+	–	–	w	+	–
Enzymatic activity (API ZYM):						
Valine arylamidase	w	–	–	w	w	+
Cystein arylamidase	–	–	–	–	–	+
Trypsin	–	w	+	+	–	+
α-Chymotrypsin	–	–	–	w	–	–
α-Galactosidase	–	–	–	w	w	–
β-Galactosidase	+	–	–	–	+	+
β-Glucuronidase	–	–	+	–	–	–
α-Glucosidase	–	–	w	–	–	+
β-Glucosidase	+	–	+	+	+	–
Carbon source utilization (API 20NE):						
Glucose	+	–	+	–	–	–
Arabinose	+	–	+	–	+	–
Mannose	–	–	–	–	–	+
Manitol	+	–	–	–	–	+
N-Acetyl-glucosamine	+	–	+	–	–	+
Maltose	+	–	–	–	–	+

Continued

Table 1. Continued

Characteristic	1	2	3	4	5	6
Potassium gluconate	w	–	–	–	–	–
Capric acid	–	–	–	–	–	+
Malic acid	w	–	–	–	–	–

*Data from [10].
†Data from [11].

Table 2. Cellular fatty acid composition (%) of strain R4DWN^T and related type strains

Strains: 1, R4DWN^T; 2, *Sphingomonas fennica* DSM 13665^T; 3, *Sphingomonas formosensis* DSM 24164^T; 4, *Sphingomonas prati* DSM 103336^T; 5, *Sphingomonas montana* DSM 103337^T; 6, *Sphingomonas oleivorans* HAMBI 3659^T. Data from strains 1, 2 and 3 are from this study, whereas data from 4, 5 and 6 are from the original species description papers [27–29]. TR, <1.0%; –, not detected

Fatty acid	1	2	3	4	5	6
Saturated						
$C_{14:0}$	1.6	1.1	5.3	TR	TR	TR
$C_{16:0}$	10.3	15.6	12.6	4.5	7.0	14.6
$C_{17:00}$	–	–	–	–	–	1.1
$C_{18:0}$	–	–	1.1	–	TR	TR
Unsaturated						
$C_{16:1}\omega5c$	1.2	1.1	4.7	1.9	1.3	TR
$C_{17:1}\omega6c$	–	2.8	–	–	TR	14.0
$C_{18:1}\omega7c$ 11-methyl	3.5	1.5	10.3	1.5	3.1	4.0
$C_{18:1}\omega5c$	–	TR	TR	–	1.3	1.0
$C_{18:1}\omega6c$	–	–	–	–	–	43.1
$C_{19:0}$ cyclo $\omega8c$	–	6.9	TR	–	TR	TR
Hydroxy						
$C_{14:0}$ 2OH	12.0	12.5	8.2	14.9	4.5	11.1
$C_{16:0}$ iso 3OH	1.3	1.0	–	–	–	
$C_{15:0}$ 2OH	–	TR	–	–	–	3.2
$C_{16:0}$ 2OH	–	–	–	1.5	–	1.3
$C_{16:1}$ 2OH				–	1.0	–
$C_{18:0}$ 2OH	–	–	–	1.1	–	–
$C_{18:1}$ 2OH				–	1.3	TR
iso-16:0 3-OH	–	–	–	2.3	1.4	–
Summed features*						
3	21.2	14.7	1.3	48.1	36.7	TR
8	48.9	41.3	54.0	21.9	39.2	–

*Summed features represent groups of two or three fatty acids that could not be separated by GLC with the MIDI system. Summed feature 3 contains $C_{16:1}\omega7c/C_{16:1}\omega6c$; and summed feature 8 contains $C_{18:1}\omega7c/C_{18:1}\omega6c$.

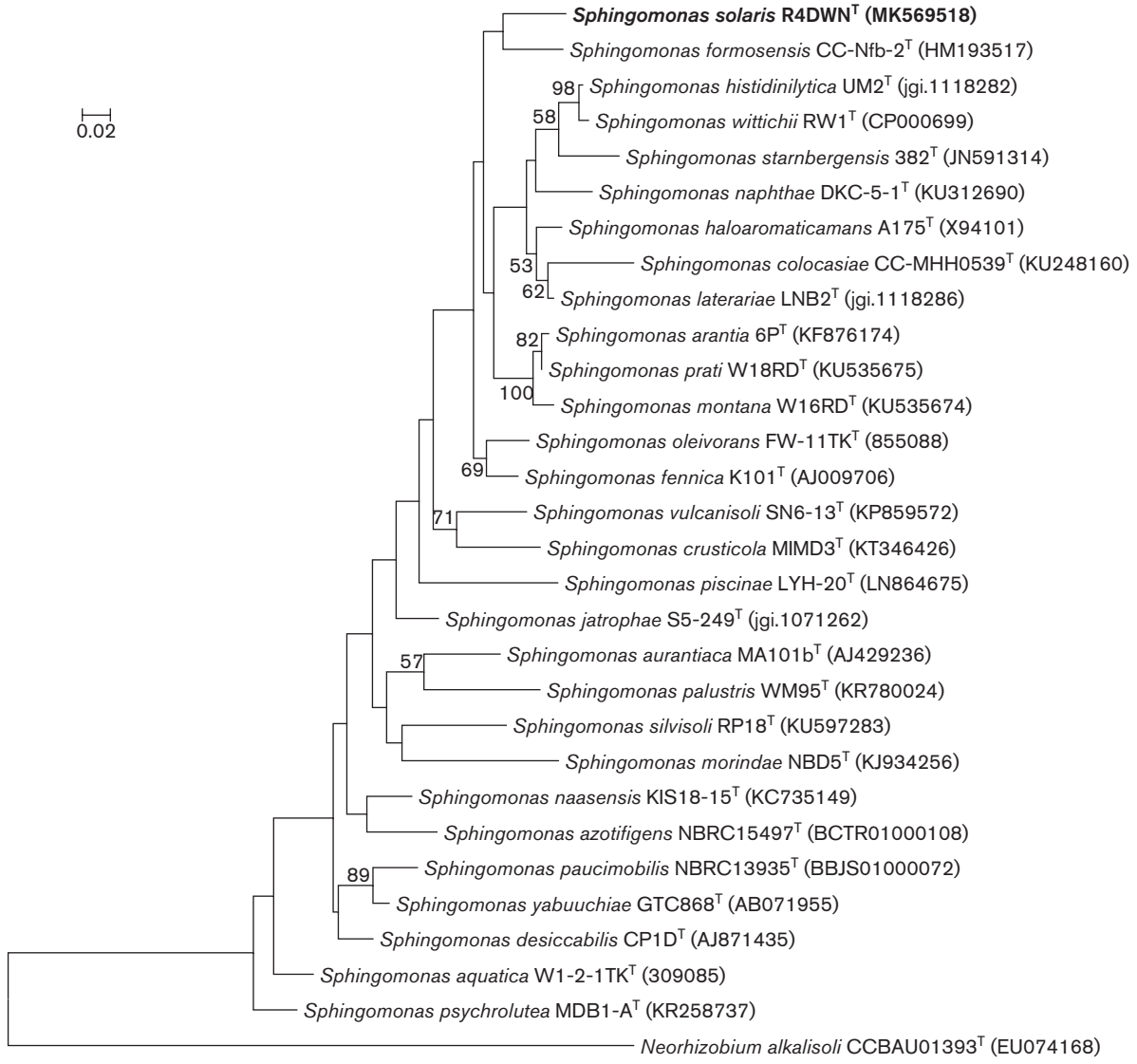

Fig. 1. Maximum-likelihood tree illustrating the phylogenetic position of strain R4DWN^T and related members of the genus *Sphingomonas* based on almost-complete 16S rRNA gene sequences. The optimal evolutionary model of nucleotide substitution applied is GTR. Bar, 0.02 expected nucleotide substitutions per site. *Neorhizobium alkalisoli* was used as an outgroup. Only bootstrap values above 50% are indicated (1000 resamplings) at branchings.

with the bioinformatic tool CheckM v1.0.6 [18], revealing values of 99.095% and 0.603, respectively. Therefore, the draft genome showed enough quality for further analyses [19]. The complete 16S rRNA gene was extracted from this draft genome and, according to the EZBioCloud online tool [4], the closest type strains of R4DWN^T are *S. fennica* K101^T, *S. formosensis* CC-Nfb-2^T, *S. prati* W18RD^T, *S. montana* W16RD^T and *S. oleivorans* FW-11^T with 96.3, 96.1, 96.0, 95.9 and 95.7% pairwise similarity, respectively. Taking into account that the similarity between R4DWN^T and the closest type strain (*S. fennica*) is lower than 98.7 %, this isolate can be considered a new species [19, 20].

With the purposes of obtaining a more accurate phylogenetic inference of strain R4DWN^T, a phylogenomic tree based on nucleotide sequences was generated. The UBCG version 3.0 pipeline (up-to-date bacterial core gene set) [21] was used to reconstruct an ML tree based on a multiple alignment of a set of 92 universal and single copy gene sequences with the tool FastTree version 2.10.1 (Fig. 2). According to the phylogenomic tree, the closest neighbour to R4DWN^T is *S. montana*, and this is supported by high bootstrap values. *S. fennica* and *S. olveirans,* two of the closest neighbours according to the 16S rRNA gene sequence, have an external position with regards to the clade formed by *S. montana* and R4DWN^T, along with other species.

In order to investigate if our isolate belongs to a known species, pairwise average nucleotide identity values (ANIb) [22] were calculated between strain R4DWN^T and its closest

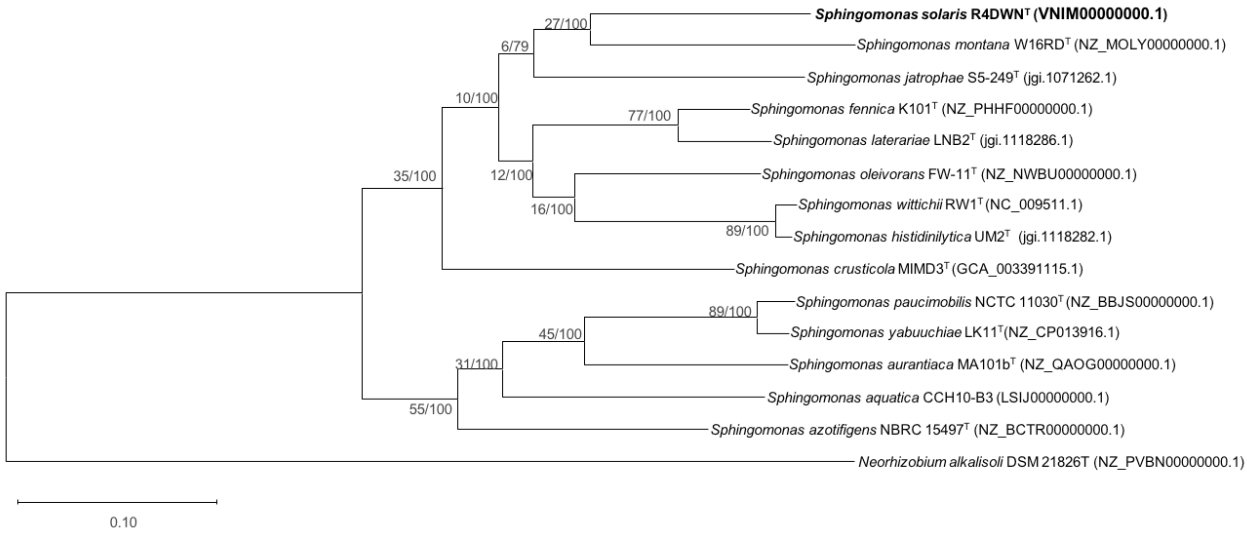

Fig. 2. Phylogenomic tree of strain R4DWN^T. Unrooted maximum-likelihood phylogenetic tree based on a multiple alignment of a set of 92 gene sequences (concatenation of 85764 nucleotides) from using the UBCG version 3.0 pipeline [21]. Bootstrap analysis was carried out using 100 replications. Gene support indices (max. value 92 genes) and percentage bootstrap values (max. value 100%) are given at branching points. Bar, 0.10 substitutions per position.

type strains, by using the JSpeciesWS online tool [23]. Additionally, digital DNA–DNA hybridization (dDDH) pairwise values were also obtained using the Genome-to-Genome Distance Calculator 2.1 (GGDC) tool [24]. As recommended for incompletely sequenced genomes, formula 2 was used for calculating the dDDH values [24]. The ANI and dDDH values between strain R4DWN^T and the type strains of phylogenetically close species were higher than the threshold established to circumscribe prokaryotic species (Table S2), namely 95% for ANI values [25] and 70% for dDDH [24]. Therefore, both genome-related indexes [26] confirmed the adscription of strain R4DWN^T to a hitherto unknown species.

Analysis of the draft genome of strain R4DWN^T allowed to predict its ability to synthesize phosphatidylethanolamine, diphosphatidilglycerol, phosphatidylglycerol, phosphatidylglycerolphosphate and a sphingolipid, due to the presence of genes coding for phosphatidylserine decarboxylase [EC 4.1.1.65], cardiolipin synthase A/B [EC:2.7.8.-], ribosomal-protein-serine acetyltransferase [EC 2.3.1.-], CDP-diacylglycerol-glycerol-3-phosphate 3-phosphatidyltransferase [EC 2.7.8.5] and serine palmitoyl transferase [EC 2.3.1.50]. This polar lipids profile is in agreement with the polar lipid analyses available for other species of the genus *Sphingomonas* with validly published names [10, 11]. As described previously in *S. fennica* [10], strain R4DWN^T is not able to synthesize phosphatidylcholine due to the absence of phosphatidylcholine synthase [EC 2.7.8.24], a unique feature of these closely related strains. Furthermore, spermidine synthase [EC 2.5.1.16] was detected in the draft genome of strain R4DWN^T, suggesting that this strain could produce spermidine as the major polyamine. On the other hand, no genes related to homospermidine synthesis were detected. Strain R4DWN^T has all the enzymatic repertory, including the enzymes 2-methoxy-6-poly prenyl-1,4-benzoquinol methylase [EC 2.1.1.201], ubiquinone biosynthesis monooxygenase Coq6 [EC 1.14.13.-] and 3-demethylubiquinol 3-O-methyltransferase [EC 2.1.1.64], to synthetize ubiquinones as the main isoprenoid quinone.

The comparison of the phenotypic, genomic and phylogenetic characteristics of strain R4DWN^T with those of its closes phylogenetic neighbours revealed that this strain represents a new species belonging to the genus *Sphingomonas* for which the name of *Sphingomonas solaris* sp. nov. is proposed.

DESCRIPTION OF *SPHINGOMONAS SOLARIS* SP. NOV.

Sphingomonas solaris (so.la.ris. N.L. fem. adj. *solaris*, pertaining to the sun, referring to the origin of the type strain, isolated from the surface of solar panels).

Cells are Gram-negative, non-motile and rod-shaped (1.2–4.5 µm long × 1.2 µm wide). In old cultures, some cells grow in the form of a long rod shape of approximately 30 µm. After 7 days of incubation at 25 °C, colonies are round-shaped, shiny, orange-coloured, convex and 1 mm in diameter. This species is able to grow between 4 and 25 °C (optimum, 15–25 °C), and tolerates up to 1% NaCl (w/v), with optimum at 0% NaCl (w/v). The pH for optimum growth ranges between 6 and 9, and oxidase and catalase tests were

positive. Alkaline phosphatase, esterase (C4), esterase lipase (C8), leucine arylamidase, valine arylamidase, acid phosphatase, naphthol-AS-BI-phosphohydrolase, β-galactosidase and β-glucosidase activities are detected, whereas lipase (C14), cystine arylamidase, trypsin, α-chymotrypsin, α-galactosidase, β-glucuronidase, α-glucosidase, *N*-acetyl-beta-glucosaminidase, α-mannosidase and α-fucosidase activities are not detected. Using API 20NE test kit, this species is positive for the assimilation of glucose, arabinose, mannitol, *N*-acetyl-glucosamine and maltose; weak for the assimilation of potassium gluconate and malic acid; and negative for the assimilation of mannose, capric acid, adipic acid, trisodium citrate and phenylacetic acid. Using Biolog GENIII MicroPlates, this species is positive for the utilization of glucuronamide, acetoacetic acid, D-fructose-6-PO4 and L-malic acid; weakly positive for the utilization of L-galactonic acid lactone, β-hydroxy-D,L-butyric acid and D-glucose-6-PO4; and negative for the utilization of raffinose, α-D-glucose, D-sorbitol, gelatin, pectin, *p*-hydroxy-phenylacetic acid, Tween 40, dextrin, lactose, D-mannose, D-mannitol, glycyl-L-proline, D-galacturonic acid, methyl pyruvate, γ-amino-butyric acid, maltose, melibiose, D-fructose, D-arabitol, L-alanine, D-lactic acid methyl ester, α-hydroxy-butyric acid, trehalose, methyl β-D-glucoside, D-galactose, myo-inositol, L-arginine, D-gluconic acid, L-lactic acid, cellobiose, D-salicin, 3-methyl glucose, glycerol, L-aspartic acid, D-glucuronic acid, citric acid, α-keto-butyric acid, gentiobiose, *N*-acetyl-D-glucosamine, D-fucose, L-glutamic acid, α-keto-glutaric acid, sucrose, *N*-acetyl-β-D-mannosamine, L-fucose, L-histidine, mucic acid, D-malic acid, propionic acid, turanose, *N*-acetyl-D-galactosamine, L-rhamnose, D-aspartic acid, L-pyroglutamic acid, quinic acid, acetic acid, stachyose, *N*-acetyl neuraminic acid, inosine, D-serine, L-serine, D-saccharic acid, bromo-succinic acid and formic acid. The major fatty acids are $C_{18:1}\omega7c$/$C_{18:1}\omega6c$, $C_{16:1}\omega7c$/$C_{16:1}\omega6c$, $C_{14:0}$ 2OH and $C_{16:0}$. The type strain is R4DWN^T (=CECT 9811^T=LMG 31344^T), isolated from the surface of a solar panel in Boston, MA, USA. The genomic G+C content of the type strain is 67.9mol%.

Funding information
Financial support from the Real Colegio Complutense at Harvard University (Visiting Research Fellowship) is acknowledged. Kristie Tanner is a recipient of a Doctorado Industrial fellowship from the Ministerio de Ciencia, Innovación y Universidades (Spain), with reference DI-16-08976. Financial support from Spanish Government (grant Helios. reference: BIO2015-66960-C3-1-R co-financed by FEDER funds and Ministerio de Economía y Competitividad) is acknowledged. Financial support from the European CSA on biological standardization BIOROBOOST (EU grant number 820699, http://standardsinsynbio.eu) is acknowledged. This work was supported by DARPA BRICS grants HR0011-15-C-0091 and HR0011-18-2-0014 (to A.S.K.) and IARPA FELIX grant N66001-18-C-4503 (to A.S.K.). A.S.K. also acknowledges funding from the NIH Director's New Innovator Award (1DP2AI131083-01) and an NSF CAREER Award (MCB-1350949).

Acknowledgements
We acknowledge the Arnold Arboretum of Harvard University for providing access to the solar panels sampled in this project. We thank Manuel Porcar for his help in writing this manuscript and his continuous support throughout this project.

Conflicts of interest
The authors declare that there are no conflicts of interest.

References

1. Yabuuchi E, Yano I, Oyaizu H, Hashimoto Y, Ezaki T *et al*. Proposals of *Sphingomonas paucimobilis* gen. nov. and comb. nov., *Sphingomonas parapaucimobilis* sp. nov., *Sphingomonas yanoikuyae* sp. nov., *Sphingomonas adhaesiva* sp. nov., *Sphingomonas capsulata* comb. nov., and two genospecies of the genus *Sphingomonas*. *Microbiol Immunol* 1990;34:99–119.
2. Takeuchi M, Sawada H, Oyaizu H, Yokota A. Phylogenetic evidence for *Sphingomonas* and *Rhizomonas* as nonphotosynthetic members of the alpha-4 subclass of the Proteobacteria. *Int J Syst Bacteriol* 1994;44:308–314.
3. White DC, Sutton SD, Ringelberg DB. The genus *Sphingomonas*: physiology and ecology. *Curr Opin Biotechnol* 1996;7:301–306.
4. Yoon S-H, Ha S-M, Kwon S, Lim J, Kim Y *et al*. Introducing EzBioCloud: a taxonomically United database of 16S rRNA gene sequences and whole-genome assemblies. *Int J Syst Evol Microbiol* 2017;67:1613–1617.
5. Zhao Q, Yue S, Bilal M, Hu H, Wang W *et al*. Comparative genomic analysis of 26 *Sphingomonas* and *Sphingobium* strains: Dissemination of bioremediation capabilities, biodegradation potential and horizontal gene transfer. *Sci Total Environ* 2017;609:1238–1247.
6. Fujiwara H, Soda S, Fujita M, Ike M. Kinetics of bisphenol A degradation by *Sphingomonas paucimobilis* FJ-4. *J Biosci Bioeng* 2016;122:341–344.
7. Gatheru Waigi M, Sun K, Gao Y. Sphingomonads in microbe-assisted phytoremediation: tackling soil pollution. *Trends Biotechnol* 2017;35:883–899.
8. Sasser M. *Identification of Bacteria by Gas Chromatography of Cellular Fatty Acids*, MIDI Technical Note 101. Newark: DE: MIDI Inc; 1990.
9. MIDI. *Sherlock Microbial Identification System Operating Manual*, version 6.1. Newark, DE: MIDI Inc; 2008.
10. Wittich R-M, Busse H-J, Kämpfer P, Macedo AJ, Tiirola M *et al*. *Sphingomonas fennica* sp. nov. and *Sphingomonas haloaromaticamans* sp. nov., outliers of the genus *Sphingomonas*. *Int J Syst Evol Microbiol* 2007;57:1740–1746.
11. Lin S-Y, Shen F-T, Lai W-A, Zhu Z-L, Chen W-M *et al*. *Sphingomonas formosensis* sp. nov., a polycyclic aromatic hydrocarbon-degrading bacterium isolated from agricultural soil. *Int J Syst Evol Microbiol* 2012;62:1581–1586.
12. Latorre A, Moya A, Ayala FJ. Evolution of mitochondrial DNA in *Drosophila subobscura*. *Proc Natl Acad Sci USA* 1986;83:8649–8653.
13. Pascual J, Wüst PK, Geppert A, Foesel BU, Huber KJ *et al*. Novel isolates double the number of chemotrophic species and allow the first description of higher taxa in Acidobacteria subdivision 4. *Syst Appl Microbiol* 2015;38:534–544.
14. Pruesse E, Peplies J, Glöckner FO. Sina: accurate high-throughput multiple sequence alignment of ribosomal RNA genes. *Bioinformatics* 2012;28:1823–1829.
15. Kozlov AM, Darriba D, Flouri T, Morel B, Stamatakis A. RAxML-NG: a fast, scalable, and user-friendly tool for maximum likelihood phylogenetic inference. *bioRxiv*2018.
16. Tamura K, Stecher G, Peterson D, Filipski A, Kumar S. MEGA6: molecular evolutionary genetics analysis version 6.0. *Mol Biol Evol* 2013;30:2725–2729.
17. Nurk S, Bankevich A, Antipov D, Gurevich A, Korobeynikov A *et al*. Assembling genomes and mini-metagenomes from highly chimeric reads. *Annual International Conference on Research in Computational Molecular Biology*. Berlin, Heidelberg: Springer; 2013. pp. 158–170.
18. Parks DH, Imelfort M, Skennerton CT, Hugenholtz P, Tyson GW. CheckM: assessing the quality of microbial genomes recovered from isolates, single cells, and metagenomes. *Genome Res* 2015;25:1043–1055.

19. Chun J, Oren A, Ventosa A, Christensen H, Arahal DR *et al*. Proposed minimal standards for the use of genome data for the taxonomy of prokaryotes. *Int J Syst Evol Microbiol* 2018;68:461–466.
20. Kim M, Oh H-S, Park S-C, Chun J. Towards a taxonomic coherence between average nucleotide identity and 16S rRNA gene sequence similarity for species demarcation of prokaryotes. *Int J Syst Evol Microbiol* 2014;64:346–351.
21. Na S-I, Kim YO, Yoon S-H, Ha S-M, Baek I *et al*. UBCG: up-to-date bacterial core gene set and pipeline for phylogenomic tree reconstruction. *J Microbiol* 2018;56:280–285.
22. Goris J, Konstantinidis KT, Klappenbach JA, Coenye T, Vandamme P *et al*. DNA-DNA hybridization values and their relationship to whole-genome sequence similarities. *Int J Syst Evol Microbiol* 2007;57:81–91.
23. Richter M, Rosselló-Mora R, Glöckner FO, Peplies J. JSpeciesWS: a web server for prokaryotic species circumscription based on pairwise genome comparison. *Bioinformatics* 2015:pii: btv681.
24. Meier-Kolthoff JP, Auch AF, Klenk H-P, Göker M. Genome sequence-based species delimitation with confidence intervals and improved distance functions. *BMC Bioinformatics* 2013;14:60.
25. Richter M, Rosselló-Móra R. Shifting the genomic gold standard for the prokaryotic species definition. *Proc Natl Acad Sci U S A* 2009;106:19126–19131.
26. Chun J, Rainey FA. Integrating genomics into the taxonomy and systematics of the bacteria and archaea. *Int J Syst Evol Microbiol* 2014;64:316–324.
27. Manandhar P, Zhang G, Hu Y, Lama A, Gao F *et al*. *Sphingomonas prati* sp. nov., isolated from alpine meadow soil. *Int J Syst Evol Microbiol* 2016;66:4269–4275.
28. Manandhar P, Zhang G, Lama A, Liu F, Hu Y. *Sphingomonas montana* sp. nov., isolated from a soil sample from the Tanggula mountain in the Qinghai Tibetan Plateau. *Antonie van Leeuwenhoek* 2017;110:1659–1668.
29. Chen L, Chen W-F, Xu Z-L, Li W, Zhang X-Y *et al*. *Sphingomonas oleivorans* sp. nov., isolated from oil-contaminated soil. *Int J Syst Evol Microbiol* 2018;68:3720–3725.

Five reasons to publish your next article with a Microbiology Society journal

1. The Microbiology Society is a not-for-profit organization.
2. We offer fast and rigorous peer review – average time to first decision is 4–6 weeks.
3. Our journals have a global readership with subscriptions held in research institutions around the world.
4. 80% of our authors rate our submission process as 'excellent' or 'very good'.
5. Your article will be published on an interactive journal platform with advanced metrics.

Find out more and submit your article at microbiologyresearch.org.

Appendix B

Supplementary tables and figures

Publication III

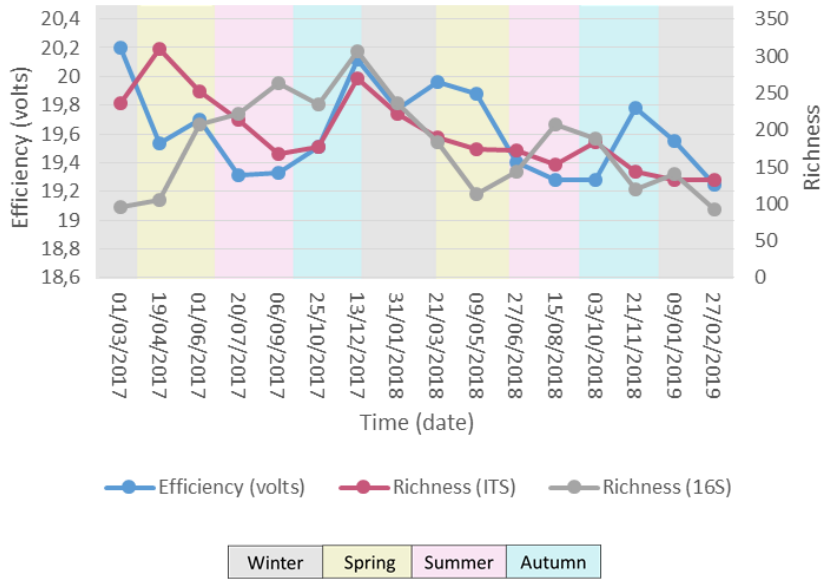

Supplementary Figure III.1. Solar panel efficiency measurements (blue dots) are shown and compared to the Richness at genus level of the detected 16S (grey dots) and ITS (pink dots) sequences (these measurements correspond to days in which samples were taken from the surface for genomic analysis). Seasons in which each sampling was performed are indicated in grey (winter), green (spring), pink (summer) and blue (autumn).

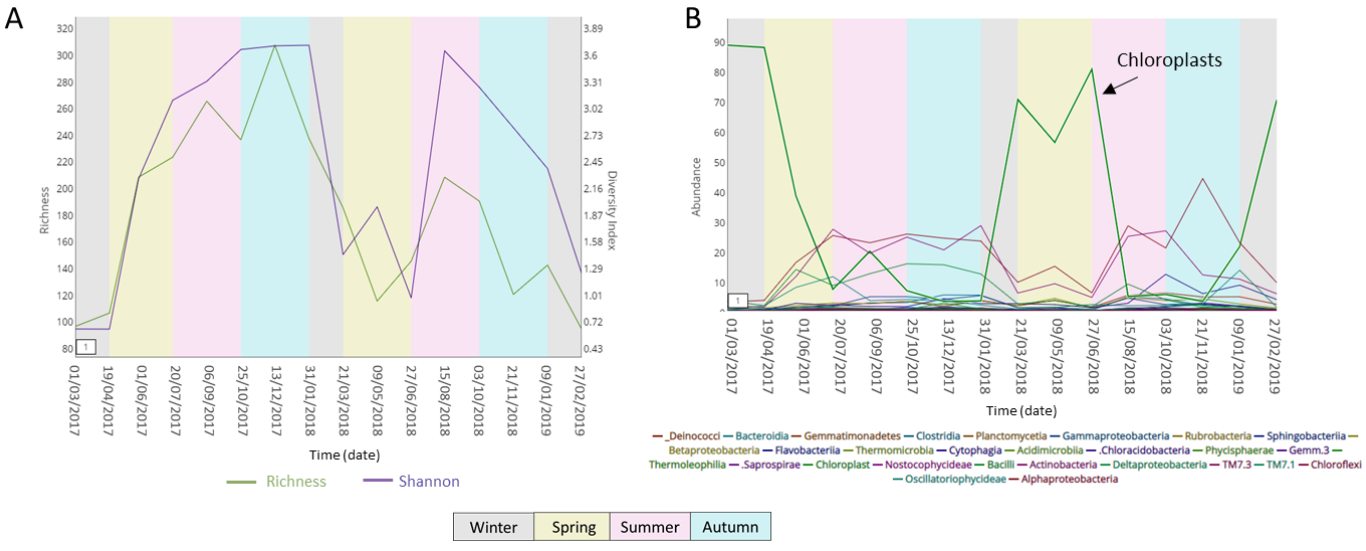

Supplementary Figure III.2. (A) Y-axes indicates bacterial Richness (green) and Shannon diversity index (purple) at genus level throughout time. (B) Taxonomic distribution of bacteria in time at class level. Seasons in which each sampling was performed are indicated in grey (winter), green (spring), pink (summer) and blue (autumn).

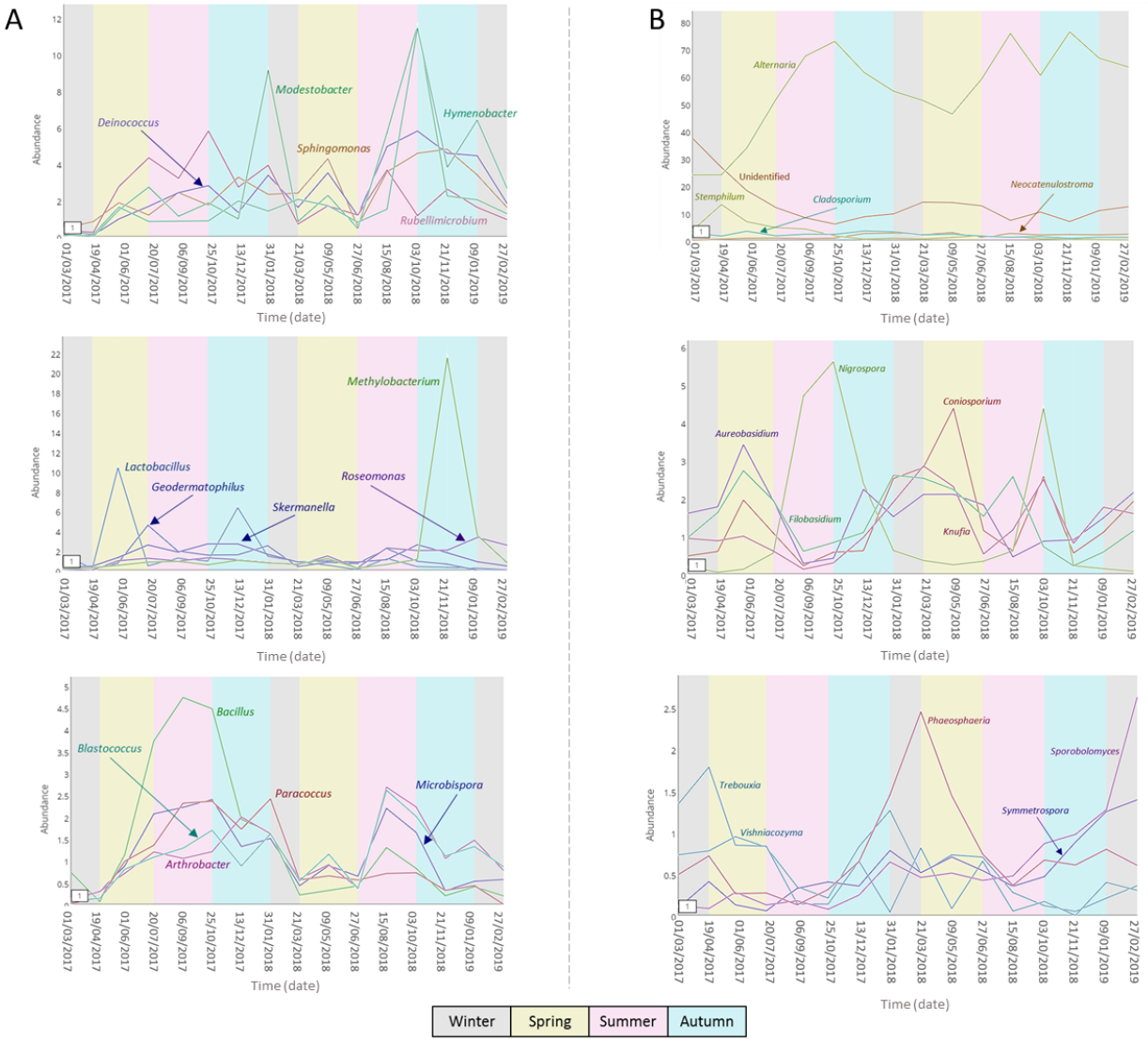

Supplementary Figure III.3. Variation in % of abundance throughout time of the 15 bacterial (A) and fungal (B) genera with highest mean abundance. Graphs are separated for 5 genera at a time to facilitate visualization of the data, and are ordered from more abundant (top) to less abundant (bottom). Seasons in which each sampling was performed are indicated in grey (winter), green (spring), pink (summer) and blue (autumn).

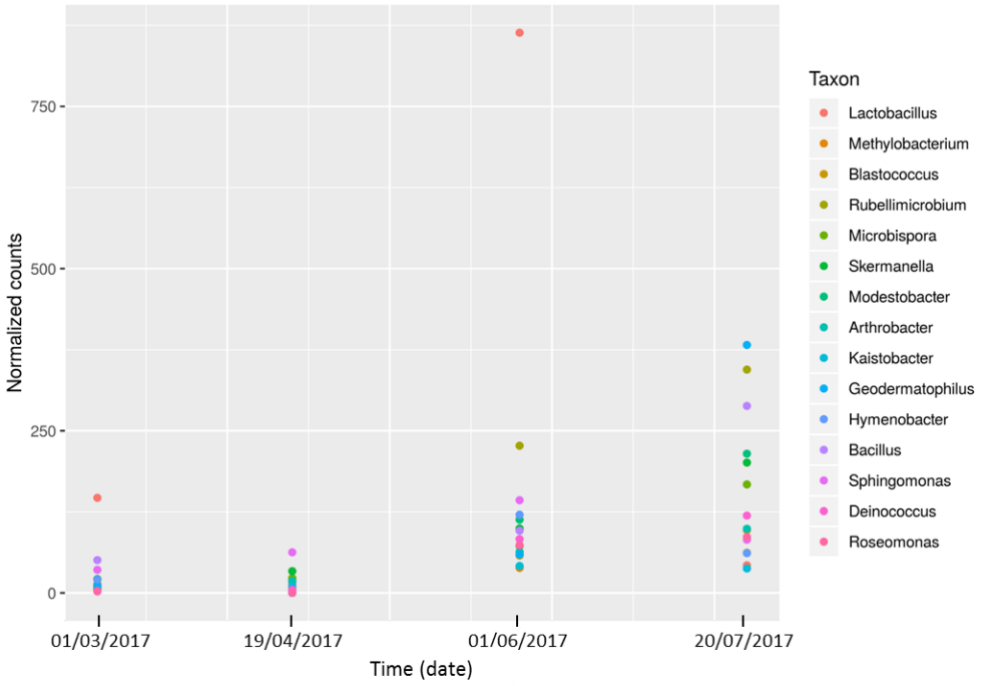

Supplementary Figure III.4. Close up of the most abundant genera in the first 21 weeks of sampling.

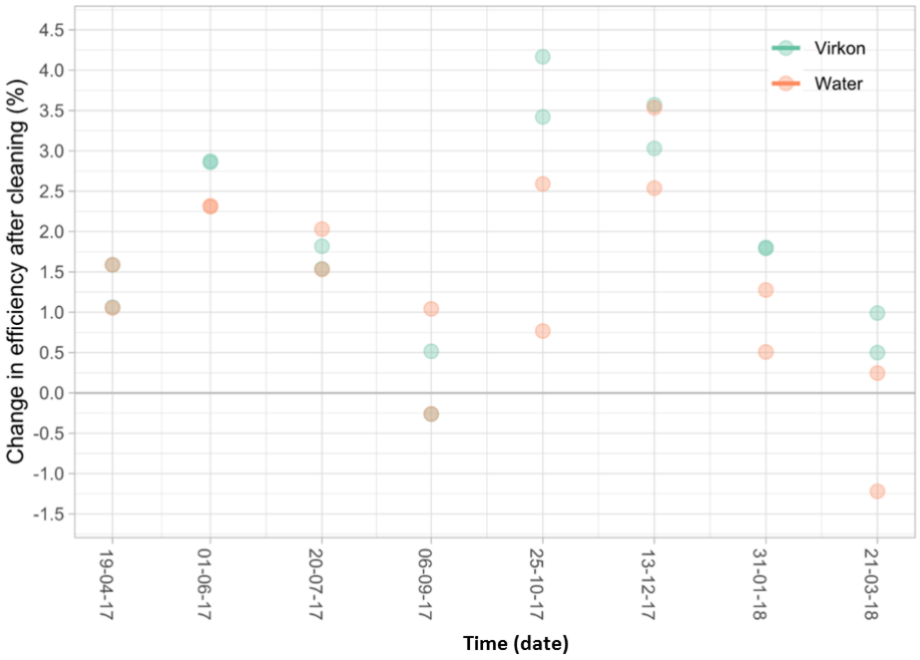

Supplementary Figure III.5. Change in open voltage (% of increase or decrease) after cleaning with Virkon or water. Values are shown for the two replicates of each conditions (blue dots for plates treated with Virkon and orange dots for plates treated with water).

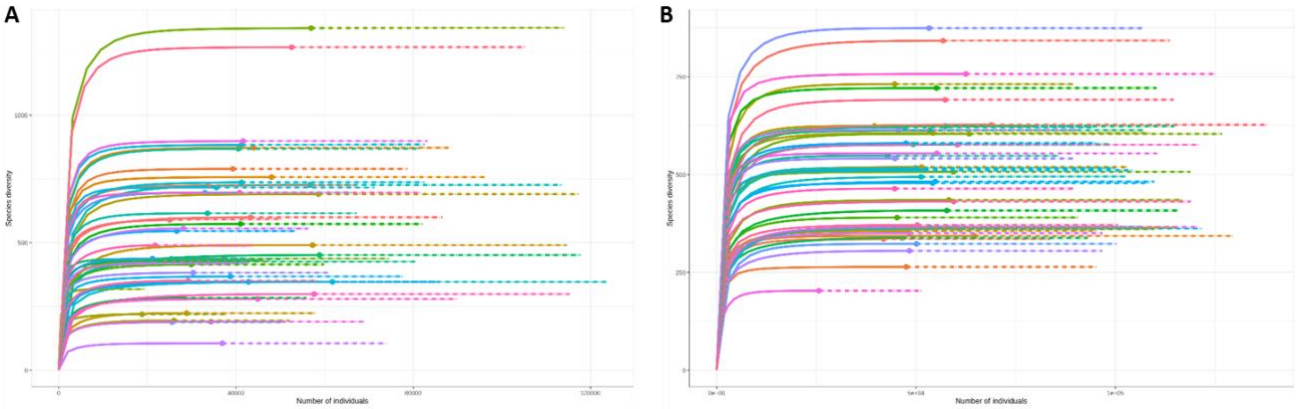

Supplementary Figure III.6. Rarefaction curves for sequences corresponding to the 16S gene (A) and ITS region (B).

Publication IV

Supplementary Table IV.1. Collection of identified bacterial isolates from solar panel surfaces. The GenBank/EMBL/DDBJ accession numbers for the partial 16S rDNA sequence of each strain is indicated, as well as the taxonomic affiliation, the closest neighbor with valid name (species, strain and accession number) and the % of similarity. Potential new species (<98.65 % similarity threshold of the 16S rRNA gene) are in bold.

Strain	Genbank accession number	Taxonomic affiliation	Closest neighbour (accession number)	% similarity
PS1	**MK621939**	***Firmicutes;Bacilli;Bacillales;Planococcaceae;Planococcus***	***Planomicrobium glaciei* 423 (EU036220)**	**97.38**
PS2	MK621940	*Actinobacteria;Actinobacteria_c;Micrococcales;Micrococcaceae;Arthrobacter*	*Arthrobacter gandavensis* R 5812 (AJ316140)	100
PS4	MK621941	*Proteobacteria;Gammaproteobacteria;Enterobacterales;Erwiniaceae;Pantoea*	*Pantoea septica* LMG 5345 (MLJJ01000077)	99.69
PS5	**MK621942**	***Actinobacteria;Actinobacteria_c;Micrococcales;Microbacteriaceae;Curtobacterium***	***Curtobacterium herbarum* P 420/07 (AJ310413)**	**98.61**
PS6	MK621943	*Actinobacteria;Actinobacteria_c;Micrococcales;Microbacteriaceae;Curtobacterium*	*Curtobacterium citreum* DSM 20528 (X77436)	99.06
PS7	**MK621944**	***Actinobacteria;Actinobacteria_c;Micrococcales;Microbacteriaceae;Curtobacterium***	***Curtobacterium herbarum* P 420/07 (AJ310413)**	**98.59**
PS8	MK621945	*Actinobacteria;Actinobacteria_c;Micrococcales;Microbacteriaceae;Frigoribacterium*	*Frigoribacterium endophyticum* EGI 6500707 (KM114212)	99.73
PS9	MK621946	*Actinobacteria;Actinobacteria_c;Micrococcales;Micrococcaceae;Kocuria*	*Kocuria rosea* DSM 20447 (X87756)	99.75
PS10	MK621947	*Actinobacteria;Actinobacteria_c;Micrococcales;Micrococcaceae;Glutamicibacter*	*Glutamicibacter arilaitensis* Re117 (FQ311875)	100
PS13	MK621948	*Actinobacteria;Actinobacteria_c;Micrococcales;Jonesiaceae;Sanguibacter*	*Sanguibacter inulinus* ST50 (X79451)	100
PS14	MK621949	*Actinobacteria;Actinobacteria_c;Micrococcales;Micrococcaceae;Kocuria*	*Kocuria rosea* DSM 20447 (X87756)	99.53
PS16	MK621950	*Actinobacteria;Actinobacteria_c;Micrococcales;Micrococcaceae;Kocuria*	*Kocuria rosea* DSM 20447 (X87756)	99.77
PS17	**MK621951**	***Actinobacteria;Actinobacteria_c;Micrococcales;Micrococcaceae;Arthrobacter***	***Arthrobacter pityocampae* Tp2 (EU855749)**	**97.77**
PS19	MK621952	*Actinobacteria;Actinobacteria_c;Micrococcales;Jonesiaceae;Sanguibacter*	*Sanguibacter inulinus* ST50 (X79451)	100
PS20	**MK621953**	***Actinobacteria;Actinobacteria_c;Micrococcales;Microbacteriaceae;Curtobacterium***	***Curtobacterium herbarum P 420/07 (AJ310413)***	**98.37**
PS21	MK621954	*Proteobacteria;Alphaproteobacteria;Rhodobacterales;Rhodobacteraceae;Rhodobacter*	*Rhodobacter maris* JA276 (AM745438)	98.89
PS22	MK621955	*Actinobacteria;Actinobacteria_c;Micrococcales;Microbacteriaceae;Curtobacterium*	*Curtobacterium flaccumfaciens*LMG 3645 (AJ312209)	99.08
PS27	MK621956	*Actinobacteria;Actinobacteria_c;Micrococcales;Microbacteriaceae;Microbacterium*	Microbacterium imperiale DSM 20530 (X77442)	100
PS28	MK621957	*Actinobacteria;Actinobacteria_c;Micrococcales;Micrococcaceae;Kocuria*	*Kocuria rosea* DSM 20447 (X87756)	99.77
PS29	MK621958	*Actinobacteria;Actinobacteria_c;Micrococcales;Micrococcaceae;Kocuria*	*Kocuria rosea* DSM 20447 (X87756)	99.77
PS30	MK621959	*Actinobacteria;Actinobacteria_c;Micrococcales;Micrococcaceae;Arthrobacter*	*Arthrobacter agilis* DSM 20550 (X80748)	99.26
PS31	MK621960	*Actinobacteria;Actinobacteria_c;Micrococcales;Micrococcaceae;Kocuria*	*Kocuria rosea* DSM 20447 (X87756)	99.77
PS33	MK621961	*Proteobacteria;Alphaproteobacteria;Rhodobacterales;Rhodobacteraceae;Paracoccus*	*Paracoccus marcusii* DSM 11574 (Y12703)	99.73
PS35	MK621962	*Actinobacteria;Actinobacteria_c;Micrococcales;Microbacteriaceae;Curtobacterium*	*Curtobacterium flaccumfaciens* LMG 3645 (AJ312209)	99.77
PS36	**MK621963**	***Actinobacteria;Actinobacteria_c;Micrococcales;Microbacteriaceae;Curtobacterium***	***Curtobacterium herbarum* P 420/07 (AJ310413)**	**97.9**

PS37	MK621964	*Actinobacteria;Actinobacteria_c;Micrococcales;Microbacteriaceae;Pseudoclavibacter*	*Pseudoclavibacter terrae* THG-MD12 (KJ769174)	99.74
PS38	MK621965	*Actinobacteria;Actinobacteria_c;Micrococcales;Microbacteriaceae;Microbacterium*	*Microbacterium yannicii* G72 (FN547412)	99.33
PS39	MK621966	*Actinobacteria;Actinobacteria_c;Micrococcales;Micrococcaceae;Arthrobacter*	*Arthrobacter agilis* DSM 20550 (X80748)	99.22
PS40	MK621967	*Actinobacteria;Actinobacteria_c;Micrococcales;Microbacteriaceae;Microbacterium*	*Microbacterium imperiale* DSM 20530 (X77442)	99.32
PS41	MK621968	*Actinobacteria;Actinobacteria_c;Micrococcales;Microbacteriaceae;Microbacterium*	*Microbacterium arborescens* DSM 20754 (X77443)	99.5
PS42	MK621969	*Actinobacteria;Actinobacteria_c;Micrococcales;Microbacteriaceae;Microbacterium*	*Microbacterium oleivorans* NBRC 103075 (BCRG01000019)	100
PS43	**MK621970**	***Actinobacteria;Actinobacteria_c;Micrococcales;Microbacteriaceae;Plantibacter***	***Plantibacter flavus* VKM Ac-2504 (jgi.1118344)**	**98.45**
PS44	MK621971	*Actinobacteria;Actinobacteria_c;Micrococcales;Microbacteriaceae;Microbacterium*	*Microbacterium foliorum* DSM12966 (JYIU01000006)	99.44
PS46	MK621972	*Actinobacteria;Actinobacteria_c;Micrococcales;Micrococcaceae;Kocuria*	*Kocuria rosea* DSM 20447 (X87756)	99.75
PS47	**MK621973**	***Actinobacteria;Actinobacteria_c;Micrococcales;Micrococcaceae;Arthrobacter***	***Arthrobacter subterraneus* CH7 (DQ097525)**	**97.95**
PS48	MK621974	*Proteobacteria;Gammaproteobacteria;Pseudomonadales;Pseudomonadaceae;Pseudomonas*	*Pseudomonas flavescens* LMG 18387 (FNDG01000047)	99.35
PS52	MK621975	*Actinobacteria;Actinobacteria_c;Micrococcales;Micrococcaceae;Arthrobacter*	*Arthrobacter ruber* MDB1-42 (JX949648)	98.71
PS53	**MK621976**	***Bacteroidetes;Cytophagia;Cytophagales;Hymenobacteraceae;Pontibacter***	***Pontibacter saemangeumensis* GCM0142 (JN607163)**	**98.2**
PS54	MK621977	*Proteobacteria;Alphaproteobacteria;Sphingomonadales;Sphingomonadaceae;Sphingomonas*	*Sphingomonas phyllosphaerae* FA2 (KE386571)	100
PS55	MK621978	*Actinobacteria;Actinobacteria_c;Micrococcales;Micrococcaceae;Kocuria*	*Kocuria rosea* DSM 20447 (X87756)	99.56
PS56	MK621979	*Actinobacteria;Actinobacteria_c;Micrococcales;Micrococcaceae;Kocuria*	*Kocuria rosea* DSM 20447 (X87756)	99.77
PS57	MK621980	*Proteobacteria;Alphaproteobacteria;Sphingomonadales;Sphingomonadaceae;Sphingomonas*	*Sphingomonas aerolata* NW12 (AJ429240)	99.76
PS58	**MK621981**	***Actinobacteria;Actinobacteria_c;Micrococcales;Microbacteriaceae;Microbacterium***	***Microbacterium terregens* IFO 12961 (AB004721)**	**97.47**
PS59	MK621982	*Actinobacteria;Actinobacteria_c;Micrococcales;Microbacteriaceae;Microbacterium*	*Microbacterium radiodurans* GIMN1.002 (GQ329713)	100
PS60	MK621983	*Proteobacteria;Alphaproteobacteria;Sphingomonadales;Sphingomonadaceae;Sphingomonas*	*Sphingomonas aerolata* NW12 (AJ429240)	100
PS62	MK621984	*Actinobacteria;Actinobacteria_c;Micrococcales;Promicromonosporaceae;Cellulosimicrobium*	*Cellulosimicrobium cellulans* LMG 16121 (CAOI01000359)	100
PS63	MK621985	*Actinobacteria;Actinobacteria_c;Micrococcales;Micrococcaceae;Arthrobacter*	*Arthrobacter agilis* DSM 20550 (X80748)	98.87
PS64	MK621986	*Proteobacteria;Alphaproteobacteria;Sphingomonadales;Sphingomonadaceae;Sphingomonas*	*Sphingomonas endophytica* YIM 65583 (HM629444)	99.75
PS65	**MK621987**	***Bacteroidetes;Sphingobacteriia;Sphingobacteriales;Sphingobacteriaceae;Pedobacter***	***Pedobacter agri* PB92 (AJLG01000244)**	**98.23**
PS66	MK621988	*Actinobacteria;Actinobacteria_c;Micrococcales;Microbacteriaceae;Agrococcus*	*Agrococcus citreus* IAM 15145 (AB279547)	99.7
PS67	**MK621989**	***Proteobacteria;Alphaproteobacteria;Rhodobacterales;Rhodobacteraceae;Paracoccus***	***Paracoccus aestuarii* B7 (EF660757)**	**97.6**
PS68	MK621990	*Actinobacteria;Actinobacteria_c;Micrococcales;Promicromonosporaceae;Cellulosimicrobium*	*Cellulosimicrobium funkei* LMG 16121 (CAOI01000359)	100
PS69	MK621991	*Actinobacteria;Actinobacteria_c;Micrococcales;Microbacteriaceae;Microbacterium*	*Microbacterium oleivorans* NBRC 103075 (BCRG01000019)	100
PS70	MK621992	*Actinobacteria;Actinobacteria_c;Micrococcales;Micrococcaceae;Kocuria*	*Kocuria rosea* DSM 20447 (X87756)	99.73
PS71	MK621993	*Actinobacteria;Actinobacteria_c;Micrococcales;Microbacteriaceae;Leucobacter*	*Leucobacter chromiiresistens* JG31 (AGCW01000231)	99.04
PS72	MK621994	*Actinobacteria;Actinobacteria_c;Micrococcales;Microbacteriaceae;Curtobacterium*	*Curtobacterium citreum* DSM 20528 (X77436)	99.25
PS74	MK621995	*Actinobacteria;Actinobacteria_c;Micrococcales;Micrococcaceae;Kocuria*	*Kocuria polaris* CMS 76or (JSUH01000031)	99.47

PS75	MK621996	*Firmicutes;Bacilli;Bacillales;Bacillaceae;Bacillus*	*Bacillus megaterium* NBRC 15308 (JJMH01000057)	100
PS76	MK621997	*Firmicutes;Bacilli;Bacillales;Bacillaceae;Bacillus*	*Bacillus endophyticus* 2DT (AF295302)	99.34
PS78	MK621998	*Firmicutes;Bacilli;Bacillales;Bacillaceae;Bacillus*	*Bacillus endophyticus* 2DT (AF295302)	99.13
PS79	MK621999	*Firmicutes;Bacilli;Bacillales;Bacillaceae;Bacillus*	*Bacillus atrophaeus* JCM 9070 (AB021181)	99.58
PS80	MK622000	*Firmicutes;Bacilli;Bacillales;Bacillaceae;Bacillus*	*Bacillus endophyticus* 2DT (AF295302)	99.55
PS81	MK622001	*Firmicutes;Bacilli;Bacillales;Bacillaceae;Bacillus*	*Bacillus megaterium* NBRC 15308 (JJMH01000057)	99.38
PS82	MK622002	*Firmicutes;Bacilli;Bacillales;Bacillaceae;Bacillus*	*Bacillus atrophaeus* JCM 9070 (AB021181)	99.56
PS83	MK622003	*Firmicutes;Bacilli;Bacillales;Bacillaceae;Bacillus*	*Bacillus aryabhattai* B8W22 (EF114313)	99.77
PS84	MK622004	*Actinobacteria;Actinobacteria_c;Micrococcales;Micrococcaceae;Arthrobacter*	*Arthrobacter ruber* MDB1-42 (JX949648)	99.29
PS85	MK622005	*Actinobacteria;Actinobacteria_c;Micrococcales;Micrococcaceae;Kocuria*	*Kocuria rosea* DSM 20447 (X87756)	99.54
PS86	MK622006	*Actinobacteria;Actinobacteria_c;Micrococcales;Micrococcaceae;Arthrobacter*	*Arthrobacter pityocampae* Tp2 (EU855749)	99.38

Supplementary Table IV.2. Carotenoids (CRTs) identified in the solar panel isolates in liquid (L) and solid (S) cultures. Numbers correspond to the chromatographic peaks represented in Supplementary Figure IV.2. Retention times, maximum wavelengths and %III/II (numeric indication of the spectral shape, specifically the relationship between the peak heights of the longest-wavelength absorption band – III – and the middle absorption band – II -, expressed as a percentage) are represented and compared with data from the literature (Britton et al., 1998; Rodrigo et al., 2003). In the final column, quantification is displayed in micrograms of each CRT per gram of cellular pellet (dry pellet in the stationary phase samples and wet pellet in the exponential phase samples). Non-identified CRTs are indicated as "NI"; s, denotes shoulder in the spectrum; *CRTs were tentatively identified (for which a standard was not available).

		Observed			Literature		
Isolate		**Carotenoid**	**λ_{max} (nm)**	**% III/II**	**λ_{max} (nm)**	**% III/II**	**µg/g**
PS1 - L	1	NI-1	440,467,498	17.5	-	-	0,2
	2	Total phytoene	278,285,301	14	276, 286, 297	10	16,9
	3	Total phytofluene	322,346,362	69	331, 348, 367	90	0,3
	4	β-cryptoxanthin	426,453,482	27	428, 450, 478	25	0,02
PS1 - S	5	Total phytoene	278,285,301	15	276, 286, 297	10	197,5
	6	Phytofluene	322,347,364	78	331, 348, 367	90	2,8
	7	NI-2	cis355,s,458,s	-	-	-	9,1
	8	NI-3	cis355,s,458,s	-	-	-	10,6
	9	β-cryptoxanthin	422,454,480	31	428, 450, 478	25	54,8
PS21 - L	10	Adonirubin*	473	-	474	-	6,4
	11	Canthaxanthin	464	-	466	-	12,0
	12	Phytoene	278,285,301	10	276, 286, 297	10	9,4
PS21 - S	13	Astaxanthin*	474	-	474	-	13,4
	14	Adonirubin*	472	-	474	-	11,9
	15	Canthaxanthin	463	-	466	-	63,9
	16	Phytoene	278,285,301	11	276, 286, 297	10	7,8
	17	Echinenone*	466	-	461	-	0,4
	18	β-carotene*	425,452,581	33	425, 450, 477	25	8,9
PS75 - L	19	NI-4	429,454, 475	75	-	-	0,03
	20	NI-5	,429,454,475	71	-	-	0,04
PS75 - S	21	NI-6	378,402,427	134	-	-	0,4
	22	Mix Phytoene-like *;and NI-7	278,285,301; s,363,390	<1	274, 286, 298	<1	mix
	23	NI-8	376,389,422	73		90	0,2
	24	NI-9	373,402,427	86	-	-	2,2
	25	NI-10	378,402,425	100	-	-	1,9
	26	NI-11	380,417,445	87	-	-	0,9
	27	NI-12	391,416,445	126	-	-	0,5

	28	NI-13	394,419,445	67	-	-	2,1
	29	NI-14	cis341,422,446,475	52	-	-	1,3
	30	NI-15	cis343,422,447,476	69	-	-	0,6
	31	NI-16	423,447,477	76	-	-	0,7
	32	NI-17	443,453,484	81	-	-	12,6

Supplementary Figure IV.1. HPLC chromatograms of the pigments extracted from the solar panel isolates grown in liquid and solid medium. Above, the MaxPlot chromatogram is represented, and the peaks of interest are numbered in accordance with the carotenoids described in Table IV.1. Spectra of peak of interests are represented below the MaxPlot chromatogram. **(A)** PS1 in liquid medium. **(B)** PS1 in solid medium. **(C)** PS21 in liquid medium. **(D)** PS21 in solid medium. **(E)** PS75 in liquid medium. **(F)** PS75 in solid medium.

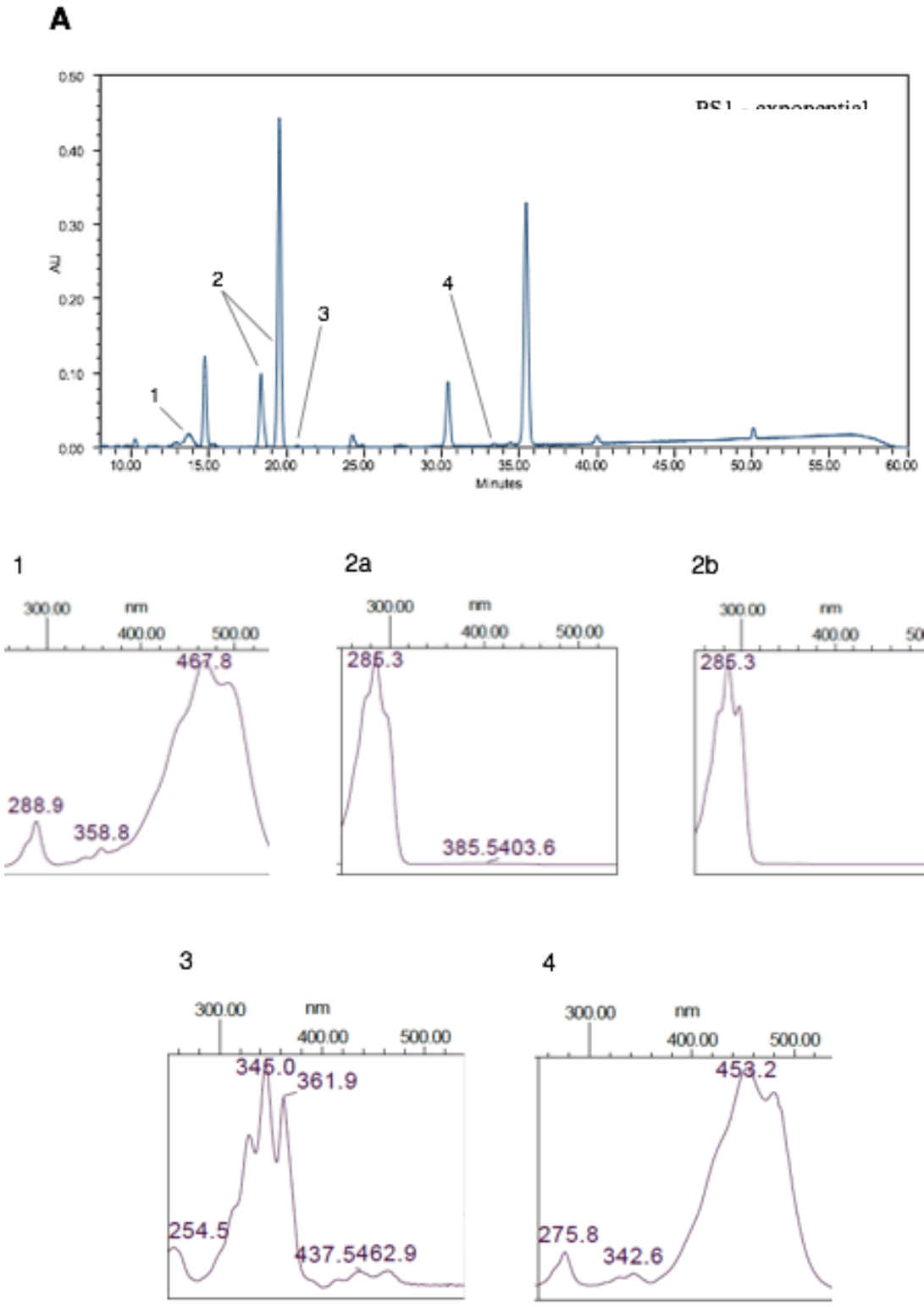

B

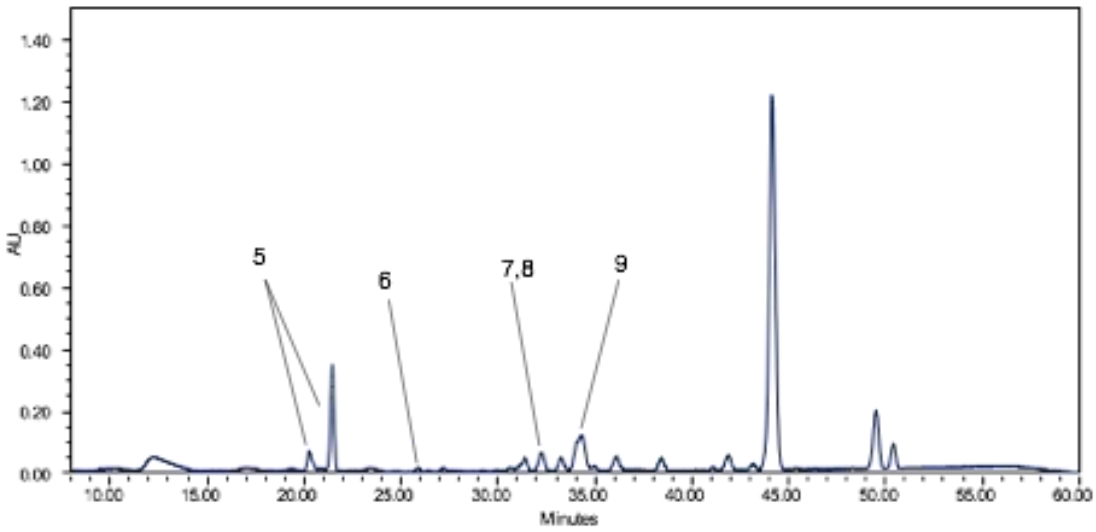
AU
Minutes
5
6
7,8
9

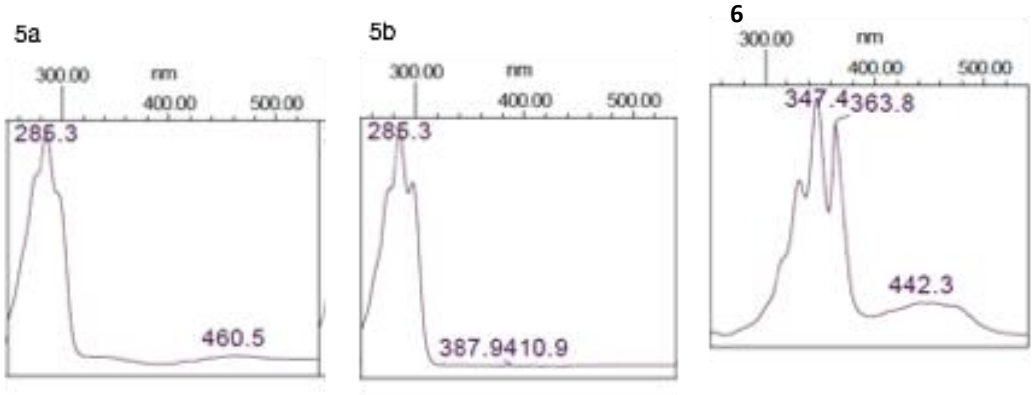
5a
5b
6
nm
285.3
460.5
387.9410.9
347.4363.8
442.3

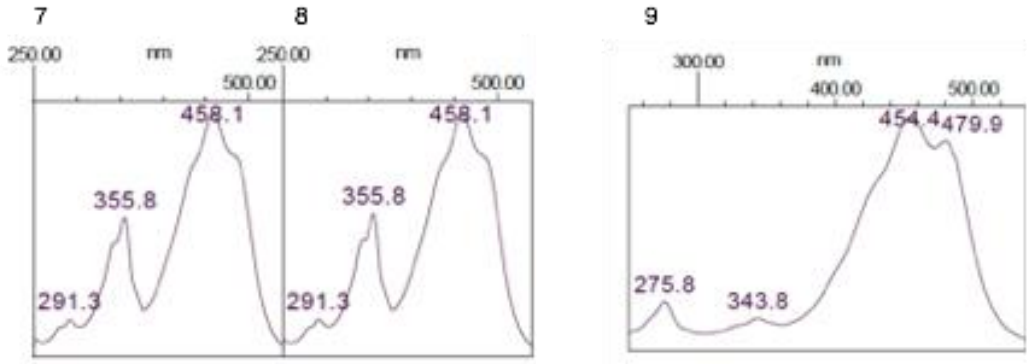
7
8
9
nm
458.1
355.8
291.3
454.4479.9
275.8
343.8

C

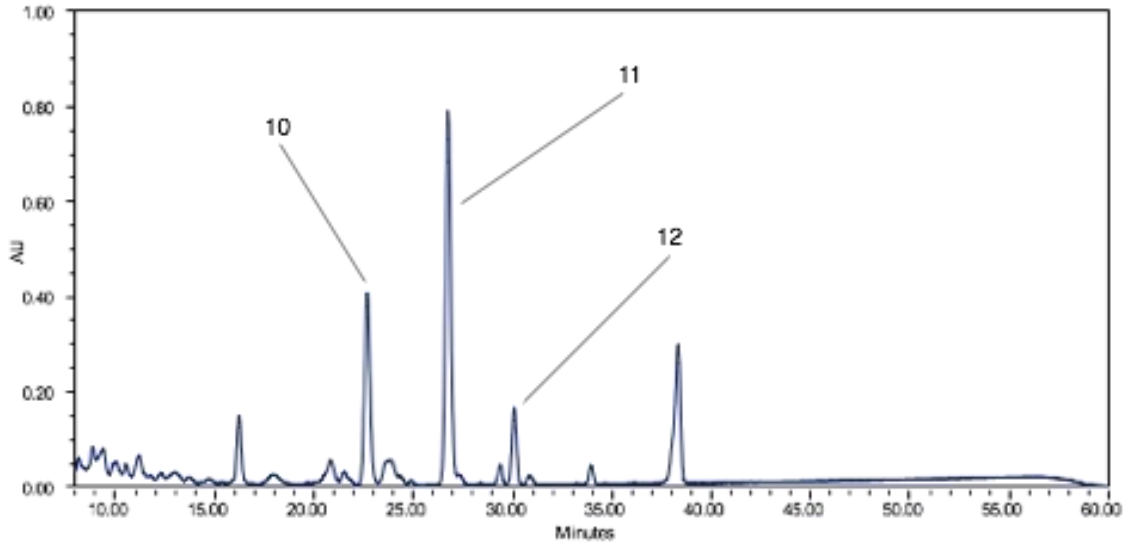
1.00
0.80
0.60
0.40
0.20
0.00
AU
10
11
12
10.00
15.00
20.00
25.00
30.00
35.00
40.00
45.00
50.00
55.00
60.00
Minutes

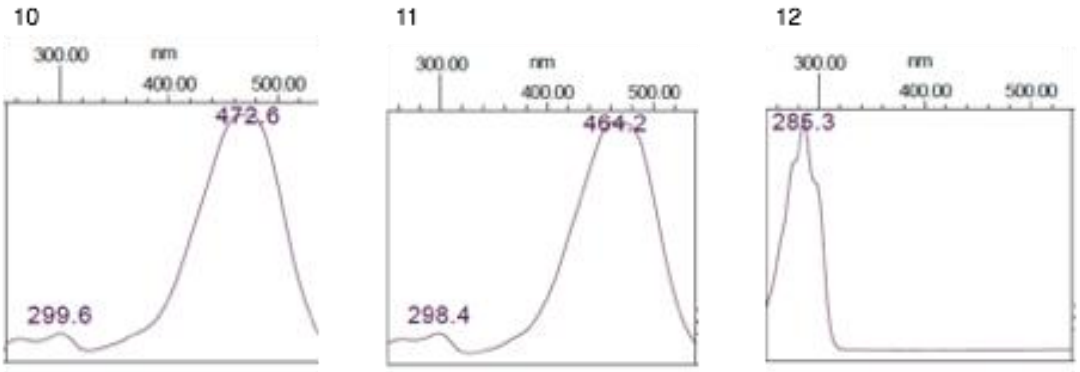
10
300.00
nm
400.00
500.00
472.6
299.6
11
300.00
nm
400.00
500.00
464.2
298.4
12
300.00
nm
400.00
500.00
285.3

D

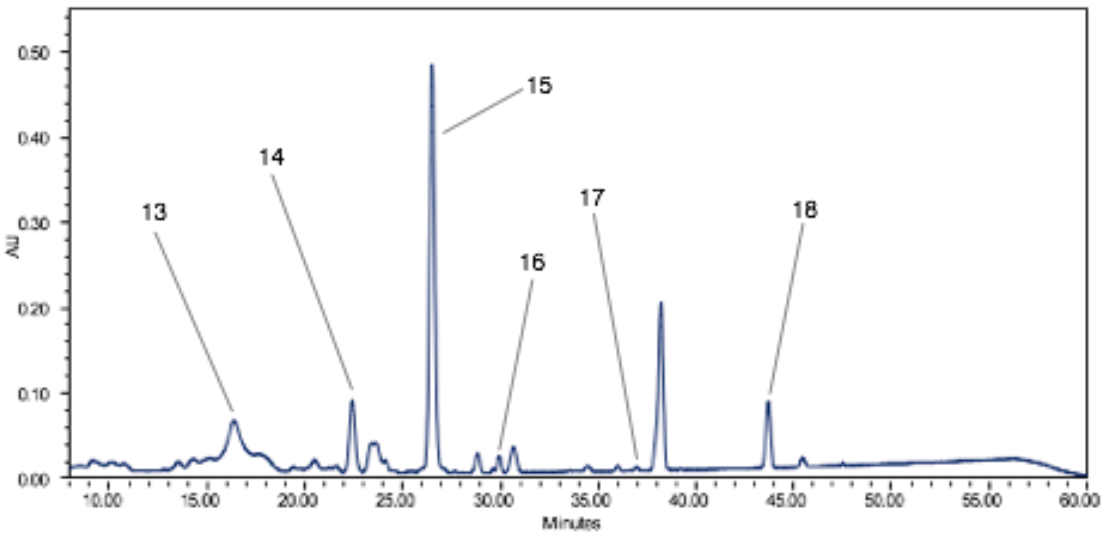
AU
Minutes
13
14
15
16
17
18

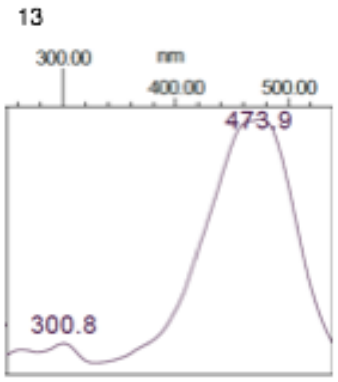
13
nm
473.9
300.8

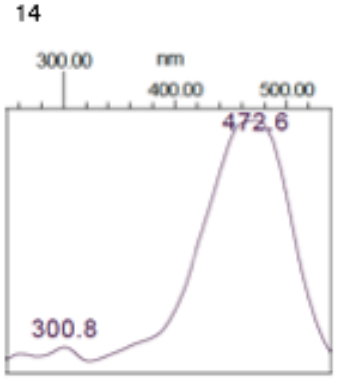
14
nm
472.6
300.8

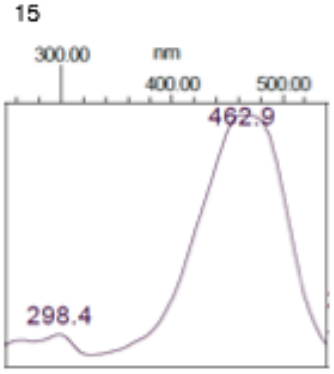
15
nm
462.9
298.4

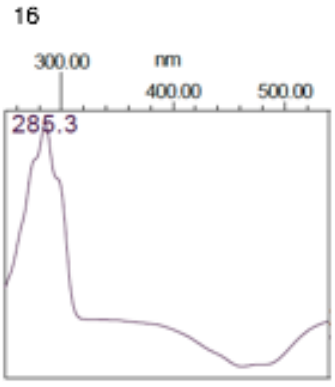
16
nm
285.3

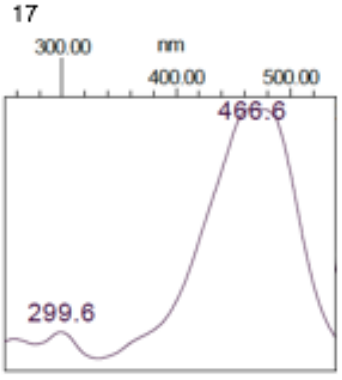
17
nm
466.6
299.6

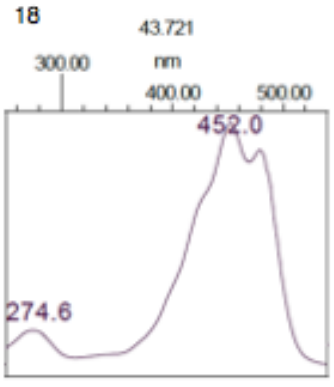
18
43.721
nm
452.0
274.6

E

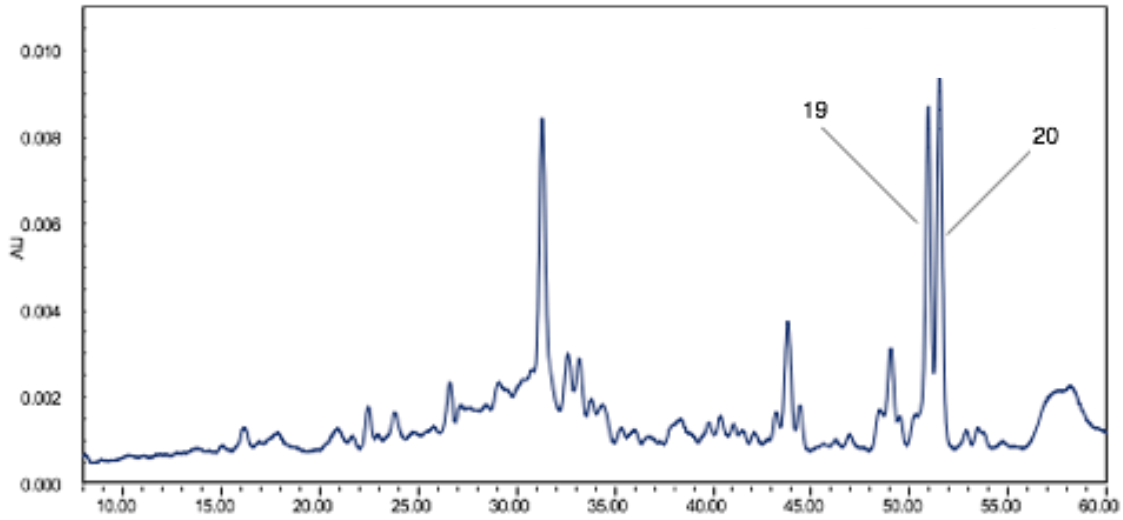
0.010
0.008
0.006
0.004
0.002
0.000
AU
19
20
10.00
15.00
20.00
25.00
30.00
35.00
40.00
45.00
50.00
55.00
60.00

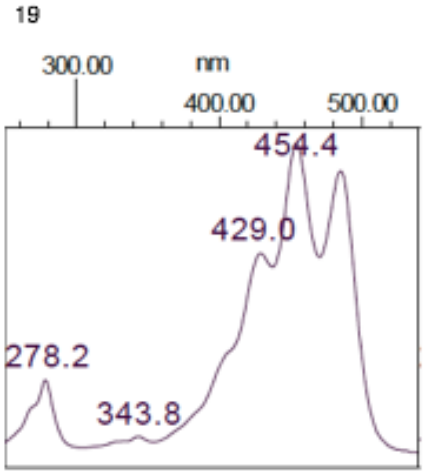
19
300.00
nm
400.00
500.00
454.4
429.0
278.2
343.8

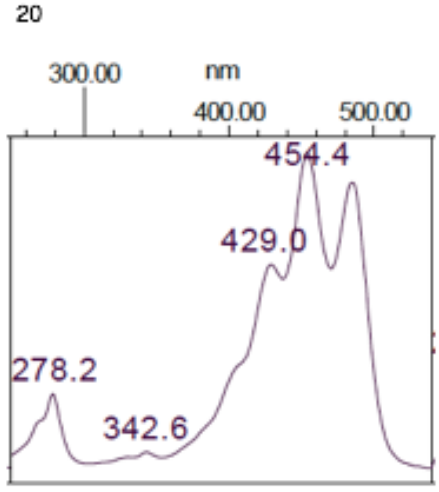
20
300.00
nm
400.00
500.00
454.4
429.0
278.2
342.6

F

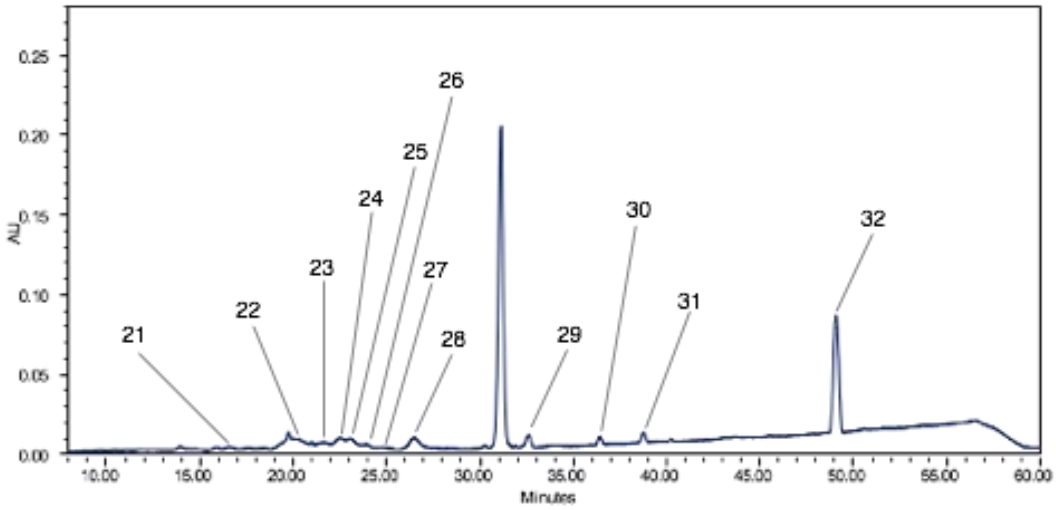
AU
Minutes
21
22
23
24
25
26
27
28
29
30
31
32

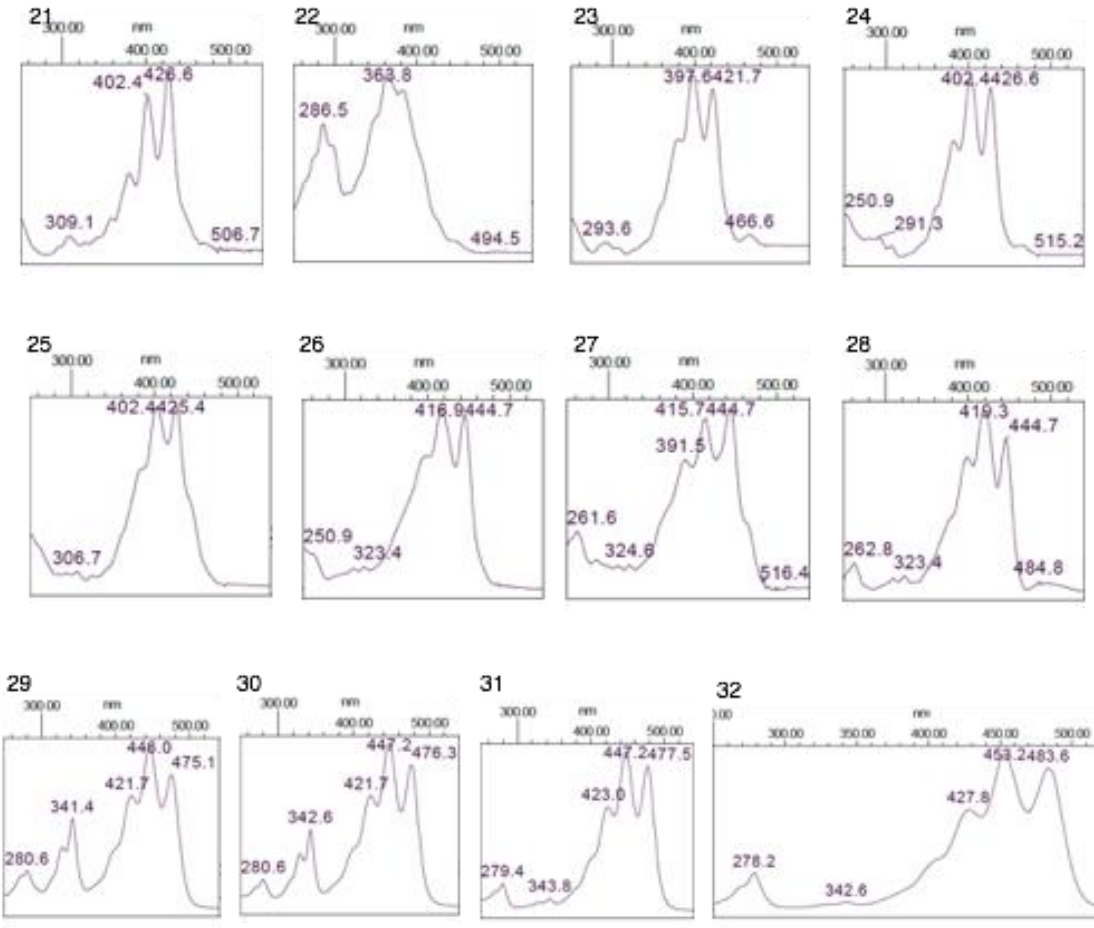
21
402.4 426.6
309.1
506.7
22
363.8
286.5
494.5
23
397.6421.7
293.6
466.6
24
402.4426.6
250.9
291.3
515.2
25
402.4425.4
306.7
26
416.9444.7
250.9
323.4
27
415.7444.7
391.5
261.6
324.6
516.4
28
419.3
444.7
262.8
323.4
484.8
29
448.0
475.1
421.7
341.4
280.6
30
447.2
476.3
421.7
342.6
280.6
31
447.2477.5
423.0
279.4
343.8
32
453.2483.6
427.8
278.2
342.6

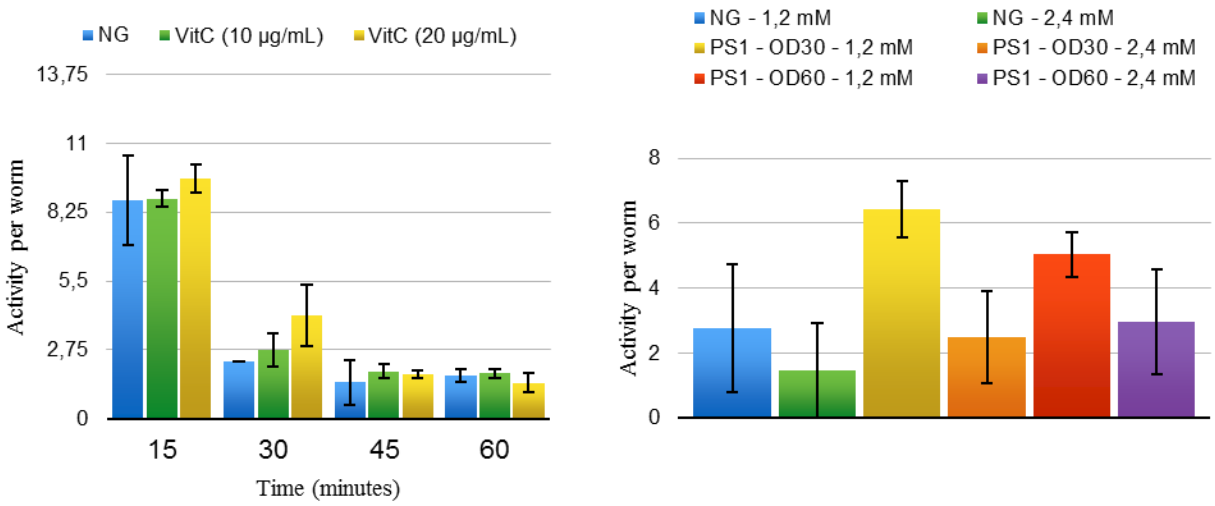

Supplementary Figure IV.1. Optimization of vitamin C and hydrogen peroxide concentrations for WormTracker assays. **(A)** Optimization of vitamin C concentration as a statistically significant positive control for WormTracker assays. Vitamin C was tested at 10 and at 20 µg/mL, resulting in significant differences in comparison to the negative control (NG) at 20 µg/mL. **(B)** Optimization of hydrogen peroxide concentrations for WormTracker assays. Hydrogen peroxide was tested at 1.2 and 2.4 mM, and activity per worm after 30 minutes of the negative control (NG) and of a positive control (PS1) can be seen in the histogram. As a result, 1.2 mM of hydrogen peroxide was selected as the optimum concentration for these assays.

Publication V

Supplementary Table V.1. Carbon source utilization comparison using Gen III Micro Plates of strain R4DWN^T and the type strains of closely related *Sphingomonas* species. Strains: 1, R4DWN^T; 2, *S. fennica* DSM 24164^T; 3, *S. formosensis* DSM 24164^T. All strains are positive for glucuronamide. All strains are negative for the following characteristics: D-raffinose, D-sorbitol, gelatin, p-hydroxy-phenylacetic acid, D-maltose, D-lactic acid methyl ester, α-hydroxy-butyric acid, β-methyl-D-glucoside, myo-inositol, D-gluconic acid, L-lactic acid, D-salicin, 3-methyl glucose, citric acid, N-acetyl-D-glucosamine, mucic acid, D-aspartic acid, L-pyroglutamic acid, quinic acid, stachyose, N-acetyl neuraminic acid, inosine, D-serine, L-serine, and D-saccharic acid. +, Positive; –, negative; W, weakly positive.

Carbon source utilization (GEN III Micro Plate)	1	2	3
Dextrin	-	W	W
α-D-Glucose	-	-	+
Pectin	-	-	+
Tween 40	-	W	+
α-D-Lactose	-	-	+
D-Mannose	-	+	+
D-Mannitol	-	-	+
Glycyl-L-Proline	-	-	+
D-Galacturonic Acid	-	-	W
Methyl Piruvate	-	-	+
ɣ-Amino-Butyric Acid	-	W	+
D-Melibiose	-	W	-
D-Fructose	-	-	+
D-Arabitol	-	+	+
L-Alanine	-	-	+
L-Galactonic Acid Lactone	W	W	-
D-Trehalose	-	-	+
D-Galactose	-	W	+
L-Arginine	-	-	+
β-Hydroxy-D,L-Butyric Acid	W	-	+
D-Cellobiose	-	-	+
Glycerol	-	-	+
L-Aspartic Acid	-	-	+
D-Glucuronic Acid	-	-	+
α-Keto-Butyric Acid	-	-	+
Gentiobiose	-	-	+
D-Fucose	-	+	+
D-Glucose-6-PO4	W	-	+
L-Glutamic Acid	-	-	+
α-Keto-Glutaric Acid	-	+	+
Acetoacetic Acid	+	-	-
Sucrose	-	W	+
N-Acetyl-β-D-Mannosamine	-	W	-
L-Fucose	-	+	W
D-Fructose-6-PO4	+	-	+
L-Histidine	-	+	+
D-Malic Acid	-	-	+

Propionic Acid	-	-	+
D-Turanose	-	W	-
N-Acetyl-D-Galactosamine	-	W	-
L-Rhamnose	-	+	-
L-Malic Acid	+	-	+
Acetic Acid	-	+	+
Bromo-Succinic Acid	-	-	+
Formic Acid	-	-	+

Supplementary Table V.2. Average nucleotide identity values (ANIb) and estimated digital DNA-DNA hybridization (dDDH) values (%) among strain R4DWN^T and its closely related type strains.

ANIb[a]	**1**	**2**	**3**	**4**	**5**	**6**	**7**
1- *Sphingomonas solaris*	100						
2- *Sphingomonas montana*	74.23	100					
3- *Sphingomonas fennica* K101^T	75.04	73.21	100				
4- *Sphingomonas oleivorans* FW-	74.71	73.34	75.36	100			
5- *Sphingomonas histidinilytica* UM2^T	73.14 (73.66)	72.73 (74.25)	74.86 (75.15)	74.82 (74.07)	100		
6- *Sphingomonas laterariae* LNB2^T	74.79 (74.48)	72.99 (73.46)	80.20 (80.21)	74.83 (74.96)	74.31 (74.19)	100	
7- *Sphingomonas wittichii* RW1^T	73.01 (70.85)	69.62 (70.98)	77.08 (78.24)	70.82 (70.05)	69.64 (71.19)	74.36 (80.49)	100
Estimated dDDH							
1- *Sphingomonas solaris*	100						
2- Sphingomonas montana	20.10	100					
3- Sphingomonas fennica K101^T	20.80	19.80	100				
4- *Sphingomonas oleivorans* FW-	20.20	19.90	20.70	100			
5- *Sphingomonas histidinilytica* UM2^T	20.40	20.60	22.20	20.80	100		
6- *Sphingomonas laterariae* LNB2^T	20.30	19.50	24.70	20.20	21.60	100	
7- *Sphingomonas wittichii* RW1^T	24.10	0.00	36.60	21.20	23.60	38.80	100

[a] Reciprocal ANIb values are shown in brackets

Supplementary Table V.3. Strains isolated from solar panel surfaces in Boston (MA, USA) and their closes neighbour, indicating % of similarity. Potential new species are in bold. IDs beginning with L indicate isolation on LB media, whereas IDs beginning with R indicate isolation on R2A media.

ID	Closest neighbor (% similarity)
L1	*Frigoribacterium faeni* (99.88 %)
L2	*Pseudomonas extremaustralis* (99.04 %)
L3	*Curtobacterium flaccumfaciens* (100 %)
L4	*Porphyrobacter mercurialis* (99.73 %)
L5	*Paracoccus marcusii* (99.72 %)
L6	*Clavibacter capsici* (99.86 %)
L7	*Arthrobacter agilis* (100 %)
L8	***Arthrobacter stackebrandtii* (98.40 %)**
L9	*Arthrobacter agilis* (100 %)
L10	*Rhodococcus fascians* (100 %)
L11	*Frigoribacterium faeni* (100 %)
L12	*Arthrobacter agilis* (99.84 %)
L13	*Plantibacter flavus* (100 %)
L14	*Arthrobacter agilis* (99.86 %)
L15	*Curtobacterium flaccumfaciens* (100 %)
L16	*Microbacterium phyllosphaerae* (100 %)
L17	*Paracoccus marcusii* (99.73 %)
L18	*Arthrobacter agilis* (99.86 %)
L19	*Microbacterium phyllosphaerae* (100 %)
L20	*Frondihabitans sucicola* (99.86 %)
R1	*Hymenobacter gelipurpurascens* (99.44 %)
R2	*Leifsonia kafniensis* (99.36 %)
R3	*Cryobacterium psychrotolerans* (100 %)
R4	***Sphingomonas formosensis* (97.29 %)**
R5	*Hymenobacter gelipurpurascens* (99.45 %)
R6	***Massilia eurypsychrophila* (97.76 %)**
R7	*Leifsonia kafniensis* (99.36 %)
R8	*Methylobacterium brachiatum* (100 %)
R9	*Sphingomonas melonis* (99.24 %)
R10	*Sphingomonas faeni* (99.73 %)
R11	*Frigoribacterium faeni* (99.44 %)
R12	*Brevundimonas intermedia* (99.73 %)
R13	*Curtobacterium flaccumfaciens* (100 %)
R14	*Sphingomonas melonis* (99.62 %)
R15	*Leifsonia kafniensis* (99.25 %)
R16	*Plantibacter flavus* (99.86 %)
R17	***Hymenobacter bucti* (97.81 %)**
R18	*Sphingomonas faeni* (99.61 %)
R19	*Brevundimonas variabilis* (98.77 %)
R20	***Sphingomonas xinjiangensis* (97.97 %)**

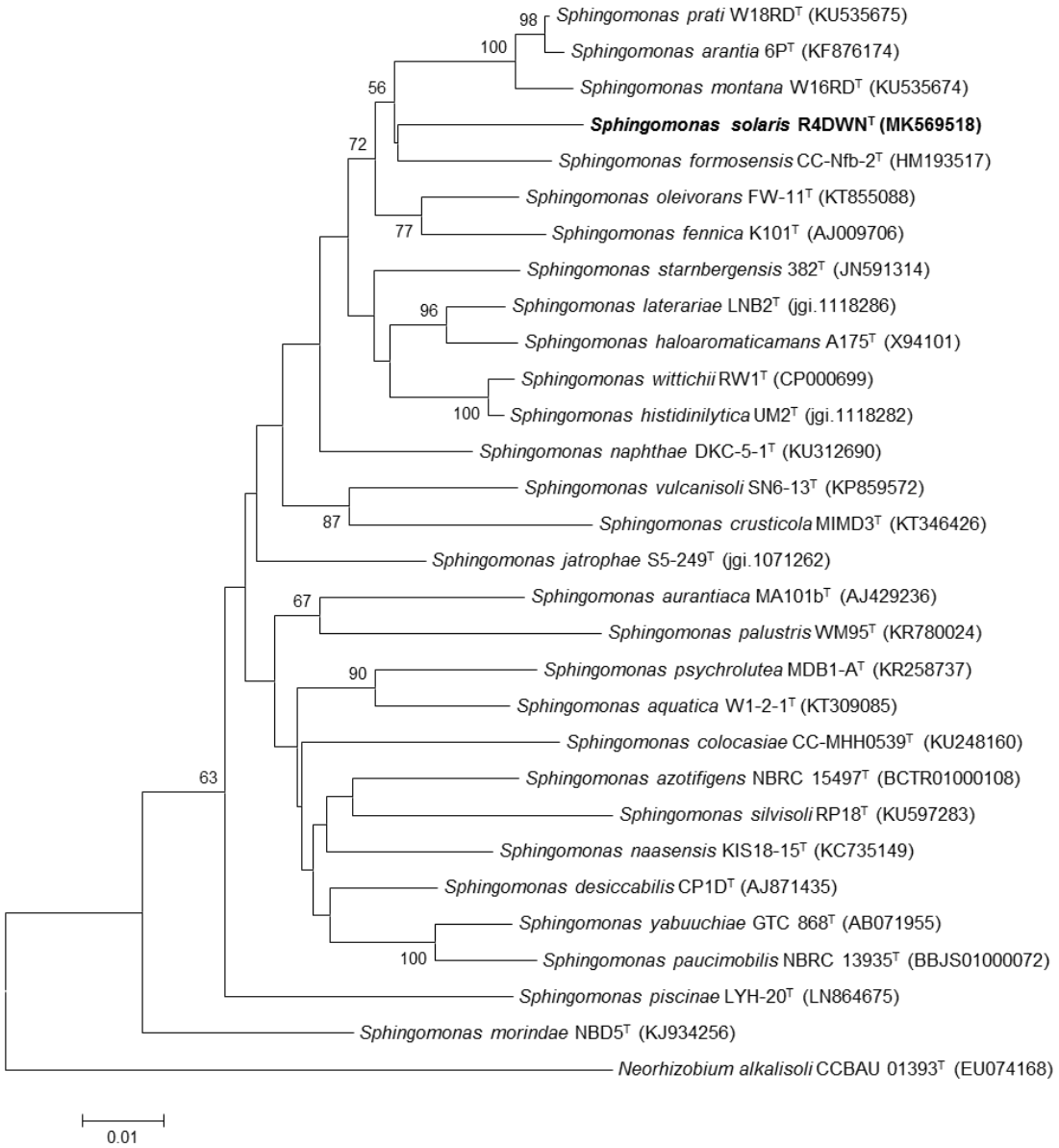

Supplementary Figure V.1. Neighbour-joining tree illustrating the phylogenetic position of strain R4DWNT and related members of the genus Sphingomonas based on almost complete 16S rRNA. The optimal evolutionary model of nucleotide substitution applied is K2P. Bar 0.01 expected nucleotide substitution per site. *Neorhizobium alkalisoli* was used as outgroup. Only bootstrap values above 50% are indicated (1000 resamplings) at branchings.

Appendix C

eVOLVING microbial strains isolated from solar panels in Boston, MA (preliminary and unpublished data)

Brief experimental procedures and results

1. Sampling of solar panels from the Arnold Arboretum at Harvard University and isolation and identification of pigmented colonies

A total of three solar panels were samples on April 10th 2018. Briefly, the solar panel surfaces were washed and scraped using squeegees and phosphate buffered saline (PBS) (Figure 1A). The resulting liquid was collected using sterile disposable pipettes and stored in sterile 50 mL Falcon tubes, which were then transported on ice back to the laboratory where the samples were then processed.

Aliquots of the three different samples were cultivated on LB and R2A media and left to grow at room temperature for 7 days. The remaining samples were mixed with glycerol, reaching a final concentration of 20 %, and stored at -20 °C until DNA extraction was performed. After the 7 days of incubation, growth of many different pigmented bacterial colonies (as well as some fungi growth) could be observed on the plates cultivated with the solar panel samples (Figure 1B). A total of 40 colonies were selected depending on their pigmentation, size and texture, and re-streaked on fresh media until obtaining pure cultures (an example can be seen in Figure 1C), which were then cryopreserved in glycerol. To identify the isolated bacteria, colony PCR was performed to amplify the 16S rRNA gene (primers prCM215 5'-CCATTGTAGCACGTGTGTAGCC-3' and prCM216 5'-ACTCCTACGGGAGGCAGC-3'), sequencing was performed using Sanger Sequencing, and the online Blast tool (NCBI) was used for taxonomic assignment. A list of all the obtained isolates with their taxonomic identification can be seen in Figure 2.

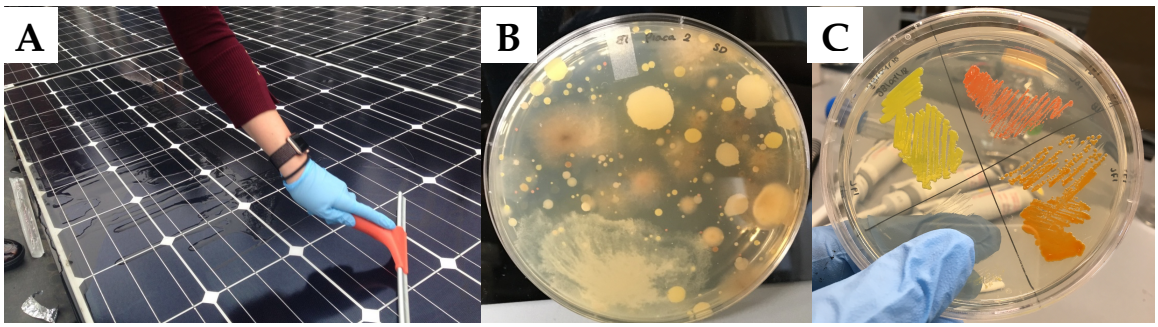

Figure 1. Solar panel sampling (A) and isolation of pigmented microorganisms through cultivation of the solar panel samples on LB media and incubation for 7 days at room temperature (B), followed by selecting and re-streaking colonies on fresh media until obtaining pure cultures (C).

2. Stress resistance assays of the isolated colonies

In order to characterize the collection of cultivable, pigmented microorganisms isolated from the solar panels, a series of stress resistance assays were performed. Specifically, and based on the harsh environmental conditions that these isolates are subjected to when inhabiting the solar panel surfaces, the following three conditions were assayed: temperature (the ability of the microorganisms to grow at temperatures between 4 and 50 degrees), desiccation-resistance (the isolates were subjected to different times of desiccation and ability to survive was assessed) and resistance to UV-light irradiation (the isolates were irradiated for different amounts of time and ability to survive was assessed) (Figure 2).

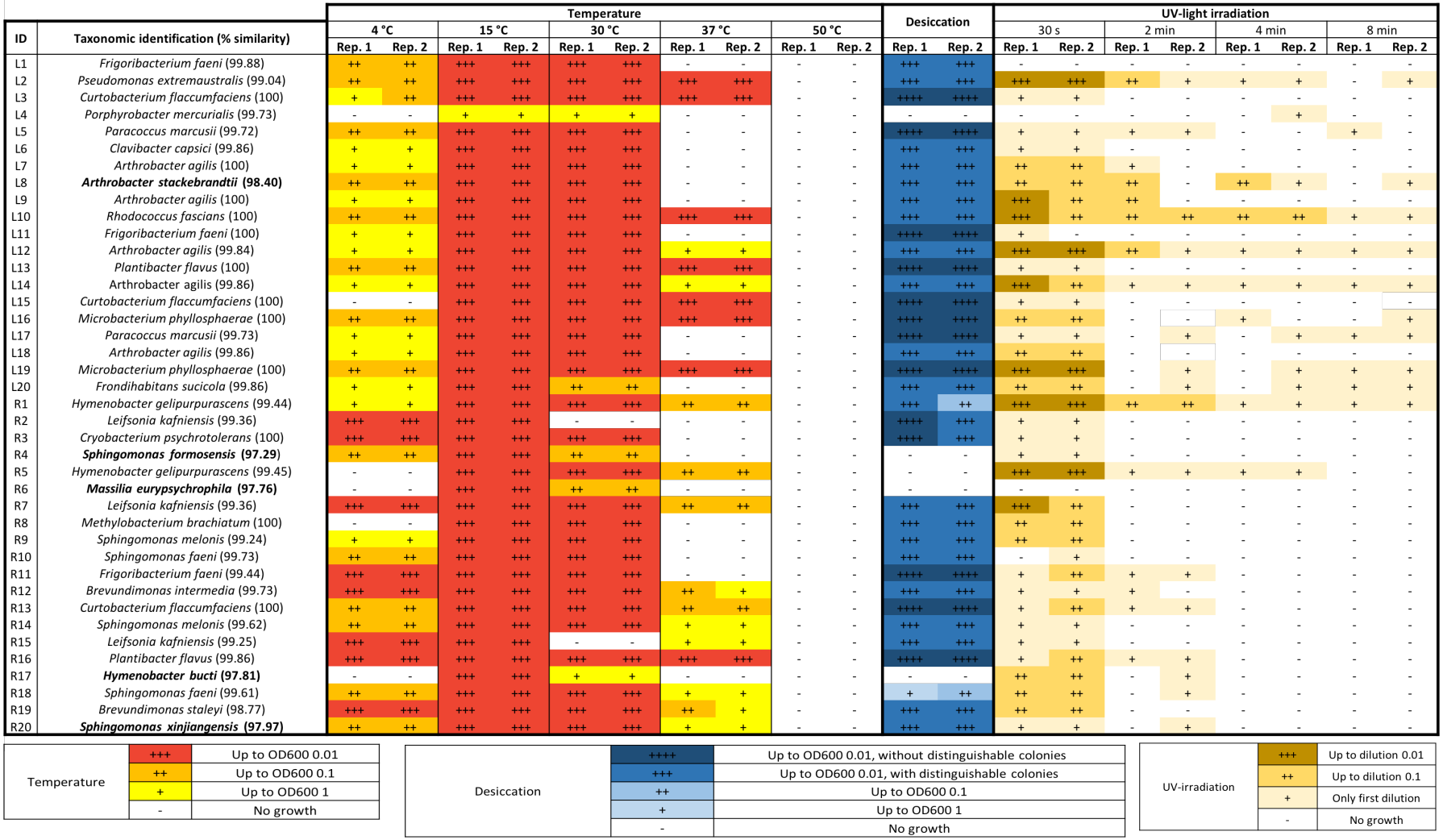

ID	Taxonomic identification (% similarity)	Temperature										Desiccation		UV-light irradiation							
		4 °C		15 °C		30 °C		37 °C		50 °C				30 s		2 min		4 min		8 min	
		Rep. 1	Rep. 2	Rep. 1	Rep. 2	Rep. 1	Rep. 2	Rep. 1	Rep. 2	Rep. 1	Rep. 2	Rep. 1	Rep. 2	Rep. 1	Rep. 2	Rep. 1	Rep. 2	Rep. 1	Rep. 2	Rep. 1	Rep. 2
L1	*Frigoribacterium faeni* (99.88)	++	++	+++	+++	+++	+++	-	-	-	-	+++	+++	-	-	-	-	-	-	-	-
L2	*Pseudomonas extremaustralis* (99.04)	++	++	+++	+++	+++	+++	+++	+++	-	-	+++	+++	+++	+++	++	+	+	+	-	+
L3	*Curtobacterium flaccumfaciens* (100)	+	++	+++	+++	+++	+++	+++	+++	-	-	++++	++++	+	+	-	-	-	-	-	-
L4	*Porphyrobacter mercurialis* (99.73)	-	-	+	+	+	+	-	-	-	-	-	-	-	-	-	-	-	+	-	-
L5	*Paracoccus marcusii* (99.72)	++	++	+++	+++	+++	+++	-	-	-	-	++++	++++	+	+	+	+	-	-	+	-
L6	*Clavibacter capsici* (99.86)	+	+	+++	+++	+++	+++	-	-	-	-	+++	+++	+	+	-	-	-	-	-	-
L7	*Arthrobacter agilis* (100)	+	+	+++	+++	+++	+++	-	-	-	-	+++	+++	++	++	+	-	-	-	-	-
L8	***Arthrobacter stackebrandtii* (98.40)**	++	++	+++	+++	+++	+++	-	-	-	-	+++	+++	++	++	++	-	++	+	-	+
L9	*Arthrobacter agilis* (100)	+	+	+++	+++	+++	+++	-	-	-	-	+++	+++	+++	++	++	-	-	-	-	-
L10	*Rhodococcus fascians* (100)	++	++	+++	+++	+++	+++	+++	+++	-	-	+++	+++	+++	++	++	++	++	++	+	+
L11	*Frigoribacterium faeni* (100)	+	+	+++	+++	+++	+++	-	-	-	-	++++	++++	+	-	-	-	-	-	-	-
L12	*Arthrobacter agilis* (99.84)	+	+	+++	+++	+++	+++	+	+	-	-	+++	+++	+++	+++	++	+	+	+	+	+
L13	*Plantibacter flavus* (100)	++	++	+++	+++	+++	+++	+++	+++	-	-	++++	++++	+	+	-	-	-	-	-	-
L14	Arthrobacter agilis (99.86)	+	+	+++	+++	+++	+++	+	+	-	-	+++	+++	+++	++	+	+	+	+	+	+
L15	*Curtobacterium flaccumfaciens* (100)	-	-	+++	+++	+++	+++	+++	+++	-	-	++++	++++	+	+	-	-	-	-	-	-
L16	*Microbacterium phyllosphaerae* (100)	++	++	+++	+++	+++	+++	+++	+++	-	-	++++	++++	++	++	-	-	+	-	-	+
L17	*Paracoccus marcusii* (99.73)	+	+	+++	+++	+++	+++	-	-	-	-	++++	++++	+	+	-	+	-	+	+	+
L18	*Arthrobacter agilis* (99.86)	+	+	+++	+++	+++	+++	-	-	-	-	+++	+++	++	++	-	-	-	-	-	-
L19	*Microbacterium phyllosphaerae* (100)	++	++	+++	+++	+++	+++	+++	+++	-	-	++++	++++	+++	+++	-	+	-	+	+	+
L20	*Frondihabitans sucicola* (99.86)	+	+	+++	+++	++	++	-	-	-	-	+++	+++	++	++	-	+	-	+	+	+
R1	*Hymenobacter gelipurpurascens* (99.44)	+	+	+++	+++	+++	+++	++	++	-	-	+++	++	+++	+++	++	++	+	+	+	+
R2	*Leifsonia kafniensis* (99.36)	+++	+++	+++	+++	-	-	-	-	-	-	++++	+++	+	+	-	-	-	-	-	-
R3	*Cryobacterium psychrotolerans* (100)	+++	+++	+++	+++	+++	+++	-	-	-	-	++++	+++	+	+	-	-	-	-	-	-
R4	***Sphingomonas formosensis* (97.29)**	++	++	+++	+++	++	++	-	-	-	-	-	-	+	+	-	-	-	-	-	-
R5	*Hymenobacter gelipurpurascens* (99.45)	-	-	+++	+++	+++	+++	++	++	-	-	-	-	+++	+++	+	+	+	+	-	-
R6	***Massilia eurypsychrophila* (97.76)**	-	-	+++	+++	++	++	-	-	-	-	-	-	-	-	-	-	-	-	-	-
R7	*Leifsonia kafniensis* (99.36)	+++	+++	+++	+++	+++	+++	++	++	-	-	+++	+++	+++	++	-	-	-	-	-	-
R8	*Methylobacterium brachiatum* (100)	-	-	+++	+++	+++	+++	-	-	-	-	+++	+++	++	++	-	-	-	-	-	-
R9	*Sphingomonas melonis* (99.24)	+	+	+++	+++	+++	+++	-	-	-	-	+++	+++	++	++	-	-	-	-	-	-
R10	*Sphingomonas faeni* (99.73)	++	++	+++	+++	+++	+++	-	-	-	-	+++	+++	-	+	-	-	-	-	-	-
R11	*Frigoribacterium faeni* (99.44)	+++	+++	+++	+++	+++	+++	-	-	-	-	++++	++++	+	++	+	+	-	-	-	-
R12	*Brevundimonas intermedia* (99.73)	+++	+++	+++	+++	+++	+++	++	+	-	-	+++	+++	+	+	+	-	-	-	-	-
R13	*Curtobacterium flaccumfaciens* (100)	++	++	+++	+++	+++	+++	++	++	-	-	++++	++++	+	++	+	+	-	-	-	-
R14	*Sphingomonas melonis* (99.62)	++	++	+++	+++	+++	+++	+	+	-	-	+++	+++	+	+	-	-	-	-	-	-
R15	*Leifsonia kafniensis* (99.25)	+++	+++	+++	+++	-	-	+	+	-	-	+++	+++	+	+	-	-	-	-	-	-
R16	*Plantibacter flavus* (99.86)	+++	+++	+++	+++	+++	+++	+++	+++	-	-	++++	++++	+	++	+	+	-	-	-	-
R17	***Hymenobacter bucti* (97.81)**	-	-	+++	+++	+	+	-	-	-	-	-	-	++	++	-	+	-	-	-	-
R18	*Sphingomonas faeni* (99.61)	++	++	+++	+++	+++	+++	+	+	-	-	+	++	++	++	-	+	-	-	-	-
R19	*Brevundimonas staleyi* (98.77)	+++	+++	+++	+++	+++	+++	++	+	-	-	+++	+++	++	++	-	-	-	-	-	-
R20	***Sphingomonas xinjiangensis* (97.97)**	++	++	+++	+++	+++	+++	+	+	-	-	+++	+++	+	+	-	+	-	-	-	-

Temperature		
	+++	Up to OD600 0.01
	++	Up to OD600 0.1
	+	Up to OD600 1
	-	No growth

Desiccation		
	++++	Up to OD600 0.01, without distinguishable colonies
	+++	Up to OD600 0.01, with distinguishable colonies
	++	Up to OD600 0.1
	+	Up to OD600 1
	-	No growth

UV-irradiation		
	+++	Up to dilution 0.01
	++	Up to dilution 0.1
	+	Only first dilution
	-	No growth

Figure 2. Cultivable microorganisms isolated from solar panel surfaces. IDs beginning with L indicate isolation on LB media, whereas IDs beginning with R indicate isolation on R2A media. Taxonomic assignation and % similarity to the closest neighbour is represented on the left. Isolates in bold represent potential new species. Characterization of their ability to resist diverse temperatures (between 4 and 50 °C), desiccation and UV-light irradiation (from 30 seconds to 8 minutes) using two biological replicates is also represented.

In general, all 40 isolates were able to grow well at temperatures between 4 and 30 °C, although only a few were able to grow at 37 °C, and none were able to grow at 50 °C. Most of the isolates proved to be desiccation resistant, in exception of isolates L4, R5, R17 and R6, and most of the isolates were able to resist 30 seconds of UV-light irradiation, in exception of L1, L4 and R6. Furthermore, a number of isolates were able to resist up to 8 minutes of irradiation, and these isolates belonged to the genera *Pseudomonas, Paracoccus, Arthrobacter, Rhodococcus, Microbacterium, Frondihabitans*, and *Hymenobacter.* These results suggest that the solar panels from the Boston area harbor a diverse microbial community that is adapted to desiccation and UV-light irradiation and that is able to grow best at temperatures between 15 and 30 °C.

3. Setting up the eVOLVER experiment

3.1 Growth test in liquid culture

The eVOLVER is a device that is coupled to a fluidics system, allowing to perform continuous cultures in liquid media. Therefore, the first step for these experiments was to test the ability of the isolates to grow in liquid medium, as not all bacteria are able to grow well in liquid medium. For these experiments, only isolates able to grow on LB were selected, and eVOLVER was used to perform growth curves and to assess the ability to grow in liquid culture. The amount of bacteria after 30 h of growth at 30 °C was quantified by measuring the optical density of the culture at 600 nm (Figure 3A), and those that grew best were selected for the following the experiments, specifically: L1, L2, L3, L8, L10, L13, L16, L17, L18, and L19. The data collected while performing the growth curves with eVOLVER was used to calculate the approximate doubling time for each isolate and, based on these results (Figure 3B), the following isolates were selected for the salt stress assay in eVOLVER: L1, L2, L3, L8, L16, L17, L18 and L19.

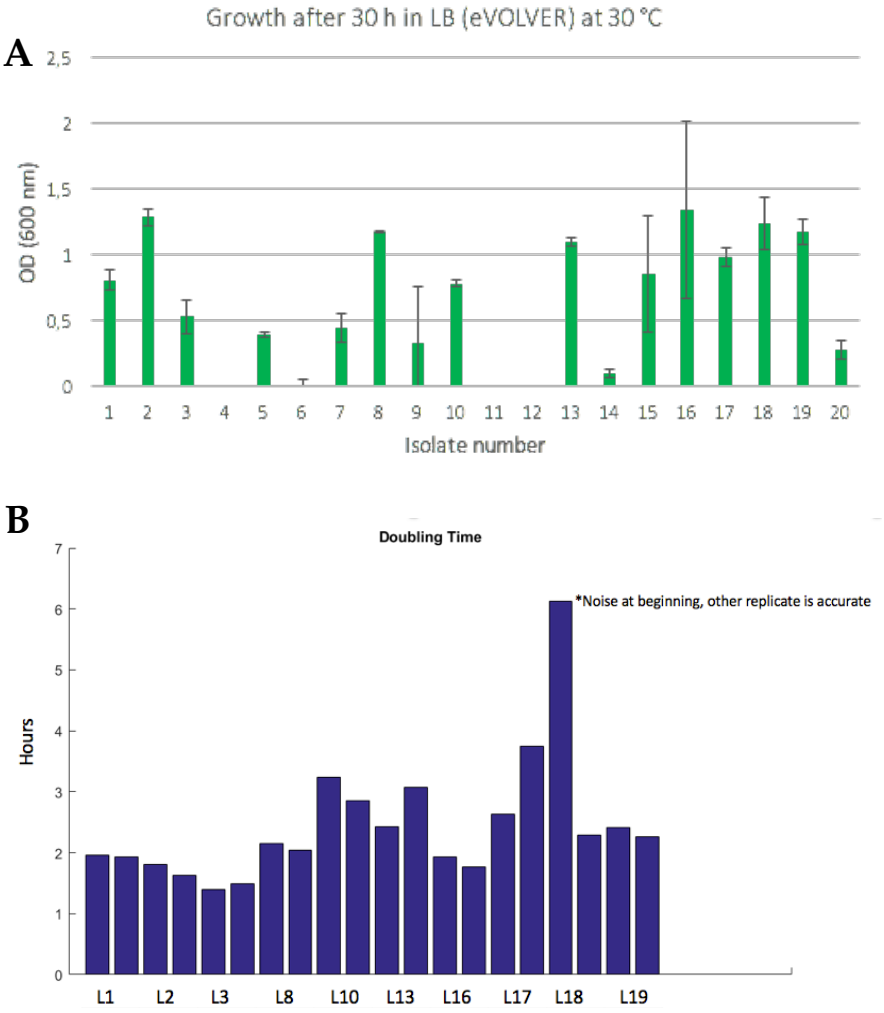

Figure 3. Growth test of the solar panel isolates in liquid LB medium using the high-throughput culture device eVOLVER. (A) Optical density at 600 nm measured after 30 hours of growth in eVOLVER at 30 ºC of the 20 strains isolated on LB medium (L1-L20). (B) Doubling time of the selected isolates calculated based on eVOLVER data.

3.2 Salt-stress test

The ten isolates selected for their ability to grow well in liquid culture were subjected to a salt stress test in order to determine their natural ability to resist saline stress. For this, the isolates were grown for 24 h at 30 °C in liquid LB medium supplemented with 1-24 % NaCl and, after, the optical density at 600 nm was measured (Figure 4). In general, all of the isolates were able to resist up to 2 % added salt, whereas addition of 4 % resulted in a growth decrease in all of the isolates, and addition of any amount above 8 % of salt to the media resulted in no growth. Based on these results, the following salt concentrations were selected for the eVOLVER experiment: 0, 2, 4, 6, 8, and 10 %.

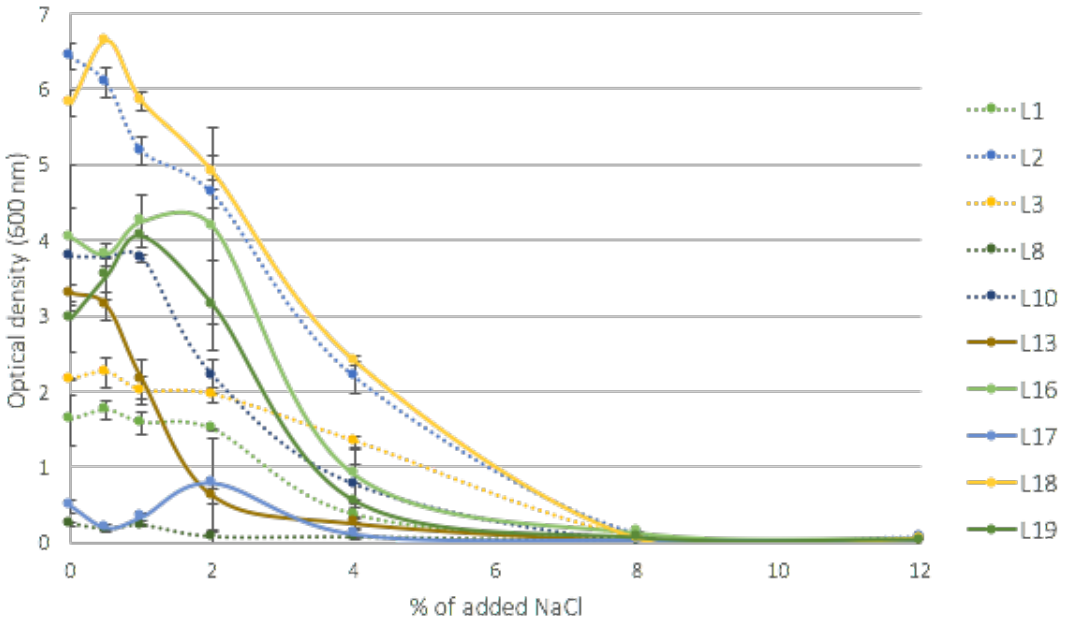

Figure 4. Salt stress test of the isolates able to grow well in liquid LB medium. Optical density at 600 nm can be seen in the Y-axis, whereas the X-axis indicates the % of salt added to regular LB medium.

4. eVOLVER experiment with continuous culture and increasing selective pressure

The eight strains (with two biological replicates) were maintained in continuous culture between an optical density at 600 nm of 0.15 and 0.2 during four weeks, gradually increasing the salt concentration after every 30-40 generations, approximately. The exact number of generations of each culture in each salt concentration can be seen in Table 1.

Table 1. Number of generations of each isolate in the eVOLVER while grown in each salt concentration (LB medium with 0 to 10 % added salt).

	L1(1)	L1(2)	L2(1)	L2(2)	L3(1)	L3(2)	L8(1)	L8(2)	L16(1)	L16(2)	L17(1)	L17(2)	L18(1)	L18(2)	L19(1)	L19(2)
LB + 0%	32,5	30,1	34,6	41,1	39,2	29,7	19,8	33,5	28,7	26,0	33,5	40,8	43,0	37,9	32,8	35,8
LB + 2%	32,8	30,4	38,1	44,9	30,3	27,7	34,9	21,8	29,9	27,7	43,2	36,3	42,6	35,9	28,2	30,7
LB + 4%	40,2	36,2	42,5	51,9	33,4	31,2	32,0	38,7	31,2	29,0	41,1	44,4	45,3	47,0	29,0	51,0
LB + 6%	25,7	22,2	31,5	29,9	31,7	28,6		1,9	10,6	12,9	15,3	41,1	6,8	6,6	16,6	39,5
LB + 8%					2,5	2,3						3,1				48,5
LB + 10%																45,5
Total	130,3	118,0	145,7	166,6	135,9	118,4	86,3	95,2	99,6	94,9	132,0	164,5	136,8	126,3	106,0	249,1

5. Salt-stress test with the evolved communities versus the non-evolved communities

Samples were collected at different time points from all the vials throughout the one-month evolution experiment, and after four weeks the final samples (evolved) were compared to the original (non-evolved) ones in terms of resistance to sodium chloride (Figure 5). Although some of the isolates displayed no change in salt resistance after the one-month evolution experiment (i.e. isolate L1, L2, L3, L16 and L19), others displayed an increase in salt resistance in the evolved cultures, as was the case of L8 and, to a lesser extent, L17 and L18.

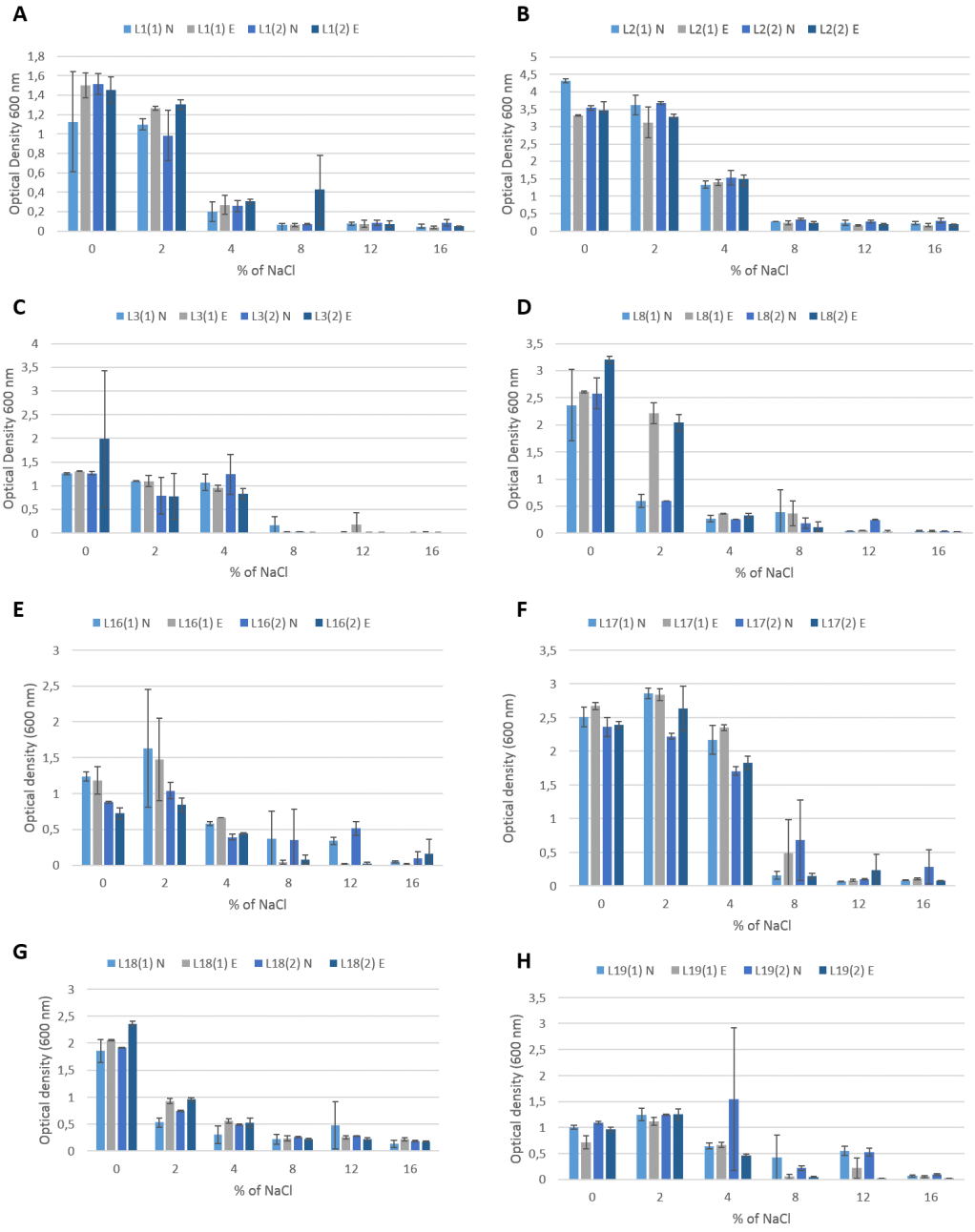

Figure 5. Growth of the selected isolates in LB medium with added NaCl (from 0% to 8 %) before (N) and after (E) being subjected to increasing salt stress in the eVOLVER during an average of 130 generations.

6. Quantification of carotenoid production

The selected non-evolved and evolved strains were grown in 2 mL liquid LB and LB + 2 and 4 % of NaCl for 72 hours. The amount of cells collected from each culture was normalized by measuring optical density of all the cultures and centrifuging the proportional amount of each one to obtain the same amount of final biomass.

After concentrating the pellet in a 1.5 mL Eppendorf tube and eliminating the growth media, the cells were washed two times with sterile PBS. Then, the pellet was resuspended in 200 µL

methanol, followed by three cycles of freeze-thaw using liquid nitrogen. Finally, the tubes were centrifuged for 3 minutes at 12.000 rpm, and the supernatants (coloured) were separated to clean Eppendorf tubes. Then, another 200 µL of methanol was added to each tube, and the same steps were repeated, in order to obtain a total coloured supernatant volume of 400 µL.

The absorbance spectra of the extractions were measured between 250 and 600 nm in UV-micro disposable cuvettes, using methanol as blank. For quantification, the absorbance value at the maximum peak wavelength was used (between 440 and 480 nm), and the following formula was applied to calculate the mg of carotenoid in the sample solution:

$$\text{carotenoid weight} = (A \times y \times 1000)/(A^{1\%\ 1cm} \times 100)$$

A: absorbance value, subtracting the base line absorbance, which should be very low

y: mL of solution (methanol solution or petroleum ether solution)

$A^{1\%\ 1cm}$: 2500

Although several of the evolved strains did not display differences in carotenoid content in comparison to the non-evolved strains (L1, L17, L19), strains L2 (Figure 6), L3 (Figure 7), L8 (Figure 8), L16 (Figure 9), and L18 (Figure 10) displayed some interesting differences especially when grown in LB + 4 % NaCl, suggesting that growing evolved strains in high salt concentrations can lead to a higher production of carotenoids.

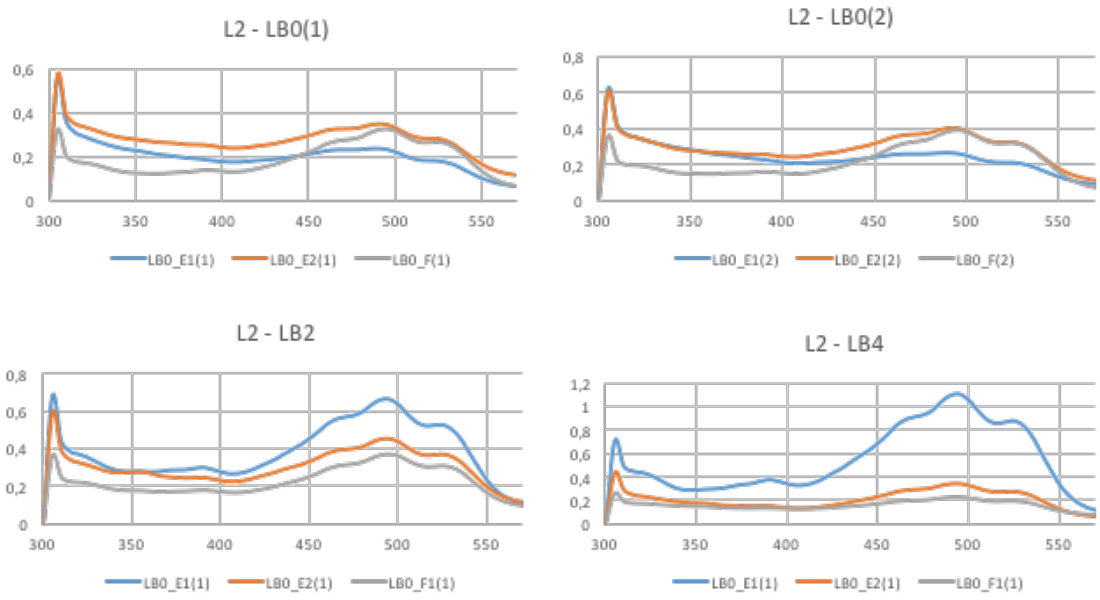

Figure 6. Absorbance spectra of L2 pigment extract after growing two evolved (E) and one non-evolved (F) strains in LB with 0, 2 and 4 % added NaCl (LB0, LB2 and LB4, respectively). Assays with LB0 were performed in duplicate, and indicated as (1) and (2), whereas only one replicate was performed in assays with LB + 2 % and LB + 4 % NaCl. Y-axis indicates absorbance values, and X-axis indicates wavelength. Grey line indicates non-evolved strain, whereas coloured lines (blue and orange) indicate evolved strains.

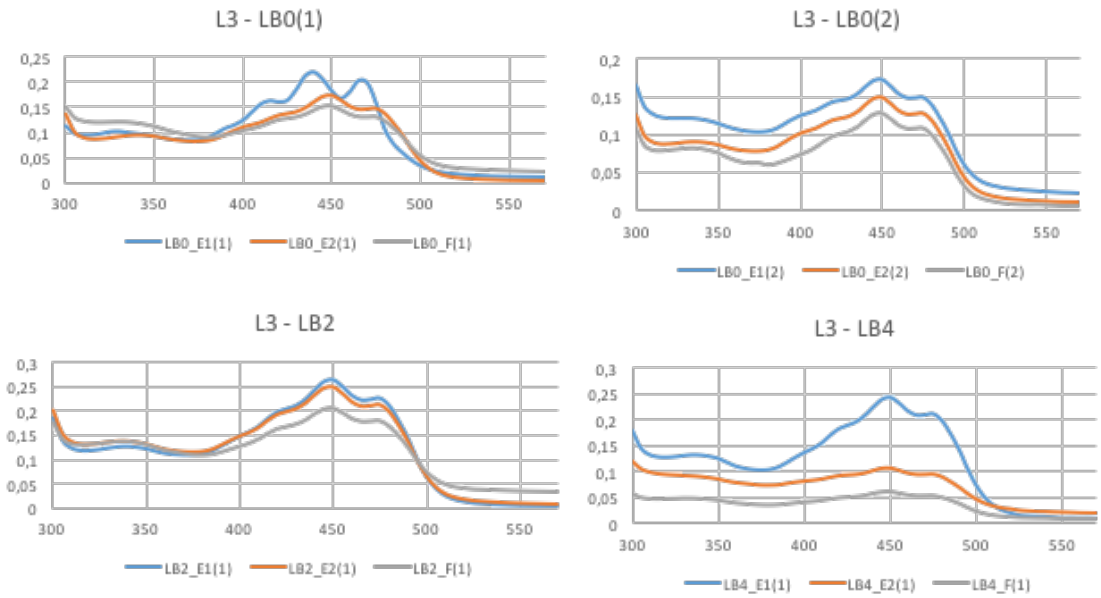

Figure 7. Absorbance spectra of L3 pigment extract after growing two evolved (E) and one non-evolved (F) strains in LB with 0, 2 and 4 % added NaCl (LB0, LB2 and LB4, respectively). Assays with LB0 were performed in duplicate, and indicated as (1) and (2), whereas only one replicate was performed in assays with LB + 2 % and LB + 4 % NaCl. Y-axis indicates absorbance values, and X-axis indicates wavelength. Grey line indicates non-evolved strain, whereas coloured lines (blue and orange) indicate evolved strains.

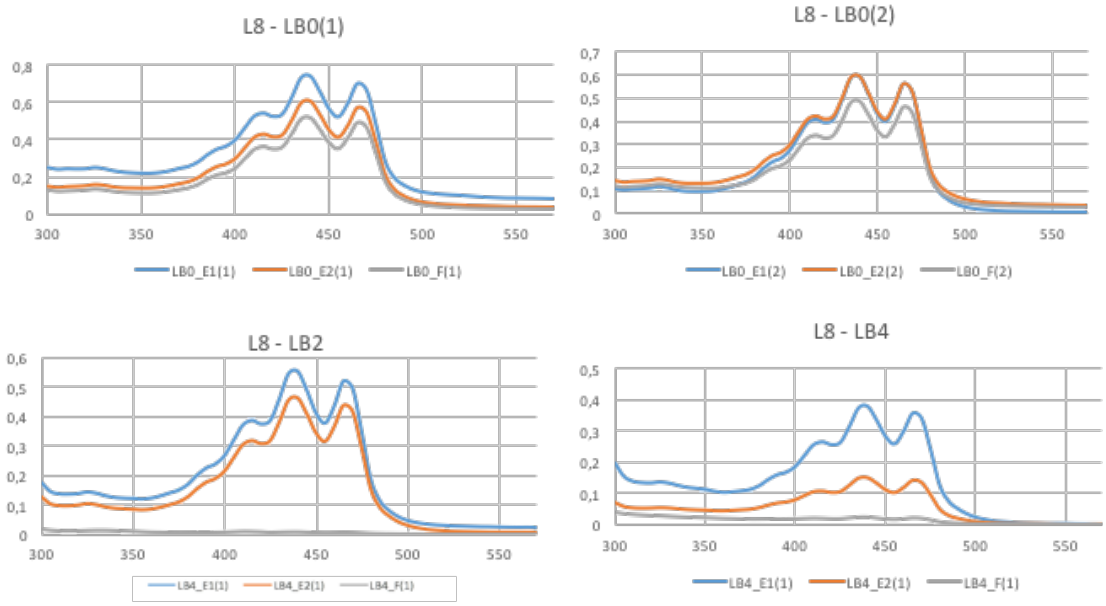

Figure 8. Absorbance spectra of L8 pigment extract after growing two evolved (E) and one non-evolved (F) strains in LB with 0, 2 and 4 % added NaCl (LB0, LB2 and LB4, respectively). Assays with LB0 were performed in duplicate, and indicated as (1) and (2), whereas only one replicate was performed in assays with LB + 2 % and LB + 4 % NaCl. Y-axis indicates absorbance values, and X-axis indicates wavelength. Grey line indicates non-evolved strain, whereas coloured lines (blue and orange) indicate evolved strains.

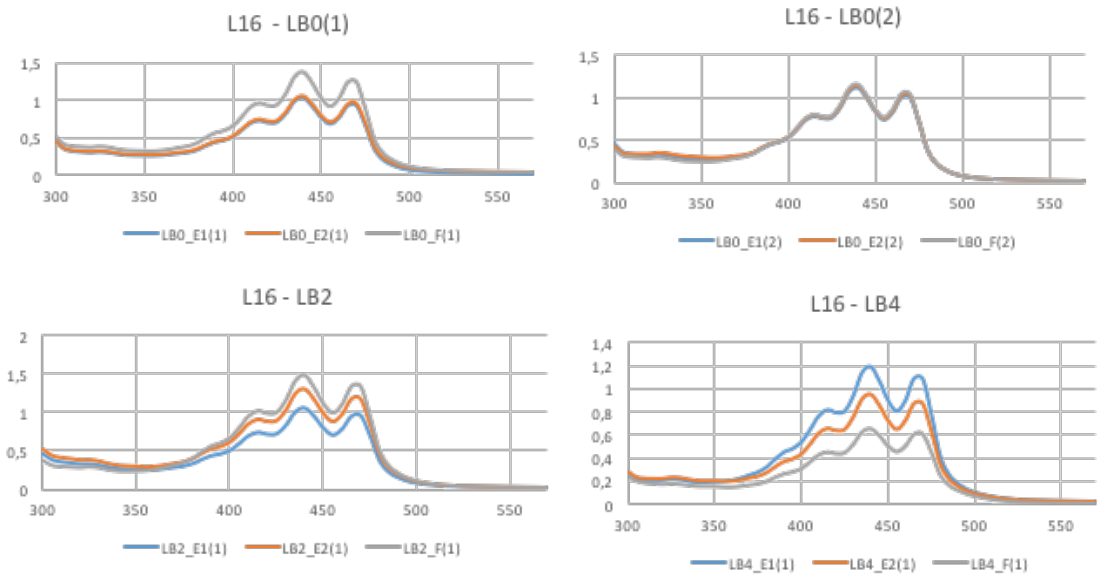

Figure 9. Absorbance spectra of L16 pigment extract after growing two evolved (E) and one non-evolved (F) strains in LB with 0, 2 and 4 % added NaCl (LB0, LB2 and LB4, respectively). Assays with LB0 were performed in duplicate, and indicated as (1) and (2), whereas only one replicate was performed in assays with LB + 2 % and LB + 4 % NaCl. Y-axis indicates absorbance values, and X-axis indicates wavelength. Grey line indicates non-evolved strain, whereas coloured lines (blue and orange) indicate evolved strains.

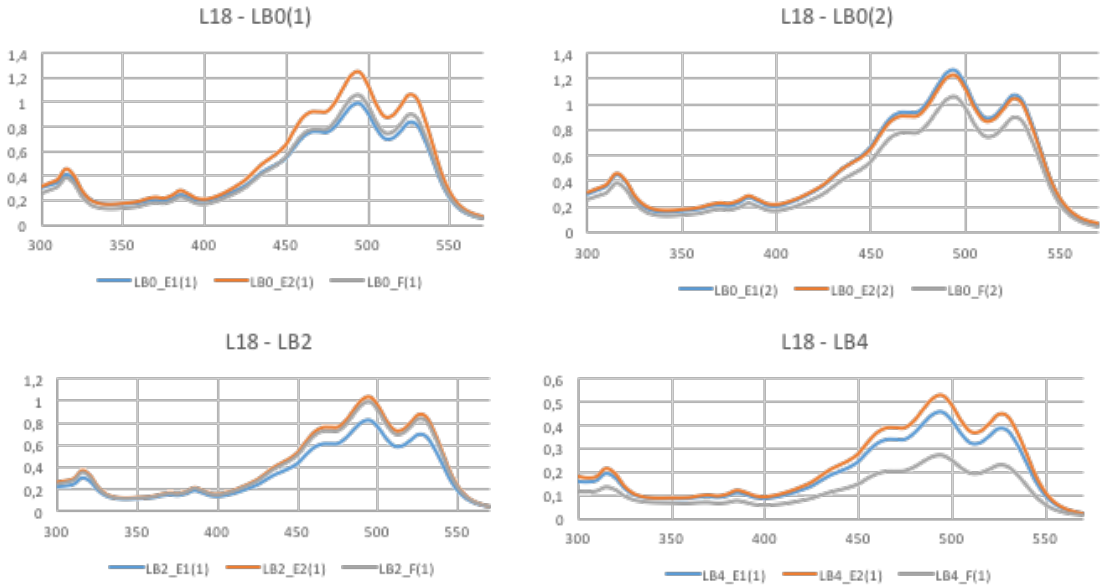

Figure 10. Absorbance spectra of L18 pigment extract after growing two evolved (E) and one non-evolved (F) strains in LB with 0, 2 and 4 % added NaCl (LB0, LB2 and LB4, respectively). Assays with LB0 were performed in duplicate, and indicated as (1) and (2), whereas only one replicate was performed in assays with LB + 2 % and LB + 4 % NaCl. Y-axis indicates absorbance values, and X-axis indicates wavelength. Grey line indicates non-evolved strain, whereas coloured lines (blue and orange) indicate evolved strains.

Appendix D

Other publications

microbial biotechnology

Open Access

doi:10.1111/1751-7915.12723

Editorial: The microbiome as a source of new enterprises and job creation

Bioprospecting challenges in unusual environments

Kristie Tanner,[1,2] Cristina Vilanova[1] and Manuel Porcar[1,2]

[1]*Darwin Bioprospecting Excellence SL, Paterna, Spain.*
[2]*I2SysBio (Institute for Integrative Systems Biology), University of Valencia-CSIC, Paterna, Spain.*

The microbial ecology field is burgeoning. Year after year, improved sampling, culturing and bioinformatics tools contribute towards an apparently endless increase in microbial diversity. Massive access to genomic data and the development of single-cell genomic techniques have re-defined the tree of life by resolving many intra- and interphylum level relationships and by including dramatic expansions such as the discovery of a new subdivision in the bacterial domain of life, or an astounding 16-fold increase in the number of known viral genes (Hug *et al.*, 2011; Rinke *et al.*, 2013; Paez-Espino *et al.*, 2016). Scaling law-based calculations have led to the prediction that Earth is the home to more than 1 trillion microbial species (Locey and Lennon, 2016) let alone the intraspecies variation. This is indeed a huge number that may be better internalized with a simple calculation: if scientists were able to summarize in a one-page genome paper each one of the bacterial species on our planet and piled the 10^{12} resulting pages one on top of another, the total height of the stacked articles would be 100 000 km, approximately a quarter of the distance from the Earth to the Moon. There is no doubt that we are dealing with a terrific amount of microbial diversity, and this puts on the table a double challenge: unveiling the myriad of microbial species still to be discovered and mining such a vast microbial diversity for novel biotechnological tools. Improving current methodologies for the analysis of omic data will be key to detect and identify novel species or gene sequences in massive datasets, whereas new culturing and screening techniques will be needed to exploit their industrial and biomedical applications (Vilanova and Porcar, 2016).

Microbial diversity is everything except random: microorganisms are the result of evolution and adaptation. This provides us with an incredible arsenal of unique and useful pre-validated tools that can be used in a wide range of industrial applications. The search of these biological tools is what we know as bioprospecting, and it is nothing new. That said, past bioprospecting efforts have mainly focused on close, well-known environments such as soil, a rich source of antibiotics (Sherpa *et al.*, 2015) and bacteria with insecticidal properties (Melo *et al.*, 2014); or human gut, from which probiotic bacteria such as *Lactobacillus spp.* can be isolated (Halimi and Mirsalehian, 2016). Nevertheless, exotic, particular environments result in particular adaptations, and the understandable ease with which human or humanized environments can be sampled should not mask that most taxonomic and functional novelties lay somewhere else. Unusual environments remain poorly or unexplored to date although they are certainly valuable sources of novel products. As illustrated by the popular illustration 'Flammarion engraving', there is a world, metaphorically, beyond those shining stars we can easily see (Fig. 1).

But, what is an unusual environment, or, more precisely, what is unusual enough? We consider an unusual environment as one that is both poorly explored, taxonomically distant from the human-associated microbiome and that is under extremophilic conditions. Interestingly, the three features tend to occur at the same time. It has to be stressed that some indoor or outdoor habitats

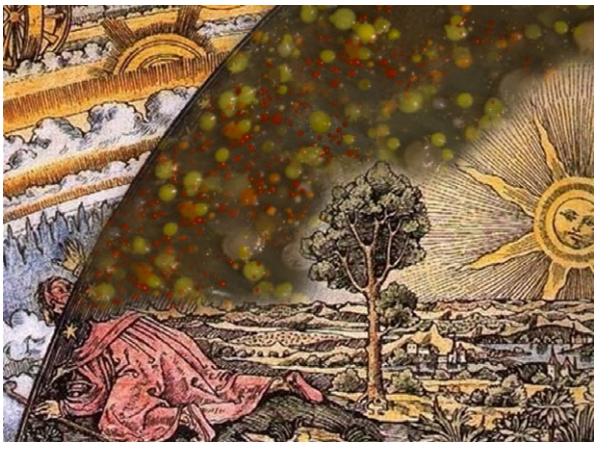

Fig. 1. Previous bioprospecting efforts have mainly focused on close environments, but beyond the comfort zone, there exist unexplored unusual niches that hold great promise as a source of biological variation that can have a key role in future biotechnological applications. The image is a collage created by blending bacterial colonies from solar panels (Dorado-Morales *et al.*, 2016) with an adapted version of the famous wood carving 'Flammarion engraving' (Flammarion, 1888).

© 2017 The Authors. *Microbial Biotechnology* published by John Wiley & Sons Ltd and Society for Applied Microbiology.
This is an open access article under the terms of the Creative Commons Attribution License, which permits use, distribution and reproduction in any medium, provided the original work is properly cited.

(electrical appliances, sun-exposed surfaces, high-temperature saunas) fall in this category.

There are three reasons making unusual environments especially interesting for bioprospecting studies. The first one is the large biodiversity they harbour, leading to a high probability of finding new taxa, as exemplified by the discovery of as many as 47 new phyla in aquifer sediments and groundwater in Colorado (Anantharaman *et al*., 2016). Second, these microorganisms are pre-adapted to stresses that often correlate with industrial needs. For example, sun-exposed environments tend to be very rich in pigmented bacteria, such as carotenoid-producing bacteria on solar panels or scytonemin-producing bacteria in microbial communities from the Atacama Desert, both of these pigment types with important applications in the food, cosmetic and pharmacological industries thanks to their antioxidant and UV-protection properties (Vítek *et al*., 2014; Rastogi *et al*., 2015; Dorado-Morales *et al*., 2016). Finally, a promising research field lies on developing new biofactories from the robust microorganisms able to resist a wide range of stresses (temperature, pH, salinity, etc.). Indeed, bacterial chassis based on *Deinococcus, Hymenobacter, Erythrobacter* and *Geobacillus* species – commonly present in extreme environments like desert soils (Rainey *et al*., 2005), Antarctic environments (Hirsch *et al*., 2004; Kojima *et al*., 2016), spacecraft surfaces (Stepanov *et al*., 2014), the troposphere (DeLeon-Rodriguez *et al*., 2013), solar salterns (Subhash *et al*., 2013) and mountain peaks (Marchant *et al*., 2002) – are already promising alternatives to classical *E. coli* models for synthetic biology (Gerber *et al*., 2015; Hussein *et al*., 2015).

Biotechnologists are indebted to thermostable polymerases, such as the immensely popular *Taq* polymerase for polymerase chain reactions (PCRs), as well as *Vent* or *Pfu* DNA polymerases, all of them isolated from the extremophilic thermophiles *Thermus aquaticus*, *Thermococcus litoralis* or *Pyrococcus furiosus* respectively (Chien *et al*., 1976; Tindall and Kunkel, 1988; Lundberg *et al*., 1991; Kong *et al*., 1993). There are many other examples of valuable products obtained from unusual environments: from silk from giant riverine orb spiders (Agnarsson *et al*., 2010), to biofuel from hyperthermophilic archaea living in deep-sea hydrothermal vent chimneys (Nishimura and Sako, 2009), or latex-degrading bacteria from pine-tree forests (Vilanova *et al*., 2014). Moreover, the recent development of innovative approaches for the mining of microbial communities is resulting in the discovery of new molecules of outstanding interest. This is the case of *Entotheonella* spp., detected through single-cell genomics approaches, and producing an unprecedented wide repertoire of bioactive compounds (Wilson *et al*., 2014), or the previously unculturable bacterium *Eleftheria terrae*, isolated from soil with innovative culturing approaches, and producer of the novel antibiotic teixobactin (Ling *et al*., 2015). It is reasonable that improving culturing techniques is first applied to well-known environments, but they will only be fully exploited on ecologically more ambitious bioprospecting efforts.

Taken together, innovative approaches applied on exotic environments will be the major source of novel microorganisms and/or metabolites in the upcoming future. Taking into account that only a fraction of global microbial diversity has been explored to date (Locey and Lennon, 2015), the number of – yet to be discovered – strains, genetic tools or metabolites with biotechnological or biomedical applications is overwhelming. This opens a great market opportunity for the biotechnology industry and particularly for microbiology-based enterprises. Highly specialized companies based on the bioprospecting of antibiotics (i.e. Prospective Research, Inc., Beverly, MA, USA) and bioactive molecules from the sea (i.e. Pharmamar, Madrid, Spain), and also new start-up companies offering improved multi-omic analysis (i.e. MicrobioMx, Barcelona, Spain) or improved culturing approaches (i.e. Darwin Bioprospecting Excellence) applied to any type of sample, are already part of the bioprospecting marketplace.

During the last two decades, the discovery of novel microbial compounds has declined significantly, mainly as a consequence of the genetic and chemical redundancy detected in commonly analysed environments (Zhang, 2005). Unusual environments hold great promise as unexploited, massively diverse targets for the discovery of biocompounds, microorganisms or consortia with potential commercial and/or industrial applications. We envisage *xenomicrobial bioprospecting* as revolutionary field for both microbial ecologists and entrepreneurs of tomorrow's bioeconomy.

References

Agnarsson, I., Kuntner, M., and Blackledge, T.A. (2010) Bioprospecting finds the toughest biological material: extraordinary silk from a giant riverine orb spider. *PLoS ONE* **5:** e11234.

Anantharaman, K., Brown, C.T., Hug, L.A., Sharon, I., Castelle, C.J., Probst, A.J., *et al.* (2016) Thousands of microbial genomes shed light on interconnected biogeochemical processes in an aquifer system. *Nat Commun* **7:** 13219.

Chien, A., Edgar, D.B., and Trela, J.M. (1976) Deoxyribonucleic acid polymerase from the extreme thermophile *Thermus aquaticus*. *J Bacteriol* **127:** 1550–1557.

DeLeon-Rodriguez, N., Lathem, T.L., Rodriguez-R, L.M., Barazesh, J.M., Anderson, B.E., Beyersdorf, A.J., *et al.* (2013) Microbiome of the upper troposphere: species

© 2017 The Authors. *Microbial Biotechnology* published by John Wiley & Sons Ltd and Society for Applied Microbiology.,

composition and prevalence, effects of tropical storms, and atmospheric implications. *Proc Nat Acad Sci USA* **110:** 2575–2580.

Dorado-Morales, P., Vilanova, C., Peretó, J., Codoñer, F.M., Ramón, D., and Porcar, M. (2016) A highly diverse, desert-like microbial biocenosis on solar panels in a Mediterranean city. *Sci Rep* **6:** 29235.

Flammarion, C. (1888) *L'atmosphère météorologie populaire*. Paris: Hachette, p. 163.

Gerber, E., Bernard, R., Castang, S., Chabot, N., Coze, F., Dreux-Zigha, A., *et al.* (2015) *Deinococcus* as new chassis for industrial biotechnology: biology, physiology and tools. *J Appl Microbiol* **119:** 1–10.

Halimi, S., and Mirsalehian, A. (2016) Assessment and comparison of probiotic potential of four *Lactobacillus* species isolated from feces samples of Iranian infants. *Microbiol Immunol* **60:** 73–81.

Hirsch, P., Gallikowski, C.A., Siebert, J., Peissl, K., Kroppenstedt, R., Schumann, P., *et al.* (2004) *Deinococcus frigens* sp. nov., *Deinococcus saxicola* sp. nov., and *Deinococcus marmoris* sp. nov., Low Temperature and Draught-tolerating, UV-resistant Bacteria from Continental Antarctica. *Syst Appl Microbiol* **27:** 636–645.

Hug, L.A., Baker, B.J., Anantharaman, K., Brown, C.T., Probst, A.J., Castelle, C.J., *et al.* (2011) A new view of the tree of life. *Nat Microbiol* **1:** 16048.

Hussein, A.H., Lisowska, B.K., and Leak, D.J. (2015) The genus geobacillus and their biotechnological potential. *Adv Appl Microbiol* **92:** 1–48.

Kojima, H., Watanabe, M., Tokizawa, R., Shinohara, A. and Fukui, M. (2016) Hymenobacter nivis sp. nov., isolated from red snow in Antarctica. *Int J Syst Evol Microbiol* **66,** 4821–4825.

Kong, H., Kucera, R.B., and Jack, W.E. (1993) Characterization of a DNA polymerase from the hyperthermophile Archaea *Thermococcus litoralis*. *J Biol Chem* **268:** 1965–1975.

Ling, L.L., Schneider, T., Peoples, A.J., Spoering, A.L., Engels, I., Conlon, B.P., *et al.* (2015) A new antibiotic kills pathogens without detectable resistance. *Nature* **517,** 455–459.

Locey, K.J., and Lennon, J.T. (2016) Scaling laws predict global microbial diversity. *PNAS* **113:** 5970–5975.

Lundberg, K.S., Shoemaker, D.D., Adams, M.W., Short, J.M., Sorge, J.A., and Mathur, E.J. (1991) High-fidelity amplification using a thermostable DNA polymerase isolated from *Pyrococcus furiosus*. *Gene* **108:** 1–6.

Marchant, R., Banat, I.M., Rahman, T.J., and Berzano, M. (2002) The frequency and characteristics of highly thermophilic bacteria in cool soil environments. *Environ Microbiol* **4:** 595–602.

Melo, A.L.D., Soccol, V.T., and Soccol, C.R. (2014) *Bacillus thuringiensis*: mechanism of action, resistance and new applications: a review. *Crit Rev Biotechnol* **36:** 317–326.

Nishimura, H. and Sako, Y. (2009) Purification and characterization of the oxygen-thermostable hydrogenase from the aerobic hyperthermophilic archaeon *Aeropyrum camini*. *J Biosci Bioeng* **108,** 299–303.

Paez-Espino, D., Eloe-Fadrosh, E.A., Pavlopoulos, G.A., Thomas, A.D., Huntemann, M., Mikhailova, N., *et al.* (2016) Uncovering Earth's virome. *Nature* **536:** 425–430.

Rainey, F.A., Ray, K., Ferreira, M., Gatz, B.Z., Nobre, M.F., Bagaley, D., *et al.* (2005) Extensive diversity of ionizing-radiation-resistant bacteria recovered from Sonoran desert soil and description of nine new species of the genus *Deinococcus* obtained from a single soil sample. *Appl Environ Microbiol* **71:** 5225–5235.

Rastogi, R.P., Sonani, R.R., and Madamwar, D. (2015) Cyanobacterial sunscreen scytonemin: role in photoprotection and biomedical research. *Appl Biochem Biotechnol* **176:** 1551–1563.

Rinke, C., Schwientek, P., Sczyrba, A., Ivanova, N.N., Anderson, I.J., Cheng, J., *et al.* (2013) Insights into the phylogeny and coding potential of microbial dark matter. *Nature* **499:** 431–437.

Sherpa, R.T., Reese, C.J., and Montazaeri, A.H. (2015) Application of iChip to grow "uncultivable" microorganisms and its impact on antibiotic discovery. *J Pharm Pharm Sci* **18:** 303–315.

Stepanov, V.G., Vaishampayan, P., Venkateswaran, K. and Fox, G.E. (2014) Draft genome sequence of *Deinococcus phoenicis*, a novel strain isolated during the Phoenix Lander spacecraft assembly. *Genome Announc* **2,** e00301-14.

Subhash, Y., Tushar, L., Sasikala, C., and Ramana, C.V. (2013) *Erythrobacter odishensis* sp. nov. and *Pontibacter odishensis* sp. nov. isolated from dry soil of a solar saltern. *Int J Syst Evol Microbiol* **63:** 4524–4532.

Tindall, K.R., and Kunkel, T.A. (1988) Fidelity of DNA synthesis by the *Thermus aquaticus* DNA polymerase. *Biochemistry* **27:** 6008–6013.

Vilanova, C., and Porcar, M. (2016) Are multi-omics enough? *Nat Microbiol* **1:** 16101.

Vilanova, C., Marín, M., Baixeras, J., Latorre, A., and Porcar, M. (2014) Selecting microbial strains from pine tree resin: biotechnological applications from a terpene world. *PLoS ONE* **9:** e100740.

Vítek, P., Jehlička, J., Ascaso, C., Mašek, V., Gómez-Silva, B., Olivares, H., and Wierzchos, J. (2014) Distribution of scytonemin in endolithic microbial communities from halite crusts in the hyperarid zone of the Atacama Desert, Chile. *FEMS Microb Ecol* **90:** 351–366.

Wilson, M.C., Mori, T., Rückert, C., Uria, A.R., Helf, M.J., Takada, K., *et al.* (2014) An environmental bacterial taxon with a large and distinct metabolic repertoire. *Nature* **506:** 58–62.

Zhang, L. (2005) Integrated approaches for discovering novel drugs from microbial natural products. *In* Natural Products. Zhang, L. and Demain, A. L. (eds). New Jersey: Humana Press, pp. 33–55.

© 2017 The Authors. *Microbial Biotechnology* published by John Wiley & Sons Ltd and Society for Applied Microbiology.,

microbial biotechnology

Open Access

Microbial communities of the Mediterranean rocky shore: ecology and biotechnological potential of the sea-land transition

Esther Molina-Menor,[1,†] Kristie Tanner,[1,2,†] Àngela Vidal-Verdú,[1] Juli Peretó[1,2,3] and Manuel Porcar[1,2,*,†]

[1]*Institute for Integrative Systems Biology I[2]SysBio, Universitat de València-CSIC, Paterna 46980, Spain.*
[2]*Darwin Bioprospecting Excellence S.L. Parc Científic Universitat de València, Paterna 46980, Spain.*
[3]*Departament de Bioquímica i Biologia Molecular, Universitat de València, Burjassot 46100, Spain.*

Summary

Microbial communities from harsh environments hold great promise as sources of biotechnologically relevant strains and compounds. In the present work, we have characterized the microorganisms from the supralittoral and splash zone in three different rocky locations of the Western Mediterranean coast, a tough environment characterized by high levels of irradiation and large temperature and salinity fluctuations. We have retrieved a complete view of the ecology and functional aspects of these communities and assessed the biotechnological potential of the cultivable microorganisms. All three locations displayed very similar taxonomic profiles, with the genus *Rubrobacter* and the families *Xenococcaceae*, *Flammeovirgaceae*, *Phyllobacteriaceae*, *Rhodobacteraceae* and *Trueperaceae* being the most abundant taxa; and *Ascomycota* and halotolerant archaea as members of the eukaryotic and archaeal community respectively. In parallel, the culture-dependent approach yielded a 100-isolates collection, out of which 12 displayed high antioxidant activities, as evidenced by two *in vitro* (hydrogen peroxide and DPPH) and confirmed *in vivo* with *Caenorhabditis elegans* assays, in which two isolates, CR22 and CR24, resulted in extended survival rates of the nematodes. This work is the first complete characterization of the Mediterranean splash-zone coastal microbiome, and our results indicate that this microbial niche is home of an extremophilic community that holds biotechnological potential.

Received 15 April, 2019; revised 30 July, 2019; accepted 31 July, 2019.
*For correspondence. E-mail manuel.porcar@uv.es; Tel. +34 963544473; Fax +34 96 3543576.
†These authors contributed equally to this work.
Microbial Biotechnology (2019) **12**(6), 1359–1370
doi:10.1111/1751-7915.13475
Funding information
Financial support from the Spanish Government (Grant Helios, Reference: BIO2015-66960-C3-1-R co-financed by FEDER funds and Ministerio de Ciencia, Innovación y Universidades) and from the European CSA on biological standardization BIOROBOOST (EU grant number 820699) is acknowledged. EMM is funded with a Formación de Profesorado Universitario (FPU) grant from the Spanish Government (Ministerio de Ciencia, Innovación y Universidades), with reference FPU17/04184. KT is a recipient of a Doctorado Industrial fellowship from the Ministerio de Ciencia, Innovación y Universidades (Spain), with reference DI-16-08976. ÀVV is funded with a Formación de Profesorado Universitario (FPU) grant from the Spanish Government (Ministerio de Ciencia, Innovación y Universidades), with reference FPU18/02578.

Introduction

The interphase between marine and land environments is an ecologically complex habitat in which selection pressures from both environments can co-occur. Some of those pressures are high salinity, dehydration, wind and sun exposition, extreme temperature oscillations and mechanical stress associated with seawater splash, often with sand or pebbles, with strong abrasive effects. The aquatic to land transition has been reported to be linked to a narrow gradient in species distribution in function of the distance to the water line, as for example in cyanobacteria in an English lake (Pentecost, 2014). Regarding marine environments, the microbial ecology of rocky shores has previously been analysed (Chan *et al*., 2003; Langenheder and Ragnarsson, 2007; Pinedo *et al*., 2007; Brandes *et al*. 2015), including its links with oil spills and biodegradation (Alonso-Gutiérrez *et al*., 2009). However, and in contrast with the well-studied microbial ecology of the intertidal zone (for a review, see Mitra *et al*., 2014), a holistic study on the microbial ecology of the marine supralittoral Mediterranean rocky shore has not been addressed previously.

Harsh, extremophilic environments can be sources of biotechnologically relevant bacteria and therefore hold great promise for the biotechnological industry (Raddadi *et al*., 2015). For example, extremophilic microorganisms can yield enzymes such as lipases and esterases that can be used under a wide range of conditions and may have relevant applications in the food, detergent and

© 2019 The Authors. *Microbial Biotechnology* published by John Wiley & Sons Ltd and Society for Applied Microbiology.
This is an open access article under the terms of the Creative Commons Attribution License, which permits use, distribution and reproduction in any medium, provided the original work is properly cited.

biofuel industries (Fuciños *et al*., 2012). There are many other examples of biotechnologically relevant microorganisms from extreme environments, including the well-known case of *Thermus aquaticus*, which produces the widely used *Taq* polymerase; or the hyperthermophilic biofuel-producing archaea that live in deep-sea hydrothermal vents (Chien *et al*., 1976; Nishimura and Sako, 2009).

The present study focuses on the microorganisms that inhabit the rocky areas of the supralittoral zone (the area just above the tide line that is subjected regularly to splash but is not permanently underwater) of the Mediterranean coast. Surface-associated microbial communities that are sun-exposed are often rich in microorganisms that produce pigments, including carotenoids (Dorado-Morales *et al*., 2015; Kumar *et al*., 2015; : Shindo and Misawa, 2014; Tanner *et al*., 2017). These pigments play a key role in radiation tolerance (Tian and Hua, 2010; Klindworth *et al*., 2013; Sandmann, 2015; Tanner *et al*., 2018), and they are valuable for the food, pharmacological and cosmetic industries as colourants, antioxidants and protectors against solar radiation respectively (Sandmann, 2015). Therefore, we hypothesized that rough conditions of the supratidal zone may be associated with the presence of biotechnologically relevant microbial taxa. From this hypothesis, we have, in the present work, compared three different supralittoral coastal locations of the Mediterranean West coast and combined culturing techniques and high throughput sequencing data (16S rRNA amplicon and metagenomic sequencing) in order to shed light on the taxonomic composition of these communities, and to explore the biotechnological potential of the culturable strains.

Results

High-throughput 16S rRNA analysis

High-throughput 16S rRNA sequencing of the samples revealed that, based on the comparison of the richness value (number of different species; Fig. 1A) and the diversity (Shannon index; Fig. 1B), the alpha diversity was not significantly different among the locations. Moreover, the shape of the rarefaction curve at OTU level (Operational Taxonomic Unit) showed that the sequences covered the majority of taxa present in the samples (Fig. S1).

However, the composition of the bacterial communities varied depending on the location, as represented in the Principal Coordinates Analysis (PCoA; Fig. 2A). Samples from Dénia showed the highest intragroup homogeneity, whereas samples from Vinaròs and Cullera displayed higher differences between replicates. Nevertheless, samples from all three locations could be distinguished in the plot. The variability explained by both axes is high enough to conclude that the microbial communities among the three locations are different. Moreover, the representation of the relative abundances (TSS) of the top 30 most abundant genera showed that the microbial composition was generally similar along the locations (Fig. 2B), although some taxa such as the genus *Rubrobacter* in Vinaròs or the genus *Rubricoccus* in Dénia allowed the differentiation of specific regions (Table 1). Eleven out of the 30 most abundant genus were significantly different at least in one location. A list of the 30 more significantly different genus is shown in (Table S1). The original data have been deposited with the NCBI SRA accession number PRJNA556782.

Shotgun metagenomic analysis

The three locations exhibited similar taxonomic profiles according to the metagenomics analysis. The most abundant bacterial phyla were the same ones observed with high-throughput 16S rRNA sequencing, with *Cyanobacteria* being the most abundant in all three locations. Moreover, other taxa, such as the families *Rhodobacteraceae*, *Flammeovirgaceae*, *Trueperaceae* and the genus *Rubrobacter*, belonging to the phyla *Proteobacteria*, *Bacteroidetes*, *Deinococcus-Thermus* and *Actinobacteria* respectively, were also detected (Figs S2A, S3A and S4A). Metagenomic sequencing allowed the identification of abundant taxa in the *Cyanobacteria* phylum, including the genera *Staniera, Pleurocapsa*, *Myxosarcina* and *Xenococcus*, in contrast to the high-throughput 16S rRNA, which mainly showed unclassified *Xennococcaceae* taxa.

Archaeal and eukaryotic communities proved very diverse, with a high number of salt-adapted microorganisms in the former and a large fraction of *Ascomycota* in the latter (Figs S2, S3, S4B and C). Salt-adapted archaea included members of *Halococcus*, *Halobacteriaceae* (*Haladaptatus* and *Halalkalicoccus*), *Haloarculaceae*, *Haloferaceae*, *Halorubraceae* and *Natrialbaceae* families, as well as methanogenic archaea (members of the *Methanosarcinaceae* family; Figs S2B, S3B and S4B). Among the diversity of *Ascomycota*, the most abundant taxa were *Glonium stellatum*, *Cenococcum geophilum*, *Coniosporium apollinis* and *Lepidopterella palustris* (Figs S2C, S3C and S4C).

The functional analysis of the samples revealed a high representation of enzymes related to oxidative stress, being peroxiredoxin (EC 1.11.1.15) and peroxidase (EC 1.11.1.7) the most abundant activities, and displaying the highest values in Cullera and Vinaròs respectively. Thioredoxin-related enzymatic activities (EC 1.8.4.8; EC 1.8.1.9; EC 1.8.4.10) were homogeneously represented in all three samples, as well as superoxide dismutase (EC 1.15.1.1). Other enzymes

© 2019 The Authors. *Microbial Biotechnology* published by John Wiley & Sons Ltd and Society for Applied Microbiology.,

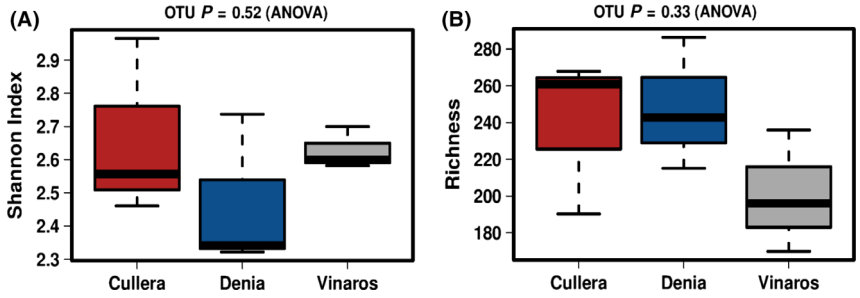

Fig. 1. Box plots showing the values of alpha diversity indexes in the sampled locations on the Mediterranean rocky-shore. (A) Observed richness at OTU level (number of OTUs). (B) Shannon index of diversity.

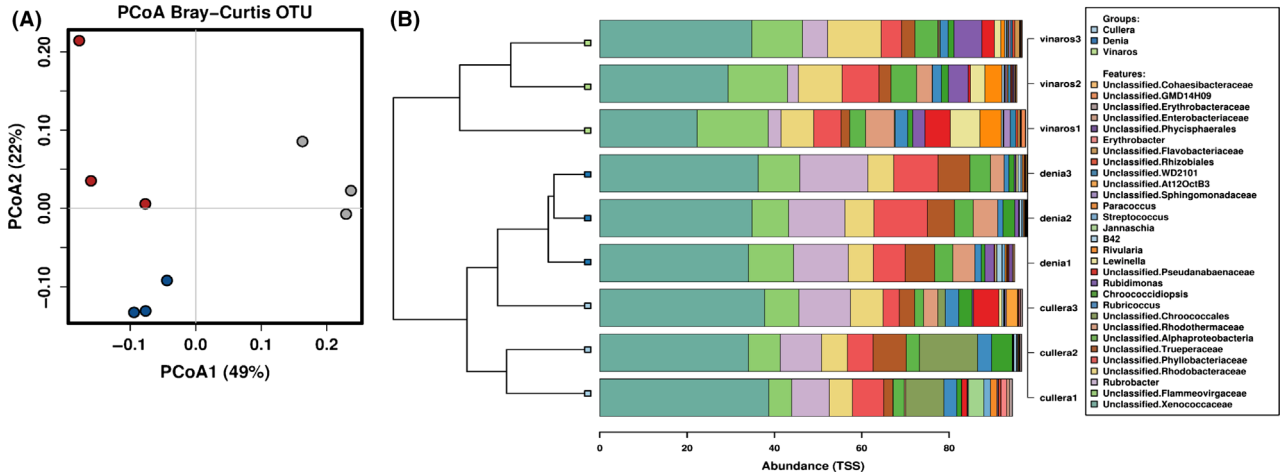

Fig. 2. (A) Principal coordinates analysis (PCoA) based on Bray–Curtis distances between OTUs in bacterial communities of three different locations. (B) Clustered-Barchart showing the top 30 most abundant genera in terms of relative abundance.

such as glutathione transferase (EC 2.5.1.18) or glutathione peroxidase (EC 1.11.1.9) varied among locations, with the former being more represented in Vinaròs and Cullera than in Dénia, and the latter being more abundant in Vinaròs. Among the genes related to carotenoid biosynthetic routes, the abscisic acid 8′-hydroxylase (EC 1.14.14.137) was particularly represented in Cullera, whereas sphingolipid-related genes such as glucosylceramidase proved to be frequent in Vinaròs (EC 3.2.1.45; Fig. 3). The original data have been deposited with the NCBI SRA accession number PRJNA556786.

Strain collection and identification

Culturing the samples on LB and Marine Agar yielded a large diversity of colonies in terms of colour, shape and morphology. A total of 100 strains were isolated and named with a code, after the location (C: Cullera, D: Dénia, V: Vinaròs) and the origin (M: Marine water, R: Rock surface). In our conditions, there was no significant fungal growth in any of the samples. The colonies observed on Marine Agar displayed the widest range of colours (wine-red, red, pink and orange, among others) in comparison with the ones observed on LB media, which were mostly yellowish and cream-coloured. Due to the known relation between the presence of pigments and antioxidant power, the main criterion for colony selection was the colour (Pawar *et al.*, 2015).

A collection of the 100 selected isolates in pure culture was established. A total of 34 isolates were initially identified through colony PCR and 16S rRNA Sanger sequencing. Although an initial step of incubation at 100°C was added to the PCR protocol of the isolates whose amplification had failed, some remained non-identified and therefore their total DNA was extracted to repeat the PCR. Finally, 56 of the isolates remained unidentified. Among the identified isolates, there were many *Bacillus* spp. (*B. oleronius*, *B. licheniformis*, *B. marisflavi*, *B. salsus* and *B. altitudinis*) and *Halobacillus* spp. (*H. trueperi* and *H. faecis*) as well as other species such as *Micrococcus antarcticus*, *Micrococcus luteus*, *Staphylococcus pasteuri*, *Vibrio tubiashii* and *Virgibacillus halodenitrificans* (Table S2).

© 2019 The Authors. *Microbial Biotechnology* published by John Wiley & Sons Ltd and Society for Applied Microbiology.,

Table 1. Top 30 most abundant genera and *P*-values for the One-Way ANOVA statistical analysis of their distributions among the three sampled locations

Taxa	*P* labelA	*P* (Tukeys) Dénia-Cullera	*P* (Tukeys) Vinaròs-Cullera	*P* (Tukeys) Vinaròs-Dénia
Rubrobacter	0.0011*	0.083	0.0096*	0.00091*
Rubricoccus	0.0018*	0.0014*	0.057	0.026*
Unclassified *Flammeovirgaceae*	0.006*	0.22	0.0051*	0.04*
Rubidimonas	0.0075*	0.58	0.0078*	0.024*
Unclassified *Erythrobacteraceae*	0.0085*	0.011*	0.018*	0.9
Unclassified *Alphaproteobacteria*	0.019*	0.052	0.02*	0.71
Unclassified *Cohaesibacteraceae*	0.021*	0.021*	0.062	0.66
Rivularia	0.026*	1	0.04*	0.038*
Unclassified *Rhodobacteraceae*	0.037*	1	0.058	0.052
Unclassified WD2101	0.039*	1	0.06	0.054
Unclassified *Chroococcales*	0.045*	0.063	0.068	1
Lewinella	0.052	1	0.073	0.075
Unclassified *Trueperaceae*	0.066	0.29	0.45	0.056
Unclassified *Phyllobacteriaceae*	0.091	0.094	0.87	0.18
Unclassified *Xenococcaceae*	0.1	0.85	0.1	0.21
Unclassified GMD14H09	0.12	1	0.17	0.16
Unclassified *Sphingomonadaceae*	0.13	0.88	0.24	0.13
Unclassified *Flavobacteriaceae*	0.13	1	0.16	0.17
B42	0.18	0.19	0.95	0.28
Unclassified *Rhodothermaceae*	0.24	0.23	0.47	0.82
Unclassified *Rhizobiales*	0.25	0.72	0.55	0.22
Chroococcidiopsis	0.28	0.4	0.3	0.97
Erythrobacter	0.28	0.29	0.42	0.95
Unclassified *Phycisphaerales*	0.32	0.29	0.66	0.73
Unclassified *Pseudanabaenaceae*	0.34	0.51	0.93	0.33
Jannaschia	0.39	0.44	0.47	1
Paracoccus	0.44	0.78	0.41	0.78
Unclassified At12OctB3	0.46	0.49	0.55	0.99
Streptococcus	0.54	0.91	0.52	0.76
Unclassified *Enterobacteriaceae*	0.77	0.91	0.75	0.95

Global *P*-values and *P*-values for the comparison by pairs is shown. Significant results are marked by an asterisk.

Antioxidant activity

In order to select and establish a collection of isolates with antioxidant properties, a high-throughput screening of the 100 isolates was performed by growing them on solid media containing H_2O_2. *Planomicrobium glaciei* and *E. coli* JM109 were used as positive and negative controls respectively. Strain JM109, with no known reports of antioxidant effect, exhibited a weak growth in the first (OD_{600} 1) and, sometimes, second dilution (OD_{600} 10^{-1}). This led us to the criterion to consider positive antioxidant producers those strains able to grow on H_2O_2-containing plates at least up to threefold dilutions (OD_{600} 10^{-2}). A total of 12 isolates were thus selected (Table 2) based on their ability to grow on 1 mM H_2O_2 plates as described above.

DPPH-based assays are widely used to detect and quantify the antioxidant power of plants or bacterial extracts. These assays are based on the decrease of DPPH absorbance at 517 nm in presence of antioxidant factors. The oxidative stress-resistant isolates selected from the H_2O_2 assay (shown in Table 2) were further tested using this method. CR17, CR21 and CR57 could not be tested due to poor growth in liquid culture, which made it impossible to obtain a concentrated extract, prepared as described in Experimental Procedures. 16S rRNA sequences were compared using NCBI BLAST tool. Isolates CR10-VR2 and CR22-CR28 were 100% identical in their 16S rRNA sequence, and therefore only one of them was selected for further assays (CR10 and CR22 respectively).

The test resulted in a general decrease in absorbance in all the samples, suggesting that the extracts were able to scavenge the DPPH. The isolates that proved more effective as antioxidants were CR22, CR24 and CR28, with values of scavenged DPPH over 30% (Fig. 4A). DR12 displayed low DPPH scavenging values maybe due to failure of the pigment extraction. Surprisingly, the control samples *P. glaciei* and JM109 did not display the expected effect. A set of three strains that had previously shown a protective effect against oxidative stress in a *Caenorhabditis elegans* model and a set of three *E. coli* strains (JM109, HB101 and DH5α) were also tested (Fig. 4D).

The two strains with the best results in the *in vitro* assays (CR22 and CR24) were selected for further *in vivo* antioxidant assays in the model organism *C. elegans,* where both proved able to display an important

© 2019 The Authors. *Microbial Biotechnology* published by John Wiley & Sons Ltd and Society for Applied Microbiology.,

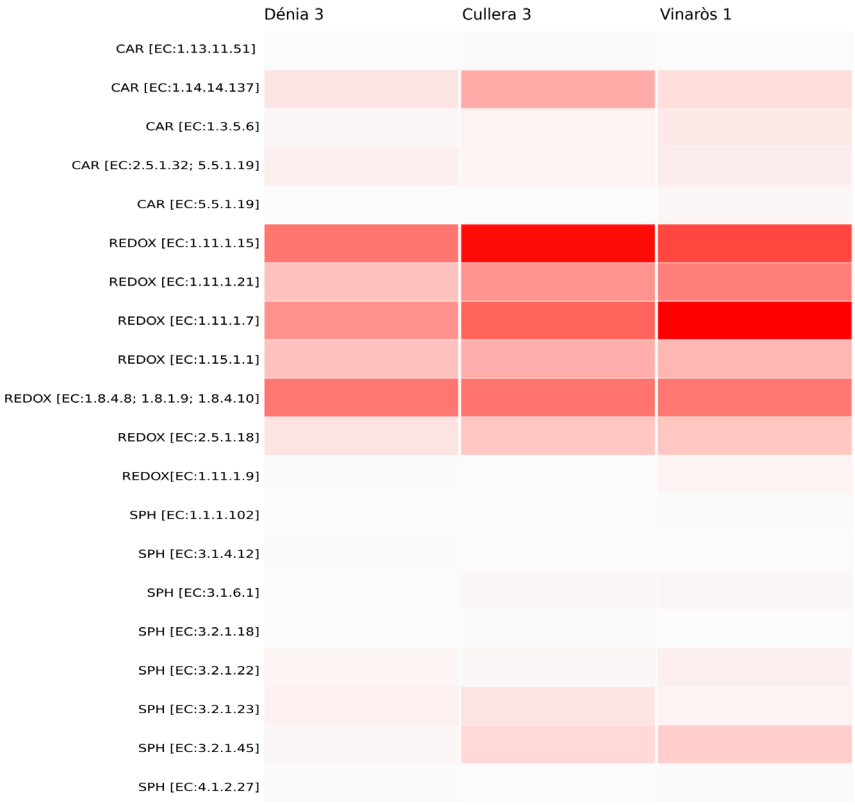

Fig. 3. Heatmap representing the functional analysis carried out through metagenomics sequencing. Enzymes related to carotenoid biosynthesis (CAR), oxidative stress (REDOX) and sphingolipid biosynthesis (SPH) are shown in the *Y*-axis.

antioxidant activity (Fig. 4B). Nematodes subjected to oxidative stress after being treated with isolates CR22 and CR24 displayed survival rates higher than the untreated worms and similar to those observed in the worms treated with vitamin C (survival rates of around 55%–65%).

Discussion

We report here, for the first time, and by using culture-dependent and independent (NGS) techniques, the microbiomes of the rocky-coastal surface of the supralittoral zone in three regions on the Mediterranean western coast. The three sampled sites, covering a coast line of about 260 km, displayed remarkably similar taxonomic profiles in terms of richness and microbial diversity, but still could perfectly be differentiated thanks to the significant difference in abundances of specific taxa, which suggest that the microbial composition of the Mediterranean supratidal zone, at least in eastern Spain, is stable but not identical within rocky locations. The studied communities were particularly dominated by bacterial strains previously described as thermophilic, halotolerant or radioresistant, such as the species within the genus *Rubrobacter* (Jurado *et al*., 2012), and pigmented isolates, as is the case of species within the *Flameovirgaceae* family, like *Tunicatimonas pelagia* and *Porifericola rhodea* (Yoon *et al*., 2011, 2012).

Truepera radiovictrix, characterized by an optimum growth temperature of 50°C and an extreme resistance to ionizing radiation, was first isolated from a hot spring in a geothermal area close to the Azores (Albuquerque *et al*., 2005; Ivanova *et al*., 2011). Moreover, the *Truepera* genus has been previously found in Lake Lucero Playa (New Mexico, USA), a particularly hostile environment as the lake dries periodically (Sirisena *et al*., 2018). This is, to the best of our knowledge, the first report of sea-inhabiting *Truepera* in a non-thermal environment, and it is tempting to hypothesize that the genus *Truepera* might have a similar ecological niche (radiation- and desiccation-resistance) than *Deinococcus*, but in saline environments, as a consequence of both its radiation resistance and halotolerance (Albuquerque *et al*., 2005).

Shotgun metagenomic analysis confirmed the similarity between the communities of the three sampled locations, as discussed above from the high-throughput 16S rRNA results, particularly at higher taxonomic (i.e. family) levels. Nevertheless, the results at lower taxonomic levels varied considerably among sequencing techniques. One of the largest differences at the species level was observed

© 2019 The Authors. *Microbial Biotechnology* published by John Wiley & Sons Ltd and Society for Applied Microbiology.,

Table 2. List of selected isolates, percentage of identity with the closest type strain, sequence similarity and results obtained in the H_2O_2 assay

Sample	Closest type strain	%	H_2O_2 Assay (dilution at which the isolate remains viable)
CR10	*Micrococcus luteus* (CP001628)	99.77	3
CR17	*Virgibacillus halodenitrificans* (AY543169)	99.58	7
CR21	Non-identified	–	4
CR22	*Virgibacillus halodenitrificans* (AY543169)	99.37	4
CR24	*Halobacillus trueperi* (AJ310349)	98.31	6
CR28	*Virgibacillus halodenitrificans* (AY543169)	100	6
CR37	*Bacillus marisflavi* (LGUE01000011)	100	4
CR44	Non-identified	–	3
CR67	*Bacillus oleronius* (X82492)	97.32	4
DM10	Non-identified	–	3
DR12	Non-identified	–	3
VR1	*Bacillus altitudinis* (ASJC011000029)	100	6
VR2	*Micrococcus luteus* (CP001628)	99.35	3
Positive control	*P. glaciei*		8
Negative control	*E. coli* (JM109)		1

within the Cyanobacterial group. In particular, high-throughput 16S rRNA revealed a large abundance of *Xennococcaceae*, whereas shotgun metagenomic sequencing revealed a more diverse population including members of *Pleurocapsa*, *Myxosarcina, Stanieria* and *Xenococcus*, as previously reported for marine environments (Burns *et al*., 2004; Alex *et al*., 2012; Yu *et al*., 2015; Brito *et al*., 2017).

The eukaryotic fraction of the samples was mainly composed of *Ascomycota*, such as *Glonium stellatum*. The genus *Glonium* includes saprophytic *Dothideomycetes* that produce darkly pigmented apothecia, which could contribute to the dark colour of the sampled rocks (Spatafora *et al*., 2012). Other species detected in the samples included as follows: *Cenococcum geophilum*, an ectomycorrhizal fungus previously described in coastal forest soils (Matsuda *et al*., 2015) and previously demonstrated to grow at up to 100 mM of NaCl (Obase *et al*., 2010); *Coniosporium apollinis*, a rock-inhabiting fungi previously isolated from the Mediterranean basin (Sterflinger *et al*., 1997); and *Lepidopterella palustris*, typically a freshwater fungus (Shearer *et al*., 2009), with this being, to the best of our knowledge, the first description of this species in a salt water habitat.

Taken together, the results obtained from both high-throughput 16S rRNA and metagenomic sequencing suggest that the sampled communities are composed of a diverse array of fungi (mainly belonging to the phylum Ascomycota), cyanobacteria (mainly *S. cyanosphaera* and *Pleurocapsa* spp., but also *Myxosarcina* spp. and *Xenococcus* spp.) and salt-adapted archaea, which remain rather stable among the three different sampled locations.

From the functional point of view, metagenomics sequencing showed abundance of enzymes involved in oxidative stress, mainly peroxidase, peroxiredoxin and thioredoxin, but also catalase and glutathione transferase. In contrast with this, enzymes involved in carotenoid or sphingolipid biosynthesis, which also play a role in the protection against oxidative stress, were less abundant and varied among locations, being abscisic acid 8′-hydroxylase (EC 1.14.14.137) in Cullera and glucosylceramidase (EC 3.2.1.45) in Vinaròs the ones with the highest values.

From the collection of cultured microorganisms, a total of 12 isolates were selected for their high antioxidant activity as measured by the oxidative stress assay performed with H_2O_2. Of those, *M. luteus* has been reported to encode genes related to resistance and tolerance to oxidative stress (superoxide dismutase and NADP reductase; Lafi *et al*., 2017). The DPPH assay was performed to dismiss false positives through the H_2O_2 assay. In general, the results correlated well with the ones previously observed in the H_2O_2 assay. It is important to note that, although DR12 displayed low scavenging in the DPPH assay, the extraction of pigments from this isolate was sub-optimal, since the pellet remained pink-coloured after the extraction process. Surprisingly, the control samples *P. glaciei* and JM109 did not display the expected effect in terms of antioxidant activity. On one hand, *P. glaciei* was expected to be one of the most antioxidant isolates, as its antioxidant activity was demonstrated in previous *in vivo* assays in *C. elegans* (Tanner *et al*., 2019) and in the H_2O_2 assay. Nevertheless, it was the worst strain in terms of DPPH scavenging. On the other hand, *E. coli* JM109, with no previous reports on antioxidant activity, resulted in high DPPH scavenging. This raises concerns on the suitability of DPPH-methods in bioprospecting for the determination of antioxidant activity and highlights the importance of using several alternative methods as the best option to have a proxy of the *in vivo* antioxidant effects. Nevertheless, the *in vivo*

© 2019 The Authors. *Microbial Biotechnology* published by John Wiley & Sons Ltd and Society for Applied Microbiology.,

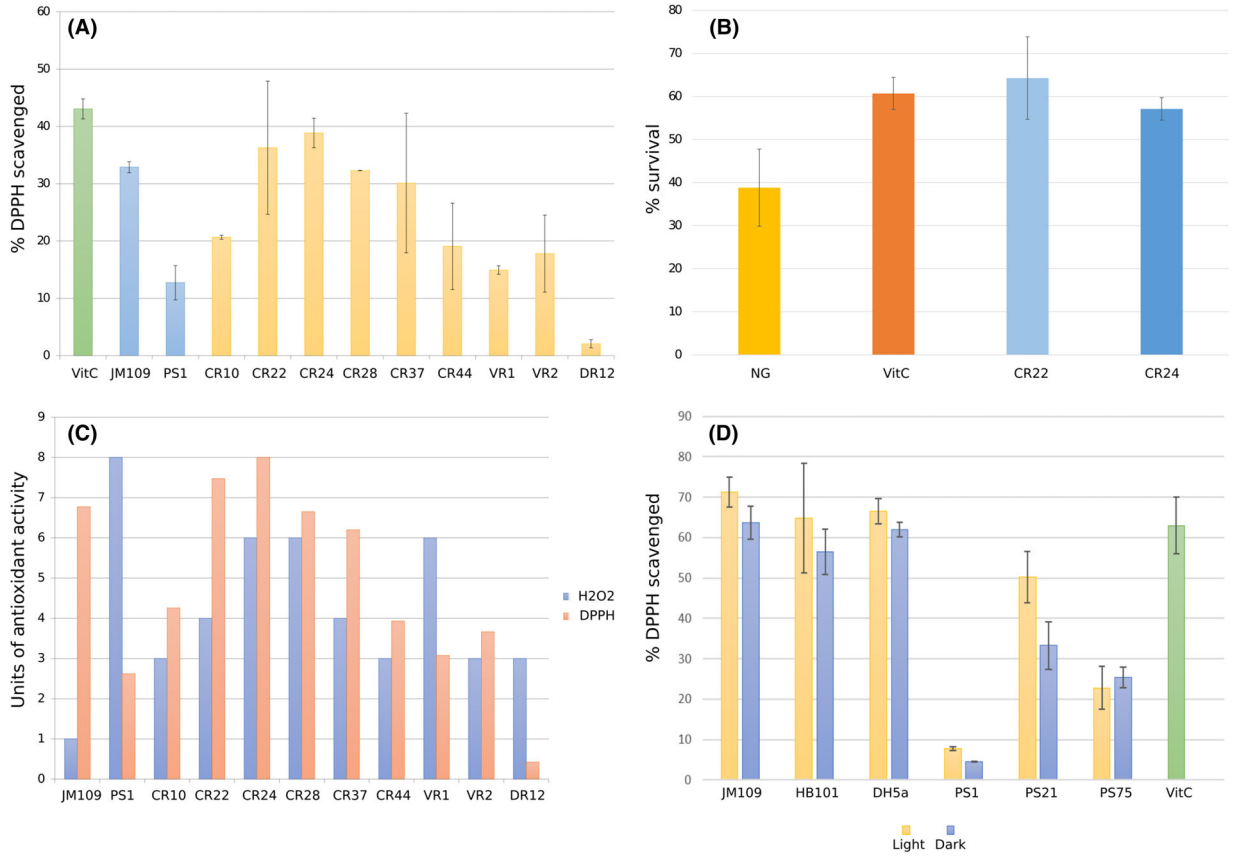

Fig. 4. (A) Antioxidant activity as measured through DPPH assay as described in EP. Absorbance was measured at 517 nm after 30 min of incubation with DPPH 50 μM. DPPH scavenged (%) is represented in *Y*-axis. VitC, vitamin C (0.5 μg ml^{-1} solution). (B) Antioxidant activity *in vivo* (using the model organism *C. elegans*). *Y*-axis indicates percentage of surviving worms after 5 h of incubation under oxidative stress (H_2O_2). Worms were treated with either a control diet (NG), a diet supplemented with the known antioxidant vitamin C as a positive control (VitC), or a diet supplemented with the selected strains CR22 and CR24. (C) Comparative analysis of the results obtained with H_2O_2 and DPPH assays. Values in *Y*-axis are normalized with respect to the highest value obtained in both assays. (D) DPPH assay with positive and negative controls. Absorbance was measured at 517 nm after 30 min of incubation with DPPH 50 μM. DPPH scavenged percentage is represented in *Y*-axis. VitC, Vitamin C, 0.5 μg ml^{-1} solution. Light and dark conditions are represented.

antioxidant assay performed in *C. elegans* allowed to confirm the antioxidant activity detected in the DPPH and H_2O_2 tests. Specifically, CR22 and CR24 displayed an antioxidant activity similar to the one observed in Vitamin C (Fig. 4B).

In general, though, the correlation between both methods was good, as the isolates with higher survival in the presence of H_2O_2 also displayed higher DPPH-scavenging ability (Fig. 4C). Nevertheless, there were some isolates that displayed different results depending on the method, in particular VR1 and CR37. Differences in VR1 could be the result of catalase activity, which may have enhanced its growth on the H_2O_2-supplemented plates. On the contrary, differences between both methods for CR37 could be caused by a deficient growth in solid medium. Once again, these results highlight the limitation of using a single screening technique for the selection of microbial strains with antioxidant activities.

A collection of both positive and negative controls (in terms of theoretical antioxidant activity) were tested using both assays (H_2O_2 and DPPH). PS1, PS21 and PS75 (*P. glaciei* 423, 97.38% ID; *Rhodobacter maris* JA276, 98.89% ID; and *Bacillus megaterium* NBRC 15308, 100% ID respectively) were the three control strains selected, all of them recovered from solar panels and previously tested in *C. elegans* for *in vivo* protection against oxidative stress (Tanner *et al.*, 2019). Three different strains of *E. coli* were chosen as negative controls (JM109, BH101, DH5α). For the DPPH assay, the isolates were grown under both light and dark conditions, in order to determine whether the light had a negative impact on the production of pigments or other antioxidant factors, as it is known that many pigments, particularly carotenoids, are prone to photodegradation (Boon *et al.*, 2010). For the *E. coli* strains, no significant differences were observed between growth in dark and light

© 2019 The Authors. *Microbial Biotechnology* published by John Wiley & Sons Ltd and Society for Applied Microbiology.,

conditions, whereas PS21 proved very sensitive to light (Fig. 4D). Moreover, the scavenging effect of the JM109 strain was also observed in the other two *E. coli* strains, confirming that the extracts obtained from *E. coli* contain compounds that are indeed able to react with DPPH. Even though *R. maris* and *B. megaterium* displayed better antioxidant properties than *P. glaciei*, which was again comparable to the negative control of methanol, they yielded lower DPPH-based activity than *E. coli* strains.

The biotechnological potential of extremophiles is well known, and saline environments are no exception to this rule (de Lourdes Moreno *et al*., 2013). However, and in contrast with the well-studied intertidal zone (Mitra *et al*., 2014), the supralittoral zone has been poorly studied to date. Interestingly, this zone experiences much higher selection pressures than the intertidal zone since while the intertidal zone is basically a marine environment which is only transiently and partially exposed to land conditions, the supralittoral zone forces organisms to adapt to a sea/land intermediate habitat where both marine and land stresses are present.

This work is the first holistic (using culture-dependent, culture-independent and biological activity assays) approach studying the microbial ecology and biotechnological potential, in terms of antioxidant properties, of the supralittoral zone of the Mediterranean rocky shore. Our results suggest that the western coastline of the Mediterranean Sea harbours a stable microbial community that is conserved among different locations, with cyanobacteria as the majoritarian bacterial taxon, followed by members of the *Flameovirgaceae* family and members of the *Rubrobacter* genus, as well as eukaryotic and archaeal members, such *Ascomycota* and halotolerant archaea. Furthermore, *in vitro* and *in vivo* assays demonstrate that this environment is a potential source of microorganisms with antioxidant activities that could hold potential for a wide range of applications in the food, cosmetic or pharmacological industries.

Experimental procedures

Sampling

Samples were collected from three different locations on the Mediterranean Western coast, in Eastern Spain: Vinaròs (Castelló), Cullera (València) and Dénia (Alacant). Three samples of dark-stained rock, at least two metres apart from each other and thus considered as biological replicates, were collected from the supralittoral (splash) zone of each location by scraping the surface with a sterile blade. Samples of the adjacent marine water were also taken, and both types of samples (scrapped rock and sea water samples) were separately stored in Falcon tubes in 15% glycerol, transported to the laboratory on ice and then stored at −20°C until required.

High-throughput rRNA and metagenomic sequencing

Total DNA was isolated from the samples with the PowerSoil DNA Isolation kit (MO BIO laboratories, Carlsbad, CA, USA) following the manufacturer's instructions. The quantity and quality of the isolated DNA was assessed using a Nanodrop-100 Spectrophotometer (Thermo Scientific, Wilmington, DE, USA) and purified DNA samples were sequenced by Life Sequencing SL (València, Spain). On one hand, the hypervariable V3-V4 regions of the 16S rRNA gene was amplified as described by Klindworth *et al*. (2013) and sequenced on the high-throughput NextSeq 500 (Illumina) platform. Greengenes database was used for the taxonomic analysis. The statistical analysis was carried out with Calypso web tool (version 8.84; http://cgenome.net). The statistical comparison of the relative abundances between locations at the genus level was calculated through One-Way Anova test (Tables 1 and S1). Richness and Shannon index box plots, PCoA, relative abundances clustering and rarefaction curve were also constructed with Calypso.

On the other hand, shotgun metagenomic sequencing was performed on the NextSeq500 Illumina platform, with paired-end sequences and reads of 150 base pairs. The obtained sequences were filtered by using 'BBtools' version 37.28 (https://jgi.doe.gov/data-and-tools/bbtools/) in order to avoid ends holding quality values under the Q20 standards. Lectures coming from human contamination were also dismissed by mapping them against the reference human genome (GRCh37d5) version 0.7.15. Assembly was carried out with 'SPAdes' (Bankevich *et al*., 2012) version 3.9. ORFs prediction was carried out by 'MegaGeneMArk' (Zhu *et al*., 2010) version 3.38 and rRNA prediction, by 'RNAmmer' (Lagesen *et al*., 2007) version 1.2. Functional annotation of the predicted CDS was carried out with *BLAST2go* (Conesa *et al*., 2005) version 4.1.9.

The Clustergrammer on-line software (Fernández *et al*., 2017) was used for the functional analysis heatmap construction, by using a correlation type distance and average linkage.

Isolation and identification of bacterial strains

Three different growth media were used for this study: Lysogenic Broth (LB, composition in g l^{-1}: 10 tryptone, 10 NaCl, 5.0 yeast extract, 15 agar); Reasoner's 2A agar (R2A, composition in g l^{-1}: peptone 0.5, casaminoacids 0.5, yeast extract 0.5, dextrose 0.5, soluble starch 0.5, K_2HPO_4 0.3, $MgSO_4$ 0.05, sodium pyruvate 0.3, 15 agar); and Marine Agar (composition in g l^{-1}: peptone 5.0, yeast extract 1.0, ferric citrate 0.1, NaCl 19.45, $MgCl_2$ 5.9, Na_2SO_4 3.24, $CaCl_2$ 1.8, KCl 0.55,

© 2019 The Authors. *Microbial Biotechnology* published by John Wiley & Sons Ltd and Society for Applied Microbiology.,

$NaHCO_3$ 0.16, KBr 0.08, $SrCl_2$ 0.034, H_3BO_3 0.022, Na_4O_4Si 0.004, NaF 0.024, NH_4NO_3 0.0016, Na_2HPO_4 0.008, 15 agar). The scraped rock samples were homogenized in the Falcon tube by vigorously mixing with a vortex, and serial dilutions were cultured on the different media and incubated at room temperature for 7 days. Marine water samples were also cultured in the same conditions. After 1 week of incubation, individual colonies were selected based on colony pigmentation and isolated by independent re-streaking on fresh medium. Pure cultures were then cryo-preserved at −80°C in 20% glycerol (vol:vol) until required.

Colony PCR and, were needed, DNA extracts of each of the isolated strains, were used for taxonomic identification through 16S rRNA gene sequencing using universal primers 28F (5′-GAG TTT GAT CNT GGC TCA G-3′) and 519R (5′-GTN TTA CNG CGG CKG CTG-3′). Colony PCR was performed with an initial step of incubation at 95°C for 5 min to lyse cells followed by PCR amplification (30 cycles of 30 s at 95°C, 30 s at 54°C, 30 s at 72°C, followed by 10 min at 72°C). The DNA extraction was done following the Latorre *et al*. (1986) protocol. Amplifications were verified by electrophoresis in a 0.8% agarose gel and then amplicons were precipitated overnight in isopropanol 1:1 (vol:vol) and potassium acetate 1:10 (vol:vol; 3 M, pH 5). DNA pellets were washed with 70% ethanol and resuspended in 30 μl Milli-Q water. BigDye® Terminator v3.1 Cycle Sequencing Kit (Applied Biosystems, Carlsbad, CA, USA) was used to tag amplicons, which were sequenced with the Sanger method by the Sequencing Service (SCSIE) of the University of Valencia (Spain). All sequences were manually edited with Pregap4 (Staden Package, 2002) to eliminate low-quality base calls, and final sequences were compared by EzBioCloud 16S tool (https://sourceforge.net/projects/staden/).

Antioxidant activity

Hydrogen peroxide assay. The collection of isolates was initially screened for antioxidant activity by applying oxidative stress to the isolated colonies through the addition of hydrogen peroxide (H_2O_2) to the growth medium. In order to do so, isolates were grown on solid media for 4 days or until reaching enough biomass. Then, the optical density at 600 nm (OD_{600}) was measured, adjusted to a value of 1, and serial dilutions prepared up to seven times fold. Two microlitres of each dilution were placed on a LB or Marine Agar place, to which 1 mM H_2O_2 had been previously added. The plates were incubated at room temperature and in the dark to avoid degradation of the H_2O_2, and results were recorded after two, four and six days. Two strains were used as controls for the assay: PS1 (*Planomicrobium glaciei* 423, 97.38% ID) and *Escherichia coli* JM109 as a positive and negative control for antioxidant activity respectively. *Planomicrobium glaciei* is a pigmented microorganism whose antioxidant activity has previously been reported *in vivo* using a *Caenorhabditis elegans* model (Tanner *et al*., 2019).

DPPH assay. Since the H_2O_2 assay can result in false-positive results due to catalase activity, a second assay using 2,2-diphenyl-1-picrylhydrazyl (DPPH) was performed to dismiss false positives in the H_2O_2 assay and to confirm the antioxidant activity of the selected strains (the ones with the best antioxidant activity according to the previous assay). Pigments were extracted from the isolates based on the protocols described by Brand-Williams *et al*. (1995), von Gadow *et al*. (1997) and Su *et al*. (2015), with the modifications suggested by Sharma and Bhat (2009). Briefly, the isolates were grown overnight in liquid LB medium and OD_{600} was measured and normalized at a value of 1.2. Cells were then harvested by centrifugation at 11,300 *g* for 3.5 min, and the pellets resuspended in 500 μL of methanol, vigorously vortexed and sonicated for 5 min (Ultrasonic bath XUBA1, Grant Instruments, Royston, UK). The supernatant was collected after centrifugation at 11,300 *g* for 3 min and kept in the dark until the assay was performed. The extraction was repeated as described until a colourless pellet was obtained.

For the DPPH assay, 600 μl of the extract in methanol were mixed with 400 μl of DPPH solution (50 μM in methanol) and incubated for 30 min in the dark. The negative control sample consisted of DPPH mixed with methanol. Absorbance was measured at 517 nm (Ultrospec 200 UV/V Visible Spectrophotometer, Pharmacia Biotech, Piscataway Township, NJ, USA).

A standard curve with a control antioxidant, ascorbic acid (vitamin C) was performed at 10, 5, 1, 0.5, 0.1, 0.05 and 0.01 μg ml^{-1} concentrations in methanol. The detection threshold was established at 0.5 μg ml^{-1} of vitamin C, as lower concentrations of vitamin C did not change DPPH absorbance (data not shown).

DPPH scavenging ability was quantified by measuring the decrease in the absorbance of this compound at 517 nm, and the percentage of scavenged DPPH was calculated using the following formula:

$$\%\,\mathrm{DPPH} = \left(1 - \frac{\mathrm{Abs\,517\,Extract}}{\mathrm{Abs\,517\,Control}}\right) \times 100.$$

In vivo *oxidative stress assays with* C. elegans

Wild-type *C. elegans* strain N2 (Bristol, UK) was routinely propagated at 20°C on Nematode Growth Medium

© 2019 The Authors. *Microbial Biotechnology* published by John Wiley & Sons Ltd and Society for Applied Microbiology.,

(NGM) plates supplemented with *E. coli* strain OP50 as the regular food source.

Nematodes were synchronized by isolating eggs from gravid adults at 20°C. Synchronization was performed on NGM plates with different treatments: *E. coli* OP50 was supplied as a negative control; *E. coli* OP50 plus vitamin C (vitC) at 10 $\mu g\ ml^{-1}$ as a positive control; and, finally, *E. coli* OP50 plus one of the selected isolates was used in order to test the effect of administrating the selected strains. Duplicates were performed for every condition. Bacterial strains were grown overnight in liquid LB medium at 28°C and 11,300 *g*. Then, OD_{600} was adjusted to 30 and 50 μl of the bacterial suspension were added to the plates.

The synchronized worms were incubated for 3 days on the previously described plates, until reaching young adult stage. Then, young adult worms were selected for each treatment ($n = 50$) and incubated at 20°C on the corresponding treatment, until reaching 5-day adult stage. The selected worms were then transferred to plates containing basal medium supplemented with 2 mM H_2O_2 and incubated for 5 h at 20°C. After incubation, survival rates for each condition (negative control, positive control and bacteria-fed worms) were recorded by manually counting the number of living versus dead worms.

Acknowledgements

We thank Adriel Latorre and Darwin Bioprospecting Excellence S.L. (Valencia, Spain) for their assistance with the bioinformatic analysis. We thank ADM-Biopolis S.L. for granting us access to their laboratory and materials for the *C. elegans* assays.

Conflict of interest

The authors declare no conflict of interest.

Author contributions

MP conceived the work. MP, KT and EMM collected the samples. EMM, KT and ÀVV performed the culture-based characterization, and KT carried out the bioinformatic analysis. All authors (MP, KT, ÀVV, EMM and JP) analysed the results, wrote and approved the manuscript.

References

Albuquerque, L., Simoes, C., Nobre, M.F., Pino, N.M., Battista, J.R., Silva, M.T., *et al*. (2005) *Truepera radiovictrix* gen. nov., sp. nov., a new radiation resistant species and the proposal of *Trueperaceae* fam. nov. *FEMS Microbiol Lett* **247:** 161–169.

Alex, A., Vasconcelos, V., Tamagnini, P., Santos, A., and Antunes, A. (2012) Unusual symbiotic cyanobacteria association in the genetically diverse intertidal marine sponge *Hymeniacidon perlevis* (demospongiae, halichondrida). *PLoS ONE* **7:** e51834.

Alonso-Gutiérrez, J., Figueras, A., Albaigés, J., Jiménez, N., Viñas, M., Solanas, A.M., and Novoa, B. (2009) Bacterial communities from shoreline environments (Costa da Morte, northwestern Spain) affected by the prestige oil spill. *Appl Environ Microbiol* **75:** 3407–3418.

Bankevich, A., Nurk, S., Antipov, D., Gurevich, A.A., Dvorkin, M., Kulikov, A.S., *et al*. (2012) SPAdes: a new genome assembly algorithm and its applications to single-cell sequencing. *J Comput Biol* **19:** 455–477.

Boon, C.S., McClements, D.J., Weiss, J., and Decker, E.A. (2010) Factors influencing the chemical stability of carotenoids in foods. *Crit Rev Food Sci Nutr* **50:** 515–532.

Brandes, M., Albach, D.C., Vogt, J.C., Mayland-Quellhorst, E., Mendieta-Leiva, G., Golubic, S., *et al*. (2015) Supratidal extremophiles-Cyanobacterial diversity in the rock pools of the Croatian Adria. *Microb Ecol* **70:** 876–888.

Brand-Williams, W., Cuvelier, M., and Berset, C. (1995) Use of a free radical method to evaluate antioxidant activity. *Lebensmittel-Wissenschaft Technol* **28:** 25–30.

Brito, A., Ramos, V., Mota, R., Lima, S., Santos, A., Vieira, J., *et al*. (2017) Description of new genera and species of marine *Cyanobacteria* from the Portuguese Atlantic coast. *Mol Phylogenet Evol* **111:** 18–34.

Burns, B.P., Goh, F., Allen, M., and Neilan, B.A. (2004) Microbial diversity of extant stromatolites in the hypersaline marine environment of Shark Bay, Australia. *Environ Microbiol* **6:** 1096–1101.

Chan, B.K., Chan, W.K., and Walker, G. (2003) Patterns of biofilm succession on a sheltered rocky shore in Hong Kong. *Biofouling*. **19:** 371–380.

Chien, A., Edgar, D.B., and Trela, J.M. (1976) Deoxyribonucleic acid polymerase from the extreme thermophile *Thermus aquaticus*. *J Bacteriol* **127:** 1550–1557.

Conesa, A., Götz, S., García-Gómez, J.M., Terol, J., Talón, M., and Robles, M. (2005) Blast2GO: a universal tool for annotation, visualization and analysis in functional genomics research. *Bioinformatics* **21:** 3674–3676.

Dorado-Morales, P., Vilanova, C., Peretó, J., Codoñer, F. M., Ramón, D., and Porcar, M. (2015) A highly diverse, desert-like microbial biocenosis on solar panels in a Mediterranean city. *Sci Rep-UK* **6:** 29235.

Fernández, N.F., Gundersen, G.W., Rahman, A., Grimes, M.L., Rikova, K., Hornbeck, P., and Ma'ayan, A. (2017) Clustergrammer, a web-based heatmap visualization and analysis tool for high-dimensional biological data. *Scientific Data* **4:** 170151.

Fuciños, P., González, R., Atanes, E., Sestelo, A.B., Pérez-Guerra, N., Pastrana, L., *et al*. (2012) Lipases and esterases from extremophiles: overview and case example of the production and purification of an esterase from *Thermus thermophilus* HB27. *Methods Mol Biol* **861:** 239–266.

von Gadow, A., Elizabeth, J., and Hansmann, C. (1997) Comparison of the antioxidant activity of aspalathin with that of other plant phenols of rooibos tea (*Aspalathus linearis*), r-tocopherol, BHT, and BHA. *J Agric Food Chem* **45:** 632–638.

© 2019 The Authors. *Microbial Biotechnology* published by John Wiley & Sons Ltd and Society for Applied Microbiology.,

Ivanova, N., Rohde, C., Munk, C., Nolan, M., Lucas, S., Rio, T.G., *et al*. (2011) Complete genome sequence of *Truepera radiovictrix*. *Stan Genomic Sci* **4:** 91–96.

Jurado, V., Miller, A., Alias-Villegas, C., Laiz, L., and Saiz-Jimenez, C. (2012) *Rubrobacter bracarensis* sp. nov., a novel member of the genus *Rubrobacter* isolated from a biodeteriorated monument. *Syst Appl Microbiol* **35:** 306–309.

Klindworth, A., Pruesse, E., Schweer, T., Peplies, J., Quast, C., Horn, M., *et al*. (2013) Evaluation of general 16S ribosomal RNA gene PCR primers for classical and next generation sequencing-based diversity studies. *Nucleic Acids Res* **41:** e1.

Kumar, V.B.N., Kampe, B., Rösch, P., and Popp, J. (2015) Characterization of carotenoids in soil bacteria and investigation of their photo degradation by UVA radiation via resonance Raman spectroscopy. *Analyst* **140:** 4584–4593.

Lafi, F.F., Ramírez-Prado, J.S., Alam, I., Bajic, V.B., Hirt, H., and Saad, M.M. (2017) Draft genome sequence of plant growth-promoting *Micrococcus luteus* strain K39 isolated from *Cyperus conglomeratus* in Saudi Arabia. *Genome Announc* **5:** pii: e01520-16.

Lagesen, K., Hallin, P.F., Rødland, E., Stærfeld, H.H., Rognes, T., and Ussery, D.W. (2007) RNAmmer: consistent annotation of rRNA genes in genomic sequences. *Nucleic Acids Res* **35:** 3100–3108.

Langenheder, S., and Ragnarsson, H. (2007) The role of environmental and spatial factors for the composition of aquatic bacterial communities. *Ecology* **88:** 2154–2161.

Latorre, A., Moya, A., and Ayala, F. (1986) Evolution of mitochondrial DNA in *Drosophila subobscura*. *P Natl Acad Sci* **83:** 8649–8653.

de Lourdes Moreno, M., Pérez, D., García, M.T., and Mellado, E. (2013) Halophilic bacteria as a source of novel hydrolytic enzymes. *Life (Basel)* **3:** 38.

Matsuda, Y., Takeuchi, K., Obase, K., and Ito, S. (2015) Spatial distribution and genetic structure of *Cenococcum geophilum* in coastal pine forests in Japan. *FEMS Microbiol Ecol* **91:fiv108.**

Mitra, S., Sana, B., and Mukherjee, J. (2014) Ecological roles and biotechnological applications of marine and intertidal microbial biofilms. *Adv Biochem Eng Biotechnol* **146:** 163–205.

Nishimura, H., and Sako, Y. (2009) Purification and characterization of the oxygen-thermostable hydrogenase from the aerobic hyperthermophilic archaeon *Aeropyrum camini*. *J Biosci Bioeng* **108:** 299–303.

Obase, K., Lee, J.K., Lee, S.K., Lee, S.Y., and Chun, K.W. (2010) Variation in sodium chloride resistance of *Cenococcum geophilum* and *Suillus granulatus* isolates in liquid culture. *Mycobiology* **38:** 225–228.

Pawar, R., Mohandass, C., Sivaperumal, E., Sabu, E., Rajasabapathy, R., and Jagtap, T. (2015) Epiphytic marine pigmented bacteria: a prospective source of natural antioxidants. *Braz J Microbiol* **46:** 29–39.

Pentecost, A. (2014) Distribution and ecology of cyanobacteria in the rocky littoral of an English lake district water body, devoke water. *Life (Basel)* **4:** 1026–1037.

Pinedo, S., García, M., Satta, M.P., and de Torres,, M., Ballesteros, E. (2007) Rocky-shore communities as indicators of water quality: a case study in the Northwestern Mediterranean. *Mar Pollut Bull* **55:** 126–135.

Raddadi, N., Cherif, A., Daffonchio, D., Neifar, M., and Fava, F. (2015) Biotechnological applications of extremophiles, extremozymes and extremolytes. *Appl Microbiol Biotechnol* **99:** 7907.

Sandmann, G. (2015) Carotenoids of biotechnological importance. *Adv Biochem Eng Biot* **148:** 449–467.

Sharma, O.P., and Bhat, T.K. (2009) DPPH antioxidant assay revisited. *Food Chem* **113:** 1202–1205.

Shearer, C.A., Raja, H. A., Miller, A.N., Nelson, P., Tanaka, K., Hirayama, K., *et al*. (2009) The molecular phylogeny of freshwater *Dothideomycetes*. *Stud Mycol* **64:** 145–153.

Shindo, K., and Misawa, N. (2014) New and rare carotenoids isolated from marine bacteria and their antioxidant activities. *Mar Drugs* **12:** 1690–1698.

Sirisena, K.A., Ramírez, S., Steele, A., and Glamodija, M. (2018) Microbial diversity of hypersaline sediments from lake Lucero playa in white sands national monument, New Mexico, USA. *Microb Ecol* **76:** 404–418.

Spatafora, J.W., Owensby, C.A., Douhan, G.W., Boehm, E.W., and Schoch, C.L. (2012) Phylogenetic placement of the ectomycorrhizal genus *Cenococcum* in *Gloniaceae* (*Dothideomycetes*). *Mycologia* **104:** 758–765.

Sterflinger, K., De Baere, R., de Hoog, G.S., De Wachter, R., Krumbein, W.E., and Haase, G. (1997) *Coniosporium perforans* and *C. apollinis*, two new rock-inhabiting fungi isolated from marble in the Sanctuary of Delos (Cyclades, Greece). *Antonie Van Leeuwenhoek* **72:** 349–363.

Su, J., Wang, T., Li, Y.-Y., Li, J., Zhang, Y., Wang, Y., *et al*. (2015) Antioxidant properties of wine lactic acid bacteria: *Oenococcus oeni*. *Appl Microbiol Biotechnol* **99:** 5189–5202.

Tanner, K., Vilanova, C., and Porcar, M. (2017) Bioprospecting challenges in unusual environments. *Microb Biotechnol* **10:** 671–673.

Tanner, K., Martí, J.M., Belliure, J., Fernández-Méndez, M., Molina-Menor, E., Peretó, J., and Porcar, M. (2018) Polar solar panels: arctic and Antarctic microbiomes display similar taxonomic profiles. *Env Microbiol Rep* **10:** 75–79.

Tanner, K., Martorell, P., Genovés, S., Ramón, D., Zacarías, L., Rodrigo, M.J., *et al*. (2019) Bioprospecting the solar panel microbiome: high-throughput screening for antioxidant bacteria in a *Caenorhabditis elegans* model. *Front Microbiol* **10:** 986.

Tian, B., and Hua, Y. (2010) Carotenoid biosynthesis in extremophilic *Deinoccocus-Thermus* bacteria. *Trends Microbiol* **18:** 512–520.

Yoon, J., Oku, N., Park, S., Kasai, H., and Yokota, A. (2011) *Porifericola rhodea* gen. nov., sp. nov., a new member of the phylum *Bacteroidetes* isolated by the bait-streaked agar technique. *Antonie Van Leeuwenhoek* **100:** 145–153.

Yoon, J., Oku, N., Park, S., Katsuta, A., and Kasai, H. (2012) *Tunicatimonas pelagia* gen. nov., sp. nov., a novel representative of the family *Flammeovirgaceae* isolated from a sea anemone by the differential growth screening method. *Antonie Van Leeuwenhoek* **101:** 133–140.

Yu, C.H., Lu, C.K., Su, H.M., Chiang, T.Y., Hwang, C.C., Liu, T., and Chen, Y.M. (2015) Draft genome of

© 2019 The Authors. *Microbial Biotechnology* published by John Wiley & Sons Ltd and Society for Applied Microbiology.,

Myxosarcina sp. strain GI1, a baeocytous cyanobacterium associated with the marine sponge *Terpios hoshinota*. *Stand Genomic Sci* **10:** 28.
Zhu, W., Lomsadze, A., and Borodovsky, M. (2010) *Ab initio* gene identification in metagenomic sequences. *Nucleic Acids Res* **38:** e132.

Supporting information

Additional supporting information may be found online in the Supporting Information section at the end of the article.

Fig. S1. Rarefaction curve at OTU level.
Fig. S2. Main bacterial (A), archaeal (B) and eukaryotic (C) groups identified in the sample obtained from Vinaròs and analysed through metagenomics sequencing.
Fig. S3. Main bacterial (A), archaeal (B) and eukaryotic (C) groups identified in the sample obtained from Cullera and analysed through metagenomics sequencing.
Fig. S4. Main bacterial (A), archaeal (B) and eukaryotic (C) groups identified in the sample obtained from Dénia and analysed through metagenomics sequencing.

Table S1. Top 30 most significant genera and *P*-values for the One-Way ANOVA statistical analysis of their distributions among the three sampled locations. Global *P*-values and *P*-values for the comparison by pairs is shown. Significant results are marked by an asterisk.
Table S2. List of the strains identified in the collection, with the closest type strain, accession number, ID percentage and the GenBank accession number for the 16S rRNA sequences. The identification code of the strains corresponds to the location from which it was isolated (V: Vinaròs, C: Cullera, D: Dènia), the sample type (R: rock, M: marine water) and a number.

© 2019 The Authors. *Microbial Biotechnology* published by John Wiley & Sons Ltd and Society for Applied Microbiology.,

Science & Society

OPEN ACCESS

EMBO reports

The long journey towards standards for engineering biosystems

Are the Molecular Biology and the Biotech communities ready to standardise?

Jacob Beal[1], Angel Goñi-Moreno[2,3], Chris Myers[4], Ariel Hecht[5], María del Carmen de Vicente[6], Maria Parco[7], Markus Schmidt[8], Kenneth Timmis[9], Geoff Baldwin[10], Steffi Friedrichs[11], Paul Freemont[10], Daisuke Kiga[12], Elena Ordozgoiti[13], Maja Rennig[14], Leonardo Rios[15], Kristie Tanner[16], Víctor de Lorenzo[17] & Manuel Porcar[18]

Standards are the basis of technology: they allow rigorous description and exact measurement of properties, reliable reproducibility and a common "language" that enables different communities to work together. Molecular biology was in part created by physicists; yet, the field did not inherit the focus on the quantitation, the definition of system boundaries and the robust, unequivocal language that is characteristic of the other natural sciences. However, synthetic biology (SynBio) increasingly requires scientific, technical, operational and semantic standards for the field to become a full-fledged engineering discipline with a high level of accuracy in the design, manufacturing and performance of biological artefacts. Although the benefits of adopting standards are clear, the community is still largely reluctant to accept them, owing to concerns about adoption costs and losses in flexibility.

> *"... Synthetic Biology (SynBio) increasingly requires scientific, technical, operational and semantic standards for the field to become a full-fledged engineering discipline ..."*

What standards are good for

In science and technology, the terms *standard* and *standardisation* describe different things: shared semantic and graphical languages for annotating the nature and the properties of systems and their components; the definition of units of relevant properties and parameters along with methods to calculate them; specifications of properties and arrangements for the physical assembly of the components of a system; and unambiguous protocols for the construction of objects. Such standards enable an abstract and precise description of a system with a suitable—also standardised—quantitative language or equivalent methods of representation.

Beyond their important role in the natural sciences, standards were also one of the key drivers for the industrial revolution as they enabled a seamless integration of product design, fabrication of its components and the final assembly—let alone tracing parts and helping to sort out matters of safety and intellectual property. Standards are for instance imperative for designing electronic circuits built from well-defined, universal simple components, such as resistors, diodes and transistors, or for software engineering that uses precompiled modules and functions. Standards enabled the rapid rise of the

1 Raytheon BBN Technologies, Cambridge, MA, USA
2 School of Computing, Newcastle University, Newcastle upon Tyne, UK
3 Centro de Biotecnología y Genómica de Plantas, (CBGP, UPM-INIA), Universidad Politécnica de Madrid, Pozuelo de Alarcón, Spain
4 University of Utah, Salt Lake City, UT, USA
5 Ginkgo Bioworks, Inc., Boston, MA, USA
6 European Commission, Directorate General for Research and Innovation, Brussels, Belgium
7 IN Srl, Udine, Italy
8 Biofaction, Wien, Austria
9 Institute of Microbiology, Technical University Braunschweig, Braunschweig, Germany
10 Imperial College, London, UK
11 AcumenIST, Brussels, Belgium
12 Waseda University, Tokyo, Japan
13 Asociación Española de Normalización (UNE), Madrid, Spain
14 Novo Nordisk Foundation Center for Biosustainability, Technical University of Denmark, Lyngby, Denmark
15 Institute for Bioengineering and Centre for Synthetic and Systems Biology, University of Edinburgh, Edinburgh, UK
16 Darwin Bioprospecting Excellence, Paterna, Spain
17 Centro Nacional de Biotecnología (CNB) CSIC, Madrid, Spain
18 Institute for Integrative Systems Biology, University of Valencia, Paterna, Spain
DOI 10.15252/embr.202050521 | The EMBO Reports (2020) 21: e50521 | Published online 26 April 2020

© 2020 The Authors. Published under the terms of the CC BY NC ND 4.0 license

personal computer industry in the 1980s and 1990s by interlinking standard components such as hard discs, memory or keyboards through standardised interfaces and protocols.

"... standards were also one of the key drivers for the industrial revolution as they enabled a seamless integration of product design, fabrication of its components and the final assembly..."

From software to nuts and bolts, the concept of a universally usable toolbox of parts to assemble more complex systems is typical for every discipline of engineering: electronics, software, mechanical design, architecture, chemical synthesis and so on. Standards enable people to work together through interoperability, coordination of labour, reproducibility and reuse of other people's efforts and achievements.

Standards must be reliable, robust and affordable, but, first and foremost, they must be agreed on by their users. Indeed, standardisation—the process of implementing and developing technical standards—requires the consensus of many different parties, such as private and public companies, organisations and policy makers. Standardisation can be driven by public acceptance/market forces (*de facto* standards), directly ordained by law (*de jure* standards) or, most commonly, arise from the combination of legal/technical requirements and recognition by potential operators since, in general, the broader the applicability of a format, the greater its market [1].

Standards in the life sciences

That said, the core standardisation process in many scientific and engineering disciplines took place decades to centuries ago, but it is still in its infancy in the life sciences. Interestingly, it is still a bottleneck for even well-developed technologies: smartphones, for instance, still lack standard key components such as batteries or electric charger cables (see e.g. https://ec.europa.eu/info/law/better-regulation/initiatives/ares-2018-6427186_en).

In this context, the conceptual frame of synthetic biology aims to making biology easier to engineer by applying principles such as modularity, orthogonality, chain production and reproducibility. Moreover, the rapid advances in wet and computational tools for genome editing, metabolic design and *in silico* modelling are opening new opportunities for genetic programming that could not have been anticipated even just a few years ago, and allow engineers to tackle increasingly complex engineering objectives. The growing demand for scaling up such technologies raises the issue of what is needed to make them work at an industrial scale [2]. Following the path of other branches of engineering, the establishment of standards appears among the key objectives of contemporary SynBio—and eventually of the life sciences as a whole—as a prerequisite for applications such as bioremediation, biomedicine, bioenergy, novel chemicals, innovative materials and cellular factories.

Although standards in SynBio have contributed to successes such as the synthesis of artemisinin or morphine (both in yeast), the problem of defining common standards is still far from being resolved. The reusability patterns of the iGEM parts database [3], the context dependence of biological components [4], the variable behaviour among strains, genetic stability or even the contested philosophical analogy between cells and machines are by no means solved issues at this point. However, there is no doubt that even partial progress on standardisation would have major consequences for bioengineering.

One bottleneck is the widespread and incorrect assumption among many researchers in the life sciences that standards may increase interoperability but necessarily limit flexibility—which is obviously important for any creative research. Rather, good standards will increase people's flexibility and creativity because it will make it easier for them to achieve their scientific objectives. A separate challenge is identifying specific systems and operations that need to be standardised, and then navigating the minefield of personal interests that typically inhibit agreement on a given format or language. As Murray Gell-Mann quipped, "a scientist would rather use someone else's toothbrush than someone else's nomenclature". Scientists and engineers will adopt standards only when they add value to their efforts to overcome the often steep costs of adoption.

Standards for engineering biology

While a number of SynBio standards have already been developed and await adoption by the broader community of users [5], others touch on core biological questions that are by no means solved from a scientific point of view. There is a legitimate concern that we still need to know more fundamental facts before we can describe engineered biosystems with a formal, unequivocal language. One typical case involves the design of genetic circuits, an archetypal product of SynBio endeavours. Habitual practices include directly transplanting toolkit for building electronic logic gates and related information-processing devices into the biological domain. However, one must be honest about how far these abstractions and their accompanying theoretical framework reflect biological reality. Boolean logic relies on values that are either true or false. In electronics, this is readily implemented using voltage levels that are separated by a larger amount than the expected noise to faithfully represent the state of the gate. In contrast, biological implementations of circuits tend to have a much higher noise-to-signal ratio, which makes it difficult to effectively distinguish true and false states and strongly limits the design of logic circuits. One way to alleviate this problem is by redesigning regulatory components to behave more digitally, but ultimately, we may need to revisit information processing in/by biological systems with other formalisms, either existing or yet to be developed, that go beyond Boolean logic [6].

"Scientists and engineers will adopt standards only when they add value to their efforts to overcome the often steep costs of adoption."

The same theory/implementation conundrum might be true for biological metrology, one of the main tenets of SynBio. Electronic circuits crucially rely on a clear definition of *potential* and *current*, their description in *volts* and *amperes*, and methods to measure these. By the same token, it is difficult to think about genetic circuits without robust measures of signal transmission through the regulation of gene expression or other core cellular processes. The concepts of RNA

© 2020 The Authors

polymerase per second (PoPS; [7]) and *ribosome per second* (RiPS) as biological counterparts of *current* were conceptualised early in the history of SynBio. Alas, very little has been done to further develop these units as practicable indicators of genetic circuit performance, perhaps due to the difficulties of measuring them accurately.

These examples showcase how developing standards for biological engineering still requires addressing a number of core scientific and technological gaps that have been left behind in the ongoing frenzy of application-focused development. Yet, such unsolved issues may strike back when the field continues to move from largely academic endeavours towards industrial realisation.

"...developing standards for biological engineering still requires addressing a number of core scientific and technological gaps that have been left behind in the ongoing frenzy of application-focused development."

Key actors in the standards conversation

International discussions about SynBio standards, mostly with US and EU stakeholders, have been going on since before 2010. Under the umbrella of the BIOROBOOST Project (http://standardsinsynbio.eu), the conversation now incorporates key actors of SynBio from Europe, North America and Asia. Much of the discussions deal with identifying key challenges for the development, promulgation and adoption of standards, and identifying stakeholders in academia, industry, research centres and politics.

The most conspicuous technical challenges include standardising simple biological parts, devices and circuits, chassis, metrology, descriptive languages (including graphical representations) and software tools. But the complexity of the endeavour also asks for the creation of a network of SynBio practitioners that share and evolve these standards together. While this is reminiscent of earlier Computational Modeling in Biology Network (COMBINE, http://co.mbine.org/), the focus of these SynBio networks needs to go beyond academic interests to include industry and commerce, and to develop strategies for educating a new generation of synthetic biologists who routinely use standards.

From the regulatory, technical and societal point of view, the challenge is complex. For example, there are practical questions such as the level of detail required in a given biological standard, which can go from light to very deep. As indicated above, *standard* is an umbrella concept, which includes a number of different approaches to harmonisation. These range from agreeing on *metrology* units and best practices to measure them, to developing standardised functional chassis—specific, formatted biological hosts for specific applications—to data formats, to safety criteria for approval by regulatory agencies and to ISO-approved reports and technical specifications.

It is necessary to distinguish between *biological standards* that could be similar to physics and engineering counterparts, such as the PoPS or RiPS units discussed above, and *standard operating procedures* (SOPs), which help users to carry out routine operations with efficiency, consistent quality and performance, and are compliant with regulations. For instance, the composition and preparation of the M9 medium would be an SOP, while the metrics for calculating containment of a given SynBio agent when released in the environment could become a biological *standard*. There are, of course, many grey zones between these two—for instance, formats for enabling communication between unrelated software, cloning methods, CRISPR-based editing and so on—that will hopefully be solved through conversations between stakeholders in the various forums just mentioned. The question remains, however, whether the wider community of potential users will see the value of adopting standards in their daily practice. Today, SynBio and systems biology practitioners are widely using the Synthetic Biology Open Language SBOL [8] and SBOL visual for describing vectors and constructs [9], and there is a great consensus on the need to go beyond the state of the art and further advance towards the standardisation of biological systems [5,10].

Stages of adoption

Is there a take-home lesson from the history of technology adoption that we can learn from for popularising biological standards? In fact, the trajectory of acceptance in the realm of engineering typically involves several stages: from an innovator phase to adoption by even the most recalcitrant laggards (Fig 1). Using this frame, it seems that most of the SynBio's standards developments are still in the innovator phase.

Many developments, even if critical for the early years in SynBio, never left the innovator state and are now outdated; advances in cloning and DNA synthesis have for instance replaced BioBricks. Others, such as SBOL [8] or the Standard European Vector Architecture (SEVA; [9]) are increasingly successful as interim formats in the early adopter stage. Yet, these may or may not become generally adopted depending on success stories and potential alternative scientific and technical solutions. Such progress will be determined by the combination of a bottom-up demand for interoperability and collaboration and a top-down implementation and enforcement by official agencies. Journal editors also have a role to play as well as reviewers of journal articles and grant proposals in insisting on the use of standards to improve reproducibility and reuse. Generally, it is important to realise that standards are ultimately social constructs to represent norms, objects or procedures, and that they become accepted by a group of individuals for practical reasons.

"... standards are ultimately social constructs to represent norms, objects or procedures, and that they become accepted by a group of individuals for practical reasons."

Low-hanging fruits

Despite the difficulties, it should be possible to come up with science-based standardisation proposals in SynBio that work across the biological, the digital and the social realms. The already existing ones at hand involve simple biological parts: devices such as promoters and other regulatory nodes and simple circuits—for instance, inverters, basic gates—such as those deposited in the repository of biological parts and other curated collections. The next stage involves definition and adoption of SynBio chassis

© 2020 The Authors

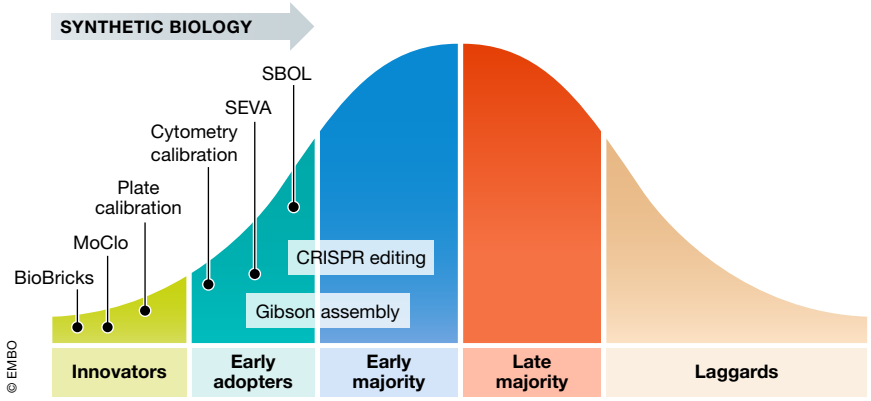

Figure 1. Adoption curve of/for biological standards.
Illustrative examples of the position of SynBio standards along the technology adoption curve: SynBio standards are largely still in the innovator phase but with a few examples having progressed to the early adopters or early majority segments. SBOL, Synthetic Biology Open Language; SEVA, Standard European Vector Architecture; MoClo, modular cloning.

other than laboratory bacteria or yeast strains. Not every species or strain that can host recombinant DNA can be considered a chassis, and this effort requires establishment of a map of requirements and functional relationships between industrially relevant practical applications and different biological platforms. Finally, standardisation would need to address the issue of metrology through the gene expression flow including fundamental units and the technologies and references to measure them, as well as computational language and software tools for easing collaborations between different actors. The main efforts to collect such low-hanging fruits would be greatly facilitated by biofoundries with good connections to policy makers with the objective of making the whole endeavour more appealing for the industrial sector.

"... the key to success is the merger of technical consistency and scientific soundness with legal requirements and consensus among end users."

The academic community cannot be a mere observer of these developments. In fact, there is much to do for endowing biological standards with a solid scientific basis, including the definition of each level of biological complexity amenable to standardisation. But the role in promoting standards is not only technical. There is ample room for networks of practitioners involving industrial players, who can provide information on how biological properties and processes could improve product development, manufacturability and consumer confidence. This could create a framework for identifying and monitoring standardisation requirements and maintaining an evolving list of scientific and industrial priorities. Ideally, such priority lists should also be considered by funding bodies to help in developing and driving adoption of standards. Relevant regulatory bodies should be involved to adapt or ease rules on the management of GMOs and/or SynBio agents. The same academic–industrial networks could also strengthen ongoing public outreach and citizen involvement to help overcoming the negative perception of genetic engineering in general.

In sum, we argue that the promise of SynBio for the benefit of global society and industry will only be met if significant advances are achieved on the standardisation front. To this end, it is not only essential to overcome national/political barriers and particular interests of given research groups, but also to gather key players in a permanent forum with the aim of making biological standards one of the ingredients of the 4th Industrial Revolution. Standards in biology will be used provided that they have intrinsic properties such as robustness, ease of use and context independence. But the key to success is the merger of technical consistency and scientific soundness with legal requirements and consensus among end users. This goes beyond the realm of research and tackles sociological and cultural issues that have been traditionally alien to the conversation. If this can be achieved, the benefits for SynBio and for society at large will be great.

Acknowledgements

Mireia Alonso is gratefully acknowledged for help in formatting the different versions of this manuscript. This work was funded by the European Union through the BioRoboost Project, H2020-NMBP-TR-IND-2018-2020/BIOTEC-01-2018 (CSA), Project ID 820699. Jake Beal was also supported in part by NSF Expeditions in Computing Program Award #1522074. This document does not contain technology or technical data controlled under either US International Traffic in Arms Regulation or US Export Administration Regulations. The information and views set out in this article are those of the authors and do not necessarily reflect the official opinion of the European Commission.

References

1. Dan SM (2019) How interface formats gain market acceptance: the role of developers and format characteristics in the development of *de facto* standards. *Technovation* 88: 102054
2. Beal J, Haddock-Angelli T, Farny N, Reggberg R (2018) Time to get serious about measurement in synthetic biology. *Trends Biotechnol* 36: 869–871
3. Vilanova C, Porcar M (2014) IGEM 2.0–refoundations for engineering biology. *Nat Biotechnol* 32: 420–424
4. Carr SB, Beal J, Densmore DM (2017) Reducing DNA context independence in bacterial promoters. *PLoS ONE* 12: e0176013
5. de Lorenzo V, Schmidt M (2018) Biological standards for the knowledge-Based BioEconomy: what is at stake. *New Biotechnol* 40: 170–180
6. Grozinger L, Amos M, Gorochowski TT, Carbonell P, Oyarzún DA, Stoof R, Fellermann H, Zuliani P, Tas H, Goñi-Moreno A (2019) Pathways to cellular supremacy in Biocomputing. *Nat Com* 10: 5250
7. Endy D (2005) Foundations for engineering biology. *Nature* 438: 449–453
8. Galdzicki M, Clancy K, Oberortner E, Pocock M, Quinn J, Rodriguez C, Roehner N, Wilson M, Adam L, Anderson JV *et al* (2014) SBOL: a community standard for communicating

 © 2020 The Authors

Further reading

Standardisation initiatives for Biology and Biotechnology

Xie Z, Hall J, McCarthy IP, Skitmore M, Shen L. Standardization efforts: The relationship between knowledge dimensions, search processes and innovation outcomes. *Technovation* 2016, 48–49: 69–78

Beal J. Bridging the Gap: A Roadmap to Breaking the Biological Design Barrier. *Front Biotechnol* 2014, *2*, 87

Knight T. Idempotent vector design for standard assembly. MIT artificial intelligent laboratory communications. https://doi.org/hdl.handle.net/1721.1/21168

Schreiber F, Sommer B, Bader GD, Gleeson P, Golebiewski M, Hucka M, Keating SM, König M, Myers C, Nickerson D, Waltemath D. Specifications of Standards in Systems and Synthetic Biology: Status and Developments in 2019. *J Integr Bioinform* 2019, 16, 20190035

Myers CJ, Beal J, Gorochowski TE, Kuwahara H, Madsen C, McLaughlin JA, *et al* (2017). A standard-enabled workflow for synthetic biology. *Biochem Soc Trans* 45, 793–803

Roehner N, Beal J, Clancy K, Bartley B, Misirli G, Grunberg R, Oberortner E, Pocock M, Bissell M, Madsen C, Nguyen T, Zhang M, Zhang Z, Zundel Z, Densmore D, Gennari J, Wipat A, Sauro H, Myers C. Sharing structure and function in biological design with SBOL 2.0", *ACS Syn Biol* 2016, 5 (6): 498–506

Beal J, Nguyen T, Gorochowski TE, Goñi-Moreno A, Scott-Brown J, McLaughlin JA, Madsen C, Aleritsch B, Bartley B, Bhakta S, Bissell M, Castillo HS, Clancy K, Luna A, Le Novère N, Palchick Z, Pocock M, Sauro H, Sexton JT, Tabor JJ, Voigt CA, Zundel Z, Myers C, Wipat A. Communicating structure and function in synthetic biology diagrams. *ACS Synth Biol* 2019, 8, 8, 1818–1825

Madsen C, Goni-Moreno A, Palchick ZPU, Roehner N, Bartley B, Bhatia S *et al* Synthetic Biology Open Language Visual (SBOL Visual) Version 2.1. *J Integr Bioinform* 2019, 16, 20180101

Quinn JY, Cox RS III, Adler A, Beal J, Bhatia S, Cai Y, *et al* (2015) SBOL Visual: A Graphical Language for Genetic Designs. *PLoS Biol* 13(12):e1002310

Walsh DI 3rd, Pavan M, Ortiz L, Wick S, Bobrow J, Guido NJ, Leinicke S, Fu D, Pandit S, Qin L, Carr PA, Densmore D. Standardizing automated DNA Assembly: best practices, metrics, and protocols using robots. *SLAS Technol* 2019, 24, 282–290

Synthetic Biology success stories

Ro D, Paradise E, Ouellet M *et al* Production of the antimalarial drug precursor artemisinic acid in engineered yeast. *Nature* 2006, 440, 940–943

DeLoache W, Russ Z, Narcross L *et al* An enzyme-coupled biosensor enables (*S*)-reticuline production in yeast from glucose. *Nat Chem Biol 2015*, 11, 465–471

Fernández-Rodríguez J, Yang L, Gorochowski TT, Gordon DB and Voigt CA. Memory and combinational logic based on DNA inversions: dynamics and evolutionary stability. *ACS Synth Biol* 2015, 4, 12, 1361–1372

Weinberg BH, Cho JH, Agarwal Y, Pham NTH, Caraballo LD, Walkosz M, Ortega C, Trexler M, Tague N, Law B, Benman WKJ, Letendre J, Beal J, Wong WW. High-performance chemical –and light-inducible recombinases in mammalian cells and mice. *Nat Commun* 2019, 10, 4845

Open questions in biological standards

Vilanova C, Tanner K, Dorado-Morales P, Villaescusa P, Chugani D, Frías A, Segredo E, Molero X, Fritschi M, Morales L, Ramón D, Peña C, Peretó J, Porcar M. Standards not that standard. *J Biol Eng* 2015, 9, 17

Nicholson DJ. Is the cell *really* a machine? *J Theor Biol* 2019, 477, 108–126

Beal J. Signal-to-Noise Ratio Measures Efficacy of Biological Computing Devices and Circuits. *Front Bioeng Biotechnol*. 2015, 3, 93

Hallinan JJ, Wipat A, Kitney R, Woods S, Taylor K and Goñi-Moreno, A. Future-proofing synthetic biology: educating the next generation. *Eng Biology* 2019, 3, 25–31

Schmidt M. A metric space for semantic containment: Towards the implementation of genetic firewalls. *Biosystems*, 2019, 185, 104015

Kitney R, Adeogun M, Fujishima Y, Goñi-Moreno A, Johnson R, Maxon M, Steedman S, Ward S, Winickoff D, Philp J. Enabling the advanced bioeconomy through public policy supporting biofoundries and engineering biology. *Trends in Biotechnol* 2019, 37, 917–920

designs in synthetic biology. *Nat Biotechnol* 32: 545 – 550

9. Martínez-García E, Goñi-Moreno A, Bartley B, McLaughlin J, Sánchez-Sampedro L, Pascual Del Pozo H, Prieto Hernández C, Marletta AS, De Lucrezia D, Sánchez-Fernández G *et al* (2020) SEVA 3.0: An update of the Standard European Vector Architecture for enabling portability of genetic constructs among diverse bacterial hosts. *Nucleic Acids Res* 8: D1164 – D1170
10. Schreiber F, Sommer B, Bader GD, Gleeson P, Golebiewski M, Hucka M, Keating SM, König M, Myers C, Nickerson D *et al* (2019) Specifications of standards in systems and synthetic biology: status and developments in 2019. *J Integr Bioinform* 16: 20190035

License: This is an open access article under the terms of the Creative Commons Attribution-NonCommercial-NoDerivs 4.0 License, which permits use and distribution in any medium, provided the original work is properly cited, the use is non-commercial and no modifications or adaptations are made.